



Earth Resources
A Continuing
Bibliography
with Indexes

NASA SP-7041(43)
October 1984

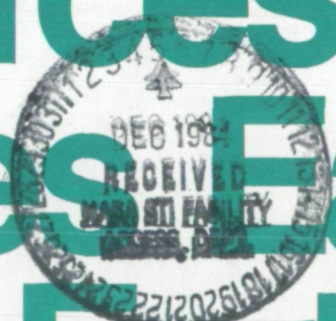
(NASA-SP-7041(43)) EARTH RESOURCES, A
CONTINUING BIBLIOGRAPHY WITH INDEXES
(National Aeronautics and Space
Administration) 136 p HC AC7/MF A01

N85-12411

CSCL 05B 00/43 Unclassified 20586

National Aeronautics and
Space Administration

es Earth Resources
s Earth Resources
Earth Resources E
th Resources Ear
Resources Earth
Resources Earth F
ources Earth Res



ACCESSION NUMBER RANGES

Accession numbers cited in this Supplement fall within the following ranges.

STAR (N-10000 Series) N84-22527 - N84-28725

IAA (A-10000 Series) A84-30009 - A84-39762

NASA SP-7041(43)

EARTH RESOURCES

A CONTINUING BIBLIOGRAPHY WITH INDEXES

Issue 43

A selection of annotated references to unclassified reports and journal articles that were introduced into the NASA scientific and technical information system and announced between July 1 and September 30, 1984 in

- *Scientific and Technical Aerospace Reports (STAR)*
- *International Aerospace Abstracts (IAA)*.



Scientific and Technical Information Branch 1984
National Aeronautics and Space Administration
Washington, DC

This supplement is available as NTISUB/038/093 from the National Technical Information Service (NTIS), Springfield, Virginia 22161 at the price of \$12.50 domestic; \$25.00 foreign for standing orders. Please note: Standing orders are subscriptions which do not terminate at the end of a year, as do regular subscriptions, but continue indefinitely unless specifically terminated by the subscriber.

INTRODUCTION

The technical literature described in this continuing bibliography may be helpful to researchers in numerous disciplines such as agriculture and forestry, geography and cartography, geology and mining, oceanography and fishing, environmental control, and many others. Until recently it was impossible for anyone to examine more than a minute fraction of the Earth's surface continuously. Now vast areas can be observed synoptically, and changes noted in both the Earth's lands and waters, by sensing instrumentation on orbiting spacecraft or on aircraft.

This literature survey lists 460 reports, articles, and other documents announced between July 1 and September 30, 1984 in *Scientific and Technical Aerospace Reports (STAR)*, and *International Aerospace Abstracts (IAA)*.

The coverage includes documents related to the identification and evaluation by means of sensors in spacecraft and aircraft of vegetation, minerals, and other natural resources, and the techniques and potentialities of surveying and keeping up-to-date inventories of such riches. It encompasses studies of such natural phenomena as earthquakes, volcanoes, ocean currents, and magnetic fields; and such cultural phenomena as cities, transportation networks, and irrigation systems. Descriptions of the components and use of remote sensing and geophysical instrumentation, their subsystems, observational procedures, signature and analyses and interpretive techniques for gathering data are also included. All reports generated under NASA's Earth Resources Survey Program for the time period covered in this bibliography will also be included. The bibliography does not contain citations to documents dealing mainly with satellites or satellite equipment used in navigation or communication systems, nor with instrumentation not used aboard aerospace vehicles.

The selected items are grouped in nine categories. These are listed in the Table of Contents with notes regarding the scope of each category. These categories were especially chosen for this publication, and differ from those found in *STAR* and *IAA*.

Each entry consists of a standard bibliographic citation accompanied by an abstract. The citations include the original accession numbers from the respective announcement journals.

Under each of the nine categories, the entries are presented in one of two groups that appear in the following order:

IAA entries identified by accession number series A84-10,000 in ascending accession number order;

STAR entries identified by accession number series N84-10,000 in ascending accession number order.

After the abstract section, there are six indexes:

subject, personal author, corporate source, contract number, report/accession number, and accession number.

AVAILABILITY OF CITED PUBLICATIONS

IAA ENTRIES (A84-10000 Series)

All publications abstracted in this Section are available from the Technical Information Service, American Institute of Aeronautics and Astronautics, Inc. (AIAA), as follows: Paper copies of accessions are available at \$8.50 per document. Microfiche⁽¹⁾ of documents announced in *IAA* are available at the rate of \$4.00 per microfiche on demand. Standing order microfiche are available at the rate of \$1.45 per microfiche for *IAA* source documents.

Minimum air-mail postage to foreign countries is \$2.50 and all foreign orders are shipped on payment of pro-forma invoices.

All inquiries and requests should be addressed to AIAA Technical Information Service. Please refer to the accession number when requesting publications.

STAR ENTRIES (N84-10000 Series)

One or more sources from which a document announced in *STAR* is available to the public is ordinarily given on the last line of the citation. The most commonly indicated sources and their acronyms or abbreviations are listed below. If the publication is available from a source other than those listed, the publisher and his address will be displayed on the availability line or in combination with the corporate source line.

Avail: NTIS. Sold by the National Technical Information Service. Prices for hard copy (HC) and microfiche (MF) are indicated by a price code preceded by the letters HC or MF in the *STAR* citation. Current values for the price codes are given in the tables on page viii.

Documents on microfiche are designated by a pound sign (#) following the accession number. The pound sign is used without regard to the source or quality of the microfiche.

Initially distributed microfiche under the NTIS SRIM (Selected Research in Microfiche) is available at greatly reduced unit prices. For this service and for information concerning subscription to NASA printed reports, consult the NTIS Subscription Section, Springfield, Va. 22161.

NOTE ON ORDERING DOCUMENTS: When ordering NASA publications (those followed by the * symbol), use the N accession number. NASA patent applications (only the specifications are offered) should be ordered by the US-Patent-Appl-SN number. Non-NASA publications (no asterisk) should be ordered by the AD, PB, or other *report* number shown on the last line of the citation, not by the N accession number. It is also advisable to cite the title and other bibliographic identification.

Avail: SOD (or GPO). Sold by the Superintendent of Documents, U.S. Government Printing Office, in hard copy. The current price and order number are given following the availability line. (NTIS will fill microfiche requests, as stated above, for those documents identified by a # symbol.)

Avail: NASA Public Document Rooms. Documents so indicated may be examined at or purchased from the National Aeronautics and Space Administration, Public Document Room (Room 126), 600 Independence Ave., S.W., Washington, D.C. 20546, or public document rooms located at each of the NASA research centers, the NASA Space Technology Laboratories, and the NASA Pasadena Office at the Jet Propulsion Laboratory.

(1) A microfiche is a transparent sheet of film, 105 by 148 mm in size containing as many as 60 to 98 pages of information reduced to micro images (not to exceed 26.1 reduction).

Avail: DOE Depository Libraries. Organizations in U.S. cities and abroad that maintain collections of Department of Energy reports, usually in microfiche form, are listed in *Energy Research Abstracts*. Services available from the DOE and its depositories are described in a booklet, *DOE Technical Information Center - Its Functions and Services* (TID-4660), which may be obtained without charge from the DOE Technical Information Center.

Avail: Univ. Microfilms. Documents so indicated are dissertations selected from *Dissertation Abstracts* and are sold by University Microfilms as xerographic copy (HC) and microfilm. All requests should cite the author and the Order Number as they appear in the citation.

Avail: USGS. Originals of many reports from the U.S. Geological Survey, which may contain color illustrations, or otherwise may not have the quality of illustrations preserved in the microfiche or facsimile reproduction, may be examined by the public at the libraries of the USGS field offices whose addresses are listed in this introduction. The libraries may be queried concerning the availability of specific documents and the possible utilization of local copying services, such as color reproduction.

Avail: HMSO. Publications of Her Majesty's Stationery Office are sold in the U.S. by Pendragon House, Inc. (PHI), Redwood City, California. The U.S. price (including a service and mailing charge) is given, or a conversion table may be obtained from PHI.

Avail: BLL (formerly NLL): British Library Lending Division, Boston Spa, Wetherby, Yorkshire, England. Photocopies available from this organization at the price shown. (If none is given, inquiry should be addressed to the BLL.)

Avail: Fachinformationszentrum, Karlsruhe. Sold by the Fachinformationszentrum Energie, Physik, Mathematik GMBH, Eggenstein Leopoldshafen, Federal Republic of Germany, at the price shown in deutschmarks (DM).

Avail: Issuing Activity, or Corporate Author, or no indication of availability. Inquiries as to the availability of these documents should be addressed to the organization shown in the citation as the corporate author of the document.

Avail: U.S. Patent and Trademark Office. Sold by Commissioner of Patents and Trademarks, U.S. Patent and Trademark Office, at the standard price of 50 cents each, postage free.

Avail: ESDU. Pricing information on specific data, computer programs, and details on ESDU topic categories can be obtained from ESDU International Ltd. Requesters in North America should use the Virginia address while all other requesters should use the London address, both of which are on page vii.

Other availabilities: If the publication is available from a source other than the above, the publisher and his address will be displayed entirely on the availability line or in combination with the corporate author line.

PUBLIC COLLECTIONS OF NASA DOCUMENTS

DOMESTIC: NASA and NASA-sponsored documents and a large number of aerospace publications are available to the public for reference purposes at the library maintained by the American Institute of Aeronautics and Astronautics, Technical Information Service, 555 West 57th Street, 12th Floor, New York, New York 10019.

EUROPEAN: An extensive collection of NASA and NASA-sponsored publications is maintained by the British Library Lending Division, Boston Spa, Wetherby, Yorkshire, England for public access. The British Library Lending Division also has available many of the non-NASA publications cited in *Star*. European requesters may purchase facsimile copy or microfiche of NASA and NASA-sponsored documents, those identified by both the symbols # and * from ESA - Information Retrieval Service European Space Agency, 8-10 rue Mario-Nikis, 75738 Paris CEDEX 15, France.

FEDERAL DEPOSITORY LIBRARY PROGRAM

In order to provide the general public with greater access to U.S. Government publications, Congress established the Federal Depository Library Program under the Government Printing Office (GPO), with 50 regional depositories responsible for permanent retention of material, inter-library loan, and reference services. Over 1,300 other depositories also exist. A list of the regional GPO libraries appears on the inside back cover.

ADDRESSES OF ORGANIZATIONS

American Institute of Aeronautics and
Astronautics
Technical Information Service
555 West 57th Street, 12th Floor
New York, New York 10019

British Library Lending Division,
Boston Spa, Wetherby, Yorkshire,
England

Commissioner of Patents and
Trademarks
U.S. Patent and Trademark Office
Washington, D.C. 20231

Department of Energy
Technical Information Center
P.O. Box 62
Oak Ridge, Tennessee 37830

ESA-Information Retrieval Service
ESRIN
Via Galileo Galilei
00044 Frascati (Rome) Italy

ESDU International, Ltd.
1495 Chain Bridge Road
McLean, Virginia 22101

ESDU International, Ltd.
251-259 Regent Street
London, W1R 7AD, England

Fachinformationszentrum Energie, Physik,
Mathematik GMBH
7514 Eggenstein Leopoldshafen
Federal Republic of Germany

Her Majesty's Stationery Office
P.O. Box 569, S.E. 1
London, England

NASA Scientific and Technical Information
Facility
P.O. Box 8757
B.W.I. Airport, Maryland 21240

National Aeronautics and Space
Administration
Scientific and Technical Information
Branch (NIT-1)
Washington, D.C. 20546

National Technical Information Service
5285 Port Royal Road
Springfield, Virginia 22161

Pendragon House, Inc.
899 Broadway Avenue
Redwood City, California 94063

Superintendent of Documents
U.S. Government Printing Office
Washington, D.C. 20402

University Microfilms
A Xerox Company
300 North Zeeb Road
Ann Arbor, Michigan 48106

University Microfilms, Ltd.
Tylers Green
London, England

U.S. Geological Survey Library
National Center - MS 950
12201 Sunrise Valley Drive
Reston, Virginia 22092

U.S. Geological Survey Library
2255 North Gemini Drive
Flagstaff, Arizona 86001

U.S. Geological Survey
345 Middlefield Road
Menlo Park, California 94025

U.S. Geological Survey Library
Box 25046
Denver Federal Center, MS 914
Denver, Colorado 80225

NTIS PRICE SCHEDULES**Schedule A**
STANDARD PAPER COPY PRICE SCHEDULE

(Effective January 1, 1983)

| Price Code | Page Range | North American Price | Foreign Price |
|------------|------------|----------------------|---------------|
| A01 | Microfiche | \$ 4.50 | \$ 9.00 |
| A02 | 001-025 | 7.00 | 14.00 |
| A03 | 026-050 | 8.50 | 17.00 |
| A04 | 051-075 | 10.00 | 20.00 |
| A05 | 076-100 | 11.50 | 23.00 |
| A06 | 101-125 | 13.00 | 26.00 |
| A07 | 126-150 | 14.50 | 29.00 |
| A08 | 151-175 | 16.00 | 32.00 |
| A09 | 176-200 | 17.50 | 35.00 |
| A10 | 201-225 | 19.00 | 38.00 |
| A11 | 226-250 | 20.50 | 41.00 |
| A12 | 251-275 | 22.00 | 44.00 |
| A13 | 276-300 | 23.50 | 47.00 |
| A14 | 301-325 | 25.00 | 50.00 |
| A15 | 326-350 | 26.50 | 53.00 |
| A16 | 351-375 | 28.00 | 56.00 |
| A17 | 376-400 | 29.50 | 59.00 |
| A18 | 401-425 | 31.00 | 62.00 |
| A19 | 426-450 | 32.50 | 65.00 |
| A20 | 451-475 | 34.00 | 68.00 |
| A21 | 476-500 | 35.50 | 71.00 |
| A22 | 501-525 | 37.00 | 74.00 |
| A23 | 526-550 | 38.50 | 77.00 |
| A24 | 551-575 | 40.00 | 80.00 |
| A25 | 576-600 | 41.50 | 83.00 |
| A99 | 601-up | -- 1 | -- 2 |

1/ Add \$1.50 for each additional 25 page increment or portion thereof for 601 pages up.

2/ Add \$3.00 for each additional 25 page increment or portion thereof for 601 pages and more.

Schedule E
EXCEPTION PRICE SCHEDULE
Paper Copy & Microfiche

| Price Code | North American Price | Foreign Price |
|------------|----------------------|---------------|
| E01 | \$ 6.50 | \$ 13.50 |
| E02 | 7.50 | 15.50 |
| E03 | 9.50 | 19.50 |
| E04 | 11.50 | 23.50 |
| E05 | 13.50 | 27.50 |
| E06 | 15.50 | 31.50 |
| E07 | 17.50 | 35.50 |
| E08 | 19.50 | 39.50 |
| E09 | 21.50 | 43.50 |
| E10 | 23.50 | 47.50 |
| E11 | 25.50 | 51.50 |
| E12 | 28.50 | 57.50 |
| E13 | 31.50 | 63.50 |
| E14 | 34.50 | 69.50 |
| E15 | 37.50 | 75.50 |
| E16 | 40.50 | 81.50 |
| E17 | 43.50 | 88.50 |
| E18 | 46.50 | 93.50 |
| E19 | 51.50 | 102.50 |
| E20 | 61.50 | 123.50 |

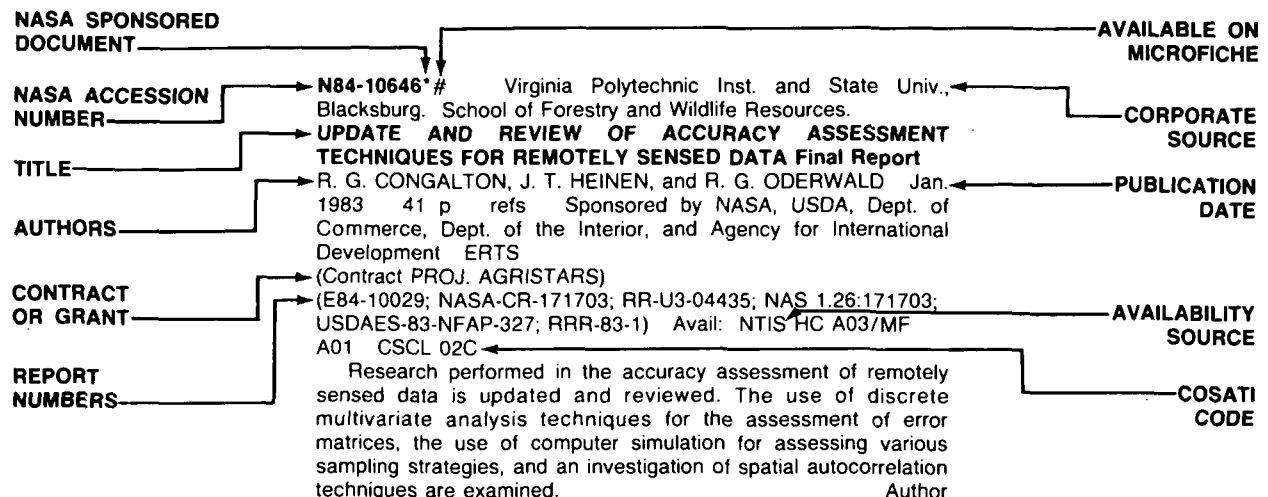
E-99 - Write for quote

N01 35.00 45.00

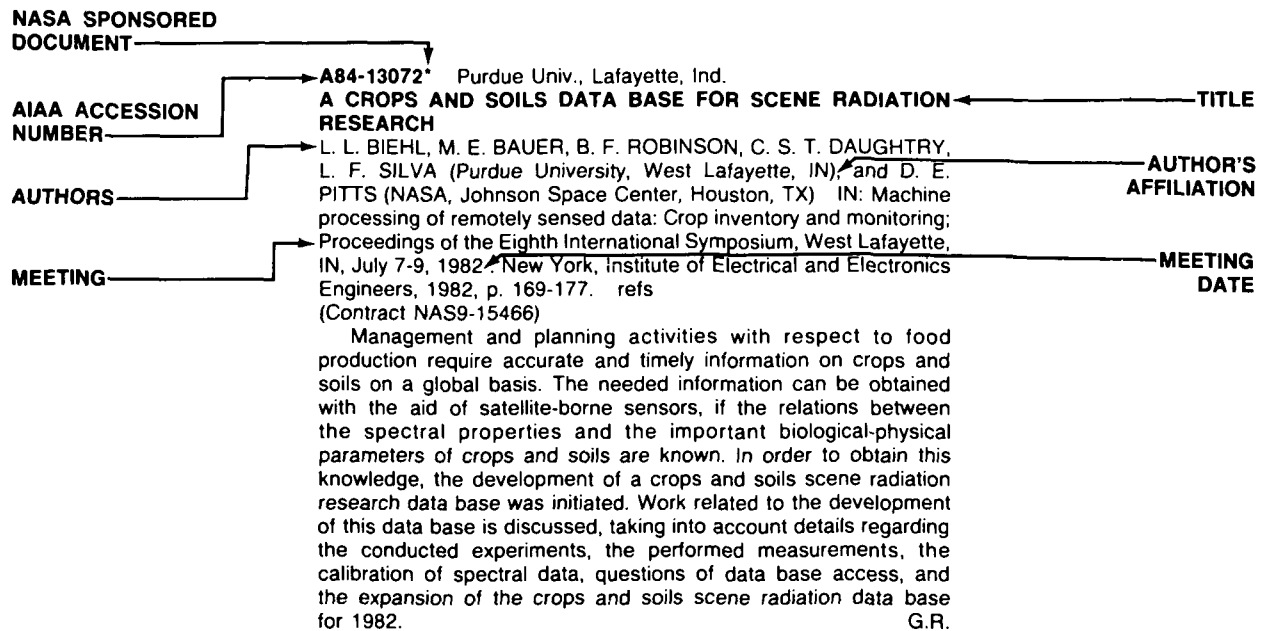
TABLE OF CONTENTS

| | Page |
|--|------------|
| Category 01 Agriculture and Forestry Includes crop forecasts, crop signature analysis, soil identification, disease detection, harvest estimates, range resources, timber inventory, forest fire detection, and wildlife migration patterns. | 1 |
| Category 02 Environmental Changes and Cultural Resources Includes land use analysis, urban and metropolitan studies, environmental impact, air and water pollution, geographic information systems, and geographic analysis. | 13 |
| Category 03 Geodesy and Cartography Includes mapping and topography. | 17 |
| Category 04 Geology and Mineral Resources Includes mineral deposits, petroleum deposits, spectral properties of rocks, geological exploration, and lithology. | 22 |
| Category 05 Oceanography and Marine Resources Includes sea-surface temperature, ocean bottom surveying imagery, drift rates, sea ice and icebergs, sea state, fish location | 30 |
| Category 06 Hydrology and Water Management Includes snow cover and water runoff in rivers and glaciers, saline intrusion, drainage analysis, geomorphology of river basins, land uses, and estuarine studies. | 50 |
| Category 07 Data Processing and Distribution Systems Includes film processing, computer technology, satellite and aircraft hardware, and imagery. | 54 |
| Category 08 Instrumentation and Sensors Includes data acquisition and camera systems and remote sensors. | 64 |
| Category 09 General Includes economic analysis. | 71 |
| Subject Index | A-1 |
| Personal Author Index | B-1 |
| Corporate Source Index | C-1 |
| Contract Number Index | D-1 |
| Report / Accession Number Index | E-1 |
| Accession Number Index | F-1 |

TYPICAL CITATION AND ABSTRACT FROM STAR



TYPICAL CITATION AND ABSTRACT FROM IAA



EARTH RESOURCES

A Continuing Bibliography (Issue 43)

OCTOBER 1984

01

AGRICULTURE AND FORESTRY

Includes crop forecasts, crop signature analysis, soil identification, disease detection, harvest estimates, range resources, timber inventory, forest fire detection, and wildlife migration patterns.

A84-30227#

MEASUREMENT OF BORO RICE ACREAGE IN NABINAGAR THANA BY REMOTE SENSING TECHNIQUE

A. K. M. FARIDUDDIN BHUIYAN, D. A. QUADIR, M. RAHMAN, and HARUN-OR-RASHID (Bangladesh Space Research and Remote Sensing Organization, Dacca, Bangladesh) IN: Asian Conference on Remote Sensing, 3rd, Dacca, Bangladesh, December 4-7, 1982, Proceedings . Tokyo, University of Tokyo, 1983, p. P-1-1 to P-1-11. refs

A program is reported which has been initiated in Bangladesh with the objective of developing a computer-based model for estimating boro rice areas using Landsat CCT data. Since some boro rice fields are smaller than the Landsat pixel, a measurement bias is introduced in those cases where only Landsat data are used. Aerial photographs can be used as initial reference material to reduce the correction factor to Landsat imagery. Estimates obtained for the boro rice acreage in Nabinagar Thana are found to be accurate to within plus or minus 5 percent. V.L.

A84-30228#

MULTISPECTRAL AND MULTITEMPORAL LANDSAT DATA FOR SOIL SURVEYS - A CASE STUDY OF PART OF NORTH WEST INDIA

H. S. IYER and M. L. MANCHANDA (Indian Photo-Interpretation Institute, Dehra Dun, India) IN: Asian Conference on Remote Sensing, 3rd, Dacca, Bangladesh, December 4-7, 1982, Proceedings . Tokyo, University of Tokyo, 1983, p. P-2-1 to P-2-13.

A84-30229#

MICROWAVE MEASUREMENTS USING ACTIVE AND PASSIVE SENSORS

S. MOHAN, V. M. MEHTA, S. MEHTA, and D. S. KAMAT (Indian Space Research Organization, Space Applications Centre, Ahmedabad, India) IN: Asian Conference on Remote Sensing, 3rd, Dacca, Bangladesh, December 4-7, 1982, Proceedings . Tokyo, University of Tokyo, 1983, p. P-3-1 to P-3-10. refs

A microwave scatterometer operating at 9.4 GHz and a passive microwave radiometer operating at 1.413 GHz have been used to sense soil moisture and vegetation growth. An analysis of the measurement results indicates that the 9.4-GHz scatterometer is capable of sensing the surface soil moisture, whereas the passive microwave sensor provides information on the integrated column of deeper layers. The 1.413-GHz passive sensor is also expected to provide information on soil moisture in the presence of vegetation, whereas the scatterometer is unsuitable for such studies. However, the 9.4-GHz scatterometer can be used for monitoring vegetation growth, while the passive sensor is yet to be exploited for such applications. V.L.

A84-30235#

MEASUREMENT OF BORO RICE ACREAGE IN SRIMANGAL THANA BY REMOTE SENSING TECHNIQUE

M. RAHMAN, A. K. M. FARIDUDDIN BHUIYAN, A. GAFOOR, and M. U. CHAUDHURY (Bangladesh Space Research and Remote Sensing Organization, Dacca, Bangladesh) IN: Asian Conference on Remote Sensing, 3rd, Dacca, Bangladesh, December 4-7, 1982, Proceedings . Tokyo, University of Tokyo, 1983, p. A-1-1 to A-1-13. refs

Black and white aerial photographs and computer-generated color-coded Landsat-2 imagery have been used to estimate the boro rice acreage in Srimangal Thana, Bangladesh. The terrain features in Srimangal Thana are examined in detail, and the methodology used is discussed along with the estimates obtained. It is concluded that real time remote sensing can provide sufficiently accurate estimates of the boro rice acreage for crop production monitoring in Bangladesh. V.L.

A84-30236#

ANALYSING FOREST STRUCTURES BY REMOTE SENSING

D. MARUOKA, S. TOMIMURA, and T. GODA (Asia Air Survey Co., Ltd, Atsugi, Kanagawa, Japan) IN: Asian Conference on Remote Sensing, 3rd, Dacca, Bangladesh, December 4-7, 1982, Proceedings . Tokyo, University of Tokyo, 1983, p. A-3-0 to A-3-10.

An interim report is presented attempting to gain a precise analysis of forest composition in two areas of Japan by means of field surveys and aerial photogrammetry. The research was conducted at Aokigahara on the foothills of Mt. Fuji and at Kobotoke on the border of the Tokyo Metropolitan area and the Yamanashi Prefecture. Since most forest areas in Japan are in hilly or mountainous terrain, it is not easy to obtain precise data on crown and tree height in a short time. Where the ground can be seen through the trees, photogrammetry can give both the treetop level and the ground height; the difference between the two yields the tree height. The method is just as accurate as the field survey (plus or minus 50 cm), and 1000 points per day can be measured vs. about 60 by the field survey method. Good quality timber can be grown more quickly when such information is used to thin the forest appropriately. D.H.

A84-30237#

IDENTIFICATION OF BROWN PLANT HOPPER AND BACTERIAL LEAF BLIGHT AFFECTED RICE CROP ON LANDSAT FALSE COLOUR COMPOSITES

P. P. N. RAO and V. R. RAO (Indian Space Research Organization, Bangalore, India) IN: Asian Conference on Remote Sensing, 3rd, Dacca, Bangladesh, December 4-7, 1982, Proceedings . Tokyo, University of Tokyo, 1983, p. A-4-1 to A-4-12.

A84-30238#

STUDY OF DESERTIFICATION/ARIDITY THROUGH REMOTE SENSING

M. A. JABBAR (Bangladesh Space Research and Remote Sensing Organization, Dacca, Bangladesh) IN: Asian Conference on Remote Sensing, 3rd, Dacca, Bangladesh, December 4-7, 1982, Proceedings . Tokyo, University of Tokyo, 1983, p. A-5-1 to A-5-9.

Phenomena leading to desertification (increased aridity) in the Barind Tract of northwest Bangladesh have been studied by means of satellite imagery, remote sensing being one of the best tools

01 AGRICULTURE AND FORESTRY

for detecting such areas. By studying the temporal changes in the images, it can be seen how solar radiation of visible and infrared bands combination with vegetation cover, distribution of annual precipitation and type of soil are the main factors in the desertification process. Human interference, in the form of deforestation, can change the energy balance-albedo of an area, raise the mean temperature, and aggravate ground water deficiencies. All of these factors have been detected in the Barind Tract. Through an extensive program of reforestation and surface/ground water management, the desertification process can be effectively checked.

D.H.

A84-30239#

AN INQUIRY INTO METHODS OF ESTIMATING YIELDS OF WHEAT AND AUTUMN CROPS IN THE PLAIN REGION WITH LANDSAT IMAGES VISUAL INTERPRETATION

F. C. JI, L. W. KE (Laboratory for Agricultural Remote Sensing, Taiyuan, People's Republic of China), C. J. CHENG, and C. L. QI (National Remote Sensing Center of China, Beijing, People's Republic of China) IN: Asian Conference on Remote Sensing, 3rd, Dacca, Bangladesh, December 4-7, 1982, Proceedings . Tokyo, University of Tokyo, 1983, p. A-7-1 to A-7-25.

The methodology for estimating crop yields (particularly for millet, cotton, wheat and sorghum) both from on-site studies and from analysis of Landsat multiwaveband photos is discussed. Such work with satellite imagery is a new undertaking in China, and interpretation at the scale of 1:250,000 has many difficulties. At the same growth stage, corn, sorghum, millet and cotton are scarcely distinguishable and so must be estimated together rather than separately. Still, testing has shown a close correlation between Landsat image tones (color) and agriculturally productive conditions, growth vigor of crops and relevant yield levels. The best dates are noted for taking the images for different crops in different areas. Visual interpretation of Landsat images has a very important reference value for providing economic and timely information - supplemented with a few ground truth investigations - for agricultural management, grain purchases and distribution by the government.

D.H.

A84-30250#

LANDSAT IMAGE USE IN FORESTRY MANAGEMENT IN CHINA

Y.-C. FANG (Nanjing Technological College of Forest Products, Nanjing, People's Republic of China) IN: Asian Conference on Remote Sensing, 3rd, Dacca, Bangladesh, December 4-7, 1982, Proceedings . Tokyo, University of Tokyo, 1983, p. Q-13-1 to Q-13-15.

A84-30253#

SPOT SIMULATIONS IN BANGLADESH FLIGHT OPERATIONS AND MAIN RESULTS

M. U. CHAUDHURY (Bangladesh Space Research and Remote Sensing Organization, Dacca, Bangladesh), C. LAYALLE, J. ROUSSEL (SocieteEuropeenne de Propulsion, Paris, France), and J. C. FAVARD (Groupement pour le Developpement de la Teledetection Aerospatiale, Toulouse, France) IN: Asian Conference on Remote Sensing, 3rd, Dacca, Bangladesh, December 4-7, 1982, Proceedings . Tokyo, University of Tokyo, 1983, p. C-6-1 to C-6-8.

First results are reported that were gained from the interpretation of data collected from an airborne remote sensing experiment over a study area in Bangladesh, namely the Hail Haor area south of Syhlet. Visible and near-infrared data from a Daedalus scanner were recorded while infrared color photographs were taken. The purpose was to allow the generation of SPOT satellite simulated data over a set of given areas. Three topics of special interest were rice, coastal areas, and cane sugar. Topography, climate, hydrology and land use of the study area are described. Studies are to be carried on in Bangladesh on an interactive image processing system.

D.H.

A84-30670* National Aeronautics and Space Administration. Goddard Space Flight Center, Greenbelt, Md.

ATMOSPHERIC EFFECT ON CLASSIFICATION OF FINITE FIELDS

Y. J. KAUFMAN (NASA, Goddard Space Flight Center, Laboratory for Atmospheric Sciences, Greenbelt; Maryland, University, College Park, MD) and R. S. FRASER (NASA, Goddard Space Flight Center, Laboratory for Atmospheric Sciences, Greenbelt, MD) Remote Sensing of Environment (ISSN 0034-4257), vol. 15, March 1984, p. 95-118. refs

The atmospheric effect on the upward radiance of sunlight scattered from the earth-atmosphere system is strongly influenced by the contrasts between fields and their sizes. In this paper, the radiances above finite fields are computed to simulate radiances measured by a satellite. A simulation case including 11 agricultural fields and four natural fields (water, soil, savannah, and forest) is used to test the effect of field size, background reflectance, and optical thickness of the atmosphere on the classification accuracy. For a given atmospheric turbidity, the atmospheric effect on classification of surface features may be much stronger for nonuniform surfaces than for uniform surfaces. Therefore, the classification accuracy of agricultural fields and urban areas is dependent not only on the optical characteristics of the atmosphere, but also on the size of the surface elements to be classified and their contrasts. It is concluded that new atmospheric correction methods, which take into account the finite size of the fields, are needed.

Author

A84-30671* Computer Sciences Corp., Silver Spring, Md.

CALCULATIONS OF RADAR BACKSCATTERING COEFFICIENT OF VEGETATION-COVERED SOILS

T. MO (Computer Sciences Corp., Silver Spring, MD), T. J. SCHMUGGE (NASA, Goddard Space Flight Center, Hydrological Sciences Branch, Greenbelt, MD), and T. J. JACKSON (U.S. Department of Agriculture, Hydrology Laboratory, Beltsville, MD) Remote Sensing of Environment (ISSN 0034-4257), vol. 15, March 1984, p. 119-133. refs

The present investigation has the objective to develop a simple 'user's' model for simulating the measured radar backscattering coefficients from vegetation-covered fields in conjunction with the data obtained by Jackson et al. (1980, 1982). The theoretical work reported by Fung and Eom (1981) provides the basis for the model. Certain modifications are related to a consideration of the effect of a vegetation canopy. The first part of the model is concerned with a description of scatter from rough bare soil, while the second part takes into account the effect of a vegetation cover. It is shown that the measured angular distribution of the backscattering coefficient of vegetation-covered fields can be satisfactorily reproduced by using the developed model.

G.R.

A84-30673

SOIL SPECTRAL EFFECTS ON 4-SPACE VEGETATION DISCRIMINATION

A. R. HUETE, D. F. POST (Arizona, University, Tucson, AZ), and R. D. JACKSON (U.S. Department of Agriculture, Water Conservation Laboratory, Phoenix, AZ) Remote Sensing of Environment (ISSN 0034-4257), vol. 15, March 1984, p. 155-165. refs

The influence of soil background on vegetation discrimination in four-band reflectance space was examined. Dry and wet reflectance data were obtained for 20 soils covering a wide range in spectral properties with a hand-held radiometer. Principal components analysis was used to study the distribution of soil spectra in 4-space and to define a mean soil line. Soil-specific background lines were similarly derived and used to examine the overall cloud of soil spectra in individual soil form. Reflectance data from a full-canopy wheat plot were used to compute unit vector coefficients in the greenness direction from the mean soil line and from the individual soil lines. Analysis of the mean soil line showed that it was not possible to discriminate bare soil from low vegetation densities. Greenness measurements were shown to be sensitive to both soil type and soil moisture condition. In contrast, the use of individual soil lines as a base to measure

greenness minimized soil background influence and improved vegetation assessment, particularly at low green plant canopy covers.

Author

A84-30674

EVALUATION OF FACTORS CAUSING REFLECTANCE DIFFERENCES BETWEEN SUN AND SHADE LEAVES

H. W. GAUSMAN (U.S. Department of Agriculture, Agricultural Research Service, Lubbock, TX) *Remote Sensing of Environment* (ISSN 0034-4257), vol. 15, March 1984, p. 177-181. refs

Shade and sun leaves of Valencia orange (*Citrus sinensis* (L.) Osbeck) were collected to evaluate comparative effects of their leaf chlorophyll concentration, water content, thickness, and mesophyll volume of air on visible light reflectance, specifically the 0.45-, 0.55-, and 0.65-micron wavelength (WLs). The reflectance at the 0.45-, 0.55-, and 0.65-micron WLs of sun leaves but not shade leaves was negatively correlated with total chlorophyll concentration. Reflectance at the 0.45-micron WL was affected by leaf water content for both sun and shade leaves. Sun leaf reflectance at the 0.45-micron WL, but not shade leaf reflectance was affected significantly by leaf mesophyll air volume. The effect of leaf thickness on reflectance was apparently of less importance than that of the chlorophyll content, air volume, and water content. The influence of shade and sun leaves on visible light reflectance/absorptance of at least Valencia orange tree canopies probably should be considered in modeling canopy reflectance and growth.

Author

A84-31498* Texas A&M Univ., College Station.

ACTIVE MICROWAVE RESPONSES - AN AID IN IMPROVED CROP CLASSIFICATION

W. D. ROSENTHAL (Texas A & M University, College Station, TX) and B. J. BLANCHARD (NASA, Goddard Space Flight Center, Greenbelt, MD) *Photogrammetric Engineering and Remote Sensing* (ISSN 0099-1112), vol. 50, April 1984, p. 461-468. refs (Contract NSG-5134)

A study determined the feasibility of using visible, infrared, and active microwave data to classify agricultural crops such as corn, sorghum, alfalfa, wheat stubble, millet, shortgrass pasture and bare soil. Visible through microwave data were collected by instruments on board the NASA C-130 aircraft over 40 agricultural fields near Guymon, OK in 1978 and Dalhart, TX in 1980. Results from stepwise and discriminant analysis techniques indicated 4.75 GHz, 1.6 GHz, and 0.4 GHz cross-polarized microwave frequencies were the microwave frequencies most sensitive to crop type differences. Inclusion of microwave data in visible and infrared classification models improved classification accuracy from 73 percent to 92 percent. Despite the results, further studies are needed during different growth stages to validate the visible, infrared, and active microwave responses to vegetation.

Author

A84-31499

ASSESSING CHANGE IN THE SURFICIAL CHARACTER OF A SEMIARID ENVIRONMENT WITH LANDSAT RESIDUAL IMAGES

T. D. FRANK (Illinois, University, Urbana, IL) *Photogrammetric Engineering and Remote Sensing* (ISSN 0099-1112), vol. 50, April 1984, p. 471-480. refs

Landsat residual images have been used to assess the relative change in land quality in a semiarid rangeland in east-central Utah. The residual images are computed as the difference between actual MSS reflectance and MSS reflectance predicted with a linear model of change between two successive Landsat scenes. The residuals represent greater than or less than expected deviations from the linear trend. MSS5, MSS6, and R6,5 residual images appear to be related to significant terrain related features. Regions of degradation and vegetation productivity that result from summer thunderstorm activity are distinguished on residual difference images. Degradation produces greater than expected reflectance in the residual image, while vegetation productivity produces less than expected reflectance. Changes in reflectance due to environmental factors which act fairly uniformly over the landscape are accounted for with the trend of the linear model.

Author

A84-33328

LANDSAT IMAGERY FOR THE INTERPRETATION OF LOUISIANA FOREST HABITAT REGIONS

D. L. EVANS, P. Y. BURNS, and J. M. HILL (Louisiana State University, Baton Rouge, LA) IN: *American Society of Photogrammetry, Annual Meeting, 49th, Washington, DC, March 13-18, 1983, Technical Papers*. Falls Church, VA, American Society of Photogrammetry, 1983, p. 33-42. refs

Bands 5 and 7, 1:250,000-scale, black-and-white Landsat prints were used for delineation of 24 forest habitat map units occurring in 8 physiographic provinces in Louisiana. Image features used to determine boundaries included: (1) drainage pattern and density, (2) degree and pattern of agricultural land use, (3) texture and tone of areas as indicated by land-use changes, and (4) other cultural features. Band-7 prints were usually sufficient, but the Band-5 prints were helpful for distinction of region boundaries implied by changes in land use. Ancillary data in the form of soil association, topographic, and geologic maps were used. High-altitude aerial photographs and ground checking were used to verify or correct some of the Landsat-derived boundaries. All boundaries were registered to a 1:1,000,000-scale, Band-7 Landsat mosaic of the state. Approximately 85 percent of the boundaries were delineated solely by use of the Landsat imagery. It was concluded that in Louisiana, a state with limited topographic variation, Landsat imagery can be used successfully for forest habitat region delineation, provided that ancillary data are available.

Author

A84-33329* Computer Sciences Corp., Silver Spring, Md.

THE STATEWIDE FOREST/NONFOREST CLASSIFICATION OF PENNSYLVANIA USING LANDSAT MSS DATA

S. A. RUSSO and M. L. STAUFFER (Computer Sciences Corp., Silver Spring, MD) IN: *American Society of Photogrammetry, Annual Meeting, 49th, Washington, DC, March 13-18, 1983, Technical Papers*. Falls Church, VA, American Society of Photogrammetry, 1983, p. 43-52. refs (Contract NAS5-24350)

A procedure is described for processing the large volume of data needed to generate a Landsat-derived forest resource map (forest/nonforest mask) for the state of Pennsylvania, for use in a defoliation assessment program. Landsat coverage of the 28 million acres encompassing Pennsylvania requires portions of ten Landsat frames, totalling approximately 76 million pixels. A prime effort of this project was to efficiently and accurately classify this data into forest or nonforest categories. A specialized approach to Bayesian classification was developed which involved the use of MSS5 and MSS7; the identification of a single class, forest; and the use of the confidence map to generate the forest/nonforest mask. Statewide, for 7-acre contiguous forest areas, the overall agreement achieved between the mask and reference data was 90 percent.

Author

A84-33330

THE USE OF LANDSAT IMAGERY IN ANALYZING THE VEGETATION AND ENERGY RESOURCES OF PICKENS COUNTY, SOUTH CAROLINA

L. R. GERING and W. A. SHAIN (Clemson University, Clemson, SC) IN: *American Society of Photogrammetry, Annual Meeting, 49th, Washington, DC, March 13-18, 1983, Technical Papers*. Falls Church, VA, American Society of Photogrammetry, 1983, p. 53-62. refs

A84-33331

VIDEOGRAPHY - SOME REMOTE SENSING APPLICATIONS

J. VLCEK (Toronto, University, Toronto, Canada) IN: *American Society of Photogrammetry, Annual Meeting, 49th, Washington, DC, March 13-18, 1983, Technical Papers*. Falls Church, VA, American Society of Photogrammetry, 1983, p. 63-69. Research supported by the Natural Sciences and Engineering Research Council of Canada and Ontario Ministry of Natural Resources.

Principal features and advantages of video imaging and video image analysis are listed and briefly discussed. Examples are given of (1) aerial video trials showing samples of imagery and image

01 AGRICULTURE AND FORESTRY

interpretation and analysis. The examples include: a drainage study, soil moisture distribution and (2) close range video analysis of spectral properties (reflectance and transmittance) of poplar leaves that was accomplished by video imaging of leaves through 8 filters of 40 mm widths spaced evenly through the visible and near IR spectrum. Author

A84-33332

ANALYSIS OF PHOTO INTERPRETATION TEST RESULTS FOR SEVEN AEROSPACE IMAGE TYPES OF THE SAN JUAN NATIONAL FOREST, COLORADO

A. S. BENSON and K. J. DUMMER (California, University, Berkeley, CA) IN: American Society of Photogrammetry, Annual Meeting, 49th, Washington, DC, March 13-18, 1983, Technical Papers . Falls Church, VA, American Society of Photogrammetry, 1983, p. 121-130. Research supported by the Nationwide Forestry Applications Program. refs

Seven interpretation tests were given to a pool of 28 photo interpreters. The objective of these tests was to measure the relative interpretability of seven aero-space image types, covering a portion of the San Juan National Forest, Colorado, with respect to point sampling for wildland management planning applications. Based on the test results, it was concluded that small scale color infrared aerial photography was more interpretable in point tests than was conventional scale aerial photography and Landsat imagery. Author

A84-33337

AUTOMATED CLASSIFICATION OF WETLANDS

J. H. HANSEN (Tennessee, University, Tullahoma, TN) IN: American Society of Photogrammetry, Annual Meeting, 49th, Washington, DC, March 13-18, 1983, Technical Papers . Falls Church, VA, American Society of Photogrammetry, 1983, p. 177-180.

As the importance of wetlands has been recognized, a need is felt for a continued study of their function and use. Such studies may be assisted by the use of remote sensing techniques to sequentially map plant and water conditions as a function of season, water levels, and upstream events. Wetlands photography and mapping allows the documentation of existing conditions as the bases for future comparisons. For limited areas, wetlands mapping done in previous years has been compared with current mapping to detect changes in wetland habitat. This study is limited to the automated inventory of land cover in terms of vegetation and associated water conditions. The area of the considered study is located in western Tennessee. Photography was taken with a RMK 15/23A camera at an altitude of 3,660 meters. Attention is given to the digitization of transparencies, plotting, and the results. The accuracy of classification indicates the feasibility of using automated remote sensing techniques for mapping wetland areas on a broad basis. G.R.

A84-33338* Department of Agriculture, Beltsville, Md.

AIRCRAFT SCATTEROMETER OBSERVATIONS OF SOIL MOISTURE ON RANGELAND WATERSHEDS

T. J. JACKSON (U.S. Department of Agriculture, Hydrology Laboratory, Beltsville, MD) and P. E. O'NEILL (NASA, Goddard Space Flight Center, Greenbelt, MD) IN: American Society of Photogrammetry, Annual Meeting, 49th, Washington, DC, March 13-18, 1983, Technical Papers . Falls Church, VA, American Society of Photogrammetry, 1983, p. 198-211. refs

Extensive studies conducted by several researchers using truck-mounted active microwave sensors have shown the sensitivity of these sensors to soil moisture variations. The logical extension of these results is the evaluation of similar systems at lower resolutions typical of operational systems. Data collected during a series of aircraft flights in 1978 and 1980 over four rangeland watersheds located near Chickasha, Oklahoma, were analyzed in this study. These data included scatterometer measurements made at 1.6 and 4.75 GHz using a NASA aircraft and ground observations of soil moisture for a wide range of moisture conditions. Data were analyzed for consistency and compared to previous truck and aircraft results. Results indicate that the sensor system is

capable of providing consistent estimates of soil moisture under the conditions tested. Author

A84-33340* Hunter Coll., New York.

SPATIAL INVENTORY INTEGRATING RASTER DATABASES AND POINT SAMPLE DATA

A. H. STRAHLER, C. E. WOODCOCK (Hunter College, New York, NY), and T. L. LOGAN (California Institute of Technology, Jet Propulsion Laboratory, Pasadena, CA) IN: American Society of Photogrammetry, Annual Meeting, 49th, Washington, DC, March 13-18, 1983, Technical Papers . Falls Church, VA, American Society of Photogrammetry, 1983, p. 225-232. refs

A timber inventory of the Eldorado National Forest, located in east-central California, provides an example of the use of a Geographic Information System (GIS) to stratify large areas of land for sampling and the collection of statistical data. The raster-based GIS format of the VICAR/IBIS software system allows simple and rapid tabulation of areas, and facilitates the selection of random locations for ground sampling. Algorithms that simplify the complex spatial pattern of raster-based information, and convert raster format data to strings of coordinate vectors, provide a link to conventional vector-based geographic information systems. Author

A84-33342

THE USE OF DIGITAL ELEVATION MODEL TOPOGRAPHIC DATA FOR SOIL EROSION MODELING WITHIN A GEOGRAPHIC INFORMATION SYSTEM

M. A. SPANNER (Technicolor Government Services, Inc., Moffett Field, CA) IN: American Society of Photogrammetry, Annual Meeting, 49th, Washington, DC, March 13-18, 1983, Technical Papers . Falls Church, VA, American Society of Photogrammetry, 1983, p. 314-323. refs

The Digital Elevation Model (DEM) topographic data are distributed by the National Cartographic Information Center (NCIC) of the U.S. Geological Survey (USGS). The data represent a valuable source of digital topographic information. DEM have been utilized for a wide variety of applications including civil engineering, solar radiation studies, and watershed analysis. The present investigation involves a soil erosion study, taking into account DEM topographic data as an integral component in a Geographic Information System (GIS) environment for the modeling of soil loss due to erosion from rain fall. A description is provided of the Universal Soil Loss Equation originally developed from soil loss data collected in 24 states, and improvements of DEM data over Defense Mapping Agency (DMA) digital terrain tapes are discussed. The Universal Soil Loss Equation is utilized in a soil erosion prediction study for an area in California. G.R.

A84-33343* Alaska Pacific Univ.

VEGETATION MONITORING AND CLASSIFICATION USING NOAA/AVHRR SATELLITE DATA

D. H. GREEGOR, JR. (Alaska Pacific University, Anchorage, AK) and J. R. NORWINE (Texas A & I University, Kingsville, TX) IN: American Society of Photogrammetry, Annual Meeting, 49th, Washington, DC, March 13-18, 1983, Technical Papers . Falls Church, VA, American Society of Photogrammetry, 1983, p. 324-333. NASA-supported research. refs

A vegetation gradient model, based on a new surface hydrologic index and NOAA/AVHRR meteorological satellite data, has been analyzed along a 1300 km east-west transect across the state of Texas. The model was developed to test the potential usefulness of such low-resolution data for vegetation stratification and monitoring. Normalized Difference values (ratio of AVHRR bands 1 and 2, considered to be an index of greenness) were determined and evaluated against climatological and vegetation characteristics at 50 sample locations (regular intervals of 0.25 deg longitude) along the transect on five days in 1980. Statistical treatment of the data indicate that a multivariate model incorporating satellite-measured spectral greenness values and a surface hydrologic factor offer promise as a new technique for regional-scale vegetation stratification and monitoring. Author

A84-33345* Cornell Univ., Ithaca, N.Y.

ANALYSIS OF LANDSAT FOR MONITORING VEGETABLES IN NEW YORK MUCKLANDS

M. H. ZHU, S. Y. YAN, W. R. PHILIPSON, C. C. YEN, and W. D. PHILPOT (Cornell University, Ithaca, NY) IN: American Society of Photogrammetry, Annual Meeting, 49th, Washington, DC, March 13-18, 1983, Technical Papers . Falls Church, VA, American Society of Photogrammetry, 1983, p. 343-353. refs
(Contract NGL-33-010-171)

This pilot study assessed the feasibility of relying on Landsat multispectral scanner data for inventoring vegetables grown in mucklands, in variably shaped, variably sized fields. Classification of muckland vegetables using a Euclidean distance classifier and a parallelepiped classifier was performed with reasonable accuracy (generally over 60 percent) based on only one date of Landsat data. Prior canonical and principal component analyses did not improve the classification accuracy but did reduce the dimensionality of the data.

Author

A84-33347* Lockheed Engineering and Management Services Co., Inc., Houston, Tex.

AUTOMATED VEGETATION CLASSIFICATION USING THEMATIC MAPPER SIMULATION DATA

K. S. NEDELMAN, R. B. CATE (Lockheed Engineering and Management Services Co., Inc., Houston, TX), and R. M. BIZZELL (NASA, Johnson Space Center, Houston, TX) IN: American Society of Photogrammetry, Annual Meeting, 49th, Washington, DC, March 13-18, 1983, Technical Papers . Falls Church, VA, American Society of Photogrammetry, 1983, p. 367-375. refs
(Contract NAS9-15800)

The present investigation is concerned with the results of a study of Thematic Mapper Simulation (TMS) data. One of the objectives of the study was related to an evaluation of the usefulness of the Thematic Mapper's (TM) improved spatial resolution and spectral coverage. The study was undertaken as part of a preparation for the efficient incorporation of Landsat 4 data into ongoing technology development in remote sensing. The study included an application of automated Landsat vegetation classification technology to TMS data. Results of comparing TMS data to Multispectral Scanner (MSS) data were found to indicate that all field definition, crop type discrimination, and subsequent proportion estimation may be greatly increased with the availability of TM data.

G.R.

A84-33348

BENCHMARK DATA ON THE SEPARABILITY BETWEEN ORCHARDS AND VINEYARDS IN THE SOUTHERN SAN JOAQUIN VALLEY OF CALIFORNIA

A. MORSE (Technicolor Government Services, Inc., Moffett Field, CA) IN: American Society of Photogrammetry, Annual Meeting, 49th, Washington, DC, March 13-18, 1983, Technical Papers . Falls Church, VA, American Society of Photogrammetry, 1983, p. 387-391.

It is pointed out that crop classification in the San Joaquin Valley of California using digitally processed Landsat data is a complex task. The crops involved include nearly 200 types and varieties, and the growing season is long. The initial problem in any crop classification effort is to make a decision which dates to use. The present investigation is concerned with information on the separability of vineyards and orchards. This information forms part of the information from a larger study involving 21 crops and eight Landsat overpass dates. This study is part of a project designed to compile baseline information on between-crop separabilities throughout the growing season. The crop separability study employed data from eight dates of Landsat acquisitions of nominal scene 45/35. The employed analysis makes use of a quadratic, maximum-likelihood algorithm in a supervised approach.

G.R.

A84-33349

PRELIMINARY DIGITAL CLASSIFICATION OF GRAZING RESOURCES IN THE SOUTHERN CHIHUAHUAHAN ARID ZONE OF MEXICO

M. K. RIDD, R. A. JAYNES, and J. A. MEROLA (Utah, University, Salt Lake City, UT) IN: American Society of Photogrammetry, Annual Meeting, 49th, Washington, DC, March 13-18, 1983, Technical Papers . Falls Church, VA, American Society of Photogrammetry, 1983, p. 392-399.

A84-33352

USING LANDSAT TO MONITOR TROPICAL FOREST ECOSYSTEMS

K. M. GREEN (Maryland, University, College Park, MD) IN: American Society of Photogrammetry, Annual Meeting, 49th, Washington, DC, March 13-18, 1983, Technical Papers . Falls Church, VA, American Society of Photogrammetry, 1983, p. 518-528. Research supported by the World Bank. refs
(Contract NIH-N01-RS-0-2125)

Estimates regarding the rate of tropical deforestation are often based on data which are obsolete or of doubtful validity. After an examination of existing data sources, it is concluded that satellite imagery must be more widely used for inventoring and monitoring tropical and subtropical forest resources. The results of some studies indicate clearly the need to monitor tropical forest ecosystems. A program designed to meet assessment needs is considered. The application of Landsat technology for the inventory and monitoring of tropical forest biomass is discussed, taking into account a case study in Bangladesh. This analysis overwhelmingly supports the contention of serious tropical forest degradation for the considered study area.

G.R.

A84-33538

SPECTRAL VARIABILITY OF LANDSAT-4 THEMATIC MAPPER AND MULTISPECTRAL SCANNER DATA FOR SELECTED CROP AND FOREST COVER TYPES

S. D. DEGLORIA (California, University, Berkeley, CA) IEEE Transactions on Geoscience and Remote Sensing (ISSN 0196-2892), vol. GE-22, May 1984, p. 303-311. refs

NASA is sponsoring a Landsat Image Data Quality Assessment (LIDQA) program to quantitatively evaluate the degree of improvement of data acquired by the Thematic Mapper (TM) sensor in comparison to the Multispectral Scanner (MSS) sensor. A part of the LIDQA program is concerned with the evaluation of digital and image products generated from computer compatible tape (CCT) data and commercially available film products for the purpose of discriminating natural targets in agricultural and forested environments. This paper presents the results of the first phase of the investigation. The objectives of this phase are related to the development of a basic understanding of the TM data with regard to spectral characteristics and variability, spatial resolution, and radiometric sensitivity. Attention is also given to the extent to which major agricultural and forest cover types can be detected and identified.

G.R.

A84-33539* National Aeronautics and Space Administration. Lyndon B. Johnson Space Center, Houston, Tex.

EVALUATION OF CORN/SOYBEANS SEPARABILITY USING THEMATIC MAPPER AND THEMATIC MAPPER SIMULATOR DATA

D. E. PITTS, G. D. BADHWAR, D. R. THOMPSON, K. E. HENDERSON (NASA, Johnson Space Center, Houston, TX), S. S. SHEN, C. T. SORENSEN, and J. G. CARNES (Lockheed Engineering and Management Co., Houston, TX) IEEE Transactions on Geoscience and Remote Sensing (ISSN 0196-2892), vol. GE-22, May 1984, p. 312-318. refs

Multitemporal Thematic Mapper, Thematic Mapper Simulator, and detailed ground truth data were collected for a 9- by 11-km sample segment in Webster County, IA, in the summer of 1982. Three dates were acquired each with Thematic Mapper Simulator (June 7, June 23, and July 31) and Thematic Mapper (August 2, September 3, and October 21). The Thematic Mapper Simulator data were converted to equivalent TM count values using TM and

01 AGRICULTURE AND FORESTRY

TMS calibration data and model based estimates of atmospheric effects. The July 31, TMS image was compared to the August 2, TM image to verify the conversion process. A quantitative measure of proportion estimation variance (Fisher information) was used to evaluate the corn/soybeans separability for each TM band as a function of time during the growing season. The additional bands in the middle infrared allowed corn and soybeans to be separated much earlier than was possible with the visible and near-infrared bands alone. Using the TM and TMS data, temporal profiles of the TM principal components were developed. The greenness and brightness exhibited behavior similar to MSS greenness and brightness for corn and soybeans.

Author

A84-33540* National Aeronautics and Space Administration. Lyndon B. Johnson Space Center, Houston, Tex.

EVALUATION OF THEMATIC MAPPER FOR DETECTING SOIL PROPERTIES UNDER GRASSLAND VEGETATION

D. R. THOMPSON and K. E. HENDERSON (NASA, Johnson Space Center, Earth Sciences and Applications Div., Houston, TX) IEEE Transactions on Geoscience and Remote Sensing (ISSN 0196-2892), vol. GE-22, May 1984, p. 319-323. NASA-supported research. refs

Analysis of Thematic Mapper data acquired November 15, 1982, over a vegetated site located in the East Texas Timbers and Claypan area of Texas has indicated that montmorillonitic clay textured soils can be separated from soils with different textures. The difference of TM band 4 (0.76-0.90 micron) and band 7 (2.08-2.35 microns) had an agreement of 55.8 percent with the USDA soil survey for upland clay soils. This compared to 55.9-percent agreement when all six bands (excluding the thermal) were used. The disagreement occurred at the boundary lines as defined by the USDA soil survey and the spectral data. This result is considered to be fairly good, considering the difficulty in placement of soil boundaries by the soil scientist in the field. While the exact influence on the vegetation, and thus the spectral response observed by TM, is not understood at this time, it appears that TM band 7 is responding to the type of mineralogy of the soil and that soil properties important to the plant can be detected using TM.

Author

A84-34385* National Aeronautics and Space Administration. Goddard Space Flight Center, Greenbelt, Md.

ALBEDO OF A FOREST MODELED AS A PLANE WITH DENSE PROTRUSIONS

J. OTTERMAN (NASA, Goddard Space Flight Center, Greenbelt, MD; Tel Aviv University, Tel Aviv, Israel) Journal of Climate and Applied Meteorology (ISSN 0733-3021), vol. 23, Feb. 1984, p. 297-307. refs

An analytical model for the absorption of solar radiation by surfaces such as a pine forest or a wheat field is presented. Objectives include understanding the parameters affecting the absorption of the solar irradiance in a complex structure, and determining the influence of the direction of illumination on light trapping. The surface is treated as a Lambertian reflectivity soil-plane; thin, vertical cylinders are regarded as Lambertian reflectors. Using a dimensionless protrusion parameter based on the height and diameter of the vertical plant elements, optical characteristics (e.g., the dependence of the albedo on the solar zenith angle) of a complex structure are well quantified.

C.M.

A84-34777

THE EFFECT OF FLUCTUATIONS IN THE OPTICAL PROPERTIES OF THE ATMOSPHERE ON SPECTRAL BRIGHTNESS RATIOS IN THE REMOTE SENSING OF AGRICULTURAL AREAS [VLIJANIE FLUKTUATSII OPTICHESKIKH SVOISTV ATMOSFERY NA OTNOSHENIIA SPEKTRAL'NYKH IARKOSTEI PRI ZONDIROVANII SEL'SKOKHOZIAISTVENNYKH UGODII]

SH. A. AKHMEDOV (Akademii Nauk Azerbaidzhanskoi SSR, Nauchno-Proizvodstvennoe Ob'edinenie Kosmicheskikh Issledovanii, Baku, Azerbaidzhan SSR) and D. A. USIKOV (Akademii Nauk SSSR, Institut Kosmicheskikh Issledovanii, Moscow, USSR) Issledovanie Zemli iz Kosmosa (ISSN 0205-9614), Mar.-Apr. 1984, p. 23, 24. In Russian.

The influence of the variability in the atmosphere's optical thickness on the decoding sign in the remote sensing of agricultural areas is considered. The ratio of the brightnesses of two spectral channels is selected as the sign. The error in the decoding sign for various cities of the USSR is estimated using the statistical properties of the optical thickness for the two wavelengths. C.R.

A84-34780

INTERPRETING MULTISPECTRAL PHOTOGRAPHS OBTAINED IN THE TELEFOTO-80 EXPERIMENT SO AS TO DISTINGUISH CROP TYPES [INTERPRETATSIIA MNOGOZONAL'NYKH SNIMKOV, POLUCHHENNYKH V KHODE EKSPERIMENTA 'TELEFOTO-80', S TSEL'IU VYDELENIIA SEL'SKOKHOZIAISTVENNYKH KUL'TUR]

R. KACZYNKI (Polska Akademia Nauk, Instytut Geodezji i Kartografii, Warsaw, Poland) Issledovanie Zemli iz Kosmosa (ISSN 0205-9614), Mar.-Apr. 1984, p. 44-47. In Russian.

A84-34783

CLASSIFYING THE COEFFICIENTS OF SPECTRAL BRIGHTNESS OF THE FOREST ZONE IN THE EUROPEAN PART OF THE SOVIET UNION [O KATALOGIZATSII KOEFFITSIENTOV SPEKTRAL'NOI IARKOSTI LESNOI ZONY EVROPEISKOI TERRITORII SOVETSKOGO SOIUZA]

IU. K. ROSS (Akademii Nauk Estonskoi SSR, Institut Astrofiziki i Fiziki Atmosfery, Tartu, Estonian SSR) and U. K. PETERSON (Tartuskii Gosudarstvennyi Universitet, Tartu, Estonian SSR) Issledovanie Zemli iz Kosmosa (ISSN 0205-9614), Mar.-Apr. 1984, p. 60-66. In Russian. refs

A84-34784

A REGRESSION ANALYSIS OF DATA FROM AIRCRAFT AND GROUND MEASUREMENTS OF A VEGETATIVE COVER [REGRESSIONNYI ANALIZ DANNYKH SAMOLETNYKH I NAZEMNYKH IZMERENII RASTITEL'NOGO POKROVA]

O. IA. KLIMENKO and V. V. KOZODEROV (Akademii Nauk SSSR, Otdel Vychislitel'noi Matematiki, Moscow, USSR) Issledovanie Zemli iz Kosmosa (ISSN 0205-9614), Mar.-Apr. 1984, p. 67-75. In Russian. refs

A84-34785

REGRESSION IN THE PRIMAL PROBLEM OF REMOTE SENSING (USING GRASS COVER AS AN EXAMPLE) [REGRESSIIA V PRIAMOI ZADACHE DISTANTSIONNOGO ZONDIROVANIIA /NA PRIMERE TRAVIANOGO POKROVA/]

B. M. BALTER and M. GANZORIG (Akademii Nauk SSSR, Institut Kosmicheskikh Issledovanii, Moscow, USSR) Issledovanie Zemli iz Kosmosa (ISSN 0205-9614), Mar.-Apr. 1984, p. 76-86. In Russian.

A description is given of a ground-based experiment that seeks to arrive at a function linking the state of a vegetative cover used as pasture with the spectral brightness of this cover. With experimental data based on regression models, an analysis is made of the effect of various factors on such a function. In addition, the accuracy possible in evaluating the condition of the object (vegetative cover) by means of remote sensing methods is calculated.

C.R.

01 AGRICULTURE AND FORESTRY

A84-34960* National Aeronautics and Space Administration. Goddard Space Flight Center, Greenbelt, Md.

POTENTIAL BENEFITS OF NEW SATELLITE SENSORS TO WETLAND MAPPING

C. L. DOTTAVIO (NASA, Goddard Space Flight Center, Greenbelt, MD) and F. D. DOTTAVIO (Clemson University, Clemson, SC) Photogrammetric Engineering and Remote Sensing (ISSN 0099-1112), vol. 50, May 1984, p. 599-606. refs

Simulated Thematic Mapper (TMS) data are compared with data from a simulated multispectral scanner to determine whether digital data from the Thematic Mapper on board Landsat will be adequate for wetland mapping. Also considered is the question whether the Thematic Mapper will in fact improve discrimination among wetland cover types. It is found that for the six cover types examined the Thematic Mapper has the greatest discriminatory power in the infrared wavelength range from 1.0 to 1.3 microns. A distinct separation was found between low marsh and high marsh species in the middle infrared band (TM5), and this is expected to assist in the inventory of wetland habitats in the future. I.H.

A84-34961* National Aeronautics and Space Administration. Goddard Space Flight Center, Greenbelt, Md.

CLASSIFYING NORTHERN FORESTS USING THEMATIC MAPPER SIMULATOR DATA

R. F. NELSON (NASA, Goddard Space Flight Center, Greenbelt, MD), R. S. LATTY (Maryland, University, College Park, MD), and G. MOTT (Maine, University, Orono, ME) Photogrammetric Engineering and Remote Sensing (ISSN 0099-1112), vol. 50, May 1984, p. 607-617. refs

Thematic Mapper Simulator data were collected over a 23,200 hectare forested area near Baxter State Park in north-central Maine. Photointerpreted ground reference information was used to drive a stratified random sampling procedure for waveband discriminant analyses and to generate training statistics and test pixel accuracies. Stepwise discriminant analyses indicated that the following bands best differentiated the thirteen level II - III cover types (in order of entry): near infrared (0.77 to 0.90 micron), blue (0.46 - 0.52 micron), first middle infrared (1.53 to 1.73 microns), second middle infrared (2.06 to 2.33 microns), red (0.63 to 0.69 micron), thermal (10.32 to 12.33 microns). Classification accuracies peaked at 58 percent for thirteen level II-III land-cover classes and at 65 percent for ten level II classes. Author

A84-36516#

THE GREEN CADASTRE - AN EXPERIMENT FOR EXPLORING THE TREE VEGETATION IN THE PARIS AREA

R. DELBARD and D. JOUANNET (Geomesure, S.A., Cachan, Val-de-Marne, France) Jena Review (ISSN 0448-9497), vol. 29, no. 1, 1984, p. 25-28.

An IR photographic study has been conducted of deciduous and conifer tree cover in the Paris area, in order to determine both the relative prevalence of the various species of tree and the state of their health. The photographs were obtained from a helicopter. Terrain exploration and numerical data extraction of IR colors were undertaken, in addition to visual interpretation. About 86 percent of all deviations detected concern tree health state determinations. O.C.

A84-36710

SURFACE ALBEDO AND THE SAHEL DROUGHT

M. F. COUREL (IBM France, S.A., Centre Scientifique, Paris, France), R. S. KANDEL (CNRS, Service d'Aeronomie, Verrières-le-Buisson, Essonne, France), and S. I. RASOOL (IBM France, S.A.; CNRS, Laboratoire de Meteorologie Dynamique, Paris, France) Nature (ISSN 0028-0836), vol. 307, Feb. 9, 1984, p. 528-531. Research supported by the Organisation for Economic Cooperation and Development, Centre National d'Etudes Spatiales, Delegation Generale a la Recherche Scientifique et Technique, and Centre National de la Recherche Scientifique. refs

The persistence of the Sahel drought can be understood in light of a strong positive feedback mechanism's operation, under the influence of changes in surface properties. Attention is presently

given to changes in the albedo of this region since 1972. It is noted that the dry season albedo in the Sahel, especially in the Ferlo and Gondo regions, declined from a maximum of nearly 0.30 in 1973 to values approaching 0.20 in 1979. This decline is consistent with plant cover changes which were determined by the analysis of Landsat MSS data, together with field studies.

O.C.

A84-37201* Kansas Univ. Center for Research, Inc., Lawrence.

A SCATTER MODEL FOR VEGETATION UP TO KU-BAND

H. J. EOM and A. K. FUNG (University of Kansas Center for Research, Inc., Lawrence, KS) Remote Sensing of Environment (ISSN 0034-4257), vol. 15, June 1984, p. 185-200. refs

(Contract NAG5-268)

A scatter model is developed based on the matrix doubling method for volume scattering and the Kirchhoff method in rough surface scattering. Scattering from vegetation is assumed to be dominated by leaves and a single leaf is modeled by a thin dielectric disk. In developing the phase matrix for the disk, field within the disk is taken to be constant over the disk thickness, but phase changes across the surface of the disk are accounted for. Comparisons of this scatter model with radar measurements indicate good agreements in polarization, angular trends, and frequency up to Ku-band. This represents a considerable improvement over low-frequency scatter models which are valid up to S-band.

Author

A84-37202* National Aeronautics and Space Administration. Goddard Space Flight Center, Greenbelt, Md.

DETERMINING FOREST CANOPY CHARACTERISTICS USING AIRBORNE LASER DATA

R. NELSON (NASA, Goddard Space Flight Center, Earth Resources Branch, Greenbelt, MD), W. KRABILL, and G. MACLEAN (NASA, Wallops Flight Center, Wallops Island, VA) Remote Sensing of Environment (ISSN 0034-4257), vol. 15, June 1984, p. 201-212. refs

A study is reported in which a profiling laser system flown at relatively low altitudes over a forested area was used to measure various forest canopy attributes, including tree heights. An analysis of the data obtained indicates that canopy closure is most strongly related to the penetration capability of the laser pulse, with the pulses attenuated more quickly in a dense canopy. Laser estimates of the average tree heights differ by less than 1 m from the photogrammetrically acquired values. It is concluded that the laser system is suitable for remotely sensing the vertical forest canopy profile. Elements of this profile are linearly related to crown closure and can be used to assess tree height. V.L.

A84-37203* New York State Univ., Binghamton.

INVERSION OF VEGETATION CANOPY REFLECTANCE MODELS FOR ESTIMATING AGRONOMIC VARIABLES. III - ESTIMATION USING ONLY CANOPY REFLECTANCE DATA AS ILLUSTRATED BY THE SUITS MODEL. IV - TOTAL INVERSION OF THE SAIL MODEL

N. S. GOEL and R. L. THOMPSON (New York, State University, Binghamton, NY) Remote Sensing of Environment (ISSN 0034-4257), vol. 15, June 1984, p. 223-253. NASA-supported research. refs

The possibility of estimating agronomic and spectral parameters for a vegetation canopy from the canopy reflectance (CR) data in the infrared region is investigated for a set of solar/view directions. It is shown that such an estimation is possible, in principle, for the Suits (1972) model for a homogeneous canopy. The technique is then applied to a more complex model, the SAIL (scattering by arbitrarily inclined leaves) model which explicitly includes the leaf angle distribution in the computation of the canopy reflectance. It is concluded that, given the expected accuracy of CR measurements and the accuracy of the SAIL model in representing CR in the infrared region, the agronomic parameters, leaf area index, and leaf angle distribution can be estimated fairly accurately using ancillary data on spectral parameters. V.L.

01 AGRICULTURE AND FORESTRY

A84-37204* National Aeronautics and Space Administration. Goddard Space Flight Center, Greenbelt, Md.

INTENSIVE FOREST CLEARING IN RONDONIA, BRAZIL, AS DETECTED BY SATELLITE REMOTE SENSING

C. J. TUCKER, B. N. HOLBEN, and T. E. GOFF (NASA, Goddard Space Flight Center, Greenbelt, MD) *Remote Sensing of Environment* (ISSN 0034-4257), vol. 15, June 1984, p. 255-261. refs

Imagery from the National Oceanic and Atmospheric Administration satellite's Advanced Very High Resolution Radiometer sensor has been used to identify an area about 100 x 400 km in Rondonia (Brazil) where massive forest clearing or deforestation is occurring. A field study verified the area of the clearing, which is associated with a large colonization program.

Author

A84-38299

LANDSAT MSS DATA USED FOR CROP IDENTIFICATION AT THE LIMIT OF ITS SPATIAL RESOLUTION

C. PATTILLO and M. SOLEDAD FERNANDEZ (Universidad de Chile, Santiago, Chile) IN: *International Symposium on Space Technology and Science*, 13th, Tokyo, Japan, June 28-July 3, 1982, *Proceedings*. Tokyo, AGNE Publishing, Inc., 1982, p. 1265-1270. Research supported by the Internal Revenue Service of Chile.

The possibility of identifying specific crops using multispectral scanner imagery from the Landsat satellite were explored. The scanned areas had to be at least 10 ha in size. The study area was in the Chilean central valley. Five intervals of imagery covering the early and middle growing season were examined. The imagery was on a 1:50,000 scale and was treated in terms of 12 control points and cubic convolution of subscenes to realize 57 x 57 m resolution. False color composites were computer-enlarged by a factor of 10. Further enhancement yielded a 1:20,000 scale image with 1 x 1 m resolution. Visual identification accuracy, relative to ground truth data, was from 43-65 percent, depending on the crop, and within 3 percent for the field size. Techniques for improving the accuracy sufficiently to use the data for government crop tax purposes are discussed.

M.S.K.

A84-38998* National Aeronautics and Space Administration. Wallops Flight Center, Wallops Island, Va.

AIRBORNE LASER TOPOGRAPHIC MAPPING RESULTS

W. B. KRABILL (NASA, Wallops Flight Center, Wallops Island, VA), J. G. COLLINS, L. E. LINK (U.S. Army, Engineer Waterways Experiment Station, Vicksburg, MS), R. N. SWIFT, and M. L. BUTLER (EG&G Washington Analytical Services Center, Inc., Pocomoke City, MD) *Photogrammetric Engineering and Remote Sensing* (ISSN 0099-1112), vol. 50, June 1984, p. 685-694. refs

The results of terrain mapping experiments utilizing the National Aeronautics and Space Administration (NASA) Airborne Oceanographic Lidar (AOL) over forested areas are presented. The flight tests were conducted as part of a joint NASA/U.S. Army Corps of Engineers (CE) investigation aimed at evaluating the potential of an airborne laser ranging system to provide cross-sectional topographic data on flood plains that are difficult and expensive to survey using conventional techniques. The data described in this paper were obtained in the Wolf River Basin located near Memphis, TN. Results from surveys conducted under winter 'leaves off' and summer 'leaves on' conditions, aspects of day and night operation, and data obtained from deciduous and coniferous tree types are compared. Data processing techniques are reviewed. Conclusions relative to accuracy and present limitations of the AOL, and airborne lidar systems in general, to terrain mapping over forested areas are discussed.

Author

A84-38999

IRRIGATED CROP INVENTORY BY CLASSIFICATION OF SATELLITE IMAGE DATA

J. A. RICHARDS (New South Wales, University, Kensington, Australia) and G. E. MORETON *Photogrammetric Engineering and Remote Sensing* (ISSN 0099-1112), vol. 50, June 1984, p. 729-737. refs

Mixed unsupervised/supervised classification of band 5, band 7 Landsat Multispectral Scanner image data is used as a procedure for determining the area of cropland under irrigation in an arid region of the state of New South Wales in Australia. Classification using two analysis systems is described. One is a dial-in bureau service which supports the ORSER software package and the other a Dipix Aries II interactive image analysis system. Results obtained agreed to within 1 to 5 percent with information provided by field studies. Density slicing using a vegetation index is also described, but with an accuracy of approximately 8 percent. A rough cost-effectiveness comparison is made with irrigated crop inventory studies of other investigators.

Author

A84-39000*

Kansas Univ. Center for Research, Inc., Lawrence. IMPROVING CROP CLASSIFICATION THROUGH ATTENTION TO THE TIMING OF AIRBORNE RADAR ACQUISITIONS

B. BRISCO, F. T. ULABY (University of Kansas Center for Research, Inc., Lawrence, KS), and R. PROTZ (Guelph, University, Guelph, Ontario, Canada) *Photogrammetric Engineering and Remote Sensing* (ISSN 0099-1112), vol. 50, June 1984, p. 739-745. Sponsorship: Department of Supply and Services. refs (Contract DSS-08SU-01525-7-0198; NAS9-1542)

Radar remote sensors may provide valuable input to crop classification procedures because of (1) their independence of weather conditions and solar illumination, and (2) their ability to respond to differences in crop type. Manual classification of multidate synthetic aperture radar (SAR) imagery resulted in an overall accuracy of 83 percent for corn, forest, grain, and 'other' cover types. Forests and corn fields were identified with accuracies approaching or exceeding 90 percent. Grain fields and 'other' fields were often confused with each other, resulting in classification accuracies of 51 and 66 percent, respectively. The 83 percent correct classification represents a 10 percent improvement when compared to similar SAR data for the same area collected at alternate time periods in 1978. These results demonstrate that improvements in crop classification accuracy can be achieved with SAR data by synchronizing data collection times with crop growth stages in order to maximize differences in the geometric and dielectric properties of the cover types of interest.

Author

N84-23004* Jet Propulsion Lab., California Inst. of Tech., Pasadena.

THE PENNSYLVANIA DEFOLIATION APPLICATION PILOT TEST

R. G. MCLEOD, A. L. ZOBRIST, and N. A. BRYANT 15 Sep. 1983 174 p refs Original contains imagery. Original photography may be purchased from the EROS Data Center, Sioux Falls, S.D. 57198 ERTS

(Contract NAS7-100)

(E84-10111; NASA-CR-173481; JPL-PUB-83-65; NAS 1.26:173481) Avail: NTIS HC A08/MF A01 CSCL 02F

Satellite imagery for the State of Pennsylvania was digitally mosaicked to provide the seed data base for monitoring defoliation of hardwood trees by the gypsy moth. Two separate mosaics for the state were prepared, one before defoliation and one after defoliation, to determine the extent, direction, and impact of gypsy moth activity in the state. The digital mosaic technology used to construct the data base was transferred to Pennsylvania State University to permit periodic updates to the data base and to assist in planning and abatement activities. Participating agencies or institutions included Goddard Space Flight Center and the Pennsylvania State University Office for Remote Sensing of Earth Resources.

Author

01 AGRICULTURE AND FORESTRY

N84-23006*# Texas A&M Univ., College Station. Remote Sensing Center.

CONSERVB: A NUMERICAL METHOD TO COMPUTE SOIL WATER CONTENT AND TEMPERATURE PROFILES UNDER A BARE SURFACE Semiannual Report, Mar. - Sep. 1982

C. H. M. VANBAVEL and R. LASCANO Sep. 1982 79 p refs Sponsored by NASA, USDA, Dept. of Commerce, Dept. of the Interior, and Agency for International Development ERTS (Contract NAG5-31; PROJ. AGRISTARS) (E84-10113; NASA-CR-173483; SM-T3-04448; NAS 1.26:173483; RSC-134) Avail: NTIS HC A05/MF A01 CSCL 02C

A comprehensive, yet fairly simple model of water disposition in a bare soil profile under the sequential impact of rain storms and other atmospheric influences, as they occur from hour to hour is presented. This model is intended mostly to support field studies of soil moisture dynamics by our current team, to serve as a background for the microwave measurements, and, eventually, to serve as a point of departure for soil moisture predictions for estimates based in part upon airborne measurements. The main distinction of the current model is that it accounts not only for the moisture flow in the soil-atmosphere system, but also for the energy flow and, hence, calculates system temperatures. Also, the model is of a dynamic nature, capable of supporting any required degree of resolution in time and space. Much critical testing of the sample is needed before the complexities of the hydrology of a vegetated surface can be related meaningfully to microwave observations.

A.R.H.

N84-23007*# Texas A&M Univ., College Station. Remote Sensing Center.

A MICROWAVE SYSTEMS APPROACH TO MEASURING ROOT ZONE SOIL MOISTURE Semiannual Report, Sep. 1982 - Mar. 1983

R. W. NEWTON, J. F. PARIS, and B. V. CLARK Mar. 1983 69 p refs Sponsored by NASA, USDA, Dept. of Commerce, Dept. of the Interior, and Agency for International Development Original contains imagery. Original photography may be purchased from the EROS Data Center, Sioux Falls, S.D. 57198 ERTS (Contract NSG-5266; NAG5-31; PROJ. AGRISTARS) (E84-10114; NASA-CR-173484; SM-T3-04447; NAS 1.26:173484; RSC-138) Avail: NTIS HC A04/MF A01 CSCL 02C

Computer microwave satellite simulation models were developed and the program was used to test the ability of a coarse resolution passive microwave sensor to measure soil moisture over large areas, and to evaluate the effect of heterogeneous ground covers with the resolution cell on the accuracy of the soil moisture estimate. The use of realistic scenes containing only 10% to 15% bare soil and significant vegetation made it possible to observe a 60% K decrease in brightness temperature from a 5% soil moisture to a 35% soil moisture at a 21 cm microwave wavelength, providing a 1.5 K to 2 K per percent soil moisture sensitivity to soil moisture. It was shown that resolution does not affect the basic ability to measure soil moisture with a microwave radiometer system. Experimental microwave and ground field data were acquired for developing and testing a root zone soil moisture prediction algorithm. The experimental measurements demonstrated that the depth of penetration at a 21 cm microwave wavelength is not greater than 5 cm.

A.R.H.

N84-23971# Technicolor Government Services, Inc., Moffett Field, Calif.

LAND COVER AND TERRAIN MAPPING FOR THE DEVELOPMENT OF DIGITAL DATA BASES FOR WILDLIFE HABITAT ASSESSMENT IN THE YUKON FLATS NATIONAL WILDLIFE REFUGE, ALASKA

M. B. SHASBY, C. MARKON (US Fish and Wildlife Service), M. D. FLEMING, D. L. MURPHY, and J. E. YORK In Geological Survey US Geological Survey Polar Res. Symp. p 43 1983 Avail: NTIS HC A04/MF A01; also available from SOD

LANDSAT multispectral scanner (MSS) data and digital elevation model (DEM) data are studied to develop and test digital land cover and terrain data bases for assessing wildlife habitat in Alaska's National Wildlife Refuges (NWR). The Yukon Flats NWR

consists of approximately 8.63 million acres of land and water in the upper watershed of the Yukon River in northeastern Alaska. Portions of seven summer and five winter LANDSAT scenes were digitally registered to a 127-meter Universal Transverse Mercator (UTM) grid and processed to derive land cover information for the refuge and an additional 4.5 million acres of adjacent lands. The lake inventory data base is developed through a series of computer programs which extract all water bodies from the land cover layer of data in raster format, to produce a new layer comprised only of water, and then convert the raster file to a vector data file from which a data base file is produced.

Author

N84-23977*# Michigan State Univ., East Lansing. Center for Remote Sensing.

USE OF REMOTE SENSING FOR LAND USE POLICY FORMULATION Annual Progress Report, 1 Jun. 1982 - 31 May 1983

31 May 1983 132 p refs Original contains imagery. Original photography may be purchased from the EROS Data Center, Sioux Falls, S.D. 57198 ERTS (Contract NGL-23-004-083) (E84-10117; NASA-CR-173487; NAS 1.26:173487) Avail: NTIS HC A07/MF A01 CSCL 08B

Multispectral scanning, infrared imagery, thematic mapping, and spectroradiometry from LANDSAT, GOES, and ground based instruments are being used to determine conifer distribution, maximum and minimum temperatures, topography, and crop diseases in Michigan's lower Peninsula. Image interpretation and automatic digital processing information from LANDSAT data are employed to classify and map the coniferous forests. Radiant temperature data from GOES were compared to temperature readings from the climatological station network. Digital data from LANDSAT is being used to develop techniques for detecting, monitoring, and modeling land surface change. Improved reflectance signatures through spectroradiometry aided in the detection of viral diseases in blueberry fields and vineyards. Soil survey maps from aerial reconnaissance are included as well as information on education, conferences, and awards.

M.A.C.

N84-23978*# Delaware Univ., Newark. Coll. of Marine Studies. **EVALUATION OF SPATIAL, RADIOMETRIC AND SPECTRAL THEMATIC MAPPER PERFORMANCE FOR COASTAL STUDIES** Quarterly Technical Status Progress Report, 1 Jan. - 31 Mar. 1984

V. KLEMAS, Principal Investigator 31 Mar. 1984 5 p ERTS (Contract NAS5-27580) (E84-10118; NASA-CR-173488; NAS 1.26:173488) Avail: NTIS HC A02/MF A01 CSCL 08B

The effect different wetland plant canopies have upon observed reflectance in Thematic Mapper bands is examined. The three major vegetation canopy types (broadleaf, gramineous and leafless) produce unique spectral responses for a similar quantity of live biomass. Biomass estimates computed from spectral data were most similar to biomass estimates determined from harvest data when models developed for a specific canopy were used. Precise determination of regression coefficients for each canopy type and modeling changes in the coefficients with various combinations of canopy types are being tested. The multispectral band scanner vegetation index estimates are very similar to the vegetation index estimates.

M.A.C.

N84-23990# Michigan State Univ., East Lansing. Center for Remote Sensing.

AERIAL PHOTOGRAPHY FOR ECOLOGICAL SITE MAPPING

W. D. HUDSON and D. P. LUSCH Mar. 1984 13 p refs Avail: NTIS HC A02/MF A01

The use of aerial imagery to classify forest lands into ecologically similar units was illustrated. An example of a regional analysis of the inter-relationships between generalized physiographic subdivisions and forest patterns, interpreted from satellite data, was contrasted with a more detailed study which utilized medium-scale photographs. Ecosystem units were distinguished on the basis of physiography, soils, and vegetation. Two of these

01 AGRICULTURE AND FORESTRY

ecosystem factors, physiography and vegetation, were identified and mapped using remotely sensed imagery data from LANDSAT 4. Vegetation/physiography profiles were generated from both studies undertaken. The photography and generalized forest cover distributions mapped at the regional level illustrate the potential for identifying broad, ecologically similar units from satellite data. Within these larger units, more detailed studies of aerial photography can provide a method of classifying individual landforms into ecological sites. R.S.F.

N84-23993# Air Force Inst. of Tech., Wright-Patterson AFB, Ohio.

A CONSTRAINED-CLUSTERING APPROACH TO THE ANALYSIS OF REMOTE SENSING DATA M.S. Thesis

C. J. RYAN 1983 136 p
(AD-A139124; AFIT/CI/NR-83-80T) Avail: NTIS HC A07/MF A01 CSCL 12A

One old and two new clustering methods were applied to the constrained-clustering problem of separating different agricultural fields based on multispectral remote sensing satellite data. (Constrained-clustering involves double clustering in multispectral measurement similarity and geographical location.) The results of applying the three methods are provided along with a discussion of their relative strengths and weaknesses and a detailed description of their algorithms. GRA

N84-25142# National Aeronautics and Space Administration, Goddard Inst. for Space Studies, New York.

VEGETATION, LAND-USE AND SEASONAL ALBEDO DATA SETS: DOCUMENTATION OF ARCHIVED DATA TAPE

E. MATTHEWS May 1984 13 p refs ERTS
(E84-10133; NASA-TM-86107; NAS 1.15:86107) Avail: NTIS HC A02/MF A01 CSCL 05B

Global data bases of vegetation, land use, and land cover were compiled at a 1 deg latitude x 1 deg longitude resolution, drawing on approximately 100 published sources complemented by a large collection of satellite imagery. Six datasets prepared and archived at NCAR are described: a vegetation data set (VEGTYPE) representing natural (pre-agricultural) vegetation based on the UNESCO classification system; a cultivation intensity data set (CULTINT) defining the areal extent (expressed as %) of presently cultivated land in the 1 x 1 cells; and four integrated surface-albedo data sets (January, April, July, October) for snow-free conditions except for permanently snow-covered continental ice, incorporating natural vegetation and cultivation characteristics from the vegetation and cultivation-intensity data sets. Non-zero data are included for permanent land only, including continental ice. Documentation of the data-tape format as well as descriptions and regional maps of the individual data sets are presented. A.R.H.

N84-26081# Instituto de Pesquisas Espaciais, Sao Jose dos Campos (Brazil).

IRRIGATED RICE AREA ESTIMATION USING REMOTE SENSING TECHNIQUES: PROJECT'S PROPOSAL AND PRELIMINARY RESULTS

N. D. J. PARADA, Principal Investigator, G. V. DEASSUNCAO, M. A. MOREIRA, and R. A. NOVAES May 1984 10 p Submitted for publication Sponsored by NASA ERTS
(E84-10131; NASA-CR-172806; NAS 1.26:172806;
INPE-3105-PRE/504) Avail: NTIS HC A02/MF A01 CSCL 02C

The development of a methodology for annual estimates of irrigated rice crop in the State of Rio Grande do Sul, Brazil, using remote sensing techniques is proposed. The project involves interpretation, digital analysis, and sampling techniques of LANDSAT imagery. Results are discussed from a preliminary phase for identifying and evaluating irrigated rice crop areas in four counties of the State, for the crop year 1982/1983. This first phase involved just visual interpretation techniques of MSS/LANDSAT images. Author

N84-26082# Purdue Univ., Lafayette, Ind. Lab. for Applications of Remote Sensing.

LANDSAT-4 IMAGE DATA QUALITY ANALYSIS Quarterly

Progress Report, 10 Nov. 1983 - 9 Feb. 1984

P. E. ANUTA 9 Feb. 1984 4 p ERTS
(Contract NAS5-26859)

(E84-10134; NASA-CR-172507; NAS 1.26:172507;

LARS-CR-020984) Avail: NTIS HC A02/MF A01 CSCL 05B

Classification performance from LANDSAT 4 TM and MSS data is evaluated using the SECHO computer program. The data accuracy is compared using forest, corn, soybeans, bare soil, grass, water, and urban areas as classes for investigation. M.A.C.

N84-26083# Instituto de Pesquisas Espaciais, Sao Jose dos Campos (Brazil).

PRINCIPAL COMPONENTS TECHNIQUE ANALYSIS FOR VEGETATION AND LAND USE DISCRIMINATION

N. D. J. PARADA, Principal Investigator, A. R. FORMAGGIO, J. R. DOSSANTOS, and L. A. V. DIAS Apr. 1984 12 p refs Submitted for publication Sponsored by NASA Original contains imagery. Original photography may be purchased from the EROS Data Center, Sioux Falls, S.D. 57198 ERTS
(E84-10135; NASA-CR-172808; NAS 1.26:172808;

INPE-3077-PRE/490) Avail: NTIS HC A02/MF A01 CSCL 02F

Automatic pre-processing technique called Principal Components (PRINCO) in analyzing LANDSAT digitized data, for land use and vegetation cover, on the Brazilian cerrados was evaluated. The chosen pilot area, 223/67 of MSS/LANDSAT 3, was classified on a GE Image-100 System, through a maximum-likelihood algorithm (MAXVER). The same procedure was applied to the PRINCO treated image. PRINCO consists of a linear transformation performed on the original bands, in order to eliminate the information redundancy of the LANDSAT channels. After PRINCO only two channels were used thus reducing computer effort. The original channels and the PRINCO channels grey levels for the five identified classes (grassland, 'cerrado', burned areas, anthropic areas, and gallery forest) were obtained through the MAXVER algorithm. This algorithm also presented the average performance for both cases. In order to evaluate the results, the Jeffreys-Matusita distance (JM-distance) between classes was computed. The classification matrix, obtained through MAXVER, after a PRINCO pre-processing, showed approximately the same average performance in the classes separability. Author

N84-26087# Instituto de Pesquisas Espaciais, Sao Jose dos Campos (Brazil).

SAMPLING SYSTEM FOR WHEAT (TRITICUM AESTIVUM L.) AREA ESTIMATION USING DIGITAL LANDSAT MSS DATA AND AERIAL PHOTOGRAPHS

N. D. J. PARADA, Principal Investigator, M. A. MOREIRA, S. C. CHEN, and G. T. BATISTA Apr. 1984 13 p refs Submitted for publication Sponsored by NASA ERTS
(E84-10139; NASA-CR-172812; NAS 1.26:172812;
INPE-3076-PRE/489) Avail: NTIS HC A02/MF A01 CSCL 02C

A procedure to estimate wheat (Triticum aestivum L.) area using sampling technique based on aerial photographs and digital LANDSAT MSS data is developed. Aerial photographs covering 720 square km are visually analyzed. To estimate wheat area, a regression approach is applied using different sample sizes and various sampling units. As the size of sampling unit decreased, the percentage of sampled area required to obtain similar estimation performance also decreased. The lowest percentage of the area sampled for wheat estimation with relatively high precision and accuracy through regression estimation is 13.90% using 10 square km as the sampling unit. Wheat area estimation using only aerial photographs is less precise and accurate than those obtained by regression estimation. M.A.C.

01 AGRICULTURE AND FORESTRY

N84-26092* # Instituto de Pesquisas Espaciais, Sao Jose dos Campos (Brazil).

FOREST INVENTORY USING MULTISTAGE SAMPLING WITH PROBABILITY PROPORTIONAL TO SIZE

N. D. J. PARADA, Principal Investigator, D. C. L. LEE, P. HERNANDEZFILHO, Y. E. SHIMABUKURO, O. R. DEASSIS, and J. S. DEMEDEIROS Apr. 1984 10 p refs Presented at the Intern. Soc. of Photogrammetry and Remote Sensing Congr., Rio de Janeiro, 18-29 Jun. 1984 Sponsored by NASA ERTS (E84-10144; NASA-CR-172817; NAS 1.26:172817; INPE-3084-PRE/494) Avail: NTIS HC A02/MF A01 CSCL 02F

A multistage sampling technique, with probability proportional to size, for forest volume inventory using remote sensing data is developed and evaluated. The study area is located in the Southeastern Brazil. The LANDSAT 4 digital data of the study area are used in the first stage for automatic classification of reforested areas. Four classes of pine and eucalypt with different tree volumes are classified utilizing a maximum likelihood classification algorithm. Color infrared aerial photographs are utilized in the second stage of sampling. In the third state (ground level) the tree volume of each class is determined. The total tree volume of each class is expanded through a statistical procedure taking into account all the three stages of sampling. This procedure results in an accurate tree volume estimate with a smaller number of aerial photographs and reduced time in field work. M.A.C.

N84-26098* # Environmental Research Inst. of Michigan, Ann Arbor. Infrared and Optics Div.

UNDERSTANDING AND UTILIZATION OF THEMATIC MAPPER AND OTHER REMOTELY SENSED DATA FOR VEGETATION MONITORING Final Report, 1 Nov. 1982 - 31 Oct. 1983

E. P. CRIST, R. C. CICONE, M. D. METZLER, T. M. PARRIS, D. P. RICE, and R. E. SAMPSON Nov. 1983 102 p refs ERTS (Contract NAS9-16538) (E84-10150; NASA-CR-171781; NAS 1.26:171781; ERIM-160300-76-F) Avail: NTIS HC A06/MF A01 CSCL 08B

The TM Tasseled Cap transformation, which provides both a 50% reduction in data volume with little or no loss of important information and spectral features with direct physical association, is presented and discussed. Using both simulated and actual TM data, some important characteristics of vegetation and soils in this feature space are described, as are the effects of solar elevation angle and atmospheric haze. A preliminary spectral haze diagnostic feature, based on only simulated data, is also examined. The characteristics of the TM thermal band are discussed, as is a demonstration of the use of TM data in energy balance studies. Some characteristics of AVHRR data are described, as are the sensitivities to scene content of several LANDSAT-MSS preprocessing techniques.

A.R.H.

N84-26099* # Texas A&M Univ., College Station. Dept. of Statistics.

AREA ESTIMATION USING MULTIYEAR DESIGNS AND PARTIAL CROP IDENTIFICATION Final Report

R. L. SIELKEN, JR. May 1984 50 p refs ERTS (Contract NAS9-16785) (E84-10151; NASA-CR-171785; NAS 1.26:171785) Avail: NTIS HC A03/MF A01 CSCL 02C

Statistical procedures were developed for large area assessments using both satellite and conventional data. Crop acreages, other ground cover indices, and measures of change were the principal characteristics of interest. These characteristics are capable of being estimated from samples collected possibly from several sources at varying times, with different levels of identification. Multiyear analysis techniques were extended to include partially identified samples; the best current year sampling design corresponding to a given sampling history was determined; weights reflecting the precision or confidence in each observation were identified and utilized, and the variation in estimates incorporating partially identified samples were quantified. A.R.H.

N84-26107* # General Electric Co., Lanham, Md. Space Systems Div.

INTERACTIVE DIGITAL IMAGE PROCESSING FOR TERRAIN DATA EXTRACTION, PHASE 4 Final Technical Report, Sep. 1982 - Nov. 1983

H. HEYDT, V. KARKHANIS, and T. WESCOTT Nov. 1983 87 p (Contract DAAK70-79-C-0153; DA PROJ. 4A1-62707-A-855) (AD-A140197; ETL-0348) Avail: NTIS HC A05/MF A01 CSCL 08B

This phase of the study concentrated on refinement of vegetation extraction techniques developed in phases 1 through 3. Software was also generated for scaling and mosaicking vegetation data derived from separate adjacent scenes, as appropriate for covering a given map area. The raster format classification files were converted to polygon vector files in the Standard Interface Format.

Author (GRA)

N84-26108* # Army Engineer Topographic Labs., Fort Belvoir, Va.

DISCRIMINATING VEGETATION AND SOILS USING LANDSAT MSS AND THEMATIC MAPPER BANDS AND BAND RATIOS

M. B. SATTERWHITE Mar. 1984 14 p (AD-A140198; ETL-R-061) Avail: NTIS HC A02/MF A01 CSCL 08F

Characterizing arid region soils and vegetation conditions from remotely sensed imagery is often limited by the low brightness contrast between soil and vegetation and between different plant communities. The purpose of this study was to determine those LANDSAT multi-spectral scanner and Thematic Mapper bands and band ratios useful for discriminating soil and vegetation in a semiarid region. Ground level reflectance spectra, 400 to 1100 nm, were taken of 35 soil and 127 vegetation samples. The sample's mean brightness values were calculated for the four MSS bands and Thematic Mapper bands 1, 2, 3 and 4. Band:band ratios were calculated. The soils were usually brighter than the vegetation in the visible region, although some gravelled soils and some gray colored species had similar values. In the visible region, brightness values ranging from 15 to 20 separated most vegetation and soils. Many soil and vegetation surfaces had similar near infrared (NIR) brightness values. The NIR:visible band ratios discriminated most soils from the vegetation samples. The soils had NIR:visible ratios less than 2.3, gray and yellow-green colored species had ratios of 2.0 to 7.5 and green vegetation had ratios 7.5. GRA

N84-27246 Iowa State Univ. of Science and Technology, Ames. USE OF TRANSFORMED LANDSAT DATA IN REGRESSION ESTIMATION OF CROP ACREAGES Ph.D. Thesis

H. M. HUNG 1983 174 p Avail: Univ. Microfilms Order No. DA8407079

The use of functions of a vector X as auxiliary variables in the regression estimation of the population mean with survey data are investigated. Functions of the vector X are estimated by estimating the unknown parameters of the transformation. Under certain assumptions, the error in the estimated parameters is order $n^{(supra-1/2)}$, where n is the sample size. The effect of estimating the auxiliary variables is investigated under the assumption that the finite population is a random sample of an infinite population. Asymptotic properties of regression estimators of the finite population mean constructed with estimated auxiliary variables are developed. The U.S. Department of Agriculture (USDA) uses satellite (LANDSAT) data to improve crop acreage estimates. LANDSAT data consist of a vector X of four radiation values in four wavelength bands of the electromagnetic spectrum. Based on these data, the USDA has developed a classification function for use as an auxiliary variable.

Dissert. Abstr.

01 AGRICULTURE AND FORESTRY

N84-27251*# Delaware Univ., Newark. Coll. of Marine Studies.
EVALUATION OF SPATIAL, RADIOMETRIC AND SPECTRAL THEMATIC MAPPER PERFORMANCE FOR COASTAL STUDIES
Quarterly Status Technical Progress Report, 1 Apr. - 30 Jun. 1984

V. KLEMAS, Principal Investigator 30 Jun. 1984 5 p ERTS
(Contract NAS5-27580)
(E84-10159; NASA-CR-173671; NAS 1.26:173671) Avail: NTIS
HC A02/MF A01 CSCL 08B

The effect different wetland plant canopies have upon observed reflectance in Thematic Mapper bands is studied. The three major vegetation canopy types (broadleaf, gramineous and leafless) produce unique spectral responses for a similar quantity of live biomass. The spectral biomass estimate of a broadleaf canopy is most similar to the harvest biomass estimate when a broadleaf canopy radiance model is used. All major wetland vegetation species can be identified through TM imagery. Simple regression models are developed equating the vegetation index and the infrared index with biomass. The spectral radiance index largely agreed with harvest biomass estimates. M.A.C.

N84-27255*# Texas A&M Univ., College Station. Remote Sensing Center.

CROP MOISTURE ESTIMATION OVER THE SOUTHERN GREAT PLAINS WITH DUAL POLARIZATION 1.66 CENTIMETER PASSIVE MICROWAVE DATA FROM NIMBUS 7 Final Report
M. J. MCFARLAND, P. H. HARDER, II, G. D. WILKE, and G. L. HUEBNER, JR. May 1984 154 p refs Original contains imagery. Original photography may be purchased from the EROS Data Center, Sioux Falls, S.D. 57198 ERTS
(Contract NAS9-16822)
(E84-10163; NASA-CR-171794; NAS 1.26:171794; RSC-4854)
Avail: NTIS HC A08/MF A01 CSCL 02C

Moisture content of snow-free, unfrozen soil is inferred using passive microwave brightness temperatures from the scanning multichannel microwave radiometer (SMMR) on Nimbus-7. Investigation is restricted to the two polarizations of the 1.66 cm wavelength sensor. Passive microwave estimates of soil moisture are of two basic categories; those based upon soil emissivity and those based upon the polarization of soil emission. The two methods are compared and contrasted through the investigation of 54 potential functions of polarized brightness temperatures and, in some cases, ground-based temperature measurements. Of these indices, three are selected for the estimated emissivity, the difference between polarized brightness temperatures, and the normalized polarization difference. Each of these indices is about equally effective for monitoring soil moisture. Using an antecedent precipitation index (API) as ground control data, temporal and spatial analyses show that emissivity data consistently give slightly better soil moisture estimates than depolarization data. The difference, however, is not statistically significant. It is concluded that polarization data alone can provide estimates of soil moisture in areas where the emissivity cannot be inferred due to nonavailability of surface temperature data. Author

N84-27256*# Instituto de Pesquisas Espaciais, Sao Jose dos Campos (Brazil).

IDENTIFICATION AND ESTIMATION OF THE AREA PLANTED WITH IRRIGATED RICE BASED ON THE VISUAL INTERPRETATION OF LANDSAT MSS DATA [IDENTIFICACAO E AVALIACAO DA AREA OCUPADA COM ARROZ IRRIGADO ATRAVES DA INTERPRETACAO VISUAL DE DADOS DO MSS DO LANDSAT]

N. D. J. PARADA, Principal Investigator, M. A. MOREIRA (Tecnicos do IRGA), G. V. ASSUNCAO, R. A. NOVAES, A. A. B. MENDOZA (Tecnicos do IRGA), C. A. BAUER, I. T. RITTER (Tecnicos do IRGA), J. A. I. BARROS, J. E. PEREZ (Tecnicos do IRGA), J. L. O. THEDY (Tecnicos do IRGA) et al. Dec. 1983 80 p refs In PORTUGUESE; ENGLISH summary Sponsored by NASA Original contains color imagery. Original photography may be purchased from the EROS Data Center, Sioux Falls, S.D. 57198 ERTS
(E84-10164; NASA-CR-173640; NAS 1.26:173640; INPE-2991-NTE/212) Avail: NTIS HC A05/MF A01 CSCL 02C

The objective was to test the feasibility of the application of MSS-LANDSAT data to irrigated rice crop identification and area evaluation, within four rice growing regions of the Rio Grande do Sul state, in order to extend the methodology for the whole state. The applied methodology was visual interpretation of the following LANDSAT products: channels 5 and 7 black and white imageries and color infrared composite imageries all at the scale of 1:250.000. For crop identification and evaluation, the multispectral criterion and the seasonal variation were utilized. Based on the results it was possible to conclude that: (1) the satellite data were efficient for crop area identification and evaluation; (2) the utilization of the multispectral criterion, allied to the seasonal variation of the rice crop areas from the other crops and, (3) the large cloud cover percentage found in the satellite data made it impossible to realize a rice crop spectral monitoring and, therefore, to define the best dates for such data acquisition for rice crop assessment. Author

N84-27257*# Instituto de Pesquisas Espaciais, Sao Jose dos Campos (Brazil).

A SAMPLING SYSTEM FOR ESTIMATING THE CULTIVATION OF WHEAT (TRITICUM AESTIVUM L) FROM LANDSAT DATA M.S. Thesis - 21 Jul. 1983 [SISTEMA DE AMOSTRAGEM PARA ESTIMAR A AREA DA CULTURA DO TRIGO (TRITICUM AESTIVUM L) ATRAVES DE DADOS DO LANDSAT]

N. D. J. PARADA, Principal Investigator and M. A. MOREIRA Oct. 1983 109 p refs In PORTUGUESE; ENGLISH summary Sponsored by NASA ERTS
(E84-10165; NASA-CR-173638; NAS 1.26:173638; INPE-2941-TDL/150) Avail: NTIS HC A06/MF A01 CSCL 02C

Using digitally processed MSS/LANDSAT data as auxiliary variable, a methodology to estimate wheat (Triticum aestivum L) area by means of sampling techniques was developed. To perform this research, aerial photographs covering 720 sq km in Cruz Alta test site at the NW of Rio Grande do Sul State, were visually analyzed. LANDSAT digital data were analyzed using non-supervised and supervised classification algorithms; as post-processing the classification was submitted to spatial filtering. To estimate wheat area, the regression estimation method was applied and different sample sizes and various sampling units (10, 20, 30, 40 and 60 sq km) were tested. Based on the four decision criteria established for this research, it was concluded that: (1) as the size of sampling units decreased the percentage of sampled area required to obtain similar estimation performance also decreased; (2) the lowest percentage of the area sampled for wheat estimation with relatively high precision and accuracy through regression estimation was 90% using 10 sq km as the sampling unit; and (3) wheat area estimation by direct expansion (using only aerial photographs) was less precise and accurate when compared to those obtained by means of regression estimation.

Author

02 ENVIRONMENTAL CHANGES AND CULTURAL RESOURCES

N84-27261# Instituto de Pesquisas Espaciais, Sao Jose dos Campos (Brazil).

RESEARCH AND APPLICATIONS OF DATA FROM ENVIRONMENTAL SATELLITES: DETERMINING PARAMETERS AND DEVELOPING INTERPRETATION TECHNIQUES FOR APPLICATIONS OF ENVIRONMENTAL SATELLITE DATA [PESQUISAS E APLICACOES EM DADOS DE SATELITES AMBIENTAIS DETERMINACAO DE PARAMETROS E DESENVOLVIMENTO DE TECNICAS INTERPRETATIVAS PARA APLICACOES DE DADOS DE SATELITES AMBIENTAIS]
G. T. BATISTA, F. C. DEALMEIDA, A. T. TARDIN, and S. D. A. F. PINTO Feb. 1984 21 p refs In PORTUGUESE; ENGLISH summary
(INPE-3005-NTE/213) Avail: NTIS HC A02/MF A01

The determination of parameters and development of techniques of interpretation of data collected by environmental satellites (Land and Meteorological Resources) emphasizing the activities carried out in the first semester of 1983 is described. This technology is highly important for the country, especially in the areas of crop production forecast, precipitation estimation, mineral and forest resources, land use and hydrographic basin management.

Author

N84-27324# National Environmental Satellite Service, Washington, D. C.

FIRE DETECTION USING THE NOAA (NATIONAL OCEANIC AND ATMOSPHERIC ADMINISTRATION)-SERIES SATELLITES
M. MATSON, S. R. SCHNEIDER, B. ALDRIDGE (National Weather Service), and B. SATCHWELL (National Weather Service) Jan. 1984 41 p refs
(PB84-176890; NOAA/TR/NESDIS-7; NOAA-84031901) Avail: NTIS HC A03/MF A01 CSCL 02F

The potential usefulness of thermal infrared sensors onboard NOAA polar orbiting satellites for detecting fires in particular, the 3.8-micrometer channel is sensitive to high temperature sources such as fires. How the 3.8-micrometer channel provides an efficient economical means of detecting and monitoring range, forest, and tundra fires is demonstrated.

GRA

02

ENVIRONMENTAL CHANGES AND CULTURAL RESOURCES

Includes land use analysis, urban and metropolitan studies, environmental impact, air and water pollution, geographic information systems, and geographic analysis.

A84-30240#

DIGITAL PROCESSING OF REMOTE SENSING DATA ON HAIL HAOR, BANGLADESH FOR LANDUSE ANALYSIS AND DEVELOPMENT POTENTIALITY ASSESSMENT

M. U. CHAUDHURY and A. K. M. SHAFIUL ALAM (Bangladesh Space Research and Remote Sensing Organization, Dacca, Bangladesh) IN: Asian Conference on Remote Sensing, 3rd, Dacca, Bangladesh, December 4-7, 1982, Proceedings . Tokyo, University of Tokyo, 1983, p. B-1 to B-11. refs

A84-30241#

APPLICATION OF MULTI-CONCEPT IN REMOTE SENSING TECHNIQUE FOR IDENTIFICATION AND MAPPING OF SOIL UNITS OF ALLUVIAL PLAIN FOR LAND USE PLANNING IN SRI LANKA

S. KUMARAKULASURIYAR (Department of Irrigation, Land Use Div., Colombo, Sri Lanka) IN: Asian Conference on Remote Sensing, 3rd, Dacca, Bangladesh, December 4-7, 1982, Proceedings . Tokyo, University of Tokyo, 1983, p. B-4-1 to B-4-10.

A84-30242#

ANALYSIS OF LAND USE CHANGES AROUND SALT LAKE CITY USING LANDSAT DIGITAL DATA - A CASE STUDY OF SANDY AREA

C.-M. LEE and S.-J. HAN (Utah, University, Salt Lake City, UT) IN: Asian Conference on Remote Sensing, 3rd, Dacca, Bangladesh, December 4-7, 1982, Proceedings . Tokyo, University of Tokyo, 1983, p. B-6-1 to B-6-15. refs

The purpose of this paper is to analyze land use changes in the Sandy area, a case study of urban growth accompanying urban encroachment into surrounding urban fringes over time by utilizing Landsat data in conjunction with aerial photographs and ground observations. This study involves two sets of imagery and digital data, these being September 12, 1972, and July 2, 1979. An up-to-date scene in 1980 was not applicable due to the low quality of the Landsat data. The conversion of agricultural lands primarily into residential land use is investigated as the phenomenon of urban sprawl. The major hypothesis is that the analysis of Landsat digital data along with aerial photographs from different dates yield an estimate of the extent and the pattern of future urban growth for the study area. The results of the study indicate that urban land is increasing extremely fast at the expense of rural land in the study area.

Author

A84-30243#

THE COMPILATION OF THE SATELLITE IMAGE MAP OF LAND-USE OF CHINA (1:2,000,000 SCALE)

L. B. HENG (National Remote Sensing Center, Information Dept., Beijing, People's Republic of China) IN: Asian Conference on Remote Sensing, 3rd, Dacca, Bangladesh, December 4-7, 1982, Proceedings . Tokyo, University of Tokyo, 1983, p. B-7-1 to B-7-10.

A84-30307

COMPUTER-AUTOMATED CO₂-LASER LONG-PATH ABSORPTION SYSTEM FOR AIR QUALITY MONITORING IN THE WORKING ENVIRONMENT

U. PERSSON, S. LUNDQVIST, B. MARTINSSON, and S. T. ENG (Chalmers Tekniska Högskola, Göteborg, Sweden) Applied Optics (ISSN 0003-6935), vol. 23, April 1, 1984, p. 998-1002. Research supported by the Styrelsen for Teknisk Utveckling. refs

A84-31024

SATELLITE CLIMATOLOGY [SPUTNIKOVAIA KLIMATOLOGIIA]

K. IA. KONDRATEV Leningrad, Gidrometeoizdat, 1983, 264 p. In Russian. refs

General requirements for observational data on climatic parameters, and for the spatial-temporal resolving power and precision of measurements are analyzed. The use of numerical weather simulation, experiments for climate sensitivity to various factors and input parameters, and multipurpose environmental surveys in meeting these requirements are discussed. The leading role of cloud cover as an energy regulator in the atmosphere (particularly in connection with cloud cover-radiation interaction) and the large volume of satellite data on clouds are seen as determining factors in setting a high priority for satellite climatology of cloud cover. Data on the water vapor and liquid content of clouds and on precipitation are studied. Considerable attention is given to the analysis of results of wind field reconstruction according to the drift of clouds and sounding balloons. Results of remote sensing are discussed for ground and ocean surface temperatures, ice and snow cover, and moisture content of soil as determined by infrared photography.

02 ENVIRONMENTAL CHANGES AND CULTURAL RESOURCES

A84-33333

SOIL EROSION MAPPING AND EVALUATION - A PHOTO-GEOMORPHOLOGICAL APPROACH

Y. I. FARHAN (Yarmouk University, Irbid, Jordan) IN: American Society of Photogrammetry, Annual Meeting, 49th, Washington, DC, March 13-18, 1983, Technical Papers . Falls Church, VA, American Society of Photogrammetry, 1983, p. 131-143. refs

A study was conducted regarding the employment of a photo-geomorphological technique for the recognition of a soil erosion potential at low cost and minimum time. Approaches to mapping soil erosion phenomena are discussed, taking into account three approaches for land erosion survey on the basis of a utilization of photogeomorphological techniques. One technique is concerned with a regional, or reconnaissance, survey level of scale 1:100000 or less. The second type of mapping is the semidetailed survey, or medium-scale mapping (scale between 1:25000 and 1:100000). The third approach is the detailed land erosion survey of scale larger than 1:25000. A solution of the problem of soil erosion in Jordan has only been possible through the use of the photo-geomorphological method, coupled with increased availability of aerial photographic coverages, and the development of photo-interpretation techniques. G.R.

A84-33344* National Aeronautics and Space Administration. Goddard Space Flight Center, Greenbelt, Md.

COMPARATIVE ACCURACIES OF AVHRR AND MSS DATA USED FOR LEVEL I LAND COVER CLASSIFICATIONS

J. C. GERVIN, R. G. WITT, A. G. KERBER (NASA, Goddard Space Flight Center, Greenbelt, MD), Y. C. LU, R. SEKHON, and B. BLY (Computer Sciences Corp., Silver Spring, MD) IN: American Society of Photogrammetry, Annual Meeting, 49th, Washington, DC, March 13-18, 1983, Technical Papers . Falls Church, VA, American Society of Photogrammetry, 1983, p. 334-342. refs

The capabilities of the Advanced Very High Resolution Radiometer (AVHRR) for land cover mapping were investigated by comparing the accuracy of land cover information for the Washington, DC area derived from NOAA-7 AVHRR data with that from Landsat Multispectral Scanner (MSS) data. Unsupervised Level I land cover classifications were performed for MSS and AVHRR data sets collected on July 11, 1981. A detailed accuracy assessment was conducted based on ground truth delineated on six USGS 7.5 minute series topographic maps. Preliminary results produced overall land cover classification accuracies of 75.6 percent and 76.1 percent for AVHRR and MSS, respectively. While the accuracies for predominant categories such as agriculture, forest, and urban were similar for both sensors, discrimination of the less commonly occurring categories such as barren, wetland, and water was improved with the MSS data set. The AVHRR, however, performed as well as or better than the MSS in classifying large homogeneous areas. The application of AVHRR data with its lower processing cost and more frequent worldwide coverage appears promising for global land cover mapping. Author

A84-33361

FINDINGS ON THE USE OF LANDSAT-3 RETURN BEAM VIDICON IMAGERY FOR DETECTING LAND USE AND LAND COVER CHANGES

V. A. MILAZZO (U.S. Geological Survey, National Mapping Div., Reston, VA) IN: American Congress on Surveying and Mapping, Annual Meeting, 43rd, Washington, DC, March 13-18, 1983, Technical Papers . Falls Church, VA, American Congress on Surveying and Mapping, 1983, p. 366-375.

Current land use and land cover maps and data are needed for gaining an understanding regarding the present use of the nation's land resources, and for the proper planning and management of these resources. In order to provide the required maps and data, research is being conducted regarding suitable methods for updating existing U.S. Geological Survey (USGS) land use and land cover data. The positional accuracy and improved resolution and quality of imagery from the return beam vidicon (RBV) camera system aboard Landsat-3 (as compared with earlier Landsat RBV and MSS imagery) suggests that such data may be useful in a USGS land use and land cover map inspection program.

In the present investigation, the RBV imagery was found to be useful in identifying a major portion of the changes which occurred in the study area. In the absence of better alternative source materials, the RBV data can be recommended as a rough estimator of change in some environments. G.R.

A84-33363

A REGIONAL RASTER DATA STUDY AT THE EXPERIMENTAL CARTOGRAPHY UNIT - THE APPLICATION OF INTERACTIVE RASTER GRAPHICS TO ENVIRONMENTAL MODELLING

J. DRUMMOND, P. GREEN, M. JACKSON, and J. PLANT (Natural Environment Research Council, London, England) IN: American Congress on Surveying and Mapping, Annual Meeting, 43rd, Washington, DC, March 13-18, 1983, Technical Papers . Falls Church, VA, American Congress on Surveying and Mapping, 1983, p. 394-401. refs

An epidemiological study into the association between degenerative diseases in man and natural trace element levels, being conducted by the Experimental Cartography Unit and the Regional Geochemical Reconnaissance Program of the Institute of Geological Sciences (both of the Natural Environment Research Council), highlights the potential application of spatial modelling techniques in environmental studies. The study area is that of Moray Buchan in northeast Scotland. A computer readable database, which includes data such as the concentrations of chemical elements, medical statistics, rainfall values, geology, and classified Landsat images, is being built up. The utilization of such very different data sets requires a system capable of handling point, line, polygon, and raster data in an integrated and registered manner. Both vector and raster systems are employed at different stages in the investigation, but the most powerful method of studying interrelationships between data sets involves the utilization of the Natural Environment Research Council's I2S Image Analysis System, which enables primary and derived data sets to be interrogated in real time. The approach used in reformatting, integrating and comparing different spatial data sets is discussed, with particular reference to the problems encountered and to sources of error.

Author

A84-33370

DEVELOPMENT OF SATELLITE DOPPLER/INERTIAL SURVEY SYSTEMS FOR BLM CADASTRAL SURVEY-RELATED APPLICATIONS IN ALASKA

W. E. BALL, JR. IN: American Congress on Surveying and Mapping, Annual Meeting, 43rd, Washington, DC, March 13-18, 1983, Technical Papers . Falls Church, VA, American Congress on Surveying and Mapping, 1983, p. 511-521.

A84-34450

RECENT INVESTIGATIONS OF OZONE AND MINOR ATMOSPHERIC GASES [O SOVREMENNYKH ISSLEDOVANIYakh OZONA I MALYKh GAZOV ATMOSFERY]

A. KH. KHRGIAN (Moskovskii Gosudarstvennyi Universitet, Moscow, USSR) Akademii Nauk SSSR, Izvestiia, Fizika Atmosfery i Okeana (ISSN 0002-3515), vol. 20, April 1984, p. 323-326. In Russian. refs

The limitations that beset the network used today for studying ozone and making predictions are discussed. These include errors in calibration, instrument drift, interruptions in observations, and the effects of volcanic eruptions. The importance of supplementing ground-based observations with satellite data is stressed. It is noted that optical studies of ozone can be distorted by SO₂, which increases in concentration during volcanic eruptions. All of the instruments used at present for ground-based studies of ozone are susceptible to some extent to the effects of minor gases. Circumspection is therefore advised in assessing the results.

C.R.

02 ENVIRONMENTAL CHANGES AND CULTURAL RESOURCES

A84-34794* Hawaii Univ., Honolulu.

FIRST ESTIMATE OF ANNUAL MERCURY FLUX AT THE KILAUEA MAIN VENT

S. M. SIEGEL and B. Z. SIEGEL (Hawaii University, Honolulu, HI) Nature (ISSN 0028-0836), vol. 309, May 10, 1984, p. 146, 147. Research supported by the Cottrell Foundation, University of Hawaii, Hawaii Natural Energy Institute, U.S. Department of Energy, and NASA. refs

Mercury and sulphur dioxide analyses were conducted from 1971 to 1980 on air samples collected immediately downwind of Halemaumau, the Kilauea main vent, in Hawaii. On the basis of these measurements, an Hg/SO₂ ratio of 0.00051 has been derived which, when applied to the recently determined SO₂ mass output of Halemaumau, yields a calculated Hg flux of 2.6×10^{-8} g annually. This rate is consistent with Varekamp and Busek's (1981) evidence suggesting that volcanic Hg significantly contributes to the atmospheric total.

O.C.

A84-38301

SPACE DISTURBANCE WARNING SYSTEM WITH THE AID OF SATELLITES

T. ONDOH, K. AIKYO (Ministry of Posts and Telecommunications, Radio Research Laboratories, Koganei, Japan), and T. OGAWA (Radio Research Laboratories, Nakaminato, Ibaraki, Japan) IN: International Symposium on Space Technology and Science, 13th, Tokyo, Japan, June 28-July 3, 1982, Proceedings. Tokyo, AGNE Publishing, Inc., 1982, p. 1277-1284.

A space environment monitoring and space warning system is proposed for forecasting space disturbances and automatically broadcasting warnings to space users. The system consists of an elliptically orbiting satellite and a GEO satellite instrumented to monitor the solar wind, polar cusp phenomena, and substorm phenomena. Measurements would be taken of solar active regions, hot plasma, high energy particles, magnetic and static electric fields, plasma waves, radio noise, plasmaspheric radio emissions, the total ionospheric electron content or scintillations, and solar X-ray fluxes. Warning would be broadcast to a ground control station using uplink/downlink frequencies of 2.1/2.2 GHz, with a 1.7 GHz link to the GEO component. An elliptical orbit with an apogee of 153,600 km and an inclination of 70 deg has been identified.

M.S.K.

A84-39455* Institute for Atmosphere Optics and Remote Sensing, Hampton, Va.

SAGE AND SAM II MEASUREMENTS OF GLOBAL STRATOSPHERIC AEROSOL OPTICAL DEPTH AND MASS LOADING

G. S. KENT (Institute for Atmospheric Optics and Remote Sensing, Hampton, VA) and M. P. MCCORMICK (NASA, Langley Research Center, Hampton, VA) Journal of Geophysical Research (ISSN 0148-0227), vol. 89, June 30, 1984, p. 5303-5314. refs

Several volcanic eruptions between November 1979 and April 1981 have injected material into the stratosphere. The SAGE and SAM II satellite systems have measured, with global coverage, the 1-micron extinction produced by this material, and examples of the data product are shown in the form of global maps of stratospheric optical depth and altitude-latitude plots of zonal mean extinction. These data, and that for the volcanically quiet period in early 1979, have been used to determine the changes in the total stratospheric mass loading. Estimates have also been made of the contribution to the total aerosol mass from each eruption. It has been found that between 1979 and mid-1981, the total stratospheric aerosol mass increased from a background level of approximately 570,000 metric tons to a peak of approximately 1,300,000 metric tons.

Author

A84-39457* National Aeronautics and Space Administration, Langley Research Center, Hampton, Va.

A COMPARATIVE STUDY OF AEROSOL EXTINCTION MEASUREMENTS MADE BY THE SAM II AND SAGE SATELLITE EXPERIMENTS

G. K. YUE (NASA, Langley Research Center; Institute for Atmospheric Optics and Remote Sensing, Hampton, VA), M. P. MCCORMICK, and W. P. CHU (NASA, Langley Research Center, Hampton, VA) Journal of Geophysical Research (ISSN 0148-0227), vol. 89, June 30, 1984, p. 5321-5327. refs (Contract NAS1-17032)

SAM II and SAGE are two satellite experiments designed to measure stratospheric aerosol extinction using the technique of solar occultation or limb extinction. Although each sensor is mounted aboard a different satellite, there are occasions when their measurement locations are nearly coincident, thereby providing opportunities for a measurement comparison. In this paper, the aerosol extinction profiles and daily contour plots for some of these events in 1979 are reported. The comparisons shown in this paper demonstrate that SAM II and SAGE are producing similar aerosol extinction profiles within their measurement errors and that since SAM II has been previously validated, these results show the validity of the SAGE aerosol measurements.

Author

N84-23983*# Utah Univ., Salt Lake City. Center for Remote Sensing and Cartography.

EPA ENVIROPOD. A SUMMARY OF THE USE OF THE ENVIROPOD UNDER A MEMORANDUM OF UNDERSTANDING AMONG EPA REGION 8, THE STATE OF UTAH, AND THE UNIVERSITY OF UTAH RESEARCH INSTITUTE Annual Report, 1 Mar. 1983 - 28 Feb. 1984

M. K. RIDD Mar. 1984 37 p Sponsored by NASA ERTS (E84-10124; NASA-CR-172799; NAS 1.26:172799; CRSC-84-2)

Avail: NTIS HC A03/MF A01 CSCL 08B

Twenty-three missions were flown using the EPA's panoramic camera to obtain color and color infrared photographs of landslide and flood damage in Utah. From the state's point of view, there were many successes. The biggest single obstacle to smooth and continued performance was unavailable aircraft. The Memorandum of Understanding between the State of Utah, the Environmental Protection Agency, and the Center for Remote Sensing and Cartography is included along with forms for planning enviropod missions, for requesting flights, and for obtaining feedback from participating agencies.

A.R.H.

N84-23984*# Utah Univ., Salt Lake City. Center for Remote Sensing and Cartography.

IDENTIFYING ENVIRONMENTAL FEATURES FOR LAND MANAGEMENT DECISIONS Semiannual Report

Apr. 1984 27 p ERTS

(Contract NAGW-95)

(E84-10125; NASA-CR-172800; NAS 1.26:172800) Avail: NTIS HC A03/MF A01 CSCL 08B

Multivariate statistical analysis and imaging processing techniques are being applied to the study of arid/semiarid environments, with emphasis on desertification. Field level indicators of land-soil biota degradation are being sifted out with staging up to the low aircraft reconnaissance level, to LANDSAT TM & MSS, and even to the AVHRR level. Three completed projects are reviewed: riparian habitat on the Humboldt River floodplain, Salt Lake County Urban expansion detection, and salinization/desertification detection in the delta area. Beginning projects summarized include: comparative condition of rangeland in Rush Valley; modeling a GIS/remote sensing data base for Cache County; universal soil loss equation applied to Pinyon-Juniper; relating MSS to ground radiometry near Battle Mountain; and riparian habitat mapping on Mary's River, Nevada.

A.R.H.

02 ENVIRONMENTAL CHANGES AND CULTURAL RESOURCES

N84-23996# Army Engineer Waterways Experiment Station, Vicksburg, Miss. Environmental Lab.

SURVEY OF AUTOMATED STATEWIDE NATURAL RESOURCE INFORMATION SYSTEMS Final Report

E. M. CAUSEY Jan. 1984 46 p

(AD-A139017; WES/MP/EL-84-1) Avail: NTIS HC A03/MF A01 CSCL 08F

This report contains the results of a survey to determine which states maintain a geographically referenced computer-based natural resource information system (NRIS). Twenty-two states currently have an NRIS in varying stages of development. A brief description of each system is included in Appendix A of this report. GRA

N84-25156# Research Inst. of National Defence, Linkoeping (Sweden).

CONTOUR-TO-GRID TRANSFORMATION: DEVELOPMENT OF A METHOD FOR GENERATION OF A SPARSE GRID STRUCTURE OUT OF TERRAIN ELEVATION CONTOURS

B. SCHMELING and E. JUNGERT Dec. 1983 34 p refs (Contract STU-83-3307)

(FOA-C-30349-E1; ISSN-0347-3708) Avail: NTIS HC A03/MF A01; Research Institute of National Defence, Stockholm KR 50

A method to transform elevation lines on a geographical map into a sparse, equidistant grid structure is described. Only those points in the grid that are closest to the elevation lines are recorded together with their elevation, which is calculated by interpolation. The important issue is to choose the distance between the grid points in such a way that: (1) no relevant information in the elevation lines will be lost; and (2) the amount of recorded grid points will be minimized. Test runs of a SIMULA program based on this method show that 12.5 meters is a suitable distance between the grid points. E.A.K.

N84-25340# Research Inst. of National Defence, Stockholm (Sweden).

A COMPUTER PROGRAM FOR MAPPING REGIONS IN A GEOGRAPHIC DATA BASE WITH RASTER STRUCTURE

J. TJERNBERG and A. WELLVING Jan. 1984 31 p. refs In SWEDISH; ENGLISH summary

(FOA-C-20529-D8; ISSN-0347-3694) Avail: NTIS HC A03/MF A01

SCOPE is a computer program that can be used for the creation of regions or landscape types in a satellite image. It uses a scanning window for a series of filtering processes and the result is a map which shows a few different regions together with existing lakes. An application of the program which is shown in the report is the study of the relation between forested and open land in an area but as a general tool for mapping out regions in geographic data bases with raster structure, the program has a large variety of applications. Author

N84-26090# Instituto de Pesquisas Espaciais, Sao Jose dos Campos (Brazil).

APPLICATION OF LANDSAT DATA TO THE STUDY OF URBAN DEVELOPMENT IN BRASILIA [APLICACOES DE DADOS DOS SATELITES LANDSAT NO ESTUDO DA EVOLUCAO URBANA DE BRASILIA]

N. D. J. PARADA, Principal Investigator, M. D. L. N. DEOLIVEIRA, C. FORESTI, M. NIERO, and E. M. D. M. F. PARREIRAS Apr. 1984 16 p refs In PORTUGUESE; ENGLISH summary Presented at the 1st Congr. Brasil. de Defesa do Meio Ambiente, 2-6 Jul. 1984 Sponsored by NASA ERTS (E84-10142; NASA-CR-172815; NAS 1.26:172815; INPE-3063-PRE/480) Avail: NTIS HC A02/MF A01 CSCL 08B

The urban growth of Brasilia within the last ten years is analyzed with special emphasis on the utilization of remote sensing orbital data and automatic image processing. The urban spatial structure and the monitoring of its temporal changes were examined in a whole and dynamic way by the utilization of MSS-LANDSAT images for June (1973, 1978 and 1983). In order to aid data interpretation, a registration algorithm implemented in the Interactive Multispectral

Image Analysis System (IMAGE-100) was utilized aiming at the overlap of multitemporal images. The utilization of suitable digital filters, combined with the images overlap, allowed a rapid identification of areas of possible urban growth and oriented the field work. The results obtained in this work permitted an evaluation of the urban growth of Brasilia, taking as reference the proposal stated for the construction of the city in the Pilot Plan elaborated by Lucio Costa. M.G.

N84-26095# Instituto de Pesquisas Espaciais, Sao Jose dos Campos (Brazil).

THE USE OF AN IMAGE REGISTRATION TECHNIQUE IN THE URBAN GROWTH MONITORING

N. D. J. PARADA, Principal Investigator, C. FORESTI, M. D. L. N. DEOLIVEIRA, M. NIERO, and E. M. D. M. F. PARREIRAS (Companhia do Desenvolvimento do Planalto Central) Apr. 1984 7 p refs Presented at the 15th Intern. Soc. of Photogrammetry and Remote Sensing Congr., Rio de Janeiro, 18-29 Jun. 1984 Submitted for publication Sponsored by NASA ERTS (E84-10147; NASA-CR-173237; NAS 1.26:173237; INPE-3089-PRE/496) Avail: NTIS HC A02/MF A01 CSCL 08B

The use of an image registration program in the studies of urban growth is described. This program permits a quick identification of growing areas with the overlap of the same scene in different periods, and with the use of adequate filters. The city of Brasilia, Brazil, is selected for the test area. The dynamics of Brasilia urban growth are analyzed with the overlap of scenes dated June 1973, 1978 and 1983. The results showed the utilization of the image registration technique for the monitoring of dynamic urban growth. M.A.C.

N84-26104# European Space Agency, Paris (France).

DIGITAL PROCESSING OF LANDSAT DATA FOR THE PREPARATION OF A LAND USE MAP OF THE RURAL DISTRICT SURROUNDING TUEBINGEN TO A SCALE OF 1:50000

H. R. GOETTING Feb. 1984 92 p refs Transl. into ENGLISH of "Fernerkundung mit LANDSAT sowie die digitale verarbeitung der daten zur herstellung einer landnutzungskarte des landkreises Tuebingen im massstab 1:50000" rept. DFVLR-FB-82-30 DFVLR, Oberpfaffenhofen, West Germany, 1982 Original language document announced as N83-285620 Original contains color illustrations

(ESA-TT-816; DFVLR-FB-82-30) Avail: NTIS HC A05/MF A01; original German report available from DFVLR, Cologne DM 44,20

Based on LANDSAT satellite remote sensing data, a 1:50,000 land use map of the rural environs of Tuebingen, West Germany was produced. The interactive digital image processing system called DIBIAS was used for the image processing. The main algorithms applied were geometrical rectification to Gauss-Krueger coordinates and Maximum Likelihood classification of the image data. The results were combined with both optical and digital topographical information and compared with a conventional vegetation map. An assessment of the usefulness of thematic mapping for regional planning is given. Aspects of data acquisition and the physical foundations of remote sensing are described. The reflection properties of various terrain types, differentiated in the wavelength bands of the electromagnetic spectrum, are discussed. The LANDSAT system and its associated sensing techniques are presented. R.S.F.

N84-26428# Instituto de Pesquisas Espaciais, Sao Jose dos Campos (Brazil).

THE USE OF PHOTointerpretation FOR SOCIO-ECONOMIC CHARACTERIZATION OF URBAN POPULATION

M. D. L. N. DEOLIVEIRA and M. S. S. BARROS Apr. 1984 8 p refs Presented at the 15th Intern. Symp. of Photogrammetry and Remote Sensing, Rio de Janeiro, Jun. 1984 (INPE-3067-PRE/484) Avail: NTIS HC A02/MF A01

The use of aerial panchromatic photography for analysis of urban residential environments in Brazilian towns is described. The lack of information about the discrimination of different segments of urban population according to their socio-economic

03 GEODESY AND CARTOGRAPHY

characteristics, as required by urban planning process, motivated the development of this work. Through the examination of relevant physical aspects of residential areas, these are classified into groups, according to their socio-economic status. This classification was validated using survey data about total family income and the main householder's income. The results showed the usefulness of aerial photography for this purpose. Author

**N84-28201# Institut Geographique National, Paris (France).
RESEARCH ON LAND USE CARTOGRAPHY BY REMOTE SENSING Final Report [RECHERCHE SUR LA CARTOGRAPHIE DE L'OCCUPATION DES SOLS PAR TELEDETECTION]**

1982 80 p In FRENCH

Avail: NTIS HC A05/MF A01

The cartography of land use obtained by LANDSAT image processing is compared with existing statistical results in order to better define the land use in agricultural areas. The Loire department in France was chosen because it could be covered by a single LANDSAT image and because of the existing cartographic data. A cartographic document on the 1:100 000 scale shows land use obtained by an image processing method. The communal thematic charts obtained from communal statistics and a surface numerical model were used to group the areas by their topographic characteristics and land occupation. The correlations between satellite images and population and geological data were established. The main error source is the cell dimension as related to the satellite space resolution. The SPOT satellite should reduce this error to 10%. Author (ESA)

03

GEODESY AND CARTOGRAPHY

Includes mapping and topography.

A84-30583

THE APPROXIMATION INTRODUCED BY REPRESENTING THE EARTH'S GRAVITY FIELD WITH A FINITE GRID OF MASCONS BOTH AT THE EARTH'S SURFACE AND AT THE BOTTOM OF THE EARTH'S CRUST

J. V. BREAKWELL (Stanford University, Stanford, CA) and W. YANG (Chinese Academy of Space Technology, Beijing, People's Republic of China) IN: Astrodynamics 1983; Proceedings of the Conference, Lake Placid, NY, August 22-25, 1983. Part 2. San Diego, CA, Univelt, Inc., 1984, p. 1023-1038.

(AAS PAPER 83-394)

It is pointed out that the error involved in representing the earth's gravity field by a large but finite number of mascons is concentrated in the short wavelength part of the gravity spectrum. For estimating this error, it is, therefore, appropriate to use the 'flat-earth' approximations considered by Breakwell (1979). The present investigation is concerned with the mascon model error. Numerical results are presented for the case in which the density fluctuations are estimated from gradiometer measurements taken in a low satellite. Attention is given to the two-layer mascon model, the mascon model and an error analysis, and the numerical results. G.R.

A84-30727

THE GEODETIC ACTIVITIES OF THE DEPARTMENT OF DEFENSE UNDER IGY PROGRAMS

O. W. WILLIAMS and K. I. DAUGHERTY (U.S. Defense Mapping Agency, Hydrographic/Topographic Center, Washington, DC) EOS (ISSN 0096-3941), vol. 64, Oct. 16, 1983, p. 593-596.

Attention is given to the U.S. Department of Defence (DOD) activities that contributed to the International Geophysical Year's active, passive, and cooperative satellite programs. The DOD continues to support the deployment, enhancement, and application of novel technology in such areas as satellite altimetry, gravity radiometry, inertial surveying, interferometry, airborne gravimetry,

inertial surveying, and CCD and laser methods for geodetic astronomy. Also noted are such major department initiatives as the Global Positioning System, which will become operational toward the end of this decade. O.C.

A84-32494

GEOMETRICAL ASPECTS OF DIFFERENTIAL GPS POSITIONING

P. VANICEK, R. B. LANGLEY, D. E. WELLS, and D. DELIKARAOGLOU (New Brunswick, University, Fredericton, Canada) Bulletin Geodesique (ISSN 0007-4632), vol. 58, no. 1, 1984, p. 37-52. Research supported by the Geodetic Survey and Natural Sciences and Engineering Research Council of Canada. refs

Differential GPS positioning is considered from the purely geometric point of view. The tetrahedron formed by two ground stations and two satellite locations is the basic geometrical building block for differential satellite positioning. Relationships between the various vectors involved in this tetrahedron are described. These relationships are used to develop linear mathematical models which relate the vector baseline between the two ground stations to various kinds of differential GPS observations. Geometrically, all proposed observation types can be considered as either differential range observations or differential range difference observations. In the absence of instrumental and refraction effects, it is found that differential range observations are geometrically superior to differential range difference observations. Some implications of these geometrical considerations to practical differential GPS positioning are discussed. Author

A84-32495

PRESENT LIMITATIONS OF ACCURATE SATELLITE DOPPLER POSITIONING FOR TECTONICS - AN EXAMPLE: DJIBOUTI

A. SOURIAU, A. PIUZZI, M. ETCHEGORY, and P. MACHETEL (Centre National d'Etudes Spatiales, Groupe de Recherche de Geodesie Spatiale, Toulouse, France) Bulletin Geodesique (ISSN 0007-4632), vol. 58, no. 1, 1984, p. 53-72. Research supported by the Institut National d'Astronomie et de Geophysique. refs

A seismic and volcanic crisis occurred in this area in November 1978. Surface geodetic measurements made in 1973 and in 1978 and 1979 revealed a 60-80 cm sinking of the graben floor and lateral extension of approximately 2 m. An analysis is presented of Doppler measurements for the period from January 1977 to November 1980. Point positions are computed for 7 to 10 intervals using a precise ephemeris, and the data are subjected to a moving window analysis. Whereas an apparent 2-m uplift preceding the November 1978 seismic crisis is detected at Djibouti, no similar phenomenon is observed at the two closest stations. Field observations, however, rule out a tectonic origin for this uplift. In Djibouti, the correlation between the apparent vertical station position and the electron density in the ionospheric F layer reveals that a bias may result from the third-order term of the ionospheric refractive index not previously taken into account or, more likely, from the ray curvature through the ionosphere. C.R.

A84-33024

A KALMAN FILTER APPROACH TO PRECISION GPS GEODESY

R. G. BROWN and P. Y. C. HWANG (Iowa State University of Science and Technology, Ames, IA) Navigation (ISSN 0028-1522), vol. 30, Winter 1983-1984, p. 338-349. refs

An alternative approach to the application of VLBI methods of radio astronomy to GPS signals is based on an adaptive filter concept developed by D. Magill (1965). The present recursive scheme uses parallel Kalman filters with each filter being modeled for a different integer wavelength assumption. Integer ambiguity is resolved in less than 10 minutes of satellite observation time using a sampling interval of 2 sec, and the estimator effectively separates the position perturbation from the integer ambiguity. As the phase measurement scheme progresses, the adaptive scheme 'learns' which filter corresponds to the correct hypothesis, simultaneously resolving the wavelength ambiguity and estimating differential

03 GEODESY AND CARTOGRAPHY

position. Simulated results for the short baseline case are presented for both single- and four-satellite systems. J.N.

A84-33357

AMERICAN CONGRESS ON SURVEYING AND MAPPING, ANNUAL MEETING, 43RD, WASHINGTON, DC, MARCH 13-18, 1983, TECHNICAL PAPERS

Falls Church, VA, American Congress on Surveying and Mapping, 1983, 734 p.

Technical, legal, and professional aspects of surveying and cartography are examined in reports and abstracts. Technological topics discussed include satellite Doppler/inertial systems for cadastral surveys, computer aids to surveyors, adaptive interpolation in digital terrain models, accuracy and classification standards for satellite Doppler surveys, VLBI and satellite laser ranging in geodynamics, application of interactive raster graphics to environmental modeling, interactive name placement for provisional maps, lithography from remote-sensing imagery, and digital processing of geographic and cartographic data. T.K.

A84-33358

ESTABLISHING HYDROGRAPHIC CONTROL USING DOPPLER

D. H. MINKEL (NOAA, National Geodetic Survey, Rockville, MD) IN: American Congress on Surveying and Mapping, Annual Meeting, 43rd, Washington, DC, March 13-18, 1983, Technical Papers . Falls Church, VA, American Congress on Surveying and Mapping, 1983, p. 69-78. refs

Two Doppler satellite surveys conducted for the purpose of establishing hydrographic control stations are reviewed. One survey was conducted in Monterey, CA, the other established shore control for an upcoming Lake Superior survey being conducted by the National Ocean Survey (NOS). A brief discussion of the positional accuracies obtained using network adjustment programs MAGNET and GEODOP V is included. The Lake Superior Project is discussed in regard to methods used and total cost incurred. Author

A84-33364

SATELLITE SURVEYING TECHNIQUES USED WITHIN GEODETIC NETWORKS

L. J. ROMEYN (Geodetic International, Inc., Houston, TX) IN: American Congress on Surveying and Mapping, Annual Meeting, 43rd, Washington, DC, March 13-18, 1983, Technical Papers . Falls Church, VA, American Congress on Surveying and Mapping, 1983, p. 402-412. refs

Geodesy may be divided into areas of global geodesy, geodetic surveying, and plane surveying. Reference systems are examined, taking into account topography, the geoid, the Cartesian coordinate system, astronomical coordinates, and plane coordinates. Attention is given to geodetic networks, the geodetic satellite Doppler stations established by the U.S. Government, datum shift procedures, and published datum shift values. It is found that the employment of satellite survey techniques on control survey projects has steadily increased. An approach involving an employment of satellite surveying techniques within geodetic networks should have even greater acceptance after certain adjustments of the geodetic network have been made. G.R.

A84-33365

A DOPPLER POSITIONING COST MODEL

J. K. CROSSFIELD (Wisconsin, University, Madison, WI) IN: American Congress on Surveying and Mapping, Annual Meeting, 43rd, Washington, DC, March 13-18, 1983, Technical Papers . Falls Church, VA, American Congress on Surveying and Mapping, 1983, p. 413-422. refs

Quality areawide geodetic survey control is a requirement for successful implementation of a multi-purpose cadastre. Doppler satellite positioning is a proven method for establishing such control. The only configuration capable of providing a substantial number of accurate positions quickly is a multiple receiver simultaneously observed network with a post mission short arc type least squares adjustment. The approximate relative positioning accuracy and time on site equation developed for this cost model was derived from documentation describing the MAGNET program.

Generalized input variables insure significant user flexibility. Limitations on model use are discussed. The cost comparison test and examples show the potential value of this cost model to the user who wishes to establish areawide control. The user may gain valuable insight into the cost benefits of Doppler satellite positioning. Author

A84-33368

ESTABLISHING FIRST-ORDER CONTROL BY GPS SATELLITE SURVEYING INSTRUMENTS

J. COLLINS (Geo/Hydro, Inc., Rockville, MD) IN: American Congress on Surveying and Mapping, Annual Meeting, 43rd, Washington, DC, March 13-18, 1983, Technical Papers . Falls Church, VA, American Congress on Surveying and Mapping, 1983, p. 449-454. refs

A totally new, revolutionary Global Positioning System (GPS) satellite surveying instrument is now available to establish first-order (and less accurate) geodetic horizontal control over both short and long distances. This instrument has been tradenamed the MACROMETER Interferometric Surveyor. The MACROMETER instrument receives and processes the GPS satellite signals, using radio interferometric techniques in a way that produces (1:100,000) accuracy. Optimum use of this system results when three or more MACROMETER instruments simultaneously observe satellite signals. Conceptually, the MACROMETER instrument can be thought of as a total station which measures precise distance, azimuth, and vertical angle from a known to an unknown point, and also has the capability to measure through intervening obstructions. Author

A84-33373

STATUS REPORT - GRAVITY ACTIVITIES WITHIN THE NATIONAL GEODETIC SURVEY (NGS)

W. T. DEWHURST (NOAA, National Geodetic Survey, Rockville, MD) IN: American Congress on Surveying and Mapping, Annual Meeting, 43rd, Washington, DC, March 13-18, 1983, Technical Papers . Falls Church, VA, American Congress on Surveying and Mapping, 1983, p. 540-548. refs

A84-33374

A FORECAST OF THE IMPACT OF GPS ON SURVEYING

A. CHRZANOWSKI, R. B. LANGLEY, D. E. WELLS, and J. D. MCCLAUGHLIN (New Brunswick, University, Fredericton, Canada) IN: American Congress on Surveying and Mapping, Annual Meeting, 43rd, Washington, DC, March 13-18, 1983, Technical Papers . Falls Church, VA, American Congress on Surveying and Mapping, 1983, p. 625-634. refs

The NAVSTAR Global Positioning System (GPS) is capable of quickly providing relative positions with centimeter-level precision over a wide range of distances without the need for intervisibility between stations. These characteristics make GPS an exceptional tool with the potential for radically affecting the surveying industry. The potential impact of GPS on surveying technology, structure, expansion, and professionalism is discussed. Author

A84-34491

MAPPING OF EXOGENIC TERRAIN DYNAMICS ON THE BASIS OF SPACE PHOTOGRAPHS (ON THE EXAMPLE OF THE BAIKAL REGION) [KARTOGRAFIROVANIE EKZOGENNOI DINAMIKI REL'efa PO KOSMICHESKIM SNIMKAM /NA PRIMERE PRIBAIKAL'IA/]

S. A. SLADKOPEVSEV (Moskovskii Institut Inzhenerov Geodezii, Aerofotos'emki i Kartografii, Moscow, USSR) Geodezii i Aerofotos'emka (ISSN 0536-101X), no. 1, 1984, p. 117-125. In Russian. refs

The mapping of exogenic terrain dynamics was carried out for the Baikal region using photographs taken from the Salyut and Soyuz-22 spacecraft. A series of conjugated thematic maps is presented which together give a comprehensive characterization of the principal factors in the development of exogenic processes, types of displacement of friable surface material, trends in the development and stability of morphological systems, and the migration of the boundaries of these systems. An assessment is

03 GEODESY AND CARTOGRAPHY

made of the significance of the mapping of exogenic terrain dynamics for the study of earth resources, environment protection, and the forecasting of environment changes.

B.J.

A84-36919#

THE GRAVSAT SIGNAL OVER TECTONIC FEATURES

C. A. WAGNER and D. T. SANDWELL (NOAA, National Geodetic Survey, Rockville, MD) *Journal of Geophysical Research* (ISSN 0148-0227), vol. 89, June 10, 1984, p. 4419-4426. refs

The range rate between two close gravitational satellites (GRAVSAT) in low earth orbit has been evaluated over model tectonic features such as mountains and ranges, fracture zones, and trenches. Models are locally compensated, and consist of both point mass dipoles and sheet mass dipoles. Masses and depths of compensation are chosen to approximate known gravity signatures. The results show that for two satellites at 160 km altitude with 3 deg separation, significant signal power (greater than 1 micron/s) remains for most extended features at wavelengths less than 200 km. Furthermore, there is strong sensitivity in the signal from these features to lateral and vertical changes of the order of 1 km and less. In addition, the signal of hidden geologic structures such as dikes, salt domes, and ore bodies may also stand above 1 micron/s for this low orbiting pair. Thus, it may prove to be efficient to model the high-frequency GRAVSAT signal directly in terms of the parameters of tectonic-topographic features and their compensation. Author

A84-37069

CONSTRUCTION OF A SYSTEM OF POINT MASSES REPRESENTING THE GRAVITATIONAL FIELD OF THE PLANET ON THE BASIS OF SATELLITE OBSERVATIONS. I - AN ALGORITHM DERIVATION [POSTROENIE SISTEMY TOCHECHNYKH MASS, PREDSTAVLIAIUSHCHIKH GRAVITATSIONNOE POLE PLANETY, PO SPUTNIKOVYM NABLUDENIAMI. I - VYVOD ALGORITMA]

S. M. POLESHCHIKOV and K. V. KHOLESHEVNIKOV Leningradskii Universitet, Vestnik, Matematika, Mekhanika, Astronomiia (ISSN 0024-0850), April 1984, p. 76-86. In Russian.

An algorithm is presented for refining the point masses representing the gravitational field of the earth. The measured quantities used are the oblique distance and its rate of change; a calculation of the matrix elements of the conditional equations is reduced to solving variational equations. The uniqueness of a potential containing complex parameters is investigated. V.L.

A84-38812* Maryland Univ., College Park.

REDUCTION OF SATELLITE MAGNETIC ANOMALY DATA

E. V. SLUD, P. J. SMITH (Maryland, University, College Park, MD), and R. A. LANGEL *Journal of Geophysics - Zeitschrift fuer Geophysik* (ISSN 0340-062X), vol. 54, 1984, p. 207-212. refs (Contract NGL-21-002-033)

Analysis of global magnetic anomaly maps derived from satellite data is facilitated by inversion to the equivalent magnetization in a constant thickness magnetic crust or, equivalently, by reduction to the pole. Previous inversions have proven unstable near the geomagnetic equator. The instability results from magnetic moment distributions which are admissible in the inversion solution but which make only small contribution to the computed values of anomaly field. Their admissibility in the solution could result from noisy or incomplete data or from small poorly resolved anomalies. The resulting magnetic moments are unrealistically large and oscillatory. Application of the method of principal components (e.g. eigenvalue decomposition and selective elimination of less significant eigenvectors) is proposed as a way of overcoming the instability and the method is demonstrated by applying it to the region around the Bangui anomaly in Central Africa. Author

N84-23048# Mathematical Geosciences, Inc., Lexington, Mass. **GEODETIC USE OF GEOSAT-A Final Report, 16 Sep. 1982 - 30 Aug. 1983**

E. M. GAPOSCHKIN Aug. 1983 69 p
(Contract F19628-82-C-0144; AF PROJ. 3201)
(AD-A137993; AFGL-TR-83-0254) Avail: NTIS HC A04/MF A01 CSCL 08E

The Molodensky Integral can be used to compute gravity anomalies from the geoid height. There are two error sources. The error due to limiting the integral to a spherical cap can, in practice, be reduced by using a low degree and order reference field. For example, with a 6 degree radius cap and a 12th degree and order reference geopotential this error is one milligal. The error due to the geoid height error depends on the gravity anomaly block size and variance of the geoid height error. In this case, a 3 cm rms geoid error will result in a one milligal error for a 28 km x 28 km mean gravity anomaly. Quantization error of replacing the integral by a summation and the singularity of the Molodensky Kernel are found to contribute in significant errors. The correction for satellite to sea surface altitude measurements due to the wet troposphere (hw) is investigated using Scanning Multichannel Microwave Radiometer (SMMR) data from SEASAT-1. The Mesoscale Eddy field is discussed, and is shown to contribute 8 to 25 cm rms noise to the mean sea surface. GRA

N84-23935# Geological Survey, Washington, D.C.

ANTARCTIC MAPPING AND INTERNATIONAL COORDINATION Abstract Only

R. B. SOUTHDARD and W. J. KOSCO *In its US Geological Survey Polar Res. Symp.* p 1-2 1983

Avail: NTIS HC A04/MF A01; also available from SOD

In the early days of mapping in Antarctica the U.S. Navy VXE-6 squadron acquired trimetrogon aerial photographs over major map features. Ground control was established by surveyors from the U.S. Geological Survey. Trimetrogon photogrammetry was used to compile maps first in the Sentinel Mountains, Thurston Peninsula, Horlich Mountains, Executive Committee Range, and McMurdo Sound. Ninety 1:250,000-scale topographic maps have been compiled by USGS over the Transantarctic Mountains and Western Antarctica. Working through the SCAR nations involved in mapping, the Antarctic standard symbols and specifications have been developed for preparing these maps. An international agreement was reached in the early 60's on the basic horizontal and vertical datums to be used for mapping. Recently, agreement was reached to include the contribution to geodesy in this age of satellites, by changing the basic geodetic reference datum in Antarctica from the international Spheroid to the World Geodetic System. J.M.S.

N84-23954# Geological Survey, Washington, D.C.

PROGRAM FOR MAPPING ANTARCTICA Abstract Only

P. F. BERMEL and C. E. MORRISON *In its US Geological Survey Polar Res. Symp., Abstracts with Program* p 18-19 1983

Avail: NTIS HC A04/MF A01; also available from SOD

The Antarctic cartographic effort undertaken at the U.S. Geological Survey (USGS) as part of the U.S. Antarctic Research Program (USARP) is described. The USGS has focused its mapping on West Antarctica and the Transantarctic Mountains to support the requirements of USARP. It has sent field parties to Antarctica every year since 1957 to establish geodetic control and has worked closely with U.S. Navy Squadron VXE-6 to acquire mapping-quality aerial photographs. The program has been very productive, resulting in over 90 1:250,000-scale topographic reconnaissance maps of West Antarctica and the Transantarctic Mountains. Other products include 1:50,000-scale topographic maps, 1:500,000-scale sketch maps, 1:1,000,000-scale topographic maps and shaded-relief reconnaissance maps, as well as satellite image maps at several mapping scales. J.M.S.

03 GEODESY AND CARTOGRAPHY

N84-23957# Geological Survey, Washington, D.C.
MODELING THE MOVEMENT AT THE POLAR ICE CAP AT THE SOUTH POLE Abstract Only
T. HENDERSON *In its US Geological Survey Polar Res. Symp.*
p 21 1983
Avail: NTIS HC A04/MF A01; also available from SOD

Winter-over teams at the South Pole provided continual geodetic satellite tracking. The coordinates computed from satellite data represent a significant improvement in both accuracy and precision over astronomic positions. By analyzing the Doppler frequency shift curves received from passing satellites, ground points are resolved to within 1 m of their true coordinates. Coordinates are provided in a geocentric X-Y-Z reference system, so the data are immediately usable in rectangular plots. Compensation is made for the slight wobble in the Earth's polar axis when reducing to the geocentric system to eliminate this source of comparison difference. Again, linear least squares fits were made to the plots of X versus time and Y versus time. The resulting three models fit the data with a standard deviation of 0.9 m in both X and Y. They indicate a movement of 10 m per year. J.M.S.

N84-25143# Instituto de Pesquisas Espaciais, Sao Jose dos Campos (Brazil).

ORBITAL IMAGERY: A CARTOGRAPHIC SOLUTION [IMAGENS ORBITAIS: UMA SOLUCAO CARTOGRAFICA]
P. C. G. DEALBUQUERQUE Jul. 1983 42 p refs In PORTUGUESE; ENGLISH summary
(INPE-2820-PRE/374) Avail: NTIS HC A03/MF A01

The use of cartography in orbital remote sensing is a useful tool to creating solutions for its immediate problems, specially those related to countries which have poor knowledge of their territorial characteristics. Satellite sensing data of first natural resources furnished the elements of cartography charts and maps. The use of the orbital data, specially the MSS imagery is presented. It is shown how available orbital data are used by cartography to correlate areas, such as those of planning where general aspect must be understood as a primary necessity to obtain reliable results. E.A.K.

N84-26069 Bayerische Akademie der Wissenschaften, Munich (West Germany). Working Group III/1 of ISP

SEMINAR ON MATHEMATICAL MODELS OF GEODETIC/PHOTOGRAMMETRIC POINT DETERMINATION WITH REGARD TO OUTLIERS AND SYSTEMATIC ERRORS
F. E. ACKERMANN, ed. 1983 130 p refs Seminar held at Stuttgart, 26-27 Nov. 1981
(SER-A-98; ISBN-3-7696-81800; ISSN-0065-5369) Avail: Issuing Activity

The achievements of practical procedures for geodesy and photogrammetric point determination rely on the consistent application of the least squares method. With the increased automation of computations and raised levels of precision the modelling of outliers and of systematic errors present problems with regard to the assessment of such errors and the quality control of results. Recent developments in photogrammetric point determination by analytical phototriangulation are described.

N84-26070 Stuttgart Univ. (West Germany). Inst. for Photogrammetry.

MATHEMATICAL MODELS OF PHOTOGRAMMETRIC POINT DETERMINATION
F. E. ACKERMANN *In Deut. Geodact. Komm. Seminar on Math. Models of Geodetic Photogrammetric Point Determination with Regard to Outliers and Systematic Errors* p 7-22 1983 refs

Avail: Issuing Activity

The development of mathematical models for photogrammetric point determination has evolved in combination with its practical application, its computational methods, and its accuracy performance. The refinement of the models did not generally originate from an overall theoretical concept but evolved step by step from inconsistencies and deficiencies of the practical models used, particularly in connection with the continuously increasing

precision performance. The step by step development of mathematical models for photo triangulation is retraced in order to show how photogrammetry has reached the stage where now a general and comprehensive theory is required. This approach was chosen deliberately for introductory and background purposes. The available theoretical tools are deployed and the general concepts of mathematical modelling are displayed. It will then be possible, hopefully, to design tests in order to provide the parameters which are essential for a comprehensive model.

Author

N84-26072 Stuttgart Univ. (West Germany). Inst. of Geodetics.
STOCHASTIC MODELS FOR POINT MANIFOLDS

E. GRAFAREN *In Deut. Geodact. Komm. Seminar on Math. Models of Geodetic Photogrammetric Point Determination with Regard to Outliers and Systematic Errors* p 29-52 1983 refs

Avail: Issuing Activity

With respect to a methodological comparison of geodetic and photogrammetric methods stochastic models for point manifolds are reviewed. At first nonlinear observational equations of photogrammetry and terrestrial/satellite geodesy are discussed with respect to first order and higher order models. Model disturbances are represented by polynomial series. Stochastic point manifolds like the point distribution in a photograph are analyzed by means of the Taylor-Karman structure for a homogeneous and isotropic random process in two and three dimensions. First order Markov processes in two and three dimensional Euclidean space characterize the characteristic functions of the Taylor-Karman structure. In detail the linearization process of a set of nonlinear observational equations under a priori information is described.

Author

N84-26073 Bonn Univ. (West Germany). Inst. for Theoretical Geodetics.

ESTIMATION OF VARIANCES AND COVARIANCES IN THE MULTIVARIATE AND IN THE INCOMPLETE MULTIVARIATE MODEL

K. R. KOCH *In Deut. Geodact. Komm. Seminar on Math. Models of Geodetic Photogrammetric Point Determination with Regard to Outliers and Systematic Errors* p 53-59 1983 refs

Avail: Issuing Activity

Systematic errors are caused by introducing too few parameters in the model for the estimation of unknown parameters. If the missing parameters are random variables with the expectation zero, they are taken into account by the variances and covariances of the observations. Full covariance matrices are therefore generally needed in the model for the estimation of parameters. In the multivariate model the variance and the covariances of measurements repeated during different epochs are estimated, while the univariate formulation of the multivariate model with unknown variance and covariance components allows the estimation of the weight matrix of the observations of one epoch. The estimation of the variances and the covariances of the repeated measurements and of the weight matrix of the observations of one epoch is also discussed in the incomplete multivariate model which has to be used for the estimation of the parameters of a photogrammetric aerotriangulation.

Author

N84-26074 Technische Univ., Hanover (West Germany). Inst. of Geodetics.

DETECTION OF ERRORS IN THE FUNCTIONAL ADJUSTMENT MODEL

H. PELZER *In Deut. Geodact. Komm. Seminar on Math. Models of Geodetic Photogrammetric Point Determination with Regard to Outliers and Systematic Errors* p 61-70 1983 refs

Avail: Issuing Activity

Among the error sources of geodetic measuring techniques the most feared are those which have an equal or similar effect on different measured variables, e.g. zero errors of distance measuring equipment. If such errors remain undetected and are disregarded in both the functional and stochastic part of an adjustment model, (systematic measuring deviations or model

03 GEODESY AND CARTOGRAPHY

disturbances) their effects on the adjustment result are discussed.

Author

N84-26077 International Inst. for Aerial Survey and Earth Sciences, Enschede (Netherlands).

SEVERAL ASPECTS OF THE SEQUENTIAL PROCESSING OF PHOTOGRAHMETRIC BUNDLE BLOCKS

M. MOLENAAR *In* Deut. Geodact. Komm. Seminar on Math. Models of Geodetic Photogrammetric Point Determination with Regard to Outliers and Systematic Errors p 105-130 1983 refs

Avail: Issuing Activity

An adjustment procedure for photogrammetric bundle blocks is presented, based on the algorithm of Tienstra's standard problem I. The method is designed so that an adjustment in steps is possible, which implies that the adjustment runs parallel to (on-line with) the measuring process of bundle blocks. The computing process is split up into two stages: first, the formation of strips by means of sequential relative orientations and triplet formations, and second, the connection of strips to ground control and other data. Condition equations are formulated for the observations in both stages. Testing procedures are then formulated for the detection of gross errors in the input data in each stage and a strategy is given for choosing optimal critical values for the tests. Finally, the possibilities of handling systematic block deformations are discussed, which leads to a modification of either the functional model or the stochastic model for the observations. Author

N84-26079 Bayerische Akademie der Wissenschaften, Munich (West Germany).

CORRELATION CALCULATION IN STEREOSCOPIC IMAGE PAIRS FOR THE AUTOMATIC ACQUISITION OF DIGITAL LAND MODELS, ORTHOPICTURES AND HEIGHT LINE PLANES Ph.D. Thesis - Karlsruhe Univ. [KORRELATIONSRECHNUNG IN STEREOBILDPAAREN ZUR AUTOMATISCHEN GEWINNUNG VON DIGITALEN GELAENDEMODELLEN ORTHOPHOTOS UND HOEHENLINIENPLAENEN]

M. CLAUS 1983 97 p refs In GERMAN
(SER-C283; ISBN-3-7696-9334-5; ISSN-0065-5325) Avail:

Issuing Activity

Photogrammetric plotting which is based on the averaging of the difference of X-image coordinates of homologous points in both images of a stereo imagery is discussed. The orthophotograph is a geometric map, however, provides more information. The graphic design of a stereo image pair in analog or analytic is still very useful. The stresses of automatic locations of homologous points by analog or digital correlations of the density value of the points and their environment in both images is outlined. The automatic calculations to which the cartographic processing and data displays are matched are examined. Transl. by E.A.K.

N84-26080 Bayerische Akademie der Wissenschaften, Munich (West Germany).

FISHEYE OBJECTIVE IN THE DOSE RANGE PHOTOGRAHMETRY: THEORETICAL AND PRACTICAL INVESTIGATIONS Ph.D. Thesis - Technische Univ. [FISHEYE-OBJEKTIVE IN DER NAHBEREICHSPHOTOGRAHMETRIE: THEORETISCHE UND PRAKТИSCHE UNTERSUCHUNGEN]

H. J. HELLMEIER 1983 72 p refs In GERMAN
(SER-C-286; ISBN-3-7696-9336-1; ISSN-0065-5325) Avail:

Issuing Activity

The nontopographic application of photogrammetry with the use of fisheye objective display was investigated. The use of fisheye objectives is only practical when used with numerical methods. The individual spot determinations are examined. A linear plotting system with the use of an analytical plotter which extended the control program does not cause difficulties. Problems which are caused by the linear initiative of a stereo model because of nonperspectiveness of the imagery and large numerical differences are indicated. Transl. by E.A.K.

N84-26687# Defense Mapping Agency, Washington, D.C.

ERROR ANALYSIS FOR MARINE GEODETIC CONTROL USING THE GLOBAL POSITIONING SYSTEM Final Report

M. KUMAR, P. J. FELL, A. VANMELLE, and N. SAXENA 9 Mar. 1984 18 p

(AD-A140566) Avail: NTIS HC A02/MF A01 CSCL 08E

The Global Positioning System (GPS) provides a new capability for establishing marine control for moored ocean bottom transponders that support precise navigation of ships, instrument packages, and submersibles. Autonomous remotely deployed marine platforms ranging to GPS satellites, which can simultaneously be triggered to measure acoustical ranges to a transponder network, can be used to establish geodetic control for the transponder array. The technique takes advantage of a dynamically changing double pyramid which is formed between GPS satellites and the transponder array linked observationally by the remote platform. An error analysis is presented for an operational scenario where marine control is established in a deep ocean area. Several designs for this experiment are considered including the effect of constraint conditions. The results indicate that the establishment of precise ocean bottom control is obtainable using the GPS system with this approach. GRA

N84-26688# Defense Mapping Agency, Washington, D.C.

APPLICATIONS OF THE GPS (GLOBAL POSITIONING SYSTEM) GEODETIC RECEIVER SYSTEM Final Report

B. HERMANN, A. G. EVANS, R. W. HILL, S. MEYERHOFF, and M. SIMS 14 Mar. 1984 20 p

(AD-A140567) Avail: NTIS HC A02/MF A01 CSCL 08E

The Defense Mapping Agency, in cooperation with the United States Geological Survey and the National Oceanic and Atmospheric Administration, is sponsoring the development of a Global Positioning System geodetic receiver (GEOSTAR). The receiver is capable of observing up to four satellites simultaneously by sampling segments of broadcast signals from different satellites in a time-multiplexing sense using a single dual frequency channel. The receiver system was designed to measure the geodetic coordinates of points to an accuracy of one meter and to provide first-order estimates of baselines of up to several hundred kilometers in length. In addition, the receiver can support positioning and attitude determination of geophysical survey platforms under low dynamic conditions. Descriptions of these applications are presented. GRA

N84-28199# Institut fuer Angewandte Geodaeie, Frankfurt am Main (West Germany).

INVESTIGATION OF THE COMBINATION OF GEODETIC POINT AGGREGATIONS Ph.D. Thesis - Technischen Hochschule, Darmstadt, West Germany [UNTERSUCHUNGEN ZUR KOMBINATION VON GEODETISCHEN PUNKTHAUFEN]

H. JOCHEMCZYK 1983 215 p refs In GERMAN
(SER-C-285; ISSN-0071-9196) Avail: NTIS HC A10/MF A01

The combination of terrestrial aggregations, partially provided for by first order ordnance survey, by modern space methods is discussed. The conventional geodetic terrestrial methods are presented. The investigation of local and global reference systems and of differential relations, and simulation calculations show a slight deviation from the geometry space, except for the height component which is referred to the gravitational space. Satellite and space observation methods leading to the determination of a purely geometric coordinate system are discussed. Combination solutions to integrate both methods are presented, enabling a strict solution. The effects of systematic errors are clarified by simulation calculations. Author (ESA)

03 GEODESY AND CARTOGRAPHY

N84-28279* # California Univ., San Diego. Inst. of Geophysics and Planetary Physics.

HIGH PRECISION MEASUREMENTS IN CRUSTAL DYNAMIC STUDIES Final Report, Feb. 1980 - Sep. 1983

F. WYATT and J. BERGER 1984 88 p refs

(Contract NAG05-11)

(NASA-CR-173680; NAS 1.26:173680) Avail: NTIS HC A05/MF A01 CSCL 08G

The development of high-precision instrumentation for monitoring benchmark stability and evaluating coseismic strain and tilt signals is reviewed. Laser strainmeter and tilt observations are presented. Examples of coseismic deformation in several geographic locations are given. Evidence suggests that the Earth undergoes elastic response to abrupt faulting. R.S.F.

data combined with aerial photography and geochemical methods can be used to direct and lead to the discovery of new mineral deposits.

D.H.

A84-30260#

REMOTE SENSING FOR BAUXITE PROSPECTING

A. K. GUPTA and V. R. RAO (Indian Space Research Organization, Bangalore, India) IN: Asian Conference on Remote Sensing, 3rd, Dacca, Bangladesh, December 4-7, 1982, Proceedings . Tokyo, University of Tokyo, 1983, p. F-3-1 to F-3-9.

Multidate Landsat MSS data were used in an attempt to identify Indian bauxite deposits on the imagery. Widely separated and well-known deposits in India (in the regions of Orissa, Madhya Pradesh and Andhra Pradesh) covering a part of the east coast bauxite deposit were selected as the test areas. Through visual interpretation of 1:1,000,000 scale black and white imagery, topography suitable for the occurrence of bauxite was delineated and correlated with the known bauxite locations. All groups of rocks having bauxite plateaus were found to be thickly vegetated while those with little or no vegetation were devoid of bauxite. Direct one-to-one correspondence between topography, plateau size and occurrence of bauxite was not seen in the areas analyzed. Only about 9 percent correlation of topography with the actual bauxite locations was noted. The bauxite occurs on the outer edges of medium to large dome-shaped folds.

D.H.

04

GEOLOGY AND MINERAL RESOURCES

Includes mineral deposits, petroleum deposits, spectral properties of rocks, geological exploration, and lithology.

A84-30247#

AN ANALYSIS OF TECTONICS AND METALLOGENY OF ORISSA STATE, INDIA WITH REMOTE SENSING TECHNIQUE

R. C. MOHARANA and B. K. MOHANTY (Directorate of Mines, Orissa, India) IN: Asian Conference on Remote Sensing, 3rd, Dacca, Bangladesh, December 4-7, 1982, Proceedings . Tokyo, University of Tokyo, 1983, p. Q-9-1 to Q-9-9. refs

A84-30254#

TYPICAL ANALYSIS OF REGIONAL STABILITY AND BLOCK STRUCTURES WITH REMOTE SENSING IMAGES

Z. CHEN and H. LIN (Chinese Academy of Sciences, Institute of Remote Sensing Applications, Beijing, People's Republic of China) IN: Asian Conference on Remote Sensing, 3rd, Dacca, Bangladesh, December 4-7, 1982, Proceedings . Tokyo, University of Tokyo, 1983, p. C-7-1 to C-7-13. refs

Landsat images of the circular block structure in the granite region along the southeastern coast of China are analyzed in a study of regional stability. Regional stability is also analyzed for a rhombic fault block structure in western Sichuan and northern Yunnan. Generally speaking, in the granite region, areas with the bigger circular blocks and complex circular blocks grouped together are relatively stable and suitable for engineering construction. In the mountainous regions studied, areas where rhombus blocks are raised rather than depressed are favorable for engineering purposes because of their relative stability. Remote sensing images are considered useful in such stability studies to aid in engineering construction site selections. D.H.

A84-30259#

REMOTE SENSING AS A TOOL FOR MINERAL PROSPECTING

W. JANTARANIPA, N. RASHATASUVAN, and S. VUDHICHTIVANICH (Department of Mineral Resources, Bangkok, Thailand) IN: Asian Conference on Remote Sensing, 3rd, Dacca, Bangladesh, December 4-7, 1982, Proceedings . Tokyo, University of Tokyo, 1983, p. F-2-1 to F-2-8.

Available unenhanced Landsat data have been studied covering an area of Paleozoic folded belts in western Thailand. The intent was to search for indications of mineralization by delineating long lineaments and seeking the highest density of intersections. A target area based primarily on lineament intersections was selected as a case study. Aerial photographs of the outline area were used to solve the problem of the Landsat data's inferior resolution. A geomorphological anomaly was recognized near the intersection within the target area, and field verification revealed a lump of galens and some magnetite veins in limestone outcrops. High anomalies of copper, lead and zinc were indicated in the geochemical samples collected. The study has shown that Landsat

A84-30261#

AN UNDETECTABLE FACTOR IN GEOMORPHOLOGICAL MAPPING FROM LAND SATELLITE IMAGES - A CASE STUDY IN THE CENTRAL HIGHLAND, THAILAND

A. EIUMNOH (Kasetsart University, Bangkok, Thailand) IN: Asian Conference on Remote Sensing, 3rd, Dacca, Bangladesh, December 4-7, 1982, Proceedings . Tokyo, University of Tokyo, 1983, p. F-4-1 to F-4-14. Research supported by the National Research Council of Thailand. refs

A84-30262#

THE USE OF HOUGH TRANSFORMATION FOR DETECTING LINEAMENTS IN SATELLITE IMAGERY

T.-S. YANG, Z.-R. LI, and L. LI (Chinese Academy of Sciences, Space Science and Technology Center, Beijing, People's Republic of China) IN: Asian Conference on Remote Sensing, 3rd, Dacca, Bangladesh, December 4-7, 1982, Proceedings . Tokyo, University of Tokyo, 1983, p. F-5-1 to F-5-8.

The way in which the Hough transformation has been used for detecting lines and curves in pictures is traced. A modified Hough transformation is described here for detecting lineaments by using the hash technique to count the maximum number of transformed intersection points in a confined region of parameter space. Before the transformation is applied, the picture is processed by a local edge detector, and a certain number of possible lineament feature points are obtained.

C.R.

A84-30263#

THE LINEAMENT FEATURES OF TARIM BASIN (WEST PART) AND ITS BEARING ON THE CHARACTERISTICS OF CENOZOIC TECTONIC STRESS FIELDS

L. CHU (National Remote Sensing Centre of China; Beijing University, Beijing, People's Republic of China) IN: Asian Conference on Remote Sensing, 3rd, Dacca, Bangladesh, December 4-7, 1982, Proceedings . Tokyo, University of Tokyo, 1983, p. F-7-1 to F-7-9.

The tectonic lineament features of the western part of the Tarim Basin in western China are characterized on the basis of Landsat images, aerial photography, and visual airborne measurements. Maps are provided, and it is found that the Basin has been subject to compression since the Cenozoic, but that the direction of stress has shifted from NE 20 to near SN. T.K.

04 GEOLOGY AND MINERAL RESOURCES

A84-30878

METALLOGENESIS - USE OF REMOTE SENSING FOR ORE DEPOSIT PROSPECTION INDICATORS LINKED TO NONOUTCROPPING LEUCOGANITIC APEXES [METALLOGENIE - UTILISATION DE LA TELEDETECTION SPATIALE POUR LA PROSPECTION MINIERE D'INDICES LIES ADES APEX LEUCOGANITIQUES NON AFFLEURANTS]

B. MARCONNET (Centre National d'Etudes Spatiales and CNRS, Laboratoire de Petrologie Structurale et Metallogenie; Nancy I, Universite, Vandoeuvre-les-Nancy, Meurthe-et-Moselle, France) Academie des Sciences (Paris), Comptes Rendus, Serie II Mecanique, Physique, Chimie, Sciences de l'Univers, Sciences de la Terre (ISSN 0249-6305), vol. 298, no. 6, Feb. 14, 1984, p. 215-218. In French. refs

A84-32590#

GEOLOGICAL INTERPRETATION FROM AERIAL REMOTE SENSING IMAGES OF TENGCHONG AREA

X. DING (Chinese Academy of Sciences, Institute of Geochemistry, Guiyang, People's Republic of China) Geochimica (ISSN 0096-3089), no. 4, 1983, p. 395-401. In Chinese with abstract in English.

A comprehensive aerial remote sensing survey was carried out over the Tengchong area in western Yunnan by research workers from the Chinese Academy of Sciences during Nov. 1978-Apr. 1979. A geological interpretation was made of the aerial black-and-white and color imagery based on the tones, colors, and landforms (including geometry, surface features, arrangement correlations, etc.), indicating that the major lithologic units in the Tengchong area covered by vegetation could be distinguished. Using fault interpretation indicators in conjunction with geological investigations and laboratory research, mantle faults, basement faults, and crust-lithosphere faults were differentiated in the Tengchong area. Finally, a general picture of the geological history of this area is outlined with the help of the rock body-structure interpretation map.

Author

A84-33327

APPLICATIONS OF THE ENVIRO-POD WITH KA-85A PANORAMIC CAMERAS IN SOUTH-EASTERN HISTORIC AND PRE-HISTORIC ARCHAEOLOGICAL SURVEY

S. L. H. MADRY (North Carolina, University, Chapel Hill, NC) IN: American Society of Photogrammetry, Annual Meeting, 49th, Washington, DC, March 13-18, 1983, Technical Papers . Falls Church, VA, American Society of Photogrammetry, 1983, p. 26-32. refs

Aerial photography has been employed in the search for archeological sites since before the first world war. However, the employed method of survey was generally random in manner. Recently, a more systematic 'Cultural Resource Management' approach has been utilized in the U.S. However, the involved technique is for economic reasons unsuited for most archeological projects. A more cost-effective means for acquiring aerial photographs for archeological sites is provided by the Environmental Protection Agency's (EPA) Enviro-pod system. This system was designed for environmental monitoring using light aircraft. A self-contained reconnaissance sensor module called the Enviro-pod was developed in 1977. The pod weighs 145 pounds and contains two KA-85A panoramic cameras. A limited series of archeological studies was conducted to determine the pod's potential use in such studies.

G.R.

A84-33350

SURFACE EXPRESSION OF HEAVILY MANTLED INSTERSTRATAL KARST BORDERING OKEFENOKEE SWAMP, GEORGIA

J. R. WADSWORTH, JR. (South Florida, University, Tampa, FL), G. A. BROOK, and R. E. CARVER (Georgia, University, Athens, GA) IN: American Society of Photogrammetry, Annual Meeting, 49th, Washington, DC, March 13-18, 1983, Technical Papers . Falls Church, VA, American Society of Photogrammetry, 1983, p. 463-470. Research supported by the University of Georgia and University of South Florida. refs (Contract NSF DEB-81-10639)

A84-34779

TOPOGRAPHY INTERPRETATION POSSIBILITIES FOR SATELLITE PHOTOS IN REGIONS WHERE THE PLATFORM MANTLE HAS A MULTITIER STRUCTURE (ON THE EXAMPLE OF THE EASTERN MARGINAL PART OF THE CASPIAN DEPRESSION) [VOZMOZHNOSTI LANDSHAFTNOGO DESHIFRIROVANIIA KOSMICHESKIKH SNIMKOV V RAIONAKH MINOGO IARUSNOGO STROENIIA PLATFORMENNOGO CHEKHLA /NA PRIMERE VOSTOCHNOI PRIBORTOVOI CHASTI PRIKASPIISKOI VPADINY/]

O. S. OBRADCHIKOV (Vsesoiuznyi Nauchno-Issledovatel'skii Geologorazvedochnyi Neftianoi Institut, Moscow, USSR) and S. E. PETROV (Issledovanie Zemli iz Kosmosa (ISSN 0205-9614), Mar.-Apr. 1984, p. 35-43. In Russian. refs

A84-34781

THE USE OF SATELLITE PHOTOS FOR ANALYZING THE STRUCTURAL AND DYNAMIC CONDITIONS SURROUNDING THE FORMATION OF ANCIENT DEPOSITS OF PHLOGOPITE AND APATITE [ISPOL'ZOVANIE KOSMICHESKIKH SNIMKOV Dlya ANALIZA STRUKTURNO-DINAMICHESKIKH USLOVII OBRAZOVANIIA DREVNICH MESTOROZHDENII FLOGOPITA I APATITA]

KH. G. ZINATOV and R. F. VAFIN (Vsesoiuznyi Nauchno-Issledovatel'skii Institut Geologii Nerudnykh Poleznykh Iskopaemykh, Kazan, USSR) Issledovanie Zemli iz Kosmosa (ISSN 0205-9614), Mar.-Apr. 1984, p. 48-54. In Russian. refs

From a tectonophysical analysis of satellite photos, the mechanism by which systems of diagonal fractures were formed in the central part of the Aldan shield is established. Reasons are also suggested to explain why the pattern has been preserved and why Precambrian fractures survived into the Phanerozoic. Attention is given to the role played by stress fields in forming structures which in the Precambrian were able to accumulate phlogopite and apatite and in the Phanerozoic ensured that these deposits were preserved. The method is shown to be applicable in regional analyses for other minerals.

C.R.

A84-34782

THE USE OF REMOTE SENSING IN THE SEARCH FOR HYDROCARBONS IN THE KERCH PENINSULA [ISPOL'ZOVANIE MATERIALOV DISTANTSIONNYKH S'EMOK PRI POISKAKH UGLEVODORODOV V USLOVIIAKH KERCHENSKOGO POLUOSTROVA]

V. I. KHNYKIN and N. V. KOLODII (Ukrainskii Nauchno-Issledovatel'skii Geologorazvedochnyi Institut, Lvov, Ukrainian SSR) Issledovanie Zemli iz Kosmosa (ISSN 0205-9614), Mar.-Apr. 1984, p. 55-59. In Russian.

04 GEOLOGY AND MINERAL RESOURCES

A84-34789

DISTINGUISHING LINEAR CONTOUR ELEMENTS ON SATELLITE PHOTOS ON THE BASIS OF A VISUAL PERCEPTION MODEL [VYDELENIE LINEINO-KONTURNYKH ELEMENTOV KOSMICHESKIH SNIMKOV NA OSNOVE MODELI VIZUAL'NOGO VOSPRIIATIIA]

M. V. SMIRNOV and L. N. ROZANOV (Vsesoiuznyi Neftianoi Nauchno-Issledovatel'skii Geologorazvedochnyi Institut, Leningrad, USSR) Issledovanie Zemli iz Kosmosa (ISSN 0205-9614), Mar.-Apr. 1984, p. 117-124. In Russian. refs

A transition from a qualitative model to a statistical one is shown to be possible in determining the parameters of a heuristically developed algorithm on the basis of the statistical characteristics of transformed satellite photos. The results obtained from processing for oil and gas bearing regions are presented. It is shown that the use of a probability distribution that allows for the objective property of actual images makes it possible in a statistical evaluation to adapt the processing. C.R.

A84-36922* Cornell Univ., Ithaca, N.Y.

COSEISMIC AND POSTSEISMIC VERTICAL MOVEMENTS ASSOCIATED WITH THE 1940 M7.1 IMPERIAL VALLEY, CALIFORNIA, EARTHQUAKE

R. REILINGER (Cornell University, Ithaca, NY) Journal of Geophysical Research (ISSN 0148-0227), vol. 89, June 10, 1984, p. 4531-4537. Sponsorship: U.S. Geological Survey. refs (Contract USGS-14-08-0001-20585; NAS5-27232)

Leveling surveys conducted along two routes that cross the Imperial fault in southern California indicate spatially coherent elevation changes attributable to coseismic and postseismic effects of the 1940, M7.1 Imperial Valley earthquake. The 1931-1941 elevation changes are consistent with theoretical models of vertical deformation of an elastic half space for a finite length strike-slip fault, using fault parameters that are consistent with the observed surface offsets following the 1940 earthquake. The elevation changes suggest an earthquake scenario consisting of a large coeismic slip in the southern half of the fault which transferred stress to the northern part as well as to the Brawley fault to the northeast. O.C.

A84-37775

APPLICATION OF LANDSAT DATA IN THE EXPLORATION OF 'CALCRETE' URANIUM DEPOSITS [EINSATZ VON LANDSAT-DATEN IN DER EXPLORATION AUF URANLAGERSTAETTEN VOM TYP 'CALCRETE']

F. QUIEL and E. U. KRISCHE (Karlsruhe, Universitaet, Karlsruhe, West Germany) Bildmessung und Luftbildwesen (ISSN 0006-2421), vol. 52, May 1984, p. 125-132. In German. refs

The successful evaluation of complete Landsat scenes using image interpretation and digital classification to identify Calcretes on a regional scale for more detailed semiregional investigations (i.e., hydrogeochemistry and shallow boreholes) is demonstrated with examples from western and central Australia. The application of the different regions of the electromagnetic spectrum in the exploration for uranium is shown. C.D.

A84-38940

RADAR GEOLOGY OF THE SHELLENG-NUMAN AREA IN NIGERIA - AN EVALUATION

S. A. ISIORHO (Michigan, University, Ann Arbor, MI) International Journal of Remote Sensing (ISSN 0143-1161), vol. 5, May-June 1984, p. 519-531. Research supported by the University of Port Harcourt. refs

A84-39379* Jet Propulsion Lab., California Inst. of Tech., Pasadena.

SPACEBORNE RADAR SUBSURFACE IMAGING IN HYPERARID REGIONS

C. ELACHI, L. E. ROTH (California Institute of Technology, Jet Propulsion Laboratory, Pasadena, CA), and G. G. SCHABER (U.S. Geological Survey, Flagstaff, AZ) IEEE Transactions on Geoscience and Remote Sensing (ISSN 0196-2892), vol. GE-22, July 1984, p. 383-388. refs (Contract NAS7-100)

Imaging data acquired with the Shuttle Imaging Radar (SIR-A) over the hyperarid region of Egypt/Sudan clearly show surface penetration through the sand cover. Even though absorption does occur in the sand layer, surface refraction leads to a steeper incidence angle at the sand/bedrock interface resulting in a stronger backscatter. A simple backscatter model shows that for a low-loss thin sand layer the presence of the covering layer enhances the capability to image the subsurface interface, particularly at large incidence angles and HH polarization.

Author

N84-23005*# Iowa Univ., Iowa City. Dept. of Geology.

USE OF MAGSAT ANOMALY DATA FOR CRUSTAL STRUCTURE AND MINERAL RESOURCES IN THE US MIDCONTINENT Final Project Report, Dec. 1980 - Sep. 1983

R. S. CARMICHAEL Oct. 1983 177 p Original contains color illustrations ERTS (Contract NAS5-26425)

(E84-10112; NASA-CR-173482; NAS 1.26:173482) Avail: NTIS HC A09/MF A01 CSCL 08G

Magnetic field data acquired by NASA's MAGSAT satellite is used to construct a long-wavelength magnetic anomaly map for the U.S. midcontinent. This aids in interpretation of gross crustal geology (structure, lithologic composition, resource potential) of the region. Magnetic properties of minerals and rocks are investigated and assessed, to help in evaluation and modelling of crustal magnetization sources and depth to the Curie-temperature isotherm.

Author

N84-23008*# Purdue Univ., Lafayette, Ind. Dept. of Geosciences.

APPLICATION OF MAGSAT LITHOSPHERIC MODELING IN SOUTH AMERICA. PART 1: PROCESSING AND INTERPRETATION OF MAGNETIC AND GRAVITY ANOMALY DATA Final Report

W. J. HINZE, L. W. BRAILE, R. R. B. VONFRESE, Principal Investigators, G. R. KELLER, and E. G. LIDIAK Jan. 1984 58 p refs Prepared in cooperation with Texas Univ., El Paso and Pittsburgh Univ. ERTS (Contract NAS5-26287)

(E84-10115; NASA-CR-173485; NAS 1.26:173485) Avail: NTIS HC A04/MF A01 CSCL 08G

Scalar magnetic anomaly data from MAGSAT, reduced to vertical polarization and long wavelength pass filtered free air gravity anomaly data of South America and the Caribbean are compared to major crustal features. The continental shields generally are more magnetic than adjacent basins, oceans and orogenic belts. In contrast, the major aulacogens are characterized by negative anomalies. Spherical earth magnetic modeling of the Amazon River and Takatu aulacogens in northeastern South America indicates a less magnetic crust associated with the aulacogens. Spherical earth modeling of both positive gravity and negative magnetic anomalies observed over the Mississippi Embayment indicate the presence of a nonmagnetic zone of high density material within the lower crust associated with the aulacogen. The MAGSAT scalar magnetic anomaly data and available free air gravity anomalies over Euro-Africa indicate several similar relationships.

M.A.C.

04 GEOLOGY AND MINERAL RESOURCES

N84-23062 State Univ. of New York, Albany.

CENOZOIC TECTONICS OF THE CARIBBEAN: STRUCTURAL AND STRATIGRAPHIC STUDIES IN JAMAICA AND HISPANIOLA

Ph.D. Thesis

W. P. MANN 1983 777 p

Avail: Univ. Microfilms Order No. DA8401427

Structural and stratigraphic field studies in Jamaica and Hispaniola (Dominican Republic and Haiti) and synthesis of published data from surrounding areas refine previously proposed models for convergent and strike-slip plate interactions in the northern Caribbean. Specifically: (1) new data and regional stratigraphic analysis of major unconformities in the Greater Antilles supports the idea of two distinct arcs that terminated by collision at slightly different times in the latest Cretaceous and Paleogene; (2) field studies in the Port Maria area of northeastern Jamaica essentially complete mapping of the Wagwater Belt, a reactivated Paleogene graben and overlying sedimentary basin; and (3) the interpretation of satellite imagery and aerial photographs and field studies in the Enriquillo Valley and Sierra el Numero, Dominican Republic; the Culde-Sac Valley and southern peninsula of Haiti; and the Clydesdale area of eastern Jamaica. Dissert. Abstr.

N84-23527*# Geological Survey, Flagstaff, Ariz.

RADAR BACKSCATTER MODELLING Progress Report.

G. G. SCHABER, R. C. KOZAK, and R. L. GURULE *In NASA. Washington Rept. of Planetary Geology Program, 1983 p 268-269*

Apr. 1984 refs

Avail: NTIS HC A15/MF A01 CSCL 171

The terrain analysis software package was restructured and documentation was added. A program was written to test Johnson Space Center's four band scatterometer data for spurious signals data. A catalog of terrain roughness statistics and calibrated four frequency multipolarization scatterometer data is being published to support the maintenance of Death Valley as a radar backscatter calibration test site for all future airborne and spacecraft missions. Test pits were dug through sand covered terrains in the Eastern Sahara to define the depth and character of subsurface interfaces responsible for either backscatter or specular response in SIR-A imagery. Blocky sandstone bedrock surfaces at about 1 m depth were responsible for the brightest SIR-A returns. Irregular very dense CaCO₃ cemented sand interfaces were responsible for intermediate grey tones. Ancient river valleys had the weakest response. Reexamination of SEASAT L-band imagery of U.S. deserts continues. A.R.H.

N84-23526*# Arizona State Univ., Tempe. Dept. of Geology.

PINACATE-GRAN DESIERTO REGION, MEXICO: SIR-A DATA ANALYSIS

P. CHRISTENSEN, R. GREELEY, J. MCHONE, Y. ASMEROM, and S. BARNETT *In NASA. Washington Rept. of Planetary Geology Program, 1983 p 270* Apr. 1984

Avail: NTIS HC A15/MF A01 CSCL 08B

Radar images (SIR-A) from the Columbia space shuttle were used to assess the radar returns of terrain shaped by volcanic, aeolian, and fluvial processes in northwest Sonora. Field studies and photointerpretation show that sand dunes are poorly imaged by SIR-A, in contrast to SEASAT, evidently a consequence of the greater SIR-A incidence angle; star dunes are visible only as small bright spots representing merging arms at dune apices which may act as corner reflectors. Desert grasses and bushes (approx. 2 m high) have little effect on radar brightness. Only larger trees with woody trunks approx. 0.5 m across are effective radar reflectors; their presence contributes to radar bright zones along some arroyos. The radar brightness of lava flows decreases with surface roughness and presence of mantling windblown sediments and weathering products; however, old uplifted (faulted) flows are of equal brightness to fresh, unmantled aa flows. Maar craters display circular patterns of varying radar brightness which represent a combination of geometry, slope, and distribution of surface materials. Some radar bright rings in the Pinacates resemble craters on radar but are observed to be playas encircled by trees.

A.R.H.

N84-23527*# Arizona State Univ., Tempe. Dept. of Geology. RADAR-VISIBLE WIND STREAKS IN THE ALTIPLANO OF BOLIVIA

R. GREELEY and P. CHRISTENSEN *In NASA. Washington Rept. of Planetary Geology Program, 1983 p 271-272* Apr. 1984 refs

Avail: NTIS HC A15/MF A01 CSCL 08B

Isolated knobs that are erosional remnants of central volcanoes or of folded rocks occur in several areas of the Altiplano are visible on both optical and images. The optically visible streaks occur in the immediate lee of the knobs, whereas the radar visible streaks occur in the zone downwind between the knobs. Aerial reconnaissance and field studies showed that the optically visible streaks consist of a series of small (100 m wide) barchan and barchanoid dunes, intradune sand sheets, and sand hummocks (large shrub coppice dunes) up to 15 m across and 5 m high. On LANDSAT images these features are poorly resolved but combine to form a bright streak. On the radar image, this area also appears brighter than the zone of the radar dark streak; evidently, the dunes and hummocks serve as radar reflectors. The radar dark streak consists of a relatively flat, smooth sand sheet which lacks organized aerolian bedforms, other than occasional ripples. Wind velocity profiles show a greater U value in the optically bright streak zone than in the radar dark streak. A.R.H.

N84-23934# Geological Survey, Washington, D.C.

US GEOLOGICAL SURVEY POLAR RESEARCH SYMPOSIUM. ABSTRACTS WITH PROGRAM

1983 62 p refs Symp. held 12-14 Oct. 1983

(USGS-CIRC-911) Avail: NTIS HC A04/MF A01; also available from SOD

Mapping, tectonic evaluation, and mineral resource exploration in the Antarctic and Arctic regions are discussed. Specific attention is given to the use of satellite data in these areas.

N84-23942# Geological Survey, Washington, D.C.

SURVEYING IN ANTARCTICA DURING THE INTERNATIONAL GEOPHYSICAL YEAR Abstract Only

W. H. CHAPMAN *In its US Geological Survey Polar Res. Symp. p 6-7 1983*

Avail: NTIS HC A04/MF A01; also available from SOD

The Antarctic International Geophysical Year (IGY) scientists discovered that the existing maps contained many errors, particularly where the original exploration was by aircraft. An expedition of two DC-3 aircraft was taken to the Ellsworth Station on the Weddell Sea. A test network of 10 control points was established 200 miles south of the Ellsworth Station on the Filchner Ice Shelf in the vicinity of the Pensacola Mountains. The positions of these points were determined by solar altitude measurements made every hour for 24 hours. U.S. Geological Survey topographic engineers were to survey any mountain ranges by establishing positions by solar altitude measurement and elevations by barometric altimetry. Aerial photographs over major mountain ranges using P-2V aircraft equipped with trimetrogon cameras was combined with the control established by the surveyors at the U.S. Geological Survey, to produce 1:250,000-scale topographic maps. The first maps produced covered the Thurston Peninsula, Sentinel Mountains, Horlick Mountains, Executive Committee Range, and McMurdo Sound. J.M.S.

N84-23943# Geological Survey, Washington, D.C.

THE DUFEEK INTRUSION OF ANTARCTICA AND A SURVEY OF ITS MINOR METALS RELATED TO POSSIBLE RESOURCES

A. B. FORD *In its US Geological Survey Polar Res. Symp. p 7-10 1983*

Avail: NTIS HC A04/MF A01; also available from SOD

The Dufek intrusion is large differentiated layered mafic igneous complex of Jurassic age in the northern Pensacola Mountains mostly covered by ice. Geologic studies determined that nearly 2 km of a lower (not lowest) part of the body is exposed in the Dufek Massif and about 1.7 km of the Fe-enriched highest part is exposed in the Forrestal Range. The rocks are generally

04 GEOLOGY AND MINERAL RESOURCES

well-layered cumulates of predominantly gabbroic composition which contain cumulus plagioclase and two pyroxenes. A reconnaissance geochemical survey shows marked enrichment in Cu, V, Ti, Pt, Pd, and S in the upper (Forrestal Range) section and corresponding depletion in Cr and Ni. Petrologic comparisons with other complexes suggest that the major pyroxenitic members of the Dufek Massif section lie at a position analogous to a level about 2 km above the chief platinum-group-metal horizons of the pyroxenitic Merensky Reef of the Bushveld Complex. Platinum-group metals would be of chief resource interest, but the absence of placers and soils will make exploration difficult. Correlation studies suggest that V may be a useful pathfinder element in a geochemical exploration for the metals within exposed units; however, drilling would be needed to explore basal layers, where metals are most likely to occur. J.M.S.

N84-23955# Geological Survey, Washington, D.C.
THE USE OF SATELLITE TECHNOLOGY IN THE SEARCH FOR METEORITES IN ANTARCTICA Abstract Only
Tony K. Meunier *In its* US Geological Survey Polar Res. Symp. p 19-20 1983 Avail: NTIS HC A04/MF A01; also available from SOD
Avail: NTIS HC A04/MF A01; also available from SOD

Delineation of surficial blue-ice patches in Antarctica is possible with K LANDSAT spacecraft and the NOAA series of weather satellites. LANDSAT 1, 2, and 3 MSS have a pixel (picture element) size of about 80 m. The images are usually acquired in four spectral bands: MSS band 4, 0.5 to 0.6 cm; MSS band 5, 0.6 to 0.7 cm; MSS band 6, 0.7 to 0.8 cm; and MSS band 7, 0.8 to 1.1 cm. In the identification of blue ice areas, MSS bands 6 and 7 are similar, with band 7 somewhat better than MSS band 6. MSS band 5, however, is best in areas of bedrock exposure, because blue ice and rock outcrops usually have a similar spectral response. All the five blue-ice areas, selected from satellite images and aerial photographs for field investigation, were found to contain concentrations of meteorites. This was totally unexpected and highly significant. The use of satellite technology proved to be effective, and its continued use will be an important tool in the systematic search for and recovery of meteorites in Antarctica. J.M.S.

N84-23962# Geological Survey, Washington, D.C.
EMERGING RECOGNITION OF THE NONFUEL MINERAL RESOURCES OF ARCTIC ALASKA Abstract Only
D. GRYBECK *In its* US Geological Survey Polar Res. Symp. p 31-32 1983
Avail: NTIS HC A04/MF A01; also available from SOD

Some of the most exciting new mineral discoveries in Alaska during the past two decades were in the Brooks Range, yet conventional wisdom 25 years ago was that northern Alaska was rather unpromising, if not geologically unfavorable for mineral deposits. Nonetheless, what has emerged in the Brooks Range is a mineral frontier, largely as a result of detailed geologic mapping, systematic mineral exploration, better accessibility, and new ore-deposit models. Author

N84-23979*# Instituto de Pesquisas Espaciais, Sao Jose dos Campos (Brazil).
UTILIZATION OF DIGITAL LANDSAT IMAGERY FOR THE STUDY OF GRANITOID BODIES IN RONDONIA: CASE EXAMPLE OF THE PEDRA BRANCA MASSIF [UTILIZACAO DE IMAGENS DIGITAIS LANDSAT NO ESTUDO DE CORPOS GRANITOIDES EM RONDONIA: CASO-EXEMPLO DO MACICO PEDRA-BRANCA]
N. D. J. PARADA, Principal Investigator, R. ALMEIDAFILHO, B. L. PAYOLLA, O. G. DEPINHO, and J. S. BETTENCOURT Jan. 1984 11 p refs In PORTUGUESE; ENGLISH summary Presented at the 2nd Simp. Amazonica, Manaus, Brazil, 8-15 Apr. 1984 Sponsored by NASA ERTS (E84-10120; NASA-CR-172795; NAS 1.26:172795; INPE-2995-PRE/447) Avail: NTIS HC A02/MF A01 CSCL 05B

Analysis of digital multispectral MSS-LANDSAT images enhanced through computer techniques and enlarged to a video

scale of 1:100,000, show the main geological and structural features of the Pedra Branca granitic massif in Rondonia. These are not observed in aerial photographs or aerial images. Field work shows that LANDSAT photogeological units correspond to different facies of granitic rocks in the Pedra Branca massif. Even under the particular characteristics of Amazonia (Tropical Forest, deep weathering, and Quaternary sedimentary covers), an adequate utilization of orbital remote sensing images can be important tools for the orientation of field works. M.A.C.

N84-24031*# National Aeronautics and Space Administration, Washington, D. C.

DISCUSSION OF THE DESIGN OF SATELLITE-LASER MEASUREMENT STATIONS IN THE EASTERN MEDITERRANEAN UNDER THE GEOLOGICAL ASPECT. CONTRIBUTION TO THE EARTHQUAKE PREDICTION RESEARCH BY THE WEGENER GROUP AND TO NASA'S CRUSTAL DYNAMICS PROJECT

A. PALUSKA and N. PAVONI Nov. 1983 18 p Transl. into ENGLISH of "Erläuterung zum Entwurf der Satelliten-Laser-Messstationen (SLR) im Oestlichen Mittelmeerraum aus Geologischer Sicht; Beitrag zur Erdbebenvorhersageforschung der Wegener Gruppe und zum Crustal Dynamics Project der NASA" rept. (West Germany), Aug. 1983 p 1-17 Transl. by Kanner (Leo) Associates, Redwood City, Calif. (Contract NASW-3541)

(NASA-TM-77412; NAS 1.15:77412) Avail: NTIS HC A02/MF A01 CSCL 08G

Research conducted for determining the location of stations for measuring crustal dynamics and predicting earthquakes is discussed. Procedural aspects, the extraregional kinematic tendencies, and regional tectonic deformation mechanisms are described. Author

N84-24691*# Business and Technological Systems, Inc., Seabrook, Md.

POTENTIAL UTILITY OF FUTURE SATELLITE MAGNETIC FIELD DATA Final Report

Feb. 1984 32 p (Contract NAS5-27597)
(NASA-CR-175230; NAS 1.26:175230; BTS07-84-05/RB) Avail: NTIS HC A03/MF A01 CSCL 05B

The requirements for a program of geomagnetic field studies are examined which will satisfy a wide range of user needs in the interim period between now and the time at which data from the Geopotential Research Mission (GRM) becomes available, and the long term needs for NASA's program in this area are considered. An overview of the subject, a justification for the recommended activities in the near term and long term, and a summary of the recommendations reached by the contributors is included. M.A.C.

N84-25128*# Texas Univ., El Paso. Dept. of Geological Sciences.

APPLICATION OF MAGSAT TO LITHOSPHERIC MODELING IN SOUTH AMERICA. PART 2: SYNTHESIS OF GEOLOGIC AND SEISMIC DATA FOR DEVELOPMENT OF INTEGRATED CRUSTAL MODELS Final Report

G. R. KELLER, E. G. LIDIAK, W. J. HINZE, L. W. BRAILE, and R. R. B. VONFRESE, Principal Investigators Jan. 1984 485 p refs Prepared in cooperation with Purdue Univ., Lafayette, Ind. and Pittsburgh Univ. ERTS (Contract NAS5-26326)
(E84-10126; NASA-CR-172801; NAS 1.26:172801) Avail: NTIS HC A21/MF A01 CSCL 08B

Research activities performed on MAGSAT scalar data over South America, Central America, and the adjacent marine areas are summarized. The geologic utility of magnetic anomalies detected by satellite is demonstrated by focusing on the spherical-Earth interpretation of scalar MAGSAT data in combination with ancillary geological and geophysical data to obtain lithospheric models for these regions related to their contemporary

04 GEOLOGY AND MINERAL RESOURCES

crustal dynamics processes, geologic history, current volcanism seismicity and natural resources.

N84-25129*# Purdue Univ., Lafayette, Ind.

EURO-AFRICAN MAGSAT ANOMALY-TECTONIC OBSERVATIONS Abstract Only

W. J. HINZE, R. R. B. VONFRESE, Principal Investigators (Ohio State Univ., Columbus), and R. OLIVIER (Lausanne Univ.) *In* Texas Univ. Appl. of MAGSAT to Lithospheric Modeling in South America, Part 2 p 25-26 Jan. 1984 ERTS

Avail: NTIS HC A21/MF A01 CSCL 08G

Preliminary satellite (MAGSAT) scalar magnetic anomaly data are compiled and differentially reduced to radial polarization by equivalent point source inversion for comparison with tectonic data of Africa, Europe and adjacent marine areas. A number of associations are evident to constrain analyses of the tectonic features and history of the region. The Precambrian shields of Africa and Europe exhibit varied magnetic signatures. All shields are not magnetic highs and, in fact, the Baltic shield is a marked minimum. The reduced-to-the-pole magnetic map shows a marked tendency for northeasterly striking anomalies in the eastern Atlantic and adjacent Africa, which is coincident to the track of several hot spots for the past 100 million years. However, there is little consistency in the sign of the magnetic anomalies and the track of the hot spots. Comparison of the radially polarized anomalies of Africa and Europe with other reduced-to-the-pole magnetic satellite anomaly maps of the Western Hemisphere support the reconstruction of the continents prior to the origin of the present-day Atlantic Ocean in the Mesozoic Era. A.R.H.

N84-25130*# Pittsburgh Univ., Pa.

CORRELATION OF TECTONIC PROVINCES OF SOUTH AMERICA AND THE CARIBBEAN REGION WITH MAGSAT ANOMALIES Abstract Only

E. G. LIDIAK, W. J. HINZE (Purdue Univ., Lafayette, Ind.), G. R. KELLER, Principal Investigators (Texas Univ., El Paso), D. W. YUAN, and M. B. LONGACRE (Purdue Univ., Lafayette, Ind.) *In* Texas Univ. Appl. of MAGSAT to Lithospheric Modeling in South America, Part 2 p 27-28 Jan. 1984 Presented at the 10th Caribbean Geol. Conf., Cartagena, Colombia, Aug. 1983 ERTS

Avail: NTIS HC A21/MF A01 CSCL 08G

Intensities of MAGSAT scalar magnetic anomaly data correlate with the main tectonic provinces of South America and the Caribbean region. Magnetic anomalies of the continents generally have higher amplitudes than oceanic anomalies. This is particularly evident in Central America and in the shield areas of South America. The Caribbean Sea and Gulf of Mexico are underlain by prominent magnetic minima. Within these oceanic areas, linear magnetic highs correlate with topographic ridges which separate the Gulf of Mexico, the Colombian Basin, and the Venezuelan Basin. The boundaries of the Caribbean plate occur along magnetic gradients which are particularly sharp along the northern and western margins of the plate, but gradational along the southern margin where they merge with the Andean Cordillera. The anomalies along the western margin of the South American plate are also distinct and appear to be separate from those of the adjacent ocean basin. Eastern South America is characterized by magnetic anomalies which commonly extend into the Atlantic Ocean. A.R.H.

N84-25131*# SOHIO Petroleum Co., Cleveland, Ohio.

SATELLITE ELEVATION MAGNETIC AND GRAVITY MODELS OF MAJOR SOUTH AMERICAN PLATE TECTONIC FEATURES Abstract Only

R. R. B. VONFRESE, W. J. HINZE (Purdue Univ., Lafayette, Ind.), L. W. BRAILE (Purdue Univ., Lafayette, Ind.), E. G. LIDIAK (Pittsburgh Univ.), G. R. KELLER, Principal Investigators (Texas Univ., El Paso), and M. B. LONGACRE (Sohio Petroleum Co.) *In* Texas Univ. Appl. of MAGSAT to Lithospheric Modeling in South America, Part 2 p 33 Jan. 1984 Presented at the 4th IAGA Sci. Assembly, Edinburgh, 3-15 Aug. 1981 ERTS

Avail: NTIS HC A21/MF A01 CSCL 08G

Some MAGSAT scalar and vector magnetic anomaly data together with regional gravity anomaly data are being used to

investigate the regional tectonic features of the South American Plate. An initial step in this analysis is three dimensional modeling of magnetic and gravity anomalies of major structures such as the Andean subduction zone and the Amazon River Aulacogen at satellite elevations over an appropriate range of physical properties using Gaus-Legendre quadrature integration method. In addition, one degree average free-air gravity anomalies of South America and adjacent marine areas are projected to satellite elevations assuming a spherical Earth and available MAGSAT data are processed to obtain compatible data sets for correlation. Correlation of these data sets is enhanced by reduction of the MAGSAT data to radial polarization because of the profound effect of the variation of the magnetic inclination over South America. A.R.H.

N84-25132*# Purdue Univ., Lafayette, Ind.

REDUCED TO POLE LONG-WAVELENGTH MAGNETIC ANOMALIES OF AFRICA AND EUROPE Abstract Only

W. J. HINZE, R. R. B. VONFRESE, Principal Investigators (Ohio State Univ., Columbus), and R. OLIVIER (Lausanne Univ.) *In* Texas Univ. Appl. of MAGSAT to Lithospheric Modeling in South America, Part 2 p 34 Jan. 1984 Presented at the Am. Geophys. Union Ann. Meeting, Baltimore, 1983 ERTS

Avail: NTIS HC A21/MF A01 CSCL 08G

To facilitate analysis of the tectonic framework for Africa, Europe and adjacent marine areas, MAGSAT scalar anomaly data are differentially reduced to the pole and compared to regional geologic information and geophysical data including surface free-air gravity anomaly data upward continued to satellite elevation (350 km) on a spherical Earth. Comparative analysis shows magnetic anomalies correspond with both ancient as well as more recent Cenozoic structural features. Anomalies associated with ancient structures are primarily caused by intra-crustal lithologic variations such as the crustal disturbance associated with the Bangui anomaly in west-central Africa. Anomalies correlative with Cenozoic tectonic elements appear to be related to Curie isotherm perturbations. A possible example of the latter is the well-defined trend of magnetic minima that characterize the Alpine orogenic belt from the Atlas mountains to Eurasia. In contrast, a well-defined magnetic satellite minimum extends across the stable craton from Finland to the Ural mountains. Prominent magnetic maxima characterize the Arabian plate, Iceland, the Kursk region of the central Russian uplift, and generally the Precambrian shields of Africa. Author

N84-25133*# Purdue Univ., Lafayette, Ind.

SATELLITE MAGNETIC ANOMALIES OF AFRICA AND EUROPE

Final Report

W. J. HINZE, R. R. B. VONFRESE, Principal Investigators (Ohio State Univ., Columbus), and R. OLIVIER (Lausanne Univ.) *In* Texas Univ. Appl. of MAGSAT to Lithospheric Modeling in South America, Part 2 p 35-44 Jan. 1984 refs Presented at the 52nd Ann. Intern. Meeting and Exposition of the Soc. of Exploration Geophysicists, Dallas, 1982 ERTS

Avail: NTIS HC A21/MF A01 CSCL 08N

Preliminary MAGSAT scalar magnetic anomaly data of Africa, Europe, and adjacent marine areas were reduced to the pole assuming a constant inducing Earth's magnetic field of 60,000 nT. This process leads to a consistent anomaly data set free from marked variations in directional and intensity effects of the Earth's magnetic field over this extensive region. The resulting data are correlated with long wave length-pass filtered free-air gravity anomalies; regional heat flow, and tectonic data to investigate megatectonic elements and the region's geologic history. Magnetic anomalies are related to both ancient as well as more recent Cenozoic structural features. A.R.H.

04 GEOLOGY AND MINERAL RESOURCES

N84-25134*# Ohio State Univ., Columbus.

DO SATELLITE MAGNETIC ANOMALY DATA ACCURATELY PORTRAY THE CRUSTAL COMPONENT? Abstract Only

R. R. B. VONFRESE and W. J. HINZE, Principal Investigators (Purdue Univ., Lafayette, Ind.) *In* Texas Univ. Appl. of MAGSAT to Lithospheric Modeling in South America, Part 2 p 45 Jan. 1984 Presented at the Geomagnetic Conf., Denver, 1982 ERTS

Avail: NTIS HC A21/MF A01 CSCL 08G

Scalar aeromagnetic data obtained during the U.S. Naval Oceanographic Office (NOO)-Vector Magnetic Survey of the conterminous United States were upward continued by equivalent point source inversion and compared with POGO satellite magnetic anomaly and preliminary scalar MAGSAT data. Initial comparisons indicate that the upward continued NOO data is dominated by long wavelength (approximately equal to 1000 to 3000 km) anomalies which are not present in the satellite anomaly data. Thus, the comparison of the data sets is poor. Several possible sources for these differences are present in the data analysis chain. However, upon removal of these long wavelengths from the upward continued NOO data, a close comparison observed between the anomalies verifies that satellite magnetic anomaly data do portray the crustal component within a range of wavelengths from roughly 1000 km down to the resolution limit of the observations.

Author

N84-25135*# Ohio State Univ., Columbus.

LONG-WAVELENGTH MAGNETIC AND GRAVITY ANOMALY CORRELATIONS OF AFRICA AND EUROPE Abstract Only

R. R. B. VONFRESE, W. J. HINZE, Principal Investigators (Purdue Univ., Lafayette, Ind.), and R. OLIVIER (Lausanne Univ.) *In* Texas Univ. Appl. of MAGSAT to Lithospheric Modeling in South America, Part 2 p 46 Jan. 1984 Presented at the 17th IUGG Gen. Assembly, Hamburg, 1983 ERTS

Avail: NTIS HC A21/MF A01 CSCL 08G

Preliminary MAGSAT scalar magnetic anomaly data were compiled for comparison with long-wavelength-pass filtered free-air gravity anomalies and regional heat-flow and tectonic data. To facilitate the correlation analysis at satellite elevations over a spherical-Earth, equivalent point source inversion was used to differentially reduce the magnetic satellite anomalies to the radial pole at 350 km elevation, and to upward continue the first radial derivative of the free-air gravity anomalies. Correlation patterns between these regional geopotential anomaly fields are quantitatively established by moving window linear regression based on Poisson's theorem. Prominent correlations include direct correspondences for the Baltic Shield, where both anomalies are negative, and the central Mediterranean and Zaire Basin where both anomalies are positive. Inverse relationships are generally common over the Precambrian Shield in northwest Africa, the Basins and Shields in southern Africa, and the Alpine Orogenic Belt. Inverse correlations also persist over the North Sea Rifts, the Benue Rift, and more generally over the East African Rifts. The results of this quantitative correlation analysis support the general inverse relationships of gravity and magnetic anomalies observed for North American continental terrain which may be broadly related to magnetic crustal thickness variations.

A.R.H.

N84-25136*# Ohio State Univ., Columbus.

US AEROMAGNETIC AND SATELLITE MAGNETIC ANOMALY COMPARISONS Abstract Only

R. R. B. VONFRESE, W. J. HINZE (Purdue Univ., Lafayette, Ind.), L. W. BRAILE, Principal Investigators (Purdue Univ., Lafayette, Ind.), and J. L. SEXTON (ARCO) *In* Texas Univ. Appl. of MAGSAT to Lithospheric Modeling in South America, Part 2 p 50-51 Jan. 1984 Presented at the 4th IAGA Sci. Assembly, Edinburgh, 3-15 Aug. 1981 ERTS

Avail: NTIS HC A21/MF A01 CSCL 08G

Scalar aeromagnetic data obtained by the U.S. Naval Oceanographic Office (NOO) Vector Magnetic Survey of the conterminous U.S. were screened for periods of intense diurnal magnetic activity and reduced to anomaly form, filtered, and continued upward. A number of correlations between the NOO,

POGO and preliminary MAGSAT data are evident at satellite elevations, including a prominent transcontinental magnetic high which extends from the Anadarko Basin to the Cincinnati Arch. The transcontinental magnetic high is breached by negative anomalies located over the Rio Grande Rift and Mississippi River Aulacogen. Differentially reduced-to-pole NOO and POGO magnetic anomaly data show that the transcontinental magnetic high corresponds to a well-defined regional trend of negative free-air gravity and enhanced crustal thickness anomalies.

A.R.H.

N84-25137*# Pittsburgh Univ., Pa. Dept. of Geology and Planetary Science.

RELATION OF MAGSAT ANOMALIES TO THE MAIN TECTONIC PROVINCES OF SOUTH AMERICA Final Report

E. G. LIDIAK, G. R. KELLER, Principal Investigators (Texas Univ., El Paso), D. W. YUAN, and M. B. LONGACRE (Purdue Univ., Lafayette, Ind.) *In* Texas Univ. Appl. of MAGSAT to Lithospheric Modeling in South America, Part 2 p 52-58 Jan. 1984 Presented at the 52nd Ann. Intern. Meeting and Exposition of the Soc. of Exploration Geophysicists, Dallas, 1982 ERTS

Avail: NTIS HC A21/MF A01 CSCL 08G

Comparison of MAGSAT scalar magnetic anomaly data to the main tectonic provinces and boundaries of South America reveals a number of geologic correlations. South America is divisible into a broad platform of Precambrian shields and cratons separated by Phanerozoic basins, grabens and aulacogens to the east, the Phanerozoic Patagonian Platform to the south, and the Mesozoic to Cenozoic Andean Fold Belt and Caribbean Mountain System to the west and north. The continental shields are mainly more magnetic than continental basins and orogenic belts. Cratons, mainly covered by younger sedimentary rocks, are generally associated with magnetic gradients. Most of the anomalies associated with the Patagonian Platform are positive and have higher amplitudes eastward away from the Andean Fold Belt. The northern Andes are coincident with positive magnetic anomalies, whereas the central and southern Andes are associated mainly with negative anomalies.

A.R.H.

N84-25138*# Pittsburgh Univ., Pa.

RELATION OF MAGSAT AND GRAVITY ANOMALIES TO THE MAIN TECTONIC PROVINCES OF SOUTH AMERICA M.S. Thesis

D. W. YUAN *In* Texas Univ. Appl. of MAGSAT to Lithospheric Modeling in South America, Part 2 177 p Jan. 1984 refs ERTS

Avail: NTIS HC A21/MF A01 CSCL 08G

Magnetic anomalies of the South American continent are generally more positive and variable than the oceanic anomalies. There is better correlation between the magnetic anomalies and the major tectonic elements of the continents than between the anomalies and the main tectonic elements of the adjacent oceanic areas. Oceanic areas generally show no direct correlation to the magnetic anomalies. Precambrian continental shields are mainly more magnetic than continental basins and orogenic belts. Shields differ markedly from major aulacogens which are generally characterized by negative magnetic anomalies and positive gravity anomalies. The Andean orogenic belt shows rather poor correlation with the magnetic anomalies. The magnetic data exhibit instead prominent east-west trends, which although consistent with some tectonic features, may be related to processing noise derived from data reduction procedures to correct for external magnetic field effects. The pattern over the Andes is sufficiently distinct from the generally north trending magnetic anomalies occurring in the adjacent Pacific Ocean to separate effectively the leading edge of the South American Plate from the Nazca Plate. Eastern South America is characterized by magnetic anomalies which commonly extend across the continental margin into the Atlantic Ocean.

A.R.H.

04 GEOLOGY AND MINERAL RESOURCES

N84-25139*# Texas Univ., El Paso.

A CRUSTAL STRUCTURE STUDY OF SOUTH AMERICA M.S. Thesis

K. S. RENBARGER *In its Appl.* of MAGSAT to Lithospheric Modeling in South America, Part 2 261 p Jan. 1984 refs ERTS

Avail: NTIS HC A21/MF A01 CSCL 08G

Variations in the average crustal thickness of the South American platform were determined by measuring fundamental mode Rayleigh wave dispersion between nine pairs of South American WWSN seismograph stations and inverting the measurements to obtain average shear wave velocity-depth models across the platform. Additional models were derived from the Rayleigh wave dispersion data previously measured over eastern South America. Both sets of models were interpreted in terms of average crustal thickness and average crustal shear wave velocity. The results obtained were depicted in a contour map of crustal thickness. Average values for seismic velocities in the crust and upper mantle were calculated and compared with maps of regional gravity models, MAGSAT magnetic anomalies, and major tectonic features. The correlations and relationships discovered are discussed.

A.R.H.

N84-26093*# Instituto de Pesquisas Espaciais, Sao Jose dos Campos (Brazil).

MULTISEASONAL VARIABLES IN DIGITAL IMAGE ENHANCEMENTS FOR GEOLOGICAL APPLICATIONS

N. D. J. PARADA, Principal Investigator, I. VITORELLO, and R. ALMEIDAFILHO Apr. 1984 13 p refs Presented at the Intern. Symp. on Photogrammetry and Remote Sensing Congr., Rio de Janeiro, 17-29 Jun. 1984 Sponsored by NASA Original contains imagery. Original photography may be purchased from the EROS Data Center, Sioux Falls, S.D. 57198 ERTS (E84-10145; NASA-CR-173235; NAS 1.26:173235; INPE-3100-PRE/499) Avail: NTIS HC A02/MF A01 CSCL 08G

Examples of enhanced multiseasonal orbital imagery illustrate the influence of multiseasonal changes in their spatial and spectral attributes, and consequently in their application to structural geology and lithological discrimination. Shadow effects associated with appropriate solar elevation and azimuth effects enhance the spatial attributes but not the spectral. In this case, variations in illumination conditions should be minimized by selecting images with high solar elevation and by the use of techniques that minimize illumination conditions. Multiseasonal imagery should be used in the identification of spectral contrast changes of rock-soil-vegetation associations which can provide evidences of related lithological units and structural features. The extraction of maximum geological information requires, at least, a fall/winter and a spring/summer scene from which spatial, spectral and multiseasonal attributes can be adequately explored.

A.R.H.

N84-26094*# Instituto de Pesquisas Espaciais, Sao Jose dos Campos (Brazil).

FIELD DATA OBSERVED DURING THE GEOLOGICAL EXCURSION IN THE WEST-CENTRAL REGION OF THE SUL-RIOGRANDE SHIELD [DADOS DE CAMPO OBSERVADOS NO CAMINHAMENTO GEOLOGICO REALIZADO NA REGIAO CENTRO-OESTE DO ESCUDO SUL-RIOGRANDENSE]

N. D. J. PARADA, Principal Investigator and T. OHARA May 1984 230 p refs In PORTUGUESE; ENGLISH summary Sponsored by NASA Original contains imagery. Original photography may be purchased from the EROS Data Center, Sioux Falls, S. D. 57198 ERTS (E84-10146; NASA-CR-173236; NAS 1.26:173236; INPE-3098-NTE/218) Avail: NTIS HC A11/MF A01 CSCL 08G

Outcrops are studied in the Copper Project test area of the Rio Grande do Sul State of Brazil. The accuracy of LANDSAT-MSS data is checked against field data. A preliminary geological map is included on a scale of 1:500,000 that describes 820 outcrops over an area of 1,700 kilometers.

M.A.C.

N84-26101# Instituto de Pesquisas Espaciais, Sao Jose dos Campos (Brazil).

METHODOLOGICAL APPROACH IN LITHOLOGICAL DISCRIMINATION BY DIGITAL PROCESSING: A CASE STUDY IN THE SERRA DO RAMALHO, STATE OF BAHIA

I. VITORELLO and W. R. PARADELLA May 1984 14 p refs Presented at the Intern. Soc. for Photogrammetry and Remote Sensing Congr., Rio de Janeiro, Brazil, 18-29 Jun. 1984 (INPE-3108-PRE/507) Avail: NTIS HC A02/MF A01

Problems related to lithologic mapping are discussed. Enhancement techniques and thematic classifications were combined and applied in the lithological discrimination of metasediments of the Bambui Super Group (Upper Proterozoic) in the region of Serra do Ramalho, representative of a widespread transitional environment between semi-arid and temperate conditions, in the southwest portion of the State of Bahia, Brazil. A preliminary methodological sequence is discussed in detail for imagery obtained during the dry season by LANDSAT satellite. Color composites of stretched original data, band ratioing and principal components allow lithological discrimination through grey level and tonal gradations of several metasedimentary sequences, to a degree superior to reconnaissance mapping. Unsupervised (K-Means classifier) and Supervised (Maximum Likelihood classifier) were also applied, and the spatial distribution of the limestone sequence, host to a fluorite mineralization, show satisfactory results for the purposes of this research. However, the effects of vegetation cover and of human activities mask and limit in several ways lithological discrimination in this kind of environment. Author

N84-27259# Instituto de Pesquisas Espaciais, Sao Jose dos Campos (Brazil).

PROJECT SERGE: BRAZIL REFERENTIAL FIELD DATA FOR THE SIR-A EXPERIMENT [PROJETO SERGE: DADOS DE CAMPO REFERENTES AO EXPERIMENTO SIR-A NO BRASIL]

M. G. BALIEIRO, P. R. MARTINI, and J. R. DOSSANTOS Nov. 1983 108 p refs In PORTUGUESE; ENGLISH summary (INPE-2973-NTE/210) Avail: NTIS HC A02/MF A01

The ground observations undertaken over the Southern of Espirito Santo State and the Southeastern of Minas Gerais State, along the SPACE SHUTTLE 2 flying orbit are investigated. Field data relates mostly with lithology, geological structures and forest cover. Specific geomorphological and pedological aspects are collected. Ground data are being applied to evaluate the SIR-A Experiment, developed in the Space Shuttle-2 mission, for natural resources mapping and prospecting.

M.A.C.

N84-28276*# Johns Hopkins Univ., Baltimore, Md. Dept. of Earth and Planetary Sciences.

PETROLOGIC AND GEOPHYSICAL SOURCES OF LONG-WAVELENGTH CRUSTAL MAGNETIC ANOMALIES Final Technical Report, 1 Jun. 1980 - 30 Apr. 1983

B. D. MARSH and C. M. SCHLINGER (Utah Univ., Salt Lake City)

1984 12 p

(Contract NAG5-35)

(NASA-CR-175245; NAS 1.26:175245) Avail: NTIS HC A02/MF A01 CSCL 08G

The magnetic mineralogy and magnetic properties of the deep crust are studied as they pertain to the interpretation of long wavelength, or regional, crustal magnetic anomalies in satellite magnetic data and near surface magnetic data. The conclusions have relevance to the understanding of regional magnetic anomalies in magnetic field measuring satellite missions data. There are two separable studies: (1) a synthesis of available information of regional magnetic anomalies and the magnetization of metamorphic and igneous rocks, and (2) a detailed field, analytical, and experimental study of *in situ* and laboratory specimens from a terrain that offers exposures of high grade granitic facies rocks that have associated regional magnetic and gravity anomalies.

M.A.C.

05 OCEANOGRAPHY AND MARINE RESOURCES

05

OCEANOGRAPHY AND MARINE RESOURCES

Includes sea-surface temperature, ocean bottom surveying imagery, drift rates, sea ice and icebergs, sea state, fish location.

A84-30024#

THE ANALYSIS AND DIGITAL SIGNAL PROCESSING OF NOAA'S SURFACE CURRENT MAPPING SYSTEM

J. A. LEISE (NOAA, Wave Propagation Laboratory, Boulder, CO) IEEE Journal of Oceanic Engineering (ISSN 0364-9059), vol. OE-9, April 1984, p. 106-113. NOAA-supported research. refs

Newly developed numerical procedures used to analyze and process sea-echo data acquired with National Oceanic and Atmospheric Administration's (NOAA) dual-site HF-radar system, called Coastal Ocean Dynamics Applications Radar (CODAR), are described. CODAR is a transportable shore-based system that can map surface currents out to a nominal range of 50 km. Since its introduction in 1976, it has performed well in a dozen major experiments. Until recently, however, the data processing was labor intensive, difficult to understand, and slow. The processing presented here largely corrects these difficulties, giving CODAR reliable real-time mapping capabilities. Author

A84-30025* Environmental Research Inst. of Michigan, Ann Arbor.

DIGITAL PROCESSING CONSIDERATIONS FOR EXTRACTION OF OCEAN WAVE IMAGE SPECTRA FROM RAW SYNTHETIC APERTURE RADAR DATA

I. J. LAHAIE, A. R. DIAS, and G. D. DARLING (Michigan, Environmental Research Institute, Ann Arbor, MI) IEEE Journal of Oceanic Engineering (ISSN 0364-9059), vol. OE-9, April 1984, p. 114-120. NASA-supported research. refs (Contract N00014-81-C-0692)

The digital processing requirements of several algorithms for extracting the spectrum of a detected synthetic aperture radar (SAR) image from the raw SAR data are described and compared. The most efficient algorithms for image spectrum extraction from raw SAR data appear to be those containing an intermediate image formation step. It is shown that a recently developed compact formulation of the image spectrum in terms of the raw data is computationally inefficient when evaluated directly, in comparison with the classical method where matched-filter image formation is an intermediate result. It is also shown that a proposed indirect procedure for digitally implementing the same compact formulation is somewhat more efficient than the classical matched-filtering approach. However, this indirect procedure includes the image formation process as part of the total algorithm. Indeed, the computational savings afforded by the indirect implementation are identical to those obtained in SAR image formation processing when the matched-filtering algorithm is replaced by the well-known 'dechirp-Fourier transform' technique. Furthermore, corrections to account for slant-to-ground range conversion, spherical earth, etc., are often best implemented in the image domain, making intermediate image formation a valuable processing feature. Author

A84-30230#

REMOTE SENSING AND STORM SURGE FORECASTING IN BANGLADESH

A. ALI (Bangladesh Space Research and Remote Sensing Organization, Dacca, Bangladesh) IN: Asian Conference on Remote Sensing, 3rd, Dacca, Bangladesh, December 4-7, 1982, Proceedings . Tokyo, University of Tokyo, 1983, p. P-6-1 to P-6-7. refs

A84-30232#

BAY MONSOON ACTIVITIES IN RELATION TO THE MONSOON IN THE WESTERN PACIFIC

A. Q. DEWAN, M. NESSA, and D. BEGUM (Bangladesh Space Research and Remote Sensing Organization, Dacca, Bangladesh) IN: Asian Conference on Remote Sensing, 3rd, Dacca, Bangladesh, December 4-7, 1982, Proceedings . Tokyo, University of Tokyo, 1983, p. P-9-1 to P-9-11. refs

A84-30258#

MONITORING THE MARINE ENVIRONMENT WITH REMOTE SENSING TECHNOLOGY

D. BOREL (United Nations, Economics and Social Commission for Asia and the Pacific, Bangkok, Thailand) IN: Asian Conference on Remote Sensing, 3rd, Dacca, Bangladesh, December 4-7, 1982, Proceedings . Tokyo, University of Tokyo, 1983, p. E-4-1 to E-4-16. refs

A general review is given of the state of the art of marine environment remote sensing. The special advantages of microwave sensing, using the altimeter, the synthetic aperture radar (SAR) and the scatterometer, are discussed; Seasat, using such sensors, although failing after 100 days of operation, proved the validity of such work and useful results are expected after the launching of similar satellites in the second half of this decade. Sea floor topography and bathymetry may be suitably studied by means of the SAR and the MSS bands 4 and 5 of Landsat. In connection with temperature measurement and thermal pollution monitoring, scanning multifrequency microwave radiometer payloads, Nimbus 7, the NOAA polar orbiting satellites, and the five Geostationary Observation Satellites (GOS) are mentioned. Means of sensing chlorophyll, sedimentation, waste pollution, oil spills, productive fishing areas, and wetlands and coastal settlements are examined. D.H.

A84-30302* National Aeronautics and Space Administration. Langley Research Center, Hampton, Va.

SENSITIVITY OF AIRBORNE FLUOROSENSOR MEASUREMENTS TO LINEAR VERTICAL GRADIENTS IN CHLOROPHYLL CONCENTRATION

D. D. VENABLE (NASA, Langley Research Center, Hampton, VA), A. R. PUNJABI, and L. R. POOLE (Hampton Institute, Hampton, VA) Applied Optics (ISSN 0003-6935), vol. 23, April 1, 1984, p. 970-972. NASA-supported research. refs

A semianalytic Monte Carlo radiative transfer simulation model for airborne laser fluorosensors has been extended to investigate the effects of inhomogeneities in the vertical distribution of phytoplankton concentrations in clear seawater. Simulation results for linearly varying step concentrations of chlorophyll are presented. The results indicate that statistically significant differences can be seen under certain conditions in the water Raman-normalized fluorescence signals between nonhomogeneous and homogeneous cases. A statistical test has been used to establish ranges of surface concentrations and/or vertical gradients in which calibration by surface samples would be inappropriate, and the results are discussed. C.D.

A84-30443

INTERPRETING THE SPECTRA OF AERIAL PHOTOGRAPHS OF THE SEA SURFACE [OB INTERPRETATSII SPEKTROV AEROFOTOGRAFIII MORSKOI POVERKHNOSTI]

A. G. LUCHININ (Akademii Nauk SSSR, Institut Prikladnoi Fiziki, Gorki, USSR) Akademii Nauk SSSR, Izvestiia, Fizika Atmosfery i Okeana (ISSN 0002-3515), vol. 20, March 1984, p. 331-334. In Russian. refs

It is pointed out that the modulation of surface brightness by waves can be conditioned by a variety of factors and that a correct interpretation of the spectra requires that the effect of each of these factors be known. Consideration is given here to the combined effect of two factors, namely angular inhomogeneity in the sea surface illumination and the double focusing arising from the twofold passage of light through an agitated air-water interface. It is found that for an extremely wide range of spatial scales and optical wavelengths, the effect of double focusing cannot be

05 OCEANOGRAPHY AND MARINE RESOURCES

neglected. It affects not only the magnitude but also the angular spectra of the fluctuations. C.R.

A84-30672* Delaware Univ., Newark.

DYNAMICS OF THE SLOPE WATER OFF NEW ENGLAND AND ITS INFLUENCE ON THE GULF STREAM AS INFERRED FROM SATELLITE IR DATA

V. KLEMAS (Delaware, University, Newark, DE), N. E. HUANG (NASA, Wallops Flight Center, Wallops Island, VA), and Q. ZHENG (Remote Sensing of Environment (ISSN 0034-4257), vol. 15, March 1984, p. 135-153. refs

A84-31193

OCEANIC FRACTURE ZONES

E. BONATTI and K. CRANE (Lamont-Doherty Geological Observatory, Palisades, NY) Scientific American (ISSN 0036-8733), vol. 250, May 1984, p. 40-51.

The origin and dynamics of oceanic fracture zones are discussed. The deep troughs in the zones are formed by the 'freezing' of upwelling hot material at a lower level than along the ocean ridge axis, forming a topographic low which is transformed into a trough by sea floor spreading. The transverse ridges flanking these troughs are deepseated rock uplifted by plate collisions. The evidence for this is presented. The physical composition of the rocks indicates they were formed at great depths. Magnetic anomalies in the oceanic crust suggest that the direction of ocean plate spreading has changed over time, leading to plate collisions; the orientation of the fracture zones also indicate such changes. The role of the fracture zones in the creation of the Atlantic Ocean is described. C.D.

A84-31431#

DUAL CHANNEL SATELLITE MEASUREMENTS OF SEA SURFACE TEMPERATURE

I. J. BARTON (Commonwealth Scientific and Industrial Research Organization, Div. of Atmospheric Physics, Aspendale, Victoria, Australia) Royal Meteorological Society, Quarterly Journal (ISSN 0035-9009), vol. 109, April 1983, p. 365-378. Research supported by the Natural Environment Research Council. refs

Results from the 11.6 micron channel on the Nimbus 5 selective chopper radiometer are presented that show ambiguity in the temperature deficit obtained for any tropical sea surface temperature (s.s.t.). The analysis indicates that to gain an accurate measurement of s.s.t. in the 10-13 micron band, further information on the water vapor content of the overlying atmosphere is required. A transmission model is used to show that for two channels a linear relation exists between the two apparent surface temperatures, and simple algorithms are derived that give s.s.t.s with an accuracy better than 0.3 K for vertically-viewing satellite radiometers. Algorithms giving s.s.t. are derived for both dual wavelength and dual angle-of-view techniques, and these are compared with those derived by other authors. Author

A84-31821

AIRCRAFT MEASUREMENTS OF CONVECTIVE DRAFT CORES IN MONEX

C. WARNER and D. P. McNAMARA (Virginia, University, Charlottesville, VA) Journal of the Atmospheric Sciences (ISSN 0022-4928), vol. 41, Feb. 1, 1984, p. 430-438. refs (Contract NSF ATM-80-12214; NSF ATM-82-10128)

The present investigation has the objective to present a survey of updraft and downdraft cores encountered by U.S. research aircraft during the Winter and Summer Monsoon Experiments. Attention is given to calculations on convective draft cores, a comparison between gust probe data and computed vertical air velocities, frequency histograms of cores, and relationships between parameters of cores. Characteristics are examined of 99 different updraft and 43 downdraft cores encountered during 16 MONEX research aircraft missions over the South China Sea, Arabian Sea, and Bay of Bengal. Empirical results about individual convective cores are provided. G.R.

A84-32266#

THE ESA OCEAN OBSERVATION SATELLITE ERS-1. I - DESCRIPTION OF THE HISTORY, GOALS, AND PAYLOAD OF ERS-1 [DE ESA-ZEEOBSERVATIESATELLIET ERS-1. I - BESCHRIJVING VAN DE VOORGESCHIEDENIS, DE DOELSTELLINGEN EN DE PAYLOAD VAN DE ERS-1]

N. J. J. BUNNIK (Nationale Lucht- en Ruimtevaartlaboratorium, Amsterdam, Netherlands) Ruimtevaart, vol. 32, Feb. 1983, p. 35-46. In Dutch.

The development of the ERS-1 satellite for remote sensing of the oceans, coasts, and sea ice (currently in the definition phase) by ESA is discussed. The history of ESA involvement in remote sensing is traced through the inception of the ERS-1 program in 1980, and the role of the NASA Landsat/Seasat and French SPOT programs in helping define the goals and payload concept of ERS-1 is stressed. The nominal payload concept finalized in the announcement of opportunity in October, 1981, comprises radar altimeter, active microwave instrumentation (wave and wind scatterometers plus SAR), along-track scanning radiometer with microwave sounder, precision range and range-rate equipment, and laser retroreflector. The user requirements submitted by governmental and scientific bodies in the Netherlands are listed and explained. T.K.

A84-33360

COASTAL MAPPING OF THE BEAUFORT SEA COAST

D. BAIN (Alaska State, Div. of Technical Services, Anchorage, AK), A. FOLLETT (North Pacific Aerial Surveys, Inc., Anchorage, AK), and J. OSWALD (International Technology, Ltd., Anchorage, AK) IN: American Congress on Surveying and Mapping, Annual Meeting, 43rd, Washington, DC, March 13-18, 1983, Technical Papers. Falls Church, VA, American Congress on Surveying and Mapping, 1983, p. 99-109.

This paper presents the details of the coastal mapping project undertaken by the State of Alaska and the Alaska Photogrammetric Consultants Group, to determine the mean high water line of about 300 miles of Beaufort Sea coastline during 1981 and 1982. The mapping was performed to determine the offshore boundaries for upcoming oil and gas lease sales. Photogrammetric manuscripts were produced, based on an extensive field survey which involved acquisition of tidal data and densification of the horizontal control network with Doppler-inertial techniques. Black and white infrared photography was obtained and used along with existing NASA color infrared photography to produce 1:50,000 scale planimetric maps. Logistical support and environmental restrictions are highlighted. Data reduction and the subsequent compilation of the tide lines are discussed. Author

A84-33774

A THEORETICAL STUDY OF AN AIRBORNE LASER TECHNIQUE FOR DETERMINING SEA WATER TURBIDITY

D. M. PHILLIPS and B. W. KOERBER (Department of Defence, Electronics Research Laboratory, Adelaide, Australia) Australian Journal of Physics (ISSN 0004-9506), vol. 37, no. 1, 1984, p. 75-90. refs

An airborne laser technique for remote measurement of sea water turbidity is studied theoretically. The limits of validity of an analytic model are established using Monte Carlo simulation computations. It is shown that, if the field of view of the airborne receiver is large enough, the backscatter signal from the water is attenuated at a rate determined by the absorption coefficient of the water. Apart from geometrical factors, the amplitude of the backscatter signal at the water surface depends on the scattering coefficient of the water. The method therefore allows both the absorption and scattering coefficients of water to be determined independently. Author

05 OCEANOGRAPHY AND MARINE RESOURCES

A84-33985

DOWNDRAFTS FROM TROPICAL OCEANIC CUMULI

R. P. ADDIS, M. GARSTANG, and G. D. EMMITT (Virginia, University, Charlottesville, VA) *Boundary-Layer Meteorology* (ISSN 0006-8314), vol. 28, Jan.-Feb. 1984, p. 23-49. refs
(Contract NSF ATM-74-21701; NSF ATM-81-15397; NSF ATM-78-08865)

A total of 49 gust fronts associated with convective clouds are simultaneously observed at up to six levels through a depth of 1100 m (from a tethered balloon and an instrumented ship's boom), in order to describe the mean and detailed characteristics of tropical oceanic cumuli outflow at both the surface and the boundary layer. Tropical gust front temperature and velocity changes are 50 percent of the magnitude of the changes observed in midlatitude convective outflows, and gust front vertical velocities of more than 1 m/sec, which are continuous through the lower 500 m for periods of up to 8 min, are held to imply that vertical displacements of at least 500 m are sufficient at the observed humidities for the initiation of new cloud growth. O.C.

A84-34164*

Woods Hole Oceanographic Institution, Mass.

RAPID EVOLUTION OF A GULF STREAM WARM-CORE RING

T. JOYCE, R. BACKUS, T. COWLES (Woods Hole Oceanographic Institution, Woods Hole, MA), K. BAKER (California, University, La Jolla, CA), P. BLACKWELDER (Nova University, Dania, FL), O. BROWN, R. EVANS, D. OLSON (Miami, University, Miami, FL), G. FRYXELL (Texas A & M University, College Station, TX), D. MOUNTAIN (NOAA, National Marine Fisheries Service, Woods Hole, MA) et al. *Nature* (ISSN 0028-0836), vol. 308, April 26, 1984, p. 837-840. Research supported by the Bedford Institute of Oceanography, NSF, NASA, and NOAA. refs

Satellite images are used to show that major alterations in the structure of Gulf Stream warm-core rings can occur during very short periods of two to five days when an interaction with the Gulf Stream is particularly intense. The role of these interactions in the evolution of a ring are discussed. C.D.

A84-34276

ARCTIC HAZE AND THE ARCTIC GAS AND AEROSOL SAMPLING PROGRAM (AGASP)

R. C. SCHNELL (Cooperative Institute for Research in Environmental Sciences, Boulder, CO) *Geophysical Research Letters* (ISSN 0094-8276), vol. 11, May 1984, p. 361-364. refs

AGASP, part of an international Arctic haze study conducted in the spring of 1983, was described along with its instrumentation. Objectives included determining the spectra, optical properties, chemical composition, distribution, and trajectories of Arctic haze aerosols; measuring the concentration and distribution of Arctic trace gases; determining the concentration, flux, and gradients of atmospheric CO₂ with regard to important Arctic sources and sinks; measuring the radiative effects of the haze; and studying the polar tropopause folds. The measurement systems carried on board the WP-3D Orion aircraft included a high-volume aerosol system, a condensation nucleus counter, an integrating nephelometer, an ozone monitor, two Particle Measuring Systems aerosol spectrometer probes, and a dropwindsonde system. C.M.

A84-34287

AIRBORNE OBSERVATIONS OF ARCTIC AEROSOL. IV - OPTICAL PROPERTIES OF ARCTIC HAZE

A. D. CLARKE, R. J. CHARLSON, and L. F. RADKE (Washington, University, Seattle, WA) *Geophysical Research Letters* (ISSN 0094-8276), vol. 11, May 1984, p. 405-408. refs
(Contract NSF DPP-82-13425; NSF DPP-82-09548)

Measurements of the horizontal and vertical distribution of aerosol light absorption and light scattering coefficients (at 550nm) for the Arctic aerosol show a high degree of correlation. Apparently originating from source areas at lower latitudes and present at various degrees of dilution, the haze observed was found to have a single scattering albedo in the range of 0.77 to 0.93 and a mean of ca. 0.86. Apart from sample periods with high seasalt concentrations at low altitudes or within ice crystal layers, the single scattering albedo values presented here are well below

values characteristic of typical crustal aerosol but are similar to continental urban and rural values. These low values are consistent with arguments for mid-latitude combustion source for this aerosol. The magnitude and variability in the observed optical parameters suggest near surface heating rates in the range of 0.01 to 0.1 degrees centigrade per day. Author

A84-34339*

National Aeronautics and Space Administration.

Goddard Space Flight Center, Greenbelt, Md.

SEASAT OBSERVATIONS OF LITHOSPHERIC FLEXURE SEAWARD OF TRENCHES

D. C. MCADOO (NASA, Goddard Space Flight Center, Geodynamics Branch, Greenbelt, MD) and C. F. MARTIN (EG&G Washington Analytical Services Center, Riverdale, MD) *Journal of Geophysical Research* (ISSN 0148-0227), vol. 89, May 10, 1984, p. 3201-3210. refs

Lithospheric flexure seaward of deep ocean trenches is evident in Seasat altimeter observations of the marine geoid. In fact, mechanical models of lithospheric flexure can be tested directly on the Seasat altimeter data. A simple elastic model has been used for the oceanic lithosphere and, after least squares adjustments, estimates have been recovered of model parameters including outer rise (OR) amplitude, OR wavelength, and effective lithospheric thickness. Effective lithospheric thicknesses have been recovered for six regions: the Mariana, the Kuril, the Philippine, the Aleutian, the Izu-Bonin, and the Middle America OR's. These results support the proposition that effective thickness Te increases with age of lithosphere in approximate accord with the relation $Te \approx C \sqrt{\text{age}}$ where C approximately 4 km/square root of (m.y.). In fact, altimetric results agree more closely with this relation than do published results based on bathymetric data. The close agreement with the thickness-age relation suggests that there is no longer any need to assume that significant horizontal compression acts across the Kuril, Marianas, and Izu-Bonin trenches. This thickness-age relation implies that flexural strength of the oceanic lithosphere is temperature controlled. Author

A84-34501

MEAN CIRCULATION AND EDDY KINETIC ENERGY IN THE EASTERN NORTH ATLANTIC

W. KRAUSS and R. H. KAESE (Kiel, Universitaet, Kiel, West Germany) *Journal of Geophysical Research* (ISSN 0148-0227), vol. 89, May 20, 1984, p. 3407-3415. refs

Sixty-two satellite-tracked buoys have been released in the northern part of the western and central North Atlantic during 1981 and 1982 and six buoys deployed in spring 1980 have been taken over. Mean values and variances about the mean have been calculated for 3 x 3-deg areas. The mean velocities confirm the large-scale gyre circulation as deduced from hydrographic data and numerical models. The center of the gyre is located at about 33 N. Eddy kinetic energy decreases eastward and southward and is concentrated along the North Atlantic Current. It appears that the North Atlantic Current (Polar Front) is the main source of eddy kinetic energy for the northern North Atlantic, whereas the Mid-Atlantic Ridge is no source of eddy energy. Eddy kinetic energy along the North Atlantic Current decreases from about 1000 sq cm/sec sq near Newfoundland to 300 sq cm/sec sq west of Scotland. A homogeneous pool of low eddy kinetic energy (less than 100 sq cm/sec sq) appears in the central North Atlantic east of the Mid-Atlantic Ridge. The level increases towards the European and African shelf where the mean southward flow also becomes stronger. The results concern the upper ocean. Author

05 OCEANOGRAPHY AND MARINE RESOURCES

A84-34502

LAGRANGIAN OBSERVATIONS OF AN ANTICYCLONIC RING IN THE WESTERN GULF OF MEXICO

A. D. KIRWAN, JR. (South Florida, University, St. Petersburg, FL), W. J. MERRELL, JR., R. E. WHITAKER (Texas A&M University, College Station, TX), and J. K. LEWIS (Science Applications, Inc., Bryan, TX) *Journal of Geophysical Research* (ISSN 0148-0227), vol. 89, May 20, 1984, p. 3417-3424. refs (Contract NOAA-NA-81QAC148; N00014-83-K-0256)

This analysis documents, for the first time, the movement and velocity characteristics of an anticyclonic ring. The ring was pinched off from the Loop Current in the fall of 1980 and moved into the western Gulf of Mexico. Lagrangian measurements obtained from satellite-tracked drifters show that typical speeds of the near-surface currents associated with this ring are about 50 cm/s. There is also a surprising amount of higher-frequency current fluctuations. These include diurnal and semidiurnal tides, a basin tidal resonance, and a free gravity mode. Author

A84-34503

A MODEL FOR THE ANALYSIS OF DRIFTER DATA WITH AN APPLICATION TO A WARM CORE RING IN THE GULF OF MEXICO

A. D. KIRWAN, JR. (South Florida, University, St. Petersburg, FL), W. J. MERRELL, JR., R. E. WHITAKER (Texas A&M University, College Station, TX), J. K. LEWIS (Science Applications, Inc., Bryan, TX), and R. LEGECKIS (NOAA, Ocean Sciences Branch, Washington, DC) *Journal of Geophysical Research* (ISSN 0148-0227), vol. 89, May 20, 1984, p. 3425-3438. refs (Contract NOAA-NA-81-QAC148; N00014-83-K-0256)

A model developed primarily for the analysis of drifter data is discussed. The model is based on a parametric representation of the drifter velocity in terms of Monge potentials, two of which are constants following the motion of the fluid. In the application presented here, one of the potentials is taken as the frequency of rotation about a ring by a parcel. A more restricted interpretation of the velocity gradient invariant for horizontal flow is also discussed. The other potential is taken as the streamline of a parcel that is locally approximated as a conic section. For the restricted interpretation, solutions to the model equations are critically dependent on the relative sizes of the squares of the vertical vorticity and total deformation rate. This model differs from drifter cluster models in that each drifter provides independent estimates of the vorticity and deformation rates. Application is made to path data from three drifters that were seeded in a warm core ring in the Gulf of Mexico in November 1980. The model provided estimates of the ring translation and swirl velocities along with the ring geometry. The analysis showed that the ring was persistently elliptical with the major axis aligned in the east-west direction. A satellite infrared photo on January 21, 1981, confirmed this orientation. Author

A84-34507

SEASONAL VARIABILITY IN MEANDERS OF THE CALIFORNIA CURRENT SYSTEM OFF VANCOUVER ISLAND

M. IKEDA, W. J. EMERY, and L. A. MYSAK (British Columbia, University, Vancouver, Canada) *Journal of Geophysical Research* (ISSN 0148-0227), vol. 89, May 20, 1984, p. 3487-3505. Research supported by the Natural Sciences and Engineering Research Council of Canada. refs

The seasonal variation of meanders in the California Current System (CCS) off Vancouver Island is investigated on the basis of IR observations obtained during 1979-1982 with the TIROS-N, NOAA-6, and NOAA-7 satellites. The data are characterized for each season and illustrated with graphs, diagrams, and satellite images. The winter and spring variations are shown to agree well with the predictions of a four-layer linear-stability-theory model of the CCS, and a nonlinear model with topographic obstacles is developed for the summer and fall variations. In this scheme, the 75-km meanders are triggered by topographic features with 75-km spatial periodicity via baroclinic instability, grow to large amplitudes, and are replaced by 150-km meanders as a result of nonlinear interactions. T.K.

A84-34509

KATABATIC WIND FORCING OF THE TERRA NOVA BAY POLYNYA

D. H. BROMWICH and D. D. KURTZ (Ohio State University, Columbus, OH) *Journal of Geophysical Research* (ISSN 0148-0227), vol. 89, May 20, 1984, p. 3561-3572. refs (Contract NSF DPP-81-00142)

A theoretical model explaining the formation of the Terra Nova Bay polynya in the Ross Sea, Antarctica, is proposed. Katabatic winds draining into the bay through the Reeves Glacier valley are identified as the primary factor, with the length of the Drygalski Ice Tongue, which acts as a shield against drifting ice, determining the width of the polynya. The details of the model are discussed and illustrated with maps, diagrams, Landsat images, and a table of predicted values for the surface energy balance of the open water. T.K.

A84-34513#

THEORY AND VALIDATION OF THE MULTIPLE WINDOW SEA SURFACE TEMPERATURE TECHNIQUE

L. M. MCMILLIN (NOAA, National Environmental Satellite, Data, and Information Service, Washington, DC) and D. S. CROSBY (American University, Washington, DC) *Journal of Geophysical Research* (ISSN 0148-0227), vol. 89, May 20, 1984, p. 3655-3661. refs

The development of the split-window approach for correcting satellite measurements of radiance for atmospheric attenuation is reviewed. The theoretical results are compared to results from actual satellite measurements in the three infrared windows of the AVHRR. Ground truth for the comparisons comes from buoys. The satellite measurements were screened for clouds, and the remaining ones were used in the analysis. Several statistical analyses showed that, when the two channels that are truly a split window are used, the result of the statistical model agrees with the one derived from theoretical considerations. When the 3.8-micron channel is combined with one in the 10-12-micron region, the result of the statistical model does not take the split-window form. Results show that the method is capable of producing sea-surface temperatures with a standard deviation of 1 K or less. Author

A84-34514

SATELLITE OBSERVATIONS OF CIRCULATION IN THE EASTERN BERING SEA

T. PALUSZKIEWICZ (Alaska, University, Fairbanks, AK; Oregon State University, Corvallis, OR) and H. J. NIEBAUER (Alaska, University, University, Fairbanks, AK) *Journal of Geophysical Research* (ISSN 0148-0227), vol. 89, May 20, 1984, p. 3663-3678. refs (Contract NSF DPP-76-23340; NOAA-NA-795AC00780)

Satellite infrared observations of the eastern Bering Sea shelf and basin were analyzed from December 1979 to August 1981. A region of warm surface water which extends from the Gulf of Alaska through the Aleutian Passes into the Bering Sea was observed coincident with a band of warm surface water and with eddies along the shelf break. The spatial and temporal relationships of these patterns imply a surface inflow through Unimak and other western Aleutian Passes, flow along the shelf break including eddies along the Bering Slope Current, and cyclonic flow in the basin. The proposed generating mechanisms for eddies along the shelf break include topographic interactions, baroclinic instabilities, and Rossby waves. Author

05 OCEANOGRAPHY AND MARINE RESOURCES

A84-34516* Remote Sensing Systems, Sausalito, Calif.

A MODEL FUNCTION FOR OCEAN RADAR CROSS SECTIONS AT 14.6 GHZ

F. J. WENTZ, L. A. THOMAS (Remote Sensing Systems, Sausalito, CA), and S. PETEHERYCH (Department of the Environment, Atmospheric Environment Service, Downsview, Ontario, Canada) Journal of Geophysical Research (ISSN 0148-0227), vol. 89, May 20, 1984, p. 3689-3704. Sponsorship: Department of the Environment of Canada. refs (Contract DE-OAJ82-00135; NASW-3606)

The relationship between the ocean's normalized radar cross section (NRCS) at 14.6 GHz and the surface wind vector is derived using the 3 months of Seasat microwave scatterometer (SASS) measurements. The derivation is based on the statistics of the SASS observations, and no in situ measurements are required, other than a mean global wind speed, which comes from climatology. The frequency distribution of the global wind vectors observed by SASS is assumed to be a bivariate normal probability function. A NRCS model function is found that maps the assumed wind vector statistics into the observed SASS NRCS statistics. This function is compared with a NRCS model coming from the Joint Air Sea Interaction Experiment (JASIN) and with aircraft scatterometer measurements. The results indicate that the statistically derived NRCS model is an improvement over the JASIN model, which was based on a limited number of in situ anemometer measurements.

Author

A84-34517# National Aeronautics and Space Administration. Goddard Space Flight Center, Greenbelt, Md.

OBSERVATIONS OF GULF STREAM-INDUCED AND WIND-DRIVEN UPWELLING IN THE GEORGIA BIGHT USING OCEAN COLOR AND INFRARED IMAGERY

C. R. MCCLAIN (NASA, Goddard Space Flight Center, Laboratory for Atmospheric Sciences, Greenbelt, MD), L. J. PIETRAFESA (North Carolina State University, Raleigh, NC), and J. A. YODER (Skidaway Institute of Oceanography, Savannah, GA) Journal of Geophysical Research (ISSN 0148-0227), vol. 89, May 20, 1984, p. 3705-3723. refs

(Contract DE-AS09-76EY-00902; DE-AS09-76EV-00936; DE-AS09-76EV-00901; DE-AS05-76EV-05163; DE-AS09-76EV-00889; NASA TASK 146-40-15-25)

Ocean color and infrared imagery from U2 aircraft and satellite sensors are used to study upwelling interaction between Gulf Stream and continental shelf waters in the Georgia Bight. The photographic data are combined with in situ measurements of currents, chlorophyll, temperature, salinity, coastal winds, and sea-level in observations of five different upwelling events including a near-short wind-driven upwelling caused by topographic effects, three filament-induced upwellings in the Gulf Stream, and a possible meander-induced upwelling event in the Gulf Stream. Chlorophyll distributions are used to trace the circulation and propagation of filaments along the advective routes by which the water moves offshore. Photographic and mooring array measurements of temperature time series are found to provide nearly identical results for the phase speeds of each event. Field measurements of surface pigments, and Nimbus/7 coastal zone color scanner (CZCS) estimates are found to agree well over the range of concentrations 0.1 to 0.7 mg/m to the third. Examples of U2/Ocean Color Scanner and Nimbus 7 CZCS photographs are provided.

I.H.

A84-34942# National Aeronautics and Space Administration. Langley Research Center, Hampton, Va.

TWO-FREQUENCY MICROWAVE RESONANCE MEASUREMENTS FROM AN AIRCRAFT - A QUANTITATIVE ESTIMATE OF THE DIRECTIONAL OCEAN SURFACE SPECTRUM

J. W. JOHNSON (NASA, Langley Research Center, Hampton, VA) and D. E. WEISSMAN (Hofstra University, Hempstead, NY) Radio Science (ISSN 0048-6604), vol. 19, May-June 1984, p. 841-854. refs

The use of the two-frequency microwave-resonance technique for airborne measurements of ocean surface-wave spectral components is examined in a summary of experiments conducted

with a coherent Ku-band radar flown on a P-3 aircraft in the 1979 MARSEN and 1980 ARSLOE projects. The 1D theoretical formulation used in the analysis of the MARSEN data by Johnson et al. (1982) is extended to the 2D case; the experimental conditions are described in detail; and typical data are presented graphically, analyzed, and compared with independent measurements obtained with a surface-contour radar. The 3.5-deg pencil-beam configuration used in ARSLOE is shown to produce spectra with good directional characteristics (strong resonances at angles of incidence 13-48 deg). It is found that the proper inversion of radar data to surface-elevation spectra requires surface-reflectivity-modulation sources in addition to the long-wave orbital velocity. T.K.

A84-35252

THE EFFECT OF OCEAN SURFACE TEMPERATURE ON THE TRAJECTORIES OF TROPICAL CYCLONES [VLIANIE TEMPERATURY POVERKHONOSTI OKEANA NA TRAEKTORII TROPICHESKIKH TSIKLONOV]

E. A. AGRENICH (Gidrometeorologicheskii Nauchno-Issledovatel'skii Tsentr SSSR, Moscow, USSR) Meteorologiya i Gidrologiya (ISSN 0130-2906), May 1984, p. 57-63. In Russian. refs

The relationship between the direction of tropical cyclone motion and the spatial distribution of ocean surface temperatures is investigated, using satellite data. In analyzing the data, derivations from initial cyclone trajectories toward warmer water were found in 87 out of 110 cases. A correlation was found between this effect and the velocity of tropical cyclone motion, the positions of the errant cyclone trajectories in relation to direct (SE-NW) and reverse (SW-NE) trajectories, and to the point of trajectory recurvature. It is expected that water temperature data will become increasingly useful in predicting the motions of tropical cyclones.

I.H.

A84-35542#

THE ACTIVE MICROWAVE INSTRUMENTATION FOR ERS-1

R. P. COX and H. JOYCE (Marconi Space and Defence Systems, Ltd., Portsmouth, England) ESA Journal (ISSN 0379-2285), vol. 8, no. 1, 1984, p. 1-18. refs

An important element of the payload of the ESA's remote sensing satellite ERS-1, which will conduct ocean area monitoring, is the Active Microwave Instrument (AMI) consisting of an imaging SAR and a scatterometer. The AMI will provide two-dimensional images of the radar reflectivity of parts of the earth's surface at 5.3 GHz once/orbit, as well as image a sea surface area of 5 x 5 km at a spacing of 100 km during a satellite orbit to provide rectangular grid sampling. The AMI will also furnish a measurement of the sea surface reflectivity perturbed by winds in the area, and a transformation of this data to that of the wind parameter. In each mode, orbital processing of the radar data will be followed by transmission to earth stations and further signal processing on the ground.

O.C.

A84-36107

REMOTE SENSING MARINE BIOLUMINESCENCE - THE ROLE OF THE IN-WATER SCALAR IRRADIANCE

H. R. GORDON (Miami, University, Coral Gables, FL) Applied Optics (ISSN 0003-6935), vol. 23, June 1, 1984, p. 1694-1696. refs

(Contract N00014-81-0388)

Radiative transfer theory is used to define optical parameters for marine bioluminescence. Emphasis is put on the important role of in-water scalar irradiance in assessing the influence of the optical properties of water on marine bioluminescence, as it is sensed from earth-orbiting satellites. It is found that in-water scalar irradiance and intensity density of the emitting sources are sufficient for determining the surface integral of the radiance at the top of the atmosphere, in cases where the duration of the flashes is at least a few tenths of a second.

I.H.

05 OCEANOGRAPHY AND MARINE RESOURCES

A84-36119

EFFECTIVE REFLECTANCE OF OCEANIC WHITECAPS

P. KOEPEK (Muenchen, Universitaet, Munich, West Germany) Applied Optics (ISSN 0003-6935), vol. 23, June 1, 1984, p. 1816-1824. Sponsorship: Bundesministerium fuer Forschung und Technologie. refs (Contract BMFT-MF-0235)

The effective reflectance of the foam on the ocean surface together with the fraction of the surface covered with foam describes the optical influence of whitecaps in the solar spectral range. This effective reflectance is found to be approximately 22 percent in the visible spectral range and is presented as a function of wavelength for the solar spectral range. With the fraction of the surface covered with foam, taken from the literature, the results lead to a good agreement with satellite measured radiances and albedo values. The effective reflectance is more than a factor of 2 lower than reflectance values used to date in remote sensing and radiation budget studies. Consequently, the optical influence of whitecaps can be assumed to be much less important than formerly supposed.

Author

A84-36289#

X TO W BAND RADIOMETRIC SIGNATURES OF NATURAL SURFACES

M. BERNABO, A. BORRANI, G. MARSIGLIA, A. RESTI (Segnalamento Marittimo ed Aereo S.p.A., Florence, Italy), P. PAMPALONI (CNR, Istituto di Analisi Ambientale e Telerilevamento Applicati alla Agricoltura, Florence, Italy), and G. TOFANI (Arcetri, Osservatorio Astrofisico, Florence, Italy) IN: Military microwaves '82, Proceedings of the Conference, London, England, October 20-22, 1982. Tunbridge Wells, Kent, England, Microwave Exhibitions and Publishers, Ltd., 1983, p. 547-552. refs

X- to W-band microwave sensors are presently applied to the radiometric investigation of land and sea surfaces. Two operational modes are investigated, the first of which uses measurements at different frequencies and the second different observational angles, for recognition of the physical and geometrical signatures of objects and images at 16 and 95 GHz. Large scale analyses of the natural environment and specific targets can be conducted on the basis of these measurements.

O.C.

A84-36684

FIRST OBSERVATIONS OF THE INTERACTION OF OCEAN SWELL WITH SEA ICE USING SATELLITE RADAR ALTIMETER DATA

C. G. RAPLEY (Centre National d'Etudes Spatiales, Groupe de Recherches de Geodesie Spatiale, Toulouse, France; London, University College, Dorking, Surrey, England) Nature (ISSN 0028-0836), vol. 307, Jan. 12, 1984, p. 150-152. Research supported by the Centre National d'Etudes Spatiales. refs

New results on the interaction of ocean swell with sea ice from the U.S. Seasat satellite are presented which suggest that radar altimetry can provide a powerful means of global synoptic monitoring of that interaction. The evolution of significant wave height and signal strength as the Seasat altimeter passes from ocean to sea ice is shown and discussed, as is the evolution of waveform shape and strength as a function of increasing distance into the ice pack.

C.D.

A84-36686

MAPPING THE SEA FLOOR BY SATELLITE

R. N. ANDERSON (Lamont-Doherty Geological Observatory, Palisades, NY) Nature (ISSN 0028-0836), vol. 307, Jan. 19, 1984, p. 208, 209. refs

Some results of the processing of SEASAT data are reviewed. A map of the earth's gravity field obtained by geoid data is shown and compared to a far more primitive construct obtained from one hundred years of oceanographic exploration. Bathymetric findings in oceanic fracture zones and seamounts using SEASAT data are described, and the methods used to make these findings are summarized.

C.D.

A84-36872* National Marine Fisheries Service, La Jolla, Calif. SATELLITE OBSERVATIONS OF THE 1982-1983 EL NINO ALONG THE U.S. PACIFIC COAST P. C. FIEDLER (NOAA, National Marine Fisheries Service, La Jolla, CA) Science (ISSN 0036-8075), vol. 224, June 15, 1984, p. 1251-1254. refs (Contract NASA ORDER W-15334)

Satellite infrared temperature images illustrate several effects of the 1982-1983 El Nino: warm sea-surface temperatures with the greatest anomalies near the coast, weakened coastal upwelling, and changes in surface circulation patterns. Phytoplankton pigment images from the Coastal Zone Color Scanner indicate reduced productivity during El Nino, apparently related to the weakened coastal upwelling. The satellite images provide direct evidence of mesoscale changes associated with the oceanwide El Nino event.

Author

A84-37095

THEORY OF RADIO WAVE PROPAGATION OVER THE SEA SURFACE [K TEORII RASPROSTRANENIIA RADIOLN NAD MOREM]

A. G. BUGROV, V. I. KLIATSKIN, and B. M. SHEVTSOV (Akademii Nauk SSSR, Tikhookeanskii Okeanologicheskii Institut, Vladivostok, USSR) Akademii Nauk SSSR, Doklady (ISSN 0002-3264), vol. 275, no. 6, 1984, p. 1372-1376. In Russian.

Problems of ultra-long-range propagation in the atmosphere and waveguide propagation over the sea surface are difficult to solve because of their boundary value nature. Some boundary value problems in acoustics and radiophysics have recently been reformulated as initial-value problems that are more convenient for numerical and statistical analyses. An attempt is made to accomplish a similar task for boundary value problems of short wave propagation in the earth's atmosphere. This is done for a simple problem, that of radio wave propagation in a spherically layered atmosphere over an ideally conducting sea surface. V.L.

A84-37299#

REMOTE SENSING OF THE OCEANS

Y. SUGIMORI Tokyo, Kurotsu Shuppan Co., Ltd., 1982, 286 p. In Japanese. refs

Analytical reports of survey research and recent advances in observational technology in the areas of basic marine science, fishery sciences, and marine meteorology are discussed. These advances have accompanied startling developments in space technology over the past several years and have occurred in fields which previously relied on earth-based systems. Observational results from NASA Landsat, Nimbus, Seasat, and the Japanese Geostationary Meteorological Satellite Himawari are considered in detail. A basic explanation is given on how data from these satellites are used.

C.D.

A84-38298

JOINT ANALYSIS OF LANDSAT-MSS AND NOAA-AVHRR DATA FOR MARINE ENVIRONMENTAL MONITORING

H. OCHIAI (Toba Merchant Marine College, Toba, Japan), K. TSUCHIYA (Chiba University, Chiba, Japan), S. TAKEUCHI (Remote Sensing Technology Center of Japan, Tokyo, Japan), and Y. SUZUKI (Fujitsu Facom Information Processing Co., Tokyo, Japan) IN: International Symposium on Space Technology and Science, 13th, Tokyo, Japan, June 28-July 3, 1982, Proceedings. Tokyo, AGNE Publishing, Inc., 1982, p. 1259-1264. refs

This paper describes the method of digital analysis of Landsat-MSS and NOAA-AVHRR data obtained nearly simultaneously and discusses the effectiveness of the combination of visible data of MSS and thermal infrared data of AVHRR for monitoring of marine environment in some coastal areas around Japan. The procedure of analysis consists of path radiance correction of Landsat-MSS data and the geometric correction and temperature calibration of NOAA-AVHRR data. From the results of analysis, the negative correlation between turbidity and sea surface temperature was found in several bays and coastal areas, which indicates that the land origin water from the specific land

05 OCEANOGRAPHY AND MARINE RESOURCES

area is the main source for water pollution in those areas.

Author

A84-38307

REMOTE SENSING OF THE OCEAN BY THE AIRBORNE MICROWAVE SCATTEROMETER/RADIOMETER SYSTEM

H. MASUKO, K. OKAMOTO, S. YOSHIKADO, T. OJIMA, H. INOMATA, N. FUGONO (Ministry of Posts and Telecommunications, Radio Research Laboratories, Tokyo, Japan), M. SHIMADA, H. YAMADA, S. NIWA (National Space Development Agency of Japan, Parts and Equipment Laboratory, Sakura, Ibaraki, Japan), and S. YAMAMOTO (National Space Development Agency of Japan, Earth Observation System Dept., Tokyo, Japan) IN: International Symposium on Space Technology and Science, 13th, Tokyo, Japan, June 28-July 3, 1982, Proceedings. Tokyo, AGNE Publishing, Inc., 1982, p. 1331-1338. refs

Preliminary results of airborne microwave scatterometer and radiometer measurements of ocean areas to identify the signal component that is affected by wind velocity are reported. The tests were run as part of the process of developing a wind speed scatterometer for the MOS-1 satellite. The trials featured X-band and Ka-band instruments aimed at nearly the same sea surfaces at 3000 m altitude and a 300 km/hr airspeed. Measurements were made of the signal differential backscattering cross-section (DBSC) and the brightness temperature. The azimuth angle periodicity and the wind speed dependence of the DBSC of the sea surface were obtained at 10 and 34.45 GHz after a comparison with buoy and shipboard data. The microwave frequency dependence of DBSC was identified for wind speeds ranging from 6-32 kt.

M.S.K.

A84-38309

MICROWAVE BACKSCATTERING CHARACTERISTICS OF WIND-GENERATED WAVES

T. KOBAYASHI and H. HIROSAWA (Tokyo, University, Tokyo, Japan) IN: International Symposium on Space Technology and Science, 13th, Tokyo, Japan, June 28-July 3, 1982, Proceedings. Tokyo, AGNE Publishing, Inc., 1982, p. 1347-1352.

Radar return from the ocean surface is useful for determining many quantities of interest: ocean conditions and wind velocities. This paper describes a wind-tunnel experiment on microwave backscatter from wind waves and discusses the backscattering mechanisms. Microwave backscatters were measured at X-band for all polarization combinations including circular polarizations. Backscattering coefficients, Fourier spectra, and probability density functions were obtained from the analyses of received signals. Microwave backscattering mechanisms were examined through these multiple aspects of the backscattering characteristics.

Author

A84-38620#

ERS-1 - AN ICE AND OCEAN MONITORING MISSION

P. GILLETT and H.-M. BRAUN Dornier-Post (English Edition) (ISSN 0012-5563), no. 2, 1984, p. 58-63.

ERS-1 is an ice and ocean monitoring mission consisting of an Ariane-launched satellite and ESA-ground directed control, data, and dissemination facilities. Short and medium-term weather forecasts and sea-ice boundary monitoring are the main mission objectives. The instruments onboard the satellite include the Active Microwave Instrumentation with SAR and a radar altimeter. Additional instruments providing significant enhancement of data include: an Along Track Scanning Radiometer and Microwave Sounder, a Precision Range and Range Rate Experiment, and a laser retroreflector. Attitude and orbit maneuvers are controlled by four tanks carrying 300 kg of hydrazine fuel. The ground segment is responsible for several main functions including satellite control, acquisition of data, production of corrected data products, archiving and calibration activities. The orbit (near-polar circular at 800 km altitude) and operational objectives are examined.

J.P.

A84-38702

THE WORLD CLIMATE RESEARCH PROGRAMME

J. T. HOUGHTON (Meteorological Office, Bracknell, Berks., England) and P. MOREL (World Meteorological Organization, Geneva, Switzerland) IN: The global climate. Cambridge and New York, Cambridge University Press, 1984, p. 1-11. refs

Three objectives or streams of research in the World Climate Research Program have been identified, namely (1) long-range weather predictions over periods of several weeks, (2) interannual variability of the global atmosphere and the tropical oceans over periods of several years, and (3) longer-term variations. Two major experiments, Tropical Oceans and Global Atmosphere and the World Ocean Circulation Experiment have been identified as the foci of the second and third streams. For these, new modeling efforts (especially coupled atmosphere-ocean models) and global observations, especially from satellites of all components (in particular the ocean) of the climate system are required.

Author

A84-38773

THE EVOLULTION OF MUSHROOM-SHAPE CURRENTS IN THE OCEAN [EVOLIUTSIIA GRIBOVIDNYKH TECHENII V OKEANE]

A. I. GINZBURG and K. N. FEDOROV (Akademii Nauk SSSR, Institut Okeanologii, Moscow, USSR) Akademii Nauk SSSR, Doklady (ISSN 0002-3264), vol. 276, no. 2, 1984, p. 481-484. In Russian.

A hypothesis is proposed to explain the origin of mushroom-shaped currents in the ocean detected by satellite-borne observations in the visible and infrared ranges. It is suggested that the mushroom-shaped currents are a result of the evolution of narrowly localized jet streams formed in the surface layer of lighter waters under the effect of a sufficiently strong locally applied impulse, such as an air jet, a level or pressure gradient, or front and current instabilities. A sequence of images documenting the evolution of a mushroom-shape current is examined, and the observed features are found to be consistent with the hypothesis proposed here.

V.L.

A84-38941

SEASAT SAR SEA-ICE IMAGERY - SUMMER MELT TO AUTUMN FREEZE-UP

R. D. KETCHUM, JR. (U.S. Navy, Polar Oceanography Branch, Bay St. Louis, MS) International Journal of Remote Sensing (ISSN 0143-1161), vol. 5, May-June 1984, p. 533-544.

Some salient aspects of Seasat L-band SAR sea-ice imagery are presented. High backscatter attributed to water-saturated surface layers reduces the ability to interpret ice conditions. Slush on water areas produces a strong backscatter which could be misinterpreted as rubble, but sequential imagery and floe sizes and shapes can be used to resolve this ambiguity. The slush effect may enhance the identification of active zones. Decreasing air temperatures during autumn freeze-up reduces background clutter increasing the ability to discern floe sizes and shapes. Higher SAR frequencies being considered for future satellites will show greater backscatter variations for different ice types, but many ambiguities will occur and the ability to discern ridges and floe sizes and shapes will be reduced in the marginal ice zones where interannual weather fluctuations will adversely affect surface scattering properties.

Author

A84-38943

DETECTION OF MARINE AEROSOL PARTICLES IN COASTAL ZONES USING SATELLITE IMAGERY

P. A. DURKEE, P. C. SINCLAIR, T. H. VONDER HAAR (Colorado State University, Fort Collins, CO), and E. E. HINDMAN International Journal of Remote Sensing (ISSN 0143-1161), vol. 5, May-June 1984, p. 577-586. refs
(Contract N00014-79-C-0793)

Regions of brightness variations are common in visible and near-infrared satellites images from clear coastal regions. The variations have been hypothesized to be caused by aerosol particles in the marine boundary layer. The hypothesis was tested using in situ particle measurements collected near the time of satellite overpasses. Boundary-layer particle concentrations related

05 OCEANOGRAPHY AND MARINE RESOURCES

to the brightness variations: high concentrations existed in bright regions and vice versa. This result indicates that, in regions over the ocean free of clouds, sunglint and whitecaps, the visible and near-infrared sensors aboard certain orbiting meteorological satellites can detect variations in the concentrations of haze particles in the marine boundary layer. Author

A84-39427 CZCS DATA ANALYSIS IN TURBID COASTAL WATER

M. VIOILLIER (CNRS, Station Biologique, France; Commission of the European Communities, Joint Research Center, Ispra, Italy) and B. STURM (Commission of the European Communities, Joint Research Center, Ispra, Italy) Journal of Geophysical Research (ISSN 0148-0227), vol. 89, June 30, 1984, p. 4977-4985. refs

Different spectral signatures of coastal waters are presented and analysed with respect to possible improvements of the CZCS algorithms. When adjusted to the prevailing oceanographic conditions, algorithms can be improved in different ways: by adjustment of the coefficients in the ratio algorithms, by use of the amplitude of reflectance, or by adjustment of the method for the aerosol correction. It is shown that the combined use of ratio and amplitude of reflectance in a sediment algorithm can be used to distinguish between offshore upwellings and turbid near shore coastal water. The processing of CZCS scenes illustrates the importance of ocean color imagery in various aspects of oceanography: fundamental biology and transport of coastal pollutants. Author

A84-39458*# Systems and Applied Sciences Corp., Hyattsville, Md.

MONTHLY DISTRIBUTIONS OF PRECIPITABLE WATER FROM THE NIMBUS 7 SMMR DATA

H. D. CHANG (Systems and Applied Sciences Corp., Hyattsville, MD), P. H. HWANG, T. T. WILHEIT, A. T. C. CHANG (NASA, Goddard Space Flight Center, Application Directorate, Greenbelt, MD), D. H. STAELIN, and P. W. ROSENKRANZ (MIT, Cambridge, MA) Journal of Geophysical Research (ISSN 0148-0227), vol. 89, June 30, 1984, p. 5328-5334. refs

The first year of data from the Nimbus 7 Scanning Multichannel Microwave Radiometer (SMMR), covering the period December 1978 through November 1979, was used to study the monthly mean distributions of precipitable water over the global oceans. The water vapor algorithm is based on a multiple regression technique, utilizing three of the higher frequency channels on SMMR. The results obtained are in good agreement with other independent studies. They reveal features associated with other independent studies. They reveal features associated with the general circulation of the atmosphere and the ocean currents. Samples of monthly and annual distributions of precipitable water over oceans are presented, and their characteristics are discussed. Author

A84-39459*# National Aeronautics and Space Administration, Goddard Space Flight Center, Greenbelt, Md.

A SUMMARY OF RESULTS FROM THE FIRST NIMBUS 7 SMMR OBSERVATIONS

P. GLOERSEN, D. J. CAVALIERI, T. T. WILHEIT, A. T. C. CHANG (NASA, Goddard Space Flight Center, Greenbelt, MD), W. J. CAMPBELL (U.S. Geological Survey, Tacoma, WA), O. M. JOHANNESSEN (Bergen, Universitetet, Bergen, Norway), K. B. KATSAROS (Washington, University, Seattle, WA), K. F. KUNZI (Bern, Universitaet, Berne, Switzerland), D. B. ROSS (NOAA, Sea-Air Interaction Laboratory, Miami, FL), D. STAELIN (MIT, Cambridge, MA) et al. Journal of Geophysical Research (ISSN 0148-0227), vol. 89, June 30, 1984, p. 5335-5344. refs

Selected data obtained during the first year of operation of the scanning multichannel microwave radiometer (SMMR) on board the Nimbus 7 satellite (launched in late October 1978) have been used to calculate, on a global basis, various geophysical parameters over open oceans, polar regions, and terrain. Over open oceans these calculations have provided values for sea surface temperatures, near-surface winds, atmospheric water vapor in a column, and rainfall rates. In polar regions, sea ice concentration,

multiyear ice fraction, and radiating temperatures have been obtained. Finally, the extent and water equivalence of snow cover over terrain have been calculated. These parameters have been compared with in situ measurements of the same geophysical parameters, where available, and the results of these comparisons are described. The self-consistency of the global displays of all the parameters is discussed along with the plans for archiving them for subsequent research purposes. A description of the SMMR calibration and data processing scheme is also given. Author

A84-39461*# National Aeronautics and Space Administration, Goddard Space Flight Center, Greenbelt, Md.

DETERMINATION OF SEA ICE PARAMETERS WITH THE NIMBUS 7 SMMR

D. J. CAVALIERI, P. GLOERSEN (NASA, Goddard Space Flight Center, Laboratory for Atmospheric Sciences, Greenbelt, MD), and W. J. CAMPBELL (U.S. Geological Survey, Tacoma, WA) Journal of Geophysical Research (ISSN 0148-0227), vol. 89, June 30, 1984, p. 5355-5369. NASA-supported research. refs

A method of determining sea ice parameters using Nimbus 7 polarized multispectral radiance data obtained with the Nimbus 7 Scanning Multichannel Microwave Radiometer (SMMR) is presented. Observed radiances from selected areas in the Arctic region for the period February 3-7, 1979 were used in computing algorithm coefficients. Polar maps of sea ice concentration, multiyear fraction, and ice temperature are illustrated for this period. The variation of the mean and standard deviation of ice concentration and multiyear ice fraction for a region of perennial ice cover over the first 11 months of SMMR operation is also presented. Comparisons are made between the calculated sea ice parameters and information obtained from previous studies using aircraft, submarine and surface observations. The absolute accuracy of the SMMR parameters remains uncertain. D.H.

A84-39523

SATELLITE OBSERVED UPPER LEVEL MOISTURE PATTERNS ASSOCIATED WITH TROPICAL CYCLONE MOVEMENT

V. DVORAK (NOAA, National Environmental Satellite, Data, and Information Service, Washington, DC) IN: Conference on Hurricanes and Tropical Meteorology, 15th, Miami, FL, January 9-13, 1984, Postprints. Boston, MA, American Meteorological Society, 1984, p. 163-168.

An examination is conducted of satellite moisture channel pictures of tropical cyclones to determine relationships between upper atmospheric moisture patterns and tropical cyclone motion. Use is made of GOES VAS-6.7 micron pictures taken at 6 hourly intervals. Attention is given to the determination of the characteristics of storms which change direction, the characteristics of nonturning storms, and the development of forecasting techniques. The results of the study indicate that changes in the upper level moisture pattern of a tropical cyclone and its environment can be used to forecast significant changes in its track. G.R.

N84-22955# European Space Agency, Paris (France).

AIRBORNE LIDAR FOR OCEANOGRAPHY AND HYDROLOGY (FLOH)

C. WERNER and H. HERRMANN Jun. 1983 52 p refs Transl. into ENGLISH of "Flugzeuglidar fuer Ozeanog. U. Hydrol." Rept. No. DFVLR-FB-82-14 DFVLR (West Germany), Oberfaffenhoffen Jun. 1982 (ESA-TT-799; DFVLR-FB-82-14) Avail: NTIS HC A04/MF A01; original German version available from DFVLR, Cologne DM 18,10

An airborne lidar for determining water depth, hydrosol distribution, and temperature was designed. The suitability of Nd: YAG and dye lasers for a two laser system is analyzed. Sea bed echo, salinity, Raman scattering temperature measurement, and detectability are discussed. A development program is outlined.

Author (ESA)

05 OCEANOGRAPHY AND MARINE RESOURCES

N84-23084# Academy of Sciences (USSR), Moscow. Soviet Geophysical Comm.

SCIENTIFIC ACTIVITY IN OCEANOGRAPHY, 1979-1982

1983 21 p refs In RUSSIAN and ENGLISH Presented at the 18th Gen. Assembly of the International Union of Geodesy and Geophysics

Avail: NTIS HC A02/MF A01

The most important theoretical and experimental investigations of the physical and geographical problems of the World oceans, completed in the period 1979-1982 by different oceanological institutes of the USSR are reported. The bibliography contains publications (monographs, collected articles, atlases) and it is listed only in Russian. E.A.K.

N84-23085*# Jet Propulsion Lab., California Inst. of Tech., Pasadena.

TOPEX: OBSERVING THE OCEANS FROM SPACE

Jul. 1982 20 p refs

(NASA-CR-173490; JPL-400-133; NAS 1.26:173490) Avail:

NTIS HC A02/MF A01 CSCL 08C

Measurement of global ocean topography by a radar altimeter aboard the TOPEX satellite is discussed. Technical aspects of satellite altimetry as they pertain to the measurement of ocean circulation are described. The TOPEX mission is explained and a general history of oceanography is included. M.A.C.

N84-23087# Royal Australian Navy Research Lab., Edgecliff.

COMPARISONS OF SEA-SURFACE TEMPERATURE OBTAINED FROM SHIP AND SATELLITE DATA

L. J. HAMILTON Oct. 1983 57 p

(AD-A138257; AD-E750826; RANRL-TM(EXT)-8/83) Avail: NTIS

HC A04/MF A01 CSCL 08J

Sea-surface-temperatures (SST) obtained by thermosalinograph on five cruises during the period 23 September 1982 to 30 January 1983 in waters east and north-east of the Australian coastline are compared graphically with SST obtained from three sources of satellite data, GOSSSTCOMP charts (Global Operational Sea Surface Temperature Computation), NWS charts (National Weather Service), and GMS (Geostationary Meteorological Satellite) tables. The data is plotted as temperatures versus cumulative ship distance travelled. For these cruises, fronts and features were seldom discernible in the satellite data but broad scale average trends were well shown. GOSSSTCOMP was found to be the most reliable temperature indicator, often closely following the graph of highly smoothed ship temperature. NWS often tended to follow peak temperatures while GMS often overestimated SST by more than 3 C. Estimates are given on the usefulness of absolute values of satellite SST in real-time analyses. GRA

N84-23089# World Meteorological Organization, Geneva (Switzerland).

INTEGRATED GLOBAL OCEAN SERVICES SYSTEM (IGOSS): GUIDE TO THE IGOSS DATA PROCESSING AND SERVICES SYSTEM

1983 61 p refs Prepared in cooperation with Intergovernmental Oceanographic Commission

(WMO-623; ISBN-92-63-10623-1) Avail: NTIS MF A01; print copy available at WMO, Geneva SWFR 8

The Integrated Global Ocean Services System (IGOSS) for the global collection and exchange of oceanic data and the preparation and dissemination of oceanic data products and services is introduced. The IGOSS data processing and services system (IDPSS) requirements for products and services are outlined. Methods and techniques used for the preparation of oceanographic products, presentation of products, organization and procedures for data collection, quality control and dissemination, implementation of an IDPSS Program in a selected ocean area, and training and assistance available to developing member states are summarized. Author (ESA)

N84-23940# Geological Survey, Washington, D.C.

SATELLITE IMAGE ATLAS OF GLACIERS: THE POLAR REGIONS Abstract Only

R. S. WILLIAMS, JR. and J. G. FERRIGNO *In its* US Geological Survey Polar Res. Symp. p 5 1983

Avail: NTIS HC A04/MF A01; also available from SOD

The Atlas involves 55 glaciologists representing 30 United States, foreign, and international organizations in an effort to produce a benchmark study of the glacierized areas of Earth. LANDSAT images provide the common data base for locating, describing, and mapping: (1) the areal extent of the Antarctic and Greenland ice sheets and ice caps in Iceland, Svalbard, the Russian Arctic islands, and northern Canada; (2) the termini of most large valley glaciers; and (3) the termini of tidal outlet glaciers. A comparison of LANDSAT images with published maps of the Arctic and Antarctic reveals many discrepancies, including incorrect positions of glacier margins, inaccuracies in geographic locations of glaciers, coastlines, and offshore islands. LANDSAT images are used as base maps to plot regional glaciological, geological, and geophysical data up to scales of 1:250,000 for LANDSAT multispectral scanner (MSS) images and up to 1:100,000 for LANDSAT 3 return beam vidicon (RBV) and LANDSAT 4 thematic mapper (TM) images. LANDSAT images have been used, in a time-lapse fashion, to monitor advance or recession of glaciers, to measure the velocity of outlet glaciers, and to monitor fluctuations in proglacial lakes. Because of the brief season and logistical costs and mobility difficulties in polar areas, satellite data are increasingly used to monitor dynamic phenomena in these areas. The Satellite Image Atlas of Glaciers, is representative of the type of multinational cooperative research possible. J.M.S.

N84-23941# Geological Survey, Washington, D.C.

WIND, WAVES AND SWELL IN THE ANTARCTIC MARGINAL ICE ZONE BY SEASAT RADAR ALTIMETER Abstract Only

W. J. CAMPBELL and N. M. MOGNARD (Centre National d'Etudes Spatiales, Toulouse) *In its* US Geological Survey Polar Res. Symp. p 6 1983

Avail: NTIS HC A04/MF A01; also available from SOD

During the Austral winter of 1978, the SEASAT satellite acquired repetitive radar altimeter observations of the oceans surrounding Antarctica. Quasi-synoptic fields of ocean surface wind speed, significant wave height, and significant swell height were computed for the entire three months the satellite operated. The generation, migration, and attenuation of swell in the southern oceans were measured for the first time. Extensive areas of pronounced significant wave height and swell height were found to occur somewhere near the Antarctic marginal ice zone every few days during the winter 1978. During the period 7 to 9 October 1978, storms between Antarctica and Australia and in the eastern South Pacific with surface wind speeds as high as 20 m/s generated large areas with significant wave heights as large as 16 m and significant swell heights as large as 12 m. Extensive wave trains with significant wave height at large as 10 to 12 m and swell as large as 8 to 10 m were observed to impact large areas of the Antarctic marginal ice zone. It is shown that phenomena within the ice can be observed with the radar altimeter. J.M.S.

N84-23956# Geological Survey, Washington, D.C.

GLACIOLOGICAL AND GEOLOGICAL STUDIES OF ANTARCTICA WITH SATELLITE REMOTE SENSING TECHNOLOGY Abstract Only

J. G. FERRIGNO, R. S. WILLIAMS, JR., C. S. SOUTHWORTH, and T. K. MEUNIER *In its* US Geological Survey Polar Res. Symp. p 20-21 1983

Avail: NTIS HC A04/MF A01; also available from SOD

Remotely sensed data were used to support a variety of glaciological and geological investigations in Antarctica. A significant attribute of the LANDSAT image is that it contains the precise time of acquisition, providing a method for making time-lapse measurements of the dynamics of the coast of Antarctica. Two LANDSAT images, 1185-13530 and 2022-13582, respectively, were used to determine the velocity of the terminus of the Pine Island Glacier, tidal outlet glacier on the Walgreen Coast, West Antarctica.

05 OCEANOGRAPHY AND MARINE RESOURCES

LANDSAT images of the Amery Ice Shelf and terminus of the Lambert Glacier were combined as a 1:500,000-scale uncontrolled image mosaic to serve as a base for compilation of 1 and 5 m contours of the shelf derived from 45 SEASAT radar altimeter traverses. The successful experiment reemphasized the fact that satellite image mosaics and maps can be effectively used as the compilation base for various types of geological, glaciological, and geophysical data. LANDSAT images of Antarctica were used to prepare 1:1,000,000 scale planimetric maps of coastal areas, bedrock exposures, and blue-ice areas of Antarctic. Digital processing of LANDSAT multispectral scanner (MSS) images of rock outcrops in Antarctica was used to map rock units from nunatak to nunatak on the basis of their spectral reflectance characteristics.

J.M.S.

N84-23969*# National Aeronautics and Space Administration. Goddard Space Flight Center, Greenbelt, Md.

A COMPARISON OF NUMERICAL RESULTS OF ARCTIC SEA ICE MODELING WITH SATELLITE IMAGES Abstract Only

C. H. LING (Geological Survey, Washington, D.C.) and C. PARKINSON /n Geological Survey US Geological Survey Polar Res. Symp. p 40 1983

Avail: NTIS HC A04/MF A01; also available from SOD CSCL 08L

Observations made from 1972 to 1976 with the Electrically Scanning Microwave Radiometer on board the Nimbus 5 Satellite provide sequential synoptic information of the Arctic sea ice cover. This 4 year data set was used to construct a fairly continuous series of 3 day average 19-GHz passive microwave images which has become a valuable source of polar information, yielding many anticipated and unanticipated discoveries of the sea ice canopy observed in its entirety through the clouds and during the polar night. Interpretation of the passive microwave satellite data set was performed by comparing selected sequential images with correspondin microwave profiles and images acquired by the NASA CV-990 airborne laboratory and with various in situ microwave and physical observations.

Author

N84-23970# National Aeronautics and Space Administration. Goddard Space Flight Center, Greenbelt, Md.

ARCTIC SEA ICE BY PASSIVE MICROWAVE OBSERVATIONS FROM THE NIMBUS-5 SATELLITE Abstract Only

W. J. CAMPBELL (Geological Survey, Washington, D.C.), P. GLOERSON, and H. J. ZWALLY (NASA. Goddard Space Flight Center, Tacoma, Wash.) /n Geological Survey US Geological Survey Polar Res. Symp. p 40-41 1983

Avail: NTIS HC A04/MF A01; also available from SOD CSCL 08L

The results of a dynamic/thermodynamic numerical model of Arctic sea ice are compared with satellite images from the Nimbus 5 electrically scanning microwave radiometer. The model combines aspects of two previous sea ice models those of Parkinson and Washington and Ling, Rasmussen, and Campbell. A solid/fluid model basically follows the formulation of the Parkinson and Washington model with the addition of the constitutive equation and equation of state from the Ling model. The Parkinson and Washington model simulates the seasonal cycle of sea ice thicknesses and concentrations with a horizontal resolution of roughly 200 km and a timestep of 8 hours. The thermodynamics are calculated through energy balances at the interfaces between ice and air, water and ice, and water and air. The ice dynamics are calculated through a momentum equation balancing air stress, water stress, dynamic topography, and Coriolis force, with an adjustment for internal ice resistance.

Author

N84-24065# Science Applications, Inc., San Diego, Calif. Electronic Vision Systems Div.

AVHRR AEROSOL GROUND TRUTH EXPERIMENT Final Report

M. GRIGGS 3 Jan. 1984 44 p refs

(Contract NA83SA-C-00106)

(PB84-157882; SAI-83/1321; NOAA-84021612) Avail: NTIS HC A03/MF A01 CSCL 04A

An experiment was conducted at ten sites around the globe in 1980, using NOAA-6. Advanced Very-High-Resolution Radiometer data and coincident ground truth measurements, to investigate the variability of the relationship that exists between upwelling visible radiance and the aerosol optical thickness in the troposphere over oceans. The esuls of the data for the remaining sites are given. The results are compared.

Author (GRA)

N84-24078*# Jet Propulsion Lab., California Inst. of Tech., Pasadena.

NASA OCEANIC PROCESSES PROGRAM, FISCAL YEAR 1983 Annual Report

R. M. NELSON, ed. and D. C. PIERI, ed. May 1984 144 p refs

(NASA-TM-86248; NAS 1.15:86248; AR-4) Avail: NTIS HC A07/MF A01 CSCL 08C

Accomplishments, activities, and plans are highlighted for studies of ocean circulation, air sea interaction, ocean productivity, and sea ice. Flight projects discussed include TOPEX, the ocean color imager, the advanced RF tracking system, the NASA scatterometer, and the pilot ocean data system. Over 200 papers generated by the program are listed.

A.R.H.

N84-25141*# Washington Univ., Seattle. Polar Science Center. **REMOTE SENSING OF FLOE SIZE DISTRIBUTION AND SURFACE TOPOGRAPHY Final Report**

D. A. ROTHROCK and A. S. THORNDIKE 1984 144 p refs ERTS

(Contract NAG5-160)

(E84-10132; NASA-CR-175155; NAS 1.26:175155) Avail: NTIS HC A07/MF A01 CSCL 08L

Floe size can be measured by several properties p- for instance, area or mean caliper diameter. Two definitions of floe size distribution seem particularly useful. $F(p)$, the fraction of area covered by floes no smaller than p ; and $N(p)$, the number of floes per unit area no smaller than p . Several summertime distributions measured are a graph, their slopes range from -1.7 to -2.5. The variance of an estimate is also calculated.

M.A.C.

N84-25235# Naval Ocean Research and Development Activity, Bay St. Louis, Miss.

ANALYSIS OF AIRBORNE ELECTROMAGNETIC SYSTEMS FOR MAPPING THICKNESS OF SEA ICE Final Report, May - Aug. 1983

A. BECKER, H. MORRISON, and K. SMITS Nov. 1983 41 p (AD-A139786; NORDA-TN-261) Avail: NTIS HC A03/MF A01

CSCL 08L

This report is part of our research program addressing AEM ice thickness determination and will demonstrate that the Navy requirements for rapid airborne methods for mapping ice thickness, in real time, can be accomplished with AEM techniques. At present, there are not reliable airborne techniques for measuring directly sea ice thickness, although impulse radar has yielded promising results by implying sea ice thickness from ice roughness measurements.

05 OCEANOGRAPHY AND MARINE RESOURCES

N84-25238# Kansas Univ. Center for Research, Inc., Lawrence.
Remote Sensing Lab.

MARGINAL ICE ZONE EXPERIMENT (1983). PART 1: ICE CHARACTERIZATION MEASUREMENTS. PART 2. HELICOPTER-BORNE AND SHIP-BASED RADAR BACKSCATTER MEASUREMENT OF SEA ICE IN THE MARGINAL ICE ZONE Technical Report

R. G. ONSTOTT Jan. 1984 30 p

(Contract N00014-76-C-1105)

(AD-A139894; CRINC/RSL-TR-331-32) Avail: NTIS HC A03/MF A01 CSCL 08L

A series of sensor-oriented characterization measurements in support of the experiment's remote sensing efforts from the Polarbjorn ice strengthened ship during the 1983 Marginal Ice Zone Experiment were conducted. Measurements describe the physical properties of the ice in this region and are reported herein. Descriptions include: ice and snow thickness; ice salinity profiles; air, ice and snow temperatures; the construction of the snow pack; and general comments about floe topography. GRA

N84-26232# Virginia Univ., Charlottesville. Dept. of Environmental Sciences.

SATELLITE OBSERVATIONS OF A MONSOON DEPRESSION Final Report

C. WARNER Jun. 1984 103 p refs

(Contract NAG5-297)

(NASA-CR-173590; NAS 1.26:173590) Avail: NTIS HC A06/MF A01 CSCL 04B

The exploration of a monsoon depression over Burma and the Bay of Bengal is discussed. Aircraft and satellite data were examined, with an emphasis on the Microwave Sounding Unit (MSU) aboard TIROS-N and the Scanning Multichannel Microwave Radiometer (SMMR) aboard Nimbus-7. The structure of the monsoon depression was found to be dominated by cumulus convection. The only systematic large scale behavior discerned was a propagation of the depression westward, and diurnal migration of contours of brightness temperature. These contours in the middle troposphere showed a gradient toward the north with the patterns migrating northward at night. From SMMR and dropwindsonde data, water vapor contents were found to be near 65 mm, increasing to more than 70 mm in the northeast Bay of Bengal. Cloud water contents reached about three mm. Rainfall rates exceeding 5.7 mm/h occurred over a small part of the storm area, while mean rainfall rates in areas of order 20,000 sq km reached approximately 0.5 mm/h. Measured MSU brightness temperatures were reconciled very well with dropwindsonde data and with airborne in situ observations of clouds (by photography) and hydrometeors (by radar). Diffuse scattering was determined to be important in computing brightness temperature. R.S.F.

N84-26233# National Aeronautics and Space Administration. Goddard Space Flight Center, Greenbelt, Md.

NIMBUS 7 SMMR DERIVED SEASONAL VARIATIONS IN THE WATER VAPOR, LIQUID WATER AND SURFACE WINDS OVER THE GLOBAL OCEANS

C. PRABHAKARA and D. A. SHORT Apr. 1984 52 p refs (NASA-TM-86080; NAS 1.15:86080) Avail: NTIS HC A04/MF A01 CSCL 04B

Monthly mean distributions of water vapor and liquid water contained in a vertical column of the atmosphere and the surface wind speed were derived from Nimbus Scanning Multichannel Microwave Radiometer (SMMR) observations over the global oceans for the period November 1978 to November 1979. The remote sensing techniques used to estimate these parameters from SMMR are presented to reveal the limitations, accuracies, and applicability of the satellite-derived information for climate studies. On a time scale of the order of a month, the distribution of atmospheric water vapor over the oceans is controlled by the sea surface temperature and the large scale atmospheric circulation. The monthly mean distribution of liquid water content in the atmosphere over the oceans closely reflects the precipitation patterns associated with the convectively and baroclinically active regions. Together with the remotely sensed surface wind speed

that is causing the sea surface stress, the data collected reveal the manner in which the ocean-atmosphere system is operating. Prominent differences in the water vapor patterns from one year to the next, or from month to month, are associated with anomalies in the wind and geopotential height fields. In association with such circulation anomalies the precipitation patterns deduced from the meteorological network over adjacent continents also reveal anomalous distributions.

Author

N84-26235# Wisconsin Univ., Milwaukee. Dept. of Geological/Geophysical Sciences.

DIAGNOSTICS OF RAINFALL ANOMALIES IN THE NORDESTE DURING THE GLOBAL WEATHER EXPERIMENT Semiannual Progress Report

D. N. SIKDAR 1983 9 p refs

(SAPR-1) Avail: NTIS HC A02/MF A01

The rainy season of Northeast Brazil (hereafter called Nordeste) is narrowly centered around March/April and is related to the southern most seasonal migration of the lower tropospheric confluence axis over the adjacent eastern tropical Atlantic. Knowledge of the influences of tropospheric circulations on drought/flood phenomena over the Nordeste is incomplete, mainly due to lack of adequate observations. This gap was narrowed by the special observing systems taken during the operational phase of the Global Weather Experiment. The behavior of the atmosphere-ocean system in the tropics in relation to extremely low rainfall events observed in Nordeste during 1979 are investigated. The observational basis includes the FGGE level IIb data set, satellite images from SMS/GOES, sea surface temperature data from the FGGE level IIb and rainfall records over land. The relationship of the daily variability of large-scale pressure, cloudiness and upper level wind patterns over the Brazil-Atlantic sector during March/April 1979 to rain fall anomalies in northern Nordeste were examined.

B.G.

N84-26255# Instituto de Pesquisas Espaciais, Sao Jose dos Campos (Brazil).

SEASONAL OSCILLATIONS OF THE SUBTROPICAL CONVERGENCE BETWEEN THE BRAZIL AND MALVINAS CURRENTS, USING OCEANOGRAPHIC AND SMS-2 SATELLITE DATA

S. S. DEGODOI (Sao Paulo Univ., Brazil) and M. R. STEVENSON (Inst. for Space Research, Sao Jose dos Campos, Brazil) May 1984 12 p refs Presented at the 15th ISPRS Intern. Soc. for Photogrammetry and Remote Sensing, Rio de Janeiro, 18-20 Jun. 1984

(INPE-3092-PRE/497) Avail: NTIS HC A02/MF A01

Seasonal variations of the Subtropical Convergence (S.C.) between the Brazil Current and Malvinas (Falkland) Current were investigated. Oceanographic and SMS-2 data were utilized for this purpose. Maps of the surface distributions of temperature and salinity were made using oceanographic data. Thermal infrared images were received from the VISSR system aboard the SMS-2 satellite. The satellite data were compared with a Gaussian Model in order to better evaluate thermal distributions. Where oceanographic data were available for comparison with SMS-2 data, the S.C. was located at or near the same position. The SMS-2 satellite data indicated, in the period of January 1980 to March 1981, the occurrence of zonal and latitudinal oscillations of the S.C. In this period, the movement of the S.C. tended to be dominated by its latitudinal fluctuations in relation to its displacement in the zonal direction. Between autumn (April to June) and spring (October to December), the mean migratory velocity in the latitudinal direction was about 1.5 cm/s; while in the zonal direction, the velocity was about 0.7 cm/s. The thermal data obtained from the VISSR system corresponded well with oceanographic data and demonstrated that temperature data from the SMS-2 satellite may be effectively used to detect and monitor the Subtropical Convergence.

Author

05 OCEANOGRAPHY AND MARINE RESOURCES

N84-26256# Instituto de Pesquisas Espaciais, Sao Jose dos Campos (Brazil).

MAPS OF FAVORABLE AREAS FOR TUNA FISHING TO THE SOUTH AND SOUTHEAST OF BRAZIL PREPARED FROM SMS-2 SATELLITE DATA

M. D. M. ABDON May 1984 12 p refs Presented at the 15th ISPRS Intern. Soc. for Photogrammetry and Remote Sensing, Rio de Janeiro, 17-29 Jun. 1984

(INPE-3102-PRE/501) Avail: NTIS HC A02/MF A01

Sea surface temperature intervals suitable for large fish catch of yellowfin tuna, albacore and bigeye tuna were defined in oceanic water to the South and Southeast of Brazil. Maps of favorable fishing areas for these species were prepared for the period of February to July of 1980. In the development of these maps, infrared images received from the SMS-2 satellite were automatically processed by computer on the Image-100 system. The favorable fishing areas and tuna CPUE data of 1980 are compared and it is observed that albacore and bigeye tuna appeared in the southern part of the study area, mainly in Malvinas Current region. Albacore and bigeye tuna CPUE data of the years 1978 and 1979, with sea surface temperature, collected in real time, for a small area influenced by Subtropical Convergence were compared. It is shown that the suitable sea surface temperature intervals for the fishing of these tuna species changes from month to month during the year. E.A.K.

N84-26257# Naval Ocean Research and Development Activity, Bay St. Louis, Miss.

PAME PROCEEDINGS, PATTERN ANALYSIS IN THE MARINE ENVIRONMENT, AN OCEAN SCIENCE AND TECHNOLOGY WORKSHOP Final Report

R. M. BROWN Oct. 1983 289 p Workshop held at Bay St. Louis, Miss., 24-26 Mar. 1982

(AD-A140195; NORDA-TN-176) Avail: NTIS HC A13/MF A01 CSCL 08C

The Pattern Analysis in the Marine Environment (PAME) Workshop Proceedings contains 10 of the papers presented at an Ocean Science and Technology Workshop sponsored by the Chief of Naval Research and hosted by the Naval Ocean Research and Development Activity, NSTL, Mississippi, 24 to 26 March 1982. The PAME Workshop topics ranged from computer science, pattern analysis, and artificial intelligence to specific problem areas, applications, and requirements in ocean science. The workshop was organized in the following five sessions: (1) image analysis techniques; (2) image analysis techniques; (3) pattern analysis techniques; (4) space technology for ocean applications; (5) ocean patterns in space time.

N84-26261# Jet Propulsion Lab., California Inst. of Tech., Pasadena.

THE USE OF SATELLITE OBSERVATIONS OF THE OCEAN SURFACE IN COMMERCIAL FISHING OPERATIONS

D. R. MONTGOMERY In Naval Ocean Res. and Develop. Activity PAME Proc., Pattern Anal. in the Marine Environ., An Ocean Sci. and Technol. Workshop p 121-155 Oct. 1983

(AD-P003120) Avail: NTIS HC A13/MF A01 CSCL 22B

Commercial fishermen are interested in the safety of their crews, boats, and gear, and in making the best catch for their time and money. Rising fuel costs, increased competition from foreign fisheries, improved knowledge about fish habits and the new 200 mile economic zone have all had an impact on the U.S. fishing industry. As a consequence, the modern fisherman, more than ever, requires reliable and timely information about the marine environment. This paper describes an experimental program to utilize satellite observations of the ocean surface, in conjunction with conventional observations and products, to prepare special fisheries aids charts for daily radio facsimile broadcasts to commercial fishermen. These special fisheries products aggregate a broad set of ocean observations, including ocean color structure, to depict oceanographic conditions of importance to commercial fishing tactics. Results to date have shown that improved safety at sea and decreased fuel costs can be achieved through the applied use of these special fisheries charts. Author (GRA)

N84-26263# McQuest Marine Research and Development Co. Ltd., Burlington (Ontario).

APPLICATION OF COMPUTER IMAGE PROCESSING TO UNDERWATER SURVEYS

P. R. PALUZZI In Naval Ocean Res. and Develop. Activity PAME Proc., Pattern Anal. in the Marine Environ., An Ocean Sci. and Technol. Workshop p 173-188 Oct. 1983

(AD-P003122) Avail: NTIS HC A13/MF A01 CSCL 20F

Computer image processing has often come to be equated with automated pattern analysis, particularly within the context of spacecraft remote-sensing. Automated pattern analysis in the form of multispectral classifications has been widely used for crop and lithologic mapping from LANDSAT images. Conversely, bottom photographs and side-scan sonar images collected during underwater surveys have rarely been subjected to automated pattern analysis. Among the reasons for this are limitations of the imaging techniques and complexity in terms of scene and pattern descriptions. It is therefore worthwhile to consider alternatives to pattern analysis for helping interpreters to work with images from underwater surveys. Computer dc notch filtering and geometric rectification by resampling are two key image processing techniques which have proved to be successful in achieving this goal. In addition, since image interpreters often compare bottom photographs and side-scan sonar records to other map based data, namely depth soundings or bathymetry, it is advantageous to also display these data as an image. Finally, while the alternative computer image processing techniques are, by themselves, powerful tools for improving image display, they also show promise for alleviating some of the problems facing automated pattern analysis as applied to underwater survey images. Author (GRA)

N84-26265# Naval Ocean Research and Development Activity, Bay St. Louis, Miss.

PRINCIPAL COMPONENTS AS A METHOD FOR ATMOSPHERICALLY CORRECTING COASTAL ZONE COLOR SCANNER DATA

R. J. HOLYER In its PAME Proc., Pattern Anal. in the Marine Environ., An Ocean and Technol. Workshop p 199-223 Oct. 1983

(AD-P003124) Avail: NTIS HC A13/MF A01 CSCL 12A

The Coastal Zone Color Scanner (CZCS) images the Earth's oceans in five visible/near-IR spectral bands. In the visible portion of the electromagnetic spectrum, satellite observed radiance typically consists of approximately 90% of atmospheric backscatter and 10% of ocean-scattered radiance. Subtle color signatures associated with oceanic features are frequently masked by this atmospheric path radiance. Accurate atmospheric correction of CZCS data is, therefore, a prerequisite to optimum information extraction from this imagery. The most widely accepted atmospheric correction scheme for CZCS data, based on a single scattering model of the atmosphere plus certain assumed optical properties of the ocean, has several inherent drawbacks that limit its effectiveness. Principal Components Analysis, a common pattern recognition tool, is offered as an alternate atmospheric correction scheme based upon a statistical rather than a modeling approach. The principal components method is applied to a representative CZCS data set and a comparison is made with corrections derived by the modeling method. Author (GRA)

N84-26266# Naval Oceanographic Office, Bay St. Louis, Miss.

WATER MASS CLASSIFICATION IN THE NORTH ATLANTIC USING IR DIGITAL DATA AND BAYESIAN DECISION THEORY

R. E. COULTER In Naval Ocean Res. and Develop. Activity PAME Proc., Pattern Anal. in the Marine Environ., An Ocean Sci. and Technol. Workshop p 225-236 Oct. 1983

(AD-P003125) Avail: NTIS HC A13/MF A01 CSCL 12A

A method is described which utilizes Bayesian decision theory and historical statistics of sea surface temperature to classify surface water masses and ocean fronts from satellite derived infrared data. Probabilities that certain features occur are determined from the normal distributions of specific statistical characteristics, known a priori, and the same characteristics computed from satellite data. The better the match between the

05 OCEANOGRAPHY AND MARINE RESOURCES

a priori information associated with a feature and the computed statistics, the higher the probability that the feature exists. The maximum probability determined by Baye's theory is subjected to two tests, based on absolute and relative threshold values, to reduce the chance of incorrect classification. The method was used for classifying satellite IR data to locate the major water masses in the Gulf Stream region. Results were compared to frontal positions obtained by conventional, subjective means.

Author (GRA)

N84-27262*# National Aeronautics and Space Administration. Marshall Space Flight Center, Huntsville, Ala.

FRONTIERS OF REMOTE SENSING OF THE OCEANS AND TROPOSPHERE FROM AIR AND SPACE PLATFORMS

Washington May 1984 615 p refs Symp. held in Shoresh, Israel, 14-23 May 1984; sponsored in cooperation with the Israel Academy of Sciences and Humanities (NASA-CP-2303; NAS 1.55:2303) Avail: NTIS HC A99/MF A01 CSCL 08C

Several areas of remote sensing are addressed including: future satellite systems; air-sea interaction/wind; ocean waves and spectra/S.A.R.; atmospheric measurements (particulates and water vapor); synoptic and weather forecasting; topography; bathymetry; sea ice; and impact of remote sensing on synoptic analysis/forecasting.

N84-27263*# Applied Physics Lab., Johns Hopkins Univ., Laurel, Md.

REMOTE SENSING FOR OCEANOGRAPHY: PAST, PRESENT, FUTURE

L. F. MCGOLDRICK *In* NASA. Marshall Space Flight Center Frontiers of Remote Sensing of the Oceans and Troposphere from Air and Space Platforms p 1-10 May 1984

Avail: NTIS HC A99/MF A01 CSCL 08C

Oceanic dynamics was traditionally investigated by sampling from instruments *in situ*, yielding quantitative measurements that are intermittent in both space and time; the ocean is undersampled. The need to obtain proper sampling of the averaged quantities treated in analytical and numerical models is at present the most significant limitation on advances in physical oceanography. Within the past decade, many electromagnetic techniques for the study of the Earth and planets were applied to the study of the ocean. Now satellites promise nearly total coverage of the world's oceans using only a few days to a few weeks of observations. Both a review of the early and present techniques applied to satellite oceanography and a description of some future systems to be launched into orbit during the remainder of this century are presented. Both scientific and technologic capabilities are discussed.

Author

N84-27264*# European Space Technology Center, Noordwijk (Netherlands).

ESA ACTIVITIES IN THE USE OF MICROWAVES FOR THE REMOTE SENSING OF THE EARTH

D. MACCOLL *In* NASA. Marshall Space Flight Center Frontiers of Remote Sensing of the Oceans and Troposphere from Air and Space Platforms p 11-17 May 1984

Avail: NTIS HC A99/MF A01 CSCL 08G

The program of activities under way in the European Space Agency (ESA) directed towards Remote Sensing of the oceans and troposphere is discussed. The initial project is the launch of a satellite named ERS-1 with a primary payload of microwave values in the C- and Ku-bands. This payload is discussed in depth. The secondary payload includes precision location experiments and an instrument to measure sea surface temperature, which are described. The important topic of calibration is extensively discussed, and a review of activities directed towards improvements to the instruments for future satellites is presented. Some discussion of the impact of the instrument payload on the spacecraft design follows and the commitment of ESA to the provision of a service of value to the ultimate user is emphasized.

Author

N84-27266*# National Aeronautics and Space Administration. Goddard Space Flight Center, Greenbelt, Md.

HIGH RESOLUTION OBSERVATIONS OF LOW CONTRAST PHENOMENA FROM AN ADVANCED GEOSYNCHRONOUS PLATFORM (AGP)

M. S. MAXWELL *In* NASA. Marshall Space Flight Center Frontiers of Remote Sensing of the Oceans and Troposphere from Air and Space Platforms p 29-40 May 1984 refs

Avail: NTIS HC A99/MF A01 CSCL 05B

Present technology allows radiometric monitoring of the Earth, ocean and atmosphere from a geosynchronous platform with good spatial, spectral and temporal resolution. The proposed system could provide a capability for multispectral remote sensing with a 50 m nadir spatial resolution in the visible bands, 250 m in the 4 micron band and 1 km in the 11 micron thermal infrared band. The diffraction limited telescope has a 1 m aperture, a 10 m focal length (with a shorter focal length in the infrared) and linear and area arrays of detectors. The diffraction limited resolution applies to scenes of any brightness but for a dark low contrast scenes, the good signal to noise ratio of the system contribute to the observation capability. The capabilities of the AGP system are assessed for quantitative observations of ocean scenes. Instrument and ground system configuration are presented and projected sensor capabilities are analyzed.

Author

N84-27267*# National Aeronautics and Space Administration. Goddard Space Flight Center, Greenbelt, Md.

REMOTE SENSING OF AIR-SEA INTERACTIONS

D. ATLAS and E. MOLLO-CHRISTENSEN *In* NASA. Marshall Space Flight Center Frontiers of Remote Sensing of the Oceans and Troposphere from Air and Space Platforms p 41-49 May 1984 refs

Avail: NTIS HC A99/MF A01 CSCL 04A

A number of preliminary concepts for the measurement or inference of fluxes across the air-sea interface through remote sensing are proposed. All the methods are achievable from aircraft with state-of-the-art technology. Only one is now ready for space implementation. The focus is on cold outbreaks. Sensible (latent) heat flux is inferred from the difference between initial surface air temperature (vapor mixing ratio) and the downwind SST (and corresponding saturation mixing ratio). The downwind growth rate of the PBL as measured by lidar also provides estimates of surface heating and the cross-inversion entrainment velocity. The lidar also provides a measure of the depth of the inversion and its penetration by surface-forced convection; this permits estimates of the surface heat flux. Lidar and radiometric measurements of cloud top height and temperature provide means of deducing the temperature sounding downstream so that heating is computed with the aid of a known sounding upstream.

Author

N84-27268*# Washington Univ., Seattle. Dept. of Atmospheric Sciences.

SCATTEROMETER CAPABILITIES IN REMOTELY SENSING GEOPHYSICAL PARAMETERS OVER THE OCEAN: THE STATUS AND THE POSSIBILITIES

R. A. BROWN *In* NASA. Marshall Space Flight Center Frontiers of Remote Sensing of the Oceans and Troposphere from Air and Space Platforms p 51-56 May 1984

Avail: NTIS HC A99/MF A01 CSCL 08C

Extensive comparison between surface measurements and satellite Scatt signal and predicted winds show successful wind and weather analysis comparable with conventional weather service analyses. However, in regions often of the most interest, e.g., fronts and local storms, inadequacies in the latter fields leaves an inability to establish the satellite sensor capabilities. Thus, comparisons must be made between wind detecting measurements and other satellite measurements of clouds, moisture, waves or any other parameter which responds to sharp gradients in the wind. At least for the windfields and the derived surface pressure field analysis, occasional surface measurements are required to anchor and monitor the satellite analyses. Their averaging times must be made compatible with the satellite sensor measurement. Careful attention must be paid to the complex fields which contain

05 OCEANOGRAPHY AND MARINE RESOURCES

many scales of turbulence and coherent structures affecting the averaging process. The satellite microwave system is capable of replacing the conventional point observation/numerical analysis for the ocean weather.

B.G.

N84-27269*# Jet Propulsion Lab., California Inst. of Tech., Pasadena.

A NEW PARAMETERIZATION OF AN EMPIRICAL MODEL FOR WIND/OCEAN SCATTEROMETRY

P. M. WOICESHYN, M. G. WURTELE (California Univ., Los Angeles), D. H. BOGGS (DB Systems Ltd., La Canada, Calif.), L. F. MCGOLDRICK (APL, Laurel, Md.), and S. PETEHERYCH (Atmospheric Environment Service, Downsview, Ontario) *In NASA*. Marshall Space Flight Center Frontiers of Remote Sensing of the Oceans and Troposphere from Air and Space Platforms p 57-74 May 1984 refs

(Contract NAS7-918)

Avail: NTIS HC A99/MF A01 CSCL 04A

The power law form of the SEASAT A Scatterometer System (SASS) empirical backscatter-to-wind model function does not uniformly meet the instrument performance over the range 4 to 24 m/s. Analysis indicates that the horizontal polarization (H-Pol) and vertical polarization (V-Pol) components of the benchmark SASS1 model function yield self-consistent results only for a small mid-range of speeds at larger incidence angles, and for a somewhat larger range of speeds at smaller incidence angles. Comparison of SASS1 to in situ data over the Gulf of Alaska region further underscores the shortcomings of the power law form. Finally, a physically based empirical SASS model is proposed which corrects some of the deficiencies of power law models like SASS1. The new model allows the mutual determination of sea surface wind stress and wind speed in a consistent manner from SASS backscatter measurements.

B.G.

N84-27272*# Remote Sensing Systems, Sausalito, Calif.

NEW ALGORITHMS FOR MICROWAVE MEASUREMENTS OF OCEAN WINDS

F. J. WENTZ and S. PETEHERYCH (Atmospheric Environment Service, Downsview, Ontario) *In NASA*. Marshall Space Flight Center Frontiers of Remote Sensing of the Oceans and Troposphere from Air and Space Platforms p 105-114 May 1984 refs

(Contract NASW-3606; N00014-83-C-0520)

Avail: NTIS HC A99/MF A01 CSCL 20N

Improved second generation wind algorithms are used to process the three month SEASAT SMMR and SASS data sets. The new algorithms are derived without using in situ anemometer measurements. All known biases in the sensors prime measurements are removed, and the algorithms prime model functions are internally self-consistent. The computed SMMR and SASS winds are collocated and compared on a 150 km cell-by-cell basis, giving a total of 115444 wind comparisons. The comparisons are done using three different sets of SMMR channels. When the 6.6H SMMR channel is used for wind retrieval, the SMMR and SASS winds agree to within 1.3 m/s over the SASS primary swath. At nadir where the radar cross section is less sensitive to wind, the agreement degrades to 1.9 m/s. The agreement is very good for winds from 0 to 15 m/s. Above 15 m/s, the off-nadir SASS winds are consistently lower than the SMMR winds, while at nadir the high SASS winds are greater than SMMR's. When 10.7H is used for the SMMR wind channel, the SMMR/SASS wind comparisons are not quite as good. When the frequency of the wind channel is increased to 18 GHz, the SMMR/SASS agreement substantially degrades to about 5 m/s.

Author

N84-27273*# Dornier-Werke G.m.b.H., Friedrichshafen (West Germany). Space Programme Dept.

OCEAN WIND FIELD MEASUREMENT PERFORMANCE OF THE ERS-1 SCATTEROMETER

P. HANS and H. SCHUESSLER *In NASA*. Marshall Space Flight Center Frontiers of Remote Sensing of the Oceans and Troposphere from Air and Space Platforms p 115-122 May 1984

Avail: NTIS HC A99/MF A01 CSCL 04B

The Active Microwave Instrumentation (AMI), which will be implemented on the ERS-1, is a 5.3 GHz multipurpose radar for land surface imaging, ocean wave spectrum measurement and wind observations over oceans. The imaging and wave measurements apply Synthetic Aperture Radar (SAR) techniques, while wind field detection is performed by the Scatterometer as part of the AMI. The Scatterometer system design was developed and optimized with the aid of a performance simulator. This paper, aimed at giving an overview, is presented about the: (1) ERS-1 Scatterometer system design; (2) Error budget; and the (3) Overall calibration concept.

M.A.C.

N84-27274*# Canada Centre for Remote Sensing, Ottawa (Ontario).

THEORY AND MEASURE OF CERTAIN IMAGE NORMS IN SAR

R. K. RANEY *In NASA*. Marshall Space Flight Center Frontiers of Remote Sensing of the Oceans and Troposphere from Air and Space Platforms p 123-136 May 1984 refs

Avail: NTIS HC A99/MF A01 CSCL 17I

The principal properties of synthetic aperture radar SAR imagery of point and distributed objects are summarized. Against this background, the response of a SAR (Synthetic Aperture Radar) to the moving surface of the sea is considered. Certain conclusions are drawn as to the mechanism of interaction between microwaves and the sea surface. Focus and speckle spectral tests may be used on selected SAR imagery for areas of the ocean. The fine structure of the sea imagery is sensitive to processor focus and adjustment. The ocean reflectivity mechanism must include point like scatterers of sufficient radar cross section to dominate the return from certain individual resolution elements. Both specular and diffuse scattering mechanisms are observed together, to varying degree. The effect is sea state dependent. Several experiments are proposed based on imaging theory that could assist in the investigation of reflectivity mechanisms.

M.A.C.

N84-27275*# Stanford Univ., Calif. Center for Radar Astronomy.

SYNTHETIC APERTURE RADAR IMAGES OF OCEAN WAVES, THEORIES OF IMAGING PHYSICS AND EXPERIMENTAL TESTS

J. F. VESECKY, S. L. DURDEN, M. P. SMITH, and D. A. NAPOLITANO *In NASA*. Marshall Space Flight Center Frontiers of Remote Sensing of the Oceans and Troposphere from Air and Space Platforms p 137-148 May 1984 refs Sponsored by NASA and ONR

Avail: NTIS HC A99/MF A01 CSCL 17I

The physical mechanism for the synthetic Aperture Radar (SAR) imaging of ocean waves is investigated through the use of analytical models. The models are tested by comparison with data sets from the SEASAT mission and airborne SAR's. Dominant ocean wavelengths from SAR estimates are biased towards longer wavelengths. The quasispecular scattering mechanism agrees with experimental data. The Doppler shift for ship wakes is that of the mean sea surface.

M.A.C.

05 OCEANOGRAPHY AND MARINE RESOURCES

N84-27276*# Nebraska Univ., Lincoln. Dept. of Electrical Engineering.

OPTIMUM BACKSCATTER CROSS SECTION OF THE OCEAN AS MEASURED BY SYNTHETIC APERTURE RADARS

E. BAHAR, C. L. RUFENACH (NOAA, Boulder, Colo.), D. BARRICK (NOAA, Boulder, Colo.), and M. A. FITZWATER *In NASA. Marshall Space Flight Center Frontiers of Remote Sensing of the Oceans and Troposphere from Air and Space Platforms* p 149-158 May 1984 refs Submitted for publication

(Contract DAAG29-83-K-0123)

Avail: NTIS HC A99/MF A01 CSCL 17I

The interaction of the radar signals from Synthetic Aperture Radar (SAR) and Side Looking Airborne Radar (SLAR) is particularly important for the ocean surface where the radar modulation can yield information about the long ocean wave field. Radar modulation measurements from fixed platforms are made in wavetanks and the open oceans. The surfaces are described in terms of two scale models. The radar modulation is considered to be principally due to: (1) geometrical tilt due to the slope of the long ocean waves, and (2) the straining of the short waves (by hydrodynamic interaction). For application to moving platforms, this modulation needs to be described in terms of a general geometry for both like and cross polarization since the long ocean waves, in general, travel in arbitrary directions. The finite resolution of the radar is considered for tilt modulation with hydrodynamic effects neglected.

M.A.C.

N84-27277*# Applied Physics Lab., Johns Hopkins Univ., Laurel, Md.

TRACKING OCEAN WAVE SPECTRUM FROM SAR IMAGES

A. D. GOLDFINGER, R. C. BEAL, F. M. MONALDO, and D. G. TILLEY *In NASA. Marshall Space Flight Center Frontiers of Remote Sensing of the Oceans and Troposphere from Air and Space Platforms* p 159-168 May 1984 refs

Avail: NTIS HC A99/MF A01 CSCL 17I

An end to end algorithm for recovery of ocean wave spectral peaks from Synthetic Aperture Radar (SAR) images is described. Current approaches allow precisions of 1 percent in wave number, and 0.6 deg in direction.

M.A.C.

N84-27278*# National Oceanic and Atmospheric Administration, Boulder, Colo. Wave Propagation Lab.

SAR IMAGERY OF OCEAN-WAVE SWELL TRAVELING IN AN ARBITRARY DIRECTION

C. L. RUFENACH, R. A. SHUCHMAN (ERIM, Ann Arbor), and D. R. LYZENGA (ERIM, Ann Arbor) *In NASA. Marshall Space Flight Center Frontiers of Remote Sensing of the Oceans and Troposphere from Air and Space Platforms* p 169-178 May 1984 refs

(Contract NASA ORDER W-15084; N00014-81-C-0692)

Avail: NTIS HC A99/MF A01 CSCL 17I

The intensity wave like patterns observed in Synthetic Aperture Radar (SAR) are known to be caused by two mechanisms: the microwave radar cross sectional amplitude modulation due to tilt and hydrodynamic interaction of the long ocean waves, and intensity modulation due to the motion of the long ocean waves. Two dimensional closed form expressions of intensity wave patterns based on ocean wave swell are developed. They illustrate the relative importance of the amplitude and motion modulations; they also show that velocity bunching and a distortion due to the phase velocity of the ocean wave field are independent of the focus adjustment, provided that the second order temporal effects are neglected. Second order effects are small only over a limited range of ocean/radar parameters.

M.A.C.

N84-27279*# Royal Norwegian Council for Scientific and Industrial Research, Kjeller. Environmental Surveillance Technology Programme.

OCEAN WAVES AND TURBULENCE AS OBSERVED WITH AN ADAPTIVE COHERENT MULTIFREQUENCY RADAR

D. T. GJESSING and J. HJELMSTAD *In NASA. Marshall Space Flight Center Frontiers of Remote Sensing of the Oceans and Troposphere from Air and Space Platforms* p 179-191 May 1984 refs

Avail: NTIS HC A99/MF A01 CSCL 17I

An adaptive coherent multifrequency radar system is developed for several applications. The velocity distribution (Doppler spectrum) and spectral intensity of 15 different irregularity scales (waves and turbulence) can be measured simultaneously. Changing the azimuth angle of the antennas at regular intervals, the directivity of the wave/turbulence pattern on the sea surface can also be studied. A series of measurements for different air/sea conditions are carried out from a coast based platform. Experiments in the Atlantic are also performed with the same equipment making use of the NASA Electra aircraft. The multifrequency radar allows the measurement of the velocity distribution ("coherent and incoherent component") associated with 15 different ocean irregularity scales simultaneously in a directional manner. It is possible to study the different air/sea mechanisms in some degree of detail. M.A.C.

N84-27280*# Naval Research Lab., Washington, D. C.

THE DUAL-FREQUENCY SCATTEROMETER REEXAMINED

W. J. PLANT and A. B. REEVES *In NASA. Marshall Space Flight Center Frontiers of Remote Sensing of the Oceans and Troposphere from Air and Space Platforms* p 193-198 May 1984 refs

Avail: NTIS HC A99/MF A01 CSCL 14B

The utility of dual frequency scatterometers in measuring ocean wave directional spectra can be increased by adding third frequency to the system. The background which effectively limits signal detectability in dual frequency operation can be made a part of the signal through the addition of this third frequency. Signal detectability is limited only by system thermal noise and space based operation becomes more feasible.

M.A.C.

N84-27281*# Naval Research Lab., Washington, D. C.

AN IMPROVED DUAL-FREQUENCY TECHNIQUE FOR THE REMOTE SENSING OF OCEAN CURRENTS AND WAVE SPECTRA

D. L. SCHULER and W. P. ENG *In NASA. Marshall Space Flight Center Frontiers of Remote Sensing of the Oceans and Troposphere from Air and Space Platforms* p 199-214 May 1984 refs

Avail: NTIS HC A99/MF A01 CSCL 08C

A two frequency microwave radar technique for the remote sensing of directional ocean wave spectra and surface currents is investigated. This technique is conceptually attractive because its operational physical principle involves a spatial electromagnetic scattering resonance with a single, but selectable, long gravity wave. Multiplexing of signals having different spacing of the two transmitted frequencies allows measurements of the entire long wave ocean spectrum to be carried out. A new scatterometer is developed and experimentally tested which is capable of making measurements having much larger signal/background values than previously possible. This instrument couples the resonance technique with coherent, frequency agility radar capabilities. This scatterometer is presently configured for supporting a program of surface current measurements.

M.A.C.

05 OCEANOGRAPHY AND MARINE RESOURCES

N84-27282*# National Aeronautics and Space Administration.

Langley Research Center, Hampton, Va.

MEASUREMENTS OF OCEAN WAVE SPECTRA AND MODULATION TRANSFER FUNCTION WITH THE AIRBORNE TWO FREQUENCY SCATTEROMETER

D. E. WEISSMAN (Hcstra Univ.) and J. W. JOHNSON *In NASA*. Marshall Space Flight Center Frontiers of Remote Sensing of the Oceans and Troposphere from Air and Space Platforms p 215-232 May 1984 refs

(Contract NAGW-468)

Avail: NTIS HC A99/MF A01 CSCL 08C

The directional spectrum and the microwave modulation transfer function of ocean waves can be measured with the airborne two frequency scatterometer technique. Similar to tower based observations, the aircraft measurements of the Modulation Transfer Function (MTF) show that it is strongly affected by both wind speed and sea state. Also detected are small differences in the magnitudes of the MTF between downwind and upwind radar look directions, and variations with ocean wavenumber. The MTF inferred from the two frequency radar is larger than that measured using single frequency, wave orbital velocity techniques such as tower based radars or ROWS measurements from low altitude aircraft. Possible reasons for this are discussed. The ability to measure the ocean directional spectrum with the two frequency scatterometer, with supporting MTF data, is demonstrated.

M.A.C.

N84-27283*# National Aeronautics and Space Administration. Goddard Space Flight Center, Greenbelt, Md.

SOME CASE STUDIES OF OCEAN WAVE PHYSICAL PROCESSES UTILIZING THE GSFC AIRBORNE RADAR OCEAN WAVE SPECTROMETER

F. C. JACKSON *In NASA*. Marshall Space Flight Center Frontiers of Remote Sensing of the Oceans and Troposphere from Air and Space Platforms p 233-245 May 1984 refs

Avail: NTIS HC A99/MF A01 CSCL 08C

The NASA K sub u band Radar Ocean Wave Spectrometer (ROWS) is an experimental prototype of a possible future satellite instrument for low data rate global waves measurements. The ROWS technique, which utilizes short pulse radar altimeters in a conical scan mode near vertical incidence to map the directional slope spectrum in wave number and azimuth, is briefly described. The potential of the technique is illustrated by some specific case studies of wave physical processes utilizing the aircraft ROWS data. These include: (1) an evaluation of numerical hindcast model performance in storm sea conditions, (2) a study of fetch limited wave growth, and (3) a study of the fully developed sea state. Results of these studies, which are briefly summarized, show how directional wave spectral observations from a mobile platform can contribute enormously to our understanding of wave physical processes.

Author

N84-27284*# National Aeronautics and Space Administration. Goddard Space Flight Center, Greenbelt, Md.

NON-GAUSSIAN STATISTICAL MODELS OF SURFACE WAVE FIELDS FOR REMOTE SENSING APPLICATIONS

N. E. HUANG *In NASA*. Marshall Space Flight Center Frontiers of Remote Sensing of the Oceans and Troposphere from Air and Space Platforms p 247-255 May 1984 refs

Avail: NTIS HC A99/MF A01 CSCL 08C

Based on the complete Stokes wave model with the bias term and using a simple mapping approach and an iteration solution method, we established a formula for the joint probability density function of the surface slope elevation of a nonlinear random wave field. The formula requires three parameters to define the whole density function: the rms surface elevation and slope values and the significant slope. This model represents the dynamics of the wave in a more direct way than the Gram-Charlier approximation. Based on this new statistical model and laboratory experiments, formula and numerical values of EM bias and dynamics bias are derived. The results indicate that various biases should be considered seriously if accuracy of the altimeter measurement is required in centimeter range.

Author

N84-27285*# Universite Catholique de Louvain (Belgium). Faculte des Sciences Appliquees.

A TENTATIVE UNIFIED SEA MODEL FOR SCATTERING AND EMISSION Abstract Only

A. GUSSARD and P. SOBIESKI *In NASA*. Marshall Space Flight Center Frontiers of Remote Sensing of the Oceans and Troposphere from Air and Space Platforms p 257 May 1984 refs

Avail: NTIS HC A99/MF A01 CSCL 08C

This work is an attempt to relate active and passive observations of the sea surface to each other, considering that more information can be obtained from a set of instruments when they are not just considered as a juxtaposition of separate and independent boxes, but as a single complex instrument. A careful review of several approaches to the solution of the scattering problem for a random rough surface has been performed. Inherent simplifications, and inconsistencies, are pointed out. To reduce the computation time to reasonable values, an approximate model is selected and some numerical results will be presented in order to illustrate the benefit that can be gained by a unified approach.

B.W.

N84-27288*# Massachusetts Univ., Amherst. Dept. of Electrical and Computer Engineering.

MICROWAVE REMOTE SENSING OF OCEAN SURFACE WIND SPEED AND RAIN RATES OVER TROPICAL STORMS

C. T. SWIFT, D. C. DEHORITY, P. G. BLACK (NOAA, Miami, Fla.), and J. Z. CHIEN (Tsinghua Univ., China) *In NASA*. Marshall Space Flight Center Frontiers of Remote Sensing of the Oceans and Troposphere from Air and Space Platforms p 281-286 May 1984 refs

Avail: NTIS HC A99/MF A01 CSCL 04B

The value of using narrowly spaced frequencies within a microwave band to measure wind speeds and rain rates over tropical storms with radiometers is reviewed. The technique focuses on results obtained in the overflights of Hurricane Allen during 5 and 8 of August, 1980.

Author

N84-27289*# National Aeronautics and Space Administration. Goddard Space Flight Center, Greenbelt, Md.

ALTIMETER HEIGHT MEASUREMENT ERRORS INTRODUCED BY THE PRESENCE OF VARIABLE CLOUD AND RAIN ATTENUATION

F. M. MONALDO, J. GOLDHIRSH, and E. J. WALSH *In NASA*. Marshall Space Flight Center Frontiers of Remote Sensing of the Oceans and Troposphere from Air and Space Platforms p 287-296 May 1984 refs Prepared in cooperation with APL, Laurel, Md.

Avail: NTIS HC A99/MF A01 CSCL 20N

It has recently been recognized that spatially inhomogeneous clouds and rain can substantially affect the height precision obtainable from a spaceborne radar altimeter system. Through computer simulation, it has been found that typical levels of cloud and rain intensities and associated spatial variabilities may degrade altimeter precision at 13.5 GHz and, in particular, cause severe degradation at 35 GHz. This degradation in precision is a result of radar signature distortion caused by variable attenuation over the beam limited altimeter footprint. Because attenuation effects increase with frequency, imprecision caused by them will significantly impact on the frequency selection of future altimeters. In this paper the degradation of altimeter precision introduced by idealized cloud and rain configurations as well as for a realistic rain configuration as measured with a ground based radar is examined.

B.W.

05 OCEANOGRAPHY AND MARINE RESOURCES

N84-27290*# Applied Physics Lab., Johns Hopkins Univ., Laurel, Md.

IMPROVED RESOLUTION RAIN MEASUREMENTS FROM SPACEBORNE RADAR ALTIMETERS

J. GOLDHIRSH and F. M. MONALDO *In NASA*. Marshall Space Flight Center Frontiers of Remote Sensing of the Oceans and Troposphere from Air and Space Platforms p 297-306 May 1984 refs Sponsored by NASA. Goddard Space Flight Center and NASA. Wallops Flight Center

Avail: NTIS HC A99/MF A01 CSCL 20N

Rain measurement of the type described here are considered vital from the standpoint of representing a flag for altimeter data that may be corrupted by rain. It also provides sorely needed rain data over the oceans where little or no such data is available. It is demonstrated that improved resolution measurements of precipitation may be obtained from satellite borne radars with antenna beams having relatively large surface footprints. The method employs deconvolution and Fourier transform procedures, and assumes a knowledge of the antenna beam pattern. As an example, the technique is specifically directed towards the application of future spaceborne radar altimeters which may contain additional range gates to enable the measurement of rain at altitude. It is demonstrated that because of the natural variability of rain in the lateral extent, the standard beam averaging over the footprint could easily produce erroneous interpretations of the intensity of rain and its extent. On the other hand, many of these ambiguities may be removed employing the deconvolution techniques described.

Author

N84-27296*# National Oceanic and Atmospheric Administration, Seattle, Wash. Pacific Marine Environmental Lab.

THE VARIABILITY OF THE SURFACE WIND FIELD IN THE EQUATORIAL PACIFIC OCEAN: CRITERIA FOR SATELLITE MEASUREMENTS

D. HALPERN *In NASA*. Marshall Space Flight Center Frontiers of Remote Sensing of the Oceans and Troposphere from Air and Space Platforms p 357-366 May 1984 refs

Avail: NTIS HC A99/MF A01 CSCL 04B

The natural variability of the equatorial Pacific surface wind field is described from long period surface wind measurements made at three sites along the equator (95 deg W, 109 deg 30 W, 152 deg 30 W). The data were obtained from surface buoys moored in the deep ocean far from islands or land, and provide criteria to adequately sample the tropical Pacific winds from satellites.

E.A.K.

N84-27297*# National Oceanic and Atmospheric Administration, Washington, D. C. National Environmental Satellite, Data, and Information Service.

RECENT ADVANCES IN MULTISPECTRAL SENSING OF OCEAN SURFACE TEMPERATURE FROM SPACE

E. P. MCCLAIN *In NASA*. Marshall Space Flight Center Frontiers of Remote Sensing of the Oceans and Troposphere from Air and Space Platforms p 367-376 May 1984 refs

Avail: NTIS HC A99/MF A01 CSCL 08C

Visual and infrared measurements from the five channel AVHRR on the NOAA-7 satellite are used operationally to derive sea surface temperatures. The multichannel data perform daytime and nighttime cloud detection tests, and the several atmospheric window channels in the thermal infrared correct for atmospheric attenuation. Monitoring of the sea surface temperature product with buoy data indicates stability in mean bias and rms difference with little variation by season or geographic area. Global mapping enables the derivation of monthly mean isotherms, monthly and annual changes, and anomaly patterns relative to climatology. Problems are associated with noise in the 3.7 micro m window channel, and with the injection of substantial volcanic aerosol into the stratosphere by the El Chichon eruption. Multichannel sea surface temperature charts are used to study phenomena such as equatorial long waves and the recent El Nino episode.

E.A.K.

N84-27298*# Applied Physics Lab., Johns Hopkins Univ., Laurel, Md.

SATELLITE TECHNIQUES FOR DETERMINING THE GEOPOTENTIAL FOR SEA-SURFACE ELEVATIONS

V. L. PISACANE *In NASA*. Marshall Space Flight Center Frontiers of Remote Sensing of the Oceans and Troposphere from Air and Space Platforms p 377-388 May 1984 refs

Avail: NTIS HC A99/MF A01 CSCL 08C

Spaceborne altimetry with measurement accuracies of a few centimeters which has the potential to determine sea surface elevations necessary to compute accurate three-dimensional geostrophic currents from traditional hydrographic observation is discussed. The limitation in this approach is the uncertainties in knowledge of the global and ocean geopotentials which produce satellite and height uncertainties about an order of magnitude larger than the goal of about 10 cm. The quantitative effects of geopotential uncertainties on processing altimetry data are described. Potential near term improvements, not requiring additional spacecraft, are discussed. Even though there are substantial improvements at the longer wavelengths, the oceanographic goal will be achieved. The geopotential research mission (GRM) is described which should produce geopotential models that are capable of defining the ocean geoid to 10 cm and near-Earth satellite position. The state of the art and the potential of spaceborne gravimetry is described as an alternative approach to improve our knowledge of the geopotential.

E.A.K.

N84-27299*# Naval Ocean Research and Development Activity, Bay St. Louis, Miss. Remote Sensing Branch.

THE SATELLITE ALTIMETER AS A PLATFORM FOR OBSERVATION OF THE OCEANIC MESOSCALE Abstract Only

J. L. MITCHELL *In NASA*. Marshall Space Flight Center Frontiers of Remote Sensing of the Oceans and Troposphere from Air and Space Platforms p 389 May 1984

Avail: NTIS HC A99/MF A01 CSCL 08C

The use of the satellite radar altimeter as a platform to provide synoptic monitoring of the oceanic mesoscale is faced with two critical issues: removal of geoid error or contamination and election of optimum space/time sampling strategies. Long wavelength orbit determination errors are not critical problems for altimeter measurements of the basin scale circulation. Both issues are addressed within the constraints provided by orbital mechanics which dictates the laydown pattern of the satellite's groundtracks in space/time. Other issues which must be assessed are: adequate mission duration scales and the problems of geophysical noise sources and instrumental noise which degrade the effective alongtrack spatial resolution of the altimeter.

E.A.K.

N84-27301*# Max-Planck-Institut fuer Meteorologie, Hamburg (West Germany).

ON THE DETECTION OF UNDERWATER BOTTOM TOPOGRAPHY BY IMAGING RADARS

W. ALPERS *In NASA*. Marshall Space Flight Center Frontiers of Remote Sensing of the Oceans and Troposphere from Air and Space Platforms p 403-413 May 1984 refs

Avail: NTIS HC A99/MF A01 CSCL 17I

A theoretical model which explains basic properties of radar imaging of underwater bottom topography in tidal channels is presented. The surface roughness modulation is described by weak hydrodynamic interaction theory in the relaxation time approximation. In contrast to previous theories on short wave modulation by long ocean waves, a different approximation is used to describe short wave modulation by tidal flow over underwater bottom topography. The modulation depth is proportional to the relaxation time of the Bragg waves. The large modulation of radar reflectivity observed in SEASAT-SAR imagery of sand banks in the Southern Bight of the North Sea are explained by assuming that the relaxation time of 34 cm Bragg waves is of the order of 30-40 seconds.

E.A.K.

05 OCEANOGRAPHY AND MARINE RESOURCES

N84-27302*# Environmental Research Inst. of Michigan, Ann Arbor. Radar Div.

MODELING OF SAR SIGNATURES OF SHALLOW WATER OCEAN TOPOGRAPHY

R. A. SHUCHMAN, A. KOZMA, E. S. KASISCHKE, and D. R. LYZENGA *In* NASA. Marshall Space Flight Center Frontiers of Remote Sensing of the Oceans and Troposphere from Air and Space Platforms p 415-430 May 1984 refs (Contract N00014-81-C-2254; DMA800-78-C-0060; N00014-81-C-2308; N00014-81-C-0692)

Avail: NTIS HC A99/MF A01 CSCL 08C

A hydrodynamic/electromagnetic model was developed to explain and quantify the relationship between the SEASAT synthetic aperture radar (SAR) observed signatures and the bottom topography of the ocean in the English Channel region of the North Sea. The model uses environmental data and radar system parameters as inputs and predicts SAR-observed backscatter changes over topographic changes in the ocean floor. The model results compare favorably with the actual SEASAT SAR observed backscatter values. The developed model is valid for only relatively shallow water areas (i.e., less than 50 meters in depth) and suggests that for bottom features to be visible on SAR imagery, a moderate to high velocity current and a moderate wind must be present.

E.A.K.

N84-27303*# Tel-Aviv Univ. (Israel). Faculty of Engineering. COASTAL BATHYMETRY AND CURRENTS FROM LANDSAT DATA Abstract Only

N. ROSENBERG *In* NASA. Marshall Space Flight Center Frontiers of Remote Sensing of the Oceans and Troposphere from Air and Space Platforms p 431 May 1984

Avail: NTIS HC A99/MF A01 CSCL 08C

LANDSAT scenes of coastal areas should be useful for bathymetry and for mapping sediment flow if scatter from bottom and suspended matter can be separated by multi-date analysis. Several filter algorithms have been developed to reduce both artifacts and random noise while retaining meaningful structures such as breakwaters and underwater reefs. Results of application of these filters to LANDSAT scenes of the Israeli coast are presented.

Author

N84-27304*# Johns Hopkins Univ., Baltimore, Md. Dept. of Earth and Planetary Sciences.

ON THE RESPONSE TO OCEAN SURFACE CURRENTS IN SYNTHETIC APERTURE RADAR IMAGERY

O. M. PHILLIPS *In* NASA. Marshall Space Flight Center Frontiers of Remote Sensing of the Oceans and Troposphere from Air and Space Platforms p 433-452 May 1984 refs (Contract NAGW-304; N00014-76-C-0184)

Avail: NTIS HC A99/MF A01 CSCL 08C

The balance of wave action spectral density for a fixed wave-number is expressed in terms of a new dimensionless function, the degree of saturation, b , and is applied to an analysis of the variations of this quantity (and local spectral level) at wave-numbers large compared to that of the spectral peak, that are produced by variations in the ocean surface currents in the presence of wind input and wave breaking. Particular care is taken to provide physically based representations of wind input and loss by wave breaking and a relatively convenient equation is derived that specifies the distribution of the degree of saturation in a current field, relative to its ambient (undisturbed) background in the absence of currents. The magnitude of the variations in b depends on two parameters, $U(o)/c$, where $U(o)$ is the velocity scale of the current and c the phase speed of the surface waves at the (fixed) wave-number considered or sampled by SAR, and $S = (L/\lambda) (u^*/c)^2$, where L is the length scale of the current distribution, λ the wavelength of the surface waves the length scale of the current distribution, λ the wavelength of the surface waves and u^* the friction velocity of the wind.

M.G.

N84-27305*# British Columbia Univ., Vancouver. Dept. of Oceanography.

VARIATIONS IN SURFACE CURRENT OFF THE COASTS OF CANADA AS INFERRED FROM INFRARED SATELLITE IMAGERY

W. J. EMERY, M. IKEDA, L. A. MYSAK, and P. H. LEBLOND *In* NASA. Marshall Space Flight Center Frontiers of Remote Sensing of the Oceans and Troposphere from Air and Space Platforms p 453-478 May 1984 refs Sponsored by Natural Sciences and Engineering Research Council of Canada

Avail: NTIS HC A99/MF A01 CSCL 08C

Infrared satellite images of sea surface temperature are used to infer changes in the surface currents off both the east and west coasts of Canada. Off the east coast, summer infrared temperature patterns suggest a close connection between the location of the continental slope and the path of the Labrador Current as marked by a strong change in the shape of the continental slope. In winter both infrared and visible imagery reveal the southward propagation of wavelike features in the ice patterns along the Labrador coast. A large number of images from the Canadian west coast were used to depict the evolution of surface temperature features. In winter and spring 150 km current meanders are fed energy by the baroclinic instability of the uniformly directed current which flows northwest in winter and southeast in spring. In summer the surface current is directed southeastward while below it an undercurrent flows to the northeast. Initiated by an interaction with the irregularities of the local continental slope 75 km current meanders begin to form. Energy is then fed non-linearly by baroclinic instability into longer scale 150 km meander which eventually shed to form separate eddies.

M.G.

N84-27306*# Naval Ocean Research and Development Activity, Bay St. Louis, Miss.

THE DEPICTION OF ALBORAN SEA GYRE DURING DONDE VA? USING REMOTE SENSING AND CONVENTIONAL DATA

P. E. LAVIOLETTE *In* NASA. Marshall Space Flight Center Frontiers of Remote Sensing of the Oceans and Troposphere from Air and Space Platforms p 479-496 May 1984 refs

Avail: NTIS HC A99/MF A01 CSCL 08C

Experienced oceanographic investigators have come to realize that remote sensing techniques are most successful when applied as part of programs of integrated measurements aimed at solving specific oceanographic problems. A good example of such integration occurred during the multi-platform international experiment, Donde Va? in the Alboran Sea during the period June through October, 1982. The objective of Donde Va? was to derive the interrelationship of the Atlantic waters entering the Mediterranean Sea and the Alboran Sea Gyre. The experimental plan conceived solely with this objective in mind consisted of a variety of remote sensing and conventional platforms: three ships, three aircraft, five current moorings, two satellites and a specialized beach radar (CODAR). Integrated analyses of these multiple-data sets are still being conducted. However, the initial results show detailed structure of the incoming Atlantic jet and Alboran Sea Gyre that would not have been possible by conventional means.

Author

N84-27307*# Institut de Physique du Globe, Paris (France). Lab. de Physique et Chimie de l'Hydrosphère.

SOMALI CURRENT STUDIED FROM SEASAT ALTIMETRY

C. PERIGAUD, J. F. MINSTER, V. ZLOTNICKI (MIT, Cambridge), and G. BALMINO (CNES, Toulouse, France) *In* NASA. Marshall Space Flight Center Frontiers of Remote Sensing of the Oceans and Troposphere from Air and Space Platforms p 497-499 May 1984

Avail: NTIS HC A99/MF A01 CSCL 08C

Mesoscale variability has been obtained for the world ocean from satellite altimetry by using the repetitive tracks data of SEASAT. No significant results were obtained for the Somali current area for two main reasons: the repetitive tracks are too sparse to cover the expected eddy pattern and these data were obtained in late September and early October when the current is strongly decaying. The non-repetitive period of SEASAT offers the possibility

05 OCEANOGRAPHY AND MARINE RESOURCES

to study a dozen of tracks parallel to the eddy axis or crossing it. These are used here to deduce the dynamic topography of the Somali current. Data error reduction and tide and orbit corrections are addressed. A local geoid was built using a collocation inverse method to combine surface gravity data and altimetry: the repetitive tracks show no variability (which confirms that the current is quasi-inexistent at that time) and can be used as data for the local geoid. This should provide a measure of the absolute dynamic topography of the Somali current. M.G.

N84-27308* # Jet Propulsion Lab., California Inst. of Tech., Pasadena.

SATELLITE REMOTE SENSING OVER ICE

R. H. THOMAS *In NASA. Marshall Space Flight Center Frontiers of Remote Sensing of the Oceans and Troposphere from Air and Space Platforms* p 501-512 May 1984 refs

Avail: NTIS HC A99/MF A01 CSCL 08L

Satellite remote sensing provides unique opportunities for observing ice-covered terrain. Passive-microwave data give information on snow extent on land, sea-ice extent and type, and zones of summer melting on the polar ice sheets, with the potential for estimating snow-accumulation rates on these ice sheets. All weather, high-resolution imagery of sea ice is obtained using synthetic aperture radars, and ice-movement vectors can be deduced by comparing sequential images of the same region. Radar-altimetry data provide highly detailed information on ice-sheet topography, with the potential for deducing thickening/thinning rates from repeat surveys. The coastline of Antarctica can be mapped accurately using altimetry data, and the size and spatial distribution of icebergs can be monitored. Altimetry data also distinguish open ocean from pack ice and they give an indication of sea-ice characteristics. Author

N84-27309* # Science Research Council, Chilton (England).

RADAR ALTIMETRY OVER SEA ICE Abstract Only

J. POWELL *In NASA. Marshall Space Flight Center Frontiers of Remote Sensing of the Oceans and Troposphere from Air and Space Platforms* p 513 May 1984

Avail: NTIS HC A99/MF A01 CSCL 08L

To study the sea-ice interactive region in the Bering and Greenland Seas a series of experimental campaigns, the Marginal Ice Zone Experiment (MIZEX) has been planned. A major objective of MIZEX is the development of a capability to relate the morphology and distribution of the sea ice to atmospheric and oceanographic parameters in an overall model. During the first part of the MIZEX, a 13.7 GHz microwave radar altimeter/scatterometer having a pulse length of 16 nanoseconds was flown over the Bering Sea Marginal ice zone. On the same aircraft were the NASA GSFC 19 GHz Electronically Scanning Microwave Radiometer (ESMR), scanning radiometers and an infrared, nadir pointing, temperature sounder. The altimeter/scatterometer was operated in nadir pointing and conically scanning modes to collect measurements of reflectivity and pulse shapes. These will be related to sea-ice classifications, ocean wave spectra and coincident microwave and infrared radiometric measurements and laser profilometer surface roughness estimates. M.G.

N84-27310* # Bar-Ilan Univ., Ramat-Gan (Israel). Dept. of Geography.

METHOD TO ESTIMATE DRAG COEFFICIENT AT THE AIR/ICE INTERFACE OVER DRIFTING OPEN PACK ICE FROM REMOTELY SENSED DATA

U. FELDMAN *In NASA. Marshall Space Flight Center Frontiers of Remote Sensing of the Oceans and Troposphere from Air and Space Platforms* p 515-526 May 1984 refs Sponsored by Natural Sciences and Engineering Research Council of Canada and Atmospheric Environment Service

Avail: NTIS HC A99/MF A01 CSCL 08L

A knowledge in near real time, of the surface drag coefficient for drifting pack ice is vital for predicting its motions. And since this is not routinely available from measurements it must be replaced by estimates. Hence, a method for estimating this variable,

as well as the drag coefficient at the water/ice interface and the ice thickness, for drifting open pack ice was developed. These estimates were derived from three-day sequences of LANDSAT-1 MSS images and surface weather charts and from the observed minima and maxima of these variables. The method was tested with four data sets in the southeastern Beaufort sea. Acceptable results were obtained for three data sets. Routine application of the method depends on the availability of data from an all-weather air or spaceborne remote sensing system, producing images with high geometric fidelity and high resolution. M.G.

N84-27311* # University Coll., Dorking (England). Dept. of Physics and Astronomy.

OBSERVATIONS OF SEA ICE AND ICEBERGS FROM SATELLITE RADAR ALTIMETERS

C. G. RAPLEY *In NASA. Marshall Space Flight Center Frontiers of Remote Sensing of the Oceans and Troposphere from Air and Space Platforms* p 527-536 May 1984 refs

Avail: NTIS HC A99/MF A01 CSCL 08L

Satellite radar altimeters can make useful contributions to the study of sea ice both by enhancing observations from other instruments and by providing a unique probe of ocean-ice interaction in the Marginal Ice Zone (MIZ). The problems, results and future potential of such observations are discussed. Author

N84-27312* # Harvard Univ., Cambridge, Mass. Center for Earth and Planetary Physics.

SIMULATION AND ASSIMILATION OF SATELLITE ALTIMETER DATA AT THE OCEANIC MESOSCALE

P. DEMAY and A. R. ROBINSON *In NASA. Marshall Space Flight Center Frontiers of Remote Sensing of the Oceans and Troposphere from Air and Space Platforms* p 537-536 May 1984 refs

(Contract N00014-75-C-0225)

Avail: NTIS HC A99/MF A01 CSCL 05B

An improved 'objective analysis' technique is used along with an altimeter signal statistical model, an altimeter noise statistical model, an orbital model, and synoptic surface current maps in the POLYMODE-SDE area, to evaluate the performance of various observational strategies in catching the mesoscale variability at mid-latitudes. In particular, simulated repetitive nominal orbits of ERS-1, TOPEX, and SPOT/POSEIDON are examined. Results show the critical importance of existence of a subcycle, scanning in either direction. Moreover, long repeat cycles (20 days) and short cross-track distances (300 km) seem preferable, since they match mesoscale statistics. Another goal of the study is to prepare and discuss sea-surface height (SSH) assimilation in quasigeostrophic models. Restored SSH maps are shown to meet that purpose, if an efficient extrapolation method or deep in-situ data (floats) are used on the vertical to start and update the model. M.G.

N84-27313* # City Coll. of the City Univ. of New York.

VECTOR WIND, HORIZONTAL DIVERGENCE, WIND STRESS AND WIND STRESS CURL FROM SEASAT-SASS AT ONE DEGREE RESOLUTION

W. J. PIERSON, JR., W. B. SYLVESTER, and R. E. SALFI (Hofstra Univ., Hempstead, N.Y.) *In NASA. Marshall Space Flight Center Frontiers of Remote Sensing of the Oceans and Troposphere from Air and Space Platforms* p 557-566 May 1984 refs

(Contract NAGW-266)

Avail: NTIS HC A99/MF A01 CSCL 04B

Conventional data obtained in 1983 are contrasted with SEASAT-A scatterometer and scanning multichannel microwave radiometer (SMMR) data to show how observations at a single station can be extended to an area of about 150,000 square km by means of remotely sensed data obtained in nine minutes. Superobservations at a one degree resolution for the vector winds were estimated along with their standard deviations. From these superobservations, the horizontal divergence, vector wind stress, and the curl of the wind stress can be found. Weather forecasting theory is discussed and meteorological charts of the North Pacific

05 OCEANOGRAPHY AND MARINE RESOURCES

Ocean are presented. Synoptic meteorology as a technique is examined.

R.S.F.

N84-27314*# National Aeronautics and Space Administration. Goddard Space Flight Center, Greenbelt, Md.

THE IMPACT OF SCATTEROMETER WIND DATA ON GLOBAL WEATHER FORECASTING

D. ATLAS, W. E. BAKER, E. KALNAY, M. HALEM, P. M. WOICESHYN (JPL, Pasadena, Calif.), and S. PETEHERYCH (Atmospheric Environment Service, Downsview, Ontario) *In NASA. Marshall Space Flight Center Frontiers of Remote Sensing of the Oceans and Troposphere from Air and Space Platforms p 567-573 May 1984 refs*

Avail: NTIS HC A99/MF A01 CSCL 04B

The impact of SEASAT-A scatterometer (SASS) winds on coarse resolution atmospheric model forecasts was assessed. The scatterometer provides high resolution winds, but each wind can have up to four possible directions. One wind direction is correct; the remainder are ambiguous or 'aliases'. In general, the effect of objectively dealiased-SASS data was found to be negligible in the Northern Hemisphere. In the Southern Hemisphere, the impact was larger and primarily beneficial when vertical temperature profile radiometer (VTPR) data was excluded. However, the inclusion of VTPR data eliminates the positive impact, indicating some redundancy between the two data sets.

R.S.F.

N84-27316*# Naval Ocean Research and Development Activity, Bay St. Louis, Miss.

THE IMPORTANCE OF ALTIMETER AND SCATTEROMETER DATA FOR OCEAN PREDICTION

H. E. HURLBURT *In NASA. Marshall Space Flight Center Frontiers of Remote Sensing of the Oceans and Troposphere from Air and Space Platforms p 587-599 May 1984 refs*

Avail: NTIS HC A99/MF A01 CSCL 08C

The prediction of ocean circulation using satellite altimeter data is discussed. Three classes of oceanic response to atmospheric forcing are outlined and examined. Storms, surface waves, eddies, and ocean currents were evaluated in terms of forecasting time requirements. Scatterometer and radiometer applications to ocean prediction are briefly reviewed.

R.S.F.

N84-27317*# Naval Ocean Research and Development Activity, Bay St. Louis, Miss. Dynamical Ocean Forecasting Branch.

SAMPLING STRATEGIES AND FOUR-DIMENSIONAL ASSIMILATION OF ALTIMETRIC DATA FOR OCEAN MONITORING AND PREDICTION

J. C. KINDLE, J. D. THOMPSON, and H. E. HURLBURT *In NASA. Marshall Space Flight Center Frontiers of Remote Sensing of the Oceans and Troposphere from Air and Space Platforms p 601-612 May 1984 refs*

Avail: NTIS HC A99/MF A01 CSCL 08C

Numerical experiments using simulated altimeter data were conducted in order to examine the assimilation of altimeter-derived sea surface heights into numerical ocean circulation models. A reduced-gravity, primitive equation circulation model of the Gulf of Mexico was utilized; the Gulf of Mexico was chosen because of its amenability to modeling and the ability of low vertical-mode models to reproduce the observed dynamical features of the Gulf circulation. The simulated data were obtained by flying an imaginary altimeter over the model ocean and sampling the model sea surface just as real altimeter would observe the true ocean. The data were used to initialize the numerical model and the subsequent forecast was compared to the true numerical solution. Results indicate that for a stationary, circular eddy, approximately three to four tracks (either ascending or descending) across the eddy are sufficient to ensure adequate spatial resolution.

Author

N84-27318*# Naval Ocean Research and Development Activity, Bay St. Louis, Miss. Dynamic Ocean Forecasting Branch.

THE INFLUENCE OF ACTUAL AND APPARENT GEOID ERROR ON OCEAN ANALYSIS AND PREDICTION Abstract Only

J. D. THOMPSON *In NASA. Marshall Space Flight Center Frontiers of Remote Sensing of the Oceans and Troposphere from Air and Space Platforms p 613-614 May 1984 refs*

Avail: NTIS HC A99/MF A01 CSCL 08C

The radar altimeter is the only satellite remote sensor with a proven capability for synoptically measuring an integral property of the dynamic ocean on a near global, all weather basis. Because acquisition of global, in situ ocean data with space/time resolution adequate to describe dynamically important ocean features is practically impossible, any attempt to develop a global ocean monitoring and forecasting system will rely heavily on altimetric data for initialization and updating. Maximizing useful information from the altimeter while minimizing error sources and developing methods for assimilating altimeter data into dynamical models are, therefore, vital areas for research and development. The limits imposed on ocean prediction by errors in the geoid or apparent errors associated with ground track variations near strong geopotential gradients are examined.

R.S.F.

N84-27319*# National Aeronautics and Space Administration. Goddard Space Flight Center, Greenbelt, Md.

MATRIX PARTITIONING AND EOF/PRINCIPAL COMPONENT ANALYSIS OF ANTARCTIC SEA ICE BRIGHTNESS TEMPERATURES

C. W. MURRAY, JR., J. L. MUELLER (Naval Post Graduate School), and H. J. ZWALLY Apr. 1984 89 p refs

(NASA-TM-83916; NAS 1.15:83916) Avail: NTIS HC A05/MF A01 CSCL 08L

A field of measured anomalies of some physical variable relative to their time averages, is partitioned in either the space domain or the time domain. Eigenvectors and corresponding principal components of the smaller dimensioned covariance matrices associated with the partitioned data sets are calculated independently, then joined to approximate the eigenstructure of the larger covariance matrix associated with the unpartitioned data set. The accuracy of the approximation (fraction of the total variance in the field) and the magnitudes of the largest eigenvalues from the partitioned covariance matrices together determine the number of local EOF's and principal components to be joined by any particular level. The space-time distribution of Nimbus-5 ESMR sea ice measurement is analyzed.

A.R.H.

N84-27320# Environmental Research Inst. of Michigan, Ann Arbor.

ANALYSIS OF SEASAT SAR IMAGERY COLLECTED DURING THE JASIN EXPERIMENT Topic Report, Aug. 1981 - May 1983

E. S. KASISCHKE, R. A. SHUCHMAN, J. D. LYDEN, and Y. C. TSENG May 1983 209 p

(Contract N00014-81-C-0692)

(AD-A140584; ERIM-155900-16-T) Avail: NTIS HC A10/MF A01 CSCL 08C

This report summarizes the analysis of SEASAT SAR imagery collected during the JASIN experiment. Studies performed on this data set include comparison of SAR-derived estimates of wavelength and direction versus surface measured values, evaluation of SAR/wave focusing algorithms and study of deep-water internal wave and frontal boundary patterns on the SAR imagery.

GRA

N84-27321# Naval Ocean Research and Development Activity, Bay St. Louis, Miss.

OCEAN OPTICAL REMOTE SENSING CAPABILITY STATEMENT

Final Technical Note

R. A. ARNONE and R. J. HOLYER Mar. 1984 30 p

(AD-A140589; NORDA-TN-264) Avail: NTIS HC A03/MF A01 CSCL 08J

The capability of the Naval Ocean Research & Development Activity Remote Sensing Branch in ocean optics is described. A summary of the facilities, programs, scientific contributions and

05 OCEANOGRAPHY AND MARINE RESOURCES

basic research issues is outlined. The application of remote sensing in the study of ocean optical properties is described in addition to present image processing software and satellite receiving capability. Different optical field instruments which the Remote Sensing Branch has obtained are presented. Results of optical data are illustrated in relation to other oceanographic parameters. Navy programs which have supported the Remote Sensing Branch's developments in water optics are described. The Navy relevance of water optics to these programs is indicated. Author (GRA)

N84-27921# Joint Publications Research Service, Arlington, Va.
SPECKLE STATISTICS IN RADAR IMAGES OF SEA SURFACE OBTAINED WITH HORIZONTAL POLARIZATION Abstract Only

F. V. BUNKIN, K. I. VOLYAK, and I. V. SHUGAN *In its USSR Report: Electronics and Electrical Engineering (JPRS-UEE-84-002) p 4 8 Mar. 1984 Transl. into ENGLISH from Izv. Vyssh. Uch. Zaved.: Radiofiz. (USSR), v. 26, no. 7, Jul. 1983 p 802-808*
Avail: NTIS HC A03/MF A01

Obtaining aerospace images of the sea surface by a scatter probing radar is analyzed, considering horizontal polarization of transmitted and received signals. The space distribution of quasi-specular speckles and its statistical characteristics are determined, taking into account those of a randomly rough sea surface. The probing angle is assumed to slide, as in the case of a lateral-scan centimetric-wave or decimetric-wave radar mounted on a low flying aircraft. The dependence of the blip statistics on the degree of wave spectrum saturation is established for a typical azimuthal distribution of sea waves and the mean signal level is calculated with only specular reflection taken into account. The effect of wind on the blip statistics is also evaluated, a typical example being modulation of wind waves by flow variations at the water surface caused by internal water waves. An indicator of changes in the blip pattern is the contrast between (ratio of) blip concentrations corresponding, in this case, to wind and water flowing in the same direction and in opposite directions, respectively. This model of image formation is valid when resonance scattering is much weaker than specular reflection. Author

N84-28298# Jet Propulsion Lab., California Inst. of Tech., Pasadena.

OBSERVING OCEAN-ATMOSPHERE EXCHANGES WITH SPACE-BORNE SENSORS, APPENDIX C

W. T. LIU *In WMO Rept. of the WMO/CAS Expert Meeting on Atmospheric Boundary Layer Parameterization Over the Oceans for Long Range Forecasting and Climate Models 4 p 1984 refs*

Avail: NTIS HC A06/MF A01 CSCL 04B

At present, space-borne sensors cannot give accurate measurements of net longwave radiation and sensible heat flux at ocean surface. The variability of ocean surface net insolation was successfully estimated from observations using geostationary satellites. Global coverages of the low frequency variation of major atmosphere-ocean exchanges, momentum, latent heat, and insolation are within reach. Data from research and defense satellites should be made available in useful form to the user community. High quality in-situ measurements are required to calibrate space-borne sensors and numerical models are needed to integrate satellite and in-situ data as well as interpolate both in space and time. Techniques that can resolve boundary layer parameters should be developed. A.R.H.

N84-28354 Institute of Oceanographic Sciences, Birkenhead (England).

PUBLICATIONS AND REPORTS OF THE INSTITUTE OF OCEANOGRAPHIC SCIENCES 1979-1982

K. D. JONES, ed. 1983 99 p refs
(IOS-170) Avail: Issuing Activity

Over 900 publications covering every aspect of oceanographic science are listed. Author (ESA)

N84-28355# Jet Propulsion Lab., California Inst. of Tech., Pasadena.

SATELLITE-DERIVED SEA SURFACE TEMPERATURE: WORKSHOP-2

E. J. NJOKU 15 Feb. 1984 148 p refs Workshop held in Pasadena, Calif., 22-24 Jun. 1983
(Contract NAS7-918)
(NASA-CR-173740; JPL-PUBL-84-5; NAS 1.26:173740) Avail: NTIS HC A07/MF A01 CSCL 08J

Global accuracies and error characteristics of presently orbiting satellite sensors are examined. The workshops are intended to lead to a better understanding of present capabilities for sea surface temperature measurement and to improve measurement concepts for the future. Data from the Advanced Very High Resolution Radiometer AVHRR and Scanning Multichannel Microwave Radiometer is emphasized. Some data from the High Resolution Infrared Sounder HIRS and AVHRR are also examined. Comparisons of satellite data with ship and expendable BathyThermograph XBT measurement show standard deviations in the range 0.5 to 1.3 C with biases of less than 0.4 C, depending on the sensor, ocean region, and spatial/temporal averaging. The Sea Surface Temperature SST anomaly maps show good agreement in some cases, but a number of sensor related problems are identified.

M.A.C.

N84-28359# Naval Ocean Research and Development Activity, Bay St. Louis, Miss.

MICROWAVE RADIOMETRIC MEASUREMENT OF SEA SURFACE SALINITY Final Report

G. STANFORD Apr. 1984 13 p
(AD-A141302; NORDA-TN-267) Avail: NTIS HC A02/MF A01 CSCL 08J

The emphasis on salinity measurements in coastal areas has obscured the development of remote sensing of salinity in the open ocean. In part, this is due to the homogeneity of haline fields in the open ocean; however, one area where salinity measurement is important is the region along the edge of polar ice, the Marginal Ice Zone (MIZ). This report discusses microwave radiometric measurements of the MIZ and other areas with similar variations in surface salinity. The physics of the S-Band radiometer is discussed.

06

HYDROLOGY AND WATER MANAGEMENT

Includes snow cover and water runoff in rivers and glaciers, saline intrusion, drainage analysis, geomorphology of river basins, land uses, and estuarine studies.

A84-30246#

TURBIDITY/SEDIMENT CONCENTRATION MAPPING IN THE COASTAL AREA OF BANGLADESH

M. A. H. PRAMANIK (Bangladesh Space Research and Remote Sensing Organization, Dacca, Bangladesh) IN: Asian Conference on Remote Sensing, 3rd, Dacca, Bangladesh, December 4-7, 1982, Proceedings . Tokyo, University of Tokyo, 1983, p. Q-6-1 to Q-6-18. refs

06 HYDROLOGY AND WATER MANAGEMENT

A84-30251#

IDENTIFICATION OF WATER-LOGGED AND SALT-AFFECTED SOILS THROUGH REMOTE SENSING TECHNIQUES

B. SAHAI, M. H. KALUBARME (Indian Space Research Organization, Space Applications Centre, Ahmedabad, India), M. V. BAPAT (Gujarat State, Irrigation Dept., Baroda, India), and K. L. JADAV (Gujarat State Land Development Corp., Ahmedabad, India) IN: Asian Conference on Remote Sensing, 3rd, Dacca, Bangladesh, December 4-7, 1982, Proceedings . Tokyo, University of Tokyo, 1983, p. Q-14-1 to Q-14-11.

An attempt has been made to delineate the water-logged and salt-affected areas associated with the Kakrapar Weir on the river Tapi and connected network of irrigation canals, by studying multiband Landsat imagery. The changes during the last ten years could be studied using multidate Landsat imagery starting with the 1972 imagery of Landsat 1. The studies were supplemented by color infrared photography over a central area of 1200 square km conducted during November 1980, May 1981 and February 1982. Water table observations during May 1981 indicate that a high water table exists in a quite sizable area, and this results in reduced crop yields and/or area under cultivation. The collation of ground truth data and the remotely sensed data shows that water-logged and salt-affected soils are identifiable within the limits of spatial resolution of remotely sensed data. D.H.

A84-30255#

THE APPLICATION OF LANDSAT IMAGE IN THE SURVEYING OF WATER RESOURCES OF DONGTING LAKE

X. LIU, S. ZHANG, and X. LI (Hunan Province, Geological Bureau, Remote Sensing Station, Hunan, People's Republic of China) IN: Asian Conference on Remote Sensing, 3rd, Dacca, Bangladesh, December 4-7, 1982, Proceedings . Tokyo, University of Tokyo, 1983, p. D-3-1 to D-3-10.

Landsat images processed at different times have been used to investigate the water surface area and the volume of China's Dongting Lake (Hunan province), the second largest body of fresh water in the country. Landsat and conventional determinations of the surface area of the lake agree within 4 percent when the outflow via the Changjiang River approaches the flood stage. Other relationships determined were that between water level and water surface area and that between water level and water volume. It is concluded that the use of Landsat MSS7 imagery and false color combination imagery for such determinations is very effective and reliable. D.H.

A84-30256#

HYDROLOGICAL DATA DENSIFICATION IN MOUNTAINOUS TERRAIN USING LANDSAT IMAGERY

A. K. BAGCHI (Kwara State College of Technology, Ilorin, Nigeria) IN: Asian Conference on Remote Sensing, 3rd, Dacca, Bangladesh, December 4-7, 1982, Proceedings . Tokyo, University of Tokyo, 1983, p. D-4-1 to D-4-7. Research supported by the Indian Space Research Organization. refs

Methods that have been proposed for obtaining hydrometeorological data in mountainous basins are reviewed. All of the methods are found to have limitations. Remote sensing is seen as holding promise, and methods are presented for the vertical and horizontal transfer of precipitation and the determination of the depth of standing snow. Reference is made to a study by Bagchi (1982), which showed the summer streamflow could be predicted when the remote sensing method was used to estimate the snow depth. C.R.

A84-30257#

SEDIMENT VOLUME MODELLING IN THE COASTAL AREA OF BANGLADESH USING TURBIDITY/SEDIMENT CONCENTRATION MAP BASED ON LANDSAT DATA

M. I. CHOWDHURY (Jahangirnagar University, Dacca, Bangladesh), F. C. POLCYN (Michigan, Environmental Research Institute, Ann Arbor, MI), and M. A. H. PRAMANIK (Bangladesh Space Research and Remote Sensing Organization, Dacca, Bangladesh) IN: Asian Conference on Remote Sensing, 3rd, Dacca, Bangladesh, December 4-7, 1982, Proceedings . Tokyo, University of Tokyo, 1983, p. E-1-1 to E-1-18. refs

A84-31948

ELEMENTS OF THE WEST AFRICAN MONSOON CIRCULATION DEDUCED FROM METEOSAT CLOUD WINDS AND SIMULTANEOUS AIRCRAFT MEASUREMENTS

M. DESBOIS (CNRS, Laboratoire de Meteorologie Dynamique, Palaiseau, Essonne, France), V. PIRCHER (Etablissement d'Etudes et de Recherches Meteorologiques, Magny-les-Hameaux, France), and B. PINTY (CNRS, LAMP, Clermont-Ferrand, France) Journal of Climate and Applied Meteorology (ISSN 0733-3021), vol. 23, Jan. 1984, p. 161-165. refs

Cloud winds derived from the European geostationary satellite Meteosat for the region of the west African monsoon are validated by DC-7 aircraft measurements for the low levels of the tropical atmosphere. Since the two sets of results are in agreement, it appears that lowest level cumuli as well as stratocumuli can be used as tracers of the actual wind field. The satellite wind fields show a large-scale circulation characterized by two opposite flows in the lower layers: the southwesterly monsoon flow near the sea surface and a northeasterly flow above, at approximately the 2000 m level. Author

A84-31950#

EURASIAN SNOW COVER VERSUS INDIAN MONSOON RAINFALL - AN EXTENSION OF THE HAHN-SHUKLA RESULTS

R. R. DICKSON (NOAA, Climate Analysis Center, Washington, DC) Journal of Climate and Applied Meteorology (ISSN 0733-3021), vol. 23, Jan. 1984, p. 171-173. refs

The apparent inverse relationship between Eurasian mean winter snow cover extent and the following warm season Indian monsoon rainfall, described by Hahn and Shukla for the 1967-75 period, is substantiated by the addition of five subsequent years of data if known deficiencies in satellite snow observations are accommodated. In this respect, elimination of a bias due to under-observation of snow cover in the Himalayan region during 1967-74 was crucial for the attainment of statistically significant correlations. Nonsignificant correlations for a shorter period (1971-80) suggest that Eurasian and Himalayan region winter snow cover extent, as well as that of Eurasia less the Himalayan region, are all about equally well related to the subsequent Indian monsoon rainfall. Furthermore, Eurasian and Himalayan snow cover extent derived from satellite observations are found to be highly correlated. Author

A84-33339* Army Cold Regions Research and Engineering Lab., Hanover, N. H.

INTEGRATION OF LANDSAT DATA INTO THE SAGINAW RIVER BASIN GEOGRAPHIC INFORMATION SYSTEM

H. L. MCKIM, C. J. MERRY (U.S. Army, Cold Regions Research and Engineering Laboratory, Hanover, NH), S. G. UNGAR (NASA, Goddard Institute for Space Studies, New York, NY), W. J. ODONOGHUE (U.S. Army, Corps of Engineers, Detroit, MI), and M. S. MILLER (M/A-COM Sigma Data, New York, NY) IN: American Society of Photogrammetry, Annual Meeting, 49th, Washington, DC, March 13-18, 1983, Technical Papers . Falls Church, VA, American Society of Photogrammetry, 1983, p. 212-224. refs

One of the objectives of the Saginaw River Basin study is related to the development of a computer model to predict flood damages. The computer model is to be operational in June 1985. In order to achieve this objective, the input of land-use data into

06 HYDROLOGY AND WATER MANAGEMENT

a data base consisting of 198,000 grid cells will be required. A planning technique using Spatial Analysis Methodology (SAM) was developed by the Corps of Engineers Hydrologic Engineering Center (HEC) to systematically handle these data. The HEC-SAM system uses the spatially oriented map data in a series of data management and analysis software programs for input to the Corps hydrologic and environmental models. Attention is given to data base development, Landsat digital data, the placement of the Landsat data into the grid cell data base, and the development of the land cover classification. The Landsat-2 MSS scene covering 85 percent of the Saginaw River Basin was geometrically corrected to a UTM coordinate system.

G.R.

A84-33353

DRAINAGE PATTERN DELINEATION - A FUNCTION OF IMAGE SCALE

B. HAGGERSTONE (MacLaren Plansearch Corp., Vancouver, Canada) IN: American Society of Photogrammetry, Annual Meeting, 49th, Washington, DC, March 13-18, 1983, Technical Papers . Falls Church, VA, American Society of Photogrammetry, 1983, p. 529-533. Research supported by Harvard University. refs

Drainage patterns delineated from imagery of five different scales were used as indices of the effects of image scale on information capture. The degree of information capture was determined by visually comparing the densities of the drainage nets delineated from each of the images with patterns derived from 1:24 000 USGS topographic maps. The selection of two adjacent watersheds, one developed in sandstone and the other in shale, facilitated comparisons between drainage nets of different densities. The study revealed a direct association between image scale and observed drainage density.

Author

A84-33355

ESTIMATION OF DEPTH OF SNOW FROM LANDSAT IMAGERY

A. K. BAGCHI (Kwara State College of Technology, Ilorin, Nigeria) IN: American Society of Photogrammetry, Annual Meeting, 49th, Washington, DC, March 13-18, 1983, Technical Papers . Falls Church, VA, American Society of Photogrammetry, 1983, p. 551-555. Research supported by the Indian Space Research Organization.

Landsat imagery has been widely used for the study of snow covered areas. However, it is not possible to determine the depth of the snow layer either by the stereoscopic method or by another approach. There is no operational method which could be used to determine the depth of snow in high mountain areas. The present investigation is concerned with a method for the determination of the depth of snow on high mountain slopes. The considered method is based on a utilization of Landsat imagery and hydrometeorological data collected at one point only. The method has been developed in Beas basin in the western Himalayas. The elevation in the considered area varies in the range from 1900 to 6000 m. Hydrometeorological data, such as maximum and minimum daily temperature, daily snowfall and rainfall, and discharge in the river Beas are recorded.

G.R.

A84-33541* California Univ., Santa Barbara.

SNOW REFLECTANCE FROM LANDSAT-4 THEMATIC MAPPER

J. DOZIER (California, University, Santa Barbara, CA) IEEE Transactions on Geoscience and Remote Sensing (ISSN 0196-2892), vol. GE-22, May 1984, p. 323-328. refs
(Contract NAS5-27463)

In California 75 percent of the agricultural water supply comes from the melting Sierra Nevada snowpack. Basin-wide spectral albedo measurements from the Landsat-4 Thematic Mapper (TM) could be used to better forecast the timing of the spring runoff, because these data can be combined with solar radiation calculations to estimate the net radiation balance. The TM is better-suited for this purpose than the Multispectral Scanner because of its larger dynamic range. Saturation still occurs in bands 1-4, but is severe only in TM1 (0.45-0.52 micron). Snow

reflectance in TM2 (0.43-0.61 micron) is typical of the visible wavelength region, where reflectance is almost insensitive to crystal size but sensitive to contamination. TM4 (0.78-0.90 micron) allows estimation of effective optical grain size and thereby spectral extension throughout the near-infrared. TM5 (1.57-1.78 microns) can discriminate clouds from snow.

Author

A84-33987

LOCATING SHORELINE CHANGES IN THE PORTTIPAHTA (FINLAND) WATER RESERVOIR BY USING MULTITEMPORAL LANDSAT DATA

H. JANTUNEN and J. RAITALA (Oulu, University, Oulu, Finland) Photogrammetria (ISSN 0031-8663), vol. 39, March 1984, p. 1-12. Research supported by the Foundation for Research of Natural Resources in Finland. refs

A84-34378

THE EFFECT OF GROUNDWATER INFLOW ON EVAPORATION FROM A SALINE LAKE

J. M. WHITING (Saskatchewan Research Council, Saskatoon, Canada) Journal of Climate and Applied Meteorology (ISSN 0733-3021), vol. 23, Feb. 1984, p. 214-221. Research supported by the Saskatchewan Research Council and Canada Centre for Inland Waters. refs

A decade study of the hydrometeorology of Big Quill Lake in Saskatchewan, a saline prairie lake, has effectively used remote sensing to delineate groundwater inflow. The lake covers an area of 250 square kilometers with the groundwater seeping through 4 square kilometers. The salinity of the lake water forces the fresher groundwater to the surface by convection and spreads the colder groundwater by diffusion over an area of 50 square kilometers. The magnitude, source and discharge rate were determined using thermal diffusivity from data supplied by thermal infrared line scanning. Two thermal scans were made of the lake and the data extended to provide a seasonal index using Landsat computer compatible tapes. The seasonal thermal index was extended further using four shore-based climatological stations to provide areal evaporation using a modified Penman equation and a diffusion equation.

Author

A84-38296

CLASSIFICATION OF SNOW SURFACE CONDITIONS BY MEANS OF LANDSAT MSS DATA UNDER COMPENSATION OF SLOPE EFFECTS

T. SAKAI, H. NISHIKAWA, M. TSUBOMATSU (Nihon University, Narashino, Japan), S. TANAKA, and H. KIMURA (Remote Sensing Technology Center of Japan, Tokyo, Japan) IN: International Symposium on Space Technology and Science, 13th, Tokyo, Japan, June 28-July 3, 1982, Proceedings . Tokyo, AGNE Publishing, Inc., 1982, p. 1245-1252. refs

Snowpack estimations were made based on surface reflectance data gathered by the Landsat multispectral scanner (MSS). The total reflected solar radiation was summed and a model was used to compensate for changes in radiance due to terrain slope. A digital terrain model was developed for the test area to effect the corrections. The MSS band 7 data differentiated between powdery snow and solid crust, the latter having a lower reflectance because of its being formed by snow that melted and then froze, thereby increasing in density. The results indicate that the solar angle must be accounted for when analyzing snowpack imagery. Reflectance increased with altitude, and snowpack classifications changed with contour.

M.S.K.

06 HYDROLOGY AND WATER MANAGEMENT

N84-22997*# California Univ., Santa Barbara. Dept. of Geography.

LANDSAT-D INVESTIGATIONS IN SNOW HYDROLOGY

Quarterly Progress Report, 1 Jan. - 31 Mar. 1984

J. DOZIER, Principal Investigator 31 Mar. 1984 9 p refs ERTS

(Contract NAS5-27463)

(E84-10094; NASA-CR-173480; NAS 1.26:173480) Avail: NTIS HC A02/MF A01 CSCL 08L

Thematic mapper radiometric characteristics, snow/cloud reflectance, and atmospheric correction are discussed with application to determining the spectral albedo of snow. The geometric characteristics of TM and digital elevation data are examined. The geometric transformations and resampling required to coregister these data are discussed.

N84-22998*# California Univ., Santa Barbara. Dept. of Geography.

ATMOSPHERIC MODEL DEVELOPMENT

In its LANDSAT-D Invest. in Snow Hydrol. p 1-6 31 Mar. 1984 refs Proposed for presentation at LARS Symp., Jun. 1984 ERTS

Avail: NTIS HC A02/MF A01 CSCL 08B

Spectral albedo measurements from the LANDSAT-4/5 thematic mappers require that spacecraft upwelling radiances be corrected for atmospheric absorption and scattering and for local surface illumination. A two-stream model is developed, with a lower boundary condition that varies with incidence angle. The TM data must be registered to digital terrain data. Reflectance from points in shadows can be used to estimate optical depth. The primary application is determination of the spectral albedo of snow. The TM is better-suited for this purpose than the MSS because of its larger dynamic range.

Author

N84-23973# Geological Survey, Washington, D.C.

HYDROLOGY OF THE NORTH SLOPE, ALASKA Abstract Only

C. E. SLOAN In its US Geological Survey Polar Res. Symp. p 44 1983

Avail: NTIS HC A04/MF A01; also available from SOD

The hydrology of the North Slope is dominated by the cold, dry climate and permafrost. Streamflow virtually ceases during the long winter. Precipitation occurs mainly as snow from September to May and is stored in the snowpack until breakup, a dynamic flow period in late May and early June. Most of the annual runoff occurs in the brief 2- to 3-week breakup period. The estimated mean annual runoff on the North Slope averages about 0.5 cubic feet per second per square mile and ranges from about 0.3 on the Coastal Plain to about 2.0 in the mountains. Peak flows usually occur during spring breakup when the height of the flood flow is significantly increased by the presence of ice jams. Maximum evident floods range from about 7 to 80 and average about 40 cubic feet per second per square mile in large streams on the North Slope.

Author

N84-23976*# Utah Univ., Salt Lake City. Center for Remote Sensing and Cartography.

RIPARIAN HABITAT ON THE HUMBOLDT RIVER, DEETH TO ELKO, NEVADA

K. P. PRICE and M. K. RIDD Dec. 1983 48 p refs ERTS

(Contract NAGW-95)

(E84-10116; NASA-CR-173486; NAS 1.26:173486; CRSC-83-3)

Avail: NTIS HC A03/MF A01 CSCL 08B

A map inventory of the major habitat types existing along the Humboldt River riparian zone in Nevada is described. Through aerialphotography, 16 riparian habitats are mapped that describe the ecological relationships between soil and vegetation types, flooding and soil erosion, and the various management practices employed to date. The specific land and water management techniques and their impact on the environment are considered.

M.A.C.

N84-25145# World Meteorological Organization, Geneva (Switzerland).

GUIDE TO HYDROLOGICAL PRACTICES. VOLUME 2: ANALYSIS, FORECASTING AND OTHER APPLICATIONS

1983 293 p refs

(WMO-168; ISBN-92-63-14168-1) Avail: NTIS MF A01; print copy available at WMO, Geneva, SWFR 40

Methods of analysis used in hydrology are discussed. The interpretation of precipitation data, including storms, rainfall frequency and intensity, and snowmelt is discussed. Stream flow data interpretation, evaporation, and evapotranspiration, runoff relations, and the modeling of hydrological systems are discussed.

R.J.F.

N84-26100# Instituto de Pesquisas Espaciais, Sao Jose dos Campos (Brazil).

RESULTS OF FIELD OBSERVATIONS OF RADIO WAVES IN ALLUVIAL DEPOSITS IN CARA STATE FROM 1:100.000: FORTALEZA, CANIRDE, TAPERUABA, SANTA QUITERIA, SOBRAL, AND SAO LUIZ DO CURU [RELATORIO DO TRABALHO DE RECONHECIMENTO DE CAMPO DE AREAS ALUVIONARES NO ESTADO DO CEARA, FOLHAS 1:100.000: FORTALEZA, CANINDE, TAPERUABA, SANTA QUITERIA, SOBRAL, IRAUCUBA E SAO LUIZ DO CURU]

M. P. BARBOSA Apr. 1984 138 p In PORTUGUESE; ENGLISH summary Original doc. contains color illustrations

(INPE-3061-NTE/216) Avail: NTIS HC A07/MF A01

The observations of the field reconnaissance accomplished in 18th and 19th October 1983, in the regions of Fortaleza, Caninde, Taperuaba, Santa Quiteria, Sobral and Sao Luiz do Curu in Ceara State are reported.

Author

N84-26106# Army Cold Regions Research and Engineering Lab., Hanover, N. H.

INTEGRATION OF LANDSAT LAND COVER DATA INTO THE SAGINAW RIVER BASIN GEOGRAPHIC INFORMATION SYSTEM FOR HYDROLOGIC MODELING

H. L. MCKIM, S. G. UNGAR, C. J. MERRY, and J. F. GAUTHIER Feb. 1984 27 p

(AD-A140185; CRREL-SP-84-1) Avail: NTIS HC A03/MF A01 CSCL 08F

A May 1977 LANDSAT-2 scene that covered approximately 85% of the Saginaw River Basin was classified into five land cover categories (urban, agriculture, forest, freshwater wetlands and open water) using a closest centroid classifier. The LANDSAT digital data were geometrically corrected to conform to a UTM (Universal Transverse Mercator) grid before classification. The 1.1-acre LANDSAT land cover classification data base was converted to 40-acre grid cells (six-by-six blocks of LANDSAT pixels) using an aggregation scheme and was integrated into the Detroit District's existing grid cell data base. A regression relationship between unit hydrograph parameters and the LANDSAT land cover classification was developed. The results indicated that the LANDSAT-2 land cover data were suitable for the Corps of Engineers hydrologic model.

GRA

N84-27258# Environmental Research Inst. of Michigan, Ann Arbor. Applications Div.

DEVELOPMENT OF GREAT LAKES ALGORITHMS FOR THE NIMBUS-G COASTAL ZONE COLOR SCANNER Final Report

F. J. TANIS and D. R. LYZENGA Jun. 1981 95 p refs

(Contract NAS3-22442)

(NASA-CR-173511; NAS 1.26:173511; ERIM-150000-11-F) Avail: NTIS HC A05/MF A01 CSCL 05B

A series of experiments in the Great Lakes designed to evaluate the application of the Nimbus G satellite Coastal Zone Color Scanner (CZCS) were conducted. Absorption and scattering measurement data were reduced to obtain a preliminary optical model for the Great Lakes. Available optical models were used in turn to calculate subsurface reflectances for expected concentrations of chlorophyll-a pigment and suspended minerals. Multiple nonlinear regression techniques were used to derive CZCS water quality prediction equations from Great Lakes simulation

06 HYDROLOGY AND WATER MANAGEMENT

data. An existing atmospheric model was combined with a water model to provide the necessary simulation data for evaluation of the preliminary CZCS algorithms. A CZCS scanner model was developed which accounts for image distorting scanner and satellite motions. This model was used in turn to generate mapping polynomials that define the transformation from the original image to one configured in a polyconic projection. Four computer programs (FORTRAN IV) for image transformation are presented.

R.S.F.

N84-27260# Instituto de Pesquisas Espaciais, Sao Jose dos Campos (Brazil).

A REPORT OF CEARA PROJECT ACTIVITIES [RELATORIO DE ATIVIDADES DO PROJETO CEARA]

M. P. BARBOSA and R. A. NOVAES Dec. 1983 62 p In PORTUGUESE; ENGLISH summary (INPE-2988-RPE/452) Avail: NTIS HC A04/MF A01

The application of remote sensing techniques and are transfer of the methodologies of applications of remote sensing data are presented. Natural resources, particularly the water resources are studied. The prolonged drought in the north eastern region of Brazil, and the obtained results from the first stage of this project are outlined.

E.A.K.

N84-28344# Atmospheric and Environmental Research, Inc., Cambridge, Mass.

OUTLOOK FOR IMPROVED NUMERICAL WEATHER PREDICTION USING SATELLITE DATA WITH A SPECIAL EMPHASIS ON THE HYDROLOGICAL VARIABLES

L. D. KAPLAN, R. N. HOFFMAN, R. G. ISAACS, R. D. ROSEN, and D. A. SALSTEIN 18 Nov. 1983 198 p (Contract F19628-83-C-0027; AF PROJ. 2310) (AD-A141233; P79-1; AFGL-TR-83-0305; SR-2) Avail: NTIS HC A09/MF A01 CSCL 04B

This review critically surveys types and accuracies of available satellite data, satellite data retrieval methodologies, and data requirements of numerical weather prediction (NWP) models. NWP modeling, parameterization and data assimilation methods are reviewed with particular attention to the hydrological variables. It is concluded that the means exist to obtain improved retrievals of cloud and moisture parameters and to better parameterize the hydrological cycle. Further advances in the retrieval of humidity profiles, the parameterizations of clouds and the objective analysis of humidity are required.

GRA

A84-30248#

REDUCTION OF HIGH DIMENSION DATA TO TWO DIMENSION USING NON LINEAR MAPPING TECHNIQUES

S. CHANDRASEKHAR (National Remote Sensing Agency, Secunderabad, India) IN: Asian Conference on Remote Sensing, 3rd, Dacca, Bangladesh, December 4-7, 1982, Proceedings . Tokyo, University of Tokyo, 1983, p. Q-10-1 to Q-10-10. refs

A description is given of the nonlinear mapping techniques available for representing data acquired with 4-12 channels on two- or three-dimensional display devices. It is pointed out, however, that these techniques involve a great deal of computation when used with fairly large data sets. A technique is described here which uses the iterative algorithm in a recursive way. The error function chosen retains both the local and global properties of the original data. It is noted that new vectors which will be useful to an analyst working on the display can be added in an interactive way. The clusters that are formed can be displayed on a two-dimensional screen.

C.R.

A84-30249#

MAKING FALSE COLOR PHOTOMAP AND ITS APPLICATION IN THEMATIC MAPPING BY USING IR PHOTOS

G.-Q. XU and T.-S. YAN (Chinese Academy of Sciences, Institute of Remote Sensing Applications, Beijing, People's Republic of China) IN: Asian Conference on Remote Sensing, 3rd, Dacca, Bangladesh, December 4-7, 1982, Proceedings . Tokyo, University of Tokyo, 1983, p. Q-12-1 to Q-12-12. refs

Resource investigation and topographic surveying in various regions of China and different seasons, using domestically produced HCJ-2 film are described. False color photographs and photomaps (photomosaic planimetric maps and differential rectification orthophoto maps) are now widely used in the Institute of Remote Sensing Applications of the Academia Sinica. The film is a kind of color infrared negative with good photographic performance and sensitivity over the wavelength range from 400 to 800 nm. The paper describes the technical procedures for making and evaluating false color photomaps which may be prepared quickly and economically and provide excellent accuracy for the user. It is hoped that interest will be stimulated for their use in resource investigation and thematic and topographic mapping.

D.H.

A84-30264#

LANDSAT PLANIMETRIC MAPS

C. WILSON and D. LOWE (Michigan, Environmental Research Institute, Ann Arbor, MI) IN: Asian Conference on Remote Sensing, 3rd, Dacca, Bangladesh, December 4-7, 1982, Proceedings . Tokyo, University of Tokyo, 1983, p. G-1-1 to G-1-10.

Techniques of geometric correction are described for generating thematic information from satellite imagery, where the information is then transferred to existing or conventionally derived base maps. The three techniques are the affine or linear technique, the nonmodel nonlinear technique, and the rigid model nonlinear technique. A map generation procedure, given exact latitude, longitude and elevation for a small number of control points, is described. A seven-step methodology is given for the generation of Landsat derived planimetric maps, and the accuracy of the correction techniques is evaluated. Maps derived for Saudi Arabia and Mali are shown as examples.

D.H.

A84-30268#

DESCRIPTION OF SEP GROUND STATION AND VIZIR IMAGE PROCESSING VIPS

L. SALTER, G. MAINCENT, G. GAYET, and D. SARRAT (Societe Europeenne de Propulsion, Vernon, Eure, France) IN: Asian Conference on Remote Sensing, 3rd, Dacca, Bangladesh, December 4-7, 1982, Proceedings . Tokyo, University of Tokyo, 1983, p. G-8-1 to G-8-16.

The benefits of receiving SPOT and Landsat-D data in a single location were reviewed, and the primary functional and performance aspects of the EXPORT concepts, which involved adapting the French National Space Research Agency station to world market requirements and adjoining it to a cartographic and thematic image

07

DATA PROCESSING AND DISTRIBUTION SYSTEMS

Includes film processing, computer technology, satellite and aircraft hardware, and imagery.

A84-30234#

BHASKARA-II TV DATA IN RESOURCE STUDIES - A CASE STUDY IN A PART OF ANDHRA PRADESH, SOUTHERN INDIA

S. K. PATHAN and A. V. KULKARNI (Indian Space Research Organization, Space Applications Centre, Ahmedabad, India) IN: Asian Conference on Remote Sensing, 3rd, Dacca, Bangladesh, December 4-7, 1982, Proceedings . Tokyo, University of Tokyo, 1983, p. P-14-1 to P-14-9.

07 DATA PROCESSING AND DISTRIBUTION SYSTEMS

processing system, were described. The modular system designed to receive data from SPOT and Landsat-D consists of a receiving station, a preprocessing station, and a Vizir Image Processing System (VIPS). The receiving station records satellite data on high density magnetic tape. The preprocessing station's functions include correcting systematic images, cataloging, and regulating the production rate. The VIPS processes for thematic and cartographic applications and produces Level 2 and S SPOT products. Technologies developed or implemented include an 8 GHz receiving antenna with zenith capability, and an 84 Megabits/s bit synchronizer. Several block diagrams are provided. C.M.

A84-32093* Jet Propulsion Lab., California Inst. of Tech., Pasadena.

DIGITAL SAR PROCESSING USING A FAST POLYNOMIAL TRANSFORM

T. K. TRUONG, R. G. LIPES, S. A. BUTMAN (California Institute of Technology, Jet Propulsion Laboratory, Pasadena, CA), I. S. REED (Southern California, University, Los Angeles, CA), and A. L. RUBIN (Aerojet Electrosystems Co., Azusa, CA) IEEE Transactions on Acoustics, Speech, and Signal Processing (ISSN 0096-3518), vol. ASSP-32, April 1984, p. 419-425. refs (Contract NAS7-100; N00039-80-C-0641; AF-AFOSR-80-0151)

A new digital processing algorithm based on the fast polynomial transform is developed for producing images from Synthetic Aperture Radar data. This algorithm enables the computation of the two dimensional cyclic correlation of the raw echo data with the impulse response of a point target, thereby reducing distortions inherent in one dimensional transforms. This SAR processing technique was evaluated on a general-purpose computer and an actual Seasat SAR image was produced. However, regular production runs will require a dedicated facility. It is expected that such a new SAR processing algorithm could provide the basis for a real-time SAR correlator implementation in the Deep Space Network. Previously announced in STAR as N82-11295 Author

A84-33334

TERRAIN ANALYSIS DATABASE GENERATION THROUGH COMPUTER-ASSISTED PHOTO INTERPRETATION

D. L. EDWARDS (U.S. Army, Engineer Topographic Laboratories, Fort Belvoir, VA) IN: American Society of Photogrammetry, Annual Meeting, 49th, Washington, DC, March 13-18, 1983, Technical Papers . Falls Church, VA, American Society of Photogrammetry, 1983, p. 152-159. refs

A program concerned with computer-assisted photo interpretation research (CAPIR) was conducted to develop methods and tools which the photo interpreter can use to perform his task more proficiently, accurately, and expeditiously. Attention is given to a system in which an analytical plotter equipped with stereo superposition graphics and linked to a minicomputer has been matched with a geographic information system. A series of microprocessors within the plotter perform real-time control functions. The plotter is equipped with a stereoscope. An investigation was conducted to demonstrate the capabilities of the considered system. High-altitude U-2 photography of the Fort Belvoir, VA, area was used for photointerpretation and digitization. The initial terrain analysis data extracted from the aerial imagery of the study area were landforms. Aspects of terrain analysis and spatial analysis are discussed. It is concluded that the capability to generate a complete digital terrain database from a single interpreter using a single workstation holds promise. G.R.

A84-33335 NON-PARALLACTIC STEREOSCOPY USING SHADOW-DISPARITY

A. F. GREGORY and H. D. MOORE (Gregory Geoscience, Ltd., Ottawa, Canada) IN: American Society of Photogrammetry, Annual Meeting, 49th, Washington, DC, March 13-18, 1983, Technical Papers . Falls Church, VA, American Society of Photogrammetry, 1983, p. 160-169. Sponsorship: Department of Energy, Mines and Resources. refs (Contract DEMR-OSQ-80-00169)

In synergistic mapping programs, use has been made of the stereoscopic viewing of seasonal Landsat images. It was found that some pairs of time-separated Landsat images for the same nominal scene produced a stereomodel for the whole scene. Observations suggest that a stereomodel can be produced in the absence of conventional parallax, while disparities in illumination may be important clues to depth. The disparities may be perceived by the human visual system in the same way as are parallactic disparities. A study of relevant literature was conducted in a search of theoretical support for these tentative conclusions. The visual perception of depth is considered along with the modelling of shadow-disparity, and some quantitative aspects of stereoscopy based on shadow-disparity. It is concluded that a stereomodel can be attained for a whole scene by selecting a pair of images with a specified range of disparities in inclination and/or azimuth of illumination but with no parallax. G.R.

A84-33356

DIGITAL COMPARISON AND CORRELATION TECHNIQUES OF REMOTE SENSING IMAGES HAVING DIFFERENT SPACE RESOLUTION

V. CAPPELLINI (Firenze, Universita; CNR, Istituto di Ricerca Sulle Onde Elettromagnetiche, Florence, Italy) IN: American Society of Photogrammetry, Annual Meeting, 49th, Washington, DC, March 13-18, 1983, Technical Papers . Falls Church, VA, American Society of Photogrammetry, 1983, p. 556-560.

Some digital techniques are proposed to compare and correlate remote sensing images having different space resolution (as obtained from sensors aboard aircrafts or satellites). To compare high space definition images with other images having lower definition, a procedure is described based on the use of a suitable low-pass digital filtering, while spectral extrapolation and approximated Shannon interpolation techniques are presented to pass from low to higher space definition. Considerations for the practical application of these techniques, in conjunction also with geometrical transformations, are developed, in particular to obtain integrated maps of the examined earth regions. Author

A84-33362

EXPERIMENTS IN LITHOGRAPHY FROM REMOTE SENSOR IMAGERY

R. KIDWELL, J. MCSWEENEY, A. WARREN, E. ZANG, and E. VICKERS (U.S. Geological Survey, National Mapping Div., Reston, VA) IN: American Congress on Surveying and Mapping, Annual Meeting, 43rd, Washington, DC, March 13-18, 1983, Technical Papers . Falls Church, VA, American Congress on Surveying and Mapping, 1983, p. 384-393. refs

Imagery from remote sensing systems such as the Landsat multispectral scanner and return beam vidicon, as well as synthetic aperture radar and conventional optical camera systems, contains information at resolutions far in excess of that which can be reproduced by the lithographic printing process. Since these imaging systems record data in various parts of the electromagnetic spectrum, the data often require special handling to produce both standard and special map products. Problems related to scan lines, pixel size, image enhancement, mosaicking, line and lettering data, and printing colors, all contribute to the complexity of these new map products. Numerous experiments have been conducted at the U.S. Geological Survey (USGS) regarding these printing problems and the potential for producing improved map products in the future. Some conclusions have been drawn regarding processing techniques, procedures for production, and printing limitations. Author

07 DATA PROCESSING AND DISTRIBUTION SYSTEMS

A84-33526* Environmental Research Inst. of Michigan, Ann Arbor.

CHARACTERIZATION OF LANDSAT-4 MSS AND TM DIGITAL IMAGE DATA

W. A. MALILA, M. D. METZLER, D. P. RICE, and E. P. CRIST (Michigan, Environmental Research Institute, Ann Arbor, MI) IEEE Transactions on Geoscience and Remote Sensing (ISSN 0196-2892), vol. GE-22, May 1984, p. 177-191. refs (Contract NAS5-27254; NAS5-27346)

The launch of Landsat-4 in July 1982 represents a continuation in the remote sensing of earth resources. The 80-m spatial resolution provided by the Multispectral Scanner (MSS) on board the satellite is fine enough to resolve many natural features and land-use details in both rural and urban settings. The second sensor of the spacecraft, the Thematic Mapper (TM), introduces a new era of sensing with refined spatial resolution (30 m) and expanded spectral coverage (7 bands). This paper describes results from engineering studies of the characteristics of digital image data from the two Landsat-4 sensors. These studies form a part of the Landsat-4 Image Data Quality Analysis program (LIDQA). The image data were generally found to be of high quality and the TM provided several improvements over the MSS, in its spatial and spectral characteristics. G.R.

A84-33527

ANALYSIS AND PROCESSING OF LANDSAT-4 SENSOR DATA USING ADVANCED IMAGE PROCESSING TECHNIQUES AND TECHNOLOGIES

R. BERNSTEIN, H. J. MYERS, H. G. KOLSKY (IBM Scientific Center, Palo Alto, CA), J. B. LOTSPIECH (IBM Laboratory, Boulder, CO), and R. D. LEES (Bechtel Corp., San Francisco, CA) IEEE Transactions on Geoscience and Remote Sensing (ISSN 0196-2892), vol. GE-22, May 1984, p. 192-221. refs

According to a NASA contract, an assessment is to be made of the performance of the Landsat-4 sensors and the associated ground processing. The assessment is to provide a basis for the recommendation of improved algorithms and procedures to process the data. This paper reports the results of the activities related to this contract. A sensor data analysis is discussed, taking into account data entropy, a histogram analysis, A/D converter nonlinearity, detector band-to-band misregistration, failed detectors, sensor resolution, and sensor noise. Questions of sensor data processing with respect to the Thematic Mapper (TM) are examined, giving attention to radiometric correction processing, noise removal, failed detector data compensation, geometric corrections, image enlargement, principal components processing results, and geological applications of TM imagery. A description of image processing technologies is also provided. G.R.

A84-33528* Purdue Univ., Lafayette, Ind.

LANDSAT-4 MSS AND THEMATIC MAPPER DATA QUALITY AND INFORMATION CONTENT ANALYSIS

P. E. ANUTA, L. A. BARTOLUCCI, M. E. DEAN, D. F. LOZANO, E. MALARET, C. D. MCGILLEM, J. A. VALDES, and C. R. VALENZUELA (Purdue University, West Lafayette, IN) IEEE Transactions on Geoscience and Remote Sensing (ISSN 0196-2892), vol. GE-22, May 1984, p. 222-236. refs (Contract NAS5-26859)

Landsat-4 Thematic Mapper and Multispectral Scanner data were analyzed to obtain information on data quality and information content. Geometric evaluations were performed to test band-to-band registration accuracy. Thematic Mapper overall system resolution was evaluated using scene objects which demonstrated sharp high contrast edge responses. Radiometric evaluation included detector relative calibration, effects of resampling, and coherent noise effects. Information content evaluation was carried out using clustering, principal components, transformed divergence separability measure, and numerous supervised classifiers on data from Iowa and Illinois. A detailed spectral class analysis (multispectral classification) was carried out on data from the Des Moines, IA area to compare the information content of the MSS and TM for a large number of scene classes.

Author

A84-33530

REVISED RADIOMETRIC CALIBRATION TECHNIQUE FOR LANDSAT-4 THEMATIC MAPPER DATA

J. M. MURPHY, T. BUTLIN, P. F. DUFF (Canada Centre for Remote Sensing, Ottawa, Canada), and A. J. FITZGERALD (Roy Ball Associates, Ottawa, Canada) IEEE Transactions on Geoscience and Remote Sensing (ISSN 0196-2892), vol. GE-22, May 1984, p. 243-251.

The Thematic Mapper (TM) sensor array consists of 100 detectors in seven spectral bands. For the radiometric calibration of Landsat-4 TM data, the Canada Centre for Remote Sensing (CCRS) has selected a procedure which is based on the method used by CCRS for Landsat Multispectral Scanner (MSS) data. On the basis of detailed observations of background reference levels it was found that line-dependent variations in raw TM image data and in the associated calibration data can be measured and corrected within an operational environment, by applying simple offset corrections on a line-by-line basis. These findings were utilized to revise the radiometric calibration procedure defined by the CCRS. G.R.

A84-33531* Arizona Univ., Tucson.

IN-FLIGHT ABSOLUTE RADIOMETRIC CALIBRATION OF THE THEMATIC MAPPER

K. R. CASTLE, R. G. HOLM, C. J. KASTNER, J. M. PALMER, P. N. SLATER (Arizona, University, Tucson, AZ), M. DINGUIRARD (ONERA, Centre d'Etudes et de Recherches de Toulouse, Toulouse, France), C. E. EZRA, R. D. JACKSON (U.S. Department of Agriculture, Agricultural Research Service, Phoenix, AZ), and R. K. SAVAGE (U.S. Army, Atmospheric Sciences Laboratory, White Sands Missile Range, NM) IEEE Transactions on Geoscience and Remote Sensing (ISSN 0196-2892), vol. GE-22, May 1984, p. 251-255. Sponsorship: U.S. Department of Agriculture. refs (Contract USDA-12-14-5001-38; NAS5-27382)

In order to determine temporal changes of the absolute radiometric calibration of the entire TM system in flight spectroradiometric measurements of the ground and the atmosphere were made simultaneously with TM image collections over the White Sands, NM area. By entering the measured values in an atmospheric radiative transfer program, the radiance levels in four of the spectral bands of the TM were determined, band 1: 0.45 to 0.52 micrometers, band 2: 0.53 to 0.61 micrometers, band 3: 0.62 to 0.70 micrometers, and 4: 0.78 to 0.91 micrometers. These levels were compared to the output digital counts from the detectors that sampled the radiometrically measured ground area, thus providing an absolute radiometric calibration of the entire TM system utilizing those detectors. Previously announced in STAR as N84-15633

A.R.H.

A84-33532* Environmental Research Inst. of Michigan, Ann Arbor.

A PHYSICALLY-BASED TRANSFORMATION OF THEMATIC MAPPER DATA THE TM TASSELED CAP

E. P. CRIST and R. C. CICONE (Michigan, Environmental Research Institute, Ann Arbor, MI) IEEE Transactions on Geoscience and Remote Sensing (ISSN 0196-2892), vol. GE-22, May 1984, p. 256-263. refs

(Contract NAS9-16538)

In an extension of previous simulation studies, a transformation of actual TM data in the six reflective bands is described which achieves three objectives: a fundamental view of TM data structures is presented, the vast majority of data variability is concentrated in a few (three) features, and the defined features can be directly associated with physical scene characteristics. The underlying TM data structure, based on three TM scenes as well as simulated data, is described, as are the general spectral characteristics of agricultural crops and other scene classes in the transformed data space.

Author

07 DATA PROCESSING AND DISTRIBUTION SYSTEMS

A84-33533* National Aeronautics and Space Administration. Ames Research Center, Moffett Field, Calif.

THEMATIC MAPPER IMAGE QUALITY - REGISTRATION, NOISE, AND RESOLUTION

R. C. WRIGLEY, D. H. CARD, C. A. HLAVKA (NASA, Ames Research Center, Moffett Field, CA), J. R. HALL, F. C. MERTZ (Technicolor Government Services, Inc., Moffett Field, CA), C. ARCHWAMETY, and R. A. SCHOWENGERDT (Arizona, University, Tucson, AZ) IEEE Transactions on Geoscience and Remote Sensing (ISSN 0196-2892), vol. GE-22, May 1984, p. 263-271. refs

The Landsat-4 satellite has two new imaging radiometers, including the redesigned Multispectral Scanner (MSS) and the Thematic Mapper (TM). The present investigation is concerned with an assessment of TM image quality on the basis of a study of band-to-band registration, periodic noise, and spatial resolution. In the TM images analyzed, the band-to-band registration accuracy of the instrument is very good. A few imperfections were found. Once a stable misregistration is removed, the TM should also meet its registration specifications between focal planes. Spatial resolution analyses in terms of MTF were performed in comparison modes. The forward and backward scans were shown to have virtually identical MTFs.

G.R.

A84-33534* Department of Agriculture, Beltsville, Md.

COMPARISON OF THE INFORMATION CONTENT OF DATA FROM THE LANDSAT-4 THEMATIC MAPPER AND THE MULTISPECTRAL SCANNER

J. C. PRICE (U.S. Department of Agriculture, Hydrology Laboratory, Beltsville, MD) IEEE Transactions on Geoscience and Remote Sensing (ISSN 0196-2892), vol. GE-22, May 1984, p. 272-281. refs

(Contract NASA ORDER S-10772-C)

There has been a steady increase with respect to the available capability to monitor the earth's surface from satellite platforms. Developments regarding instrumentation should now be considered in the context of the possible commercialization of space systems. The satellite data user is to select his data with many variables in mind, including cost. The present investigation provides a statistical comparison of simultaneously acquired data from the Landsat-4 Thematic Mapper (TM) and the Multispectral Scanner (MSS) for five scenes acquired over agricultural areas. Simple examination of photographic products and manipulation and display of image data suggests that the utility of the TM data will be far greater than that of the MSS. However, factors of cost and frequency of observations can also be important. The approach employed in the investigation should facilitate evaluation of future remote sensing systems.

G.R.

A84-33535* Georgia Univ., Athens.

CARTOGRAPHIC ACCURACY OF LANDSAT-4 MSS AND TM IMAGE DATA

R. WELCH and E. L. USERY (Georgia, University, Athens, GA) IEEE Transactions on Geoscience and Remote Sensing (ISSN 0196-2892), vol. GE-22, May 1984, p. 281-288. refs

(Contract NAS5-27383)

Investigations of the cartographic quality of Landsat-4 MSS and TM image data in CCT-p formats have produced rectification accuracies (rmse/xy/ values) of + or - 2/3 to + or - 1 data pixel for both whole and subscene areas using polynomials of the first through third degree. In order to achieve these accuracies with MSS data, 15 or more Ground Control Points (GCPs) are required, whereas with the TM data sets as few as 5-10 GCPs will suffice. Factors which limit the cartographic rectification accuracies of the Landsat-4 data include: (1) spatial resolution of the data; (2) map and digitizing errors; and (3) terrain relief. Of these factors, data resolution is the most significant, limiting the location of GCPs to about + or - 0.5 pixel. Horizontal displacements due to terrain relief can be minimized by selecting GCPs at or near midrange elevations. Overall, the representative rmse(xy) values of + or - 25 and + or - 55 m for TM and MSS data sets are within U.S. National Map Accuracy Standards for cartographic products of 1:100,000 and 1:200,000 scale, respectively.

G.R.

A84-33536* Jet Propulsion Lab., California Inst. of Tech., Pasadena.

AN ANALYSIS OF LANDSAT-4 THEMATIC MAPPER GEOMETRIC PROPERTIES

R. E. WALKER, A. L. ZOBRIST, N. A. BRYANT, B. GOHKMAN, S. Z. FRIEDMAN, and T. L. LOGAN (California Institute of Technology, Jet Propulsion Laboratory, Pasadena, CA) IEEE Transactions on Geoscience and Remote Sensing (ISSN 0196-2892), vol. GE-22, May 1984, p. 288-293. NASA-supported research. refs

Landsat-4 Thematic Mapper data of Washington, DC, Harrisburg, PA, and Salton Sea, CA were analyzed to determine geometric integrity and conformity of the data to known earth surface geometry. Several tests were performed. Intraband correlation and interband registration were investigated. No problems were observed in the intraband analysis, and aside from indications of slight misregistration between bands of the primary versus bands of the secondary focal planes, interband registration was well within the specified tolerances. A substantial number of ground control points were found and used to check the images' conformity to the Space Oblique Mercator (SOM) projection of their respective areas. The means of the residual offsets, which included nonprocessing related measurement errors, were close to the one pixel level in the two scenes examined. The Harrisburg scene residual mean was 28.38 m (0.95 pixels) with a standard deviation of 19.82 m (0.66 pixels), while the mean and standard deviation for the Salton Sea scene were 40.46 (1.35 pixels) and 30.57 m (1.02 pixels), respectively. Overall, the data were judged to be a high geometric quality with errors close to those targeted by the TM sensor design specifications.

Author

A84-33537* National Aeronautics and Space Administration. Goddard Space Flight Center, Greenbelt, Md.

A STATISTICAL EVALUATION OF THE ADVANTAGES OF LANDSAT THEMATIC MAPPER DATA IN COMPARISON TO MULTISPECTRAL SCANNER DATA

D. L. WILLIAMS, J. R. IRONS, B. L. MARKHAM, R. F. NELSON, D. L. TOLL (NASA, Goddard Space Flight Center, Earth Resources Branch, Greenbelt, MD), R. S. LATTY (Maryland, University, College Park, MD), and M. L. STAUFFER (Computer Sciences Corp., Silver Spring, MD) IEEE Transactions on Geoscience and Remote Sensing (ISSN 0196-2892), vol. GE-22, May 1984, p. 294-302. refs

On July 16, 1982, the second decade of land remote sensing from space was inaugurated with the successful launch of Landsat-4. This satellite carries the Multispectral Scanner (MSS) and a new sensor, the Thematic Mapper (TM). The TM represents the result of an effort in which all of the major improvements in remote-sensing capability were simultaneously integrated into one system. An experiment was developed and conducted to quantify the effect of each TM sensor parameter on classification accuracy. This paper discusses the experimental design and summarizes the results obtained using TM data acquired over the Washington, DC area on November 2, 1982. Attention is given to a study site/data description, the experimental design, photointerpretation and digitization, spectral simulation, radiometric simulation, and spatial simulation.

G.R.

A84-33542 THEMATIC MAPPER - THE ESA-EARTHNET GROUND SEGMENT AND PROCESSING EXPERIENCE

L. FUSCO (ESA, Earthnet Programme Office, Frascati, Italy) IEEE Transactions on Geoscience and Remote Sensing (ISSN 0196-2892), vol. GE-22, May 1984, p. 329-335. refs

The Landsat-4 upgrading project within the European Space Agency's Earthnet Programme Office (EPO) had the objective to allow both the Landsat stations of Fucino (Italy) and Kiruna (Sweden) to acquire, record, preprocess, and distribute Landsat-4 data. The upgrading required to handle Thematic Mapper (TM) data were rather extensive. The TM ground segment is discussed, taking into account the acquisition system, the synchronization and preprocessing system, and processing algorithms and system performance. The procurement of the different systems in the TM

07 DATA PROCESSING AND DISTRIBUTION SYSTEMS

ground processing chain was based on the utilization of off-the-shelf equipment. G.R.

A84-33629

CORRELATIONS BETWEEN THE NONTHERMAL EMISSION OF QUASARLIKE NUCLEI AND THEIR BALMER-LINE WIDTHS

B. V. KOMBERG and E. IU. SHEFER (Akademii Nauk SSSR, Institut Kosmicheskikh Issledovanii, Moscow, USSR) (Pis'ma v Astronomicheskii Zhurnal, vol. 9, Sept. 1983, p. 529-534) Soviet Astronomy Letters (ISSN 0360-0327), vol. 9, Sept.-Oct. 1983, p. 277-279. Translation. refs

Correlations between the nonthermal X-ray and radio luminosities and the full widths of the Balmer emission lines are established for the active-nucleus galaxies cataloged by Steiner. The existence of such correlations would be compatible with an equipartition of energy between the nonthermal radiation and the motion of the gas clouds in the broad-line formation zone. Vaiana has found a similar correlation for the X rays emitted by the hot coronas of rapidly rotating single stars, suggesting that, as in the SS 433 binary system, the radiation from active nuclei may be anisotropic, and their structure might be double. Author

A84-33798

SIMPLE ENHANCEMENT TECHNIQUES IN DIGITAL IMAGE PROCESSING

S. HAHN (IBM de Mexico, S.A.; Instituto Politecnico Nacional, Mexico City, Mexico) and E. E. MENDOZA (Universidad Nacional Autonoma de Mexico, Villa Obregon, Mexico) Computer Vision, Graphics, and Image Processing (ISSN 0734-189X), vol. 26, May 1984, p. 233-241.

Operators based upon partial derivatives are very useful in digital image processing. In this paper results using a gradient-like map and a three-parameter family of filters are presented. An important parameter of this family is the fraction of original data to be combined simultaneously with an enhanced image obtained through the use of a generalized Laplacian-like map. By superposing different sets of data new images are obtained with highly enhanced edges and contours, while still preserving the original texture. The results are illustrated by using Landsat images of Mexico. Author

A84-34786

INTERACTIVE PROCEDURES FOR DISTINGUISHING AND RECONSTRUCTING CONTOUR NETWORKS [INTERAKTIVNYE PROTSEDURY VYDELENIIA I VOSSTANOVLENIIA KONTURNYKH SETEI]

R. I. ELMAN (Vsesoiuznoe Aerofotolesoustroitel'noe Ob'edinenie Lesproekt, Moscow, USSR) Issledovanie Zemli iz Kosmosa (ISSN 0205-9614), Mar.-Apr. 1984, p. 87-97. In Russian.

A method is outlined for the interactive detection and reconstruction of the contour lines that are drawn on aerospace photos after interpretation. Smooth masks and logic masks are used to distinguish the contour lines. The reconstruction of the lines involves a sequence of procedures based on an analysis of the vicinities of the contour points. C.R.

A84-34959

A SEMI-AUTOMATED PROCEDURE FOR IDENTIFYING LANDSAT MSS SUBREGION COORDINATES

D. L. CIVCO (Connecticut, University, Storrs, CT) Photogrammetric Engineering and Remote Sensing (ISSN 0099-1112), vol. 50, May 1984, p. 597, 598.

A84-37773

RABIVE - A REAL TIME PROGRAM SYSTEM FOR RADIOMETRIC IMAGE PROCESSING [RABIVE - EIN ECHTZEITPROGRAMMSYSTEM ZUR RADIOMETRISCHEN BILDVERARBEITUNG]

M. KAEHLER and G. KOENIG (Berlin, Technische Universitaet, Berlin, West Germany) Bildmessung und Luftbildwesen (ISSN 0006-2421), vol. 52, May 1984, p. 107-114. In German. refs

A system which reduces the response time of a digital image processing system is presented. This software package permits

simultaneous radiometric image enhancement of up to four pictures of 512 by 512 pixels each. The hardware environment of the system is described, and some examples of radiometric corrections are presented. C.D.

A84-38300

PERFORMANCE EVALUATION AND A DEDICATED SYSTEM FOR SAR IMAGE DATA PROCESSING

K. HOMMA, F. KOMURA, S. YAMAGATA (Hitachi Ltd., Systems Development Laboratory, Kawasaki, Japan), and Y. KUBO (Hitachi Ltd., Omika Works, Hitachi, Japan) IN: International Symposium on Space Technology and Science, 13th, Tokyo, Japan, June 28-July 3, 1982, Proceedings . Tokyo, AGNE Publishing, Inc., 1982, p. 1271-1276. Research supported by the Earth Resource Satellite.

The performance of a synthetic aperture radar (SAR) image reconstruction system for spaceborne SAR is assessed, along with the requirements of a dedicated system. A returned microwave pulse carries a reflection intensity pattern of the surface in hologram pattern. The pulse has, however, time duration and a lack of sharpness in the orbital direction. Data processing proceeds by range compression, range migration correction, and compression in the along-track direction. The first and last stages are performed by cross-correlating spread point target information. An estimate of the Doppler shift is made and the frequency modulation rate is evaluated as a constant value. Application of the technique with data from the Seasat-1 SAR imagery is shown to require a multiprocessor capability. A processor pipeline concept, i.e., an aggregate network of processing algorithm flow, is asserted capable of 80 images per day. M.S.K.

A84-38302

TWO-STAGE CLUSTER ANALYSIS OF A LANDSAT IMAGE

K. MATSUMOTO, M. NAKA, H. YAMAMOTO (National Aerospace Laboratory, Chofu, Tokyo, Japan), and I. OHNUKI (Forestry and Forest Products National Research Institute, Ushiku, Ibaraki, Japan) IN: International Symposium on Space Technology and Science, 13th, Tokyo, Japan, June 28-July 3, 1982, Proceedings . Tokyo, AGNE Publishing, Inc., 1982, p. 1285-1290. refs

The two-stage clustering program CASIM for analysis of remotely sensed imagery is described. A satellite image is first subjected to histogram clustering (HC), which involves segmentation of the multidimensional space using local maxima and minima of a spectral distribution function. The cluster is correctly identified if the center of a cluster is observed as a peak of the histogram frequency. The HC results are then processed by splitting and merging functions as 'seeds' representing the spectral distribution of the scene. Adjacent areas with similar spectral characteristics can then be discerned according to a priori-determined boundaries, cluster size, the number of clusters, etc. CASIM performance is illustrated using 60,000 synthetic samples from a 10-cluster mixture in four-dimensional space representing a forested area. The overall classification accuracy obtained is about 73 percent for seven categories of forest type. M.S.K.

A84-38304

A SAR IMAGE AUTO-FOCUSING USING LINEAR DISTORTION AZIMUTH MATCHED FILTER

A. TSUBOI, T. IIJIMA, H. KIMURA, and N. KODAIRA (Remote Sensing Technology Center of Japan, Tokyo, Japan) IN: International Symposium on Space Technology and Science, 13th, Tokyo, Japan, June 28-July 3, 1982, Proceedings . Tokyo, AGNE Publishing, Inc., 1982, p. 1299-1304.

The estimation error in an azimuth matched filter used for the azimuth compression of SAR raw data causes image slip between looks. The image slip gives rise to most degradation of SAR multi-look image in look summation operation. In order to reduce the degradation and produce a high resolution SAR multi-look image, an auto-focusing method that minimizes the degradation by measuring the image slip is proposed and proved feasible by being applied for the Seasat SAR data processing. In this method,

07 DATA PROCESSING AND DISTRIBUTION SYSTEMS

a linear distortion matched filter is used for the azimuth compression so that the image slip may be measured precisely. Author

A84-38305

FAST PROCESSING OF SYNTHETIC APERTURE RADAR SIGNAL WITHOUT DATA TRANSPOSITION

M. ONOE (Tokyo, University, Tokyo, Japan), I. KUBOTA, and Y. MASUBUCHI IN: International Symposium on Space Technology and Science, 13th, Tokyo, Japan, June 28-July 3, 1982, Proceedings . Tokyo, AGNE Publishing, Inc., 1982, p. 1305-1310. Research supported by Toray Science and Technology. refs

An algorithm is presented for processing Seasat SAR imagery. The code was devised to raise the efficiency of processing the data which, although gathered for only three months, would require a decade to process using existing techniques. A method for computing large-scale two-dimensional Fourier transforms (FFT) without transposing the data matrix is reviewed. The algorithm permits applications of FFT functions to each row element, thus eliminating the necessity of transposing whole rows. The matrix obtained is then transformed for azimuth compression to account for range curvature corrections and the multiple look operations. Experimental results generated with a minicomputer demonstrate the efficacy of the CASIM code. M.S.K.

A84-38313

STUDY ON TEMPORAL GEOMETRIC-DISTORTION VARIATION OF LANDSAT MSS AND RBV IMAGERIES AND ATTITUDE DETERMINATION PROGRAM

Y. YAMAURA (National Space Development Agency of Japan, Ohashi, Saitama, Japan) and K. TSUCHIYA (Chiba University, Chibashi, Japan) IN: International Symposium on Space Technology and Science, 13th, Tokyo, Japan, June 28-July 3, 1982, Proceedings . Tokyo, AGNE Publishing, Inc., 1982, p. 1371-1380. refs

The results and problems which arose in analyses of Landsat MSS, return beam vidicon (RBV) and telemetry data to determine the spacecraft attitude as a prelude to correcting for geometric distortions are reported. The analyses revealed the presence of image offsets in across- and along-track directions as well as skewness and rotation of images. The temporal variations in the imagery amounted to 3.4 km offsets, while MSS image skew and RBV rotation amounted to 2.1 deg. The causative agent was inaccuracy in the IR horizon model. The error was possibly introduced by a sudden stratospheric warming in winter. Techniques used to quantify the attitude measurement sensor yaw determination and geometric distortion factors are detailed. It is concluded that the present CO2 IR horizon model must be upgraded to include zonal variation factors in order to reduce yaw errors. M.S.K.

A84-38314

DATA COMPRESSION OF REMOTELY SENSED DATA FROM SPACE

K. MAEDA (National Space Development Agency of Japan, Earth Observation Systems Dept., Tokyo, Japan) IN: International Symposium on Space Technology and Science, 13th, Tokyo, Japan, June 28-July 3, 1982, Proceedings . Tokyo, AGNE Publishing, Inc., 1982, p. 1381-1391. refs

Comparisons are made among original remotely sensed images and images treated with data compression clustering (DCC) techniques to identify parameters which lead to high classification accuracy. Imagery generated with the Landsat MSS and airborne SAR apparatus was considered. DCC consists of subdividing the images into subimages (windows) and applying clustering analysis to each window. A second clustering state is then imposed on clusters obtained in the first stage. The images examined included seven classes of farm crops and trees. A cascading cluster method was used to eliminate the generation of artificial boundaries in the first set of windows. Mean square errors were calculated for the resulting classifications. The effect of window shape was quantified. The compression ratio yielded by the cascade technique commends the method to inclusion in on-board data compressors on future spacecraft. M.S.K.

A84-38315

IMAGE ANALYSIS RESEARCHES OF REMOTELY SENSED DATA AT NAL

H. KOSHIISHI, M. NAKA, H. YAMAMOTO, K. MATSUMOTO, and K. HOMMA (National Aerospace Laboratory, Chofu, Tokyo, Japan) IN: International Symposium on Space Technology and Science, 13th, Tokyo, Japan, June 28-July 3, 1982, Proceedings . Tokyo, AGNE Publishing, Inc., 1982, p. 1393-1400. Research supported by the Science and Technology Agency. refs

This paper describes some of the results obtained in image analysis researches at National Aerospace Laboratory (NAL) for effective utilization of earth observation satellite data. As an advanced image analysis technique of parallel form and/or spatial information processing, three classifiers (maximum likelihood analysis, clustering analysis and relaxation analysis) have been studied, and these computer softwares have been implemented on the vector type parallel processor. The implemented softwares are successfully applied to vegetation analysis of forestry and good classification color maps are obtained. Author

A84-38316

A SIMULATION PROGRAM FOR THE INTEGRATION OF AEROSPACE REMOTE SENSING SYSTEMS WITH A DIGITAL TERRAIN MODEL

S. VETRELLA and A. MOCCIA (Napoli, Universita, Naples, Italy) IN: International Symposium on Space Technology and Science, 13th, Tokyo, Japan, June 28-July 3, 1982, Proceedings . Tokyo, AGNE Publishing, Inc., 1982, p. 1401-1407. Research supported by the Consiglio Nazionale delle Ricerche. refs

A simulation program for obtaining the principal orbital orientation and viewing parameters for remote sensing satellites is described. The program takes into account the orbital geometry, the pointing accuracy, and the drift. The subsatellite and Doppler track, the local time, the instantaneous line of sight or the slant range and its intersection with illumination and atmospheric conditions are obtained. The fundamental equations of orbital dynamics are defined. A sample simulation was performed with SPOT satellite data, demonstrating that a minimum number of ground control points will be required where extensive cartography has already been performed. The program can be applied to preprocessing incoming satellite imagery data. M.S.K.

A84-38942

ATMOSPHERIC CORRECTION OF LANDSAT MSS DATA FOR A MULTIDATE SUSPENDED SEDIMENT ALGORITHM

N. MACFARLANE and I. S. ROBINSON (Southampton, University, Southampton, England) International Journal of Remote Sensing (ISSN 0143-1161), vol. 5, May-June 1984, p. 561-576. refs

This paper describes the application of various processing methods to a synoptic set of satellite-sea data obtained from the Solent area on the south coast of England. The methods include 'darkest pixel' correction, sun angle and radiometric corrections, chromaticity analysis, atmospheric and surface corrections and the use of the satellite sensor response curves. It is shown that the use of a simple atmospheric/surface correction algorithm, based on atmospheric optical transmission theory, provides the most accurate method of estimating estuarine suspended sediment concentration from the satellite data above. Author

A84-38944

EQUIDENSITOMETRY AND REMOTE SENSING IMAGERY

R. HARRIS (Durham, University, Durham, England) International Journal of Remote Sensing (ISSN 0143-1161), vol. 5, May-June 1984, p. 619-622. refs

In connection with the interpretation of remotely sensed imagery, there is now a need for inexpensive methods which will provide objective statements of relative image densities. Such methods can be based on the photographic processing of imagery. The principal advantages of such an approach would be related to low cost, high spatial resolution, and objectivity. The present investigation is concerned with a form of photographic processing which generates density contours from imagery, taking into account the technique of equidensitometry. This technique involves the

07 DATA PROCESSING AND DISTRIBUTION SYSTEMS

linking of all points of the same density on an image by a line. The resulting image is a contour map of the original image, with contours representing lines of equal density. The application of equidensitometry is illustrated with the aid of a case study involving a NOAA2 thermal infrared image composite. G.R.

A84-39044

A BISPECTRAL METHOD FOR THE HEIGHT DETERMINATION OF OPTICALLY THIN ICE CLOUDS

W. POLLINGER and P. WENDLING (Deutsche Forschungs- und Versuchsanstalt fuer Luft- und Raumfahrt, Institut fuer Physik der Atmosphaere, Oberpfaffenhofen, West Germany) Beitraege zur Physik der Atmosphaere (ISSN 0005-8173), vol. 57, May 1984, p. 269-281. Research supported by the Deutsche Forschungsgemeinschaft and Deutsche Forschungs- und Versuchsanstalt fur Luft- und Raumfahrt. refs

A technique for determining the height of ice clouds of emissivity less than one from temperature and humidity profiles plus satellite IR (6.3-micron and 11-micron) measurements is developed and demonstrated using simulated data from a radiative-transfer model and NOAA-6 HIRS/2 data. The principle of the method is explained, and the fundamental equations are derived, taking the water vapor above the cloud into account. A flow chart of the computation scheme is shown, and the results of the simulation are presented in graphs. Comparison of actual satellite measurements with airborne lidar data reveals good agreement. T.K.

N84-22999*# California Univ., Santa Barbara. Dept. of Geography.

REGISTRATION OF TM DATA TO DIGITAL ELEVATION MODELS

In its LANDSAT-D Invest. in Snow Hydrol. p 6-9 31 Mar. 1984 refs Proposed for presentation at the LARS Symp., Jun. 1984 ERTS

Avail: NTIS HC A02/MF A01 CSCL 08B

Several problems arise when attempting to register LANDSAT thematic mapper data to U.S. Geological Survey digital elevation models (DEMs). The TM data are currently available only in a rotated variant of the Space Oblique Mercator (SOM) map projection. Geometric transforms are thus required to access TM data in the geodetic coordinates used by the DEMs. Due to positional errors in the TM data, these transforms require some sort of external control. The spatial resolution of TM data exceeds that of the most commonly DEM data. Oversampling DEM data to TM resolution introduces systematic noise. Common terrain processing algorithms (e.g., close computation) compound this problem by acting as high-pass filters. Author

N84-23003*# EROS Data Center, Sioux Falls, S. Dak.

LANDSAT 4 INVESTIGATIONS OF THEMATIC MAPPER AND MULTISPECTRAL SCANNER APPLICATIONS Quarterly Report

D. T. LAUER, Principal Investigator 26 Apr. 1984 19 p refs Original contains imagery. Original photography may be purchased from the EROS Data Center, Sioux Falls, S.D. 57198 ERTS (Contract NASA ORDER S-10757-C) (E84-10100; NASA-CR-173369; NAS 1.26:173369) Avail: NTIS HC A02/MF A01 CSCL 08B

The optimum index factor package was used to choose TM band for color compositing. Processing techniques were also used on TM data over several sites to: (1) reduce the amount of data that needs to be processed and analyzed by using statistical methods or by combining full-resolution products with spatially compressed products; (2) digitally process small subareas to improve the visual appearance of large-scale products or to merge different-resolution image data; and (3) evaluate and compare the information content of the different three-band combinations that can be made using the TM data. Results indicate that for some applications the added spectral information over MSS is even more important than the TM's increased spatial resolution. A.R.H.

N84-23009*# Rochester Inst. of Tech., N. Y. Coll. of Graphic Arts and Photography.

LANDSAT 4 BAND 6 DATA EVALUATION Quarterly Report

15 Mar. 1984 3 p ERTS

(Contract NAS5-27323)

(E84-10119; NASA-CR-173489; NAS 1.26:173489; QR-6) Avail: NTIS HC A02/MF A01 CSCL 05B

Previously experienced data collection problems were successfully resolved. A limited effort, directed at improved methods of display of TM Band 6 data, has concentrated on implementation of intensity hue and saturation displays using the Band 6 data to control hue. These displays tend to give the appearance of high resolution thermal data and make whole scene thermal interpretation easier by color coding thermal data in a manner that aids visual interpretation. More quantitative efforts were directed at utilizing the reflected bands to define land cover classes and then modifying the thermal displays using long wave optical properties associated with cover type. A.R.H.

N84-23980*# Instituto de Pesquisas Espaciais, Sao Jose dos Campos (Brazil).

EVALUATION OF THE EFFECTS OF THE SEASONAL VARIATION OF SOLAR ELEVATION ANGLE AND AZIMUTH ON THE PROCESSES OF DIGITAL FILTERING AND THEMATIC CLASSIFICATION OF RELIEF UNITS [AVALIACAO DOS EFEITOS DA VARIACAO SAZONAL DO ANGULO DE ELEVACAO SOLAR E AZIMUTE SOBRE PROCESSOS DE FILTRAGEM DIGITAL E CLASSIFICACAO TEMATICA DO RELEVO]

N. D. J. PARADA, Principal Investigator and E. M. L. M. NOVO Aug. 1983 36 p refs In PORTUGUESE; ENGLISH summary Sponsored by NASA Original contains color imagery. Original photography may be purchased from the EROS Data Center, Sioux Falls, S.D. 57198 ERTS (E84-10121; NASA-CR-172796; NAS 1.26:172796; INPE-2858-RPE/440) Avail: NTIS HC A03/MF A01 CSCL 05B

The effects of the seasonal variation of illumination over digital processing of LANDSAT images are evaluated. Two sets of LANDSAT data referring to the orbit 150 and row 28 were selected with illumination parameters varying from 43 deg to 64 deg for azimuth and from 30 deg to 36 deg for solar elevation respectively. IMAGE-100 system permitted the digital processing of LANDSAT data. Original images were transformed by means of digital filtering so as to enhance their spatial features. The resulting images were used to obtain an unsupervised classification of relief units. Topographic variables (declivity, altitude, relief range and slope length) were used to identify the true relief units existing on the ground. The LANDSAT over pass data show that digital processing is highly affected by illumination geometry, and there is no correspondence between relief units as defined by spectral features and those resulting from topographic features. M.A.C.

N84-23981*# Arizona Univ., Tucson.

INVESTIGATION OF SEVERAL ASPECTS OF LANDSAT-4 DATA QUALITY Quarterly Progress Report

R. C. WRIGLEY, Principal Investigator 20 Mar. 1984 10 p

Sponsored by NASA ERTS

(E84-10122; NASA-CR-172797; NAS 1.26:172797) Avail: NTIS HC A02/MF A01 CSCL 05B

The Thematic Mapper scene of Sacramento, CA acquired during the TDRSS test was received in TIPS format. Quadrants for both scenes were tested for band-to-band registration using reimplemented block correlation techniques. Summary statistics for band-to-band registrations of TM band combinations for Quadrant 4 of the NE Arkansas scene in TIPS format are tabulated as well as those for Quadrant 1 of the Sacramento scene. The system MTF analysis for the San Francisco scene is completed. The thermal band did not have sufficient contrast for the targets used and was not analyzed. A.R.H.

07 DATA PROCESSING AND DISTRIBUTION SYSTEMS

N84-24499# Institute for Image Processing Computer Mapping, Graz (Austria).

EXPERIMENTS TO CORRECT A DIGITAL MAP DATA BASE USING SCENE ANALYSIS Progress Report, 1 Sep. - 31 Dec. 1983

F. LEBERL Mar. 1984 39 p

(Contract DAJA45-83-C-0022; DA PROJ. IT1-61102-BH-57)
(AD-A139447; PR-4) Avail: NTIS HC A03/MF A01 CSCL 09B

Concepts and methods used in correcting a digital map base with scene analysis are presented in summary form. This study is concerned with one special aspect of computer vision: How can knowledge in the form of a digital map serve in automatic image interpretation, and, on the other hand, how can interpretation results be used to change or update the map? In a wider sense, map may mean any graphic representation of a scene that is imaged. Here, in particular, this document deals with maps in the cartographic sense, and with images from airborne photographic systems. One of the obvious applications is the correction or densification of a map data base using time series of aerial surveying imagery. The aim of this study therefore is the design of a strategy to evaluate the usefulness of image-map correspondence to aid the interpretation of digital aerial photography. This is the first step to be taken towards a photo-interpretation expert system, which shall be called henceforth name PHIX.

GRA

N84-25140*# Environmental Research Inst. of Michigan, Ann Arbor.

STUDY ON SPECTRAL/RADIOMETRIC CHARACTERISTICS OF THE THEMATIC MAPPER FOR LAND USE APPLICATIONS

Quarterly Status Technical Progress Report, 21 Dec. 1983 - 20 Mar. 1984

W. A. MALILA, Principal Investigator Apr. 1984 29 p refs ERTS

(Contract NAS5-27346)

(E84-10130; NASA-CR-172805; NAS 1.26:172805;

ERIM-16400-10-P) Avail: NTIS HC A03/MF A01 CSCL 08B

An information theoretic measure of multispectral information content is developed and applied to a simultaneous LANDSAT TM and MSS data set. The entropy based function measures the dispersion and concentration of signal values in various data spaces, irrespective of specific class memberships. It is used to compare the information content of TM and MSS and of various subsets of TM and MSS bands, as well as tasseled cap transformations of the band values. Differences exist between the information measure results and results using variance based measures. System design information capacities and data space volumes are also compared. The results and observations presented are considered preliminary in nature since only one real and one simulated data set are analyzed. M.A.C.

N84-25148# Royal Inst. of Tech., Stockholm (Sweden). Dept. of Photogrammetry.

MATHEMATICAL ASPECTS OF DIGITAL TERRAIN INFORMATION. A PROGRESS REPORT FROM ISPRS WORKING GROUP III:3

K. TORLEGAARD *In its* Photogrammetric Res. 3 p 1983

Avail: NTIS HC A10/MF A01

An international experiment to compare photogrammetrically measured digital elevation models (DEM) is started. Terrain classification and mathematical aspects on planimetric data were examined.

Author

N84-26085*# California Univ., Berkeley. Space Sciences Lab. **ANALYSIS OF THE QUALITY OF IMAGE DATA ACQUIRED BY THE LANDSAT-4 THEMATIC MAPPER AND MULTISPECTRAL SCANNERS** Quarterly Status Technical Progress Report, 1 Jan. - 31 Mar. 1984

R. N. COLWELL, Principal Investigator 15 Apr. 1984 22 p ERTS

(Contract NAS5-27377)

(E84-10137; NASA-CR-172810; NAS 1.26:172810; QSTPR-5)

Avail: NTIS HC A02/MF A01 CSCL 05B

The geometric quality of TM film and digital products is evaluated by making selective photomeasurements and by measuring the coordinates of known features on both the TM products and map products. These paired observations are related using a standard linear least squares regression approach. Using regression equations and coefficients developed from 225 (TM film product) and 20 (TM digital product) control points, map coordinates of test points are predicted. The residual error vectors and analysis of variance (ANOVA) were performed on the east and north residual using nine image segments (blocks) as treatments. Based on the root mean square error of the 223 (TM film product) and 22 (TM digital product) test points, users of TM data expect the planimetric accuracy of mapped points to be within 91 meters and within 117 meters for the film products, and to be within 12 meters and within 14 meters for the digital products.

M.A.C.

N84-26086*# Georgia Univ., Athens. Dept. of Geography.

COMPARATIVE ASSESSMENT OF LANDSAT-D MSS AND TM DATA QUALITY FOR MAPPING APPLICATIONS IN THE SOUTHEAST Report, 15 Oct. 1983 - 15 Jul. 1984

6 Jun. 1984 3 p ERTS

(Contract NAS5-27383)

(E84-10138; NASA-CR-172811; NAS 1.26:172811) Avail: NTIS

HC A02/MF A01 CSCL 05B

Rectifications of multispectral scanner and thematic mapper data sets for full and subscene areas, analyses of planimetric errors, assessments of the number and distribution of ground control points required to minimize errors, and factors contributing to error residual are examined. Other investigations include the generation of three dimensional terrain models and the effects of spatial resolution on digital classification accuracies.

M.A.C.

N84-26088*# Instituto de Pesquisas Espaciais, Sao Jose dos Campos (Brazil).

EVALUATION OF SOLAR ANGLE VARIATION OVER DIGITAL PROCESSING OF LANDSAT IMAGERY

N. D. J. PARADA, Principal Investigator and E. M. L. M. NOVO May 1984 10 p refs Submitted for publication Sponsored by NASA ERTS

(E84-10140; NASA-CR-172813; NAS 1.26:172813;

INPE-3101-PRE/500) Avail: NTIS HC A02/MF A01 CSCL 05B

The effects of the seasonal variation of illumination over digital processing of LANDSAT images are evaluated. Original images are transformed by means of digital filtering to enhance their spatial features. The resulting images are used to obtain an unsupervised classification of relief units. After defining relief classes, which are supposed to be spectrally different, topographic variables (declivity, altitude, relief range and slope length) are used to identify the true relief units existing on the ground. The samples are also clustered by means of an unsupervised classification option. The results obtained for each LANDSAT overpass are compared. Digital processing is highly affected by illumination geometry. There is no correspondence between relief units as defined by spectral features and those resulting from topographic features.

M.A.C.

07 DATA PROCESSING AND DISTRIBUTION SYSTEMS

N84-26089*# Instituto de Pesquisas Espaciais, Sao Jose dos Campos (Brazil).

EVALUATION OF ENTROPY AND JM-DISTANCE CRITERIONS AS FEATURES SELECTION METHODS USING SPECTRAL AND SPATIAL FEATURES DERIVED FROM LANDSAT IMAGES

N. D. J. PARADA, Principal Investigator, L. V. DUTRA, F. A. M. II, and N. D. A. MASCARENHAS May 1984 10 p refs Presented at the Intern. Soc. for Photogrammetry and Remote Sensing Congr., Rio de Janeiro, 18-29 Jun. 1984 Sponsored by NASA ERTS (E84-10141; NASA-CR-172814; NAS 1.26:172814; INPE-3122-PRE/515) Avail: NTIS HC A02/MF A01 CSCL 12A

A study area near Ribeirao Preto in Sao Paulo state was selected, with predominance in sugar cane. Eight features were extracted from the 4 original bands of LANDSAT image, using low-pass and high-pass filtering to obtain spatial features. There were 5 training sites in order to acquire the necessary parameters. Two groups of four channels were selected from 12 channels using JM-distance and entropy criterions. The number of selected channels was defined by physical restrictions of the image analyzer and computacional costs. The evaluation was performed by extracting the confusion matrix for training and tests areas, with a maximum likelihood classifier, and by defining performance indexes based on those matrixes for each group of channels. Results show that in spatial features and supervised classification, the entropy criterion is better in the sense that allows a more accurate and generalized definition of class signature. On the other hand, JM-distance criterion strongly reduces the misclassification within training areas.

Author

N84-26091*# Instituto de Pesquisas Espaciais, Sao Jose dos Campos (Brazil).

AN INTEGRATED SOFTWARE SYSTEM FOR GEOMETRIC CORRECTION OF LANDSAT MSS IMAGERY

N. D. J. PARADA, Principal Investigator, A. J. F. M. ESILVA, F. A. M. II, G. CAMARA-NETO, P. R. M. SERRA, and R. C. M. DESOUZA Apr. 1984 12 p refs Presented at the 15th Intern. Congr. of Photogrammetry and Remote Sensing, Rio de Janeiro, 17-20 Jun. 1984 Sponsored by NASA ERTS (E84-10143; NASA-CR-172816; NAS 1.26:172816; INPE-3078-PRE/491) Avail: NTIS HC A02/MF A01 CSCL 09B

A system for geometrically correcting LANDSAT MSS imagery includes all phases of processing, from receiving a raw computer compatible tape (CCT) to the generation of a corrected CCT (or UTM mosaic). The system comprises modules for: (1) control of the processing flow; (2) calculation of satellite ephemeris and attitude parameters, (3) generation of uncorrected files from raw CCT data; (4) creation, management and maintenance of a ground control point library; (5) determination of the image correction equations, using attitude and ephemeris parameters and existing ground control points; (6) generation of corrected LANDSAT file, using the equations determined beforehand; (7) union of LANDSAT scenes to produce and UTM mosaic; and (8) generation of output tape, in super-structure format.

A.R.H.

N84-26096*# Instituto de Pesquisas Espaciais, Sao Jose dos Campos (Brazil).

EVALUATION OF SIR-A (SHUTTLE IMAGING RADAR) IMAGES FROM THE TRES MARIAS REGION (MINAS GERAIS STATE, BRAZIL) USING DERIVED SPATIAL FEATURES AND REGISTRATION WITH MSS-LANDSAT IMAGES

N. D. J. PARADA, Principal Investigator, H. J. H. KUX, and L. V. DUTRA May 1984 8 p refs Presented at the Intern. Soc. for Photogrammetry and Remote Sensing Congr., Rio de Janeiro, 18-29 Jun. 1984 Sponsored by NASA ERTS (E84-10148; NASA-CR-173238; NAS 1.26:173238; INPE-3113-PRE/510) Avail: NTIS HC A02/MF A01 CSCL 05B

Two image processing experiments are described using a MSS-LANDSAT scene from the Tres Marias region and a shuttle Imaging Radar SIR-A image digitized by a vidicon scanner. In the first experiment the study area is analyzed using the original and

preprocessed SIR-A image data. The following thematic classes are obtained: (1) water, (2) dense savanna vegetation, (3) sparse savanna vegetation, (4) reforestation areas and (5) bare soil areas. In the second experiment, the SIR-A image was registered together with MSS-LANDSAT bands five, six, and seven. The same five classes mentioned above are obtained. These results are compared with those obtained using solely MSS-LANDSAT data. The spatial information as well as coregistered SIR-A and MSS-LANDSAT data can increase the separability between classes, as compared to the use of raw SIR-A data solely.

M.A.C.

N84-26097*# California Univ., Davis. Dept. of Electrical and Computer Engineering.

LANDSAT-D THEMATIC MAPPER IMAGE DIMENSIONALITY REDUCTION AND GEOMETRIC CORRECTION ACCURACY Quarterly Status Technical Progress Report, 3 Dec. 1983 - 3 Mar. 1984

G. E. FORD, Principal Investigator 3 Mar. 1984 7 p refs ERTS (Contract NAS5-27577) (E84-10149; NASA-CR-173239; NAS 1.26:173239) Avail: NTIS HC A02/MF A01 CSCL 08B

Principal components transformations was applied to a Walnut Creek, Texas subscene to reduce the dimensionality of the multispectral sensor data. This transformation was also applied to a LANDSAT 3 MSS subscene of the same area acquired in a different season and year. Results of both procedures are tabulated and allow for comparisons between TM and MSS data. The TM correlation matrix shows that visible bands 1 to 3 exhibit a high degree of correlation in the range 0.92 to 0.96. Correlation for bands 5 to 7 is 0.93. Band 4 is not highly correlated with any other band, with corrections in the range 0.13 to 0.52. The thermal band (6) is not highly correlated with other bands in the range 0.13 to 0.46. The MSS correlation matrix shows that bands 4 and 5 are highly correlated (0.96) as are bands 6 and 7 with a correlation of 0.92.

A.R.H.

N84-26102*# European Space Agency, Paris (France).

EARTHNET: THE STORY OF IMAGES

N. LONGDON, ed. Mar. 1984 60 p Original contains color illustrations

(ESA-BR-18; ISSN-0250-1589) Avail: NTIS HC A04/MF A01

Earthnet, the European-based program involved with the acquisition, archiving, preprocessing, and distribution of satellite remote sensing data, is discussed in terms of scope and experience with NASA satellites. Interface with the SEASAT 1 satellite, the Nimbus 7, the Heat Capacity Mapping Mission (HCMM), and LANDSAT satellites is described. The cataloging and transmission of image data at Earthnet facilities are reviewed. The ERS-1 satellite of the European Space Agency (ESA) and the Spacelab project are discussed with respect to Earthnet.

R.S.F.

N84-26103*# Societe d'Etudes Techniques et d'Entreprises Generales, Leplessis-Robinson (France).

COMPARATIVE STUDY OF IMAGE DATA PRODUCED BY SATELLITES WITH DIFFERENT CHARACTERISTICS Final Report [ETUDE SUR LA COMPARAISON DES DONNEES IMAGES PRODUITES PAR DES SATELLITES DE CARACTERISTIQUES DIFFERENTES]

Paris ESA Oct. 1983 82 p refs

(Contract ESA-4524/81/D-JS(SC))

(ESA-CR(P)-1867) Avail: NTIS HC A05/MF A01

The methodology for combining imagery from different satellites involves choosing a reference and, by appropriate transformations, associating several spectral responses of a target, and then reducing these responses to conditions which permit the juxtaposition in space (geometry and resolution), in time, and from the point of view of their radiometric calibration. Procedures are reviewed using examples from oceanography, geology, and the natural milieu to demonstrate feasibility and interest combining imagery from satellite imagery.

A.R.H.

07 DATA PROCESSING AND DISTRIBUTION SYSTEMS

N84-26105# European Space Agency, Paris (France). THE THEORY OF EARTH OBSERVATION USING MULTIPLE-FREQUENCY RADAR

E. SAPPL Sep. 1983 58 p refs Transl. into ENGLISH of "Theorie der erdbeobachtung mit mehrfrequenzradar" rept. DFVLR-FB-82-31 DFVLR, Goettingen, West Germany, Sep. 1982 Original language document announced as N83-30856 (ESA-TT-819; DFVLR-FB-82-31) Avail: NTIS HC A04/MF A01; Original Germany report available from DFVLR, Cologne DM 22,50

The backscattering from the Earth's surface using multiple-frequency radar is described by a generalized backscattering coefficient. The measurement of this coefficient is discussed. A surface whose characteristic scattering is both homogeneous and stationary is considered and thereafter the study is extended to any type of surface. The general case includes the observation of water surfaces by means of a dual frequency radar.

E.A.K.

N84-26112# Army Engineer Topographic Labs., Fort Belvoir, Va.

CARTOGRAPHIC FEATURE EXTRACTION ON ETL'S (ENGINEER TOPOGRAPHIC LABORATORIES') DIAL (DIGITAL IMAGE ANALYSIS LABORATORY) SYSTEM

R. S. RAND Mar. 1984 9 p (AD-A140230; ETL-R-060) Avail: NTIS HC A02/MF A01 CSCL 08B

A number of feature extraction techniques have been developed and tested on the Digital Image Analysis Laboratory (DIAL) at ETL. These techniques include stereo matching, edge detection, texture extraction, and statistical pattern recognition on digitized aerial imagery, as well as interactive binary image cleansing (raster processing) on the derived results. Experiments have shown that each of these techniques has some limited success at performing its task, but as isolated entities, they fail to perform at a level needed in a cartographic feature extraction system. This paper discusses some of the capabilities of DIAL and concludes that a method of coordinating simple feature extraction techniques under the management of a heuristic rule-based system should be investigated.

GRA

N84-27245 Missouri Univ., Columbia.

CONTEXTUAL CLASSIFICATION OF REMOTELY SENSED DATA Ph.D. Thesis

S. HONBOONHERM 1983 168 p Avail: Univ. Microfilms Order No. DA8406203

Contextual information currently is utilized to modify pixel classification data derived from digital remotely sensed data. A contextual procedure was applied to classified digital imagery to improve the contextual integrity and the utility of the classification. Classification results achieved in a LANDSAT satellite analysis of north central Missouri were used. The probabilities of pixel classification were iteratively updated as a function of the set of probabilities found in the local area. In updating the probabilities, two factors were considered: (1) the initial probabilities, and (2) the compatibility coefficients. A method for generating the compatibility coefficients for a relaxation labeling process was developed. Techniques for generating the contextual influence for the updating algorithm employed in the relaxation labeling process and the stopping criteria were proposed. The reclassification method proved to be effective in improving the contextual integrity and the accuracies of individual classes. The experimental convergence algorithm was effective in reducing processing time.

Dissert. Abstr.

N84-27247*# EROS Data Center, Sioux Falls, S. Dak. LANDSAT 4 INVESTIGATIONS OF THEMATIC MAPPER AND MULTISPECTRAL SCANNER APPLICATIONS Quarterly Report

D. T. LAUER, Principal Investigator 3 Jul. 1984 3 p

(Contract NASA ORDER S-10757-C)
(E84-10152; NASA-CR-173223; NAS 1.26:173223) Avail: NTIS HC A02/MF A01 CSCL 08B

Interband detector noise was suppressed in the TIPS TM North Dakota data by median filtering. Procedures were developed to optimize the visual information content of thematic mapper data and evaluate the resulting photographic products by visual interpretation. A digital to analog TM transfer function was developed which properly placed the digital values on the most useable portion of film response curve. Utilizing the calculated minimum, mean, and maximum and the respective standard deviations of the bands from 50 sample scenes of TM data, look up tables were designed which resulted in acceptable photographic products. These products were evaluated by generation of color composites of selected band combinations using standard photo production procedures, and visual interpretation of scene features.

A.R.H.

N84-27249*# Canada Centre for Remote Sensing, Ottawa (Ontario).

EVALUATING LANDSAT-4 MSS AND TM DATA Progress Report, 3 Jan. - 2 May 1984

W. M. STROME, J. CIHLAR, D. G. GOODENOUGH, F. E. GUERTIN, Principal Investigator, J. M. MURPHY, G. GRIEVE, R. SIMARD, D. HORLER, and F. J. AHERN 12 Jun. 1984 9 p refs Sponsored by NASA ERTS
(E84-10157; NASA-CR-173669; NAS 1.26:173669; PR-3) Avail: NTIS HC A02/MF A01 CSCL 05B

Interband line pixel misregistrations were determined for the four MSS bands of the Mistassini, Ontario scene and multitemporal registration of LANDSAT-4 products were tested for two different geocoded scenes. Line and pixel misregistrations are tabulated as determined by the manual ground control points and the digital band to band correlation techniques. A method was developed for determining the spectral information content of TM images for forestry applications.

A.R.H.

N84-27250*# Purdue Univ., Lafayette, Ind. Lab. for Applications of Remote Sensing.

LANDSAT-4 IMAGE DATA QUALITY ANALYSIS Quarterly Progress Report, 10 Feb. - 9 May 1984

P. E. ANUTA 9 May 1984 3 p ERTS
(Contract NAS5-26859)

(E84-10158; NASA-CR-173670; NAS 1.26:173670; LARS-CR-050984) Avail: NTIS HC A02/MF A01 CSCL 05B

Methods were developed for estimating point spread functions from image data. Roads and bridges in dark backgrounds are being examined as well as other smoothing methods for reducing noise in the estimated point spread function. Tomographic techniques were used to estimate two dimensional point spread functions. Reformating software changes were implemented to handle formats for LANDSAT-5 data.

A.R.H.

N84-28202# Institut Geographique National, Paris (France). Dept. de Teledetection et de Cartographie Spatiale.

REMOTE SENSING OF THE SANTONGE LITTORAL. PROCESSING AND INTERPRETATION OF SATELLITE IMAGES [TELEDETECTION DU LITTORAL SAINTOGEAIS. METHODES DE TRAITEMENTS ET INTERPRETATION D'IMAGES SATELLITAIRES]

F. CUQ 1983 224 p refs In FRENCH Original contains color illustrations
(ISBN-2-85929-016-8) Avail: NTIS HC A10/MF A01; Ecole Normale Supérieure de Jeunes Filles, Paris FF 90

Remote sensing hardware and software are described. Interpretation of 13 images obtained from LANDSAT 1 and 2; of data acquisition; labeling; color mapping; and automatic mapping are summarized. It is concluded that after 10 years of experiments

08 INSTRUMENTATION AND SENSORS

the surveillance and management of land resources by satellite detection are possible. Author (ESA)

08

INSTRUMENTATION AND SENSORS

Includes data acquisition and camera systems and remote sensors.

A84-30226

ASIAN CONFERENCE ON REMOTE SENSING, 3RD, DACCA, BANGLADESH, DECEMBER 4-7, 1982, PROCEEDINGS

Conference sponsored by the Bangladesh Space Research and Remote Sensing Organization, Japan Association of Remote Sensing, International Society for Photogrammetry and Remote Sensing, et al. Tokyo, University of Tokyo, 1983, 668 p.

The papers presented in this volume provide an overview of remote sensing activities in Asian countries, with emphasis on the unique problems encountered in these countries. Topics discussed include multispectral and multitemporal Landsat data for soil surveys, the development of an automated area measurement system, analyzing forest structures by remote sensing, and the use of satellite pictures in aviation meteorology. Papers are also presented on the detectability of subpixel size features through ideal imaging sensors, the reduction of high-dimension data to two dimensions using nonlinear mapping techniques, and identification of water-logged and salt-affected soils through remote sensing techniques. V.L.

A84-30265#

A REMOTE SENSING DATA PROCESSING SYSTEM BASED ON A MICRO-COMPUTER

J. IISAKA (IBM Japan, Tokyo Scientific Center, Tokyo, Japan), T. OSHIMA, and K. MIYASHITA (Hosei University, Koganei, Tokyo, Japan) IN: Asian Conference on Remote Sensing, 3rd, Dacca, Bangladesh, December 4-7, 1982, Proceedings . Tokyo, University of Tokyo, 1983, p. G-4-1 to G-4-12.

A newly developed man-machine communications system for analyzing remote sensing data uses a 64 microcomputer with a GPIB interface bus. The language used is Fortran-F80, and the software is CP/M-based. Two double-density floppy disks, each with 1.2 Mb capacity, are used. The cost of the system is estimated to be less than 18,000 U.S. dollars because generally standard components are used. The accuracy of experimental results using such a system is similar to results using a large capacity computer, but the data conversion service from computer compatible tape to floppy disk, the requirements for preprocessing images, the long calculation time, and the limited color range of the CRT are not always satisfactory for all purposes. Some flow charts and block diagrams are included.

D.H.

A84-30233#

THE EXPERIENCE OF ORGANISING A UTILISATION PROGRAMME FOR BHASKARA

R. K. GOEL and A. R. DASGUPTA (Indian Space Research Organization, Space Applications Centre, Ahmedabad, India) IN: Asian Conference on Remote Sensing, 3rd, Dacca, Bangladesh, December 4-7, 1982, Proceedings . Tokyo, University of Tokyo, 1983, p. P-13-1 to P-13-11.

A program for the utilization of the TV and SAMIR (a three-frequency microwave radiometer) data provided by Bhaskara-I and Bhaskara-II, Indian experimental satellites, is discussed. Attention is given to the infrastructure and expertise developed for data acquisition, processing, and dissemination. Data products and user services, as well as interaction with user agencies, are also discussed. V.L.

A84-30266#

APPLICATION OF THE VIZIR IMAGE PROCESSING SYSTEM TO THE REMOTE SENSING STUDIES IN BANGLADESH

A. K. M. S. ALAM, K. FARUQUI, N. HOQUE, and A. H. HOWLADER (Bangladesh Space Research and Remote Sensing Organization, Dacca, Bangladesh) IN: Asian Conference on Remote Sensing, 3rd, Dacca, Bangladesh, December 4-7, 1982, Proceedings . Tokyo, University of Tokyo, 1983, p. G-6-1 to G-6-15.

A84-30516#

THE RADAR ALTIMETER FOR ERS-1 SATELLITE

G. LOSQUADRO, R. SOMMA, G. POZZOLINI (Selenia S.p.A., Rome, Italy), and G. PICARDI (Rome, Universita, Rome, Italy) IETE, IEEE, SEE, and Institution of Engineers of India, International Radar Symposium, Bangalore, India, Oct. 9-12, 1983, Paper. 7 p. refs

This paper deals with the Radar Altimeter for the ERS-1 Satellite. After a review of the main system concepts, the attention is focussed on the parameters estimation process, which is the key for the instrument performances. In particular, simulation results are given in terms of accuracy and tracking capability. Author

A84-30252#

BENEFITS AND PROBLEMS IN OPERATIONAL REMOTE SENSING

B. L. DEEKSHATULU (National Remote Sensing Agency, Hyderabad, India) IN: Asian Conference on Remote Sensing, 3rd, Dacca, Bangladesh, December 4-7, 1982, Proceedings . Tokyo, University of Tokyo, 1983, p. C-5-1 to C-5-9.

In discussing the remote sensing of soil moisture, it is pointed out that existing operational satellites operate in the visible and near infrared regions and that these bands give only a qualitative assessment of soil moisture. Whereas there is a relationship between reflectance and soil moisture content, factors other than moisture, such as factors related to organic matter and particle size, affect the reflectance. What is more, reflectance is affected by surface roughness, viewing angle, and illumination. In discussing remote sensing of the oceans, it is noted that there is no working altimeter flying in space today. The Geosat scheduled for 1983 does not have an orbit determination precision sufficient for quantitative ocean circulation research. Other limitations of remote sensing are discussed. These have to do with complex surfaces, cloud cover, pollution monitoring, and the continuity of data.

C.R.

A84-31072

AN AIRBORNE RADAR STATION FOR STUDYING THE REFLECTION PROPERTIES OF THE EARTH'S SURFACE [RADIOLOKATSIONNAIA STANTSIIA DLIA ISSLEDOVANIIA OTRAZHAIUSHCHIKH SVOISTV ZEMNOI POVERKHNOSTI S SAMOLETA]

O. N. RZHIGA, N. A. ARMANA, Iu. N. ALEKSARDROV, S. M. BARABOSHKIN, V. S. BARINOV, L. F. BORODIN, A. L. ZAITSEV, A. I. ZAKHAROV, V. E. ZIMOV, V. I. KAEVITSER et al. Radiotekhnika i Elektronika (ISSN 0033-8494), vol. 29, March 1984, p. 573-578. In Russian.

A radar station for studying the reflection properties of the earth's surface has been designed for installation on board the IL-18 flying laboratory. The design and performance characteristics of the radar are discussed, as are the computer-aided signal processing and imagery synthesis. Examples of actual images obtained with the radar system are presented.

V.L.

08 INSTRUMENTATION AND SENSORS

A84-31741* National Aeronautics and Space Administration. Langley Research Center, Hampton, Va.

A RAPID METHOD FOR OBTAINING FREQUENCY-RESPONSE FUNCTIONS FOR MULTIPLE INPUT PHOTOGRAHMETRIC DATA

M. L. KROEN and J. S. TRIPP (NASA, Langley Research Center, Instrument Research Div., Hampton, VA) IN: Structures, Structural Dynamics and Materials Conference, 25th, Palm Springs, CA, May 14-16, 1984, and AIAA Dynamics Specialists Conference, Palm Springs, CA, May 17, 18, 1984, Technical Papers. Part 2. New York, American Institute of Aeronautics and Astronautics, 1984, p. 510-527. refs (AIAA PAPER 84-1060)

A two-digital-camera photogrammetric technique for measuring the motion of a vibrating spacecraft structure or wing surface and an applicable data-reduction algorithm are presented. The 3D frequency-response functions are obtained by coordinate transformation from averaged cross and autopower spectra derived from the 4D camera coordinates by Fourier transformation. Error sources are investigated analytically, and sample results are shown in graphs. T.K.

A84-31947* National Aeronautics and Space Administration. Langley Research Center, Hampton, Va.

COMPARISON OF LONGWAVE DIURNAL MODELS APPLIED TO SIMULATIONS OF THE EARTH RADIATION BUDGET EXPERIMENT

D. R. BROOKS and P. MINNIS (NASA, Langley Research Center, Atmospheric Sciences Div., Hampton, VA) Journal of Climate and Applied Meteorology (ISSN 0733-3021), vol. 23, Jan. 1984, p. 155-160. refs

The Earth Radiation Budget Experiment (ERBE) is a multisatellite experiment which is to be implemented in the mid 1980s. The experiment involves a utilization of instruments on one or more sun-synchronous satellites in the NOAA series, and the employment of a dedicated spacecraft, the ERBS, in a 57 deg orbit. One of the objectives of ERBE is related to an improvement of knowledge regarding the diurnal variability in the earth's radiation balance. In the present investigation, satellite samples of longwave (LW) radiation over land are simulated for both sun-synchronous and non-sun-synchronous orbits. Three different LW diurnal models are then applied to the sampled data, and the resulting modeled monthly net LW radiant exitances are compared against reference values based on complete hourly sampling of the area for a month. The results demonstrate the general usefulness of a trigonometric diurnal LW model for land regions with daytime heating trends. G.R.

A84-32938*

GLOBAL DATA ASSIMILATION EXPERIMENTS WITH SCATTEROMETER WINDS FROM SEASAT-A

T.-W. YU and R. D. MCPHERSON (NOAA, National Meteorological Center, Washington, DC) Monthly Weather Review (ISSN 0027-0644), vol. 112, Feb. 1984, p. 368-376. refs

Two days of global scatterometer-derived oceanic surface winds during the period of 0000 GMT 16 July-0000 GMT 18 July 1978 from the SEASAT-A satellite are used in the NMC's global data assimilation and forecast experiments to gain a preliminary appreciation of the impact of this dataset. The NMC's global data assimilation system used in this study is described. The nature of the scatterometer winds and their error characteristics are discussed. Two parallel 48-hour data assimilation experiments are conducted: one including scatterometer wind data (SASS), the other without (NOSASS). After 48 hours of assimilation, large differences have evolved between SASS and NOSASS analyses due to the scatterometer winds. Comparison of the analyses with the operational analysis generated by the Australian Bureau of Meteorology suggests that the influence of scatterometer winds was beneficial in the Southern Hemisphere. Author

A84-33326

AMERICAN SOCIETY OF PHOTOGRAHMETRY, ANNUAL MEETING, 49TH, WASHINGTON, DC, MARCH 13-18, 1983, TECHNICAL PAPERS

Falls Church, VA, American Society of Photogrammetry, 1983, 410 p.

Methods of vegetation change mapping using Landsat MSS data are considered along with an estimation of depth of snow from Landsat imagery, circular structures of earth, digital comparison and correlation techniques of remote sensing images having different space resolution, the construction of new area sampling frames using Landsat imagery, Shuttle earth remote sensing experiments for the 1980's, and terrain analysis database generation through computer-assisted photo interpretation. Attention is also given to a photo-geomorphological approach to soil erosion mapping and evaluation, specifications for aerial photography, temporal image normalization, analytical photogrammetry from small format photography, and the geometric fidelity of aircraft scanner data for automated mapping of agricultural features. Other topics explored are related to a multipurpose approach to urban mapping, a chained data structure for efficient extraction and display of information from polygon maps, and a matrix camera with digital image processing in photogrammetric applications. G.R.

A84-34157

FOG RECOGNITION IN DAYLIGHT 3.7-MICRON-BAND TIROS-N AND NOAA IMAGES [NEBELERKENNUNG IN TAG-AUFGNAHMEN DES 3.7-MICRON-SPEKTRALBEREICH DER TIROS N/NOAA-SERIE]

G. GROSS (Amt fuer Wehrgeophysik, Traben-Trarbach, West Germany) Meteorologische Rundschau (ISSN 0026-1211), vol. 37, April 1984, p. 33-42. In German. refs

A technique for detecting the extent and thickness of ground fog and low stratus formations from daylight AVHRR images is developed and demonstrated on two test cases. The 3.55-3.93-micron band (channel 3) is found to give satisfactory results if the general cloud cover is light and the sun angle is high, and if the characteristics of the underlying terrain are well known. Comparison of images from different orbital passes permits the monitoring of fog evolution. Sample images and geopotential and ground-weather maps are provided. T.K.

A84-34787

CONDITIONS FOR THE ILLUMINATION OF AN AREA IN SATELLITE SCANNER SURVEYS [USLOVIA OSVESHCHENIIA MESTNOSTI PRI KOSMICHESKOI SKANERNOI S'EMKE]

A. M. KUZINA, I. G. MALTSEVA, and N. S. RAMM (Proizvodstvennoe Geologicheskoe Ob'edinenie Aerogeologii, Leningrad, USSR) Issledovaniye Zemli iz Kosmosa (ISSN 0205-9614), Mar.-Apr. 1984, p. 98-106. In Russian. refs

Consideration is given to the illumination of terrain in scanner surveys from satellites designed to study natural resources and placed in circular solar synchronous orbits at heights of 600-900 km. The expediency of allowing for variability in the conditions of illumination in interpreting the images obtained in the survey is demonstrated. C.R.

A84-34958

USER GUIDE FOR THE USGS AERIAL CAMERA REPORT OF CALIBRATION

W. P. TAYMAN (U.S. Geological Survey, National Mapping Div., Reston, VA) Photogrammetric Engineering and Remote Sensing (ISSN 0099-1112), vol. 50, May 1984, p. 577-584. refs

A guide for using the USGS Aerial Camera Calibration Report is presented. Attention is focused on USGS specifications for aerial photography procurement, with respect to equipment standardization. Calibration and testing of aerial cameras includes procedures for measuring optical constants and for ensuring that major mechanical and electronic camera parts function normally. I.H.

08 INSTRUMENTATION AND SENSORS

A84-37873* National Aeronautics and Space Administration. Goddard Space Flight Center, Greenbelt, Md.

LARGE-SCALE ANALYSIS AND FORECAST EXPERIMENTS WITH WIND DATA FROM THE SEASAT A SCATTEROMETER

W. E. BAKER, R. ATLAS, E. KALNAY, M. HALEM (NASA, Goddard Space Flight Center, Laboratory for Atmospheric Sciences, Greenbelt, MD), P. M. WOICESHYN (California Institute of Technology, Jet Propulsion Laboratory, Pasadena, CA), S. PETEHERYCH (Department of the Environment, Atmospheric Environment Service, Downsview, Ontario, Canada), and D. EDELMANN (M/A-COM Sigma Data, Inc., Greenbelt, MD) *Journal of Geophysical Research* (ISSN 0148-0227), vol. 89, June 20, 1984, p. 4927-4936. refs (Contract NAS7-918)

A series of data assimilation experiments is performed to assess the impact of Seasat A satellite scatterometer (SASS) wind data on Goddard Laboratory for Atmospheric Sciences (GLAS) model forecasts. The SASS data are dealiased as part of an objective analysis system utilizing a three-pass procedure. The impact of the SASS data is evaluated with and without temperature soundings from the NOAA 4 Vertical Temperature Profile Radiometer (VTPR) instrument in order to study possible redundancy between surface wind data and upper air temperature data. In the northern hemisphere the SASS data are generally found to have a negligible effect on the forecasts. In the southern hemisphere the forecast impact from SASS data is somewhat larger and primarily beneficial in the absence of VTPR data. However, the inclusion of VTPR data effectively eliminates the positive impact over Australia and South America. This indicates that SASS data can be beneficial for numerical weather prediction in regions with large data gaps, but in the presence of satellite soundings the usefulness of SASS data is significantly reduced. Author

A84-38310

MICROWAVE SCATTEROMETER

H. YAMADA, M. SHIMADA (National Space Development Agency of Japan, Sakura, Ibaraki, Japan), M. KONDO, A. HISANAGA, and M. SASANUMA (Mitsubishi Electric Co., Kamakura, Japan) IN: *International Symposium on Space Technology and Science*, 13th, Tokyo, Japan, June 28-July 3, 1982, *Proceedings* . Tokyo, AGNE Publishing, Inc., 1982, p. 1353-1357. refs

Design features and operational parameters of a microwave scatterometer (MS) intended as a spaceborne surface wind speed and direction sensor are presented. The MS has beams distributed along the 45, 75, 135, 225, and 315 deg angles. Each complementary pair has VV and HH polarized components. The MS has a low aliasing production probability, a variable resolution cell to decrease the precipitation error, and redundancy because of the dual polarization channels. An on-board Doppler filter accounts for satellite movement and the beam-surface incident angles. A computer simulation has indicated that highly accurate results may be generated by the MS. M.S.K.

A84-38311

DESIGN AND DEVELOPMENT OF CCD PUSHBROOM CAMERA FOR EARTH RESOURCES SURVEY

G. JOSEPH, K. NAGACHENCHAIAH, and A. S. KIRAN KUMAR (Indian Space Research Organization, Sensor Development Div., Ahmedabad, India) IN: *International Symposium on Space Technology and Science*, 13th, Tokyo, Japan, June 28-July 3, 1982, *Proceedings* . Tokyo, AGNE Publishing, Inc., 1982, p. 1359-1364.

Design considerations and performance expectations for a multiband pushbroom scanner for remote sensing of the earth are discussed. Attention is given to the radiometric accuracy, spatial resolution and band-to-band registration. It is shown that an increased data acquisition rate can lower image smear and reduce the SNR. A filter wheel provides the band-to-band registration and an improved modulation transfer function, while still having a single CCD detector array. Airborne test data from two single-band test cameras are provided. The results have encouraged work on a spaceborne multiband camera operating in the 0.45-0.9 spectral region with 35 m resolution from sun-synchronous orbit. M.S.K.

A84-38312

PERFORMANCE STUDY OF MULTICOLOR VISUAL SENSOR SYSTEM

S. J. MORIZUMI (Hughes Aircraft Co., Electro-Optic and Data Systems Group, El Segundo, CA) IN: *International Symposium on Space Technology and Science*, 13th, Tokyo, Japan, June 28-July 3, 1982, *Proceedings* . Tokyo, AGNE Publishing, Inc., 1982, p. 1365-1370. refs

The purpose of the paper is to show the design procedures for an optimization of performance capability of a multicolor visual sensing system. The system may be used on board an aircraft or a spacecraft to scan the land or the ocean surface to explore the spectral characteristics of the earth surface and its environment. The components of the sensor system are carefully selected and their performances are optimized. The total system performance in terms of signal to noise ratio and noise equivalent difference in reflectivity is evaluated. Author

A84-38922

CLIMATE RESEARCH FROM SPACE

D. L. CROOM (Science and Engineering Research Council, Rutherford Appleton Laboratory, Didcot, Oxon, England) *British Interplanetary Society, Journal (Space Science)* (ISSN 0007-084X), vol. 37, July 1984, p. 323-329. refs

The Rutherford Appleton Laboratory is involved in several space projects related to studies of global climate. This paper describes these activities, past, current and planned, the principal of which are the Along Track Scanning Radiometer, accepted by ESA for inclusion on the ERS-1 remote sensing satellite, proposals for a joint NERC-SERC-University Advanced Space Radar Altimetry Programme, and involvement in the Meteorological Office contribution to the planned joint UK-USA Advanced Microwave Sounding Unit for meteorology from space. An outline of proposals for coping with the massive data flow from these and other space projects is given. Author

A84-38923

ATMOSPHERIC SCIENCE

J. E. HARRIES (Science and Engineering Research Council, Rutherford Appleton Laboratory, Didcot, Oxon, England) *British Interplanetary Society, Journal (Space Science)* (ISSN 0007-084X), vol. 37, July 1984, p. 330-336. refs

This paper presents a review of the use of satellite remote sounding experiments for studies of the earth in both the stratosphere and mesosphere. A brief summary of the main scientific objectives involved is followed by a description of space projects in this area in which the RAL has played a role. The paper seeks to demonstrate the important role which observations from space have played, and will continue to play, in advancing our understanding of the complex scientific processes in the atmosphere of our planet. Author

A84-39440* National Center for Atmospheric Research, Boulder, Colo.

THE LIMB INFRARED MONITOR OF THE STRATOSPHERE - EXPERIMENT DESCRIPTION, PERFORMANCE, AND RESULTS

J. C. GILLE (National Center for Atmospheric Research, Boulder, CO) and J. M. RUSSELL, III (NASA, Langley Research Center, Hampton, VA) *Journal of Geophysical Research* (ISSN 0148-0227), vol. 89, June 30, 1984, p. 5125-5140. refs (Contract NASA ORDER L-36446-A; NASA ORDER L-86651-A; NASA ORDER S-70994-A; NASA ORDER L-9469-B; NASA ORDER W-15439)

An experiment and results, using a six-channel infrared radiometer aboard the Nimbus 7 spacecraft to sound the composition and structure of the middle atmosphere, are described. The measurement requirements are discussed, and critical instrument parameters are identified. Next, the instrument and its laboratory calibration are described. Temperature accuracy and precision are estimated to be 2 K and about 0.4 K respectively. Accuracy of the trace gas measurements is about 25 percent, comparable to the estimated accuracy of the in situ comparison data; their precision is about 0.25 ppmv for ozone and water

08 INSTRUMENTATION AND SENSORS

vapor and 0.2 ppbv for nitric acid and nitrogen dioxide. Examples of the vertical profiles, maps, and cross sections of the data show previously unobserved variations with latitude, altitude, and time. The results demonstrate that infrared limb scanning is an extremely powerful method for sounding the middle atmosphere. D.H.

A84-39443* National Aeronautics and Space Administration. Langley Research Center, Hampton, Va.

THE VALIDATION OF NIMBUS 7 LIMS MEASUREMENTS OF OZONE

E. E. REMSBERG, J. M. RUSSELL, III (NASA, Langley Research Center, Hampton, VA), J. C. GILLE, P. L. BAILEY (National Center for Atmospheric Research, Boulder, CO), L. L. GORDLEY (Systems and Applied Sciences Corp., Hampton, VA), W. G. PLANET (NOAA, Washington, DC), and J. E. HARRIES (Science and Engineering Research Council, Rutherford Appleton Laboratory, Didcot, Oxon., England) *Journal of Geophysical Research* (ISSN 0148-0227), vol. 89, June 30, 1984, p. 5161-5178. refs

Approximately seven and one half months of stratospheric ozone profiles have been processed from the LIMS (Limb Infrared Monitor of the Stratosphere) experiment on the Nimbus 7 satellite. Data profiles cover the stratosphere and mesosphere from 100 to 0.1 mbar and from 84 degrees N to 64 degrees S latitude. Topics covered include the ozone channel characteristics, precision, systematic uncertainties, and comparisons with data from balloon and rocket underflights, Umkehr soundings, and Dobson measurements. Comparisons with Dobson total ozone are made by integrating combined LIMS plus balloon profiles. The estimated on-orbit precision is 0.02-0.16 ppmv. Simulations of the experiment indicate potential systematic uncertainties ranging from 15 percent in the 1-mbar region to an upper limit of 40 percent at 100 mbar and 0.1 mbar. Results are well within the uncertainties for the correlative sensors themselves. LIMS detects significant vertical structure in the ozone profile even below the ozone mixing ratio peak. Several other comparisons showing good agreement are noted. D.H.

A84-39444* National Center for Atmospheric Research, Boulder, Colo.

ACCURACY AND PRECISION OF THE NITRIC ACID CONCENTRATIONS DETERMINED BY THE LIMB INFRARED MONITOR OF THE STRATOSPHERE EXPERIMENT ON NIMBUS 7

J. C. GILLE, P. L. BAILEY, B. W. GANDRUD (National Center for Atmospheric Research, Boulder, CO), J. M. RUSSELL, E. E. REMSBERG (NASA, Langley Research Center, Hampton, VA), L. L. GORDLEY (Systems and Applied Sciences Corp., Hampton, VA), W. F. J. EVANS (Department of the Environment, Atmospheric Environment Service, Downsview, Ontario, Canada), H. FISCHER (Muenchen, Universitaet, Munich, West Germany), A. GIRARD (ONERA, Chatillon-sous-Bagneux, Hauts-de-Seine, France), J. E. HARRIES (Science and Engineering Research Council, Rutherford Appleton Laboratory, Didcot, Oxon., England) et al. *Journal of Geophysical Research* (ISSN 0148-0227), vol. 89, June 30, 1984, p. 5179-5190. refs
(Contract NASA ORDER L-36446-A; NASA ORDER L-86651-A; NASA ORDER S-70994-A; NASA ORDER L-9469-B; NASA ORDER W-15439)

A84-39447*

HIGH-PRECISION ATMOSPHERIC OZONE MEASUREMENTS USING WAVELENGTHS BETWEEN 290 AND 305 NM

R. D. SAUNDERS, H. J. KOSTKOWSKI, J. F. WARD, C. H. POPENO (National Bureau of Standards, Washington, DC), and A. E. S. GREEN (Florida, University, Gainesville, FL) *Journal of Geophysical Research* (ISSN 0148-0227), vol. 89, June 30, 1984, p. 5215-5226. Research supported by the U.S. Environmental Protection Agency. refs

It is shown theoretically that many errors are significantly less when determining atmospheric ozone thicknesses from measurements of solar terrestrial spectral irradiance in the wavelength region between 290 and 305 nm as compared to the 305- to 340-nm region employed by the Dobson spectrophotometer.

In order to test this conclusion experimentally, an elaborate set of state-of-the-art measurements have been made in the shorter wavelength region in Gainesville, Florida, between June 13 and June 18, 1980. Details of these measurements, including an extensive error analysis, are presented and indicate that such short-wavelength measurements, particularly between 295 and 305 nm, can be used to detect long-term changes of atmospheric ozone with an uncertainty not exceeding 1 percent. Observing conditions restricted the Gainesville measurements to zenith angles of less than 35 deg. Author

A84-39449* Systems and Applied Sciences Corp., Hyattsville, Md.

INTERCOMPARISON OF THE NIMBUS 7 SBUV/TOMS TOTAL OZONE DATA SETS WITH DOBSON AND M83 RESULTS

P. K. BHARTIA, K. F. KLENK, C. K. WONG, D. GORDON (Systems and Applied Sciences Corp., Hyattsville, MD), and A. J. FLEIG (NASA, Goddard Space Flight Center, Laboratory for Atmospheric Sciences, Greenbelt, MD) *Journal of Geophysical Research* (ISSN 0148-0227), vol. 89, June 30, 1984, p. 5239-5247. refs
(Contract NAS5-27393-14; NAS5-26753-20)

Two years of SBUV/TOMS (Solar Backscattered Ultraviolet/Total Ozone Mapping Spectrometer) data spanning the period November 1978 to October 1980 have been processed and compared with ground-based ozone measurements made at 62 Dobson spectrophotometer and 18 M83 filter photometer ozone stations. Results show that the satellite ozone values are consistently smaller than those measured by the stations; most of this difference is probably due to an error in the currently accepted ozone absorption cross sections at ultraviolet wavelengths. Dobson-derived ozone amounts agree extremely well with those derived from each of the satellite instruments. Long-term stability of the ozone derived by the two instruments is expected to be better than 0.5 percent per year. D.H.

N84-22873* SRI International Corp., Menlo Park, Calif.

PROPAGATION EFFECTS IN SATELLITE-BASED SYNTHETIC APERTURE RADARS

C. L. RINO and V. H. GONZALEZ 1 Mar. 1983 48 p
(Contract DNA001-81-C-0010; S99-QAXH)
(AD-A138681; AD-E301336; DNA-TR-81-253) Avail: NTIS HC A03/MF A01 CSCL 171

This report describes the effects of propagation disturbances on space-based synthetic aperture radars (SAR). Using a model developed earlier, we performed simulations to show the distortion of the radar ambiguity function for the SEASAT-A SAR. For moderate disturbance, an elevated sidelobe level causes a reduction in contrast. The SEASAT-A library of high-latitude data showed examples of this effect, one example of which is analyzed here in detail. GRA

N84-23000* Arizona Univ., Tucson, Optical Sciences Center. *SPECTRORADIOMETRIC CALIBRATION OF THE THEMATIC MAPPER AND MULTISPECTRAL SCANNER SYSTEM* Quarterly Report, 1 Nov. 1983 - 1 Feb. 1984

J. PALMER, Principal Investigator and P. SLATER 1 Feb. 1984 35 p refs ERTS
(Contract NAS5-27382)
(E84-10098; NASA-CR-173367; NAS 1.26:173367; QR-5) Avail: NTIS HC A03/MF A01 CSCL 08B

Results of an analysis that relates TM saturation level to ground reflectance, calendar date, latitude, and atmospheric conditions are reported. The determination of the spectral reflectance at the entrance pupil of the LANDSAT 4 pupil of the thematic mapper is described.

08 INSTRUMENTATION AND SENSORS

N84-23001*# Arizona Univ., Tucson. Optical Sciences Center. SENSOR RADIANCE FOR A MIDLATITUDE ATMOSPHERIC MODEL

In its Spectroradiometric Calibration of the Thematic Mapper and Multispectral Scanner System p 1-14 1 Feb. 1984 refs ERTS

Avail: NTIS HC A03/MF A01 CSCL 08B

The Herman radiative transfer code which iteratively traces solar radiance through a discrete number of scattering angles and many atmospheric layers was transferred to a personnel computer to reduce time in recompiling the source code. The code was then used to predict what ground reflectance would saturate the TM sensor output given a standard midlatitude atmospheric model. Output radiance is tabulated for the first four bands. Plots show radiance at the sensor as a function of solar zenith angle from a visibility of 40 km; solar zenith angle as a function of time of year for four latitudes over a typical portion of the descending node of a LANDSAT orbit; and values of ground reflectance required to saturate the TM sensor from three different aerosol loading conditions (corresponding to about 20 km, 40 km. and greater than 100 km visibility). A.R.H.

N84-23002*# Arizona Univ., Tucson. Optical Sciences Center. IN-FLIGHT ABSOLUTE RADIOMETRIC CALIBRATION OF THE THEMATIC MAPPER

J. PALMER, P. N. SLATER, Principal Investigators, K. R. CASTLE, R. G. HOLM, C. J. KASTNER, M. DINGUIRARD (Centre d'Etudes et de Recherches de Toulouse, France), C. E. EZRA (Agriculture Dept., Phoenix, Ariz.), R. D. JACKSON (Agriculture Dept., Phoenix, Ariz.), and R. K. SAVAGE (Atmospheric Sciences Lab., White Sands Missile Range, N. Mex.) *In its* Spectroradiometric Calibration of the Thematic Mapper and Multispectral Scanner System p 15-34 1 Feb. 1984 refs Submitted for publication ERTS

Avail: NTIS HC A03/MF A01 CSCL 08B

Ground spectral reflectance and atmospheric spectral optical depth measurements made at White Sands, New Mexico were used with an atmospheric radiative transfer program to determine the spectral radiance at the entrance pupil of the LANDSAT-4 TM. Comparison with the output digital counts of the TM, when imaging the measured ground area, provided an absolute calibration for five detectors in TM bands 2, 3, and 4. By reference to an adjacent, larger uniform area, the calibration was extended to all 16 detectors in each of three bands. Preflight calibration results agreed with these inflight measurements to 6.6%, 2.4%, and 12.9% in bands 2,3, and 4, respectively. Author

N84-23982*# Utah Univ., Salt Lake City. Center for Remote Sensing and Cartography.

ENVIROPOD HANDBOOK: A GUIDE TO PREPARATION AND USE OF THE ENVIRONMENTAL PROTECTION AGENCY'S LIGHT-WEIGHT AERIAL CAMERA SYSTEM

S. J. BROWER and M. K. RIDD Mar. 1984 67 p ERTS
(Contract NAGW-95)

(E84-10123; NASA-CR-172798; NAS 1.26:172798; CRSC-84-1)

Avail: NTIS HC A04/MF A01 CSCL 14E

The use of the Environmental Protection Agency (EPA) Enviropod camera system is detailed in this handbook which contains a step-by-step guide for mission planning, flights, film processing, indexing, and documentation. Information regarding Enviropod equipment and specifications is included. A.R.H.

N84-23986*# Mississippi State Univ., Mississippi State. Mississippi Remote Sensing Center.

APPLICATION OF REMOTE SENSING TO STATE AND REGIONAL PROBLEMS Semiannual Progress Report, 1 Nov. 1983 - 30 Apr. 1984

W. F. MILLER, Principal Investigator, J. TINGLE, L. H. WRIGHT, and B. TEBBS 1 May 1984 60 p ERTS
(Contract NGL-25-001-054)

(E84-10128; NASA-CR-172803; NAS 1.26:172803; SAPR-21)

Avail: NTIS HC A04/MF A01 CSCL 05B

Progress was made in the hydroclimatology, habitat modeling and inventory, computer analysis, wildlife management, and data

comparison programs that utilize LANDSAT and SEASAT data provided to Mississippi researchers through the remote sensing applications program. Specific topics include water runoff in central Mississippi, habitat models for the endangered gopher tortoise, coyote, and turkey. Geographic Information Systems (GIS) development, forest inventory along the Mississippi River, and the merging of LANDSAT and SEASAT data for enhanced forest type discrimination. M.A.C.

N84-23987*# City Univ. Inst. of Marine and Atmospheric Sciences, New York.

A SEASAT SASS SIMULATION EXPERIMENT TO QUANTIFY THE ERRORS RELATED TO A + OR - 3 HOUR INTERMITTENT ASSIMILATION TECHNIQUE

W. B. SYLVESTER May 1984 92 p refs ERTS
(Contract NAGW-266)

(E84-10129; NASA-CR-3799; NAS 1.26:3799) Avail: NTIS HC A05/MF A01 CSCL 05B

A series of SEASAT repeat orbits over a sequence of best Low center positions is simulated by using the Seatrak satellite calculator. These Low centers are, upon appropriate interpolation to hourly positions, located at various times during the + or - 3 hour assimilation cycle. Error analysis for a sample of best cyclone center positions taken from the Atlantic and Pacific oceans reveals a minimum average error of 1.1 deg of Longitude and a standard deviation of 0.9 deg of Longitude. The magnitude of the average error seems to suggest that by utilizing the + or - 3 hour window in the assimilation cycle, the quality of the SASS data is degraded to the level of the background. A further consequence of this assimilation scheme is the effect which is manifested as a result of the blending of two or more more juxtaposed vector winds, generally possessing different properties (vector quantity and time). The outcome of this is to reduce gradients in the wind field and to deform isobaric and frontal patterns of the initial field. A.R.H.

N84-24679*# National Aeronautics and Space Administration. Langley Research Center, Hampton, Va.

EFFECT OF SPACE EXPOSURE ON PYROELECTRIC INFRARED DETECTORS (A0135)

J. B. ROBERTSON, I. O. CLARK, and R. K. CROUCH *In its* Long Duration Exposure Facility (LDEF) p 158 Feb. 1984
Avail: NTIS HC A09/MF A01; also available SOD HC CSCL 20F

The effects of long-duration space exposure and launch environment on the performance of pyroelectric detectors which is important for the prediction of performance degradation, setting exposure limits, or determining shielding requirements was investigated. Air pollution monitoring and thermal mapping of the Earth, which includes the remote sensing of aerosols and limb scanning infrared radiometer projects, requires photodetection in the 6- to 20 micro m region of the spectrum. Pyroelectric detectors can detect radiation in the 1- to 100 micro m region while operating at room temperature. This makes the pyroelectric detector a prime candidate to fill the thermal infrared detector requirements.

E.A.K.

N84-24693# Deutsche Forschungs- und Versuchsanstalt fuer Luft- und Raumfahrt, Oberpfaffenhofen (West Germany). Abt. HF-Systeme.

PRELIMINARY INVESTIGATIONS CONCERNING A 90 GHZ RADIOMETER SATELLITE EXPERIMENT

F. HEEL and H. KIETZMANN Oct. 1983 64 p refs
(DFVLR-FB-84-02) Avail: NTIS HC A04/MF A01; DFVLR, Cologne DM 20,50

The preliminary investigations in this paper are aimed to realize a satellite experiment by means of a 90 GHz radiometer. Therefore, on the basis of a computer model the radiation temperatures of the object classes sand, vegetation, concrete and water are determined for different atmospheric conditions. Measurements with an uncooled airborne 90 GHz radiometer allow a quality test with respect to the model results. To accomplish the planned experiment a special null-balancing radiometer is proposed. In the case of null-balancing failure this system also can be operated as

08 INSTRUMENTATION AND SENSORS

total power radiometer. This procedure reduces the probability of a complete system drop out. Author

N84-25034# National Academy of Sciences - National Research Council, Washington, D. C. Board on Physics and Astronomy.

PROCEEDINGS OF A WORKSHOP: MULTIDISCIPLINARY USE OF THE VERY LONG BASELINE ARRAY Final Report, 1 Nov. 1982 - 31 Mar. 1984

Feb. 1984 202 p refs Sponsored in part by NASA and Defense Advanced Research Projects Agency (Contract MDA903-83-M-5896; NSF AST-83-03119; NA83AA-A-02632) (NASA-CR-173541; NAS 1.26:173541; PB84-163690) Avail: NTIS HC A10/MF A01 CSCL 14B

The National Research Council organized a workshop to gather together experts in very long baseline interferometry, astronomy, space navigation, general relativity and the earth sciences. The purpose of the workshop was to provide a forum for consideration of the various possible multi-disciplinary uses of the very long baseline array. Geophysical investigations received major attention. Geodesic uses of the very long baseline array were identified as were uses for fundamental astronomy investigations. Numerous specialized uses were identified. GRA

N84-25144# European Space Agency, Frascati (Italy).

PROCEEDINGS OF THE FOURTH MEETING OF THE LANDSAT TECHNICAL WORKING GROUP (LTWG), VOLUME 1

Apr. 1983 49 p Meeting held at Frascati, Italy, 19-21 Apr. 1983 2 Vol.

(LIB-PRO-0012-VOL-1) Avail: NTIS HC A03/MF A01

The performance of LANDSAT remote sensing and data transmission systems is assessed and methods are discussed for radiometric and geometric correction. Standard formats for data products and options for LANDSAT 4 tm data distribution to ground stations are considered. Author

N84-25146# Royal Inst. of Tech., Stockholm (Sweden). Dept. of Photogrammetry.

PHOTOGRAMMETRIC RESEARCH [FOTOGRAFMETRISKA MEDDELANDEN]

1983 206 p refs

(TRITA-FMI-47) Avail: NTIS HC A10/MF A01

The following topics are addressed: geometrical testing of x-y plotters; the question of accuracy in transition from analog to analytic photogrammetry; digital elevation models; adjustment problems and accuracy problems in analytical photogrammetry; and testing of instruments and non-topographical applications of photogrammetry.

N84-25147# Royal Inst. of Tech., Stockholm (Sweden). **PHOTOGRAMMETRIC RESEARCH AT THE ROYAL INSTITUTE OF TECHNOLOGY, STOCKHOLM, SWEDEN**

K. TORLEGAARD *In its* Photogrammetric Res. 9 p 1983 refs

Avail: NTIS HC A10/MF A01

During the past few years the special weight was placed on analytic photogrammetry, computer-aided stereo-mapping, and special applications. With this in mind stress was placed on the acquisition of a powerful minicomputer and a number of peripheral units which may be used on-line with several stereo instruments. For the period 1980 to 1984 priority is being placed on the following: analytic photogrammetry and its accuracy; map data bases and digital elevation models; cartographic remote sensing and data bases for physical planning; and non-topographic applications of photogrammetry. Author

N84-25150# Royal Inst. of Tech., Stockholm (Sweden). Dept. of Photogrammetry.

CORRELATING AERIAL PHOTOGRAPHS TO LANDSAT MULTISPECTRAL SENSOR (MSS) DATA TO MEASURE GROUND CONTROL POINTS

L. LARSSON and H. MALMSTROEM *In its* Photogrammetric Res. 8 p 1983 refs

Avail: NTIS HC A10/MF A01

The geometric rectification of MSS-data (MSS = Multi Spectral Sensor) is studied to improve the accuracy. This improvement is done by using an aerial photograph as a step between the MSS-data and the GCP (Ground Control Points) in the map coordinate system. Aerial photographs digitized to higher resolution than LANDSAT can after resampling to LANDSAT pixel size be positioned in the LANDSAT-scene using digital image correlation. The photograph coordinates are also transformed to the map coordinate system. With this sequence of transformations MSS-data in the map coordinate system are calculated without having to manually define GCP in the digital image. By moving the resampling grid net when resampling the aerial photography to LANDSAT pixel size we try to improve the correlation to subpixel accuracy.

Author

N84-25151# Royal Inst. of Tech., Stockholm (Sweden). Dept. of Photogrammetry.

GENERAL TRIANGULATION: INCORPORATING PHOTOGRAMMETRIC AND OTHER OBSERVATIONS

R. LARSSON *In its* Photogrammetric Res. 10 p 1983 refs Presented at ISP Comm. 3 Symp., Helsinki, 7-11 Jun. 1982 and 9th Nordic Geodetic Meeting, Gaevel, Sweden, 13-17 Sep. 1982

Avail: NTIS HC A10/MF A01

The facilities of and the possibilities with the GENTRI adjustment system are described. The underlying principles and data structures are explained. Several types of observations can be entered in the system and a few of them are discussed. The general way to treat observations handles such extra observations as lake surfaces, stastoscope observations, flight platform orientation, slope distances, height differences, angle measurements and observations of any parameter in the solution. Results from testruns with a few of these observations implemented are presented. A preview of the possibilities to detect blunders and predict reliability is also discussed.

Author

N84-25152# Royal Inst. of Tech., Stockholm (Sweden). Dept. of Photogrammetry.

GENTRI: A SYSTEM FOR SIMULTANEOUS ADJUSTMENT OF PHOTOGRAMMETRIC AND OTHER OBSERVATIONS

R. LARSSON *In its* Photogrammetric Res. 10 p 1983 refs Presented at ISP Comm. 5 Symp., York, England, 5-10 Sep. 1984

Avail: NTIS HC A10/MF A01

The program and data structures as realized in the GENTRI system are reported. Implementation and results from some tests using real data and further modifications by adding new types of information are discussed.

Author

N84-25153# Royal Inst. of Tech., Stockholm (Sweden). Dept. of Photogrammetry.

THE QUESTION OF ACCURACY IN THE TRANSITION FROM ANALOGUE TO ANALYTIC PHOTOGRAMMETRY

K. TORLEGAARD *In its* Photogrammetric Res. 19 p 1983 refs

Avail: NTIS HC A10/MF A01

In Sweden, photogrammetric detail measurement is performed exclusively with analog instruments of type WILD A7, A8, B8, A10, Jena Stereometrograph, Gallileo Stereosimplex, etc. In these instruments a stereoscopic model, similar to the terrain, and oriented in the ground coordinate system, is reconstructed either optically or mechanically. Measurement is characterized by the fact that each single model, covering a particular portion of the terrain is dealt with individually, resulting in a map with both planimetric details and contours for that particular area. In the case of orthophoto production, profiles are measured in each individual model. In the case of engineering planning it is often so

08 INSTRUMENTATION AND SENSORS

that digital elevation models, derived from individual stereoscopic models in analog instruments, are used. The result, when, for example, the Gigas-Zeiss system with so-called profile plates for the measuring of orthophoto profiles is used, will be graphical, while the result will be digital if, for example, the WILD OR1 orthophoto projector is used. Author

N84-25154# Royal Inst. of Tech., Stockholm (Sweden). Dept. of Photogrammetry.

MULTI-MODELS TO INCREASE ACCURACY

K. TORLEGAARD *In its Photogrammetric Res.* 109 p 1983 refs

Avail: NTIS HC A10/MF A01

Classical theory of error for photogrammetry divides errors in three groups: blunders, systematic errors and random errors. Systematic errors are caused by the lacking fidelity of the functional part of the mathematical model to the real geometric relations. Block adjustment with additional parameters, multiple photographic coverage and snooping after blunders provide results with high reliability, fidelity and precision. Results based on multi-models formed by averaging two or more single stereo-models are presented. The comprising single models are calculated without correction to lens distortion, atmospheric refraction and earth curvature. The improvement of accuracy by forming multi-models is studied. The precision of photogrammetric stereo-models is decomposed into components related to ground coordinates, image coordinates and image motion due to aircraft speed. The multi-model method provides an increase of the accuracy which is similar to the additional parameters in photogrammetric block adjustment, because both methods are based on multiple photographic coverage. Author

N84-26003 Institut d'Aeronomie Spatiale de Belgique, Brussels. **A SAMPLE PERFORMANCE OF THE GRILLE SPECTROMETER ABOARD SPACELAB**

M. P. LEMAIRE, J. LAURENT, J. BESSON, A. GIRARD, C. LIPPENS, C. MULLER, J. VERCHEVAL, and M. ACKERMAN 1984 13 p refs Submitted for publication Sponsored by Belgian Ministries of Education and Science Policy, CNES and French Ministry of Research and Industry (AERONOMICA-ACTA-A-281-1984) Avail: Issuing Activity

Preliminary results of the grille spectrometer flown on the Spacelab One mission intend only to show the quality of the obtained spectral data. Among ten trace species observed in the atmosphere, methane was chosen for the spectacular aspect of Q branch of the intense upsilon 3 band. Other molecules, as well as the atmospheric significance of the results, will be discussed elsewhere. Author

N84-26084* Arizona Univ., Tucson. Optical Sciences Center. **SPECTRORADIOMETRIC CALIBRATION OF THE THEMATIC MAPPER AND MULTISPECTRAL SCANNER SYSTEM** Quarterly Report, 1 Feb. - 1 May 1984

J. M. PALMER, Principal Investigator and P. N. SLATER 1 May 1984 24 p refs ERTS (Contract NAS5-27382)

(E84-10136; NASA-CR-172809; NAS 1.26:172809; QR-6) Avail: NTIS HC A02/MF A01 CSCL 14B

The newly built Caste spectropolarimeters gave satisfactory performance during tests in the solar radiometer and helicopter modes. A bandwidth normalization technique based on analysis of the moments of the spectral responsivity curves was used to analyze the spectral bands of the MSS and TM subsystems of LANDSAT 4 and 5 satellites. Results include the effective wavelength, the bandpass, the wavelength limits, and the normalized responsivity for each spectral channel. Temperature coefficients for TM PF channel 6 were also derived. The moments normalization method used yields sensor parameters whose derivation is independent of source characteristics (i.e., incident solar spectral irradiance, atmospheric transmittance, or ground reflectance). The errors expected using these parameters are lower than those expected using other normalization methods. A.R.H.

N84-26217# Boston Univ., Mass. Dept. of Astronomy. **A STUDY OF GEOMAGNETIC PULSATIONS USING THE AFGL (AIR FORCE GEOPHYSICS LABORATORY) MAGNETOMETER NETWORK** Final Report, 15 Nov. 1980 - 14 Nov. 1983 W. J. HUGHES, H. J. SINGER, and M. LESTER 13 Jan. 1983 56 p (Contract F19628-81-K-0003; AF PROJ. 7601) (AD-A140507; AFGL-TR-84-0027) Avail: NTIS HC A04/MF A01 CSCL 08N

The objective of this work has been to study the midlatitude magnetic signatures of magnetospheric substorm onsets with the aim of using these signals to time and locate substorm onsets. The primary data source was the AFGL Magnetometer Network, a unique facility in that it spans over four hours in local magnetic time, a far greater extent than any other high-time-resolution network. Using this capability we have found that pi2 pulsation polarizations are ordered in longitude or local time. The direction of the major axis of the polarizations ellipse varies with longitude, and points due north on the central meridian of the D.C. substorm current system. We have made use of this pattern to locate particular substorms. We have also shown that substorm onset signatures near geostationary orbit are far more localized than at midlatitudes on the ground. The geostationary orbit signature is usually localized to within the two meridians on which the main substorm field-aligned currents flow, whereas the ground signature is usually seen over the entire nightside of the Earth. The latter we have shown by using data from Northern Europe in conjunction with the AFGL data. In addition to these studies, we have also made some theoretical contributions and participated in two data analysis. GRA

N84-26237# Battelle Inst., Frankfurt am Main (West Germany). **APPLICATIONS OF LASER FOR CLIMATOLOGY AND ATMOSPHERIC RESEARCH**

M. ENDEMANN, ed. Paris ESA Oct. 1983 367 p refs (Contract ESTEC-4868/81/NL-HP(SC)) (BLEV-R-65.169-5; ESA-CR(P)-1868) Avail: NTIS HC A16/MF A01

Sensor parameters, specific applications, and conceptual design studies are examined for various Light Detection And Ranging (LIDAR) systems as they effect climatology and general meteorological research. Atmospheric measurements are subjected to error analysis and comparison with passive radiometric data from satellite and ground based stations. The instrument classes are used to investigate such phenomena as planetary and surface albedo, cloud height, atmospheric composition, wind and temperature profiles, and sea surface temperature.

N84-26238# Battelle Inst., Frankfurt am Main (West Germany). **FUNDAMENTALS OF SPACEBORNE REMOTE SENSING: APPLICATIONS OF LASERS, VOLUME 1**

M. ENDEMANN *In its Appl. of Laser for Climatol. and Atmospheric Res.* 149 p Oct. 1983 refs (Contract ESTEC-4868/81/NL-HP(SC)) Avail: NTIS HC A16/MF A01

The measurement capabilities of spaceborne, laser based sensors are examined. After a review of the interactions with light and the atmosphere, performance capabilities of Light Detection And Ranging (LIDAR) systems are discussed with emphasis on atmospheric modeling and definition of the system limitations. The feasibility of spaceborne atmospheric probing with LIDAR systems is determined and an error analysis performed on a Differential Absorption Lidar (DIAL) system. Atmospheric measurements that concern climatology research are compared for the two systems. M.A.C.

N84-27248*# National Aeronautics and Space Administration. Goddard Space Flight Center, Greenbelt, Md.

HEAT CAPACITY MAPPING RADIOMETER (HCMR) DATA PROCESSING ALGORITHM, CALIBRATION, AND FLIGHT PERFORMANCE EVALUATION

J. R. BOHSE (Computer Sciences Corp.), M. BEWTRA (Computer Sciences Corp.), and W. L. BARNES Apr. 1979 173 p refs HCMM

(E84-10153; NASA-TM-80258; NAS 1.15:80258) Avail: NTIS

HC A08/MF A01 CSCL 14B

The rationale and procedures used in the radiometric calibration and correction of Heat Capacity Mapping Mission (HCMM) data are presented. Instrument-level testing and calibration of the Heat Capacity Mapping Radiometer (HCMR) were performed by the sensor contractor ITT Aerospace/Optical Division. The principal results are included. From the instrumental characteristics and calibration data obtained during ITT acceptance tests, an algorithm for post-launch processing was developed. Integrated spacecraft-level sensor calibration was performed at Goddard Space Flight Center (GSFC) approximately two months before launch. This calibration provided an opportunity to validate the data calibration algorithm. Instrumental parameters and results of the validation are presented and the performances of the instrument and the data system after launch are examined with respect to the radiometric results. Anomalies and their consequences are discussed. Flight data indicates a loss in sensor sensitivity with time. The loss was shown to be recoverable by an outgassing procedure performed approximately 65 days after the infrared channel was turned on. It is planned to repeat this procedure periodically.

M.G.

N84-27286*# National Center for Atmospheric Research, Boulder, Colo.

APPLICATIONS OF AIRBORNE REMOTE SENSING IN ATMOSPHERIC SCIENCES RESEARCH

R. J. SERAFIN, G. SZEJWACH (Lab. de Meteorologie Dynamique, Palaiseau, France), and B. B. PHILLIPS /n NASA. Marshall Space Flight Center Frontiers of Remote Sensing of the Oceans and Troposphere from Air and Space Platforms p 259-269 May 1984 refs Sponsored by NSF

Avail: NTIS HC A99/MF A01 CSCL 04A

This paper explores the potential for airborne remote sensing for atmospheric sciences research. Passive and active techniques from the microwave to visible bands are discussed. It is concluded that technology has progressed sufficiently in several areas that the time is right to develop and operate new remote sensing instruments for use by the community of atmospheric scientists as general purpose tools. Promising candidates include Doppler radar and lidar, infrared short range radiometry, and microwave radiometry.

Author

09

GENERAL

Includes economic analysis.

A84-34575#

STATUS OF THE TERS PROJECT [STAND VAN ZAKEN IN HET TERS PROJEKT]

R. VAN KONIJNENBURG (Nederlands Instituut voor Vliegtuigontwikkeling en Ruimtevaart, Delft, Netherlands) Ruimtevaart, vol. 33, Feb. 1984, p. 19-23. In Dutch.

The Tropic Earth Resources Satellite (TERS) being developed in Dutch-Indonesian cooperation is characterized. The planned TERS orbit is equatorial at 1680 km altitude, permitting 11 passes per day. The instrumentation is to be derived from the IRAS experience and permit 60-km-swath images at 16 m resolution in three spectral bands and at 8-m resolution in a panchromatic channel; coverage of 10 deg latitude on each side of the equator

is to be provided by a swath-selection mirror aided by a forward-looking cloud detector (to identify cloud-free regions). User needs in agriculture, forestry, navigation, city planning, and migration studies are being considered in the current phase-A1 studies.

T.K.

A84-37049

HIGH RESOLUTION OBSERVATION OF THE EARTH'S SURFACE FROM SPACE - PROGRAMS, PROBLEMS AND PERSPECTIVES [L'OBSERVATION A HAUTE RESOLUTION DE LA SURFACE DE LA TERRE A PARTIR DE L'ESPACE - PROGRAMMES, PROBLEMES ET PERSPECTIVES]

G. BRACHET (Spot Image, Toulouse, France) Air et Cosmos (ISSN 0044-6971), May 5, 1984, p. 299-304. In French.

Although no follow-on U.S. programs are planned to continue developing the technologies defined by the Landsat series of satellites, other nations have initiated projects. The French have the SPOT (1985), the Japanese the MOS-1 (1986), the Indians the IRS-1 (1986), ESA has the ERS-1 (1988), and Canada has Radarsat (1990). Data from the Landsat satellites sold for more than \$7 million in 1982, substantiating the presence of a market for the imagery. The SPOT satellites will have high resolution visible and near-IR capabilities. Resolution will be 20 m in the multispectral mode and 10 m in the panchromatic mode. Time-delay stereoscopic imagery will also be afforded due to lens positioning capabilities. A 10-yr payback is hoped for SPOT investors, although the size and long-term nature of the market for remotely sensed images are still unknown quantities, as are reactions of UN member nations to the marketing of imagery of regions within their national boundaries.

M.S.K.

N84-23985*# Council of State Governments, Washington, D.C. **STATE REMOTE SENSING (LANDSAT) PROGRAMS CATALOG**

Mar. 1981 71 p Sponsored by NASA and Council of State Planning Agencies ERTS

(E84-10127; NASA-CR-172802; NAS 1.26:172802) Avail: NTIS HC A04/MF A01 CSCL 05B

This directory lists the technical capabilities, personnel, and program structure for remote sensing activities as they existed in each state in late 1980. The institutional framework, participating agencies, applications, status, equipment, software, and funding sources are also indicated.

A.R.H.

N84-25159# National Commission on Libraries and Information Science, Washington, D. C. Panel on the Information Policy Implications of Archiving Satellite Data.

PRESERVE THE SENSE OF EARTH FROM SPACE

Dec. 1983 84 p refs

(DE84-900854; NP-4900854) Avail: NTIS HC A05/MF A01

The information policy implications of archiving satellite data, which was convened by the National Commission on Libraries and Information Science in September 1983 are reported. The archiving requirements that should be imposed in the event of a transfer of the US land remote sensing satellite systems to the private sector are considered. Recommendations are made to the archiving requirements that should be included in the government's request for proposals (RFP) from potential bidders.

DOE

N84-25510*# Jet Propulsion Lab., California Inst. of Tech., Pasadena.

PUBLICATIONS OF THE JET PROPULSION LABORATORY 1982

15 Sep. 1983 26 p Sponsored by NASA (NASA-CR-173539; JPL-BIBL-39-24; NAS 1.26:173539) Avail: NTIS HC A03/MF A01 CSCL 05B

A bibliography of articles concerning topics on the deep space network, data acquisition, telecommunication, and related aerospace studies is presented. A sample of the diverse subjects include, solar energy remote sensing, computer science, Earth resources, astronomy, and satellite communication.

M.A.C.

09 GENERAL

N84-25737*# National Aeronautics and Space Administration, Washington, D. C.

LIVING AND WORKING IN SPACE. A HISTORY OF SKYLAB

W. D. COMPTON and C. D. BENSON 1983 466 p refs

Original document contains color illustrations

(NASA-SP-4208; NAS 1.21:4208; LC-81-22424) Avail: NTIS MF A01; SOD HC \$20.00 as 033-000-00847-3

The history of Skylab is examined with emphasis on program development from previous Apollo missions, modifications to spacecraft, onboard experiments, and flight crew training. A listing of the missions and an evaluation of results are included with a brief description of the workshop's reentry.

M.A.C.

N84-26467*# National Aeronautics and Space Administration, Goddard Space Flight Center, Greenbelt, Md.

TECHNICAL PUBLICATIONS OF THE NASA WALLOPS FLIGHT FACILITY, 1980 THROUGH 1983

J. N. FOSTER Jun. 1984 47 p

(NASA-TM-84421; NAS 1.15:84421) Avail: NTIS HC A03/MF

A01 CSCL 05B

This bibliography lists the publications sponsored by the NASA Wallops Flight Center/NASA Goddard Space Flight Center, Wallops Flight Facility during the period 1980 through 1983. The compilation contains citations listed by type of publication; i.e., NASA formal report, NASA contractor report, journal article, or presentation; by contract/grant number; and by accession number. Oceanography, astrophysics, artificial satellites, fluid mechanics, and sea ice are among the topics covered.

R.J.F.

N84-26563*# National Aeronautics and Space Administration, Washington, D. C.

NASA, THE FIRST 25 YEARS: 1958 - 1983

J. DALEIO, comp., J. TULLY, comp., and W. CORTESE, comp.

1983 130 p

(NASA-EP-182; NAS 1.19:182) Avail: NTIS MF A01; SOD HC

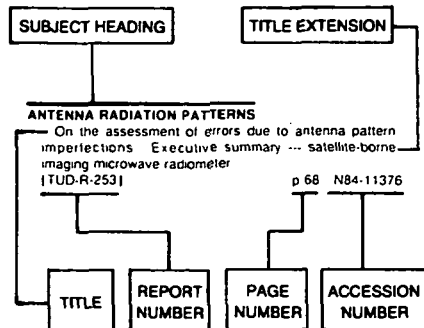
\$8.00 as 033-000-00909-7 CSCL 05D

Because it is impossible to describe the 25 years of NASA's research and missions in detail, this book is designed to provide a reference base from which teachers can develop classroom concepts and activities. It begins with a prologue, a brief history of the National Advisory Committee for Aeronautics, NASA's predecessor. Succeeding chapters are devoted to major NASA programs, in alphabetical order; within the chapters projects are listed chronologically. Each chapter concludes with ideas for the classroom and space for notes and new information the user may wish to add.

Author

SUBJECT INDEX

Typical Subject Index Listing



The subject heading is a key to the subject content of the document. The title is used to provide a description of the subject matter. When the title is insufficiently descriptive of the document content, the title extension is added, separated from the title by three hyphens. The (NASA or AIAA) accession number and the page number are included in each entry to assist the user in locating the abstract in the abstract section (of this supplement). If applicable, a report number is also included as an aid in identifying the document. Under any one subject heading, the accession numbers are arranged in sequence with the AIAA accession numbers appearing first.

A

ACCURACY

Comparative accuracies of AVHRR and MSS data used for Level I land cover classifications p 14 N84-33344

ACTIVE SATELLITES

The active microwave instrumentation for ERS-1 p 34 N84-35542

ADAPTIVE FILTERS

Distinguishing linear contour elements on satellite photos on the basis of a visual perception model p 24 N84-34789

AERIAL PHOTOGRAPHY

Measurement of boro rice acreage in Srimangal Thana by remote sensing technique p 1 N84-30235

Analysing forest structures by remote sensing p 1 N84-30236

Analysis of land use changes around Salt Lake City using Landsat digital data - A case study of Sandy area p 13 N84-30242

Interpreting the spectra of aerial photographs of the sea surface p 30 N84-30443

Elements of the west African monsoon circulation deduced from Meteosat cloud winds and simultaneous aircraft measurements p 51 N84-31948

Geological interpretation from aerial remote sensing images of Tengchong area p 23 N84-32590

American Society of Photogrammetry, Annual Meeting, 49th, Washington, DC, March 13-18, 1983, Technical Papers p 65 N84-33326

Applications of the Enviro-pod with KA-85A panoramic cameras in south-eastern historic and pre-historic archaeological survey p 23 N84-33327

Analysis of photo interpretation test results for seven aerospace image types of the San Juan National Forest, Colorado p 4 N84-33328

Automated classification of wetlands p 4 N84-33337

Interpreting multispectral photographs obtained in the Telefoto-80 experiment so as to distinguish crop types p 6 N84-34780

A regression analysis of data from aircraft and ground measurements of a vegetative cover p 6 N84-34784

User guide for the USGS aerial camera report of calibration p 65 N84-34958

Performance study of multicolor visual sensor system p 66 N84-38312

Enviropod handbook: A guide to preparation and use of the Environmental Protection Agency's light-weight aerial camera system --- Weber River, Utah [E84-10123] p 68 N84-23982

Aerial photography for ecological site mapping p 9 N84-23990

Experiments to correct a digital map data base using scene analysis [AD-A139447] p 61 N84-24499

Correlating aerial photographs to LANDSAT Multispectral Sensor (MSS) data to measure ground control points p 69 N84-25150

Correlation calculation in stereoscopic image pairs for the automatic acquisition of digital land models, orthophotos and height line planes [SER-C-283] p 21 N84-26079

Fisheye objective in the dose range photogrammetry: Theoretical and practical investigations [SER-C-286] p 21 N84-26080

Cartographic feature extraction on ETL's (Engineer Topographic Laboratories') DIAL (Digital Image Analysis Laboratory) system [AD-A140230] p 63 N84-26112

The use of photointerpretation for socio-economic characterization of urban population [INPE-3067-PRE/484] p 16 N84-26428

AERIAL RECONNAISSANCE

EPA Enviropod. A summary of the use of the Enviropod under a Memorandum of Understanding among EPA Region 8, the State of Utah, and the University of Utah Research Institute [E84-10124] p 15 N84-23983

Sampling system for wheat (*Triticum aestivum* L) area estimation using digital LANDSAT MSS data and aerial photographs --- Brazil [E84-10139] p 10 N84-26087

Forest inventory using multistage sampling with probability proportional to size --- Brazil [E84-10144] p 11 N84-26092

Ocean waves and turbulence as observed with an adaptive coherent multifrequency radar p 44 N84-27279

Measurements of ocean wave spectra and modulation transfer function with the airborne frequency scatterometer p 45 N84-27282

AERODYNAMIC COEFFICIENTS

Method to estimate drag coefficient at the air/ice interface over drifting open pack ice from remotely sensed data p 48 N84-27310

AERODYNAMIC DRAG

Method to estimate drag coefficient at the air/ice interface over drifting open pack ice from remotely sensed data p 48 N84-27310

AEROMAGNETISM

Do satellite magnetic anomaly data accurately portray the crustal component? p 28 N84-25134

Long-wavelength magnetic and gravity anomaly correlations of Africa and Europe p 28 N84-25135

US aeromagnetic and satellite magnetic anomaly comparisons p 28 N84-25136

AEROSOLS

Arctic haze and the Arctic gas and aerosol sampling program (AGASP) p 32 N84-34276

Airborne observations of Arctic aerosol. IV - Optical properties of Arctic haze p 32 N84-34287

Detection of marine aerosol particles in coastal zones using satellite imagery p 36 N84-38943

SAGE and SAM II measurements of global stratospheric aerosol optical depth and mass loading p 15 N84-39455

A comparative study of aerosol extinction measurements made by the SAM II and SAGE satellite experiments p 15 N84-39457

AVHRR aerosol ground truth experiment [PB84-157882] p 39 N84-24065

AFRICA

Euro-African MAGSAT anomaly-tectonic observations p 27 N84-25129

Reduced to pole long-wavelength magnetic anomalies of Africa and Europe p 27 N84-25132

Satellite magnetic anomalies of Africa and Europe p 27 N84-25133

Long-wavelength magnetic and gravity anomaly correlations of Africa and Europe p 28 N84-25135

AGRICULTURE

A constrained-clustering approach to the analysis of remote sensing data [AD-A139124] p 10 N84-23993

AGRISTARS PROJECT

CONSERVB: A numerical method to compute soil water content and temperature profiles under a bare surface [E84-10113] p 9 N84-23006

A microwave systems approach to measuring root zone soil moisture [E84-10114] p 9 N84-23007

AIR POLLUTION

Arctic haze and the Arctic gas and aerosol sampling program (AGASP) p 32 N84-34276

Airborne observations of Arctic aerosol. IV - Optical properties of Arctic haze p 32 N84-34287

First estimate of annual mercury flux at the Kilauea vent p 15 N84-34794

AIR QUALITY

Computer-automated CO₂-laser long-path absorption system for air quality monitoring in the working environment p 13 N84-30307

AIR SAMPLING

Arctic haze and the Arctic gas and aerosol sampling program (AGASP) p 32 N84-34276

AIR SEA ICE INTERACTIONS

Katabatic wind forcing of the Terra Nova Bay polynya p 33 N84-34509

Climate research from space p 66 N84-38922

Wind, waves and swell in the Antarctic marginal ice zone by SEASAT radar altimeter p 38 N84-23941

Radar altimetry over sea ice p 48 N84-27309

Method to estimate drag coefficient at the air/ice interface over drifting open pack ice from remotely sensed data p 48 N84-27310

AIR WATER INTERACTIONS

Interpreting the spectra of aerial photographs of the sea surface p 30 N84-30443

Katabatic wind forcing of the Terra Nova Bay polynya p 33 N84-34509

Effective reflectance of oceanic whitecaps p 35 N84-36119

Remote sensing of the ocean by the airborne microwave scatterometer/radiometer system p 36 N84-38307

Detection of marine aerosol particles in coastal zones using satellite imagery p 36 N84-38943

Arctic Sea ice by passive microwave observations from the Nimbus-5 Satellite p 39 N84-23970

NASA Oceanic Processes Program, fiscal year 1983 [NASA-TM-86248] p 39 N84-24078

Nimbus 7 SMMR derived seasonal variations in the water vapor, liquid water and surface winds over the global oceans [NASA-TM-86080] p 40 N84-26233

Frontiers of Remote Sensing of the Oceans and Troposphere from Air and Space Platforms [NASA-CP-2303] p 42 N84-27262

Remote sensing for oceanography. Past, present, future p 42 N84-27263

Remote sensing of air-sea interactions p 42 N84-27267

A new parameterization of an empirical model for wind/ocean scatterometry p 43 N84-27269

Observing ocean-atmosphere exchanges with space-borne sensors, appendix C p 50 N84-28298

AIRBORNE EQUIPMENT

Sensitivity of airborne fluorosensor measurements to linear vertical gradients in chlorophyll concentration p 30 N84-30302

An airborne radar station for studying the reflection properties of the earth's surface p 64 N84-31072

S
U
B
J
E
C
T

AIRBORNE SURVEILLANCE RADAR

SUBJECT INDEX

Aircraft scatterometer observations of soil moisture on rangeland watersheds p 4 A84-3338

A theoretical study of an airborne laser technique for determining sea water turbidity p 31 A84-33774

Determining forest canopy characteristics using airborne laser data p 7 A84-37202

Airborne laser topographic mapping results p 8 A84-38998

Airborne lidar for oceanography and hydrology (FLOH) [ESA-TT-799] p 37 N84-22955

GENTRI: A system for simultaneous adjustment of photogrammetric and other observations p 69 N84-25152

Analysis of airborne electromagnetic systems for mapping thickness of sea ice [AD-A139786] p 39 N84-25235

AIRBORNE SURVEILLANCE RADAR

Preliminary investigations concerning a 90 GHz radiometer satellite experiment [DFVLR-FB-84-02] p 68 N84-24693

AIRBORNE/SPACEBORNE COMPUTERS

Application of the Vizir Image Processing System to the remote sensing studies in Bangladesh p 64 A84-30266

ALABAMA

Application of remote sensing to state and regional problems [E84-10128] p 68 N84-23986

ALASKA

Emerging recognition of the nonfuel mineral resources of Arctic Alaska p 26 N84-23962

Land cover and terrain mapping for the development of digital data bases for wildlife habitat assessment in the Yukon Flats National Wildlife Refuge, Alaska p 9 N84-23971

Hydrology of the North Slope, Alaska p 53 N84-23973

ALBEDO

Snow reflectance from Landsat-4 Thematic Mapper p 52 A84-33541

Albedo of a forest modeled as a plane with dense protrusions p 6 A84-34385

Surface albedo and the Sahel drought p 7 A84-36710

Atmospheric model development p 53 N84-22998

Vegetation, land-use and seasonal albedo data sets: Documentation of archived data tape [E84-10133] p 10 N84-25142

ALGORITHMS

Digital SAR processing using a fast polynomial transform p 55 A84-32093

A constrained-clustering approach to the analysis of remote sensing data [AD-A139124] p 10 N84-23993

Several aspects of the sequential processing of photogrammetric bundle blocks p 21 N84-26077

Development of Great Lakes algorithms for the Nimbus-G coastal zone color scanner [NASA-CR-173511] p 53 N84-27258

New algorithms for microwave measurements of ocean winds p 43 N84-27272

Tracking ocean wave spectrum from SAR images p 44 N84-27277

ALLUVIUM

Results of field observations of radio waves in alluvial deposits in Cara state from 1:100,000: Fortaleza, Canirde, Taperuaba, Santa Quiteria, Sobral, and Sao Luiz do Curu [INPE-3061-NTE/216] p 53 N84-26100

ALTIMETERS

Topex: Observing the oceans from Space [NASA-CR-173490] p 38 N84-23085

Satellite techniques for determining the geopotential for sea-surface elevations p 46 N84-27298

The importance of altimeter and scatterometer data for ocean prediction p 49 N84-27316

AMAZON REGION (SOUTH AMERICA)

Application of MagSat lithospheric modeling in South America. Part 1: Processing and interpretation of magnetic and gravity anomaly data [E84-10115] p 24 N84-23008

Satellite elevation magnetic and gravity models of major South American plate tectonic features p 27 N84-25131

ANDES MOUNTAINS (SOUTH AMERICA)

Radar-visible wind streaks in the Altiplano of Bolivia p 25 N84-23527

Correlation of tectonic provinces of South America and the Caribbean region with MAGSAT anomalies p 27 N84-25130

Satellite elevation magnetic and gravity models of major South American plate tectonic features p 27 N84-25131

ANNUAL VARIATIONS

Seasonal variability in meanders of the California Current System off Vancouver Island p 33 A84-34507

Evaluation of the effects of the seasonal variation of solar elevation angle and azimuth on the processes of digital filtering and thematic classification of relief units [E84-10121] p 60 N84-23980

Vegetation, land-use and seasonal albedo data sets: Documentation of archived data tape [E84-10133] p 10 N84-25142

Evaluation of solar angle variation over digital processing of LANDSAT imagery --- Brazil [E84-10140] p 61 N84-26088

Multiseasonal variables in digital image enhancements for geological applications [E84-10145] p 29 N84-26093

Nimbus 7 SMMR derived seasonal variations in the water vapor, liquid water and surface winds over the global oceans [NASA-TM-86080] p 40 N84-26233

Seasonal oscillations of the subtropical convergence between the Brazil and Malvinas currents, using oceanographic and SMS-2 satellite data [INPE-3092-PRE/497] p 40 N84-26255

Maps of favorable areas for tuna fishing to the South and Southeast of Brazil prepared from SMS-2 satellite data [INPE-3102-PRE/501] p 41 N84-26256

Recent advances in multispectral sensing of ocean surface temperature from space p 46 N84-27297

ANOMALIES

Diagnostics of rainfall anomalies in the Nordeste during the global weather experiment [SAPR-1] p 40 N84-26235

ANOMALOUS TEMPERATURE ZONES

Nimbus 7 SMMR derived seasonal variations in the water vapor, liquid water and surface winds over the global oceans [NASA-TM-86080] p 40 N84-26233

ANTARCTIC REGIONS

US Geological Survey Polar Research Symposium. Abstracts with program [USGS-CIRC-911] p 25 N84-23934

Antarctic mapping and international coordination p 19 N84-23935

Satellite image atlas of glaciers: The Polar regions p 38 N84-23940

Wind, waves and swell in the Antarctic marginal ice zone by SEASAT radar altimeter p 38 N84-23941

Surveying in Antarctica during the International Geophysical Year p 25 N84-23942

The Dufek intrusion of Antarctica and a survey of its minor metals related to possible resources p 25 N84-23943

Program for mapping Antarctica p 19 N84-23954

The use of satellite technology in the search for meteorites in Antarctica aut 01Meunier, Tony K. p 26 N84-23955

Glaciological and geological studies of Antarctica with satellite remote sensing technology p 38 N84-23956

Modeling the movement at the polar ice cap at the South Pole p 20 N84-23957

Satellite remote sensing over ice p 48 N84-27308

Matrix partitioning and EOF/principal component analysis of Antarctic Sea ice brightness temperatures [NASA-TM-83916] p 49 N84-27319

ANTICYCLONES

Lagrangian observations of an anticyclonic ring in the western Gulf of Mexico p 33 A84-34502

APPLICATIONS EXPLORER SATELLITES

Heat Capacity Mapping Radiometer (HCMR) data processing algorithm, calibration, and flight performance evaluation [E84-10153] p 71 N84-27248

APPROXIMATION

The approximation introduced by representing the earth's gravity field with a finite grid of mascons both at the earth's surface and at the bottom of the earth's crust [AAS PAPER 83-394] p 17 A84-30583

ARCHAEOLOGY

Applications of the Enviro-pod with KA-85A panoramic cameras in south-eastern historic and pre-historic archaeological survey p 23 A84-33327

ARCTIC OCEAN

Seasat SAR sea-ice imagery - Summer melt to autumn freeze-up p 36 A84-38941

A comparison of numerical results of Arctic Sea ice modeling with satellite images p 39 N84-23969

Arctic Sea ice by passive microwave observations from the Nimbus-5 Satellite p 39 N84-23970

Remote sensing of floe size distribution and surface topography [E84-10132] p 39 N84-25141

ARCTIC REGIONS

Arctic haze and the Arctic gas and aerosol sampling program (AGASP) p 92 A84-34276

Airborne observations of Arctic aerosol. IV - Optical properties of Arctic haze p 32 A84-34287

US Geological Survey Polar Research Symposium. Abstracts with program [USGS-CIRC-911] p 25 N84-23934

Satellite image atlas of glaciers: The Polar regions p 38 N84-23940

ARID LANDS

Study of desertification/aridity through remote sensing p 1 A84-30238

Assessing change in the surficial character of a semiarid environment with Landsat residual images p 3 A84-31499

Preliminary digital classification of grazing resources in the Southern Chihuahuan Arid Zone of Mexico p 5 A84-33349

Surface albedo and the Sahel drought p 7 A84-36710

Identifying environmental features for land management decisions [E84-10125] p 15 N84-23984

Discriminating vegetation and soils using LANDSAT MSS and Thematic Mapper bands and band ratios [AD-A140198] p 11 N84-26108

ARTIFICIAL SATELLITES

Comparisons of sea-surface temperature obtained from ship and satellite data [AD-A138257] p 38 N84-23087

ASIA

Asian Conference on Remote Sensing, 3rd, Dacca, Bangladesh, December 4-7, 1982, Proceedings p 64 A84-30226

ASTRONOMY

Proceedings of a workshop: Multidisciplinary Use of the Very Long Baseline Array [NASA-CR-173541] p 69 N84-25034

ATLANTIC OCEAN

Dynamics of the slope water off New England and its influence on the Gulf Stream as inferred from satellite IR data p 31 A84-30672

Mean circulation and eddy kinetic energy in the eastern North Atlantic p 32 A84-34501

Diagnostics of rainfall anomalies in the Nordeste during the global weather experiment [SAPR-1] p 40 N84-26235

Seasonal oscillations of the subtropical convergence between the Brazil and Malvinas currents, using oceanographic and SMS-2 satellite data [INPE-3092-PRE/497] p 40 N84-26255

The depiction of Alboran Sea Gyre during Donde Va? using remote sensing and conventional data p 47 N84-27306

ATMOSPHERIC BOUNDARY LAYER

Detection of marine aerosol particles in coastal zones using satellite imagery p 36 A84-38943

Observing ocean-atmosphere exchanges with space-borne sensors, appendix C p 50 N84-28298

ATMOSPHERIC CHEMISTRY

Accuracy and precision of the nitric acid concentrations determined by the limb infrared monitor of the stratosphere experiment on NIMBUS 7 p 67 A84-39444

Applications of airborne remote sensing in atmospheric sciences research p 71 N84-27286

ATMOSPHERIC CIRCULATION

Observations of Gulf Stream-induced and wind-driven upwelling in the Georgia Bight using ocean color and infrared imagery p 34 A84-34517

Monthly distributions of precipitable water from the Nimbus 7 SMMR data p 37 A84-39458

Satellite observed upper level moisture patterns associated with tropical cyclone movement p 37 A84-39523

ATMOSPHERIC COMPOSITION

Recent investigations of ozone and minor atmospheric gases p 14 A84-34450

Accuracy and precision of the nitric acid concentrations determined by the limb infrared monitor of the stratosphere experiment on NIMBUS 7 p 67 A84-39444

High-precision atmospheric ozone measurements using wavelengths between 290 and 305 nm p 67 A84-39447

Intercomparison of the Nimbus 7 SBUV/TOMS total ozone data sets with Dobson and M83 results -- Solar Backscattered Ultraviolet/Total Ozone Mapping Spectrometer p 67 A84-39449

SAGE and SAM II measurements of global stratospheric aerosol optical depth and mass loading p 15 A84-39455

A comparative study of aerosol extinction measurements made by the SAM II and SAGE satellite experiments p 15 A84-39457

A sample performance of the grille spectrometer aboard Spacelab [AERONOMICA-ACTA-A-281-1984] p 70 N84-26003

ATMOSPHERIC CORRECTION

Atmospheric correction of Landsat MSS data for a multidate suspended sediment algorithm p 59 A84-38942

SUBJECT INDEX

LANDSAT-D investigations in snow hydrology
[E84-10094] p 53 N84-22997

LANDSAT 4 band 6 data evaluation
[E84-10119] p 60 N84-23009

Understanding and utilization of Thematic Mapper and other remotely sensed data for vegetation monitoring
[E84-10150] p 11 N84-26098

Development of Great Lakes algorithms for the Nimbus-G coastal zone color scanner
[NASA-CR-173511] p 53 N84-27258

ATMOSPHERIC EFFECTS

Atmospheric effect on classification of finite fields --- satellite-imaged agricultural areas p 2 A84-30670

ATMOSPHERIC GENERAL CIRCULATION EXPERIMENT

A sample performance of the grille spectrometer aboard Spacelab
[AERONOMICA-ACTA-A-281-1984] p 70 N84-26003

ATMOSPHERIC LASERS

Applications of laser for climatology and atmospheric research
[BLEV-R-65-169-5] p 70 N84-26237

Fundamentals of spaceborne remote sensing: Applications of lasers, volume 1 p 70 N84-26238

ATMOSPHERIC MODELS

Atmospheric model development p 53 N84-22998

Nimbus 7 SMMR derived seasonal variations in the water vapor, liquid water and surface winds over the global oceans
[NASA-TM-86080] p 40 N84-26233

The impact of scatterometer wind data on global weather forecasting p 49 N84-27314

ATMOSPHERIC MOISTURE

Fog recognition in daylight 3.7-micron-band Tires-N and NOAA images p 65 A84-34157

Monthly distributions of precipitable water from the Nimbus 7 SMMR data p 37 A84-39458

Satellite observed upper level moisture patterns associated with tropical cyclone movement p 37 A84-39523

Satellite observations of a monsoon depression
[NASA-CR-173590] p 40 N84-26232

Nimbus 7 SMMR derived seasonal variations in the water vapor, liquid water and surface winds over the global oceans
[NASA-TM-86080] p 40 N84-26233

ATMOSPHERIC OPTICS

The effect of fluctuations in the optical properties of the atmosphere on spectral brightness ratios in the remote sensing of agricultural areas p 6 A84-34777

Effective reflectance of oceanic whitecaps p 35 A84-36119

Detection of marine aerosol particles in coastal zones using satellite imagery p 36 A84-38943

Applications of laser for climatology and atmospheric research
[BLEV-R-65-169-5] p 70 N84-26237

ATMOSPHERIC SCATTERING

Fundamentals of spaceborne remote sensing: Applications of lasers, volume 1 p 70 N84-26238

ATMOSPHERIC SOUNDING

Atmospheric science --- overview of stratosphere and mesosphere satellite remote sounding experiments p 66 A84-38923

The Limb Infrared Monitor of the Stratosphere - Experiment description, performance, and results p 66 A84-39440

The validation of Nimbus 7 LIMS measurements of ozone p 67 A84-39443

ATMOSPHERIC WINDOWS

Theory and validation of the multiple window sea surface temperature technique p 33 A84-34513

ATMOSPHERICS

Principal components as a method for atmospherically correcting coastal zone color scanner data
[AD-P003124] p 41 N84-26265

ATTITUDE INDICATORS

Study on temporal geometric-distortion variation of Landsat MSS and RBV imageries and attitude determination program p 59 A84-38313

AUTOMATIC CONTROL

Error analysis for marine geodetic control using the global positioning system
[AD-A140566] p 21 N84-26687

AZIMUTH

Evaluation of the effects of the seasonal variation of solar elevation angle and azimuth on the processes of digital filtering and thematic classification of relief units
[E84-10121] p 60 N84-23980

Multiseasonal variables in digital image enhancements for geological applications
[E84-10145] p 29 N84-26093

B

BACKSCATTERING

Calculations of radar backscattering coefficient of vegetation-covered soils p 2 A84-30671

Microwave backscattering characteristics of wind-generated waves p 36 A84-38309

Radar backscatter modelling p 25 N84-23525

Marginal ice zone experiment (1983). Part 1: Ice characterization measurements. Part 2. Helicopter-borne and ship-based radar backscatter measurement of sea ice in the marginal ice zone
[AD-A139894] p 40 N84-25238

The theory of Earth observation using multiple-frequency radar
[ESA-TT-819] p 63 N84-26105

A new parameterization of an empirical model for wind/ocean scatterometry p 43 N84-27269

New algorithms for microwave measurements of ocean winds p 43 N84-27272

Optimum backscatter cross section of the ocean as measured by synthetic aperture radars p 44 N84-27276

Non-Gaussian statistical models of surface wave fields for remote sensing applications p 45 N84-27284

BALMER SERIES

Correlations between the nonthermal emission of quasimolecular nuclei and their Balmer-line widths p 58 A84-33629

BAND RATIOING

Methodological approach in lithological discrimination by digital processing: A case study in the Serra do Ramalho, state of Bahia
[INPE-3108-PRE/507] p 29 N84-26101

BANDWIDTH

Spectroradiometric calibration of the Thematic Mapper and Multispectral Scanner system --- White Sands, New Mexico
[E84-10136] p 70 N84-26084

BANGLADESH

Measurement of boro rice acreage in Nabinagar Thana by remote sensing technique p 1 A84-30227

SPOT simulations in Bangladesh flight operations and main results p 2 A84-30253

BARREN LAND

CONSERVB: A numerical method to compute soil water content and temperature profiles under a bare surface
[E84-10113] p 9 N84-23006

A microwave systems approach to measuring root zone soil moisture
[E84-10114] p 9 N84-23007

BATHYMETERS

Airborne lidar for oceanography and hydrology (FLOH)
[ESA-TT-799] p 37 N84-22955

Coastal bathymetry and currents from LANDSAT data p 47 N84-27303

BAUXITE

Remote sensing for bauxite prospecting p 22 A84-30260

BAYES THEOREM

Water mass classification in the North Atlantic using IR digital data and Bayesian decision theory
[AD-P003125] p 41 N84-26266

BAYS (TOPOGRAPHIC FEATURES)

Bay monsoon activities in relation to the monsoon in the western Pacific p 30 A84-30232

Observations of Gulf Stream-induced and wind-driven upwelling in the Georgia Bight using ocean color and infrared imagery p 34 A84-34517

BEAUFORT SEA (NORTH AMERICA)

Coastal mapping of the Beaufort Sea coast p 31 A84-33360

Method to estimate drag coefficient at the air/ice interface over drifting open pack ice from remotely sensed data p 48 N84-27310

BEDROCK

Euro-African MAGSAT anomaly-tectonic observations p 27 N84-25129

Reduced to pole long-wavelength magnetic anomalies of Africa and Europe p 27 N84-25132

Relation of MAGSAT anomalies to the main tectonic provinces of South America p 28 N84-25137

BERING SEA

Satellite observations of circulation in the eastern Bering Sea p 33 A84-34514

Radar altimetry over sea ice p 48 N84-27309

BIBLIOGRAPHIES

Scientific activity in oceanography, 1979-1982 p 38 N84-23084

Publications of the Jet Propulsion Laboratory 1982
[NASA-CR-173539] p 71 N84-25510

Technical publications of the NASA Wallops Flight Facility, 1980 through 1983
[NASA-TM-84421] p 72 N84-26467

BRIGHTNESS TEMPERATURE

BIOLUMINESCENCE

Remote sensing marine bioluminescence - The role of the in-water scalar irradiance p 34 A84-36107

BIOASSAY

The use of Landsat imagery in analyzing the vegetation and energy resources of Pickens County, South Carolina p 3 A84-33330

BIONICS

Distinguishing linear contour elements on satellite photos on the basis of a visual perception model p 24 A84-34789

BRIGHT

Identification of brown plant hopper and bacterial leaf blight affected rice crop on Landsat false colour composites p 1 A84-30237

BOLIVIA

Radar-visible wind streaks in the Altiplano of Bolivia p 25 N84-23527

BOUNDARY LAYERS

Remote sensing of air-sea interactions p 42 N84-27267

BOUNDARY VALUE PROBLEMS

Theory of radio wave propagation over the sea surface p 35 A84-37095

BRAGG CURVE

On the detection of underwater bottom topography by imaging radars p 46 N84-27301

BRAZIL

Utilization of digital LANDSAT imagery for the study of granitoid bodies in Rondonia: Case example of the Pedra Branca massif
[E84-10120] p 26 N84-23979

Evaluation of the effects of the seasonal variation of solar elevation angle and azimuth on the processes of digital filtering and thematic classification of relief units
[E84-10121] p 60 N84-23980

Irrigated rice area estimation using remote sensing techniques: Project's proposal and preliminary results --- Rio Grande do Sul, Brazil

[E84-10131] p 10 N84-26081

Sampling system for wheat (*Triticum aestivum* L) area estimation using digital LANDSAT MSS data and aerial photographs --- Brazil

[E84-10139] p 10 N84-26087

Evaluation of solar angle variation over digital processing of LANDSAT imagery --- Brazil

[E84-10140] p 61 N84-26088

Application of LANDSAT data to the study of urban development in Brasilia

[E84-10142] p 16 N84-26090

Forest inventory using multistage sampling with probability proportional to size --- Brazil

[E84-10144] p 11 N84-26092

Field data observed during the geological excursion in the west-central region of the Sui-RioGrande Shield

[E84-10146] p 29 N84-26094

The use of an image registration technique in the urban growth monitoring

[E84-10147] p 16 N84-26095

Evaluation of SIR-A (Shuttle Imaging Radar) images from the Tres Marias region (Minas Gerais State, Brazil) using derived spatial features and registration with MSS-LANDSAT images

[E84-10148] p 62 N84-26096

Results of field observations of radio waves in alluvial deposits in Cara state from 1:100,000: Fortaleza, Canirde, Taperuaba, Santa Quiteria, Sobral, and Sao Luiz do Curu

[INPE-3061-NTE/216] p 53 N84-26100

Methodological approach in lithological discrimination by digital processing: A case study in the Serra do Ramalho, state of Bahia

[INPE-3108-PRE/507] p 29 N84-26101

Diagnostics of rainfall anomalies in the Nordeste during the global weather experiment

[SAPR-1] p 40 N84-26235

The use of photointerpretation for socio-economic characterization of urban population

[INPE-3067-PRE/484] p 16 N84-26428

Identification and estimation of the area planted with irrigated rice based on the visual interpretation of LANDSAT MSS data

[E84-10164] p 12 N84-27256

A sampling system for estimating the cultivation of wheat (*Triticum aestivum* L) from LANDSAT data

[E84-10165] p 12 N84-27257

BRIGHTNESS TEMPERATURE

A microwave systems approach to measuring root zone soil moisture

[E84-10114] p 9 N84-23007

Use of remote sensing for land use policy formulation

[E84-10117] p 9 N84-23977

Satellite observations of a monsoon depression

[NASA-CR-173590] p 40 N84-26232

BUNDLES

Crop moisture estimation over the southern Great Plains with dual polarization 1.66 centimeter passive microwave data from Nimbus 7
[E84-10163] p 12 N84-27255
Matrix partitioning and EOF/principal component analysis of Antarctic Sea ice brightness temperatures [NASA-TM-83916] p 49 N84-27319

BUNDLES

Several aspects of the sequential processing of photogrammetric bundle blocks p 21 N84-26077

BOUYOS

A model for the analysis of drifter data with an application to a warm core ring in the Gulf of Mexico
p 33 A84-34503

The variability of the surface wind field in the equatorial Pacific Ocean: Criteria for satellite measurements p 46 N84-27296

C

CADASTRAL MAPPING

A Doppler positioning cost model --- for cadastral geodetic surveys p 18 A84-33365
Development of satellite Doppler/inertial survey systems for BLM cadastral survey-related applications in Alaska p 14 A84-33370
The Green Cadastre - An experiment for exploring the tree vegetation in the Paris area p 7 A84-36516

CALIBRATING

In-flight absolute radiometric calibration of the Thematic Mapper p 56 A84-33531
User guide for the USGS aerial camera report of calibration p 65 A84-34958
Spectroradiometric calibration of the Thematic Mapper and multispectral scanner system [E84-10098] p 67 N84-23000
Sensor radiance for a midlatitude atmospheric model p 68 N84-23001
In-flight absolute radiometric calibration of the Thematic Mapper --- White Sands, New Mexico p 68 N84-23002

Spectroradiometric calibration of the Thematic Mapper and Multispectral Scanner system --- White Sands, New Mexico [E84-10136] p 70 N84-26084

Heat Capacity Mapping Radiometer (HCMR) data processing algorithm, calibration, and flight performance evaluation [E84-10153] p 71 N84-27248

CAMERAS

User guide for the USGS aerial camera report of calibration p 65 A84-34958
Enviropod handbook: A guide to preparation and use of the Environmental Protection Agency's light-weight aerial camera system --- Weber River, Utah [E84-10123] p 68 N84-23982

CANOPIES (VEGETATION)

Calculations of radar backscattering coefficient of vegetation-covered soils p 2 A84-30671
Soil spectral effects on 4-space vegetation discrimination p 2 A84-30673
Determining forest canopy characteristics using airborne laser data p 7 A84-37202

Inversion of vegetation canopy reflectance models for estimating agronomic variables. III - Estimation using only canopy reflectance data as illustrated by the suits model. IV - Total inversion of the SAIL model --- Scattering by Arbitrarily Inclined Leaves p 7 A84-37203

Evaluation of spatial, radiometric and spectral Thematic Mapper performance for coastal studies [E84-10118] p 9 N84-23978

Evaluation of spatial, radiometric and spectral Thematic Mapper performance for coastal studies [E84-10159] p 12 N84-27251

CARBON DIOXIDE LASERS

Computer-automated CO₂-laser long-path absorption system for air quality monitoring in the working environment p 13 A84-30307

CARIBBEAN REGION

Correlation of tectonic provinces of South America and the Caribbean region with MAGSAT anomalies p 27 N84-25130

CARIBBEAN SEA

Application of Magsat lithospheric modeling in South America. Part 1: Processing and interpretation of magnetic and gravity anomaly data [E84-10115] p 24 N84-23008

CATALOGS (PUBLICATIONS)

Publications and reports of the Institute of Oceanographic Sciences 1979-1982 [IOS-170] p 50 N84-28354

CELESTIAL GEODESY

Geometrical aspects of differential GPS positioning p 17 A84-32494

SUBJECT INDEX

Present limitations of accurate satellite Doppler positioning for tectonics - An example: Djibouti p 17 A84-32495

A Kalman filter approach to precision GPS geodesy p 17 A84-33024
The GRAVSAT signal over tectonic features p 19 A84-36919

CHANGE DETECTION

Use of remote sensing for land use policy formulation [E84-10117] p 9 N84-23977

Application of LANDSAT data to the study of urban development in Brasilia [E84-10142] p 16 N84-26090

CHARGE COUPLED DEVICES

Design and development of CCD pushbroom camera for earth resources survey p 66 A84-38311

CHESAPEAKE BAY (US)

Evaluation of spatial, radiometric and spectral Thematic Mapper performance for coastal studies [E84-10118] p 9 N84-23978

Evaluation of spatial, radiometric and spectral Thematic Mapper performance for coastal studies [E84-10159] p 12 N84-27251

CHINA

The compilation of the satellite image map of land-use of China (1:2,000,000 scale) p 13 A84-30243

The application of Landsat image in the surveying of water resources of Dongting Lake p 51 A84-30255

CHLOROPHYLLS

Sensitivity of airborne fluorosensor measurements to linear vertical gradients in chlorophyll concentration p 30 A84-30302

Development of Great Lakes algorithms for the Nimbus-G coastal zone color scanner [NASA-CR-173511] p 53 N84-27258

CITIES

Application of LANDSAT data to the study of urban development in Brasilia [E84-10142] p 16 N84-26090

CLASSIFICATIONS

Atmospheric effect on classification of finite fields --- satellite-imaged agricultural areas p 2 A84-30670

Automated classification of wetlands p 4 A84-33337

Improving crop classification through attention to the timing of airborne radar acquisitions p 8 A84-39000

Aerial photography for ecological site mapping p 9 N84-23990

Principal components technique analysis for vegetation and land use discrimination --- Brazilian cerrados [E84-10135] p 10 N84-26083

Evaluation of entropy and JM-distance criterions as features selection methods using spectral and spatial features derived from LANDSAT images [E84-10141] p 62 N84-26089

CLIMATOLOGY

Satellite climatology --- Russian book p 13 A84-31024

The World Climate Research Programme p 36 A84-38702

Climate research from space p 66 A84-38922

Hydrology of the North Slope, Alaska p 53 N84-23973

Applications of laser for climatology and atmospheric research [BLEV-R-65.169-5] p 70 N84-26237

CLOUD COVER

A bispectral method for the height determination of optically thin ice clouds p 60 A84-39044

CLOUD HEIGHT INDICATORS

A bispectral method for the height determination of optically thin ice clouds p 60 A84-39044

CLOUDS

Altimeter height measurement errors introduced by the presence of variable cloud and rain attenuation p 45 N84-27289

CLUMPS

A constrained-clustering approach to the analysis of remote sensing data [AD-A139124] p 10 N84-23993

CLUSTER ANALYSIS

Two-stage cluster analysis of a Landsat image p 58 A84-38302

COASTAL CURRENTS

Seasonal variability in meanders of the California Current System off Vancouver Island p 33 A84-34507

Coastal bathymetry and currents from LANDSAT data p 47 N84-27303

Variations in surface current off the coasts of Canada as inferred from infrared satellite imagery p 47 N84-27305

COASTAL ECOLOGY

Evaluation of spatial, radiometric and spectral Thematic Mapper performance for coastal studies [E84-10118] p 9 N84-23978

Evaluation of spatial, radiometric and spectral Thematic Mapper performance for coastal studies [E84-10159] p 12 N84-27251

COASTAL PLAINS

Sediment volume modelling in the coastal area of Bangladesh using turbidity/sediment concentration map based on Landsat data p 51 N84-30257

COASTAL WATER

The analysis and digital signal processing of NOAA's surface current mapping system p 30 A84-30024

Turbidity/sediment concentration mapping in the coastal area of Bangladesh p 50 A84-30246

Atmospheric correction of Landsat MSS data for a multidate suspended sediment algorithm p 59 A84-38942

CZCS data analysis in turbid coastal water p 37 A84-39427

Coastal bathymetry and currents from LANDSAT data p 47 N84-27303

COASTAL ZONE COLOR SCANNER

CZCS data analysis in turbid coastal water p 37 A84-39427

Principal components as a method for atmospherically correcting coastal zone color scanner data [AD-P003124] p 41 N84-26265

Development of Great Lakes algorithms for the Nimbus-G coastal zone color scanner [NASA-CR-173511] p 53 N84-27258

COASTS

Establishing hydrographic control using Doppler --- shore control stations for geodetic surveys p 18 A84-33358

Coastal mapping of the Beaufort Sea coast p 31 A84-33360

COHERENT RADAR

Ocean waves and turbulence as observed with an adaptive coherent multifrequency radar p 44 N84-27279

COLOR CODING

LANDSAT 4 investigations of Thematic Mapper and multispectral scanner applications --- Death Valley, California; Silver Bell Copper Mine, Arizona, and Dulles Airport near Washington, D.C. [E84-10100] p 60 N84-23003

COLOR INFRARED PHOTOGRAPHY

Sampling system for wheat (*Triticum aestivum* L) area estimation using digital LANDSAT MSS data and aerial photographs --- Brazil [E84-10139] p 10 N84-26087

Forest inventory using multistage sampling with probability proportional to size --- Brazil [E84-10144] p 11 N84-26092

COLOR PHOTOGRAPHY

Making false color photomap and its application in thematic mapping by using IR photos p 54 A84-30249

Performance study of multicolor visual sensor system p 66 A84-38312

COMPUTER AIDED MAPPING

Sediment volume modelling in the coastal area of Bangladesh using turbidity/sediment concentration map based on Landsat data p 51 A84-30257

Interactive procedures for distinguishing and reconstructing contour networks --- in aerospace computer aided photomapping p 58 A84-34786

Development of Great Lakes algorithms for the Nimbus-G coastal zone color scanner [NASA-CR-173511] p 53 N84-27258

COMPUTER COMPATIBLE TAPES

Cartographic accuracy of Landsat-4 MSS and TM image data p 57 A84-33535

COMPUTER GRAPHICS

Terrain analysis database generation through computer-assisted photo interpretation p 55 A84-33334

Photogrammetric research

[TRITA-FMI-47] p 69 N84-25146

COMPUTER PROGRAMS

Two-stage cluster analysis of a Landsat image p 58 A84-38302

A computer program for mapping regions in a geographic data base with raster structure [FOA-C-20529-D8] p 16 N84-25340

An integrated software system for geometric correction of LANDSAT MSS imagery [E84-10143] p 62 N84-26091

The use of an image registration technique in the urban growth monitoring p 16 N84-26095

Development of Great Lakes algorithms for the Nimbus-G coastal zone color scanner [NASA-CR-173511] p 53 N84-27258

COMPUTER SYSTEMS PROGRAMS

Integration of LANDSAT land cover data into the Saginaw River basin geographic information system for hydrologic modeling [AD-A140185] p 53 N84-26106

SUBJECT INDEX

COMPUTER TECHNIQUES

A semi-automated procedure for identifying Landsat MSS subregion coordinates p 58 A84-34959
Photogrammetric research at the Royal Institute of Technology, Stockholm, Sweden p 69 N84-25147
Application of computer image processing to underwater surveys [AD-P003122] p 41 N84-26263

COMPUTER VISION

Experiments to correct a digital map data base using scene analysis [AD-A139447] p 61 N84-24499

COMPUTERIZED SIMULATION

Microwave scatterometer p 66 A84-38310
Application of remote sensing to state and regional problems [E84-10128] p 68 N84-23986

CONFERENCES

Asian Conference on Remote Sensing, 3rd, Dacca, Bangladesh, December 4-7, 1982, Proceedings p 64 A84-30226

American Society of Photogrammetry, Annual Meeting, 49th, Washington, DC, March 13-18, 1983, Technical Papers p 65 A84-33326

American Congress on Surveying and Mapping, Annual Meeting, 43rd, Washington, DC, March 13-18, 1983, Technical Papers p 18 A84-33357

US Geological Survey Polar Research Symposium. Abstracts with program [USGS-CIRC-911] p 25 N84-23934

Proceedings of a workshop: Multidisciplinary Use of the Very Long Baseline Array [NASA-CR-173541] p 69 N84-25034

Proceedings of the Fourth Meeting of the LANDSAT Technical Working Group (LTWG), volume 1 [LIB-PRO-0012-VOL-1] p 69 N84-25144

PAME Proceedings, Pattern Analysis in the Marine Environment, An Ocean Science and Technology Workshop [AD-A140195] p 41 N84-26257

CONIFERS

The Green Cadastre - An experiment for exploring the tree vegetation in the Paris area p 7 A84-36516

CONTOURS

Contour-to-grid transformation: Development of a method for generation of a sparse grid structure out of terrain elevation contours [FOA-C-30349-E1] p 16 N84-25156

CONVECTION CLOUDS

Aircraft measurements of convective draft cores in MONEX p 31 A84-31821
Downdrafts from tropical oceanic cumuli p 32 A84-33985

CONVOLUTION INTEGRALS

Improved resolution rain measurements from spaceborne radar altimeters p 46 N84-27290

COORDINATES

A semi-automated procedure for identifying Landsat MSS subregion coordinates p 58 A84-34959

CORRELATION

Correlations between the nonthermal emission of quasarlike nuclei and their Balmer-line widths p 58 A84-33629

COST ANALYSIS

A Doppler positioning cost model --- for cadastral geodetic surveys p 18 A84-33365

COVARIANCE

Detection of errors in the functional adjustment model p 20 N84-26074

CRATERS

Radar-visible wind streaks in the Altiplano of Bolivia p 25 N84-23527

CRATONS

Relation of MAGSAT anomalies to the main tectonic provinces of South America p 28 N84-25137

CRITERIA

Evaluation of entropy and JM-distance criterions as features selection methods using spectral and spatial features derived from LANDSAT images [E84-10141] p 62 N84-26089

CROP CALENDARS

Evaluation of corn/soybeans separability using Thematic Mapper and Thematic Mapper Simulator data p 5 A84-33539

CROP GROWTH

Use of transformed LANDSAT data in regression estimation of crop acreages p 11 N84-27246

Research and applications of data from environmental satellites: Determining parameters and developing interpretation techniques for applications of environmental satellite data [INPE-3005-NTE/213] p 13 N84-27261

CROP IDENTIFICATION

SPOT simulations in Bangladesh flight operations and main results p 2 A84-30253

Soil spectral effects on 4-space vegetation discrimination p 2 A84-30673

Active microwave responses - An aid in improved crop classification p 3 A84-31498

Analysis of Landsat for monitoring vegetables in New York mucklands p 5 A84-33345

Automated vegetation classification using Thematic Mapper Simulation data p 5 A84-33347

Benchmark data on the separability between orchards and vineyards in the southern San Joaquin Valley of California p 5 A84-33348

A physically-based transformation of Thematic Mapper data The TM tasseled cap p 56 A84-33532

Spectral variability of Landsat-4 Thematic Mapper and Multispectral Scanner data for selected crop and forest cover types p 5 A84-33538

Evaluation of corn/soybeans separability using Thematic Mapper and Thematic Mapper Simulator data p 5 A84-33539

The effect of fluctuations in the optical properties of the atmosphere on spectral brightness ratios in the remote sensing of agricultural areas p 6 A84-34777

Interpreting multispectral photographs obtained in the Telefoto-80 experiment so as to distinguish crop types p 6 A84-34780

Landsat MSS data used for crop identification at the limit of its spatial resolution p 8 A84-38299

Improving crop classification through attention to the timing of airborne radar acquisitions p 8 A84-39000

LANDSAT-4 image data quality analysis [E84-10134] p 10 N84-26082

Area estimation using multiyear designs and partial crop identification [E84-10151] p 11 N84-26099

Identification and estimation of the area planted with irrigated rice based on the visual interpretation of LANDSAT MSS data [E84-10164] p 12 N84-27256

A sampling system for estimating the cultivation of wheat (*Triticum aestivum* L) from LANDSAT data [E84-10165] p 12 N84-27257

CROP INVENTORIES

Measurement of boro rice acreage in Nabinnagar Thana by remote sensing technique p 1 A84-30227

Measurement of boro rice acreage in Srimangal Thana by remote sensing technique p 1 A84-30235

An inquiry into methods of estimating yields of wheat and autumn crops in the plain region with Landsat images visual interpretation p 2 A84-30239

A regression analysis of data from aircraft and ground measurements of a vegetative cover p 6 A84-34784

Irrigated crop inventory by classification of satellite image data p 8 A84-38999

Irrigated rice area estimation using remote sensing techniques: Project's proposal and preliminary results --- Rio Grande do Sul, Brazil [E84-10131] p 10 N84-26081

Sampling system for wheat (*Triticum aestivum* L) area estimation using digital LANDSAT MSS data and aerial photographs --- Brazil [E84-10139] p 10 N84-26087

Area estimation using multiyear designs and partial crop identification [E84-10151] p 11 N84-26099

CROP VIGOR

Use of remote sensing for land use policy formulation [E84-10117] p 9 N84-23977

CRUSTAL FRACTURES

The use of satellite photos for analyzing the structural and dynamic conditions surrounding the formation of ancient deposits of phlogopite and apatite p 23 A84-34781

High precision measurements in crustal dynamic studies [NASA-CR-173680] p 22 N84-28279

CUMULUS CLOUDS

Downdrafts from tropical oceanic cumuli p 32 A84-33985

Satellite observations of a monsoon depression [NASA-CR-173590] p 40 N84-26232

CYCLOCLES

The effect of ocean surface temperature on the trajectories of tropical cyclones p 34 A84-35252

Satellite observed upper level moisture patterns associated with tropical cyclone movement p 37 A84-39523

A SEASAT SASS simulation experiment to quantify the errors related to a + or - 3 hour intermittent assimilation technique [E84-10129] p 68 N84-23987

DATA PROCESSING

D

DATA ACQUISITION

Status report - Gravity activities within the National Geodetic Survey (NGS) p 18 A84-33373

Orbital imagery: A cartographic solution [INPE-2820-PRE/374] p 20 N84-25143

Preserve the sense of Earth from space [DE84-900854] p 71 A84-25159

Publications of the Jet Propulsion Laboratory 1982 [NASA-CR-173539] p 71 N84-25510

Earthnet: The story of images [ESA-BR-18] p 62 N84-26102

DATA BASES

Terrain analysis database generation through computer-assisted photo interpretation p 55 A84-33334

Spatial inventory integrating raster databases and point sample data --- Geographic Information System for timber inventory p 4 A84-33340

A regional raster data study at the Experimental Cartography Unit - The application of interactive raster graphics to environmental modelling p 14 A84-33363

Survey of automated statewide natural resource information systems [AD-A139017] p 16 N84-23996

Experiments to correct a digital map data base using scene analysis [AD-A139447] p 61 N84-24499

Vegetation, land-use and seasonal albedo data sets: Documentation of archived data tape [E84-10133] p 10 N84-25142

Photogrammetric research at the Royal Institute of Technology, Stockholm, Sweden p 69 N84-25147

A computer program for mapping regions in a geographic data base with raster structure [FOCA-C-20529-D8] p 16 N84-25340

DATA COMPRESSION

Data compression of remotely sensed data from space p 59 A84-38314

DATA CORRELATION

Digital comparison and correlation techniques of remote sensing images having different space resolution p 55 A84-33356

Evaluation of solar angle variation over digital processing of LANDSAT imagery --- Brazil p 61 N84-26088

Field data observed during the geological excursion in the west-central region of the Sul-RioGrande Shield [E84-10146] p 29 N84-26094

Evaluation of SIR-A (Shuttle Imaging Radar) images from the Trez Marias region (Minas Gerais State, Brazil) using derived spatial features and registration with MSS-LANDSAT images [E84-10148] p 62 N84-26096

Satellite-Derived Sea Surface Temperature: Workshop-2 [NASA-CR-173740] p 50 N84-28355

DATA INTEGRATION

A SEASAT SASS simulation experiment to quantify the errors related to a + or - 3 hour intermittent assimilation technique [E84-10129] p 68 N84-23987

Comparative study of image data produced by satellites with different characteristics [ESA-CR(P)-1867] p 62 N84-26103

DATA MANAGEMENT

Integrated Global Ocean Services System (IGOSS): Guide to the IGOSS data processing and services system [WMO-623] p 38 N84-23089

DATA PROCESSING

Digital processing considerations for extraction of ocean wave image spectra from raw synthetic aperture radar data p 30 A84-30025

The statewide forest/nonforest classification of Pennsylvania using Landsat MSS data p 3 A84-33329

Preliminary digital classification of grazing resources in the Southern Chihuahuan Arid Zone of Mexico p 5 A84-33349

Integrated Global Ocean Services System (IGOSS): Guide to the IGOSS data processing and services system [WMO-623] p 38 N84-23089

Application of MAGSAT to lithospheric modeling in South America. Part 2: Synthesis of geologic and seismic data for development of integrated crustal models [E84-10126] p 26 N84-25128

Proceedings of the Fourth Meeting of the LANDSAT Technical Working Group (LTWG), volume 1 [LIB-PRO-0012-VOL-1] p 69 N84-25144

Understanding and utilization of Thematic Mapper and other remotely sensed data for vegetation monitoring [E84-10150] p 11 N84-26098

Earthnet: The story of images [ESA-BR-18] p 62 N84-26102

DATA PROCESSING EQUIPMENT

Contextual classification of remotely sensed data p 63 N84-27245
 Heat Capacity Mapping Radiometer (HCMR) data processing algorithm, calibration, and flight performance evaluation
 [E84-10153] p 71 N84-27248

Research and applications of data from environmental satellites: Determining parameters and developing interpretation techniques for applications of environmental satellite data
 [INPE-3005-NTE/213] p 13 N84-27261

DATA PROCESSING EQUIPMENT

Application of the Vizir Image Processing System to the remote sensing studies in Bangladesh p 64 A84-30266

Thematic Mapper - The ESA-Earthnet ground segment and processing experience p 57 A84-33542

DATA REDUCTION

Reduction of satellite magnetic anomaly data p 19 A84-38812
 LANDSAT 4 investigations of Thematic Mapper and multispectral scanner applications --- Death Valley, California; Silver Bell Copper Mine, Arizona, and Dulles Airport near Washington, D.C.
 [E84-10100] p 60 N84-23003

DATA RETRIEVAL

Earthnet: The story of images p 62 N84-26102

DATA SAMPLING

Forest inventory using multistage sampling with probability proportional to size --- Brazil
 [E84-10144] p 11 N84-26092
 Area estimation using multiyear designs and partial crop identification
 [E84-10155] p 11 N84-26099

DATA SIMULATION

SPOT simulations in Bangladesh flight operations and main results p 2 A84-30253

Evaluation of corn/soybeans separability using Thematic Mapper and Thematic Mapper Simulator data p 5 A84-33539

A SEASAT SASS simulation experiment to quantify the errors related to a + or - 3 hour intermittent assimilation technique
 [E84-10129] p 68 N84-23987

DATA STORAGE

Earthnet: The story of images p 62 N84-26102

DATA SYSTEMS

A remote sensing data processing system based on a micro-computer p 64 A84-30265

DATA TRANSMISSION

Study on spectral/radiometric characteristics of the Thematic Mapper for land use applications
 [E84-10130] p 61 N84-25140

Earthnet: The story of images p 62 N84-26102

DECIDUOUS TREES

The Green Cadastre - An experiment for exploring the tree vegetation in the Paris area p 7 A84-36516

DEEP SPACE NETWORK

Digital SAR processing using a fast polynomial transform p 55 A84-32093

Publications of the Jet Propulsion Laboratory 1982
 [NASA-CR-173539] p 71 N84-25510

DEFENSE PROGRAM

The geodetic activities of the Department of Defense under IGY programs p 17 A84-30727

DEFOLIATION

The Pennsylvania defoliation application pilot test
 [E84-10111] p 8 N84-23004

DEFORESTATION

Intensive forest clearing in Rondonia, Brazil, as detected by satellite remote sensing p 8 A84-37204

DEGRADATION

Assessing change in the surficial character of a semiarid environment with Landsat residual images p 3 A84-31499

DENSITY MEASUREMENT

Equidensitometry and remote sensing imagery p 59 A84-38944

DEPTH MEASUREMENT

Estimation of depth of snow from Landsat imagery p 52 A84-33555

Airborne lidar for oceanography and hydrology (FLOH)
 [ESA-TT-799] p 37 N84-22955

Ocean optical remote sensing capability statement
 [AD-A10589] p 49 N84-27321

DESERTIFICATION

Study of desertification/aridity through remote sensing p 1 A84-30238

Identifying environmental features for land management decisions
 [E84-10125] p 15 N84-23984

DESERTS

Spaceborne radar subsurface imaging in hyperarid regions p 24 A84-39379
 Pinacate-Gran Desierto Region, Mexico: SIR-A data analysis p 25 N84-23526

DESIGN ANALYSIS

Design and development of CCD pushbroom camera for earth resources survey p 66 A84-38311

DIGITAL DATA

The use of digital elevation model topographic data for soil erosion modeling within a geographic information system p 4 A84-33342

Preliminary digital classification of grazing resources in the Southern Chihuahuan Arid Zone of Mexico p 5 A84-33349

Registration of TM data to digital elevation models p 60 N84-22999

LANDSAT 4 investigations of Thematic Mapper and multispectral scanner applications --- Death Valley, California; Silver Bell Copper Mine, Arizona, and Dulles Airport near Washington, D.C.
 [E84-10100] p 60 N84-23003

Experiments to correct a digital map data base using scene analysis p 61 N84-24499

Analysis of the quality of image data acquired by the LANDSAT-4 Thematic Mapper and Multispectral Scanners p 61 N84-24499

[E84-10137] p 61 N84-26085

Multiseasonal variables in digital image enhancements for geological applications p 29 N84-26093

Integration of LANDSAT land cover data into the Saginaw River basin geographic information system for hydrologic modeling p 53 N84-26106

Contextual classification of remotely sensed data p 63 N84-27245

DIGITAL FILTERS

Simple enhancement techniques in digital image processing p 58 A84-33798

DIGITAL RADAR SYSTEMS

Performance evaluation and a dedicated system for SAR image data processing p 58 A84-38300

DIGITAL SYSTEMS

Application of the Vizir Image Processing System to the remote sensing studies in Bangladesh p 64 A84-30266

Photogrammetric research p 69 N84-25146

[TRITA-FMI-47] p 61 N84-25148

Mathematical aspects of digital terrain information. A progress report from ISPRS Working Group III:3 p 69 N84-25153

DIGITAL TECHNIQUES

Digital processing of remote sensing data on Hail Haor, Bangladesh for landuse analysis and development potentiality assessment p 13 A84-30240

Digital comparison and correlation techniques of remote sensing images having different space resolution p 55 A84-33356

RABIVE - A real time program system for radiometric image processing p 58 A84-37773

Joint analysis of Landsat-MSS and NOAA-AVHRR data for marine environmental monitoring p 35 A84-38298

A simulation program for the integration of aerospace remote sensing systems with a digital terrain model p 59 A84-38316

Irrigated rice area estimation using remote sensing techniques: Project's proposal and preliminary results --- Rio Grande do Sul, Brazil
 [E84-10131] p 10 N84-26081

Digital processing of LANDSAT data for the preparation of a land use map of the rural district surrounding Tuebingen to a scale of 1:50000 p 16 N84-26104

[ESA-TT-816] p 11 N84-26107

Interactive digital image processing for terrain data extraction, phase 4 p 71 N84-23985

DIRECTORIES

State remote sensing (LANDSAT) programs catalog p 71 N84-23985

DISASTERS

EPA Enviropod. A summary of the use of the Enviropod under a Memorandum of Understanding among EPA Region 8, the State of Utah, and the University of Utah Research Institute p 15 N84-23983

[E84-10124] p 15 N84-23983

DISPLACEMENT MEASUREMENT

A rapid method for obtaining frequency-response functions for multiple input photogrammetric data p 65 A84-31741

DIURNAL VARIATIONS

Comparison of longwave diurnal models applied to simulations of the Earth Radiation Budget Experiment p 65 A84-31947

DOMINICAN REPUBLIC

Cenozoic tectonics of the Caribbean: Structural and stratigraphic studies in Jamaica and Hispaniola p 25 N84-23062

DOPPLER EFFECT

Present limitations of accurate satellite Doppler positioning for tectonics - An example: Djibouti p 17 A84-32495

DOPPLER NAVIGATION

A Doppler positioning cost model --- for cadastral geodetic surveys p 18 A84-33365
 Development of satellite Doppler/inertial survey systems for BLM cadastral survey-related applications in Alaska p 14 A84-33370

DRAINAGE PATTERNS

Drainage pattern delineation - A function of image scale p 52 A84-3353

DRIFT RATE

A model for the analysis of drifter data with an application to a warm core ring in the Gulf of Mexico p 33 A84-34503

DROUGHT

Surface albedo and the Sahel drought p 7 A84-36710

A report of Ceara Project activities p 54 N84-27260

DYNAMIC MODELS

CONSERVB: A numerical method to compute soil water content and temperature profiles under a bare surface p 9 N84-23006

E

EARTH (PLANET)

Construction of a system of point masses representing the gravitational field of the planet on the basis of satellite observations. I - An algorithm derivation p 19 A84-37069

EARTH ATMOSPHERE

X to W band radiometric signatures of natural surfaces p 35 A84-36289

EARTH CRUST

Typical analysis of regional stability and block structures with remote sensing images p 22 A84-30254

The approximation introduced by representing the earth's gravity field with a finite grid of mascons both at the earth's surface and at the bottom of the earth's crust

[AAS PAPER 83-394] p 17 A84-30583

Use of MAGSAT anomaly data for crustal structure and mineral resources in the US midcontinent p 24 N84-23005

[E84-10112] Application of Magsat lithospheric modeling in South America. Part 1: Processing and interpretation of magnetic and gravity anomaly data p 24 N84-23008

[E84-10115] Discussion of the design of satellite-laser measurement stations in the eastern Mediterranean under the geological aspect. Contribution to the earthquake prediction research by the Wegener Group and to NASA's Crustal Dynamics Project p 26 N84-24031

[NASA-TM-77412] Application of MAGSAT to lithospheric modeling in South America. Part 2: Synthesis of geologic and seismic data for development of integrated crustal models p 26 N84-25128

[E84-10126] Do satellite magnetic anomaly data accurately portray the crustal component? p 28 N84-25134

US aeromagnetic and satellite magnetic anomaly comparisons p 28 N84-25136

A crustal structure study of South America p 29 N84-25139

Petrologic and geophysical sources of long-wavelength crustal magnetic anomalies p 29 N84-28276

EARTH MOVEMENTS

Coseismic and postseismic vertical movements associated with the 1940 M7.1 Imperial Valley, California, earthquake p 24 A84-36922

High precision measurements in crustal dynamic studies p 22 N84-28279

[NASA-CR-173680] Conditions for the illumination of an area in satellite scanner surveys p 65 A84-34787

X to W band radiometric signatures of natural surfaces p 35 A84-36289

High resolution observation of the earth's surface from space - Programs, problems and perspectives p 71 A84-37049

SUBJECT INDEX

Data compression of remotely sensed data from space p 59 N84-38314

Image analysis researches of remotely sensed data at NAL p 59 N84-38315

Climate research from space p 66 N84-38922

Radar backscatter modelling p 25 N84-23525

Pinacate-Gran Desierto Region, Mexico: SIR-A data analysis p 25 N84-23526

NASA Oceanic Processes Program, fiscal year 1983 [NASA-TM-86248] p 39 N84-24078

Preserve the sense of Earth from space [DE84-900854] p 71 N84-25159

The theory of Earth observation using multiple-frequency radar [ESA-TT-819] p 63 N84-26105

Remote sensing of the Santonge littoral. Processing and interpretation of satellite images [ISBN-2-85929-016-8] p 63 N84-28202

EARTH RADIATION BUDGET EXPERIMENT

Comparison of longwave diurnal models applied to simulations of the Earth Radiation Budget Experiment p 65 N84-31947

EARTH RESOURCES

Preliminary digital classification of grazing resources in the Southern Chihuahuan Arid Zone of Mexico p 5 N84-33349

Findings on the use of Landsat-3 return beam vidicon imagery for detecting land use and land cover changes p 14 N84-33361

Status of the TERS project p 71 N84-34575

Performance study of multicolor visual sensor system p 66 N84-38312

Survey of automated statewide natural resource information systems [AD-A139017] p 16 N84-23996

Orbital imagery: A cartographic solution [INPE-2820-PRE/374] p 20 N84-25143

Publications of the Jet Propulsion Laboratory 1982 [NASA-CR-173539] p 71 N84-25510

Project SERGE: Brazil referential field data for the SIR-A experiment [INPE-2973-NTE/210] p 29 N84-27259

Remote sensing of the Santonge littoral. Processing and interpretation of satellite images [ISBN-2-85929-016-8] p 63 N84-28202

EARTH RESOURCES PROGRAM

Design and development of CCD pushbroom camera for earth resources survey p 66 N84-38311

EARTH RESOURCES SHUTTLE IMAGING RADAR

Spaceborne radar subsurface imaging in hyperarid regions p 24 N84-39379

EARTH SURFACE

The approximation introduced by representing the earth's gravity field with a finite grid of mascons both at the earth's surface and at the bottom of the earth's crust [AAS PAPER 83-394] p 17 N84-30583

An airborne radar station for studying the reflection properties of the earth's surface p 64 N84-31072

Surface expression of heavily mantled interstratal Karst bordering Okefenokee Swamp, Georgia p 23 N84-33350

High resolution observation of the earth's surface from space - Programs, problems and perspectives p 71 N84-37049

High-precision atmospheric ozone measurements using wavelengths between 290 and 305 nm p 67 N84-39447

The theory of Earth observation using multiple-frequency radar [ESA-TT-819] p 63 N84-26105

High precision measurements in crustal dynamic studies [NASA-CR-173680] p 22 N84-28279

EARTHQUAKE DAMAGE

Coseismic and postseismic vertical movements associated with the 1940 M7.1 Imperial Valley, California, earthquake p 24 N84-36922

EARTHQUAKES

Discussion of the design of satellite-laser measurement stations in the eastern Mediterranean under the geological aspect. Contribution to the earthquake prediction research by the Wegener Group and to NASA's Crustal Dynamics Project [NASA-TM-77412] p 26 N84-24031

High precision measurements in crustal dynamic studies [NASA-CR-173680] p 22 N84-28279

ECOLOGY

Riparian habitat on the Humboldt River, Deeth to Elko, Nevada [E84-10116] p 53 N84-23976

ECOSYSTEMS

Using Landsat to monitor tropical forest ecosystems p 5 N84-33352

Identifying environmental features for land management decisions [E84-10125] p 15 N84-23984

Aerial photography for ecological site mapping p 9 N84-23990

EDUCATION

NASA, the first 25 years: 1958 - 1983 [NASA-EP-182] p 72 N84-26563

ELECTROMAGNETIC MEASUREMENT

Analysis of airborne electromagnetic systems for mapping thickness of sea ice [AD-A139786] p 39 N84-25235

ELEVATION

Coseismic and postseismic vertical movements associated with the 1940 M7.1 Imperial Valley, California, earthquake p 24 N84-36922

Contour-to-grid transformation: Development of a method for generation of a sparse grid structure out of terrain elevation contours [FOA-C-30349-E1] p 16 N84-25156

ELEVATION ANGLE

Evaluation of the effects of the seasonal variation of solar elevation angle and azimuth on the processes of digital filtering and thematic classification of relief units [E84-10121] p 60 N84-23980

EMISSION

A tentative unified sea model for scattering and emission p 45 N84-27285

END-TO-END DATA SYSTEMS

Tracking ocean wave spectrum from SAR images p 44 N84-27277

ENTROPY (STATISTICS)

Study on spectral/radiometric characteristics of the Thematic Mapper for land use applications [E84-10130] p 61 N84-25140

ENVIRONMENT MODELS

Albedo of a forest modeled as a plane with dense protrusions p 6 N84-34385

Evaluation of spatial, radiometric and spectral Thematic Mapper performance for coastal studies [E84-10118] p 9 N84-23978

Application of remote sensing to state and regional problems [E84-10128] p 68 N84-23986

Evaluation of spatial, radiometric and spectral Thematic Mapper performance for coastal studies [E84-10159] p 12 N84-27251

ENVIRONMENTAL MONITORING

Satellite climatology -- Russian book p 13 N84-31024

Using Landsat to monitor tropical forest ecosystems p 5 N84-33352

Joint analysis of Landsat-MSS and NOAA-AVHRR data for marine environmental monitoring p 35 N84-38298

Space disturbance warning system with the aid of satellites p 15 N84-38301

Enviropod handbook: A guide to preparation and use of the Environmental Protection Agency's light-weight aerial camera system --- Weber River, Utah [E84-10123] p 68 N84-23982

EPA Enviropod. A summary of the use of the Enviropod under a Memorandum of Understanding among EPA Region 8, the State of Utah, and the University of Utah Research Institute p 15 N84-23983

Identifying environmental features for land management decisions [E84-10125] p 15 N84-23984

State remote sensing (LANDSAT) programs catalog [E84-10127] p 71 N84-23985

ENVIRONMENTAL RESEARCH SATELLITES

Potential utility of future satellite magnetic field data [NASA-CR-175230] p 26 N84-24691

ENVIRONMENTAL SURVEYS

A regional raster data study at the Experimental Cartography Unit - The application of interactive raster graphics to environmental modeling p 14 N84-33363

EPIDEMIOLOGY

A regional raster data study at the Experimental Cartography Unit - The application of interactive raster graphics to environmental modeling p 14 N84-33363

EQUIPMENT SPECIFICATIONS

User guide for the USGS aerial camera report of calibration p 65 N84-34958

Enviropod handbook: A guide to preparation and use of the Environmental Protection Agency's light-weight aerial camera system --- Weber River, Utah [E84-10123] p 68 N84-23982

EROS (SATELLITES)

ERS-1 - An ice and ocean monitoring mission p 36 N84-38620

ERROR ANALYSIS

A SEASAT SASS simulation experiment to quantify the errors related to a + or - 3 hour intermittent assimilation technique [E84-10129] p 68 N84-23987

The question of accuracy in the transition from analogue to analytic photogrammetry p 69 N84-25153

Multi-models to increase accuracy p 70 N84-25154

Stochastic models for point manifolds p 20 N84-26072

Estimation of variances and covariances in the multivariate and in the incomplete multivariate model p 20 N84-26073

Detection of errors in the functional adjustment model p 20 N84-26074

Several aspects of the sequential processing of photogrammetric bundle blocks p 21 N84-26077

Altimeter height measurement errors introduced by the presence of variable cloud and rain attenuation p 45 N84-27289

Satellite-Derived Sea Surface Temperature: Workshop-2 [NASA-CR-173740] p 50 N84-28355

ERRORS

Altimeter height measurement errors introduced by the presence of variable cloud and rain attenuation p 45 N84-27289

ERS-1 (ESA SATELLITE)

The radar altimeter for ERS-1 Satellite p 64 N84-30516

The ESA ocean observation satellite ERS-1. I - Description of the history, goals, and payload of ERS-1 p 31 N84-32266

The active microwave instrumentation for ERS-1 p 34 N84-35542

Climate research from space p 66 N84-38922

ESTIMATING

A sampling system for estimating the cultivation of wheat (*Triticum aestivum* L) from LANDSAT data [E84-10165] p 12 N84-27257

EUROPE

Euro-African MAGSAT anomaly-tectonic observations p 27 N84-25129

Reduced to pole long-wavelength magnetic anomalies of Africa and Europe p 27 N84-25132

Satellite magnetic anomalies of Africa and Europe p 27 N84-25133

Long-wavelength magnetic and gravity anomaly correlations of Africa and Europe p 28 N84-25135

EUROPEAN SPACE AGENCY

Thematic Mapper - The ESA-Earthnet ground segment and processing experience p 57 N84-33542

ESA activities in the use of microwaves for the remote sensing of the Earth p 42 N84-27264

EUROPEAN SPACE PROGRAMS

The ESA ocean observation satellite ERS-1. I - Description of the history, goals, and payload of ERS-1 p 31 N84-32266

Earthnet: The story of images [ESA-BR-18] p 62 N84-26102

EVAPORATION

The effect of groundwater inflow on evaporation from a saline lake p 52 N84-34378

EXPERIMENT DESIGN

Living and working in space. A history of Skylab [NASA-SP-4208] p 72 N84-25737

EXPERT SYSTEMS

Experiments to correct a digital map data base using scene analysis [AD-A139447] p 61 N84-24499

EXTINCTION

A comparative study of aerosol extinction measurements made by the SAM II and SAGE satellite experiments p 15 N84-39457

EXTRACTION

Cartographic feature extraction on ETL's (Engineer Topographic Laboratories') DIAL (Digital Image Analysis Laboratory) system [AD-A140230] p 63 N84-26112

F

FARM CROPS

Atmospheric effect on classification of finite fields --- satellite-imaged agricultural areas p 2 N84-30670

Analysis of Landsat for monitoring vegetables in New York mucklands p 5 N84-33345

Automated vegetation classification using Thematic Mapper Simulation data p 5 N84-33347

Inversion of vegetation canopy reflectance models for estimating agronomic variables. III - Estimation using only canopy reflectance data as illustrated by the suits model. IV - Total inversion of the SAIL model --- Scattering by Arbitrarily Inclined Leaves p 7 N84-37203

Irrigated crop inventory by classification of satellite image data p 8 N84-38999

Improving crop classification through attention to the timing of airborne radar acquisitions p 8 N84-39000

FAST FOURIER TRANSFORMATIONS

Digital SAR processing using a fast polynomial transform p 55 A84-32093

FIELD STRENGTH

Petrologic and geophysical sources of long-wavelength crustal magnetic anomalies [NASA-CR-175245] p 29 N84-28276

FILE MAINTENANCE (COMPUTERS)

GENTRI: A system for simultaneous adjustment of photogrammetric and other observations p 69 N84-25152

FIRES

Fire detection using the NOAA (National Oceanic and Atmospheric Administration)-series satellites [PB84-176890] p 13 N84-27324

FISHERIES

Maps of favorable areas for tuna fishing to the South and Southeast of Brazil prepared from SMS-2 satellite data [INPE-3102-PRE/501] p 41 N84-26256

The use of satellite observations of the ocean surface in commercial fishing operations [AD-P003120] p 41 N84-26261

FISHES

Maps of favorable areas for tuna fishing to the South and Southeast of Brazil prepared from SMS-2 satellite data [INPE-3102-PRE/501] p 41 N84-26256

FLEXING

Seasat observations of lithospheric flexure seaward of trenches p 32 A84-34339

FLOOD CONTROL

The application of Landsat image in the surveying of water resources of Dongting Lake p 51 A84-30255

Riparian habitat on the Humboldt River, Deeth to Elko, Nevada [E84-10116] p 53 N84-23976

FLOODS

EPA Enviropod. A summary of the use of the Enviropod under a Memorandum of Understanding among EPA Region 8, the State of Utah, and the University of Utah Research Institute [E84-10124] p 15 N84-23983

FLOW GEOMETRY

The evolution of mushroom-shape currents in the ocean p 36 A84-38773

FLOW VELOCITY

Seasonal oscillations of the subtropical convergence between the Brazil and Malvinas currents, using oceanographic and SMS-2 satellite data [INPE-3092-PRE/497] p 40 N84-26255

FLUORESCENCE

Sensitivity of airborne fluorosensor measurements to linear vertical gradients in chlorophyll concentration p 30 A84-30302

FOG

Fog recognition in daylight 3.7-micron-band Tiros-N and NOAA images p 65 A84-34157

FOLDS (GEOLGY)

The use of remote sensing in the search for hydrocarbons in the Kerch peninsula p 23 A84-34782

FORECASTING

Research and applications of data from environmental satellites: Determining parameters and developing interpretation techniques for applications of environmental satellite data [INPE-3005-NTE/213] p 13 N84-27261

The importance of altimeter and scatterometer data for ocean prediction p 49 N84-27316

The influence of actual and apparent geoid error on ocean analysis and prediction p 49 N84-27318

FOREST FIRE DETECTION

Fire detection using the NOAA (National Oceanic and Atmospheric Administration)-series satellites [PB84-176890] p 13 N84-27324

FOREST MANAGEMENT

Landsat image use in forestry management in China p 2 A84-30250

Using Landsat to monitor tropical forest ecosystems p 5 A84-33352

Spectral variability of Landsat-4 Thematic Mapper and Multispectral Scanner data for selected crop and forest cover types p 5 A84-33538

Classifying the coefficients of spectral brightness of the forest zone in the European part of the Soviet Union p 6 A84-34783

The Pennsylvania defoliation application pilot test [E84-10111] p 8 N84-23004

Use of remote sensing for land use policy formulation [E84-10117] p 9 N84-23977

Forest inventory using multistage sampling with probability proportional to size -- Brazil [E84-10144] p 11 N84-26092

FORESTS

Analysing forest structures by remote sensing p 1 A84-30236

Landsat imagery for the interpretation of Louisiana forest habitat regions p 3 A84-33328

The statewide forest/nonforest classification of Pennsylvania using Landsat MSS data p 3 A84-33329

Analysis of photo interpretation test results for seven aerospace image types of the San Juan National Forest, Colorado p 4 A84-33332

Spatial inventory integrating raster databases and point sample data -- Geographic Information System for timber inventory p 4 A84-33340

Albedo of a forest modeled as a plane with dense protrusions p 6 A84-34385

Classifying northern forests using Thematic Mapper Simulator data p 7 A84-34961

Determining forest canopy characteristics using airborne laser data p 7 A84-37202

Intensive forest clearing in Rondonia, Brazil, as detected by satellite remote sensing p 8 A84-37204

Aerial photography for ecological site mapping p 9 N84-23990

Evaluating LANDSAT-4 MSS and TM data [E84-10157] p 63 N84-27249

FREQUENCY RESPONSE

A rapid method for obtaining frequency-response functions for multiple input photogrammetric data [AIAA PAPER 84-1060] p 65 A84-31741

FREQUENCY SCANNING

The dual-frequency scatterometer reexamined p 44 N84-27280

G

GALACTIC NUCLEI

Correlations between the nonthermal emission of quasarlike nuclei and their Balmer-line widths p 58 A84-33629

GAS COMPOSITION

Arctic haze and the Arctic gas and aerosol sampling program (AGASP) p 32 A84-34276

GEOCHEMISTRY

The Dufek intrusion of Antarctica and a survey of its minor metals related to possible resources p 25 N84-23943

GEOCHRONOLOGY

US Geological Survey Polar Research Symposium. Abstracts with program [USGS-CIRC-911] p 25 N84-23934

GEODESY

The geodetic activities of the Department of Defense under IGY programs p 17 A84-30727

A Kalman filter approach to precision GPS geodesy p 17 A84-33024

American Congress on Surveying and Mapping, Annual Meeting, 43rd, Washington, DC, March 13-18, 1983, Technical Papers p 18 A84-33357

Scientific activity in oceanography, 1979-1982 p 38 N84-23084

Stochastic models for point manifolds p 20 N84-26072

Detection of errors in the functional adjustment model p 20 N84-26074

Investigation of the combination of geodetic point aggregations [SER-C-285] p 21 N84-28199

GEODETIC COORDINATES

Investigation of the combination of geodetic point aggregations [SER-C-285] p 21 N84-28199

GEODETIC SATELLITES

The geodetic activities of the Department of Defense under IGY programs p 17 A84-30727

Error analysis for marine geodetic control using the global positioning system [AD-A10566] p 21 N84-26687

Establishing hydrographic control using Doppler -- shore control stations for geodetic surveys p 18 A84-33358

Satellite surveying techniques used within geodetic networks p 18 A84-33364

A Doppler positioning cost model -- for cadastral geodetic surveys p 18 A84-33365

Establishing first-order control by GPS satellite surveying instruments p 18 A84-33368

Status report - Gravity activities within the National Geodetic Survey (NGS) p 18 A84-33373

A forecast of the impact of GPS on surveying p 18 A84-33374

Antarctic mapping and international coordination p 19 N84-23935

Modeling the movement at the polar ice cap at the South Pole p 20 N84-23957

Altimeter height measurement errors introduced by the presence of variable cloud and rain attenuation p 45 N84-27289

Investigation of the combination of geodetic point aggregations [SER-C-285] p 21 N84-28199

GEODYNAMICS

Discussion of the design of satellite-laser measurement stations in the eastern Mediterranean under the geological aspect. Contribution to the earthquake prediction research by the Wegener Group and to NASA's Crustal Dynamics Project [NASA-TM-77412] p 26 N84-24031

High precision measurements in crustal dynamic studies [NASA-CR-173680] p 22 N84-28279

GEOGRAPHIC INFORMATION SYSTEMS

The use of Landsat imagery in analyzing the vegetation and energy resources of Pickens County, South Carolina p 3 A84-33330

Integration of Landsat data into the Saginaw River Basin geographic information system p 51 A84-33339

Spatial inventory integrating raster databases and point sample data -- Geographic Information System for timber inventory p 4 A84-33340

The use of digital elevation model topographic data for soil erosion modeling within a geographic information system p 4 A84-33342

Survey of automated statewide natural resource information systems [AD-A139017] p 16 N84-23996

Contour-to-grid transformation: Development of a method for generation of a sparse grid structure out of terrain elevation contours [FOA-C-30349-E1] p 16 N84-25156

GEOGRAPHY

A computer program for mapping regions in a geographic data base with raster structure [FOA-C-20529-D8] p 16 N84-25340

GEOIDS

Geodetic use of GEOSAT-A [AD-A137993] p 19 N84-23048

The influence of actual and apparent geoid error on ocean analysis and prediction p 49 N84-27318

GEOLOGICAL FAULTS

Oceanic fracture zones p 31 A84-31193

Coseismic and postseismic vertical movements associated with the 1940 M7.1 Imperial Valley, California, earthquake p 24 A84-36922

High precision measurements in crustal dynamic studies [NASA-CR-173680] p 22 N84-28279

GEOLOGICAL SURVEYS

Typical analysis of regional stability and block structures with remote sensing images p 22 A84-30254

Geological interpretation from aerial remote sensing images of Tengchong area p 23 A84-32590

US Geological Survey Polar Research Symposium. Abstracts with program [USGS-CIRC-911] p 25 N84-23934

Surveying in Antarctica during the International Geophysical Year p 25 N84-23942

The Duffek intrusion of Antarctica and a survey of its minor metals related to possible resources p 25 N84-23943

Emerging recognition of the nonfuel mineral resources of Arctic Alaska p 26 N84-23962

Land cover and terrain mapping for the development of digital data bases for wildlife habitat assessment in the Yukon Flats National Wildlife Refuge, Alaska p 9 N84-23971

Potential utility of future satellite magnetic field data [NASA-CR-175230] p 26 N84-24691

Field data observed during the geological excursion in the west-central region of the Sul-Riogrande Shield [E84-10146] p 29 N84-26094

GEOMAGNETIC PULSATIONS

A study of geomagnetic pulsations using the AFGL (Air Force Geophysics Laboratory) magnetometer network [AD-A140507] p 70 N84-26217

GEOMAGNETISM

Use of MAGSAT anomaly data for crustal structure and mineral resources in the US midcontinent [E84-10112] p 24 N84-23005

Potential utility of future satellite magnetic field data [NASA-CR-175230] p 26 N84-24691

Euro-African MAGSAT anomaly-tectonic observations p 27 N84-25129

Reduced to pole long-wavelength magnetic anomalies of Africa and Europe p 27 N84-25132

Satellite magnetic anomalies of Africa and Europe p 27 N84-25133

Relation of MAGSAT anomalies to the main tectonic provinces of South America p 28 N84-25137

Relation of MAGSAT and gravity anomalies to the main tectonic provinces of South America p 28 N84-25138

Petrologic and geophysical sources of long-wavelength crustal magnetic anomalies [NASA-CR-175245] p 29 N84-28276

SUBJECT INDEX

GEOMETRIC ACCURACY

Landsat-4 MSS and Thematic Mapper data quality and information content analysis p 56 A84-33528
An analysis of Landsat-4 Thematic Mapper geometric properties p 57 A84-33536
Study on temporal geometric-distortion variation of Landsat MSS and RBV imageries and attitude determination program p 59 A84-38313
Investigation of several aspects of LANDSAT-4 data quality -- Sacramento, San Francisco, and NE Arkansas [E84-10122] p 60 N84-23981
Proceedings of the Fourth Meeting of the LANDSAT Technical Working Group (LTWG), volume 1 [LIB-PRO-0012-VOL-1] p 69 N84-25144
Analysis of the quality of image data acquired by the LANDSAT-4 Thematic Mapper and Multispectral Scanners [E84-10137] p 61 N84-26085
LANDSAT-D Thematic Mapper image dimensionality reduction and geometric correction accuracy -- Walnut Creek Watershed, Texas [E84-10149] p 62 N84-26097

GEOMETRIC RECTIFICATION (IMAGERY)

Landsat planimetric maps p 54 A84-30264
Cartographic accuracy of Landsat-4 MSS and TM image data p 57 A84-33535
A simulation program for the integration of aerospace remote sensing systems with a digital terrain model p 59 A84-38316
LANDSAT-D investigations in snow hydrology [E84-10094] p 53 N84-22997
Registration of TM data to digital elevation models p 60 N84-22999
Comparative assessment of LANDSAT-D MSS and TM data quality for mapping applications in the Southeast [E84-10138] p 61 N84-26086
An integrated software system for geometric correction of LANDSAT MSS imagery [E84-10143] p 62 N84-26091
LANDSAT-D Thematic Mapper image dimensionality reduction and geometric correction accuracy -- Walnut Creek Watershed, Texas [E84-10149] p 62 N84-26097
Comparative study of image data produced by satellites with different characteristics [ESA-CR(P)-1867] p 62 N84-26103
Evaluating LANDSAT-4 MSS and TM data [E84-10157] p 63 N84-27249
Development of Great Lakes algorithms for the Nimbus-G coastal zone color scanner [NASA-CR-173511] p 53 N84-27258

GEOMORPHOLOGY

An undetectable factor in geomorphological mapping from land satellite images - A case study in the central highland, Thailand p 22 A84-30261
Soil erosion mapping and evaluation - A photo-geomorphological approach p 14 A84-33333
GEOPHYSICS

Surface expression of heavily mantled interstratal Karst bordering Okefenokee Swamp, Georgia p 23 A84-33350
Seasat observations of lithospheric flexure seaward of trenches p 32 A84-34339
Construction of a system of point masses representing the gravitational field of the planet on the basis of satellite observations. I - An algorithm derivation p 19 A84-37069
A summary of results from the first Nimbus 7 SMMR observations p 37 A84-39459
Scientific activity in oceanography, 1979-1982 p 38 N84-23084
Scatterometer capabilities in remotely sensing geophysical parameters over the ocean: The status and the possibilities p 42 N84-27268

GEOPOTENTIAL

Construction of a system of point masses representing the gravitational field of the planet on the basis of satellite observations. I - An algorithm derivation p 19 A84-37069

Potential utility of future satellite magnetic field data [NASA-CR-175230] p 26 N84-24691
Satellite techniques for determining the geopotential for sea-surface elevations p 46 N84-27298
The influence of actual and apparent geoid error on ocean analysis and prediction p 49 N84-27318

GEORGIA

Comparative assessment of LANDSAT-D MSS and TM data quality for mapping applications in the Southeast [E84-10138] p 61 N84-26086

GEOSTROPHIC WIND

Satellite techniques for determining the geopotential for sea-surface elevations p 46 N84-27298

GEOSYNCHRONOUS ORBITS

High resolution observations of low contrast phenomena from an Advanced Geosynchronous Platform (AGP) p 42 N84-27266

GLACIOLOGY

Satellite image atlas of glaciers: The Polar regions p 38 N84-23940
Glaciological and geological studies of Antarctica with satellite remote sensing technology p 38 N84-23956

GLOBAL ATMOSPHERIC RESEARCH PROGRAM

The World Climate Research Programme p 36 A84-38702

SATELLITE OBSERVATIONS OF A MONSOON DEPRESSION

[NASA-CR-173590] p 40 N84-26232

GLOBAL POSITIONING SYSTEM

Geometrical aspects of differential GPS positioning p 17 A84-32494

A Kalman filter approach to precision GPS geodesy p 17 A84-33024

ESTABLISHING FIRST-ORDER CONTROL BY GPS SATELLITE SURVEYING INSTRUMENTS

A forecast of the impact of GPS on surveying p 18 A84-33368

Error analysis for marine geodetic control using the global positioning system p 18 A84-33374

APPLICATIONS OF THE GPS (GLOBAL POSITIONING SYSTEM)

Geodetic Receiver System p 21 N84-26687

[AD-A140566] p 21 N84-26688

GRANITE

Typical analysis of regional stability and block structures with remote sensing images p 22 A84-30254

Metallogenesis - Use of remote sensing for ore deposit prospection: Indicators linked to nonoutcropping leucogranitic apexes p 23 A84-30878

Utilization of digital LANDSAT imagery for the study of granitoid bodies in Rondonia: Case example of the Pedra Branca massif p 26 N84-23979

GRASSLANDS

Preliminary digital classification of grazing resources in the Southern Chihuahuan Arid Zone of Mexico p 5 A84-33349

Evaluation of Thematic Mapper for detecting soil properties under grassland vegetation p 6 A84-33540

Regression in the primal problem of remote sensing (using grass cover as an example) p 6 A84-34785

GRAVIMETRY

Status report - Gravity activities within the National Geodetic Survey (NGS) p 18 A84-33373

GRAVITATIONAL FIELDS

The approximation introduced by representing the earth's gravity field with a finite grid of mascons both at the earth's surface and at the bottom of the earth's crust p 17 A84-30583

Construction of a system of point masses representing the gravitational field of the planet on the basis of satellite observations. I - An algorithm derivation p 19 A84-37069

GRAVITY ANOMALIES

Mapping the sea floor by satellite p 35 A84-36686

The GRAVSAT signal over tectonic features p 19 A84-36919

Application of MagSat lithospheric modeling in South America. Part 1: Processing and interpretation of magnetic and gravity anomaly data p 24 N84-23008

[E84-10115] p 19 N84-23048

Geodetic use of GEOSAT-A p 27 N84-25131

Satellite elevation magnetic and gravity models of major South American plate tectonic features p 28 N84-25135

Relation of MAGSAT and gravity anomalies to the main tectonic provinces of South America p 28 N84-25138

A crustal structure study of South America p 29 N84-25139

GRAVITY WAVES

Non-Gaussian statistical models of surface wave fields for remote sensing applications p 45 N84-27284

GRAVSAT SATELLITE

The GRAVSAT signal over tectonic features p 19 A84-36919

GREAT LAKES (NORTH AMERICA)

Development of Great Lakes algorithms for the Nimbus-G coastal zone color scanner [NASA-CR-173511] p 53 N84-27258

GREAT PLAINS CORRIDOR (NORTH AMERICA)

Crop moisture estimation over the southern Great Plains with dual polarization 1.66 centimeter passive microwave data from Nimbus 7 p 12 N84-27255

GRIDS

Contour-to-grid transformation: Development of a method for generation of a sparse grid structure out of terrain elevation contours [FOA-C-30349-E1] p 16 N84-25156

HISTORIES

GROUND STATIONS

Description of SEP ground station and Vizir image processing VIPS -- for Spot and Landsat 4 satellites p 54 A84-30268

Establishing hydrographic control using Doppler -- shore control stations for geodetic surveys p 18 A84-33358

Thematic Mapper - The ESA-Earthnet ground segment and processing experience p 57 A84-33542

GROUND SUPPORT SYSTEMS

Space disturbance warning system with the aid of satellites p 15 A84-38301

GROUND TRUTH

Analysing forest structures by remote sensing p 1 A84-30236

AVHRR aerosol ground truth experiment [P884-157882] p 39 N84-24065

Forest inventory using multistage sampling with probability proportional to size -- Brazil [E84-10144] p 11 N84-26092

Results of field observations of radio waves in alluvial deposits in Cara state from 1:100,000: Fortaleza, Canirde, Taperuaba, Santa Quiteria, Sobral, and Sao Luiz do Curu [INPE-3061-NTE/216] p 53 N84-26100

Project SERGE: Brazil referential field data for the SIR-A experiment [INPE-2973-NTE/210] p 29 N84-27259

GROUND WATER

The effect of groundwater inflow on evaporation from a saline lake p 52 A84-34378

GROUND WIND

Nimbus 7 SMMR derived seasonal variations in the water vapor, liquid water and surface winds over the global oceans [NASA-TM-86080] p 40 N84-26233

GULF OF MEXICO

Sampling strategies and four-dimensional assimilation of altimetric data for ocean monitoring and prediction p 49 N84-27317

GULF STREAM

Dynamics of the slope water off New England and its influence on the Gulf Stream as inferred from satellite IR data p 31 A84-30672

Rapid evolution of a Gulf Stream warm-core ring p 32 A84-34164

Water mass classification in the North Atlantic using IR digital data and Bayesian decision theory [AD-P003125] p 41 N84-26266

GUSTS

Downdrafts from tropical oceanic cumuli p 32 A84-33985

H

HABITATS

Riparian habitat on the Humboldt River, Deeth to Elko, Nevada [E84-10116] p 53 N84-23976

HAITI

Cenozoic tectonics of the Caribbean: Structural and stratigraphic studies in Jamaica and Hispaniola p 25 N84-23062

HAZE

Understanding and utilization of Thematic Mapper and other remotely sensed data for vegetation monitoring [E84-10150] p 11 N84-26098

HAZE DETECTION

Arctic haze and the Arctic gas and aerosol sampling program (AGASP) p 32 A84-34276

Airborne observations of Arctic aerosol. IV - Optical properties of Arctic haze p 32 A84-34287

HEAT CAPACITY MAPPING MISSION

Heat Capacity Mapping Radiometer (HCMR) data processing algorithm, calibration, and flight performance evaluation [E84-10153] p 71 N84-27248

HEAT FLUX

Observing ocean-atmosphere exchanges with space-borne sensors, appendix C p 50 N84-28298

HELICOPTERS

Marginal ice zone experiment (1983). Part 1: Ice characterization measurements. Part 2: Helicopter-borne and ship-based radar backscatter measurement of sea ice in the marginal ice zone [AD-A139894] p 40 N84-25238

HIGH RESOLUTION

High resolution observation of the earth's surface from space - Programs, problems and perspectives p 71 A84-37049

Improved resolution rain measurements from spaceborne radar altimeters p 46 N84-27290

HISTORIES

Living and working in space. A history of Skylab [NASA-SP-4208] p 72 N84-25737

HYDROCARBONS

NASA, the first 25 years: 1958 - 1983
 [NASA-EP-182] p 72 N84-26563
 Remote sensing for oceanography: Past, present, future p 42 N84-27263

HYDROCARBONS

The use of remote sensing in the search for hydrocarbons in the Kerch peninsula p 23 A84-34782

HYDROCLIMATOLOGY

Application of remote sensing to state and regional problems
 [E84-10128] p 68 N84-23986

HYDRODYNAMICS

On the detection of underwater bottom topography by imaging radars p 46 N84-27301

Modeling of SAR signatures of shallow water ocean topography p 47 N84-27302

HYDROGEOLGY

Mapping the sea floor by satellite p 35 A84-36686
 HYDROGRAPHY

The experience of organising a utilisation programme for Bhaskara --- Indian experimental satellite p 64 A84-30233

Integration of Landsat data into the Saginaw River Basin geographic information system p 51 A84-33339

Drainage pattern delineation - A function of image scale p 52 A84-33335

Establishing hydrographic control using Doppler --- shore control stations for geodetic surveys p 18 A84-33358

Locating shoreline changes in the Portipahtau (Finland) water reservoir by using multitemporal Landsat data p 52 A84-33987

Classification of snow surface conditions by means of Landsat MSS data under compensation of slope effects p 52 A84-38296

Results of field observations of radio waves in alluvial deposits in Cara state from 1:100,000: Fortaleza, Canirde, Taperuaba, Santa Quiteria, Sobral, and Sao Luiz do Curu

[INPE-3061-NTE/216] p 53 N84-26100

HYDROLOGY

LANDSAT-D investigations in snow hydrology
 [E84-10094] p 53 N84-22997

Atmospheric model development p 53 N84-22998

Hydrology of the North Slope, Alaska p 53 N84-23973

Guide to hydrological practices. Volume 2: Analysis, forecasting and other applications

[WMO-168] p 53 N84-25145

Outlook for improved numerical weather prediction using satellite data with a special emphasis on the hydrological variables

[AD-A141233] p 54 N84-28344

HYDROLOGY MODELS

Integration of LANDSAT land cover data into the Saginaw River basin geographic information system for hydrologic modeling

[AD-A140185] p 53 N84-26106

HYDROMETEOROLOGY

Hydrological data densification in mountainous terrain using Landsat imagery p 51 A84-30256

The effect of groundwater inflow on evaporation from a saline lake p 52 A84-34378

ICE FLOES

Method to estimate drag coefficient at the air/ice interface over drifting open pack ice from remotely sensed data p 48 N84-27310

ICE MAPPING

Satellite image atlas of glaciers: The Polar regions p 38 N84-23940

Remote sensing of floe size distribution and surface topography

[E84-10132] p 39 N84-25141

ICE REPORTING

Seasat SAR sea-ice imagery - Summer melt to autumn freeze-up p 36 A84-38941

A bispectral method for the height determination of optically thin ice clouds p 60 A84-39044

Determination of sea ice parameters with the Nimbus 7 SMMR p 37 A84-39461

ICEBERGS

Observations of sea ice and icebergs from satellite radar altimeters p 48 N84-27311

IMAGE ANALYSIS

An analysis of tectonics and metallogeny of Orissa state, India with remote sensing technique p 22 A84-30247

Reduction of high dimension data to two dimension using non linear mapping techniques p 54 A84-30248

The use of Hough transformation for detecting lineaments in satellite imagery p 22 A84-30262

Geological interpretation from aerial remote sensing images of Tengchong area p 23 A84-32590

Analysis of photo interpretation test results for seven aerospace image types of the San Juan National Forest, Colorado p 4 A84-33332

Characterization of Landsat-4 MSS and TM digital image data p 56 A84-33526

Landsat-4 MSS and Thematic Mapper data quality and information content analysis p 56 A84-33528

Thematic Mapper image quality - Registration, noise, and resolution p 57 A84-33533

Comparison of the information content of data from the Landsat-4 Thematic Mapper and the Multispectral Scanner p 57 A84-33534

A statistical evaluation of the advantages of Landsat Thematic Mapper data in comparison to Multispectral Scanner data p 57 A84-33537

A semi-automated procedure for identifying Landsat MSS subregion coordinates p 58 A84-34959

Joint analysis of Landsat-MSS and NOAA-AVHRR data for marine environmental monitoring p 35 A84-38298

Landsat MSS data used for crop identification at the limit of its spatial resolution p 8 A84-38299

Two-stage cluster analysis of a Landsat image p 58 A84-38302

Image analysis researches of remotely sensed data at NAL p 59 A84-38315

Application of LANDSAT data to the study of urban development in Brasilia p 16 N84-26090

[E84-10142] PAME Proceedings, Pattern Analysis in the Marine Environment, An Ocean Science and Technology Workshop p 16 N84-26090

[AD-A140195] p 41 N84-26257

LANDSAT-4 image data quality analysis p 63 N84-27250

Analysis of SEASAT SAR imagery collected during the JASIN experiment p 49 N84-27320

IMAGE ENHANCEMENT

Analysis and processing of Landsat-4 sensor data using advanced image processing techniques and technologies p 56 A84-33527

Revised radiometric calibration technique for Landsat-4 Thematic Mapper data p 56 A84-33530

Simple enhancement techniques in digital image processing p 58 A84-33798

Utilization of digital LANDSAT imagery for the study of granitoid bodies in Rondonia: Case example of the Pedra Branca massif p 26 N84-23979

[E84-10120] Analysis of the quality of image data acquired by the LANDSAT-4 Thematic Mapper and Multispectral Scanners p 61 N84-26085

Comparative assessment of LANDSAT-D MSS and TM data quality for mapping applications in the Southeast [E84-10138] p 61 N84-26086

Multiseasonal variables in digital image enhancements for geological applications p 29 N84-26093

[E84-10145] Methodological approach in lithological discrimination by digital processing: A case study in the Serra do Ramalho, state of Bahia p 29 N84-26101

IMAGE FILTERS

Simple enhancement techniques in digital image processing p 58 A84-33798

IMAGE PROCESSING

Digital processing of remote sensing data on Hail Haor, Bangladesh for landuse analysis and development potentiality assessment p 13 A84-30240

A remote sensing data processing system based on a micro-computer p 64 A84-30265

Application of the Vizir Image Processing System to the remote sensing studies in Bangladesh p 64 A84-30266

Description of SEP ground station and Vizir image processing VIPS --- for Spot and Landsat 4 satellites p 54 A84-30268

Digital comparison and correlation techniques of remote sensing images having different space resolution p 55 A84-33356

Characterization of Landsat-4 MSS and TM digital image data p 56 A84-33526

Analysis and processing of Landsat-4 sensor data using advanced image processing techniques and technologies p 56 A84-33527

A physically-based transformation of Thematic Mapper data The TM tasseled cap p 56 A84-33532

Comparison of the information content of data from the Landsat-4 Thematic Mapper and the Multispectral Scanner p 57 A84-33534

Thematic Mapper - The ESA-Earthnet ground segment and processing experience p 57 A84-33542

Simple enhancement techniques in digital image processing p 58 A84-33798

Distinguishing linear contour elements on satellite photos on the basis of a visual perception model p 24 A84-34789

RABIVE - A real time program system for radiometric image processing p 58 A84-37773

Performance evaluation and a dedicated system for SAR image data processing p 58 A84-38300

A SAR image auto-focusing using linear distortion azimuth matched filter p 58 A84-38304

Equidensitometry and remote sensing imagery p 59 A84-38944

LANDSAT-D investigations in snow hydrology [E84-10094] p 53 N84-22997

Registration of TM data to digital elevation models p 60 N84-22999

LANDSAT 4 investigations of Thematic Mapper and multispectral scanner applications --- Death Valley, California; Silver Bell Copper Mine, Arizona, and Dulles Airport near Washington, D.C. [E84-10100] p 60 N84-23003

The Pennsylvania defoliation application pilot test [E84-10111] p 8 N84-23004

LANDSAT 4 band 6 data evaluation [E84-10119] p 60 N84-23009

Evaluation of the effects of the seasonal variation of solar elevation angle and azimuth on the processes of digital filtering and thematic classification of relief units [E84-10121] p 60 N84-23980

A constrained-clustering approach to the analysis of remote sensing data [AD-A139124] p 10 N84-23993

Experiments to correct a digital map data base using scene analysis [AD-A139447] p 61 N84-24499

Study on spectral/radiometric characteristics of the Thematic Mapper for land use applications [E84-10130] p 61 N84-25140

Photogrammetric research [TRITA-FMI-47] p 69 N84-25146

General triangulation: Incorporating photogrammetric and other observations p 69 N84-25151

Publications of the Jet Propulsion Laboratory 1982 [NASA-CR-173539] p 71 N84-25510

Principal components technique analysis for vegetation and land use discrimination --- Brazilian cerrados [E84-10135] p 10 N84-26083

Analysis of the quality of image data acquired by the LANDSAT-4 Thematic Mapper and Multispectral Scanners [E84-10137] p 61 N84-26085

Sampling system for wheat (*Triticum aestivum* L.) area estimation using digital LANDSAT MSS data and aerial photographs --- Brazil [E84-10139] p 10 N84-26087

An integrated software system for geometric correction of LANDSAT MSS imagery [E84-10143] p 62 N84-26091

Earthnet: The story of images [ESA-BR-18] p 62 N84-26102

Digital processing of LANDSAT data for the preparation of a land use map of the rural district surrounding Tuebingen to a scale of 1:50000 [ESA-TT-816] p 16 N84-26104

Interactive digital image processing for terrain data extraction, phase 4 [AD-A140197] p 11 N84-26107

PAME Proceedings, Pattern Analysis in the Marine Environment, An Ocean Science and Technology Workshop [AD-A140195] p 41 N84-26257

Application of computer image processing to underwater surveys [AD-P003122] p 41 N84-26263

Contextual classification of remotely sensed data p 63 N84-27245

LANDSAT 4 investigations of Thematic Mapper and Multispectral Scanner applications [E84-10152] p 63 N84-27247

Evaluating LANDSAT-4 MSS and TM data [E84-10157] p 63 N84-27249

Research on land use cartography by remote sensing p 17 N84-28201

Remote sensing of the Santonge littoral. Processing and interpretation of satellite images p 17 N84-28201

[ISBN-2-85929-016-8] p 63 N84-28202

IMAGE RECONSTRUCTION

Interactive procedures for distinguishing and reconstructing contour networks --- in aerospace computer aided photomapping p 58 A84-34788

IMAGE RESOLUTION

Thematic Mapper image quality - Registration, noise, and resolution p 57 A84-33533

Investigation of several aspects of LANDSAT-4 data quality --- Sacramento, San Francisco, and NE Arkansas [E84-10122] p 60 N84-23981

SUBJECT INDEX

LAND USE

LANDSAT-4 image data quality analysis [E84-10134] p 10 N84-26082

Analysis of the quality of image data acquired by the LANDSAT-4 Thematic Mapper and Multispectral Scanners [E84-10137] p 61 N84-26085

Comparative assessment of LANDSAT-D MSS and TM data quality for mapping applications in the Southeast [E84-10138] p 61 N84-26086

Evaluation of solar angle variation over digital processing of LANDSAT imagery --- Brazil [E84-10140] p 61 N84-26088

Evaluation of SIR-A (Shuttle Imaging Radar) images from the Tres Marias region (Minas Gerais State, Brazil) using derived spatial features and registration with MSS-LANDSAT images [E84-10148] p 62 N84-26096

Comparative study of image data produced by satellites with different characteristics [ESA-CR(P)-1867] p 62 N84-26103

LANDSAT-4 image data quality analysis [E84-10158] p 63 N84-27250

IMAGERY

Satellite image atlas of glaciers: The Polar regions p 38 N84-23940

The use of satellite technology in the search for meteorites in Antarctica aut 01Meunier, Tony K. p 26 N84-23955

Glaciological and geological studies of Antarctica with satellite remote sensing technology p 38 N84-23956

Correlation calculation in stereoscopic image pairs for the automatic acquisition of digital land models, orthopictures and height line planes [SER-C283] p 21 N84-26079

IMAGING TECHNIQUES

Application of the Vizir Image Processing System to the remote sensing studies in Bangladesh p 64 A84-30266

Digital SAR processing using a fast polynomial transform p 55 A84-32093

Experiments in lithography from remote sensor imagery p 55 A84-33362

A comparison of numerical results of Arctic Sea ice modeling with satellite images p 39 N84-23969

Utilization of digital LANDSAT imagery for the study of granitoid bodies in Rondonia: Case example of the Pedra Branca massif [E84-10120] p 26 N84-23979

Seminar on mathematical models of geodetic/photogrammetric point determination with regard to outliers and systematic errors [SER-A-98] p 20 N84-26069

Mathematical models of photogrammetric point determination p 20 N84-26070

Several aspects of the sequential processing of photogrammetric bundle blocks p 21 N84-26077

Analysis of the quality of image data acquired by the LANDSAT-4 Thematic Mapper and Multispectral Scanners [E84-10137] p 61 N84-26085

Comparative assessment of LANDSAT-D MSS and TM data quality for mapping applications in the Southeast [E84-10138] p 61 N84-26086

Evaluation of solar angle variation over digital processing of LANDSAT imagery --- Brazil [E84-10140] p 61 N84-26088

The use of an image registration technique in the urban growth monitoring [E84-10147] p 16 N84-26095

Theory and measure of certain image norms in SAR p 43 N84-27274

The dual-frequency scatterometer reexamined p 44 N84-27280

An improved dual-frequency technique for the remote sensing of ocean currents and wave spectra p 44 N84-27281

IMPERIAL VALLEY (CA)

Coseismic and postseismic vertical movements associated with the 1940 M7.1 Imperial Valley, California, earthquake p 24 A84-36922

INDIA

Multispectral and multitemporal Landsat data for soil surveys - A case study of part of north west India p 1 A84-30228

INDIAN OCEAN

Somali current studied from SEASAT altimetry p 47 N84-27307

INDIAN SPACECRAFT

The experience of organising a utilisation programme for Bhaskara --- Indian experimental satellite p 64 A84-30233

Bhaskara-II TV data in resource studies - A case study in a part of Andhra Pradesh, southern India p 54 A84-30234

INFESTATION

Identification of brown plant hopper and bacterial leaf blight affected rice crop on Landsat false colour composites p 1 A84-30237

The Pennsylvania defoliation application pilot test [E84-10111] p 6 N84-23004

INFORMATION DISSEMINATION

Earthnet: The story of images [ESA-BR-18] p 62 N84-26102

INFORMATION MANAGEMENT

Earthnet: The story of images [ESA-BR-18] p 62 N84-26102

INFORMATION RETRIEVAL

Preserve the sense of Earth from space [DE84-900854] p 71 N84-25159

INFORMATION SYSTEMS

Integration of LANDSAT land cover data into the Saginaw River basin geographic information system for hydrologic modeling [AD-A104185] p 53 N84-26106

INFORMATION THEORY

Study on spectral/radiometric characteristics of the Thematic Mapper for land use applications [E84-10130] p 61 N84-25140

INFRARED DETECTORS

Fog recognition in daylight 3.7-micron-band Tiros-N and NOAA images p 65 A84-34157

Effect of space exposure on pyroelectric infrared detectors (A0135) p 68 N84-24679

Fire detection using the NOAA (National Oceanic and Atmospheric Administration)-series satellites [PB84-176890] p 13 N84-27324

INFRARED IMAGERY

Making false color photomap and its application in thematic mapping by using IR photos p 54 A84-30249

Dynamics of the slope water off New England and its influence on the Gulf Stream as inferred from satellite IR data p 31 A84-30672

Satellite observations of circulation in the eastern Bering Sea p 33 A84-34514

Observations of Gulf Stream-induced and wind-driven upwelling in the Georgia Bight using ocean color and infrared imagery p 34 A84-34517

Satellite observations of the 1982-1983 El Nino along the U.S. Pacific coast p 35 A84-36872

Maps of favorable areas for tuna fishing to the South and Southeast of Brazil prepared from SMS-2 satellite data [INPE-3102-PRE/501] p 41 N84-26256

Variations in surface current off the coasts of Canada as inferred from infrared satellite imagery p 47 N84-27305

INFRARED PHOTOGRAPHY

The Green Cadastre - An experiment for exploring the tree vegetation in the Paris area p 7 A84-36516

INFRARED RADIOMETERS

Dual channel satellite measurements of sea surface temperature p 31 A84-31431

Atmospheric science -- overview of stratosphere and mesosphere satellite remote sounding experiments p 66 A84-38923

The Limb Infrared Monitor of the Stratosphere - Experiment description, performance, and results p 66 A84-39440

Accuracy and precision of the nitric acid concentrations determined by the limb infrared monitor of the stratosphere experiment on NIMBUS 7 p 67 A84-39444

Heat Capacity Mapping Radiometer (HCMR) data processing algorithm, calibration, and flight performance evaluation [E84-10153] p 71 N84-27248

Applications of airborne remote sensing in atmospheric sciences research p 71 N84-27286

INFRARED SCANNERS

Accuracy and precision of the nitric acid concentrations determined by the limb infrared monitor of the stratosphere experiment on NIMBUS 7 p 67 A84-39444

INFRARED SIGNATURES

Evaluation of corn/soybeans separability using Thematic Mapper and Thematic Mapper Simulator data p 5 A84-33539

INFRARED SPECTRA

Active microwave responses - An aid in improved crop classification p 3 A84-31498

LANDSAT 4 band 6 data evaluation [E84-10119] p 60 N84-23009

INSOLATION

Albedo of a forest modeled as a plane with dense protrusions p 6 A84-34385

INSTRUCTORS

NASA, the first 25 years: 1958 - 1983 [NASA-EP-182] p 72 N84-26563

INSTRUMENT ERRORS

Microwave scatterometer p 66 A84-38310

INTERNATIONAL GEOPHYSICAL YEAR

The geodetic activities of the Department of Defense under IGY programs p 17 A84-30727

IONOSPHERIC DISTURBANCES

Space disturbance warning system with the aid of satellites p 15 A84-38301

IONOSPHERIC PROPAGATION

Propagation effects in satellite-based synthetic aperture radars [AD-A138681] p 67 N84-22873

Geodetic use of GEOSAT-A [AD-A137993] p 19 N84-23048

IRRADIANCE

High-precision atmospheric ozone measurements using wavelengths between 290 and 305 nm p 67 A84-39447

ISRAEL

Coastal bathymetry and currents from LANDSAT data p 47 N84-27303

ITERATION

Non-Gaussian statistical models of surface wave fields for remote sensing applications p 45 N84-27284

J

JAMAICA

Cenozoic tectonics of the Caribbean: Structural and stratigraphic studies in Jamaica and Hispaniola p 25 N84-23062

JAPAN

Analysing forest structures by remote sensing p 1 A84-30236

JAPANESE SPACE PROGRAM

Remote sensing of the oceans --- Japanese book p 35 A84-37299

JET STREAMS (METEOROLOGY)

The evolution of mushroom-shape currents in the ocean p 36 A84-38773

K

KALMAN FILTERS

A Kalman filter approach to precision GPS geodesy p 17 A84-30244

KARHUNEN-LOEVE EXPANSION

Principal components technique analysis for vegetation and land use discrimination --- Brazilian cerrados [E84-10135] p 10 N84-26083

KARST

Surface expression of heavily mantled interstratal Karst bordering Okefenokee Swamp, Georgia p 23 A84-33350

KINETIC ENERGY

Mean circulation and eddy kinetic energy in the eastern North Atlantic p 32 A84-34501

L

LAKES

The application of Landsat image in the surveying of water resources of Dongting Lake p 51 A84-30255

The effect of groundwater inflow on evaporation from a saline lake p 52 A84-34378

LAND ICE

Vegetation, land-use and seasonal albedo data sets: Documentation of archived data tape [E84-10133] p 10 N84-25142

Satellite remote sensing over ice p 48 N84-27308

LAND MANAGEMENT

Application of multi-concept in remote sensing technique for identification and mapping of soil units of alluvial plain for land use planning in Sri Lanka p 13 A84-30241

Development of satellite Doppler/inertial survey systems for BLM cadastral survey-related applications in Alaska p 14 A84-33370

Land cover and terrain mapping for the development of digital data bases for wildlife habitat assessment in the Yukon Flats National Wildlife Refuge, Alaska p 9 N84-23971

Identifying environmental features for land management decisions [E84-10125] p 15 N84-23984

LAND USE

Digital processing of remote sensing data on Hail Haor, Bangladesh for landuse analysis and development potentiality assessment p 13 A84-30240

Application of multi-concept in remote sensing technique for identification and mapping of soil units of alluvial plain for land use planning in Sri Lanka p 13 A84-30241

Analysis of land use changes around Salt Lake City using Landsat digital data - A case study of Sandy area p 13 A84-30242

The compilation of the satellite image map of land-use of China (1:2,000,000 scale) p 13 A84-30243

The use of Landsat imagery in analyzing the vegetation and energy resources of Pickens County, South Carolina p 3 A84-33330

Soil erosion mapping and evaluation - A photo-geomorphological approach p 14 A84-33333

Findings on the use of Landsat-3 return beam vidicon imagery for detecting land use and land cover changes p 14 A84-33361

A statistical evaluation of the advantages of Landsat Thematic Mapper data in comparison to Multispectral Scanner data p 57 A84-33537

Identifying environmental features for land management decisions (E84-10125) p 15 N84-23984

Vegetation, land-use and seasonal albedo data sets: Documentation of archived data tape (E84-10133) p 10 N84-25142

Principal components technique analysis for vegetation and land use discrimination --- Brazilian cerrados (E84-10135) p 10 N84-26083

Comparative assessment of LANDSAT-D MSS and TM data quality for mapping applications in the Southeast (E84-10138) p 61 N84-26086

Integration of LANDSAT land cover data into the Saginaw River basin geographic information system for hydrologic modeling (AD-A140185) p 53 N84-26106

Use of transformed LANDSAT data in regression estimation of crop acreages p 11 N84-27246

Research on land use cartography by remote sensing p 17 N84-28201

Remote sensing of the Santonge littoral. Processing and interpretation of satellite images [ISBN-2-85929-016-8] p 63 N84-28202

LANDFORMS

An undetectable factor in geomorphological mapping from land satellite images - A case study in the central highland, Thailand p 22 A84-30261

X to W band radiometric signatures of natural surfaces p 35 A84-36289

LANDSAT SATELLITES

Multispectral and multitemporal Landsat data for soil surveys - A case study of part of north west India p 1 A84-30228

Identification of brown plant hopper and bacterial leaf blight affected rice crop on Landsat false colour composites p 1 A84-30237

An inquiry into methods of estimating yields of wheat and autumn crops in the plain region with Landsat images visual interpretation p 2 A84-30239

Analysis of land use changes around Salt Lake City using Landsat digital data - A case study of Sandy area p 13 A84-30242

Landsat image use in forestry management in China p 2 A84-30250

The application of Landsat image in the surveying of water resources of Dongting Lake p 51 A84-30255

Landsat planimetric maps p 54 A84-30264

A remote sensing data processing system based on a micro-computer p 64 A84-30265

Landsat imagery for the interpretation of Louisiana forest habitat regions p 3 A84-33328

Non-parallactic stereoscopy using shadow-disparity --- time separated Landsat photos p 55 A84-33335

Integration of Landsat data into the Saginaw River Basin geographic information system p 51 A84-33339

Application of Landsat data in the exploration of 'Calcrete' uranium deposits p 24 A84-37775

Landsat MSS data used for crop identification at the limit of its spatial resolution p 8 A84-38299

Two-stage cluster analysis of a Landsat image p 58 A84-38302

Study on temporal geometric-distortion variation of Landsat MSS and RBV imageries and attitude determination program p 59 A84-38313

Irrigated crop inventory by classification of satellite image data p 8 A84-38999

Land cover and terrain mapping for the development of digital data bases for wildlife habitat assessment in the Yukon Flats National Wildlife Refuge, Alaska p 9 N84-23971

Hydrology of the North Slope, Alaska p 53 N84-23973

Proceedings of the Fourth Meeting of the LANDSAT Technical Working Group (LTWG), volume 1 [LIB-PRO-0012-VOL-1] p 69 N84-25144

Correlating aerial photographs to LANDSAT Multispectral Sensor (MSS) data to measure ground control points p 69 N84-25150

Preserve the sense of Earth from space [DE84-900854] p 71 N84-25159

Digital processing of LANDSAT data for the preparation of a land use map of the rural district surrounding Tuebingen to a scale of 1:50000 (ESA-TT-816) p 16 N84-26104

Use of transformed LANDSAT data in regression estimation of crop acreages p 11 N84-27246

Research on land use cartography by remote sensing p 17 N84-28201

Remote sensing of the Santonge littoral. Processing and interpretation of satellite images [ISBN-2-85929-016-8] p 63 N84-28202

LANDSAT 4

Description of SEP ground station and Vizir image processing VIPS --- for Spot and Landsat 4 satellites p 54 A84-30268

Characterization of Landsat-4 MSS and TM digital image data p 56 A84-33526

Analysis and processing of Landsat-4 sensor data using advanced image processing techniques and technologies p 56 A84-33527

Landsat-4 MSS and Thematic Mapper data quality and information content analysis p 56 A84-33528

Revised radiometric calibration technique for Landsat-4 Thematic Mapper data p 56 A84-33530

In-flight absolute radiometric calibration of the Thematic Mapper p 56 A84-33531

Comparison of the information content of data from the Landsat-4 Thematic Mapper and the Multispectral Scanner p 57 A84-33534

Cartographic accuracy of Landsat-4 MSS and TM image data p 57 A84-33535

An analysis of Landsat-4 Thematic Mapper geometric properties p 57 A84-33536

A statistical evaluation of the advantages of Landsat Thematic Mapper data in comparison to Multispectral Scanner data p 57 A84-33537

Spectral variability of Landsat-4 Thematic Mapper and Multispectral Scanner data for selected crop and forest cover types p 5 A84-33538

Snow reflectance from Landsat-4 Thematic Mapper p 52 A84-33541

Thematic Mapper - The ESA-Earthnet ground segment and processing experience p 57 A84-33542

Spectroradiometric calibration of the Thematic Mapper and multispectral scanner system [E84-10098] p 67 N84-23000

In-flight absolute radiometric calibration of the Thematic Mapper --- White Sands, New Mexico p 68 N84-23002

LANDSAT 4 investigations of Thematic Mapper and multispectral scanner applications --- Death Valley, California; Silver Bell Copper Mine, Arizona, and Dulles Airport near Washington, D.C. [E84-10100] p 60 N84-23003

LANDSAT 4 band 6 data evaluation [E84-10119] p 60 N84-23009

Investigation of several aspects of LANDSAT-4 data quality --- Sacramento, San Francisco, and NE Arkansas [E84-10122] p 60 N84-23981

LANDSAT-D Thematic Mapper image dimensionality reduction and geometric correction accuracy --- Walnut Creek Watershed, Texas [E84-10149] p 62 N84-26097

LANDSAT 4 investigations of Thematic Mapper and Multispectral Scanner applications [E84-10152] p 63 N84-27247

Evaluating LANDSAT-4 MSS and TM data [E84-10157] p 63 N84-27249

LANDSAT-4 image data quality analysis [E84-10158] p 63 N84-27250

LANDSAT 5

Spectroradiometric calibration of the Thematic Mapper and multispectral scanner system [E84-10098] p 67 N84-23000

LASER APPLICATIONS

Computer-automated CO₂-laser long-path absorption system for air quality monitoring in the working environment p 13 A84-30307

A theoretical study of an airborne laser technique for determining sea water turbidity p 31 A84-33774

Determining forest canopy characteristics using airborne laser data p 7 A84-37202

Airborne laser topographic mapping results p 8 A84-38998

LAUNCH VEHICLES

NASA, the first 25 years: 1958 - 1983 [NASA-EP-182] p 72 N84-26563

LEAST SQUARES METHOD

Seminar on mathematical models of geodetic/photogrammetric point determination with regard to outliers and systematic errors [SER-A-98] p 20 N84-26069

Area estimation using multiyear designs and partial crop identification [E84-10151] p 11 N84-26099

LEAVES

Evaluation of factors causing reflectance differences between sun and shade leaves p 3 A84-30674

Inversion of vegetation canopy reflectance models for estimating agronomic variables. III - Estimation using only canopy reflectance data as illustrated by the suits model. IV - Total inversion of the SAIL model --- Scattering by Arbitrarily Inclined Leaves p 7 A84-37203

LENSES

Fisheye objective in the dose range photogrammetry: Theoretical and practical investigations [SER-C-286] p 21 N84-26080

LIMP BRIGHTENING

The Limb Infrared Monitor of the Stratosphere - Experiment description, performance, and results p 66 A84-39440

LIMNOLOGY

Locating shoreline changes in the Porttipahta (Finland) water reservoir by using multitemporal Landsat data p 52 A84-33987

LITHOGRAPHY

Experiments in lithography from remote sensor imagery p 55 A84-33362

LITHOLOGY

Reduced to pole long-wavelength magnetic anomalies of Africa and Europe p 27 N84-25132

Relation of MAGSAT anomalies to the main tectonic provinces of South America p 28 N84-25137

LITHOSPHERE

Seasat observations of lithospheric flexure seaward of trenches p 32 A84-34339

Application of Magsat lithospheric modeling in South America. Part 1: Processing and interpretation of magnetic and gravity anomaly data [E84-10115] p 24 N84-23008

Application of MAGSAT to lithospheric modeling in South America. Part 2: Synthesis of geologic and seismic data for development of integrated crustal models [E84-10126] p 26 N84-25128

Euro-African MAGSAT anomaly-tectonic observations p 27 N84-25129

Relation of MAGSAT and gravity anomalies to the main tectonic provinces of South America p 28 N84-25138

LONG DURATION EXPOSURE FACILITY

Effect of space exposure on pyroelectric infrared detectors (A0135) p 68 N84-24679

LONG WAVE RADIATION

Comparison of longwave diurnal models applied to simulations of the Earth Radiation Budget Experiment p 65 A84-31947

LUMINOSITY

Correlations between the nonthermal emission of quasars like nuclei and their Balmer-line widths p 58 A84-33629

M

MAGNETIC ANOMALIES

Reduction of satellite magnetic anomaly data p 19 A84-38812

Use of MAGSAT anomaly data for crustal structure and mineral resources in the US midcontinent [E84-10112] p 24 N84-23005

Application of Magsat lithospheric modeling in South America. Part 1: Processing and interpretation of magnetic and gravity anomaly data [E84-10115] p 24 N84-23008

Application of MAGSAT to lithospheric modeling in South America. Part 2: Synthesis of geologic and seismic data for development of integrated crustal models [E84-10126] p 26 N84-25128

Euro-African MAGSAT anomaly-tectonic observations p 27 N84-25129

Correlation of tectonic provinces of South America and the Caribbean region with MAGSAT anomalies p 27 N84-25130

Satellite elevation magnetic and gravity models of major South American plate tectonic features p 27 N84-25131

Reduced to pole long-wavelength magnetic anomalies of Africa and Europe p 27 N84-25132

Satellite magnetic anomalies of Africa and Europe p 27 N84-25133

Do satellite magnetic anomaly data accurately portray the crustal component? p 28 N84-25134

Long-wavelength magnetic and gravity anomaly correlations of Africa and Europe p 28 N84-25135

US aeromagnetic and satellite magnetic anomaly comparisons p 28 N84-25136

Relation of MAGSAT anomalies to the main tectonic provinces of South America p 28 N84-25137

Relation of MAGSAT and gravity anomalies to the main tectonic provinces of South America p 28 N84-25138

A crustal structure study of South America p 29 N84-25139

Petrologic and geophysical sources of long-wavelength crustal magnetic anomalies [NASA-CR-175245] p 29 N84-28276

SUBJECT INDEX

MAGNETIC SIGNATURES

A study of geomagnetic pulsations using the AFGL (Air Force Geophysics Laboratory) magnetometer network [AD-A140507] p 70 N84-26217

MAGNETIC STORMS

A study of geomagnetic pulsations using the AFGL (Air Force Geophysics Laboratory) magnetometer network [AD-A140507] p 70 N84-26217

MAGNETOMETERS

A study of geomagnetic pulsations using the AFGL (Air Force Geophysics Laboratory) magnetometer network [AD-A140507] p 70 N84-26217

MAGNETOSPHERE

A study of geomagnetic pulsations using the AFGL (Air Force Geophysics Laboratory) magnetometer network [AD-A140507] p 70 N84-26217

MAPPING

The compilation of the satellite image map of land-use of China (1:2,000,000 scale) p 13 A84-30243

American Congress on Surveying and Mapping, Annual Meeting, 43rd, Washington, DC, March 13-18, 1983, Technical Papers p 18 A84-33557

Coastal mapping of the Beaufort Sea coast p 31 A84-33560

A regional raster data study at the Experimental Cartography Unit - The application of interactive raster graphics to environmental modelling p 14 A84-33563

Airborne laser topographic mapping results p 8 A84-38998

Antarctic mapping and international coordination p 19 N84-23935

Surveying in Antarctica during the International Geophysical Year p 25 N84-23942

Program for mapping Antarctica p 19 N84-23954

Glaciological and geological studies of Antarctica with satellite remote sensing technology p 38 N84-23956

Emerging recognition of the nonfuel mineral resources of Arctic Alaska p 26 N84-23962

Orbital imagery: A cartographic solution [INPE-2820-PRE/374] p 20 N84-25143

Photogrammetric research at the Royal Institute of Technology, Stockholm, Sweden p 69 N84-25147

Correlating aerial photographs to LANDSAT Multispectral Sensor (MSS) data to measure ground control points p 69 N84-25150

General triangulation: Incorporating photogrammetric and other observations p 69 N84-25151

GENTRI: A system for simultaneous adjustment of photogrammetric and other observations p 69 N84-25152

Multi-models to increase accuracy p 70 N84-25154

Contour-to-grid transformation: Development of a method for generation of a sparse grid structure out of terrain elevation contours [FOA-C-30349-E1] p 16 N84-25156

Analysis of airborne electromagnetic systems for mapping thickness of sea ice [AD-A139786] p 39 N84-25235

A computer program for mapping regions in a geographic data base with raster structure [FOA-C-20529-D8] p 16 N84-25340

Correlation calculation in stereoscopic image pairs for the automatic acquisition of digital land models, orthoimages and height line planes [SER-C-283] p 21 N84-26079

Fisheye objective in the dose range photogrammetry: Theoretical and practical investigations [SER-C-286] p 21 N84-26080

Integration of LANDSAT land cover data into the Saginaw River basin geographic information system for hydrologic modeling [AD-A140185] p 53 N84-26106

Cartographic feature extraction on ETL's (Engineer Topographic Laboratories) DIAL (Digital Image Analysis Laboratory) system [AD-A140230] p 63 N84-26112

Non-Gaussian statistical models of surface wave fields for remote sensing applications p 45 N84-27284

Research on land use cartography by remote sensing p 17 N84-28201

Remote sensing of the Santonge littoral. Processing and interpretation of satellite images [ISBN-2-85929-016-8] p 63 N84-28202

MAPS

Experiments to correct a digital map data base using scene analysis [AD-A139447] p 61 N84-24499

MARINE BIOLOGY

Remote sensing marine bioluminescence - The role of the in-water scalar irradiance p 34 A84-36107

MARINE ENVIRONMENTS

Monitoring the marine environment with remote sensing technology p 30 N84-30258

Joint analysis of Landsat-MSS and NOAA-AVHRR data for marine environmental monitoring p 35 A84-38298

Scientific activity in oceanography, 1979-1982

p 38 N84-23084

PAME Proceedings, Pattern Analysis in the Marine Environment, An Ocean Science and Technology Workshop [AD-A140195] p 41 N84-26257

MARINE METEOROLOGY

Remote sensing and storm surge forecasting in Bangladesh p 30 A84-30230

The effect of ocean surface temperature on the trajectories of tropical cyclones p 34 A84-35252

Large-scale analysis and forecast experiments with wind data from the Seasat A scatterometer p 66 A84-37873

Detection of marine aerosol particles in coastal zones using satellite imagery p 36 A84-38943

MARINE TECHNOLOGY

PAME Proceedings, Pattern Analysis in the Marine Environment, An Ocean Science and Technology Workshop [AD-A140195] p 41 N84-26257

MARITIME SATELLITES

The ESA ocean observation satellite ERS-1. I - Description of the history, goals, and payload of ERS-1 p 31 A84-32266

MASCONS

The approximation introduced by representing the earth's gravity field with a finite grid of mascons both at the earth's surface and at the bottom of the earth's crust

[AAS PAPER 83-394] p 17 A84-30583

MASS

Water mass classification in the North Atlantic using IR digital data and Bayesian decision theory [AD-P003125] p 41 N84-26266

MASS DISTRIBUTION

SAGE and SAM II measurements of global stratospheric aerosol optical depth and mass loading p 15 A84-39455

MASSIFS

Utilization of digital LANDSAT imagery for the study of granitoid bodies in Rondonia: Case example of the Pedra Branca massif

[E84-10120] p 26 N84-23979

MATCHED FILTERS

A SAR image auto-focusing using linear distortion azimuth matched filter p 58 A84-38304

MATHEMATICAL MODELS

CONSERVB: A numerical method to compute soil water content and temperature profiles under a bare surface [E84-10113] p 9 N84-23006

Radar backscatter modelling p 25 N84-23525

Arctic Sea ice by passive microwave observations from the Nimbus-5 Satellite p 39 N84-23970

Potential utility of future satellite magnetic field data [NASA-CR-175230] p 26 N84-24691

Application of MAGSAT to lithospheric modeling in South America. Part 2: Synthesis of geologic and seismic data for development of integrated crustal models [E84-10126] p 26 N84-25128

Satellite elevation magnetic and gravity models of major South American plate tectonic features p 27 N84-25131

Photogrammetric research [TRITA-FMI-47] p 69 N84-25146

Mathematical aspects of digital terrain information. A progress report from ISPRS Working Group III:3 p 61 N84-25148

Multi-models to increase accuracy p 70 N84-25154

Seminar on mathematical models of geodetic/photogrammetric point determination with regard to outliers and systematic errors [SER-A-98] p 20 N84-26069

Mathematical models of photogrammetric point determination p 20 N84-26070

Stochastic models for point manifolds p 20 N84-26072

Estimation of variances and covariances in the multivariate and in the incomplete multivariate model p 20 N84-26073

Detection of errors in the functional adjustment model p 20 N84-26074

SAR imagery of ocean-wave swell traveling in an arbitrary direction p 44 N84-27278

Measurements of ocean wave spectra and modulation transfer function with the airborne two frequency scatterometer p 45 N84-27282

MATRICES (MATHEMATICS)

Matrix partitioning and EOF/principal component analysis of Antarctic Sea ice brightness temperatures [NASA-TM-83916] p 49 N84-27319

MEANDERS

Seasonal variability in meanders of the California Current System off Vancouver Island p 33 A84-34507

MICROWAVE IMAGERY

MEDITERRANEAN SEA

Discussion of the design of satellite-laser measurement stations in the eastern Mediterranean under the geological aspect. Contribution to the earthquake prediction research by the Wegener Group and to NASA's Crustal Dynamics Project [NASA-TM-77412] p 26 N84-24031

The depiction of Alboran Sea Gyre during Donde Va? using remote sensing and conventional data p 47 N84-27306

MERCURY VAPOR

First estimate of annual mercury flux at the Kilauea main vent p 15 N84-34794

MESOSCALE PHENOMENA

The satellite altimeter as a platform for observation of the oceanic mesoscale p 46 N84-27299

Simulation and assimilation of satellite altimeter data at the oceanic mesoscale p 48 N84-27312

METEORITES

The use of satellite technology in the search for meteorites in Antarctica aut 01Meunier, Tony K. p 26 N84-23955

METEOROLOGICAL PARAMETERS

The World Climate Research Programme p 36 A84-38702

Outlook for improved numerical weather prediction using satellite data with a special emphasis on the hydrological variables

[AD-A141233] p 54 N84-28344

METEOROLOGICAL RESEARCH AIRCRAFT

Aircraft measurements of convective draft cores in MONEX p 31 A84-31821

METEOROLOGICAL SATELLITES

Bay monsoon activities in relation to the monsoon in the western Pacific p 30 N84-30232

Satellite climatology --- Russian book p 13 A84-31024

Applications of laser for climatology and atmospheric research

[BLEV-R-65-169-5] p 70 N84-26237

METEOROLOGY

Guide to hydrological practices. Volume 2: Analysis, forecasting and other applications [WMO-168] p 53 N84-25145

Tracking ocean wave spectrum from SAR images p 44 N84-27277

A tentative unified sea model for scattering and emission p 45 N84-27285

MEXICO

Pinacate-Gran Desierto Region, Mexico: SIR-A data analysis p 25 N84-23526

Identifying environmental features for land management decisions [E84-10125] p 15 N84-23984

MICHIGAN

Use of remote sensing for land use policy formulation [E84-10117] p 9 N84-23977

Aerial photography for ecological site mapping p 9 N84-23990

Integration of LANDSAT land cover data into the Saginaw River basin geographic information system for hydrologic modeling [AD-A140185] p 53 N84-26106

MICROCOMPUTERS

A remote sensing data processing system based on a micro-computer p 64 A84-30265

MICROWAVE EMISSION

A microwave systems approach to measuring root zone soil moisture [E84-10114] p 9 N84-23007

Crop moisture estimation over the southern Great Plains with dual polarization 1.66 centimeter passive microwave data from Nimbus 7 [E84-10163] p 12 N84-27255

MICROWAVE EQUIPMENT

The active microwave instrumentation for ERS-1 p 34 A84-35542

Microwave radiometric measurement of sea surface salinity

[AD-A141302] p 50 N84-28359

MICROWAVE IMAGERY

Crop moisture estimation over the southern Great Plains with dual polarization 1.66 centimeter passive microwave data from Nimbus 7 [E84-10163] p 12 N84-27255

Ocean wind field measurement performance of the ERS-1 scatterometer p 43 N84-27273

Theory and measure of certain image norms in SAR p 43 N84-27274

Synthetic aperture radar images of ocean waves, theories of imaging physics and experimental tests p 43 N84-27275

SAR imagery of ocean-wave swell traveling in an arbitrary direction p 44 N84-27278

MICROWAVE RADIOMETERS

Ocean waves and turbulence as observed with an adaptive coherent multifrequency radar
p 44 N84-27279
An improved dual-frequency technique for the remote sensing of ocean currents and wave spectra
p 44 N84-27281

Measurements of ocean wave spectra and modulation transfer function with the airborne two frequency scatterometer
p 45 N84-27282

MICROWAVE RADIOMETERS

X to W band radiometric signatures of natural surfaces
p 35 A84-36289
Remote sensing of the ocean by the airborne microwave scatterometer/radiometer system
p 36 A84-38307
Monthly distributions of precipitable water from the Nimbus 7 SMMR data
p 37 A84-39458
A summary of results from the first Nimbus 7 SMMR observations
p 37 A84-39459
Determination of sea ice parameters with the Nimbus 7 SMMR
p 37 A84-39461
Applications of airborne remote sensing in atmospheric sciences research
p 71 N84-27286

MICROWAVE RESONANCE

Two-frequency microwave resonance measurements from an aircraft - A quantitative estimate of the directional ocean surface spectrum
p 34 A84-34942
Measurements of ocean wave spectra and modulation transfer function with the airborne two frequency scatterometer
p 45 N84-27282

MICROWAVE SCATTERING

A scatter model for vegetation up to Ku-band
p 7 A84-37201
Microwave backscattering characteristics of wind-generated waves
p 36 A84-38309
Ocean wind field measurement performance of the ERS-1 scatterometer
p 43 N84-27273
SAR imagery of ocean-wave swell traveling in an arbitrary direction
p 44 N84-27278

MICROWAVE SENSORS

Microwave measurements using active and passive sensors --- for agriculture in India
p 1 A84-30229
Microwave scatterometer
p 66 A84-38310
ESA activities in the use of microwaves for the remote sensing of the Earth
p 42 N84-27264
High resolution observations of low contrast phenomena from an Advanced Geosynchronous Platform (AGP)
p 42 N84-27266

New algorithms for microwave measurements of ocean winds
p 43 N84-27272

MICROWAVE SOUNDING

Satellite observations of a monsoon depression
[NASA-CR-173590] p 40 N84-26232

MICROWAVE SPECTRA

Active microwave responses - An aid in improved crop classification
p 3 A84-31498
Two-frequency microwave resonance measurements from an aircraft - A quantitative estimate of the directional ocean surface spectrum
p 34 A84-34942

MICROWAVES

Microwave remote sensing of ocean surface wind speed and rain rates over tropical storms
p 45 N84-27288

MIDDLE ATMOSPHERE

Atmospheric science --- overview of stratosphere and mesosphere satellite remote sounding experiments
p 66 A84-38923

MINERAL DEPOSITS

Application of Landsat data in the exploration of 'Calcrete' uranium deposits
p 24 A84-37775

MINERAL EXPLORATION

Remote sensing as a tool for mineral prospecting
p 22 A84-30259
Remote sensing for bauxite prospecting
p 22 A84-30260

Metallogenesis - Use of remote sensing for ore deposit prospecting indicators linked to nonoutcropping leucogranitic apexes
p 23 A84-30878

The use of satellite photos for analyzing the structural and dynamic conditions surrounding the formation of ancient deposits of phlogopite and apatite
p 23 A84-34781

Application of Landsat data in the exploration of 'Calcrete' uranium deposits
p 24 A84-37775
Radar geology of the Shelleng-Numan area in Nigeria - An evaluation
p 24 A84-38940

The Duffek intrusion of Antarctica and a survey of its minor metals related to possible resources
p 25 N84-23943

Emerging recognition of the nonfuel mineral resources of Arctic Alaska
p 26 N84-23962

Project SERGE: Brazil referential field data for the SIR-A experiment
[INPE-2973-NTF/210] p 29 N84-27259

MINERALOGY

An analysis of tectonics and metallogeny of Orissa state, India with remote sensing technique
p 22 A84-30247

SUBJECT INDEX

Petrologic and geophysical sources of long-wavelength crustal magnetic anomalies
[NASA-CR-175245] p 29 N84-28276

MINERALS
Use of MAGSAT anomaly data for crustal structure and mineral resources in the US midcontinent
[E84-10112] p 24 N84-23005

MISSISSIPPI
Application of remote sensing to state and regional problems
[E84-10128] p 68 N84-23986

MISSISSIPPI RIVER (US)
Application of remote sensing to state and regional problems
[E84-10128] p 68 N84-23986

MODULATION
On the detection of underwater bottom topography by imaging radars
p 46 N84-27301

MOISTURE CONTENT
CONSERVB: A numerical method to compute soil water content and temperature profiles under a bare surface
[E84-10113] p 9 N84-23006

MONSOONS
Bay monsoon activities in relation to the monsoon in the western Pacific
p 30 A84-30232
Aircraft measurements of convective draft cores in MONEX
p 31 A84-31821
Elements of the west African monsoon circulation deduced from Meteosat cloud winds and simultaneous aircraft measurements
p 51 A84-31948
Eurasian snow cover versus Indian monsoon rainfall - An extension of the Hahn-Shukla results
p 51 A84-31950
Satellite observations of a monsoon depression
[NASA-CR-173590] p 40 N84-26232

MOTHS
The Pennsylvania defoliation application pilot test
[E84-10111] p 8 N84-23004

MOUNTAINS
Hydrological data densification in mountainous terrain using Landsat imagery
p 51 A84-30256
Surveying in Antarctica during the International Geophysical Year
p 25 N84-23942
Program for mapping Antarctica
p 19 N84-23954

MULTICHANNEL COMMUNICATION
A summary of results from the first Nimbus 7 SMMR observations
p 37 A84-39459

MULTISPECTRAL BAND SCANNERS
Assessing change in the surficial character of a semiarid environment with Landsat residual images
p 3 A84-31499
Comparative accuracies of AVHRR and MSS data used for Level I land cover classifications
p 14 A84-33344
Characterization of Landsat-4 MSS and TM digital image data
p 56 A84-33526
Analysis and processing of Landsat-4 sensor data using advanced image processing techniques and technologies
p 56 A84-33527
Landsat-4 MSS and Thematic Mapper data quality and information content analysis
p 56 A84-33528
Revised radiometric calibration technique for Landsat-4 Thematic Mapper data
p 56 A84-33530
In-flight absolute radiometric calibration of the Thematic Mapper
p 56 A84-33531
A physically-based transformation of Thematic Mapper data The TM tasseled cap
p 56 A84-33532
Thematic Mapper image quality - Registration, noise, and resolution
p 57 A84-33533
Comparison of the information content of data from the Landsat-4 Thematic Mapper and the Multispectral Scanner
p 57 A84-33534
Cartographic accuracy of Landsat-4 MSS and TM image data
p 57 A84-33535
An analysis of Landsat-4 Thematic Mapper geometric properties
p 57 A84-33536
A statistical evaluation of the advantages of Landsat Thematic Mapper data in comparison to Multispectral Scanner data
p 57 A84-33537
Spectral variability of Landsat-4 Thematic Mapper and Multispectral Scanner data for selected crop and forest cover types
p 5 A84-33538
Evaluation of corn/soybeans separability using Thematic Mapper and Thematic Mapper Simulator data
p 5 A84-33539
Classification of snow surface conditions by means of Landsat MSS data under compensation of slope effects
p 52 A84-38296
Landsat MSS data used for crop identification at the limit of its spatial resolution
p 8 A84-38299
Study on temporal geometric-distortion variation of Landsat MSS and RBV imageries and attitude determination program
p 59 A84-38313
Atmospheric correction of Landsat MSS data for a multiday suspended sediment algorithm
p 59 A84-38942

Spectroradiometric calibration of the Thematic Mapper and multispectral scanner system
[E84-10098] p 67 N84-23000
Sensor radiance for a midlatitude atmospheric model
p 68 N84-23001
In-flight absolute radiometric calibration of the Thematic Mapper --- White Sands, New Mexico
p 68 N84-23002
Correlating aerial photographs to LANDSAT Multispectral Sensor (MSS) data to measure ground control points
p 69 N84-23150
Spectroradiometric calibration of the Thematic Mapper and Multispectral Scanner system --- White Sands, New Mexico
[E84-10136] p 70 N84-26084
Discriminating vegetation and soils using LANDSAT MSS and Thematic Mapper bands and band ratios
[AD-A140198] p 11 N84-26108

MULTISPECTRAL PHOTOGRAPHY
The effect of fluctuations in the optical properties of the atmosphere on spectral brightness ratios in the remote sensing of agricultural areas
p 6 A84-34777
Interpreting multispectral photographs obtained in the Telefoto-80 experiment so as to distinguish crop types
p 6 A84-34780
Regression in the primal problem of remote sensing (using grass cover as an example)
p 6 A84-34785
LANDSAT 4 investigations of Thematic Mapper and multispectral scanner applications --- Death Valley, California; Silver Bell Copper Mine, Arizona, and Dulles Airport near Washington, D.C.
[E84-10100] p 60 N84-23003

MULTISPECTRAL RADAR
The theory of Earth observation using multiple-frequency radar
[ESA-TT-819] p 63 N84-26105

MULTIVARIATE STATISTICAL ANALYSIS
Estimation of variances and covariances in the multivariate and in the incomplete multivariate model
p 20 N84-26073

N

NASA PROGRAMS
Remote sensing of the oceans --- Japanese book
p 35 A84-37299
NASA Oceanic Processes Program, fiscal year 1983
[NASA-TM-86248] p 39 N84-24078
NASA, the first 25 years: 1958 - 1983
[NASA-EP-182] p 72 N84-26563

NATURAL GAS EXPLORATION
Topography interpretation possibilities for satellite photos in regions where the platform mantle has a multilayer structure (on the example of the eastern marginal part of the Caspian depression)
p 23 A84-34779
The use of remote sensing in the search for hydrocarbons in the Kerch peninsula
p 23 A84-34782

NEARSHORE WATER
Dynamics of the slope water off New England and its influence on the Gulf Stream as inferred from satellite IR data
p 31 A84-30672

NETWORK CONTROL
General triangulation: Incorporating photogrammetric and other observations
p 69 N84-25151

NEVADA
Riparian habitat on the Humboldt River, Deeth to Elko, Nevada
[E84-10116] p 53 N84-23976

NERGERIA
Radar geology of the Shelleng-Numan area in Nigeria - An evaluation
p 24 A84-38940

NIMBUS 5 SATELLITE
Dual channel satellite measurements of sea surface temperature
p 31 A84-31431
A comparison of numerical results of Arctic Sea ice modeling with satellite images
p 39 N84-23969

NIMBUS 7 SATELLITE
The validation of Nimbus 7 LIMS measurements of ozone
p 67 A84-39443
Intercomparison of the Nimbus 7 SBUV/TOMS total ozone data sets with Dobson and M83 results --- Solar Backscattered Ultraviolet/Total Ozone Mapping Spectrometer
p 67 A84-39449
A summary of results from the first Nimbus 7 SMMR observations
p 37 A84-39459
Development of Great Lakes algorithms for the Nimbus-G coastal zone color scanner
[NASA-CR-173511] p 53 N84-27258

NITRIC ACID
Accuracy and precision of the nitric acid concentrations determined by the limb infrared monitor of the stratosphere experiment on NIMBUS 7
p 67 A84-39444

NOAA SATELLITES
The analysis and digital signal processing of NOAA's surface current mapping system
p 30 A84-30024

SUBJECT INDEX

Vegetation monitoring and classification using NOAA/AVHRR satellite data p 4 A84-33343
 Intensive forest clearing in Rondonia, Brazil, as detected by satellite remote sensing p 8 A84-37204
 Joint analysis of Landsat-MSS and NOAA-AVHRR data for marine environmental monitoring p 35 A84-38298

NOAA 6 SATELLITE
 AVHRR aerosol ground truth experiment [PB84-157882] p 39 N84-24065

NORTHERN HEMISPHERE
 The impact of scatterometer wind data on global weather forecasting p 49 N84-27314

NUMERICAL CONTROL
 Photogrammetric research (TRITA-FMI-47) p 69 N84-25146
 The question of accuracy in the transition from analogue to analytic photogrammetry p 69 N84-25153

NUMERICAL WEATHER FORECASTING
 Global data assimilation experiments with scatterometer winds from SEASAT-A p 65 A84-32938
 The impact of scatterometer wind data on global weather forecasting p 49 N84-27314
 Outlook for improved numerical weather prediction using satellite data with a special emphasis on the hydrological variables [AD-A141233] p 54 N84-28344

O

OCEAN BOTTOM
 Oceanic fracture zones p 31 A84-31193
 Seasat observations of lithospheric flexure seaward of trenches p 32 A84-34339
 Mapping the sea floor by satellite p 35 A84-36686
 Error analysis for marine geodetic control using the global positioning system [AD-A140566] p 21 N84-26687
 On the detection of underwater bottom topography by imaging radars p 46 N84-27301
 Modeling of SAR signatures of shallow water ocean topography p 47 N84-27302

OCEAN COLOR SCANNER
 Observations of Gulf Stream-induced and wind-driven upwelling in the Georgia Bight using ocean color and infrared imagery p 34 A84-34517

OCEAN CURRENTS
 The analysis and digital signal processing of NOAA's surface current mapping system p 30 A84-30024
 Rapid evolution of a Gulf Stream warm-core ring p 32 A84-34164
 Mean circulation and eddy kinetic energy in the eastern North Atlantic p 32 A84-34501
 Lagrangian observations of an anticyclonic ring in the western Gulf of Mexico p 33 A84-34502
 The evolution of mushroom-shape currents in the ocean p 36 A84-38773
 Topex: Observing the oceans from Space [NASA-CR-173490] p 38 N84-23085
 Seasonal oscillations of the subtropical convergence between the Brazil and Malvinas currents, using oceanographic and SMS-2 satellite data [INPE-3092-PRE/497] p 40 N84-26255
 Frontiers of Remote Sensing of the Oceans and Troposphere from Air and Space Platforms [NASA-CP-2303] p 42 N84-27262
 On the response to ocean surface currents in synthetic aperture radar imagery p 47 N84-27304
 The depiction of Alboran Sea Gyre during *Donde Va?* using remote sensing and conventional data p 47 N84-27306
 Somali current studied from SEASAT altimetry p 47 N84-27307
 Simulation and assimilation of satellite altimeter data at the oceanic mesoscale p 48 N84-27312
 The importance of altimeter and scatterometer data for ocean prediction p 49 N84-27316
 Sampling strategies and four-dimensional assimilation of altimetric data for ocean monitoring and prediction p 49 N84-27317

OCEAN DATA ACQUISITIONS SYSTEMS

A theoretical study of an airborne laser technique for determining sea water turbidity p 31 A84-33774
 Airborne lidar for oceanography and hydrology (FLOH) [ESA-TT-799] p 37 N84-22955
 Comparisons of sea-surface temperature obtained from ship and satellite data [AD-A138257] p 38 N84-23087
 Integrated Global Ocean Services System (IGOSS): Guide to the IGOSS data processing and services system [WMO-623] p 38 N84-23089
 Recent advances in multispectral sensing of ocean surface temperature from space p 46 N84-27297

OCEAN DYNAMICS

Rapid evolution of a Gulf Stream warm-core ring p 32 A84-34164
 First observations of the interaction of ocean swell with sea ice using satellite radar altimeter data p 35 A84-36684

OCEAN MODELS

A model for the analysis of drifter data with an application to a warm core ring in the Gulf of Mexico p 33 A84-34503

Nimbus 7 SMMR derived seasonal variations in the water vapor, liquid water and surface winds over the global oceans [NASA-TM-86080] p 40 N84-26233

Synthetic aperture radar images of ocean waves, theories of imaging physics and experimental tests p 43 N84-27275

Optimum backscatter cross section of the ocean as measured by synthetic aperture radars p 44 N84-27276

Tracking ocean wave spectrum from SAR images p 44 N84-27277

On the detection of underwater bottom topography by imaging radars p 46 N84-27301

The importance of altimeter and scatterometer data for ocean prediction p 49 N84-27316

Sampling strategies and four-dimensional assimilation of altimetric data for ocean monitoring and prediction p 49 N84-27317

The influence of actual and apparent geoid error on ocean analysis and prediction p 49 N84-27318

OCEAN SURFACE

Digital processing considerations for extraction of ocean wave image spectra from raw synthetic aperture radar data p 30 A84-30025

Interpreting the spectra of aerial photographs of the sea surface p 30 A84-30443

The radar altimeter for ERS-1 Satellite p 64 A84-30516

Global data assimilation experiments with scatterometer winds from SEASAT-A p 65 A84-32938

Downdrafts from tropical oceanic cumuli p 32 A84-33985

Theory and validation of the multiple window sea surface temperature technique p 33 A84-34513

A model function for ocean radar cross sections at 14.6 GHz p 34 A84-34516

Two-frequency microwave resonance measurements from an aircraft - A quantitative estimate of the directional ocean surface spectrum p 34 A84-34942

The effect of ocean surface temperature on the trajectories of tropical cyclones p 34 A84-35252

Effective reflectance of oceanic whitecaps p 35 A84-36119

Satellite observations of the 1982-1983 El Nino along the U.S. Pacific coast p 35 A84-36872

Theory of radio wave propagation over the sea surface p 35 A84-37095

Remote sensing of the ocean by the airborne microwave scatterometer/radiometer system p 36 A84-38307

Microwave backscattering characteristics of wind-generated waves p 36 A84-38309

Topex: Observing the oceans from Space [NASA-CR-173490] p 38 N84-23085

Comparisons of sea-surface temperature obtained from ship and satellite data [AD-A138257] p 38 N84-23087

Wind, waves and swell in the Antarctic marginal ice zone by SEASAT radar altimeter p 38 N84-23941

The use of satellite observations of the ocean surface in commercial fishing operations [AD-P003120] p 41 N84-26261

Ocean wind field measurement performance of the ERS-1 scatterometer p 43 N84-27273

Theory and measure of certain image norms in SAR p 43 N84-27274

Synthetic aperture radar images of ocean waves, theories of imaging physics and experimental tests p 43 N84-27275

Optimum backscatter cross section of the ocean as measured by synthetic aperture radars p 44 N84-27276

Tracking ocean wave spectrum from SAR images p 44 N84-27277

SAR imagery of ocean-wave swell traveling in an arbitrary direction p 44 N84-27278

Ocean waves and turbulence as observed with an adaptive coherent multifrequency radar p 44 N84-27279

The dual-frequency scatterometer reexamined p 44 N84-27280

An improved dual-frequency technique for the remote sensing of ocean currents and wave spectra p 44 N84-27281

OCEANOGRAPHY

Measurements of ocean wave spectra and modulation transfer function with the airborne two frequency scatterometer p 45 N84-27282

Some case studies of ocean wave physical processes utilizing the GSFC airborne radar ocean wave spectrometer p 45 N84-27283

Microwave remote sensing of ocean surface wind speed and rain rates over tropical storms p 45 N84-27288

Recent advances in multispectral sensing of ocean surface temperature from space p 46 N84-27297

Satellite techniques for determining the geopotential for sea-surface elevations p 46 N84-27298

On the response to ocean surface currents in synthetic aperture radar imagery p 47 N84-27304

Variations in surface current off the coasts of Canada as inferred from infrared satellite imagery p 47 N84-27305

Sampling strategies and four-dimensional assimilation of altimetric data for ocean monitoring and prediction p 49 N84-27317

The influence of actual and apparent geoid error on ocean analysis and prediction p 49 N84-27318

Ocean optical remote sensing capability statement [AD-A140589] p 49 N84-27321

Speckle statistics in radar images of sea surface obtained with horizontal polarization p 50 N84-27921

Observing ocean-atmosphere exchanges with space-borne sensors, appendix C p 50 N84-28298

Satellite-Derived Sea Surface Temperature: Workshop-2 [NASA-CR-173740] p 50 N84-28355

Microwave radiometric measurement of sea surface salinity [AD-A141302] p 50 N84-28359

OCEAN TEMPERATURE

Dual channel satellite measurements of sea surface temperature p 31 A84-31431

Theory and validation of the multiple window sea surface temperature technique p 33 A84-34513

Satellite observations of the 1982-1983 El Nino along the U.S. Pacific coast p 35 A84-36872

Airborne lidar for oceanography and hydrology (FLOH) [ESA-TT-799] p 37 N84-22955

Comparisons of sea-surface temperature obtained from ship and satellite data [AD-A138257] p 38 N84-23087

Seasonal oscillations of the subtropical convergence between the Brazil and Malvinas currents, using oceanographic and SMS-2 satellite data [INPE-3092-PRE/497] p 40 N84-26255

Variations in surface current off the coasts of Canada as inferred from infrared satellite imagery p 47 N84-27305

Satellite-Derived Sea Surface Temperature: Workshop-2 [NASA-CR-173740] p 50 N84-28355

OCEANOGRAPHIC PARAMETERS

Monitoring the marine environment with remote sensing technology p 30 A84-30258

The ESA ocean observation satellite ERS-1. I - Description of the history, goals, and payload of ERS-1 p 31 A84-32266

CZCS data analysis in turbid coastal water p 37 A84-39427

Integrated Global Ocean Services System (IGOSS): Guide to the IGOSS data processing and services system [WMO-623] p 38 N84-23089

Maps of favorable areas for tuna fishing to the South and Southeast of Brazil prepared from SMS-2 satellite data [INPE-3102-PRE/501] p 41 N84-26256

OCEANOGRAPHY

The analysis and digital signal processing of NOAA's surface current mapping system p 30 A84-30024

Mapping the sea floor by satellite p 35 A84-36686

Remote sensing of the oceans -- Japanese book p 35 A84-37299

Scientific activity in oceanography, 1979-1982 p 38 N84-23084

Topex: Observing the oceans from Space [NASA-CR-173490] p 38 N84-23085

NASA Oceanic Processes Program, fiscal year 1983 [NASA-TM-86248] p 39 N84-24078

PAME Proceedings, Pattern Analysis in the Marine Environment, An Ocean Science and Technology Workshop [AD-A140195] p 41 N84-26257

Remote sensing for oceanography: Past, present, future p 42 N84-27263

High resolution observations of low contrast phenomena from an Advanced Geosynchronous Platform (AGP) p 42 N84-27266

A tentative unified sea model for scattering and emission p 45 N84-27285

Altimeter height measurement errors introduced by the presence of variable cloud and rain attenuation p 45 N84-27289

Publications and reports of the Institute of Oceanographic Sciences 1979-1982 [IOS-170] p 50 N84-28354

OCEANS

Monthly distributions of precipitable water from the Nimbus 7 SMMR data p 37 A84-39458

AVHRR aerosol ground truth experiment [PB84-157882] p 39 N84-24065

Nimbus 7 SMMR derived seasonal variations in the water vapor, liquid water and surface winds over the global oceans [NASA-TM-86080] p 40 N84-26233

PAME Proceedings, Pattern Analysis in the Marine Environment, An Ocean Science and Technology Workshop [AD-A140195] p 41 N84-26257

Frontiers of Remote Sensing of the Oceans and Troposphere from Air and Space Platforms [NASA-CP-2303] p 42 N84-27262

ESA activities in the use of microwaves for the remote sensing of the Earth p 42 N84-27264

Scatterometer capabilities in remotely sensing geophysical parameters over the ocean: The status and the possibilities p 42 N84-27268

New algorithms for microwave measurements of ocean winds p 43 N84-27272

Some case studies of ocean wave physical processes utilizing the GSFC airborne radar ocean wave spectrometer p 45 N84-27283

Improved resolution rain measurements from spaceborne radar altimeters p 46 N84-27290

The importance of altimeter and scatterometer data for ocean prediction p 49 N84-27316

OIL EXPLORATION

Topography interpretation possibilities for satellite photos in regions where the platform mantle has a multilayer structure (on the example of the eastern marginal part of the Caspian depression) p 23 A84-34779

The use of remote sensing in the search for hydrocarbons in the Kerch peninsula p 23 A84-34782

OPERATIONAL PROBLEMS

Benefits and problems in operational remote sensing p 64 A84-30252

OPERATORS (MATHEMATICS)

Simple enhancement techniques in digital image processing p 58 A84-33798

OPTICAL CORRECTION PROCEDURE

Atmospheric correction of Landsat MSS data for a multilayer suspended sediment algorithm p 59 A84-38942

OPTICAL MEASUREMENT

Sensitivity of airborne fluorosensor measurements to linear vertical gradients in chlorophyll concentration p 30 A84-30302

OPTICAL PROPERTIES

Airborne observations of Arctic aerosol. IV - Optical properties of Arctic haze p 32 A84-34287

OPTICAL RADAR

Airborne lidar for oceanography and hydrology (FLOH) [ESA-TT-799] p 37 N84-22955

Applications of laser for climatology and atmospheric research [BLEV-R-65.169-5] p 70 N84-26237

Fundamentals of spaceborne remote sensing: Applications of lasers, volume 1 p 70 N84-26238

Applications of airborne remote sensing in atmospheric sciences research p 71 N84-27286

OPTICAL SCANNERS

Conditions for the illumination of an area in satellite scanner surveys p 65 A84-34787

Principal components as a method for atmospherically correcting coastal zone color scanner data [AD-P003124] p 41 N84-26265

OPTICAL THICKNESS

A bispectral method for the height determination of optically thin ice clouds p 60 A84-39044

High-precision atmospheric ozone measurements using wavelengths between 290 and 305 nm p 67 A84-39447

SAGE and SAM II measurements of global stratospheric aerosol optical depth and mass loading p 15 A84-39455

ORBITAL POSITION ESTIMATION

A Doppler positioning cost model --- for cadastral geodetic surveys p 18 A84-33365

ORCHARDS

Benchmark data on the separability between orchards and vineyards in the southern San Joaquin Valley of California p 5 A84-33348

ORTHOGONAL FUNCTIONS

Matrix partitioning and EOF/principal component analysis of Antarctic Sea ice brightness temperatures [NASA-TM-83916] p 49 N84-27319

ORTHOPHOTOGRAPHY

Correlation calculation in stereoscopic image pairs for the automatic acquisition of digital land models, orthopictures and height line planes [SER-C283] p 21 N84-26079

OUTCROPS

Field data observed during the geological excursion in the west-central region of the Sul-RioGrande Shield [E84-10146] p 29 N84-26094

OUTLIERS (STATISTICS)

Seminar on mathematical models of geodetic/photogrammetric point determination with regard to outliers and systematic errors [SER-A-98] p 20 N84-26069

OZONOMETRY

Recent investigations of ozone and minor atmospheric gases p 14 A84-34450

The validation of Nimbus 7 LIMS measurements of ozone p 67 A84-39443

High-precision atmospheric ozone measurements using wavelengths between 290 and 305 nm p 67 A84-39447

Intercomparison of the Nimbus 7 SBUV/TOMS total ozone data sets with Dobson and M83 results --- Solar Backscattered Ultraviolet/Total Ozone Mapping Spectrometer p 67 A84-39449

P

PACIFIC OCEAN

Bay monsoon activities in relation to the monsoon in the western Pacific p 30 A84-30232

Comparisons of sea-surface temperature obtained from ship and satellite data [AD-A138257] p 38 N84-23087

The variability of the surface wind field in the equatorial Pacific Ocean: Criteria for satellite measurements p 46 N84-27296

Vector wind, horizontal divergence, wind stress and wind stress curl from SEASAT-SASS at one degree resolution p 48 N84-27313

PANORAMIC CAMERAS

Applications of the Enviro-pod with KA-85A panoramic cameras in south-eastern historic and pre-historic archaeological survey p 23 A84-33327

PARAMETER IDENTIFICATION

The radar altimeter for ERS-1 Satellite p 64 A84-30516

Research and applications of data from environmental satellites: Determining parameters and developing interpretation techniques for applications of environmental satellite data [INPE-3005-NTE/213] p 13 N84-27261

Scatterometer capabilities in remotely sensing geophysical parameters over the ocean: The status and the possibilities p 42 N84-27268

PARAMETERIZATION

A new parameterization of an empirical model for wind/ocean scatterometry p 43 N84-27269

PATTERN RECOGNITION

Interactive procedures for distinguishing and reconstructing contour networks --- in aerospace computer aided photomapping p 58 A84-34786

Distinguishing linear contour elements on satellite photos on the basis of a visual perception model p 24 A84-34789

Evaluation of entropy and JM-distance criterions as features selection methods using spectral and spatial features derived from LANDSAT images [E84-10141] p 62 N84-26089

Cartographic feature extraction on ETL's (Engineer Topographic Laboratories') DIAL (Digital Image Analysis Laboratory) system [AD-A140230] p 63 N84-26112

PAME Proceedings, Pattern Analysis in the Marine Environment, An Ocean Science and Technology Workshop [AD-A140195] p 41 N84-26257

Principal components as a method for atmospherically correcting coastal zone color scanner data [AD-P003124] p 41 N84-26265

PATTERN REGISTRATION

Thematic Mapper image quality - Registration, noise, and resolution p 57 A84-33533

Investigation of several aspects of LANDSAT-4 data quality --- Sacramento, San Francisco, and NE Arkansas [E84-10122] p 60 N84-23981

The use of an image registration technique in the urban growth monitoring [E84-10147] p 16 N84-26095

Evaluation of SIR-A (Shuttle Imaging Radar) images from the Tres Mares region (Minas Gerais State, Brazil) using derived spatial features and registration with MSS-LANDSAT images [E84-10148] p 62 N84-26096

PENNSYLVANIA

The Pennsylvania defoliation application pilot test [E84-10111] p 8 N84-23004

PERFORMANCE PREDICTION

The radar altimeter for ERS-1 Satellite p 64 A84-30516

PERMAFROST

Hydrology of the North Slope, Alaska p 53 N84-23973

PETROLOGY

An analysis of tectonics and metallogeny of Orissa state, India with remote sensing technique p 22 A84-30247

PHENOLogy

Sampling system for wheat (*Triticum aestivum* L) area estimation using digital LANDSAT MSS data and aerial photographs --- Brazil [E84-10139] p 10 N84-26087

PHOTOABSORPTION

Computer-automated CO₂-laser long-path absorption system for air quality monitoring in the working environment p 13 A84-30307

PHOTOGEOLogy

An analysis of tectonics and metallogeny of Orissa state, India with remote sensing technique p 22 A84-30247

Topography interpretation possibilities for satellite photos in regions where the platform mantle has a multilayer structure (on the example of the eastern marginal part of the Caspian depression) p 23 A84-34779

The use of satellite photos for analyzing the structural and dynamic conditions surrounding the formation of ancient deposits of phlogopite and apatite p 23 A84-34781

The use of remote sensing in the search for hydrocarbons in the Kerch peninsula p 23 A84-34782

Distinguishing linear contour elements on satellite photos on the basis of a visual perception model p 24 A84-34789

Radar geology of the Shelleng-Numan area in Nigeria - An evaluation p 24 A84-38940

Utilization of digital LANDSAT imagery for the study of granitoid bodies in Rondonia: Case example of the Pedra Branca massif [E84-10120] p 26 N84-23979

Multiseasonal variables in digital image enhancements for geological applications [E84-10145] p 29 N84-26093

Field data observed during the geological excursion in the west-central region of the Sul-RioGrande Shield [E84-10146] p 29 N84-26094

Methodological approach in lithological discrimination by digital processing: A case study in the Serra do Ramalho, state of Bahia [INPE-3108-PRE/507] p 29 N84-26101

PHOTOGAMMOMETRY

Analysing forest structures by remote sensing p 1 A84-30236

A rapid method for obtaining frequency-response functions for multiple input photogrammetric data [AIAA PAPER 84-1060] p 65 A84-31741

American Society of Photogrammetry, Annual Meeting, 49th, Washington, DC, March 13-18, 1983, Technical Papers p 65 A84-33326

American Congress on Surveying and Mapping, Annual Meeting, 43rd, Washington, DC, March 13-18, 1983, Technical Papers p 18 A84-33357

Coastal mapping of the Beaufort Sea coast p 31 A84-33360

A forecast of the impact of GPS on surveying p 18 A84-33374

Equidensitometry and remote sensing imagery p 59 A84-38944

Antarctic mapping and international coordination p 19 A84-23935

Photogrammetric research [TRITA-FMI-47] p 69 N84-25146

Photogrammetric research at the Royal Institute of Technology, Stockholm, Sweden p 69 N84-25147

Mathematical aspects of digital terrain information. A progress report from ISPRS Working Group III:3 p 61 N84-25148

General triangulation: Incorporating photogrammetric and other observations p 69 N84-25151

GENTRI: A system for simultaneous adjustment of photogrammetric and other observations p 69 N84-25152

The question of accuracy in the transition from analogue to analytic photogrammetry p 69 N84-25153

Multi-models to increase accuracy p 70 N84-25154

Seminar on mathematical models of geodetic/photogrammetric point determination with regard to outliers and systematic errors [SER-A-98] p 20 N84-26069

Mathematical models of photogrammetric point determination p 20 N84-26070

Stochastic models for point manifolds p 20 N84-26072

SUBJECT INDEX

Estimation of variances and covariances in the multivariate and in the incomplete multivariate model p 20 N84-26073

Several aspects of the sequential processing of photogrammetric bundle blocks p 21 N84-26077

Correlation calculation in stereoscopic image pairs for the automatic acquisition of digital land models, orthopictures and height line planes [SER-C283] p 21 N84-26079

Fisheye objective in the dose range photogrammetry: Theoretical and practical investigations [SER-C-286] p 21 N84-26080

PHOTOGRAPHIC PROCESSING

Experiments in lithography from remote sensor imagery p 55 A84-33362

Equidensitometry and remote sensing imagery p 59 A84-38944

PHOTOINTERPRETATION

Application of multi-concept in remote sensing technique for identification and mapping of soil units of alluvial plain for land use planning in Sri Lanka p 13 A84-30241

Interpreting the spectra of aerial photographs of the sea surface p 30 A84-30443

Atmospheric effect on classification of finite fields --- satellite-imaged agricultural areas p 2 A84-30670

Geological interpretation from aerial remote sensing images of Tengchong area p 23 A84-32590

Landsat imagery for the interpretation of Louisiana forest habitat regions p 3 A84-33328

Analysis of photo interpretation test results for seven aerospace image types of the San Juan National Forest, Colorado p 4 A84-33332

Terrain analysis database generation through computer-assisted photo interpretation p 55 A84-33334

Automated classification of wetlands p 4 A84-33337

Automated vegetation classification using Thematic Mapper Simulation data p 5 A84-33347

Benchmark data on the separability between orchards and vineyards in the southern San Joaquin Valley of California p 5 A84-33348

Topography interpretation possibilities for satellite photos in regions where the platform mantle has a multilayer structure (on the example of the eastern marginal part of the Caspian depression) p 23 A84-34779

Interpreting multispectral photographs obtained in the Telefoto-80 experiment so as to distinguish crop types p 6 A84-34780

Interactive procedures for distinguishing and reconstructing contour networks -- in aerospace computer aided photomapping p 58 A84-34786

Classifying northern forests using Thematic Mapper Simulator data p 7 A84-34961

Experiments to correct a digital map data base using scene analysis [AD-A139447] p 61 N84-24499

Irrigated rice area estimation using remote sensing techniques: Project's proposal and preliminary results --- Rio Grande do Sul, Brazil [E84-10131] p 10 N84-26081

Results of field observations of radio waves in alluvial deposits in Cara state from 1:100.000: Fortaleza, Caninde, Taperuaba, Santa Quiteria, Sobral, and Sao Luiz do Curi [INPE-3061-NTE/216] p 53 N84-26100

The use of photointerpretation for socio-economic characterization of urban population [INPE-3067-PRE/484] p 16 N84-26428

LANDSAT 4 investigations of Thematic Mapper and Multispectral Scanner applications [E84-10152] p 63 N84-27247

Evaluation of spatial, radiometric and spectral Thematic Mapper performance for coastal studies [E84-10159] p 12 N84-27251

Ocean waves and turbulence as observed with an adaptive coherent multifrequency radar p 44 N84-27279

PHOTOMAPPING

Reduction of high dimension data to two dimension using non linear mapping techniques p 54 A84-30248

An undetectable factor in geomorphological mapping from land satellite images - A case study in the central highland, Thailand p 22 A84-30261

Landsat planimetric maps p 54 A84-30264

Description of SEP ground station and Vizir image processing VIPS -- for Spot and Landsat 4 satellites p 54 A84-30268

Applications of the Enviro-pod with KA-85A panoramic cameras in south-eastern historic and pre-historic archaeological survey p 23 A84-33327

Soil erosion mapping and evaluation - A photo-geomorphological approach p 14 A84-33333

Drainage pattern delineation - A function of image scale p 52 A84-33353

Estimation of depth of snow from Landsat imagery p 52 A84-33355

Cartographic accuracy of Landsat-4 MSS and TM image data p 57 A84-33535

An analysis of Landsat-4 Thematic Mapper geometric properties p 57 A84-33536

Mapping of exogenic terrain dynamics on the basis of space photographs (on the example of the Baikal region) p 18 A84-34491

User guide for the USGS aerial camera report of calibration p 65 A84-34958

Potential benefits of new satellite sensors to wetland mapping p 7 A84-34960

Satellite image atlas of glaciers: The Polar regions p 38 N84-23940

EPA Enviropod. A summary of the use of the Enviropod under a Memorandum of Understanding among EPA Region 8, the State of Utah, and the University of Utah Research Institute [E84-10124] p 15 N84-23983

Aerial photography for ecological site mapping p 9 N84-23990

Ocean wind field measurement performance of the ERS-1 scatterometer p 43 N84-27273

PHOTOMAPS

Making false color photomap and its application in thematic mapping by using IR photos p 54 A84-30249

PHOTOMETERS

A comparative study of aerosol extinction measurements made by the SAM II and SAGE satellite experiments p 15 A84-39457

PHOTORECONNAISSANCE

Riparian habitat on the Humboldt River, Death to Elko, Nevada [E84-10116] p 53 N84-23976

Fisheye objective in the dose range photogrammetry: Theoretical and practical investigations [SER-C-286] p 21 N84-26080

PHOTORESISTIVITY

Sensitivity of airborne fluorosensor measurements to linear vertical gradients in chlorophyll concentration p 30 A84-30302

PHOTOVOLTAIC CELLS

Publications of the Jet Propulsion Laboratory 1982 [NASA-CR-173539] p 71 N84-25510

PLANETARY GRAVITATION

Construction of a system of point masses representing the gravitational field of the planet on the basis of satellite observations. I - An algorithm derivation p 19 A84-37069

PLANT ROOTS

A microwave systems approach to measuring root zone soil moisture [E84-10114] p 9 N84-23007

PLATES (TECTONICS)

Oceanic fracture zones p 31 A84-31193

Cenozoic tectonics of the Caribbean: Structural and stratigraphic studies in Jamaica and Hispaniola p 25 N84-23062

Discussion of the design of satellite-laser measurement stations in the eastern Mediterranean under the geological aspect. Contribution to the earthquake prediction research by the Wegener Group and to NASA's Crustal Dynamics Project [NASA-TM-77412] p 26 N84-24031

Correlation of tectonic provinces of South America and the Caribbean region with MAGSAT anomalies p 27 N84-25130

Satellite elevation magnetic and gravity models of major South American plate tectonic features p 27 N84-25131

POINT SPREAD FUNCTIONS

LANDSAT-4 image data quality analysis [E84-10158] p 63 N84-27250

POLAR WANDERING (GEOLOGY)

Modeling the movement at the polar ice cap at the South Pole p 20 N84-23957

POLARIMETERS

Spectroradiometric calibration of the Thematic Mapper and Multispectral Scanner system -- White Sands, New Mexico [E84-10136] p 70 N84-26084

POLARIZATION (WAVES)

Crop moisture estimation over the southern Great Plains with dual polarization 1.66 centimeter passive microwave data from Nimbus 7 [E84-10163] p 12 N84-27255

POLLUTION MONITORING

Computer-automated CO₂-laser long-path absorption system for air quality monitoring in the working environment p 13 A84-30307

Recent investigations of ozone and minor atmospheric gases p 14 A84-34450

RADAR GEOLGY

POLYSTATION DOPPLER TRACKING SYSTEM

Development of satellite Doppler/inertial survey systems for BLM cadastral survey-related applications in Alaska p 14 A84-33370

POPULATIONS

The use of an image registration technique in the urban growth monitoring [E84-10147] p 16 N84-26095

POSITIONING

Present limitations of accurate satellite Doppler positioning for tectonics - An example: Djibouti p 17 A84-32495

PRECAMBRIAN PERIOD

The use of satellite photos for analyzing the structural and dynamic conditions surrounding the formation of ancient deposits of phlogopite and apatite p 23 A84-34781

PRECIPITATION (METEOROLOGY)

Monthly distributions of precipitable water from the Nimbus 7 SMMR data p 37 A84-39458

PRINCIPAL COMPONENTS ANALYSIS

Matrix partitioning and EOF/principal component analysis of Antarctic Sea ice brightness temperatures [NASA-TM-83916] p 49 N84-27319

PROBABILITY DENSITY FUNCTIONS

Non-Gaussian statistical models of surface wave fields for remote sensing applications p 45 N84-27284

PROCEDURES

Guide hydrological practices. Volume 2: Analysis, forecasting and other applications [WMO-168] p 53 N84-25145

PRODUCT DEVELOPMENT

Airborne lidar for oceanography and hydrology (FLOH) [ESA-TT-799] p 37 N84-22955

PROJECT MANAGEMENT

Living and working in space. A history of Skylab [NASA-SP-4208] p 72 N84-25737

PUBLIC HEALTH

A regional raster data study at the Experimental Cartography Unit - The application of interactive raster graphics to environmental modelling p 14 A84-33363

PUERTO RICO

Application of remote sensing to state and regional problems [E84-10128] p 68 N84-23986

PULSE DOPPLER RADAR

An airborne radar station for studying the reflection properties of the earth's surface p 64 A84-31072

PUSHBROOM SENSOR MODES

Design and development of CCD pushbroom camera for earth resources survey p 66 A84-38311

PYROELECTRICITY

Effect of space exposure on pyroelectric infrared detectors (A0135) p 68 N84-24679

Q

QUASARS

Correlations between the nonthermal emission of quasarlike nuclei and their Balmer-line widths p 58 A84-33629

R

RADAR CROSS SECTIONS

A model function for ocean radar cross sections at 14.6 GHz p 34 A84-34516

Optimum backscatter cross section of the ocean as measured by synthetic aperture radars p 44 N84-27276

SAR imagery of ocean-wave swell traveling in an arbitrary direction p 44 N84-27278

RADAR DATA

Digital processing considerations for extraction of ocean wave image spectra from raw synthetic aperture radar data p 30 A84-30025

Fast processing of synthetic aperture radar signal without data transposition p 59 A84-38305

RADAR ECHOES

The radar altimeter for ERS-1 Satellite p 64 A84-30516

An airborne radar station for studying the reflection properties of the earth's surface p 64 A84-31072

RADAR EQUIPMENT

Non-Gaussian statistical models of surface wave fields for remote sensing applications p 45 N84-27284

RADAR GEOLOGY

Radar geology of the Shelleng-Numan area in Nigeria

- An evaluation p 24 A84-38940

Radar backscatter modelling p 25 N84-23525

Pinacate-Gran Desierto Region, Mexico: SIR-A data analysis p 25 N84-23526

Radar-visible wind streaks in the Altiplano of Bolivia p 25 N84-23527

RADAR IMAGERY

RADAR IMAGERY

An airborne radar station for studying the reflection properties of the earth's surface p 64 A84-31072
Digital SAR processing using a fast polynomial transform p 55 A84-32093

Performance evaluation and a dedicated system for SAR image data processing p 58 A84-38300
A SAR image auto-focusing using linear distortion azimuth matched filter p 58 A84-38304

Seasat SAR sea-ice imagery - Summer melt to autumn freeze-up p 36 A84-38941

Improving crop classification through attention to the timing of airborne radar acquisitions p 8 A84-39000

Spaceborne radar subsurface imaging in hyperarid regions p 24 A84-39379

Pinacate-Gran Desierto Region, Mexico: SIR-A data analysis p 25 N84-23526

On the detection of underwater bottom topography by imaging radars p 46 N84-27301

On the response to ocean surface currents in synthetic aperture radar imagery p 47 N84-27304

Satellite remote sensing over ice p 48 N84-27308

Analysis of SEASAT SAR imagery collected during the JASIN experiment p 49 N84-27320

Speckle statistics in radar images of sea surface obtained with horizontal polarization p 50 N84-27921

RADAR MAPS

Radar geology of the Shelling-Numan area in Nigeria - An evaluation p 24 A84-38940

RADAR MEASUREMENT

Microwave measurements using active and passive sensors -- for agriculture in India p 1 A84-30229

A model function for ocean radar cross sections at 14.6 GHz p 34 A84-34516

Two-frequency microwave resonance measurements from an aircraft - A quantitative estimate of the directional ocean surface spectrum p 34 A84-34942

First observations of the interaction of ocean swell with sea ice using satellite radar altimeter data p 35 A84-36684

RADAR SCATTERING

Calculations of radar backscattering coefficient of vegetation-covered soils p 2 A84-30671

Spaceborne radar subsurface imaging in hyperarid regions p 24 A84-39379

Radar backscatter modelling p 25 N84-23525

RADIANCE

In-flight absolute radiometric calibration of the Thematic Mapper --- White Sands, New Mexico p 68 N84-23002

RADIANT FLUX DENSITY

Correlations between the nonthermal emission of quasarlike nuclei and their Balmer-line widths p 58 A84-33629

RADIATIVE TRANSFER

In-flight absolute radiometric calibration of the Thematic Mapper p 56 A84-33531

Remote sensing marine bioluminescence - The role of the in-water scalar irradiance p 34 A84-36107

Spectroradiometric calibration of the Thematic Mapper and multispectral scanner system p 64 A84-10098

Sensor radiance for a midlatitude atmospheric model p 67 N84-23000

In-flight absolute radiometric calibration of the Thematic Mapper --- White Sands, New Mexico p 68 N84-23002

RADAR ALTIMETERS

The radar altimeter for ERS-1 Satellite p 64 A84-30516

Some case studies of ocean wave physical processes utilizing the GSFC airborne radar ocean wave spectrometer p 45 N84-27283

Altimeter height measurement errors introduced by the presence of variable cloud and rain attenuation p 45 N84-27289

Improved resolution rain measurements from spaceborne radar altimeters p 46 N84-27290

The satellite altimeter as a platform for observation of the oceanic mesoscale p 46 N84-27299

Somali current studied from SEASAT altimetry p 47 N84-27307

Satellite remote sensing over ice p 48 N84-27308

Radar altimetry over sea ice p 48 N84-27309

Observations of sea ice and icebergs from satellite radar altimeters p 48 N84-27311

Simulation and assimilation of satellite altimeter data at the oceanic mesoscale p 48 N84-27312

RADIO INTERFEROMETERS

Establishing first-order control by GPS satellite surveying instruments p 18 A84-33368

RADIO NAVIGATION

Applications of the GPS (Global Positioning System) Geodetic Receiver System [AD-A140567] p 21 N84-26688

RADIO RECEIVERS

Applications of the GPS (Global Positioning System) Geodetic Receiver System [AD-A140567] p 21 N84-26688

RADIO WAVE REFRACTION

Theory of radio wave propagation over the sea surface p 35 A84-37095

RADIOMETERS

Comparative accuracies of AVHRR and MSS data used for Level I land cover classifications p 14 A84-33344

Climate research from space p 66 A84-38922

Preliminary investigations concerning a 90 GHz radiometer satellite experiment [DFVLR-FB-84-02] p 68 N84-24693

Microwave radiometric measurement of sea surface salinity [AD-A141302] p 50 N84-28359

RADIOMETRIC CORRECTION

Dual channel satellite measurements of sea surface temperature p 31 A84-31431

Characterization of Landsat-4 MSS and TM digital image data p 56 A84-33526

Analysis and processing of Landsat-4 sensor data using advanced image processing techniques and technologies p 56 A84-33527

Revised radiometric calibration technique for Landsat-4 Thematic Mapper data p 56 A84-33530

RABIVE - A real time program system for radiometric image processing p 58 A84-37773

Heat Capacity Mapping Radiometer (HCMR) data processing algorithm, calibration, and flight performance evaluation [E84-10153] p 71 N84-27248

Evaluating LANDSAT-4 MSS and TM data p 63 N84-27249

RADIOMETRIC RESOLUTION

Landsat-4 MSS and Thematic Mapper data quality and information content analysis p 56 A84-33528

Spectroradiometric calibration of the Thematic Mapper and multispectral scanner system [E84-10098] p 67 N84-23000

Sensor radiance for a midlatitude atmospheric model p 68 N84-23001

In-flight absolute radiometric calibration of the Thematic Mapper --- White Sands, New Mexico p 68 N84-23002

LANDSAT 4 band 6 data evaluation [E84-10119] p 60 N84-23009

Proceedings of the Fourth Meeting of the LANDSAT Technical Working Group (LTWG), volume 1 [LIB-PRO-0012-VOL-1] p 69 N84-25144

Spectroradiometric calibration of the Thematic Mapper and Multispectral Scanner system --- White Sands, New Mexico [E84-10136] p 70 N84-26084

Heat Capacity Mapping Radiometer (HCMR) data processing algorithm, calibration, and flight performance evaluation [E84-10153] p 71 N84-27248

RAIN

Diagnostics of rainfall anomalies in the Nordeste during the global weather experiment [SAPR-1] p 40 N84-26235

Microwave remote sensing of ocean surface wind speed and rain rates over tropical storms p 45 N84-27288

Improved resolution rain measurements from spaceborne radar altimeters p 46 N84-27290

RANGEFINDING

Discussion of the design of satellite-laser measurement stations in the eastern Mediterranean under the geological aspect. Contribution to the earthquake prediction research by the Wegener Group and to NASA's Crustal Dynamics Project [NASA-TM-77412] p 26 N84-24031

RANGELEANDS

Aircraft scatterometer observations of soil moisture on rangeland watersheds p 4 A84-33338

REAL TIME OPERATION

Error analysis for marine geodetic control using the global positioning system [AD-A140566] p 21 N84-26687

REFERENCE SYSTEMS

Investigation of the combination of geodetic point aggregations [SER-C-285] p 21 N84-28199

REFLECTANCE

Assessing change in the surficial character of a semiarid environment with Landsat residual images p 3 A84-31499

Albedo of a forest modeled as a plane with dense protrusions p 6 A84-34385

Theory and measure of certain image norms in SAR p 43 N84-27274

REGRESSION ANALYSIS

A regression analysis of data from aircraft and ground measurements of a vegetative cover p 6 A84-34784

Regression in the primal problem of remote sensing (using grass cover as an example) p 6 A84-34785

Use of transformed LANDSAT data in regression estimation of crop acreages p 11 N84-27246

RELATIVITY

Proceedings of a workshop: Multidisciplinary Use of the Very Long Baseline Array [NASA-CR-173541] p 69 N84-25034

RELAXATION TIME

On the detection of underwater bottom topography by imaging radars p 46 N84-27301

RELIEF MAPS

Mapping of exogenic terrain dynamics on the basis of space photographs (on the example of the Baikal region) p 18 A84-34491

Mapping the sea floor by satellite p 35 A84-36686

Fish-eye objective in the dose range photogrammetry: Theoretical and practical investigations [SER-C-286] p 21 N84-26080

REMOTE SENSING

Asian Conference on Remote Sensing, 3rd, Dacca, Bangladesh, December 4-7, 1982, Proceedings p 64 A84-30226

Measurement of boro rice acreage in Nabinagar Thana by remote sensing technique p 1 A84-30227

Multispectral and multitemporal Landsat data for soil surveys - A case study of part of north west India p 1 A84-30228

Microwave measurements using active and passive sensors -- for agriculture in India p 1 A84-30229

Remote sensing and storm surge forecasting in Bangladesh p 30 A84-30230

Bay monsoon activities in relation to the monsoon in the western Pacific p 30 A84-30232

The experience of organising a utilisation programme for Bhaskara --- Indian experimental satellite p 64 A84-30233

Bhaskara-II TV data in resource studies - A case study in a part of Andhra Pradesh, southern India p 54 A84-30234

Measurement of boro rice acreage in Srimangal Thana by remote sensing technique p 1 A84-30235

Study of desertification/aridity through remote sensing p 1 A84-30238

An inquiry into methods of estimating yields of wheat and autumn crops in the plain region with Landsat images visual interpretation p 2 A84-30239

Application of multi-concept in remote sensing technique for identification and mapping of soil units of alluvial plain for land use planning in Sri Lanka p 13 A84-30241

Analysis of land use changes around Salt Lake City using Landsat digital data - A case study of Sandy area p 13 A84-30242

The compilation of the satellite image map of land-use of China (1:2,000,000 scale) p 13 A84-30243

Turbidity/sediment concentration mapping in the coastal area of Bangladesh p 50 A84-30246

Reduction of high dimension data to two dimension using non linear mapping techniques p 54 A84-30248

Making false color photomap and its application in thematic mapping by using IR photos p 54 A84-30249

Identification of water-logged and salt-affected soils through remote sensing techniques p 51 A84-30251

Benefits and problems in operational remote sensing p 64 A84-30252

SPOT simulations in Bangladesh flight operations and main results p 2 A84-30253

Typical analysis of regional stability and block structures with remote sensing images p 22 A84-30254

Hydrological data densification in mountainous terrain using Landsat imagery p 51 A84-30256

Monitoring the marine environment with remote sensing technology p 30 A84-30258

Remote sensing as a tool for mineral prospecting p 22 A84-30259

Remote sensing for bauxite prospecting p 22 A84-30260

The lineament features of Tarim Basin (west part) and its bearing on the characteristics of Cenozoic tectonic stress fields p 22 A84-30263

A remote sensing data processing system based on a micro-computer p 64 A84-30265

Application of the Vizir Image Processing System to the remote sensing studies in Bangladesh p 64 A84-30266

Metallogenesis - Use of remote sensing for ore deposit prospecting indicators linked to nonoutcropping leucogranitic apexes p 23 A84-30878

A rapid method for obtaining frequency-response functions for multiple input photogrammetric data [AIAA PAPER 84-1060] p 65 A84-31741

Geological interpretation from aerial remote sensing images of Tengchong area p 23 A84-32590

SUBJECT INDEX

American Society of Photogrammetry, Annual Meeting, 49th, Washington, DC, March 13-18, 1983, Technical Papers p 65 A84-3326

The statewide forest/nonforest classification of Pennsylvania using Landsat MSS data p 3 A84-3329

Videography - Some remote sensing applications p 3 A84-3331

Aircraft scatterometer observations of soil moisture on rangeland watersheds p 4 A84-3338

Spatial inventory integrating raster databases and point sample data -- Geographic Information System for timber inventory p 4 A84-3340

The use of digital elevation model topographic data for soil erosion modeling within a geographic information system p 4 A84-3342

Vegetation monitoring and classification using NOAA/AVHRR satellite data p 4 A84-3343

Preliminary digital classification of grazing resources in the Southern Chihuahuan Arid Zone of Mexico p 5 A84-3349

Surface expression of heavily mantled interstratal Karst bordering Okefenokee Swamp, Georgia p 23 A84-3350

Digital comparison and correlation techniques of remote sensing images having different space resolution p 55 A84-3356

Experiments in lithography from remote sensor imagery p 55 A84-3362

Satellite surveying techniques used within geodetic networks p 18 A84-3364

Evaluation of Thematic Mapper for detecting soil properties under grassland vegetation p 6 A84-3350

Snow reflectance from Landsat-4 Thematic Mapper p 52 A84-3354

A theoretical study of an airborne laser technique for determining sea water turbidity p 31 A84-33774

Observations of Gulf Stream-induced and wind-driven upwelling in the Georgia Bight using ocean color and infrared imagery p 34 A84-34517

The effect of fluctuations in the optical properties of the atmosphere on spectral brightness ratios in the remote sensing of agricultural areas p 6 A84-34777

The use of remote sensing in the search for hydrocarbons in the Kerch peninsula p 23 A84-34782

Regression in the primal problem of remote sensing (using grass cover as an example) p 6 A84-34785

Two-frequency microwave resonance measurements from an aircraft - A quantitative estimate of the directional ocean surface spectrum p 34 A84-34942

A semi-automated procedure for identifying Landsat MSS subregion coordinates p 58 A84-34959

Remote sensing marine bioluminescence - The role of the in-water scalar irradiance p 34 A84-36107

X to W band radiometric signatures of natural surfaces p 35 A84-36289

The Green Cadastre - An experiment for exploring the tree vegetation in the Paris area p 7 A84-36516

High resolution observation of the earth's surface from space - Programs, problems and perspectives p 71 A84-37049

A scatter model for vegetation up to Ku-band p 7 A84-37201

Determining forest canopy characteristics using airborne laser data p 7 A84-37202

Inversion of vegetation canopy reflectance models for estimating agronomic variables. III - Estimation using only canopy reflectance data as illustrated by the suits model. IV - Total inversion of the SAIL model -- Scattering by Arbitrarily Inclined Leaves p 7 A84-37203

Remote sensing of the oceans --- Japanese book p 35 A84-37299

RABIVE - A real time program system for radiometric image processing p 58 A84-37773

Two-stage cluster analysis of a Landsat image p 58 A84-38302

Fast processing of synthetic aperture radar signal without data transposition p 59 A84-38305

Remote sensing of the ocean by the airborne microwave scatterometer/radiometer system p 36 A84-38307

Design and development of CCD pushbroom camera for earth resources survey p 66 A84-38311

Performance study of multicolor visual sensor system p 66 A84-38312

Data compression of remotely sensed data from space p 59 A84-38314

Image analysis researches of remotely sensed data at NAL p 59 A84-38315

A simulation program for the integration of aerospace remote sensing systems with a digital terrain model p 59 A84-38316

Equidensitometry and remote sensing imagery p 59 A84-38944

A summary of results from the first Nimbus 7 SMMR observations p 37 A84-39459

Determination of sea ice parameters with the Nimbus 7 SMMR p 37 A84-39461

Topex: Observing the oceans from Space [NASA-CR-173490] p 38 N84-23085

A comparison of numerical results of Arctic Sea ice modeling with satellite images p 39 N84-23969

Arctic Sea ice by passive microwave observations from the Nimbus-5 Satellite p 39 N84-23970

State remote sensing (LANDSAT) programs catalog [E84-10127] p 71 N84-23985

Aerial photography for ecological site mapping p 9 N84-23990

A constrained-clustering approach to the analysis of remote sensing data [AD-A139124] p 10 N84-23993

Orbital imagery: A cartographic solution [INPE-2820-PRE/374] p 20 N84-25143

Marginal ice zone experiment (1983). Part 1: Ice characterization measurements. Part 2. Helicopter-borne and ship-based radar backscatter measurement of sea ice in the marginal ice zone [AD-A139894] p 40 N84-25238

A computer program for mapping regions in a geographic data base with raster structure [FOA-C-20529-D8] p 16 N84-25340

Publications of the Jet Propulsion Laboratory 1982 [NASA-CR-173539] p 71 N84-25510

Earthnet: The story of images [ESA-BR-18] p 62 N84-26102

Digital processing of LANDSAT data for the preparation of land use map of the rural district surrounding Tuebingen to a scale of 1:50000 [ESA-TT-816] p 16 N84-26104

Integration of LANDSAT land cover data from the Saginaw River basin geographic information system for hydrologic modeling [AD-A140185] p 53 N84-26106

Satellite observations of a monsoon depression [NASA-CR-173590] p 40 N84-26232

Maps of favorable areas for tuna fishing to the South and Southeast of Brazil prepared from SMS-2 satellite data [INPE-3102-PRE/501] p 41 N84-26256

Contextual classification of remotely sensed data p 63 N84-27245

Development of Great Lakes algorithms for the Nimbus-G coastal zone color scanner [NASA-CR-173511] p 53 N84-27258

A report of Ceara Project activities [INPE-2988-RPE/452] p 54 N84-27260

Frontiers of Remote Sensing of the Oceans and Troposphere from Air and Space Platforms [NASA-CP-2303] p 42 N84-27262

Remote sensing for oceanography: Past, present, future p 42 N84-27263

ESA activities in the use of microwaves for the remote sensing of the Earth p 42 N84-27264

High resolution observations of low contrast phenomena from an Advanced Geosynchronous Platform (AGP) p 42 N84-27266

Remote sensing of air-sea interactions p 42 N84-27267

Scatterometer capabilities in remotely sensing geophysical parameters over the ocean: The status and the possibilities p 42 N84-27268

Synthetic aperture radar images of ocean waves, theories of imaging physics and experimental tests p 43 N84-27275

An improved dual-frequency technique for the remote sensing of ocean currents and wave spectra p 44 N84-27281

A tentative unified sea model for scattering and emission p 45 N84-27285

Applications of airborne remote sensing in atmospheric sciences research p 71 N84-27286

Microwave remote sensing of ocean surface wind speed and rain rates over tropical storms p 45 N84-27288

Recent advances in multispectral sensing of ocean surface temperature from space p 46 N84-27297

Vector wind, horizontal divergence, wind stress and wind stress curl from SEASAT-SASS at one degree resolution p 48 N84-27313

The impact of scatterometer wind data on global weather forecasting p 49 N84-27314

The importance of altimeter and scatterometer data for ocean prediction p 49 N84-27316

Sampling strategies and four-dimensional assimilation of altimetric data for ocean monitoring and prediction p 49 N84-27317

The influence of actual and apparent geoid error on ocean analysis and prediction p 49 N84-27318

Research on land use cartography by remote sensing p 17 N84-28201

Remote sensing of the Santonge littoral. Processing and interpretation of satellite images [ISBN-2-85929-016-8] p 63 N84-28202

Observing ocean-atmosphere exchanges with space-borne sensors, appendix C p 50 N84-28298

SALINITY

REMOTE SENSORS

Sensitivity of airborne fluorosensor measurements to linear vertical gradients in chlorophyll concentration p 30 A84-30302

The ESA ocean observation satellite ERS-1. I - Description of the history, goals, and payload of ERS-1 p 31 A84-32266

Comparative accuracies of AVHRR and MSS data used for Level I land cover classifications p 14 A84-33344

Analysis of airborne electromagnetic systems for mapping thickness of sea ice [AD-A139786] p 39 N84-25235

Ocean optical remote sensing capability statement [AD-A140589] p 49 N84-27321

REPORTS

Technical publications of the NASA Wallops Flight Facility, 1980 through 1983 [NASA-TM-84421] p 72 N84-26467

Publications and reports of the Institute of Oceanographic Sciences 1979-1982 [IOS-170] p 50 N84-28354

RESEARCH FACILITIES

Technical publications of the NASA Wallops Flight Facility, 1980 through 1983 [NASA-TM-84421] p 72 N84-26467

RESEARCH PROJECTS

The World Climate Research Programme p 36 A84-38702

RESERVOIRS

Locating shoreline changes in the Porttipahta (Finland) water reservoir by using multitemporal Landsat data p 52 A84-33987

RESIDENTIAL AREAS

The use of photointerpretation for socio-economic characterization of urban population [INPE-3067-PRE/484] p 16 N84-26428

RESOURCES MANAGEMENT

Landsat image use in forestry management in China p 2 A84-30250

State remote sensing (LANDSAT) programs catalog [E84-10127] p 71 N84-23985

RETURN BEAM VIDICONS

Findings on the use of Landsat-3 return beam vidicon imagery for detecting land use and land cover changes p 14 A84-33361

Study on temporal geometric-distortion variation of Landsat MSS and RBV imageries and attitude determination program p 59 A84-38313

RICE

Measurement of boro rice acreage in Nabinagar Thana by remote sensing technique p 1 A84-30227

Measurement of boro rice acreage in Srimangal Thana by remote sensing technique p 1 A84-30235

Identification of brown plant hopper and bacterial leaf blight affected rice crop on Landsat false colour composites p 1 A84-30237

Irrigated rice area estimation using remote sensing techniques: Project's proposal and preliminary results --- Rio Grande do Sul, Brazil [E84-10131] p 10 N84-26081

Identification and estimation of the area planted with irrigated rice based on the visual interpretation of LANDSAT MSS data [E84-10164] p 12 N84-27256

RING STRUCTURES

Rapid evolution of a Gulf Stream warm-core ring p 32 A84-34164

RIVER BASINS

Riparian habitat on the Humboldt River, Deeth to Elko, Nevada [E84-10116] p 53 N84-23976

Integration of LANDSAT land cover data into the Saginaw River basin geographic information system for hydrologic modeling [AD-A140185] p 53 N84-26106

ROSS ICE SHELF

Katabatic wind forcing of the Terra Nova Bay polynya p 33 A84-34509

RURAL LAND USE

Comparison of the information content of data from the Landsat-4 Thematic Mapper and the Multispectral Scanner p 57 A84-33534

Digital processing of LANDSAT data for the preparation of a land use map of the rural district surrounding Tuebingen to a scale of 1:50000 [ESA-TT-816] p 16 N84-26104

S

SAHARA DESERT (AFRICA)

Surface albedo and the Sahel drought p 7 A84-36710

SALINITY

Identification of water-logged and salt-affected soils through remote sensing techniques p 51 A84-30251

SAMPLING

The effect of groundwater inflow on evaporation from a saline lake p 52 A84-34378
Airborne lidar for oceanography and hydrology (FLOH) [ESA-TT-799] p 37 N84-22955

SAMPLING
A sampling system for estimating the cultivation of wheat (*Triticum aestivum L.*) from LANDSAT data [E84-10165] p 12 N84-27257
Remote sensing for oceanography: Past, present, future p 42 N84-27263

SATELLITE IMAGERY

Measurement of boro rice acreage in Nabinagar Thana by remote sensing technique p 1 A84-30227
Multispectral and multitemporal Landsat data for soil surveys - A case study of part of north west India

p 1 A84-30228
Bay monsoon activities in relation to the monsoon in the western Pacific p 30 A84-30232

Bhaskara-II TV data in resource studies - A case study in a part of Andhra Pradesh, southern India p 54 A84-30234
Measurement of boro rice acreage in Srimangal Thana by remote sensing technique p 1 A84-30235
Study of desertification/aridity through remote sensing p 1 A84-30238

An inquiry into methods of estimating yields of wheat and autumn crops in the plain region with Landsat images visual interpretation p 2 A84-30239
Digital processing of remote sensing data in Hall Haor, Bangladesh for landuse analysis and development potentiality assessment p 13 A84-30240
Analysis of land use changes around Salt Lake City using Landsat digital data - A case study of Sandy area p 13 A84-30242

The compilation of the satellite image map of land-use of China (1:2,000,000 scale) p 13 A84-30243
Turbidity/sediment concentration mapping in the coastal area of Bangladesh p 50 A84-30246

An analysis of tectonics and metallogeny of Orissa state, India with remote sensing technique p 22 A84-30247
Reduction of high dimension data to two dimension using non linear mapping techniques p 54 A84-30248
Landsat image use in forestry management in China p 2 A84-30250

Identification of water-logged and salt-affected soils through remote sensing techniques p 51 A84-30251
SPOT simulations in Bangladesh flight operations and main results p 2 A84-30253

Typical analysis of regional stability and block structures with remote sensing images p 22 A84-30254
The application of Landsat image in the surveying of water resources of Dongting Lake p 51 A84-30255

Monitoring the marine environment with remote sensing technology p 30 A84-30258
Remote sensing as a tool for mineral prospecting p 22 A84-30259

Remote sensing for bauxite prospecting p 22 A84-30260

An undetectable factor in geomorphological mapping from land satellite images - A case study in the central highland, Thailand p 22 A84-30261
The use of Hough transformation for detecting lineaments in satellite imagery p 22 A84-30262

Landsat planimetric maps p 54 A84-30264
Description of SEP ground station and Vizir image processing VIPS --- for Spot and Landsat 4 satellites p 54 A84-30268

Atmospheric effect on classification of finite fields --- satellite-imaged agricultural areas p 2 A84-30670
Dynamics of the slope water off New England and its influence on the Gulf Stream as inferred from satellite IR data p 31 A84-30672

Soil spectral effects on 4-space vegetation discrimination p 2 A84-30673
Assessing change in the surficial character of a semiarid environment with Landsat residual images p 3 A84-31499

Landsat imagery for the interpretation of Louisiana forest habitat regions p 3 A84-33328
The use of Landsat imagery in analyzing the vegetation and energy resources of Pickens County, South Carolina p 3 A84-33330

Non-parallactic stereoscopy using shadow-disparity --- time separated Landsat photos p 55 A84-33335
Integration of Landsat data into the Saginaw River Basin geographic information system p 51 A84-33339
Vegetation monitoring and classification using NOAA/AVHRR satellite data p 4 A84-33343

Comparative accuracies of AVHRR and MSS data used for Level I land cover classifications p 14 A84-33344
Analysis of Landsat for monitoring vegetables in New York mucklands p 5 A84-33345
Using Landsat to monitor tropical forest ecosystems p 5 A84-33352

Drainage pattern delineation - A function of image scale p 52 A84-33353

Estimation of depth of snow from Landsat imagery p 52 A84-33355
Findings on the use of Landsat-3 return beam vidicon imagery for detecting land use and land cover changes p 14 A84-33361

Revised radiometric calibration technique for Landsat-4 Thematic Mapper data p 56 A84-33350
A physically-based transformation of Thematic Mapper data The TM tasseled cap p 56 A84-33352

A statistical evaluation of the advantages of Landsat Thematic Mapper data in comparison to Multispectral Scanner data p 57 A84-33357
Evaluation of Thematic Mapper for detecting soil properties under grassland vegetation p 6 A84-33540

Locating shoreline changes in the Porttipahta (Finland) water reservoir by using multitemporal Landsat data p 28 A84-33987

Fog recognition in daylight 3.7-micron-band Tiros-N and NOAA images p 65 A84-34157
Seasonal variability in meanders of the California Current System off Vancouver Island p 33 A84-34507

Satellite observations of circulation in the eastern Bering Sea p 33 A84-34514
Topography interpretation possibilities for satellite photos in regions where the platform mantle has a multilayer structure (on the example of the eastern marginal part of the Caspian depression) p 23 A84-34779

The use of satellite photos for analyzing the structural and dynamic conditions surrounding the formation of ancient deposits of phlogopite and apatite p 23 A84-34781

Interactive procedures for distinguishing and reconstructing contour networks --- in aerospace computer aided photomapping p 58 A84-34786
Conditions for the illumination of an area in satellite scanner surveys p 65 A84-34787

Distinguishing linear contour elements on satellite photos on the basis of a visual perception model p 24 A84-34789
A semi-automated procedure for identifying Landsat MSS subregion coordinates p 58 A84-34959
Potential benefits of new satellite sensors to wetland mapping p 7 A84-34960

Surface albedo and the Sahel drought p 7 A84-36710
Satellite observations of the 1982-1983 El Nino along the U.S. Pacific coast p 35 A84-36872

Intensive forest clearing in Rondonia, Brazil, as detected by satellite remote sensing p 8 A84-37204
RABIVE - A real time program system for radiometric image processing p 58 A84-37773

Application of Landsat data in the exploration of 'Calcrete' uranium deposits p 24 A84-37775
Classification of snow surface conditions by means of Landsat MSS data under compensation of slope effects p 52 A84-38296

Joint analysis of Landsat-MSS and NOAA-AVHRR data for marine environmental monitoring p 35 A84-38298
Landsat MSS data used for crop identification at the limit of its spatial resolution p 8 A84-38299

Two-stage cluster analysis of a Landsat image p 58 A84-38302
A SAR image auto-focusing using linear distortion azimuth matched filter p 58 A84-38304

Performance study of multicolor visual sensor system p 66 A84-38312
Study on temporal geometric-distortion variation of Landsat MSS and RBV imageries and attitude determination program p 59 A84-38313

Image analysis researches of remotely sensed data at NAL p 59 A84-38315
A simulation program for the integration of aerospace remote sensing systems with a digital terrain model p 59 A84-38316

Atmospheric correction of Landsat MSS data for a multidate suspended sediment algorithm p 59 A84-38942
Detection of marine aerosol particles in coastal zones using satellite imagery p 36 A84-38943

Irrigated crop inventory by classification of satellite image data p 8 A84-38999
Proceedings of the Fourth Meeting of the LANDSAT Technical Working Group (LTWG), volume 1 [LIB-PRO-0012-VOL-1] p 69 N84-25144

An integrated software system for geometric correction of LANDSAT MSS imagery [E84-10143] p 62 N84-26091
Comparative study of image data produced by satellites with different characteristics [ESA-CR(P)-1867] p 62 N84-26103

Coastal bathymetry and currents from LANDSAT data p 47 N84-27303
On the response to ocean surface currents in synthetic aperture radar imagery p 47 N84-27304

SUBJECT INDEX

Variations in surface current off the coasts of Canada as inferred from infrared satellite imagery p 47 N84-27305

Satellite remote sensing over ice p 48 N84-27308
Method to estimate drag coefficient at the air/ice interface over drifting open pack ice from remotely sensed data p 48 N84-27310

Analysis of SEASAT SAR imagery collected during the JASIN experiment [AD-A140584] p 49 N84-27320

SATELLITE INSTRUMENTS

Status of the TERS project p 71 A84-34575
Satellite techniques for determining the geopotential for sea-surface elevations p 46 N84-27298

The satellite altimeter as a platform for observation of the oceanic mesoscale p 46 N84-27299

SATELLITE OBSERVATION

Benefits and problems in operational remote sensing p 64 A84-30252
Satellite climatology --- Russian book p 13 A84-31024

Elements of the west African monsoon circulation deduced from Meteosat cloud winds and simultaneous aircraft measurements p 51 A84-31948
Eurasian snow cover versus Indian monsoon rainfall - An extension of the Hahn-Shukla results p 51 A84-31950

Status of the TERS project p 71 A84-34575
First observations of the interaction of ocean swell with sea ice using satellite radar altimeter data p 35 A84-36684

High resolution observation of the earth's surface from space - Programs, problems and perspectives p 71 A84-37049

Remote sensing of the oceans --- Japanese book p 35 A84-37299

Large-scale analysis and forecast experiments with wind data from the Seasat A scatterometer p 66 A84-37873

Data compression of remotely sensed data from space p 59 A84-38314
The evolution of mushroom-shape currents in the ocean p 36 A84-38773

Reduction of satellite magnetic anomaly data p 19 A84-38812
A bispectral method for the height determination of optically thin ice clouds p 60 A84-39044

The validation of Nimbus 7 LIMS measurements of ozone p 67 A84-39443
SAGE and SAM II measurements of global stratospheric aerosol optical depth and mass loading p 15 A84-39455

A summary of results from the first Nimbus 7 SMMR observations p 37 A84-39459
Determination of sea ice parameters with the Nimbus 7 SMMR p 37 A84-39461

Satellite observed upper level moisture patterns associated with tropical cyclone movement p 37 A84-39523

Topex: Observing the oceans from Space [NASA-CR-173490] p 38 N84-23085
Arctic Sea ice by passive microwave observations from the Nimbus 5 Satellite p 39 N84-23970

AVHRR aerosol ground truth experiment [PB84-157882] p 39 N84-24065
Preliminary investigations concerning a 90 GHz radiometer satellite experiment [DFVLR-FB-84-02] p 68 N84-24693

Stochastic models for point manifolds p 20 N84-26072
The use of satellite observations of the ocean surface in commercial fishing operations [AD-P003120] p 41 N84-26261

Research and applications of data from environmental satellites: Determining parameters and developing interpretation techniques for applications of environmental satellite data [INPE-3005-NTE/213] p 13 N84-27261

Frontiers of Remote Sensing of the Oceans and Troposphere from Air and Space Platforms [NASA-CP-2303] p 42 N84-27262

Remote sensing of air-sea interactions p 42 N84-27267
Ocean wind field measurement performance of the ERS-1 scatterometer p 43 N84-27273

Theory and measure of certain image norms in SAR p 43 N84-27274
Synthetic aperture radar images of ocean waves, theories of imaging physics and experimental tests p 43 N84-27275

Satellite techniques for determining the geopotential for sea-surface elevations p 46 N84-27298
Observations of sea ice and icebergs from satellite radar altimeters p 48 N84-27311

Simulation and assimilation of satellite altimeter data at the oceanic mesoscale p 48 N84-27312

SUBJECT INDEX

Fire detection using the NOAA (National Oceanic and Atmospheric Administration)-series satellites [PB84-176890] p 13 N84-27324

Petrologic and geophysical sources of long-wavelength crustal magnetic anomalies [NASA-CR-175245] p 29 N84-28276

Observing ocean-atmosphere exchanges with space-borne sensors, appendix C p 50 N84-28288

Outlook for improved numerical weather prediction using satellite data with a special emphasis on the hydrological variables [AD-A141233] p 54 N84-28344

Satellite-Derived Sea Surface Temperature: Workshop-2 [NASA-CR-173740] p 50 N84-28355

SATELLITE ORBITS

The approximation introduced by representing the earth's gravity field with a finite grid of mascons both at the earth's surface and at the bottom of the earth's crust [AAS PAPER 83-394] p 17 A84-30583

A simulation program for the integration of aerospace remote sensing systems with a digital terrain model p 59 A84-38316

SATELLITE SOUNDING

The analysis and digital signal processing of NOAA's surface current mapping system p 30 A84-30024

Comparison of longwave diurnal models applied to simulations of the Earth Radiation Budget Experiment p 65 A84-31947

The ESA ocean observation satellite ERS-1. I - Description of the history, goals, and payload of ERS-1 p 31 A84-32266

Satellite surveying techniques used within geodetic networks p 18 A84-33364

Seasat observations of lithospheric flexure seaward of trenches p 32 A84-34339

Theory and validation of the multiple window sea surface temperature technique p 33 A84-34513

Atmospheric science --- overview of stratosphere and mesosphere satellite remote sounding experiments p 66 A84-38923

Intercomparison of the Nimbus 7 SBUV/TOMS total ozone data sets with Dobson and M83 results --- Solar Backscattered Ultraviolet/Total Ozone Mapping Spectrometer p 67 A84-39449

SATELLITE TRACKING

A Doppler positioning cost model --- for cadastral geodetic surveys p 18 A84-33365

Development of satellite Doppler/inertial survey systems for BLM cadastral survey-related applications in Alaska p 14 A84-33370

Modeling the movement at the polar ice cap at the South Pole p 20 N84-23957

SATELLITE-BORNE INSTRUMENTS

Establishing first-order control by GPS satellite surveying instruments p 18 A84-33368

The active microwave instrumentation for ERS-1 p 34 A84-35542

Microwave scatterometer p 66 A84-38310

ERS-1 - An ice and ocean monitoring mission p 36 A84-38620

Climate research from space p 66 A84-38922

Atmospheric science --- overview of stratosphere and mesosphere satellite remote sounding experiments p 66 A84-38923

The Limb Infrared Monitor of the Stratosphere - Experiment description, performance, and results p 66 A84-39440

The validation of Nimbus 7 LIMS measurements of ozone p 67 A84-39443

Accuracy and precision of the nitric acid concentrations determined by the limb infrared monitor of the stratosphere experiment on NIMBUS 7 p 67 A84-39444

A comparative study of aerosol extinction measurements made by the SAM II and SAGE satellite experiments p 15 A84-39457

SATELLITE-BORNE PHOTOGRAPHY

American Society of Photogrammetry, Annual Meeting, 49th, Washington, DC, March 13-18, 1983, Technical Papers p 65 A84-33326

Analysis of photo interpretation test results for seven aerospace image types of the San Juan National Forest, Colorado p 4 A84-33332

Estimation of depth of snow from Landsat imagery p 52 A84-33355

Mapping of exogenic terrain dynamics on the basis of space photographs (on the example of the Baikal region) p 18 A84-34491

SATELLITE-BORNE RADAR

A model function for ocean radar cross sections at 14.6 GHz p 34 A84-34516

Performance evaluation and a dedicated system for SAR image data processing p 58 A84-38300

SATELLITE-TO-SATELLITE TRACKING

The GRASAT signal over tectonic features p 19 A84-36919

SCALE (RATIO)

Drainage pattern delineation - A function of image scale p 52 A84-33353

SCALE MODELS

Optimum backscatter cross section of the ocean as measured by synthetic aperture radars p 44 N84-27276

SCATTERING CROSS SECTIONS

Fundamentals of spaceborne remote sensing: Applications of lasers, volume 1 p 70 N84-26238

A tentative unified sea model for scattering and emission p 45 N84-27285

SCATTERING FUNCTIONS

Fundamentals of spaceborne remote sensing: Applications of lasers, volume 1 p 70 N84-26238

SCATTEROMETERS

Aircraft scatterometer observations of soil moisture on rangeland watersheds p 4 A84-33338

The active microwave instrumentation for ERS-1 p 34 A84-35542

Remote sensing of the ocean by the airborne microwave scatterometer/radiometer system p 36 A84-38307

Microwave scatterometer p 66 A84-38310

A SEASAT SASS simulation experiment to quantify the errors related to a + or - 3 hour intermittent assimilation technique [E84-10129] p 68 N84-23987

Scatterometer capabilities in remotely sensing geophysical parameters over the ocean: The status and the possibilities p 42 N84-27268

A new parameterization of an empirical model for wind/ocean scatterometry p 43 N84-27269

Ocean wind field measurement performance of the ERS-1 scatterometer p 43 N84-27273

The dual-frequency scatterometer reexamined p 44 N84-27280

An improved dual-frequency technique for the remote sensing of ocean currents and wave spectra p 44 N84-27281

The importance of altimeter and scatterometer data for ocean prediction p 49 N84-27316

SCENE ANALYSIS

Identification of brown plant hopper and bacterial leaf blight affected rice crop on Landsat false colour composites p 1 A84-30237

Remote sensing for bauxite prospecting p 22 A84-30260

Experiments to correct a digital map data base using scene analysis [AD-A139447] p 61 N84-24499

SCHOOLS

NASA, the first 25 years: 1958 - 1983 [NASA-EP-182] p 72 N84-26563

SEA ICE

First observations of the interaction of ocean swell with sea ice using satellite radar altimeter data p 35 A84-36684

ERS-1 - An ice and ocean monitoring mission p 36 A84-38620

Seasat SAR sea-ice imagery - Summer melt to autumn freeze-up p 36 A84-38941

Determination of sea ice parameters with the Nimbus 7 SMMR p 37 A84-39461

Wind, waves and swell in the Antarctic marginal ice zone by SEASAT radar altimeter p 38 N84-23941

A comparison of numerical results of Arctic Sea ice modeling with satellite images p 39 N84-23969

Arctic Sea ice by passive microwave observations from the Nimbus-5 Satellite p 39 N84-23970

Remote sensing of floe size distribution and surface topography [E84-10132] p 39 N84-25141

Analysis of airborne electromagnetic systems for mapping thickness of sea ice [AD-A139786] p 39 N84-25235

Marginal ice zone experiment (1983). Part 1: Ice characterization measurements. Part 2. Helicopter-borne and ship-based radar backscatter measurement of sea ice in the marginal ice zone [AD-A139894] p 40 N84-25238

Frontiers of Remote Sensing of the Oceans and Troposphere from Air and Space Platforms [NASA-CP-2303] p 42 N84-27262

Satellite remote sensing over ice p 48 N84-27308

Radar altimetry over sea ice p 48 N84-27309

Observations of sea ice and icebergs from satellite radar altimeters p 48 N84-27311

Matrix partitioning and EOF/principal component analysis of Antarctic Sea ice brightness temperatures [NASA-TM-83916] p 49 N84-27319

Microwave radiometric measurement of sea surface salinity [AD-A141302] p 50 N84-28359

SEA ROUGHNESS

Effective reflectance of oceanic whitecaps p 35 A84-36119

Ocean waves and turbulence as observed with an adaptive coherent multifrequency radar p 44 N84-27279

The dual-frequency scatterometer reexamined p 44 N84-27280

An improved dual-frequency technique for the remote sensing of ocean currents and wave spectra p 44 N84-27281

SEA STATES

Remote sensing and storm surge forecasting in Bangladesh p 30 A84-30230

X to W band radiometric signatures of natural surfaces p 35 A84-36289

Microwave backscattering characteristics of wind-generated waves p 36 A84-38309

Wind, waves and swell in the Antarctic marginal ice zone by SEASAT radar altimeter p 38 N84-23941

Some case studies of ocean wave physical processes utilizing the GSFC airborne radar ocean wave spectrometer p 45 N84-27283

SEA TRUTH

Satellite-Derived Sea Surface Temperature: Workshop-2 [NASA-CR-173740] p 50 N84-28355

SEA WATER

A theoretical study of an airborne laser technique for determining sea water turbidity p 31 A84-33774

SEAS

The depiction of Alboran Sea Gyre during Donde Va? using remote sensing and conventional data p 47 N84-27306

SEASAT SATELLITES

Mapping the sea floor by satellite p 35 A84-36686

A SEASAT SASS simulation experiment to quantify the errors related to a + or - 3 hour intermittent assimilation technique [E84-10129] p 68 N84-23987

Scatterometer capabilities in remotely sensing geophysical parameters over the ocean: The status and the possibilities p 42 N84-27268

A new parameterization of an empirical model for wind/ocean scatterometry p 43 N84-27269

SEASAT 1

Global data assimilation experiments with scatterometer winds from SEASAT-A p 65 A84-32938

Large-scale analysis and forecast experiments with wind data from the Seasat A scatterometer p 66 A84-37873

Seasat SAR sea-ice imagery - Summer melt to autumn freeze-up p 36 A84-38941

Propagation effects in satellite-based synthetic aperture radars [AD-A136861] p 67 N84-22873

SEDIMENT TRANSPORT

Sediment volume modelling in the coastal area of Bangladesh using turbidity/sediment concentration map based on Landsat data p 51 A84-30257

Atmospheric correction of Landsat MSS data for a multiday suspended sediment algorithm p 59 A84-38942

Coastal bathymetry and currents from LANDSAT data p 47 N84-27303

SEDIMENTARY ROCKS

Topography interpretation possibilities for satellite photos in regions where the platform mantle has a multilayer structure (on the example of the eastern marginal part of the Caspian depression) p 23 A84-34779

Methodological approach in lithological discrimination by digital processing: A case study in the Serra do Ramalho, state of Bahia [INPE-3108-PRE/507] p 29 N84-26101

SEDIMENTS

Turbidity/sediment concentration mapping in the coastal area of Bangladesh p 50 A84-30246

Sediment volume modelling in the coastal area of Bangladesh using turbidity/sediment concentration map based on Landsat data p 51 A84-30257

SEISMIC WAVES

A crustal structure study of South America p 29 N84-25139

SEISMOLOGY

Typical analysis of regional stability and block structures with remote sensing images p 22 A84-30254

Coseismic and postseismic vertical movements associated with the 1940 M7.1 Imperial Valley, California, earthquake p 24 A84-36922

SELF FOCUSING

A SAR image auto-focusing using linear distortion azimuth matched filter p 58 A84-38304

SHADOWS

Evaluation of factors causing reflectance differences between sun and shade leaves p 3 A84-30674

SHALLOW WATER

Non-parallactic stereoscopy using shadow-disparity --- time separated Landsat photos p 55 N84-33335

SHALLOW WATER

Modeling of SAR signatures of shallow water ocean topography p 47 N84-27302

SHIPS

Comparisons of sea-surface temperature obtained from ship and satellite data [AD-A138257] p 38 N84-23087

Marginal ice zone experiment (1983). Part 1: Ice characterization measurements. Part 2. Helicopter-borne and ship-based radar backscatter measurement of sea ice in the marginal ice zone [AD-A139894] p 40 N84-25238

SHORELINES

Locating shoreline changes in the Porttipahta (Finland) water reservoir by using multitemporal Landsat data p 52 N84-33987

SHORT WAVE RADIO TRANSMISSION

Theory of radio wave propagation over the sea surface p 35 N84-37095

SIDE-LOOKING RADAR

Optimum backscatter cross section of the ocean as measured by synthetic aperture radars p 44 N84-27276

SIGNAL ANALYSIS

Study on spectral/radiometric characteristics of the Thematic Mapper for land use applications [E84-10130] p 61 N84-25140

SIGNAL PROCESSING

The analysis and digital signal processing of NOAA's surface current mapping system p 30 N84-30024

Fast processing of synthetic aperture radar signal without data transposition p 59 N84-38305

The dual-frequency scatterometer reexamined p 44 N84-27280

SIGNAL TRANSMISSION

Speckle statistics in radar images of sea surface obtained with horizontal polarization p 50 N84-27921

SIGNATURE ANALYSIS

LANDSAT-4 image data quality analysis [E84-10134] p 10 N84-26082

Analysis of the quality of image data acquired by the LANDSAT-4 Thematic Mapper and Multispectral Scanners [E84-10137] p 61 N84-26085

Comparative assessment of LANDSAT-D MSS and TM data quality for mapping applications in the Southeast [E84-10138] p 61 N84-26086

Field data observed during the geological excursion in the west-central region of the Sul-RioGrande Shield [E84-10146] p 29 N84-26094

Applications of laser for climatology and atmospheric research [BLEV-R-65-169-5] p 70 N84-26237

Fundamentals of spaceborne remote sensing: Applications of lasers, volume 1 p 70 N84-26238

SIGNATURES

Principal components as a method for atmospherically correcting coastal zone color scanner data [AD-P003124] p 41 N84-26265

SITE SELECTION

Discussion of the design of satellite-laser measurement stations in the eastern Mediterranean under the geological aspect. Contribution to the earthquake prediction research by the Wegener Group and to NASA's Crustal Dynamics Project [NASA-TM-77412] p 26 N84-24031

SIZE DETERMINATION

Remote sensing of floe size distribution and surface topography [E84-10132] p 39 N84-25141

SIZE DISTRIBUTION

Remote sensing of floe size distribution and surface topography [E84-10132] p 39 N84-25141

SKYLAB PROGRAM

Living and working in space. A history of Skylab [NASA-SP-4208] p 72 N84-25737

SNOW

Estimation of depth of snow from Landsat imagery p 52 N84-33355

LANDSAT-D investigations in snow hydrology [E84-10094] p 53 N84-22997

Atmospheric model development p 53 N84-22998

SNOW COVER

Eurasian snow cover versus Indian monsoon rainfall - An extension of the Hahn-Shukla results p 51 N84-31950

Snow reflectance from Landsat-4 Thematic Mapper p 52 N84-33541

Classification of snow surface conditions by means of Landsat MSS data under compensation of slope effects p 52 N84-38296

SUBJECT INDEX

Correlation of tectonic provinces of South America and the Caribbean region with MAGSAT anomalies

p 27 N84-25130

Satellite elevation magnetic and gravity models of major South American plate tectonic features

p 27 N84-25131

Relation of MAGSAT anomalies to the main tectonic provinces of South America

p 28 N84-25137

Relation of MAGSAT and gravity anomalies to the main tectonic provinces of South America

p 28 N84-25138

A crustal structure study of South America

p 29 N84-25139

SOUTHERN HEMISPHERE

The impact of scatterometer wind data on global weather forecasting

p 49 N84-27314

SPACE COMMUNICATION

Digital SAR processing using a fast polynomial transform

p 55 N84-32093

SPACE FLIGHT

NASA, the first 25 years: 1958 - 1983

[NASA-EP-182] p 72 N84-26563

SPACE MISSIONS

Living and working in space. A history of Skylab

[NASA-SP-4208] p 72 N84-25737

SPACE NAVIGATION

Proceedings of a workshop: Multidisciplinary Use of the Very Long Baseline Array

[NASA-CR-173541] p 69 N84-25034

SPACE SHUTTLE PAYLOADS

Evaluation of SIR-A (Shuttle Imaging Radar) images from the Tres Marias region (Minas Gerais State, Brazil) using derived spatial features and registration with MSS-LANDSAT images

[E84-10148] p 62 N84-26096

Project SERGE: Brazil referential field data for the SIR-A experiment

[INPE-2973-NTE/210] p 29 N84-27259

SPACEBORNE EXPERIMENTS

Effect of space exposure on pyroelectric infrared detectors (A0135) p 68 N84-24679

Living and working in space. A history of Skylab

[NASA-SP-4208] p 72 N84-25737

Applications of laser for climatology and atmospheric research

[BLEV-R-65-169-5] p 70 N84-26237

Fundamentals of spaceborne remote sensing: Applications of lasers, volume 1 p 70 N84-26238

SPACECRAFT ENVIRONMENTS

Living and working in space. A history of Skylab

[NASA-SP-4208] p 72 N84-25737

SPACELAB PAYLOADS

A sample performance of the grille spectrometer aboard Spacelab

[AERONOMICA-ACTA-A-281-1984] p 70 N84-26003

SPATIAL DISTRIBUTION

Remote sensing of floe size distribution and surface topography

[E84-10132] p 39 N84-25141

Evaluation of entropy and JM-distance criterions as features selection methods using spectral and spatial features derived from LANDSAT images

[E84-10141] p 62 N84-26089

SPATIAL RESOLUTION

Digital comparison and correlation techniques of remote sensing images having different space resolution

p 55 N84-33356

Thematic Mapper image quality - Registration, noise, and resolution

p 57 A84-33533

Landsat MSS data used for crop identification at the limit of its spatial resolution

p 8 A84-38299

Registration of TM data to digital elevation models

p 60 N84-22999

LANDSAT-4 image data quality analysis

[E84-10134] p 10 N84-26082

Evaluation of solar angle variation over digital processing of LANDSAT imagery --- Brazil

[E84-10140] p 61 N84-26088

Multiseasonal variables in digital image enhancements for geological applications

[E84-10145] p 29 N84-26093

Evaluation of SIR-A (Shuttle Imaging Radar) images from the Tres Marias region (Minas Gerais State, Brazil) using derived spatial features and registration with MSS-LANDSAT images

[E84-10148] p 62 N84-26096

The satellite altimeter as a platform for observation of the oceanic mesoscale

p 46 N84-27299

SPECKLE PATTERNS

Speckle statistics in radar images of sea surface obtained with horizontal polarization

p 50 N84-27921

SPECTRAL BANDS

Classifying northern forests using Thematic Mapper Simulator data

p 7 A84-34961

LANDSAT 4 band 6 data evaluation

[E84-10119] p 60 N84-23009

SUBJECT INDEX

Investigation of several aspects of LANDSAT-4 data quality --- Sacramento, San Francisco, and NE Arkansas [E84-10122] p 60 N84-23981

Spectroradiometric calibration of the Thematic Mapper and Multispectral Scanner system --- White Sands, New Mexico [E84-10136] p 70 N84-26084

LANDSAT-D Thematic Mapper image dimensionality reduction and geometric correction accuracy --- Walnut Creek Watershed, Texas [E84-10149] p 62 N84-26097

Discriminating vegetation and soils using LANDSAT MSS and Thematic Mapper bands and band ratios [AD-A140198] p 11 N84-26108

LANDSAT 4 investigations of Thematic Mapper and Multispectral Scanner applications [E84-10152] p 63 N84-27247

SPECTRAL METHODS

A bispectral method for the height determination of optically thin ice clouds p 60 A84-39044

SPECTRAL RECONNAISSANCE

The use of satellite technology in the search for meteorites in Antarctica aut 01Meunier, Tony K. p 26 N84-23955

SPECTRAL REFLECTANCE

Soil spectral effects on 4-space vegetation discrimination p 2 A84-30673

Evaluation of factors causing reflectance differences between sun and shade leaves p 3 A84-30674

An airborne radar station for studying the reflection properties of the earth's surface p 64 A84-31072

In-flight absolute radiometric calibration of the Thematic Mapper p 56 A84-33531

A physically-based transformation of Thematic Mapper data The TM tasseled cap p 56 A84-33532

Spectral variability of Landsat-4 Thematic Mapper and Multispectral Scanner data for selected crop and forest cover types p 5 A84-33538

Snow reflectance from Landsat-4 Thematic Mapper p 52 A84-33541

Classifying the coefficients of spectral brightness of the forest zone in the European part of the Soviet Union p 6 A84-34783

A regression analysis of data from aircraft and ground measurements of a vegetative cover p 6 A84-34784

Regression in the primal problem of remote sensing (using grass cover as an example) p 6 A84-34785

Effective reflectance of oceanic whitecaps p 35 A84-36119

Inversion of vegetation canopy reflectance models for estimating agronomic variables. III - Estimation using only canopy reflectance data as illustrated by the suits model. IV - Total inversion of the SAIL model --- Scattering by Arbitrarily Inclined Leaves p 7 A84-37203

Classification of snow surface conditions by means of Landsat MSS data under compensation of slope effects p 52 A84-38296

Atmospheric model development p 53 N84-22998

Spectroradiometric calibration of the Thematic Mapper and multispectral scanner system [E84-10098] p 67 N84-23000

Sensor radiance for a midlatitude atmospheric model p 68 N84-23001

In-flight absolute radiometric calibration of the Thematic Mapper --- White Sands, New Mexico p 68 N84-23002

Giacological and geological studies of Antarctica with satellite remote sensing technology p 38 N84-23956

Discriminating vegetation and soils using LANDSAT MSS and Thematic Mapper bands and band ratios [AD-A140198] p 11 N84-26108

Identification and estimation of the area planted with irrigated rice based on the visual interpretation of LANDSAT MSS data [E84-10164] p 12 N84-27256

SPECTRAL RESOLUTION

Multiseasonal variables in digital image enhancements for geological applications [E84-10145] p 29 N84-26093

SPECTRAL SIGNATURES

Identification of brown plant hopper and bacterial leaf blight affected rice crop on Landsat false colour composites p 1 A84-30237

The effect of fluctuations in the optical properties of the atmosphere on spectral brightness ratios in the remote sensing of agricultural areas p 6 A84-34777

CZCS data analysis in turbid coastal water p 37 A84-39427

LANDSAT 4 investigations of Thematic Mapper and multispectral scanner applications --- Death Valley, California; Silver Bell Copper Mine, Arizona, and Dulles Airport near Washington, D.C. [E84-10100] p 60 N84-23003

Study on spectral/radiometric characteristics of the Thematic Mapper for land use applications [E84-10130] p 61 N84-25140

SYNTHETIC APERTURE RADAR

SUPERHIGH FREQUENCIES

A scatter model for vegetation up to Ku-band p 7 A84-37201

SURFACE NAVIGATION

Error analysis for marine geodetic control using the global positioning system [AD-A140566] p 21 N84-26687

SURFACE PROPERTIES

Surface expression of heavily mantled interstratal Karst bordering Okefenokee Swamp, Georgia p 23 A84-33350

SURFACE TEMPERATURE

Theory and validation of the multiple window sea surface temperature technique p 33 A84-34513

The effect of ocean surface temperature on the trajectories of tropical cyclones p 34 A84-35252

CONSERVB: A numerical method to compute soil water content and temperature profiles under a bare surface [E84-10113] p 9 N84-23006

Comparisons of sea-surface temperature obtained from ship and satellite data [AD-A138257] p 38 N84-23087

Recent advances in multispectral sensing of ocean surface temperature from space p 46 N84-27297

Variations in surface current off the coasts of Canada as inferred from infrared satellite imagery p 47 N84-27305

SURFACES

The variability of the surface wind field in the equatorial Pacific Ocean: Criteria for satellite measurements p 46 N84-27296

SURVEYS

American Congress on Surveying and Mapping, Annual Meeting, 43rd, Washington, DC, March 13-18, 1983, Technical Papers p 18 A84-33357

Development of satellite Doppler/inertial survey systems for BLM cadastral survey-related applications in Alaska p 14 A84-33370

SYNCHRONOUS PLATFORMS

High resolution observations of low contrast phenomena from an Advanced Geosynchronous Platform (AGP) p 42 N84-27266

SYNCHRONOUS SATELLITES

Space disturbance warning system with the aid of satellites p 15 A84-38301

SYNOPTIC METEOROLOGY

Eurasian snow cover versus Indian monsoon rainfall - An extension of the Hahn-Shukla results p 51 A84-31950

A SEASAT SASS simulation experiment to quantify the errors related to a + or - 3 hour intermittent assimilation technique [E84-10129] p 68 N84-23987

Vector wind, horizontal divergence, wind stress and wind stress curl from SEASAT-SASS at one degree resolution p 48 N84-27313

SYNTHETIC APERTURE RADAR

Digital processing considerations for extraction of ocean wave image spectra from raw synthetic aperture radar data p 30 A84-30025

Digital SAR processing using a fast polynomial transform p 55 A84-32093

The active microwave instrumentation for ERS-1 p 34 A84-35542

Performance evaluation and a dedicated system for SAR image data processing p 58 A84-38300

A SAR image auto-focusing using linear distortion azimuth matched filter p 58 A84-38304

Fast processing of synthetic aperture radar signal without data transposition p 59 A84-38305

Seasat SAR sea-ice imagery - Summer melt to autumn freeze-up p 36 A84-38941

Improving crop classification through attention to the timing of airborne radar acquisitions p 8 A84-39000

Propagation effects in satellite-based synthetic aperture radars [AD-A138681] p 67 N84-22873

Evaluation of SIR-A (Shuttle Imaging Radar) images from the Tres Marias region (Minas Gerais State, Brazil) using derived spatial features and registration with MSS-LANDSAT images [E84-10148] p 62 N84-26096

Project SERGE: Brazil referential field data for the SIR-A experiment [INPE-2973-NTE/210] p 29 N84-27259

Ocean wind field measurement performance of the ERS-1 scatterometer p 43 N84-27273

Theory and measure of certain image norms in SAR p 43 N84-27274

Synthetic aperture radar images of ocean waves, theories of imaging physics and experimental tests p 43 N84-27275

Optimum backscatter cross section of the ocean as measured by synthetic aperture radars p 44 N84-27276

TECHNOLOGY ASSESSMENT

Tracking ocean wave spectrum from SAR images p 44 N84-27277
 SAR imagery of ocean-wave swell traveling in an arbitrary direction p 44 N84-27278
 Modeling of SAR signatures of shallow water ocean topography p 47 N84-27302
 On the response to ocean surface currents in synthetic aperture radar imagery p 47 N84-27304
 Analysis of SEASAT SAR imagery collected during the JASIN experiment [AD-A140584] p 49 N84-27320

T

TECHNOLOGY ASSESSMENT

Remote sensing of the oceans --- Japanese book p 35 A84-37299

TECHNOLOGY TRANSFER

Proceedings of the Fourth Meeting of the LANDSAT Technical Working Group (LTWG), volume 1 [LIB-PRO-0012-VOL-1] p 69 N84-25144

TECHNOLOGY UTILIZATION

Videography - Some remote sensing applications p 3 A84-33331

Satellite surveying techniques used within geodetic networks p 18 A84-33364

TECTONICS

An analysis of tectonics and metallogenesis of Orissa state, India with remote sensing technique p 22 A84-30247

The lineament features of Tarim Basin (west part) and its bearing on the characteristics of Cenozoic tectonic stress fields p 22 A84-30263

Present limitations of accurate satellite Doppler positioning for tectonics - An example: Djibouti p 17 A84-32495

The use of satellite photos for analyzing the structural and dynamic conditions surrounding the formation of ancient deposits of phlogopite and apatite p 23 A84-34781

The GRAVSAT signal over tectonic features p 19 A84-36919

Discussion of the design of satellite-laser measurement stations in the eastern Mediterranean under the geological aspect. Contribution to the earthquake prediction research by the Wegener Group and to NASA's Crustal Dynamics Project [NASA-TM-77412] p 26 N84-24031

Application of MAGSAT to lithospheric modeling in South America. Part 2: Synthesis of geologic and seismic data for development of integrated crustal models [E84-10126] p 26 N84-25128

Euro-African MAGSAT anomaly-tectonic observations p 27 N84-25129

Correlation of tectonic provinces of South America and the Caribbean region with MAGSAT anomalies p 27 N84-25130

Satellite elevation magnetic and gravity models of major South American plate tectonic features p 27 N84-25131

Long-wavelength magnetic and gravity anomaly correlations of Africa and Europe p 28 N84-25135

Relation of MAGSAT anomalies to the main tectonic provinces of South America p 28 N84-25137

Relation of MAGSAT and gravity anomalies to the main tectonic provinces of South America p 28 N84-25138

A crustal structure study of South America p 29 N84-25139

TELECOMMUNICATION

Publications of the Jet Propulsion Laboratory 1982 [NASA-CR-175359] p 71 N84-25510

TEMPERATURE DISTRIBUTION

Seasonal oscillations of the subtropical convergence between the Brazil and Malvinas currents, using oceanographic and SMS-2 satellite data [INPE-3092-PRE/497] p 40 N84-26255

The variability of the surface wind field in the equatorial Pacific Ocean: Criteria for satellite measurements p 46 N84-27296

Recent advances in multispectral sensing of ocean surface temperature from space p 46 N84-27297

TEMPERATURE MEASUREMENT

Theory and validation of the multiple window sea surface temperature technique p 33 A84-34513

TERRADYNAMICS

Mapping of exogenic terrain dynamics on the basis of space photographs (on the example of the Baikal region) p 18 A84-34491

TERRAIN

Registration of TM data to digital elevation models p 60 N84-22999

Mathematical aspects of digital terrain information. A progress report from ISPRS Working Group III:3 p 61 N84-25148

The question of accuracy in the transition from analogue to analytic photogrammetry p 69 N84-25153

TERRAIN ANALYSIS

Terrain analysis database generation through computer-assisted photo interpretation p 55 A84-33334

An analysis of Landsat-4 Thematic Mapper geometric properties p 57 A84-33536

Mapping of exogenic terrain dynamics on the basis of space photographs (on the example of the Baikal region) p 18 A84-34491

A simulation program for the integration of aerospace remote sensing systems with a digital terrain model p 59 A84-38316

Radar backscatter modelling p 25 N84-23525

Pinacate-Gran Desierto Region, Mexico: SIR-A data analysis p 25 N84-23526

Radar-visible wind streaks in the Altiplano of Bolivia p 25 N84-23527

TETRAHEDRONS

Geometrical aspects of differential GPS positioning p 17 A84-32494

THEMATIC MAPPING

Turbidity/sediment concentration mapping in the coastal area of Bangladesh p 50 A84-30246

Making false color photomap and its application in thematic mapping by using IR photos p 17 A84-32494

THICKNESS

Landsat planimetric maps p 54 A84-30249

Soil erosion mapping and evaluation - A photo-geomorphological approach p 14 A84-33333

Automated classification of wetlands p 4 A84-33337

Automated vegetation classification using Thematic Mapper Simulation data p 5 A84-33347

Characterization of Landsat-4 MSS and TM digital image data p 56 A84-33526

Analysis and processing of Landsat-4 sensor data using advanced image processing techniques and technologies p 56 A84-33527

Landsat-4 MSS and Thematic Mapper data quality and information content analysis p 56 A84-33528

Revised radiometric calibration technique for Landsat-4 Thematic Mapper data p 56 A84-33530

A physically-based transformation of Thematic Mapper data The TM tasseled cap p 56 A84-33532

Thematic Mapper image quality - Registration, noise, and resolution p 57 A84-33533

Comparison of the information content of data from the Landsat-4 Thematic Mapper and the Multispectral Scanner p 57 A84-33534

Cartographic accuracy of Landsat-4 MSS and TM image data p 57 A84-33535

An analysis of Landsat-4 Thematic Mapper geometric properties p 57 A84-33536

A statistical evaluation of the advantages of Landsat Thematic Mapper data in comparison to Multispectral Scanner data p 57 A84-33537

Spectral variability of Landsat-4 Thematic Mapper and Multispectral Scanner data for selected crop and forest cover types p 5 A84-33538

Evaluation of corn/soybeans separability using Thematic Mapper and Thematic Mapper Simulator data p 5 A84-33539

Evaluation of Thematic Mapper for detecting soil properties under grassland vegetation p 6 A84-33540

Snow reflectance from Landsat-4 Thematic Mapper p 52 A84-33541

Thematic Mapper - The ESA-Earthnet ground segment and processing experience p 57 A84-33542

Interactive procedures for distinguishing and reconstructing contour networks --- in aerospace computer aided photomapping p 58 A84-34786

Potential benefits of new satellite sensors to wetland mapping p 7 A84-34960

Classifying northern forests using Thematic Mapper Simulator data p 7 A84-34961

LANDSAT-D investigations in snow hydrology [E84-10094] p 53 A84-22997

Atmospheric model development p 53 N84-22998

The Pennsylvania defoliation application pilot test [E84-10111] p 8 A84-23004

Evaluation of spatial, radiometric and spectral Thematic Mapper performance for coastal studies [E84-10118] p 9 N84-23978

Evaluation of the effects of the seasonal variation of solar elevation angle and azimuth on the processes of digital filtering and thematic classification of relief units [E84-10121] p 60 N84-23980

Investigation of several aspects of LANDSAT-4 data quality --- Sacramento, San Francisco, and NE Arkansas [E84-10122] p 60 N84-23981

Aerial photography for ecological site mapping p 9 A84-23990

Potential utility of future satellite magnetic field data [NASA-CR-175230] p 26 N84-24691

SUBJECT INDEX

Study on spectral/radiometric characteristics of the Thematic Mapper for land use applications [E84-10130] p 61 N84-25140

Remote sensing of floe size distribution and surface topography [E84-10132] p 39 N84-25141

Vegetation, land-use and seasonal albedo data sets: Documentation of archived data tape [E84-10133] p 10 N84-25142

LANDSAT-4 image data quality analysis [E84-10134] p 10 N84-26082

Analysis of the quality of image data acquired by the LANDSAT-4 Thematic Mapper and Multispectral Scanners [E84-10137] p 61 N84-26085

Comparative assessment of LANDSAT-D MSS and TM data quality for mapping applications in the Southeast [E84-10138] p 61 N84-26086

Sampling system for wheat (Triticum aestivum L) area estimation using digital LANDSAT MSS data and aerial photographs --- Brazil [E84-10139] p 10 N84-26087

Forest inventory using multistage sampling with probability proportional to size --- Brazil [E84-10144] p 11 N84-26092

Field data observed during the geological excursion in the west-central region of the Sul-Riogrande Shield [E84-10146] p 29 N84-26094

The use of an image registration technique in the urban growth monitoring [E84-10147] p 16 N84-26095

Evaluation of SIR-A (Shuttle Imaging Radar) images from the Tres Marias region (Minas Gerais State, Brazil) using derived spatial features and registration with MSS-LANDSAT images [E84-10148] p 62 N84-26096

LANDSAT-D Thematic Mapper image dimensionality reduction and geometric correction accuracy --- Walnut Creek Watershed, Texas [E84-10149] p 62 N84-26097

Understanding and utilization of Thematic Mapper and other remotely sensed data for vegetation monitoring [E84-10150] p 11 N84-26098

Results of field observations of radio waves in alluvial deposits in Cara state from 1:100,000: Fortaleza, Caniride, Taperuaba, Santa Quiteria, Sobral, and Sao Luiz do Curu [INPE-3061-NTE/216] p 53 N84-26100

Comparative study of image data produced by satellites with different characteristics [ESA-CR(P)-1867] p 62 N84-26103

Digital processing of LANDSAT data for the preparation of a land use map of the rural district surrounding Tuebingen to a scale of 1:50,000 [ESA-TT-816] p 16 N84-26104

LANDSAT 4 investigations of Thematic Mapper and Multispectral Scanner applications [E84-10152] p 63 N84-27247

Evaluation of spatial, radiometric and spectral Thematic Mapper performance for coastal studies [E84-10159] p 12 N84-27251

Project SERGE: Brazil referential field data for the SIR-A experiment [INPE-2973-NTE/210] p 29 N84-27259

TERMAL MAPPING

Seasonal oscillations of the subtropical convergence between the Brazil and Malvinas currents, using oceanographic and SMS-2 satellite data [INPE-3092-PRE/497] p 40 N84-26255

THICKNESS

Analysis of airborne electromagnetic systems for mapping thickness of sea ice [AD-A139786] p 39 N84-25235

TIMBER IDENTIFICATION

Analysis of photo interpretation test results for seven aerospace image types of the San Juan National Forest, Colorado p 4 A84-33332

Classifying northern forests using Thematic Mapper Simulator data p 7 A84-34961

Use of remote sensing for land use policy formulation [E84-10117] p 9 N84-23977

TIMBER INVENTORY

Spacial inventory integrating raster databases and point sample data --- Geographic Information System for timber inventory p 4 A84-33340

Application of remote sensing to state and regional problems [E84-10128] p 68 N84-23986

Forest inventory using multistage sampling with probability proportional to size --- Brazil [E84-10144] p 11 N84-26092

TIME DIVISION MULTIPLEXING

Applications of the GPS (Global Positioning System) Geodetic Receiver System [AD-A140567] p 21 N84-26688

SUBJECT INDEX

TOPEX
Topex: Observing the oceans from Space
[NASA-CR-173490] p 38 N84-23085

TOPOGRAPHY
Albedo of a forest modeled as a plane with dense protrusions p 6 N84-34385
The GRAVAT signal over tectonic features p 19 N84-36919
Airborne laser topographic mapping results p 8 N84-38998
Scientific activity in oceanography, 1979-1982 p 38 N84-23084
Program for mapping Antarctica p 19 N84-23954
Utilization of digital LANDSAT imagery for the study of granitoid bodies in Rondonia: Case example of the Pedra Branca massif [E84-10120] p 26 N84-23979
Evaluation of the effects of the seasonal variation of solar elevation angle and azimuth on the processes of digital filtering and thematic classification of relief units [E84-10121] p 60 N84-23980
Photogrammetric research at the Royal Institute of Technology, Stockholm, Sweden p 69 N84-25147
GENTRI: A system for simultaneous adjustment of photogrammetric and other observations p 69 N84-25152
Correlation calculation in stereoscopic image pairs for the automatic acquisition of digital land models, orthoimages and height line planes [SER-C283] p 21 N84-26079
Comparative assessment of LANDSAT-D MSS and TM data quality for mapping applications in the Southeast [E84-10138] p 61 N84-26086
Field data observed during the geological excursion in the west-central region of the Sul-Rio Grande Shield [E84-10146] p 29 N84-26094
Frontiers of Remote Sensing of the Oceans and Troposphere from Air and Space Platforms [NASA-CP-2303] p 42 N84-27262
On the detection of underwater bottom topography by imaging radars p 46 N84-27301
Modeling of SAR signatures of shallow water ocean topography p 47 N84-27302

TRAJECTORY ANALYSIS
A model for the analysis of drifter data with an application to a warm core ring in the Gulf of Mexico p 33 N84-34503
The effect of ocean surface temperature on the trajectories of tropical cyclones p 34 N84-35252

TRANSFER FUNCTIONS
Measurements of ocean wave spectra and modulation transfer function with the airborne two frequency scatterometer p 45 N84-27282

TRANSFORMATIONS (MATHEMATICS)
The use of Hough transformation for detecting lineaments in satellite imagery p 22 N84-30262

TRANSPODERS
Error analysis for marine geodetic control using the global positioning system [AD-A140566] p 21 N84-26687

TREES (PLANTS)
Evaluation of factors causing reflectance differences between sun and shade leaves p 3 N84-30674

TRIANGULATION
Estimation of variances and covariances in the multivariate and in the incomplete multivariate model p 20 N84-26073
Error analysis for marine geodetic control using the global positioning system [AD-A140566] p 21 N84-26687

TROPICAL METEOROLOGY
Aircraft measurements of convective draft cores in MONEX p 31 N84-31821
Elements of the west African monsoon circulation deduced from Meteosat cloud winds and simultaneous aircraft measurements p 51 N84-31948
Downdrafts from tropical oceanic cumuli p 32 N84-33985
The effect of ocean surface temperature on the trajectories of tropical cyclones p 34 N84-35252

TROPICAL REGIONS
Using Landsat to monitor tropical forest ecosystems p 5 N84-33352
Intensive forest clearing in Rondonia, Brazil, as detected by satellite remote sensing p 8 N84-37204

TROPICAL STORMS
Satellite observed upper level moisture patterns associated with tropical cyclone movement p 37. N84-39523
Microwave remote sensing of ocean surface wind speed and rain rates over tropical storms p 45 N84-27288

TROPOSPHERE
AVHRR aerosol ground truth experiment [PB84-157882] p 39 N84-24065
ESA activities in the use of microwaves for the remote sensing of the Earth p 42 N84-27264

TURBIDITY
Turbidity/sediment concentration mapping in the coastal area of Bangladesh p 50 N84-30246
A theoretical study of an airborne laser technique for determining sea water turbidity p 31 N84-33774
CZCS data analysis in turbid coastal water p 37 N84-39427

U

UNDERWATER OPTICS
Remote sensing marine bioluminescence - The role of the in-water scalar irradiance p 34 N84-36107
Atmospheric correction of Landsat MSS data for a multistate suspended sediment algorithm p 59 N84-38942
Ocean optical remote sensing capability statement [AD-A140589] p 49 N84-27321

UNDERWATER PHOTOGRAPHY
Application of computer image processing to underwater surveys [AD-P003122] p 41 N84-26263

UNITED STATES
State remote sensing (LANDSAT) programs catalog [E84-10127] p 71 N84-23985
US aeromagnetic and satellite magnetic anomaly comparisons p 28 N84-25136

UPPER ATMOSPHERE
Satellite observed upper level moisture patterns associated with tropical cyclone movement p 37 N84-39523

UPWELLING WATER
Observations of Gulf Stream-induced and wind-driven upwelling in the Georgia Bight using ocean color and infrared imagery p 34 N84-34517

URANIUM
Application of Landsat data in the exploration of 'Calcrete' uranium deposits p 24 N84-37775

URBAN DEVELOPMENT
Analysis of land use changes around Salt Lake City using Landsat digital data - A case study of Sandy area p 13 N84-30242

URBAN RESEARCH
The use of an image registration technique in the urban growth monitoring [E84-10147] p 16 N84-26095

USER REQUIREMENTS
Multi-models to increase accuracy p 70 N84-25154

UTAH
Enviropod handbook: A guide to preparation and use of the Environmental Protection Agency's light-weight aerial camera system -- Weber River, Utah [E84-10123] p 68 N84-23982
EPA Enviropod. A summary of the use of the Enviropod under a Memorandum of Understanding among EPA Region 8, the State of Utah, and the University of Utah Research Institute [E84-10124] p 15 N84-23983
Identifying environmental features for land management decisions [E84-10125] p 15 N84-23984

V

VALLEYS
Radar-visible wind streaks in the Altiplano of Bolivia p 25 N84-23527

VEGETABLES
Analysis of Landsat for monitoring vegetables in New York mucklands p 5 N84-33345

VEGETATION
The use of Landsat imagery in analyzing the vegetation and energy resources of Pickens County, South Carolina p 3 N84-33330
Vegetation monitoring and classification using NOAA/AVHRR satellite data p 4 N84-33343
Automated vegetation classification using Thematic Mapper Simulation data p 5 N84-33347
A scatter model for vegetation up to Ku-band p 7 N84-37201
Riparian habitat on the Humboldt River, Deeth to Elko, Nevada [E84-10116] p 53 N84-23976
Vegetation, land-use and seasonal albedo data sets: Documentation of archived data tape [E84-10133] p 10 N84-25142

WATER CIRCULATION
Principal components technique analysis for vegetation and land use discrimination -- Brazilian cerrados [E84-10135] p 10 N84-26083
Understanding and utilization of Thematic Mapper and other remotely sensed data for vegetation monitoring [E84-10150] p 11 N84-26098
Interactive digital image processing for terrain data extraction, phase 4 [AD-A140197] p 11 N84-26107
Discriminating vegetation and soils using LANDSAT MSS and Thematic Mapper bands and band ratios [AD-A140198] p 11 N84-26108

VEGETATION GROWTH
Microwave measurements using active and passive sensors -- for agriculture in India p 1 N84-30229
Assessing change in the surficial character of a semiarid environment with Landsat residual images p 3 N84-31499
A regression analysis of data from aircraft and ground measurements of a vegetative cover p 6 N84-34784
Regression in the primal problem of remote sensing (using grass cover as an example) p 6 N84-34785
The Green Cadastre - An experiment for exploring the tree vegetation in the Paris area p 7 N84-36516

VEGETATIVE INDEX
Evaluation of spatial, radiometric and spectral Thematic Mapper performance for coastal studies [E84-10118] p 9 N84-23978
Evaluation of spatial, radiometric and spectral Thematic Mapper performance for coastal studies [E84-10159] p 12 N84-27251

VERTICAL AIR CURRENTS
Aircraft measurements of convective draft cores in MONEX p 31 N84-31821
Downdrafts from tropical oceanic cumuli p 32 N84-33985

VERTICAL DISTRIBUTION
A sample performance of the grille spectrometer aboard Spacelab [AERONOMICA-ACTA-A-281-1984] p 70 N84-26003

VERY LONG BASE INTERFEROMETRY
Proceedings of a workshop: Multidisciplinary Use of the Very Long Baseline Array [NASA-CR-173541] p 69 N84-25034

VIDEO DATA
Videography - Some remote sensing applications p 3 N84-33331

VINEYARDS
Benchmark data on the separability between orchards and vineyards in the southern San Joaquin Valley of California p 5 N84-33348
Use of remote sensing for land use policy formulation [E84-10117] p 9 N84-23977

VISIBLE SPECTRUM
Interpreting the spectra of aerial photographs of the sea surface p 30 N84-30443
Active microwave responses - An aid in improved crop classification p 3 N84-31498

VOLCANOES
First estimate of annual mercury flux at the Kilauea main vent p 15 N84-34794

VORTICES
Mean circulation and eddy kinetic energy in the eastern North Atlantic p 32 N84-34501
The importance of altimeter and scatterometer data for ocean prediction p 49 N84-27316
Sampling strategies and four-dimensional assimilation of altimetric data for ocean monitoring and prediction p 49 N84-27317

W

WARNING SYSTEMS
Space disturbance warning system with the aid of satellites p 15 N84-38301
Fire detection using the NOAA (National Oceanic and Atmospheric Administration)-series satellites [PB84-176890] p 13 N84-27324

WATER
Nimbus 7 SMMR derived seasonal variations in the water vapor, liquid water and surface winds over the global oceans [NASA-TM-86080] p 40 N84-26233
Water mass classification in the North Atlantic using IR digital data and Bayesian decision theory [AD-P003125] p 41 N84-26266

WATER CIRCULATION
Dynamics of the slope water of New England and its influence on the Gulf Stream as inferred from satellite IR data p 31 N84-30672
Mean circulation and eddy kinetic energy in the eastern North Atlantic p 32 N84-34501
Lagrangian observations of an anticyclonic ring in the western Gulf of Mexico p 33 N84-34502

WATER MANAGEMENT

A model for the analysis of drifter data with an application to a warm core ring in the Gulf of Mexico
p 33 A84-34503
Satellite observations of circulation in the eastern Bering Sea
p 33 A84-34514
NASA Oceanic Processes Program, fiscal year 1983
[NASA-TM-86248] p 39 N84-24078

WATER MANAGEMENT

Locating shoreline changes in the Porttipahta (Finland) water reservoir by using multitemporal Landsat data
p 52 A84-33987

WATER RESOURCES

The application of Landsat image in the surveying of water resources of Dongting Lake p 51 A84-30255
A report of Ceara Project activities
[INPE-2988-RPE/452] p 54 N84-27260

WATER RUNOFF

Atmospheric model development p 53 N84-22998

WATER TEMPERATURE

Rapid evolution of a Gulf Stream warm-core ring
p 32 A84-34164

WATER VAPOR

Monthly distributions of precipitable water from the Nimbus 7 SMMR data p 37 A84-39458
Satellite observations of a monsoon depression [NASA-CR-173590] p 40 N84-26232
Nimbus 7 SMMR derived seasonal variations in the water vapor, liquid water and surface winds over the global oceans
[NASA-TM-86080] p 40 N84-26233

WATER WAVES

Digital processing considerations for extraction of ocean wave image spectra from raw synthetic aperture radar data p 30 A84-30025
First observations of the interaction of ocean swell with sea ice using satellite radar altimeter data
p 35 A84-36684

Microwave backscattering characteristics of wind-generated waves p 36 A84-38309
Wind, waves and swell in the Antarctic marginal ice zone by SEASAT radar altimeter p 38 N84-23941
Some case studies of ocean wave physical processes utilizing the GSFC airborne radar ocean wave spectrometer p 45 N84-27283

WATERSHEDS

Aircraft scatterometer observations of soil moisture on rangeland watersheds p 4 A84-33338
Drainage pattern delineation - a function of image scale p 52 A84-33535
Riparian habitat on the Humboldt River, Deeth to Elko, Nevada
[E84-10116] p 53 N84-23976

WAVEGUIDE WINDOWS

Recent advances in multispectral sensing of ocean surface temperature from space p 46 N84-27297

WAVELENGTHS

Reduced to pole long-wavelength magnetic anomalies of Africa and Europe p 27 N84-25132
Long-wavelength magnetic and gravity anomaly correlations of Africa and Europe p 28 N84-25135

WEATHER FORECASTING

Remote sensing and storm surge forecasting in Bangladesh p 30 A84-30230
ERS-1 - An ice and ocean monitoring mission p 36 A84-38620

Diagnostics of rainfall anomalies in the Nordeste during the global weather experiment
[SAPR-1] p 40 N84-26235

Vector wind, horizontal divergence, wind stress and wind stress curl from SEASAT-SASS at one degree resolution p 48 N84-27313

WEST GERMANY

Digital processing of LANDSAT data for the preparation of a land use map of the rural district surrounding Tuebingen to a scale of 1:50000
[ESA-TT-816] p 16 N84-26104

WETLANDS

Automated classification of wetlands p 4 A84-33337
Potential benefits of new satellite sensors to wetland mapping p 7 A84-34960

Evaluation of spatial, radiometric and spectral Thematic Mapper performance for coastal studies
[E84-10118] p 9 N84-23978

Evaluation of spatial, radiometric and spectral Thematic Mapper performance for coastal studies
[E84-10159] p 12 N84-27251

WHEAT

Sampling system for wheat (*Triticum aestivum* L) area estimation using digital LANDSAT MSS data and aerial photographs -- Brazil
[E84-10139] p 10 N84-26087

A sampling system for estimating the cultivation of wheat (*Triticum aestivum* L) from LANDSAT data
[E84-10165] p 12 N84-27257

WILDERNESS

Land cover and terrain mapping for the development of digital data bases for wildlife habitat assessment in the Yukon Flats National Wildlife Refuge, Alaska
p 9 N84-23971

WILDLIFE

Land cover and terrain mapping for the development of digital data bases for wildlife habitat assessment in the Yukon Flats National Wildlife Refuge, Alaska
p 9 N84-23971

Application of remote sensing to state and regional problems
[E84-10128] p 68 N84-23986

WIND (METEOROLOGY)

New algorithms for microwave measurements of ocean winds
The variability of the surface wind field in the equatorial Pacific Ocean: Criteria for satellite measurements
p 46 N84-27296

Vector wind, horizontal divergence, wind stress and wind stress curl from SEASAT-SASS at one degree resolution p 48 N84-27313

The impact of scatterometer wind data on global weather forecasting p 49 N84-27314

The importance of altimeter and scatterometer data for ocean prediction p 49 N84-27316

WIND DIRECTION

The impact of scatterometer wind data on global weather forecasting p 49 N84-27314

WIND EFFECTS

Katabatic wind forcing of the Terra Nova Bay polynya p 33 A84-34509

Microwave backscattering characteristics of wind-generated waves p 36 A84-38309

WIND EROSION

Radar-visible wind streaks in the Altiplano of Bolivia p 25 N84-23527

WIND MEASUREMENT

Elements of the west African monsoon circulation deduced from Meteosat cloud winds and simultaneous aircraft measurements p 51 A84-31948

Global data assimilation experiments with scatterometer winds from SEASAT-A p 65 A84-32938

A model function for ocean radar cross sections at 14.6 GHz p 34 A84-34516

Large-scale analysis and forecast experiments with wind data from the Seasat A scatterometer p 66 A84-37873

Remote sensing of the ocean by the airborne microwave scatterometer/radiometer system p 36 A84-38307

Microwave scatterometer p 66 A84-38310

The variability of the surface wind field in the equatorial Pacific Ocean: Criteria for satellite measurements
p 46 N84-27296

WIND PROFILES

Vector wind, horizontal divergence, wind stress and wind stress curl from SEASAT-SASS at one degree resolution p 48 N84-27313

WIND VELOCITY

Microwave remote sensing of ocean surface wind speed and rain rates over tropical storms p 45 N84-27288

WIND VELOCITY MEASUREMENT

Aircraft measurements of convective draft cores in MONEX p 31 A84-31821

Ocean wind field measurement performance of the ERS-1 scatterometer p 43 N84-27273

WINTER

Hydrology of the North Slope, Alaska p 53 N84-23973

WORLD DATA CENTERS

Integrated Global Ocean Services System (IGOSS): Guide to the IGOSS data processing and services system
[WMO-623] p 38 N84-23089

WORLD METEOROLOGICAL ORGANIZATION

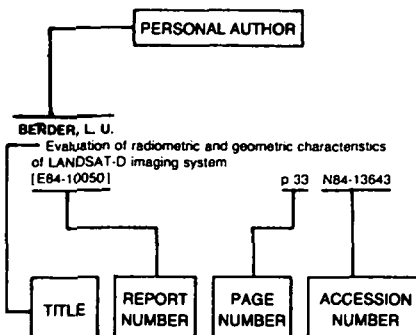
Integrated Global Ocean Services System (IGOSS): Guide to the IGOSS data processing and services system
[WMO-623] p 38 N84-23089

PERSONAL AUTHOR INDEX

EARTH RESOURCES / A Continuing Bibliography (Issue 43)

OCTOBER 1984

Typical Personal Author Index Listing



Listings in this index are arranged alphabetically by personal author. The title of the document provides the user with a brief description of the subject matter. The report number helps to indicate the type of document listed (e.g., NASA report, translation, NASA contractor report). The page and accession numbers are located beneath and to the right of the title. Under any one author's name the accession numbers are arranged in sequence with the AIAA accession numbers appearing first.

A

ABDON, M. D. M. Maps of favorable areas for tuna fishing to the South and Southeast of Brazil prepared from SMS-2 satellite data [INPE-3102-PRE/501] p 41 N84-26256

ACKERMAN, M. A sample performance of the grille spectrometer aboard Spacelab [AERONOMICA-ACTA-A-281-1984] p 70 N84-26003

ACKERMANN, F. E. Seminar on mathematical models of geodetic/photogrammetric point determination with regard to outliers and systematic errors [SER-A-98] p 20 N84-26069

Mathematical models of photogrammetric point determination p 20 N84-26070

ADDIS, R. P. Downdrafts from tropical oceanic cumuli p 32 N84-33985

AGRENICH, E. A. The effect of ocean surface temperature on the trajectories of tropical cyclones p 34 N84-35252

AHERN, F. J. Evaluating LANDSAT-4 MSS and TM data [E84-10157] p 63 N84-27249

AIKYO, K. Space disturbance warning system with the aid of satellites p 15 N84-38301

AKHMEDOV, SH. A. The effect of fluctuations in the optical properties of the atmosphere on spectral brightness ratios in the remote sensing of agricultural areas p 6 N84-34777

ALAM, A. K. M. S. Application of the Vizir Image Processing System to the remote sensing studies in Bangladesh p 64 N84-30266

ALDRIDGE, B. Fire detection using the NOAA (National Oceanic and Atmospheric Administration)-series satellites [PB84-176890] p 13 N84-27324

ALEKSARDROV, IU. N. An airborne radar station for studying the reflection properties of the earth's surface p 64 N84-31072

ALI, A. Remote sensing and storm surge forecasting in Bangladesh p 30 N84-30230

ALMEIDAFLHO, R. Utilization of digital LANDSAT imagery for the study of granitoid bodies in Rondonia: Case example of the Pedra Branca massif [E84-10120] p 26 N84-23979

Multiseasonal variables in digital image enhancements for geological applications [E84-10145] p 29 N84-26093

ALPERS, W. On the detection of underwater bottom topography by imaging radars p 46 N84-27301

ANDERSON, R. N. Mapping the sea floor by satellite p 35 N84-36686

ANUTA, P. E. Landsat-4 MSS and Thematic Mapper data quality and information content analysis p 56 N84-33528

LANDSAT-4 image data quality analysis [E84-10134] p 10 N84-26082

LANDSAT-4 image data quality analysis [E84-10158] p 63 N84-27250

ARCHWAMETY, C. Thematic Mapper image quality - Registration, noise, and resolution p 57 N84-33533

ARMANA, N. A. An airborne radar station for studying the reflection properties of the earth's surface p 64 N84-31072

ARNONE, R. A. Ocean optical remote sensing capability statement [AD-A140589] p 49 N84-27321

ASMEROM, Y. Pinacate-Gran Desierto Region, Mexico: SIR-A data analysis p 25 N84-23526

ASSUNCAO, G. V. Identification and estimation of the area planted with irrigated rice based on the visual interpretation of LANDSAT MSS data [E84-10164] p 12 N84-27256

ATLAS, D. Remote sensing of air-sea interactions p 42 N84-27267

The impact of scatterometer wind data on global weather forecasting p 49 N84-27314

ATLAS, R. Large-scale analysis and forecast experiments with wind data from the Seasat A scatterometer p 66 N84-37873

B

BACKUS, R. Rapid evolution of a Gulf Stream warm-core ring p 32 N84-34164

BADHWAR, G. D. Evaluation of corn/soybeans separability using Thematic Mapper and Thematic Mapper Simulator data p 5 N84-33539

BAGCHI, A. K. Hydrological data densification in mountainous terrain using Landsat imagery p 51 N84-30256

Estimation of depth of snow from Landsat imagery p 52 N84-33355

BAHAR, E. Optimum backscatter cross section of the ocean as measured by synthetic aperture radars p 44 N84-27276

BAILEY, P. L. The validation of Nimbus 7 LIMS measurements of ozone p 67 N84-39443

Accuracy and precision of the nitric acid concentrations determined by the limb infrared monitor of the stratosphere experiment on NIMBUS 7 p 67 N84-39444

BAIN, D. Coastal mapping of the Beaufort Sea coast p 31 N84-33360

BAKER, K. Rapid evolution of a Gulf Stream warm-core ring p 32 N84-34164

BAKER, W. E. Large-scale analysis and forecast experiments with wind data from the Seasat A scatterometer p 66 N84-37873

The impact of scatterometer wind data on global weather forecasting p 49 N84-27314

BALIEIRO, M. G. Project SERGE: Brazil referential field data for the SIR-A experiment [INPE-2973-NTE/210] p 29 N84-27259

BALL, W. E., JR. Development of satellite Doppler/inertial survey systems for BLM cadastral survey-related applications in Alaska p 14 N84-33370

BALMINO, G. Somali current studied from SEASAT altimetry p 47 N84-27307

BALTER, B. M. Regression in the primal problem of remote sensing (using grass cover as an example) p 6 N84-34785

BAPAT, M. V. Identification of water-logged and salt-affected soils through remote sensing techniques p 51 N84-30251

BARABOSHIN, S. M. An airborne radar station for studying the reflection properties of the earth's surface p 64 N84-31072

BARBOSA, M. P. Results of field observations of radio waves in alluvial deposits in Cara state from 1:100,000: Fortaleza, Canirde, Taperuba, Santa Quiteria, Sobral, and Sao Luiz do Curu [INPE-3061-NTE/216] p 53 N84-26100

A report of Ceara Project activities [INPE-2988-RPE/452] p 54 N84-27260

BARINOV, V. S. An airborne radar station for studying the reflection properties of the earth's surface p 64 N84-31072

BARNES, W. L. Heat Capacity Mapping Radiometer (HCMR) data processing algorithm, calibration, and flight performance evaluation [E84-10153] p 71 N84-27248

BARNETT, S. Pinacate-Gran Desierto Region, Mexico: SIR-A data analysis p 25 N84-23526

BARRICK, D. Optimum backscatter cross section of the ocean as measured by synthetic aperture radars p 44 N84-27276

BARROS, J. A. I. Identification and estimation of the area planted with irrigated rice based on the visual interpretation of LANDSAT MSS data [E84-10164] p 12 N84-27256

BARROS, M. S. The use of photointerpretation for socio-economic characterization of urban population [INPE-3067-PRE/484] p 16 N84-26428

BARTOLUCCI, L. A. Landsat-4 MSS and Thematic Mapper data quality and information content analysis p 56 N84-33528

BARTON, I. J. Dual channel satellite measurements of sea surface temperature p 31 N84-31431

BATISTA, G. T. Sampling system for wheat (*Triticum aestivum* L) area estimation using digital LANDSAT MSS data and aerial photographs [E84-10139] p 10 N84-26087

Research and applications of data from environmental satellites: Determining parameters and developing interpretation techniques for applications of environmental satellite data [INPE-3005-NTE/213] p 13 N84-27261

BAUER, C. A. Identification and estimation of the area planted with irrigated rice based on the visual interpretation of LANDSAT MSS data [E84-10164] p 12 N84-27256

BEAL, R. C. Tracking ocean wave spectrum from SAR images p 44 N84-27277

A
U
T
H
O
R

BECKER, A.

BECKER, A.
Analysis of airborne electromagnetic systems for mapping thickness of sea ice
[AD-A139786] p 39 N84-25235

BEGUM, D.
Bay monsoon activities in relation to the monsoon in the western Pacific p 30 N84-30232

BENSON, A. S.
Analysis of photo interpretation test results for seven aerospace image types of the San Juan National Forest, Colorado p 4 A84-33332

BENSON, C. D.
Living and working in space. A history of Skylab [NASA-SP-4208] p 72 N84-25737

BERGER, J.
High precision measurements in crustal dynamic studies [NASA-CR-173680] p 22 N84-28279

BERMEL, P. F.
Program for mapping Antarctica p 18 N84-23954

BERNABO, M.
X to W band radiometric signatures of natural surfaces p 35 A84-36289

BERNSTEIN, R.
Analysis and processing of Landsat-4 sensor data using advanced image processing techniques and technologies p 56 A84-33527

BESSON, J.
A sample performance of the grille spectrometer aboard Spacelab [AERONOMICA-ACTA-A-281-1984] p 70 N84-26003

BETTENCOURT, J. S.
Utilization of digital LANDSAT imagery for the study of granitoid bodies in Rondonia: Case example of the Pedra Branca massif [E84-10120] p 26 N84-23979

BEWTRA, M.
Heat Capacity Mapping Radiometer (HCMR) data processing algorithm, calibration, and flight performance evaluation [E84-10153] p 71 N84-27248

BHARTIA, P. K.
Intercomparison of the Nimbus 7 SBUV/TOMS total ozone data sets with Dobson and M83 results p 67 A84-39449

BIZZELL, R. M.
Automated vegetation classification using Thematic Mapper Simulation data p 5 A84-33347

BLACK, P. G.
Microwave remote sensing of ocean surface wind speed and rain rates over tropical storms p 45 N84-27288

BLACKWELDER, P.
Rapid evolution of a Gulf Stream warm-core ring p 32 A84-34164

BLANCHARD, B. J.
Active microwave responses - An aid in improved crop classification p 3 A84-31498

BLY, B.
Comparative accuracies of AVHRR and MSS data used for Level I land cover classifications p 14 A84-33344

BOGGS, D. H.
A new parameterization of an empirical model for wind/ocean scatterometry p 43 N84-27269

BOHSE, J. R.
Heat Capacity Mapping Radiometer (HCMR) data processing algorithm, calibration, and flight performance evaluation [E84-10153] p 71 N84-27248

BONATTI, E.
Oceanic fracture zones p 31 A84-31193

BOREL, D.
Monitoring the marine environment with remote sensing technology p 30 A84-30258

BORODIN, L. F.
An airborne radar station for studying the reflection properties of the earth's surface p 64 A84-31072

BORRANI, A.
X to W band radiometric signatures of natural surfaces p 35 A84-36289

BRACHET, G.
High resolution observation of the earth's surface from space - Programs, problems and perspectives p 71 A84-37049

BRAILE, L. W.
Application of Magsat lithospheric modeling in South America. Part 1: Processing and interpretation of magnetic and gravity anomaly data [E84-10115] p 24 N84-23008

Application of Magsat to lithospheric modeling in South America. Part 2: Synthesis of geologic and seismic data for development of integrated crustal models [E84-10126] p 26 N84-25128

Satellite elevation magnetic and gravity models of major South American plate tectonic features p 27 N84-25131

PERSONAL AUTHOR INDEX

CARMICHAEL, R. S.
Use of Magsat anomaly data for crustal structure and mineral resources in the US midcontinent [E84-10112] p 24 N84-23005

CARNES, J. G.
Evaluation of corn/soybeans separability using Thematic Mapper and Thematic Mapper Simulator data p 5 A84-33539

CARVER, R. E.
Surface expression of heavily mantled interstratal Karst bordering Okefenokee Swamp, Georgia p 23 A84-33350

CASTLE, K. R.
In-flight absolute radiometric calibration of the Thematic Mapper p 56 A84-33531

CHEM, Z.
In-flight absolute radiometric calibration of the Thematic Mapper p 68 N84-23002

CATE, R. B.
Automated vegetation classification using Thematic Mapper Simulation data p 5 A84-33347

CAUSEY, E. M.
Survey of automated statewide natural resource information systems [AD-A139017] p 16 N84-23996

CAVALIERI, D. J.
A summary of results from the first Nimbus 7 SMMR observations
Determination of sea ice parameters with the Nimbus 7 SMMR p 37 A84-39461

CHANDRASEKHAR, S.
Reduction of high dimension data to two dimension using non linear mapping techniques p 54 A84-30248

CHANG, A. T. C.
Monthly distributions of precipitable water from the Nimbus 7 SMMR data p 37 A84-39458

A summary of results from the first Nimbus 7 SMMR observations p 37 A84-39459

CHANG, H. D.
Monthly distributions of precipitable water from the Nimbus 7 SMMR data p 37 A84-39458

CHAPMAN, W. H.
Surveying in Antarctica during the International Geophysical Year p 25 N84-23942

CHARLSON, R. J.
Airborne observations of Arctic aerosol. IV - Optical properties of Arctic haze p 32 A84-34287

CHAUDHURY, M. U.
Measurement of boro rice acreage in Srimangal Thana by remote sensing technique p 1 A84-30235

Digital processing of remote sensing data on Hail Haor, Bangladesh for landuse analysis and development potential assessment p 13 A84-30240

SPOT simulations in Bangladesh flight operations and main results p 2 A84-30253

CHEN, S. C.
Sampling system for wheat (*Triticum aestivum* L) area estimation using digital LANDSAT MSS data and aerial photographs [E84-10139] p 10 N84-26087

CHEN, Z.
Typical analysis of regional stability and block structures with remote sensing images p 22 A84-30254

CHENG, C. J.
An inquiry into methods of estimating yields of wheat and autumn crops in the plain region with Landsat images visual interpretation p 2 A84-30239

CHIEN, J. Z.
Microwave remote sensing of ocean surface wind speed and rain rates over tropical storms p 45 N84-27288

CHOWDHURY, M. I.
Sediment volume modelling in the coastal area of Bangladesh using turbidity/sediment concentration map based on Landsat data p 51 A84-30257

CHRISTENSEN, P.
Pinacate-Gran Desierto Region, Mexico: SIR-A data analysis p 25 N84-23526

Radar-visible wind streaks in the Altiplano of Bolivia p 25 N84-23527

CHRZANOWSKI, A.
A forecast of the impact of GPS on surveying p 18 A84-33374

CHU, L.
The lineament features of Tarim Basin (west part) and its bearing on the characteristics of Cenozoic tectonic stress fields p 22 A84-30263

CHU, W. P.
A comparative study of aerosol extinction measurements made by the SAM II and SAGE satellite experiments p 15 A84-39457

CICONE, R. C.
A physically-based transformation of Thematic Mapper data The TM tasseled cap p 56 A84-33532

Understanding and utilization of Thematic Mapper and other remotely sensed data for vegetation monitoring [E84-10150] p 11 N84-26098

C

CAMARA-NETO, G.
An integrated software system for geometric correction of LANDSAT MSS imagery [E84-10143] p 62 N84-26091

CAMPBELL, W. J.
A summary of results from the first Nimbus 7 SMMR observations p 37 A84-39459

Determination of sea ice parameters with the Nimbus 7 SMMR p 37 A84-39461

Wind, waves and swell in the Antarctic marginal ice zone by SEASAT radar altimeter p 38 N84-23941

Arctic Sea ice by passive microwave observations from the Nimbus-5 Satellite p 39 N84-23970

CAPPELLINI, V.
Digital comparison and correlation techniques of remote sensing images having different space resolution p 55 A84-33356

CARD, D. H.
Thematic Mapper image quality - Registration, noise, and resolution p 57 A84-33533

PERSONAL AUTHOR INDEX

ENG, W. P.

CIHLAR, J.
Evaluating LANDSAT-4 MSS and TM data [E84-10157] p 63 N84-27249

CIVCO, D. L.
A semi-automated procedure for identifying Landsat MSS subregion coordinates p 58 A84-34959

CLARK, B. V.
A microwave systems approach to measuring root zone soil moisture [E84-10114] p 9 N84-23007

CLARK, I. O.
Effect of space exposure on pyroelectric infrared detectors (A0135) p 68 N84-24679

CLARKE, A. D.
Airborne observations of Arctic aerosol. IV - Optical properties of Arctic haze p 32 A84-34287

CLAUS, M.
Correlation calculation in stereoscopic image pairs for the automatic acquisition of digital land models, orthophotos and height line planes [SER-C283] p 21 N84-26079

COLLINS, J.
Establishing first-order control by GPS satellite surveying instruments p 18 A84-33368

COLLINS, J. G.
Airborne laser topographic mapping results p 8 A84-38998

COLWELL, R. N.
Analysis of the quality of image data acquired by the LANDSAT-4 Thematic Mapper and Multispectral Scanners [E84-10137] p 61 N84-26085

COMPTON, W. D.
Living and working in space. A history of Skylab [NASA-SP-4208] p 72 N84-25737

CORTESI, W.
NASA, the first 25 years: 1958 - 1983 [NASA-EP-182] p 72 N84-26563

COULTER, R. E.
Water mass classification in the North Atlantic using IR digital data and Bayesian decision theory [AD-P003125] p 41 N84-26266

COUREL, M. F.
Surface albedo and the Sahel drought p 7 A84-36710

COWLES, T.
Rapid evolution of a Gulf Stream warm-core ring p 32 A84-34164

COX, R. P.
The active microwave instrumentation for ERS-1 p 34 A84-35542

CRANE, K.
Oceanic fracture zones p 31 A84-31193

CRIST, E. P.
Characterization of Landsat-4 MSS and TM digital image data p 56 A84-33526

A physically-based transformation of Thematic Mapper data The TM tasseled cap p 56 A84-33532

Understanding and utilization of Thematic Mapper and other remotely sensed data for vegetation monitoring [E84-10150] p 11 N84-26098

CROOM, D. L.
Climate research from space p 66 A84-38922

CROSBY, D. S.
Theory and validation of the multiple window sea surface temperature technique p 33 A84-34513

CROSSFIELD, J. K.
A Doppler positioning cost model p 18 A84-33365

CRUCH, R. K.
Effect of space exposure on pyroelectric infrared detectors (A0135) p 68 N84-24679

CUQ, F.
Remote sensing of the Santonge littoral. Processing and interpretation of satellite images [ISBN-2-85929-016-8] p 63 N84-28202

D

DALELIO, J.
NASA, the first 25 years: 1958 - 1983 [NASA-EP-182] p 72 N84-26563

DARLING, G. D.
Digital processing considerations for extraction of ocean wave image spectra from raw synthetic aperture radar data p 30 A84-30025

DASGUPTA, A. R.
The experience of organising a utilisation programme for Bhaskara p 64 A84-30233

DAUGHERTY, K. I.
The geodetic activities of the Department of Defense under IGY programs p 17 A84-30727

DEALBUQUERQUE, P. C. G.
Orbital imagery: A cartographic solution [INPE-2820-PRE/374] p 20 N84-25143

DEALMEIDA, F. C.
Research and applications of data from environmental satellites: Determining parameters and developing interpretation techniques for applications of environmental satellite data [INPE-3005-NTE/213] p 13 N84-27261

DEAN, M. E.
Landsat-4 MSS and Thematic Mapper data quality and information content analysis p 56 A84-33528

DEASIS, O. R.
Forest inventory using multistage sampling with probability proportional to size [E84-10144] p 11 N84-26092

DEASSUNCAO, G. V.
Irrigated rice area estimation using remote sensing techniques: Project's proposal and preliminary results [E84-10131] p 10 N84-26081

DEEKSHATULU, B. L.
Benefits and problems in operational remote sensing p 64 A84-30252

DEGLORIA, S. D.
Spectral variability of Landsat-4 Thematic Mapper and Multispectral Scanner data for selected crop and forest cover types p 5 A84-33538

DEGODOI, S. S.
Seasonal oscillations of the subtropical convergence between the Brazil and Malvinas currents, using oceanographic and SMS-2 satellite data [INPE-3092-PRE/497] p 40 N84-26255

DEHORITY, D. C.
Microwave remote sensing of ocean surface wind speed and rain rates over tropical storms p 45 N84-27288

DELBARD, R.
The Green Cadastre - An experiment for exploring the tree vegetation in the Paris area p 7 A84-36516

DELIKARAOGLU, D.
Geometrical aspects of differential GPS positioning p 17 A84-32494

DEMAY, P.
Simulation and assimilation of satellite altimeter data at the oceanic mesoscale p 48 N84-27312

DEMEDIOS, J. S.
Forest inventory using multistage sampling with probability proportional to size [E84-10144] p 11 N84-26092

DEOLIVEIRA, M. D. L. N.
Application of LANDSAT data to the study of urban development in Brasilia [E84-10142] p 16 N84-26090

DEOLIVEIRA, M. D. L. N.
The use of an image registration technique in the urban growth monitoring [E84-10147] p 16 N84-26095

DEOLIVEIRA, M. D. L. N.
The use of photointerpretation for socio-economic characterization of urban population [INPE-3067-PRE/484] p 16 N84-26428

DEPINHO, O. G.
Utilization of digital LANDSAT imagery for the study of granitoid bodies in Rondonia: Case example of the Pedra Branca massif [E84-10120] p 26 N84-23979

DESOBIS, M.
Elements of the west African monsoon circulation deduced from Meteosat cloud winds and simultaneous aircraft measurements p 51 A84-31948

DESOUSA, R. C. M.
An integrated software system for geometric correction of LANDSAT MSS imagery [E84-10143] p 62 N84-26091

DEWAN, A. Q.
Bay monsoon activities in relation to the monsoon in the western Pacific p 30 A84-30232

DEWHURST, W. T.
Status report - Gravity activities within the National Geodetic Survey (NGS) p 18 A84-33373

DIAS, A. R.
Digital processing considerations for extraction of ocean wave image spectra from raw synthetic aperture radar data p 30 A84-30025

DIAS, L. A. V.
Principal components technique analysis for vegetation and land use discrimination [E84-10135] p 10 N84-26083

DICKSON, R. R.
Eurasian snow cover versus Indian monsoon rainfall - An extension of the Hahn-Shukla results p 51 A84-31950

DING, X.
Geological interpretation from aerial remote sensing images of Tengchong area p 23 A84-32590

DINGUIRARD, M.
In-flight absolute radiometric calibration of the Thematic Mapper p 56 A84-33531

DINGUIRARD, M.
In-flight absolute radiometric calibration of the Thematic Mapper p 68 N84-23002

DOSSANTOS, J. R.
Principal components technique analysis for vegetation and land use discrimination [E84-10135] p 10 N84-26083

Project SERGE: Brazil referential field data for the SIR-A experiment [INPE-2973-NTE/210] p 29 N84-27259

DOTTAVIO, C. L.
Potential benefits of new satellite sensors to wetland mapping p 7 A84-34960

DOTTAVIO, F. D.
Potential benefits of new satellite sensors to wetland mapping p 7 A84-34960

DOZIER, J.
Snow reflectance from Landsat-4 Thematic Mapper p 52 A84-33541

LANDSAT-D investigations in snow hydrology [E84-10094] p 53 N84-22997

DRUMMOND, J.
A regional raster data study at the Experimental Cartography Unit - The application of interactive raster graphics to environmental modelling p 14 A84-33363

DUFF, P. F.
Revised radiometric calibration technique for Landsat-4 Thematic Mapper data p 56 A84-33530

DUMMER, K. J.
Analysis of photo interpretation test results for seven aerospace image types of the San Juan National Forest, Colorado p 4 A84-3332

DURDEN, S. L.
Synthetic aperture radar images of ocean waves, theories of imaging physics and experimental tests p 43 N84-27275

DURKEE, P. A.
Detection of marine aerosol particles in coastal zones using satellite imagery p 36 A84-38943

DUTRA, L. V.
Evaluation of entropy and JM-distance criterions as features selection methods using spectral and spatial features derived from LANDSAT images [E84-10141] p 62 N84-26089

Evaluation of SIR-A (Shuttle Imaging Radar) images from the Tres Marias region (Minas Gerais State, Brazil) using derived spatial features and registration with MSS-LANDSAT images [E84-10148] p 62 N84-26096

DVORAK, V.
Satellite observed upper level moisture patterns associated with tropical cyclone movement p 37 A84-39523

E

EDELMANN, D.
Large-scale analysis and forecast experiments with wind data from the Seasat A scatterometer p 66 A84-37873

EDWARDS, D. L.
Terrain analysis database generation through computer-assisted photo interpretation p 55 A84-33334

EJUMNOH, A.
An undetectable factor in geomorphological mapping from land satellite images - A case study in the central highland, Thailand p 22 A84-30261

ELACHI, C.
Spaceborne radar subsurface imaging in hyperarid regions p 24 A84-39379

ELMAN, R. I.
Interactive procedures for distinguishing and reconstructing contour networks p 58 A84-34786

EMERY, W. J.
Seasonal variability in meanders of the California Current System off Vancouver Island p 33 A84-34507

Variations in surface current off the coasts of Canada as inferred from infrared satellite imagery p 47 N84-27305

EMMITT, G. D.
Downdrafts from tropical oceanic cumuli p 32 A84-33985

ENDEMANN, M.
Applications of laser for climatology and atmospheric research [BLEV-R-65.169-5] p 70 N84-26237

Fundamentals of spaceborne remote sensing: Applications of lasers, volume 1 p 70 N84-26238

ENG, S. T.
Computer-automated CO₂-laser long-path absorption system for air quality monitoring in the working environment p 13 A84-30307

ENG, W. P.
An improved dual-frequency technique for the remote sensing of ocean currents and wave spectra p 44 N84-27281

EOM, H. J.

EOM, H. J.
A scatter model for vegetation up to Ku-band
p 7 A84-37201

ESILVA, A. J. F. M.
An integrated software system for geometric correction of LANDSAT MSS imagery
[E84-10143] p 62 N84-26091

ETCHEGORRY, M.
Present limitations of accurate satellite Doppler positioning for tectonics - An example: Djibouti
p 17 A84-32495

EVANS, A. G.
Applications of the GPS (Global Positioning System) Geodetic Receiver System
[AD-A140567] p 21 N84-26688

EVANS, D. L.
Landsat imagery for the interpretation of Louisiana forest habitat regions
p 3 A84-33328

EVANS, R.
Rapid evolution of a Gulf Stream warm-core ring
p 32 A84-34164

EVANS, W. F. J.
Accuracy and precision of the nitric acid concentrations determined by the limb infrared monitor of the stratosphere experiment on NIMBUS 7 p 67 A84-39444

EZRA, C. E.
In-flight absolute radiometric calibration of the Thematic Mapper p 56 A84-33531
In-flight absolute radiometric calibration of the Thematic Mapper p 68 N84-23002

F

FANG, Y.-C.
Landsat image use in forestry management in China
p 2 A84-30250

FARHAN, Y. I.
Soil erosion mapping and evaluation - A photo-geomorphological approach p 14 A84-33333

FARIODDIN BHUIYAN, A. K. M.
Measurement of boro rice acreage in Nabinagar Thana by remote sensing technique p 1 A84-30227
Measurement of boro rice acreage in Srimangal Thana by remote sensing technique p 1 A84-30235

FARUQUI, K.
Application of the Vizir Image Processing System to the remote sensing studies in Bangladesh
p 64 A84-30266

FAVARD, J. C.
SPOT simulations in Bangladesh flight operations and main results p 2 A84-30253

FEDOROV, K. N.
The evolution of mushroom-shape currents in the ocean p 36 A84-38773

FELDMAN, U.
Method to estimate drag coefficient at the air/ice interface over drifting open pack ice from remotely sensed data p 48 N84-27310

FELL, P. J.
Error analysis for marine geodetic control using the global positioning system
[AD-A140566] p 21 N84-26687

FERRIGNO, J. G.
Satellite image atlas of glaciers: The Polar regions p 38 N84-23940
Glaciological and geological studies of Antarctica with satellite remote sensing technology p 38 N84-23956

FIEDLER, P. C.
Satellite observations of the 1982-1983 El Nino along the U.S. Pacific coast p 35 A84-36872

FISCHER, H.
Accuracy and precision of the nitric acid concentrations determined by the limb infrared monitor of the stratosphere experiment on NIMBUS 7 p 67 A84-39444

FITZGERALD, A. J.
Revised radiometric calibration technique for Landsat-4 Thematic Mapper data p 56 A84-33530

FITZWATER, M. A.
Optimum backscatter cross section of the ocean as measured by synthetic aperture radars
p 44 N84-27276

FLEIG, A. J.
Intercomparison of the Nimbus 7 SBUV/TOMS total ozone data sets with Dobson and M83 results p 67 A84-39449

FLEMING, M. D.
Land cover and terrain mapping for the development of digital data bases for wildlife habitat assessment in the Yukon Flats National Wildlife Refuge, Alaska
p 9 N84-23971

FOLLETT, A.
Coastal mapping of the Beaufort Sea coast p 31 A84-33360

FORD, A. B.

The Duffek intrusion of Antarctica and a survey of its minor metals related to possible resources
p 25 N84-23943

FORD, G. E.
LANDSAT-D Thematic Mapper image dimensionality reduction and geometric correction accuracy
[E84-10149] p 62 N84-26097

FORESTI, C.
Application of LANDSAT data to the study of urban development in Brasilia
[E84-10142] p 16 N84-26090

The use of an image registration technique in the urban growth monitoring
[E84-10147] p 16 N84-26095

FORMAGGIO, A. R.
Principal components technique analysis for vegetation and land use discrimination
[E84-10135] p 10 N84-26083

FOSTER, J. N.
Technical publications of the NASA Wallops Flight Facility, 1980 through 1983
[NASA-TM-84421] p 72 N84-26467

FRANK, T. D.
Assessing change in the surficial character of a semiarid environment with Landsat residual images
p 3 A84-31499

FRASER, R. S.
Atmospheric effect on classification of finite fields
p 2 A84-30670

FRIEDMAN, S. Z.
An analysis of Landsat-4 Thematic Mapper geometric properties
p 57 A84-33536

FRYXELL, G.
Rapid evolution of a Gulf Stream warm-core ring
p 32 A84-34164

FUGONO, N.
Remote sensing of the ocean by the airborne microwave scatterometer/radiometer system p 36 A84-38307

FUNG, A. K.
A scatter model for vegetation up to Ku-band
p 7 A84-37201

FUSCO, L.
Thematic Mapper - The ESA-Earthnet ground segment and processing experience p 57 A84-33542

G

GAFOOR, A.
Measurement of boro rice acreage in Srimangal Thana by remote sensing technique p 1 A84-30235

GANDRUD, B. W.
Accuracy and precision of the nitric acid concentrations determined by the limb infrared monitor of the stratosphere experiment on NIMBUS 7 p 67 A84-39444

GANZORIG, M.
Regression in the primal problem of remote sensing (using grass cover as an example) p 6 A84-34785

GAPOSCHKIN, E. M.
Geodetic use of GEOSAT-A
[AD-A137993] p 19 N84-23048

GARSTANG, M.
Downdrafts from tropical oceanic cumuli
p 32 A84-33985

GAUSMAN, H. W.
Evaluation of factors causing reflectance differences between sun and shade leaves p 3 A84-30674

GAUTHIER, J. F.
Integration of LANDSAT land cover data into the Saginaw River basin geographic information system for hydrologic modeling
[AD-A140185] p 53 N84-26106

GAYET, G.
Description of SEP ground station and Vizir image processing VIPS p 54 A84-30268

GERING, L. R.
The use of Landsat imagery in analyzing the vegetation and energy resources of Pickens County, South Carolina
p 3 A84-33330

GERVIN, J. C.
Comparative accuracies of AVHRR and MSS data used for Level I land cover classifications p 14 A84-33344

GILLE, J. C.
The Limb Infrared Monitor of the Stratosphere - Experiment description, performance, and results
p 66 A84-39440

The validation of Nimbus 7 LIMS measurements of ozone p 67 A84-39443

Accuracy and precision of the nitric acid concentrations determined by the limb infrared monitor of the stratosphere experiment on NIMBUS 7 p 67 A84-39444

GILLETT, P.
ERS-1 - An ice and ocean monitoring mission
p 36 A84-38620

GINZBURG, A. I.

The evolution of mushroom-shape currents in the ocean p 36 A84-38773

GIRARD, A.
Accuracy and precision of the nitric acid concentrations determined by the limb infrared monitor of the stratosphere experiment on NIMBUS 7 p 67 A84-39444

A sample performance of the grille spectrometer aboard Spacelab
[AERONOMICA-ACTA-A-281-1984] p 70 N84-26003

GJESSING, D. T.
Ocean waves and turbulence as observed with an adaptive coherent multifrequency radar
p 44 N84-27279

GLOERSEN, P.
A summary of results from the first Nimbus 7 SMMR observations p 37 A84-39459

Determination of sea ice parameters with the Nimbus 7 SMMR p 37 A84-39461

GLOERSEN, P.
Arctic Sea ice by passive microwave observations from the Nimbus-5 Satellite p 39 N84-23970

GODA, T.
Analysing forest structures by remote sensing p 1 A84-30236

GOEL, N. S.
Inversion of vegetation canopy reflectance models for estimating agronomic variables. III - Estimation using only canopy reflectance data as illustrated by the suits model. IV - Total inversion of the SAIL model p 7 A84-37203

GOEL, R. K.
The experience of organising a utilisation programme for Bhaskara p 64 A84-30233

GOETTING, H. R.
Digital processing of LANDSAT data for the preparation of a land use map of the rural district surrounding Tuebingen to a scale of 1:50000
[ESA-TT-816] p 16 N84-26104

GOFF, T. E.
Intensive forest clearing in Rondonia, Brazil, as detected by satellite remote sensing p 8 A84-37204

GOHKMAN, B.
An analysis of Landsat-4 Thematic Mapper geometric properties p 57 A84-33536

GOLDINGER, A. D.
Tracking ocean wave spectrum from SAR images p 44 N84-27277

GOLDHIRSH, J.
Altimeter height measurement errors introduced by the presence of variable cloud and rain attenuation p 45 N84-27289

Improved resolution rain measurements from spaceborne radar altimeters p 46 N84-27290

GONZALEZ, V. H.
Propagation effects in satellite-based synthetic aperture radars
[AD-A138681] p 67 N84-22873

GOODENOUGH, D. G.
Evaluating LANDSAT-4 MSS and TM data
[E84-10157] p 63 N84-27249

GORDLEY, L. L.
The validation of Nimbus 7 LIMS measurements of ozone p 67 A84-39443

Accuracy and precision of the nitric acid concentrations determined by the limb infrared monitor of the stratosphere experiment on NIMBUS 7 p 67 A84-39444

GORDON, D.
Intercomparison of the Nimbus 7 SBUV/TOMS total ozone data sets with Dobson and M83 results p 67 A84-39449

GORDON, H. R.
Remote sensing marine bioluminescence - The role of the in-water scalar irradiance p 34 A84-36107

GRAFAREND, E.
Stochastic models for point manifolds p 20 N84-26072

GREEGOR, D. H., JR.
Vegetation monitoring and classification using NOAA/AVHRR satellite data p 4 A84-33343

GREELEY, R.
Pinacate-Gran Desierto Region, Mexico: SIR-A data analysis p 25 N84-23526

Radar-visible wind streaks in the Altiplano of Bolivia p 25 N84-23527

GREEN, A. E. S.
High-precision atmospheric ozone measurements using wavelengths between 290 and 305 nm p 67 A84-39447

GREEN, K. M.
Using Landsat to monitor tropical forest ecosystems p 5 A84-33352

GREEN, P.
A regional raster data study at the Experimental Cartography Unit - The application of interactive raster graphics to environmental modelling p 14 A84-33363

PERSONAL AUTHOR INDEX

IYER, H. S.

GREGORY, A. F.
Non-parallactic stereoscopy using shadow-disparity
p 55 N84-33335

GRIEVE, G.
Evaluating LANDSAT-4 MSS and TM data
[E84-10157] p 63 N84-27249

GRIGGS, M.
AVHRR aerosol ground truth experiment
[PB84-157882] p 39 N84-24065

GROSS, G.
Fog recognition in daylight 3.7-micron-band Ticos-N and
NOAA images p 65 N84-34157

GRYBECK, D.
Emerging recognition of the nonfuel mineral resources
of Arctic Alaska p 26 N84-23962

GUERTIN, F. E.
Evaluating LANDSAT-4 MSS and TM data
[E84-10157] p 63 N84-27249

GUSSARD, A.
A tentative unified sea model for scattering and
emission p 45 N84-27285

GUPTA, A. K.
Remote sensing for bauxite prospecting p 22 N84-30260

GURULE, R. L.
Radar backscatter modelling p 25 N84-23525

H

HAGGERSTONE, B.
Drainage pattern delineation - A function of image
scale p 52 N84-33353

HAHN, S.
Simple enhancement techniques in digital image
processing p 58 N84-33798

HALEM, M.
Large-scale analysis and forecast experiments with wind
data from the Seasat A scatterometer
p 66 N84-37873

The impact of scatterometer wind data on global weather
forecasting p 49 N84-27314

HALL, J. R.
Thematic Mapper image quality - Registration, noise,
and resolution p 57 N84-33533

HALPERN, D.
The variability of the surface wind field in the equatorial
Pacific Ocean: Criteria for satellite measurements
p 46 N84-27296

HAMILTON, L. J.
Comparisons of sea-surface temperature obtained from
ship and satellite data
[AD-A138257] p 38 N84-23087

HAN, S.-J.
Analysis of land use changes around Salt Lake City using
Landsat digital data - A case study of Sandy area
p 13 N84-30242

HANS, P.
Ocean wind field measurement performance of the
ERS-1 scatterometer p 43 N84-27273

HANSEN, J. H.
Automated classification of wetlands p 4 N84-33337

HARDER, P. H., II
Crop moisture estimation over the southern Great Plains
with dual polarization 1.66 centimeter passive microwave
data from Nimbus 7
[E84-10163] p 12 N84-27255

HARRIES, J. E.
Atmospheric science p 66 N84-38923

The validation of Nimbus 7 LIMS measurements of
ozone p 67 N84-39443

Accuracy and precision of the nitric acid concentrations
determined by the limb infrared monitor of the stratosphere
experiment on NIMBUS 7 p 67 N84-39444

HARRIS, R.
Equidensitometry and remote sensing imagery p 59 N84-38944

HARUN-OR-RASHID
Measurement of boro rice acreage in Nabinagar Thana
by remote sensing technique p 1 N84-30227

HEEL, F.
Preliminary investigations concerning a 90 GHz
radiometer satellite experiment
[DFVLR-FB-84-02] p 68 N84-24693

HELLMEIER, H. J.
Fish-eye objective in the dose range photogrammetry:
Theoretical and practical investigations
[SER-C-286] p 21 N84-26080

HENDERSON, K. E.
Evaluation of corn/soybeans separability using Thematic
Mapper and Thematic Mapper Simulator data
p 5 N84-33539

Evaluation of Thematic Mapper for detecting soil
properties under grassland vegetation p 6 N84-33540

HENDERSON, T.
Modeling the movement at the polar ice cap at the South
Pole p 20 N84-23957

HENG, L. B.
The compilation of the satellite image map of land-use
of China (1:2,000,000 scale) p 13 N84-30243

HERMANN, B.
Applications of the GPS (Global Positioning System)
Geodetic Receiver System
[AD-A140567] p 21 N84-26688

HERNANDEZFILHO, P.
Forest inventory using multistage sampling with
probability proportional to size
[E84-10144] p 11 N84-26092

HERRMANN, H.
Airborne lidar for oceanography and hydrology (FLOH)
[ESA-TT-799] p 37 N84-22955

HEYDT, H.
Interactive digital image processing for terrain data
extraction, phase 4
[AD-A140197] p 11 N84-26107

HILL, J. M.
Landsat imagery for the interpretation of Louisiana forest
habitat regions p 3 N84-33328

HILL, R. W.
Applications of the GPS (Global Positioning System)
Geodetic Receiver System
[AD-A140567] p 21 N84-26688

HINDMAN, E. E.
Detection of marine aerosol particles in coastal zones
using satellite imagery p 36 N84-38943

HINZE, W. J.
Application of Magsat lithospheric modeling in South
America. Part 1: Processing and interpretation of magnetic
and gravity anomaly data
[E84-10115] p 24 N84-23008

Application of MAGSAT to lithospheric modeling in South
America. Part 2: Synthesis of geologic and seismic data
for development of integrated crustal models
[E84-10126] p 26 N84-25128

Euro-African MAGSAT anomaly-tectonic observations
p 27 N84-25129

Correlation of tectonic provinces of South America and
the Caribbean region with MAGSAT anomalies
p 27 N84-25130

Satellite elevation magnetic and gravity models of major
South American plate tectonic features
p 27 N84-25131

Reduced to pole long-wavelength magnetic anomalies
of Africa and Europe p 27 N84-25132

Satellite magnetic anomalies of Africa and Europe
p 27 N84-25133

Do satellite magnetic anomaly data accurately portray
the crustal component? p 28 N84-25134

Long-wavelength magnetic and gravity anomaly
correlations of Africa and Europe p 28 N84-25135

US aeromagnetic and satellite magnetic anomaly
comparisons p 28 N84-25136

HIROSAWA, H.
Microwave backscattering characteristics of
wind-generated waves p 36 N84-38309

HISANAGA, A.
Microwave scatterometer p 66 N84-38310

HJELMSTAD, J.
Ocean waves and turbulence as observed with an
adaptive coherent multifrequency radar
p 44 N84-27279

HLAVKA, C. A.
Thematic Mapper image quality - Registration, noise,
and resolution p 57 N84-33533

HOFFMAN, R. N.
Outlook for improved numerical weather prediction using
satellite data with a special emphasis on the hydrological
variables
[AD-A141233] p 54 N84-28344

HOLBEN, B. N.
Intensive forest clearing in Rondonia, Brazil, as detected
by satellite remote sensing p 8 N84-37204

HOLM, R. G.
In-flight absolute radiometric calibration of the Thematic
Mapper p 56 N84-33531

In-flight absolute radiometric calibration of the Thematic
Mapper p 68 N84-23002

HOLYER, R. J.
Principal components as a method for atmospherically
correcting coastal zone color scanner data
[AD-P003124] p 41 N84-26265

Ocean optical remote sensing capability statement
[AD-A140589] p 49 N84-27321

HOMMA, K.
Performance evaluation and a dedicated system for SAR
image data processing p 58 N84-38300

Image analysis researches of remotely sensed data at
NAL p 59 N84-38315

HONBOONHERM, S.
Contextual classification of remotely sensed data
p 63 N84-27245

HOQUE, N.
Application of the Vizir Image Processing System to the
remote sensing studies in Bangladesh
p 64 N84-30266

HORLER, D.
Evaluating LANDSAT-4 MSS and TM data
[E84-10157] p 63 N84-27249

HOUGHTON, J. T.
The World Climate Research Programme
p 36 N84-38702

HOWLADER, A. H.
Application of the Vizir Image Processing System to the
remote sensing studies in Bangladesh
p 64 N84-30266

HUANG, N. E.
Dynamics of the slope water off New England and its
influence on the Gulf Stream as inferred from satellite IR
data p 31 N84-30672

Non-Gaussian statistical models of surface wave fields
for remote sensing applications p 45 N84-27284

HUDSON, W. D.
Aerial photography for ecological site mapping
p 9 N84-23990

HUEBNER, G. L., JR.
Crop moisture estimation over the southern Great Plains
with dual polarization 1.66 centimeter passive microwave
data from Nimbus 7
[E84-10163] p 12 N84-27255

HUETE, A. R.
Soil spectral effects on 4-space vegetation
discrimination p 2 N84-30673

HUGHES, W. J.
A study of geomagnetic pulsations using the AFGL (Air
Force Geophysics Laboratory) magnetometer network
[AD-A140507] p 70 N84-26217

HUNG, H. M.
Use of transformed LANDSAT data in regression
estimation of crop acreages p 11 N84-27246

HURLBURT, H. E.
The importance of altimeter and scatterometer data for
ocean prediction p 49 N84-27316

Sampling strategies and four-dimensional assimilation
of altimetric data for ocean monitoring and prediction
p 49 N84-27317

HWANG, P. H.
Monthly distributions of precipitable water from the
Nimbus 7 SMMR data p 37 N84-39458

HWANG, P. Y. C.
A Kalman filter approach to precision GPS geodesy
p 17 N84-33024

I

II, F. A. M.
Evaluation of entropy and JM-distance criterions as
features selection methods using spectral and spatial
features derived from LANDSAT images
[E84-10141] p 62 N84-26089

An integrated software system for geometric correction
of LANDSAT MSS imagery
[E84-10143] p 62 N84-26091

IIJIMA, T.
A SAR image auto-focusing using linear distortion
azimuth matched filter p 58 N84-38304

IIISAKA, J.
A remote sensing data processing system based on a
micro-computer p 64 N84-30265

IKEDA, M.
Seasonal variability in meanders of the California Current
System off Vancouver Island p 33 N84-34507

Variations in surface current off the coasts of Canada
as inferred from infrared satellite imagery
p 47 N84-27305

INOMATA, H.
Remote sensing of the ocean by the airborne microwave
scatterometer/radiometer system p 36 N84-38307

IRONS, J. R.
A statistical evaluation of the advantages of Landsat
Thematic Mapper data in comparison to Multispectral
Scanner data p 57 N84-33537

ISAACS, R. G.
Outlook for improved numerical weather prediction using
satellite data with a special emphasis on the hydrological
variables
[AD-A141233] p 54 N84-28344

ISIORHO, S. A.
Radar geology of the Shelleng-Numan area in Nigeria
- An evaluation p 24 N84-38940

IYER, H. S.
Multispectral and multitemporal Landsat data for soil
surveys - A case study of part of north west India
p 1 N84-30228

J

JABBAR, M. A.

Study of desertification/aridity through remote sensing
p 1 A84-30238

JACKSON, F. C.

Some case studies of ocean wave physical processes utilizing the GSFC airborne radar ocean wave spectrometer
p 45 N84-27283

JACKSON, M.

A regional raster data study at the Experimental Cartography Unit - The application of interactive raster graphics to environmental modelling
p 14 A84-33363

JACKSON, R. D.

Soil spectral effects on 4-space vegetation discrimination
p 2 A84-30673
In-flight absolute radiometric calibration of the Thematic Mapper
p 56 A84-33531
In-flight absolute radiometric calibration of the Thematic Mapper
p 68 N84-23002

JACKSON, T. J.

Calculations of radar backscattering coefficient of vegetation-covered soils
p 2 A84-30671
Aircraft scatterometer observations of soil moisture on rangeland watersheds
p 4 A84-33338

JADAV, K. L.

Identification of water-logged and salt-affected soils through remote sensing techniques
p 51 A84-30251

JANTARANIPA, W.

Remote sensing as a tool for mineral prospecting
p 22 A84-30259

JANTUNEN, H.

Locating shoreline changes in the Porttipahta (Finland) water reservoir by using multitemporal Landsat data
p 52 A84-33987

JAYNES, R. A.

Preliminary digital classification of grazing resources in the Southern Chihuahuan Arid Zone of Mexico
p 5 A84-33349

JI, F. C.

An inquiry into methods of estimating yields of wheat and autumn crops in the plain region with Landsat images visual interpretation
p 2 A84-30239

JOCHEMCZYK, H.

Investigation of the combination of geodetic point aggregations
[SER-C-285] p 21 N84-28199

JOHANNESSEN, O. M.

A summary of results from the first Nimbus 7 SMMR observations
p 37 A84-39459

JOHNSON, J. W.

Two-frequency microwave resonance measurements from an aircraft - A quantitative estimate of the directional ocean surface spectrum
p 34 A84-34942

Measurements of ocean wave spectra and modulation transfer function with the airborne two frequency scatterometer
p 45 N84-27282

JONES, K. D.

Publications and reports of the Institute of Oceanographic Sciences 1979-1982
[IOS-170] p 50 N84-28354

JOSEPH, G.

Design and development of CCD pushbroom camera for earth resources survey
p 66 A84-38311

JOUANNET, D.

The Green Cadastre - An experiment for exploring the tree vegetation in the Paris area
p 7 A84-36516

JOYCE, H.

The active microwave instrumentation for ERS-1
p 34 A84-35542

JOYCE, T.

Rapid evolution of a Gulf Stream warm-core ring
p 32 A84-34164

JUNGERT, E.

Contour-to-grid transformation: Development of a method for generation of a sparse grid structure out of terrain elevation contours
[FOA-C-30349-E1] p 16 N84-25156

K

KACZYNSKI, R.

Interpreting multispectral photographs obtained in the Telefoto-80 experiment so as to distinguish crop types
p 6 A84-34780

KAEHLER, M.

RABIVE - A real time program system for radiometric image processing
p 58 A84-37773

KAESE, R. H.

Mean circulation and eddy kinetic energy in the eastern North Atlantic
p 32 A84-34501

KAEVITSER, V. I.

An airborne radar station for studying the reflection properties of the earth's surface
p 64 A84-31072

KALNAY, E.

Large-scale analysis and forecast experiments with wind data from the Seasat A scatterometer
p 66 A84-37873

The impact of scatterometer wind data on global weather forecasting
p 49 N84-27314

KALUBARME, M. H.

Identification of water-logged and salt-affected soils through remote sensing techniques
p 51 A84-30251

KAMAT, D. S.

Microwave measurements using active and passive sensors
p 1 A84-30229

KANDEL, R. S.

Surface albedo and the Sahel drought
p 7 A84-36710

KAPLAN, L. D.

Outlook for improved numerical weather prediction using satellite data with a special emphasis on the hydrological variables
[AD-A141233] p 54 N84-28344

KARKHANIS, V.

Interactive digital image processing for terrain data extraction, phase 4
[AD-A104197] p 11 N84-26107

KASISCHKE, E. S.

Modeling of SAR signatures of shallow water ocean topography
p 47 N84-27302

KASTNER, C. J.

In-flight absolute radiometric calibration of the Thematic Mapper
p 56 A84-33531
In-flight absolute radiometric calibration of the Thematic Mapper
p 68 N84-23002

KATSAROS, K. B.

A summary of results from the first Nimbus 7 SMMR observations
p 37 A84-39459

KAUFMAN, Y. J.

Atmospheric effect on classification of finite fields
p 2 A84-30670

KE, L. W.

An inquiry into methods of estimating yields of wheat and autumn crops in the plain region with Landsat images visual interpretation
p 2 A84-30239

KELLER, G. R.

Application of Magsat lithospheric modeling in South America. Part 1: Processing and interpretation of magnetic and gravity anomaly data
[E84-10115] p 24 N84-23008

Application of MAGSAT to lithospheric modeling in South America. Part 2: Synthesis of geologic and seismic data for development of integrated crustal models
[E84-10126] p 26 N84-25128

Correlation of tectonic provinces of South America and the Caribbean region with MAGSAT anomalies
p 27 N84-25130

Satellite elevation magnetic and gravity models of major South American plate tectonic features
p 27 N84-25131

Relation of MAGSAT anomalies to the main tectonic provinces of South America
p 28 N84-25137

KENT, G. S.

SAGE and SAM II measurements of global stratospheric aerosol optical depth and mass loading
p 15 A84-39455

KERBER, A. G.

Comparative accuracies of AVHRR and MSS data used for Level I land cover classifications
p 14 A84-33344

KETCHUM, R. D., JR.

Seasat SAR sea-ice imagery - Summer melt to autumn freeze-up
p 36 A84-38941

KHNYKIN, V. I.

The use of remote sensing in the search for hydrocarbons in the Kerch peninsula
p 23 A84-34782

KHOLSHEVNIKOV, K. V.

Construction of a system of point masses representing the gravitational field of the planet on the basis of satellite observations. I - An algorithm derivation
p 19 A84-37069

KHRIGIAN, A. KH.

Recent investigations of ozone and minor atmospheric gases
p 14 A84-34450

KIDWELL, R.

Experiments in lithography from remote sensor imagery
p 55 A84-33362

KIEITZMANN, H.

Preliminary investigations concerning a 90 GHz radiometer satellite experiment
[DFVLR-FB-84-02] p 68 N84-24693

KIMURA, H.

Classification of snow surface conditions by means of Landsat MSS data under compensation of slope effects
p 52 A84-38296

A SAR image auto-focusing using linear distortion azimuth matched filter
p 58 A84-38304

KINDLE, J. C.

Sampling strategies and four-dimensional assimilation of altimetric data for ocean monitoring and prediction
p 49 N84-2717

KIRAN KUMAR, A. S.

Design and development of CCD pushbroom camera for earth resources survey
p 66 A84-38311

KIRWAN, A. D., JR.

Lagrangian observations of an anticyclonic ring in the western Gulf of Mexico
p 33 A84-34502

A model for the analysis of drifter data with an application to a warm core ring in the Gulf of Mexico
p 33 A84-34503

KLEMAS, V.

Dynamics of the slope water off New England and its influence on the Gulf Stream as inferred from satellite IR data
p 31 A84-30672

Evaluation of spatial, radiometric and spectral Thematic Mapper performance for coastal studies
[E84-10118] p 9 N84-23978

Evaluation of spatial, radiometric and spectral Thematic Mapper performance for coastal studies
[E84-10159] p 12 N84-27251

KLEINER, K. F.

Intercomparison of the Nimbus 7 SBUV/TOMS total ozone data sets with Dobson and M83 results
p 67 A84-39449

KLIATSKIN, V. I.

Theory of radio wave propagation over the sea surface
p 35 A84-37095

KLIMENKO, O. IA.

A regression analysis of data from aircraft and ground measurements of a vegetative cover
p 6 A84-34784

KOBAYASHI, T.

Microwave backscattering characteristics of wind-generated waves
p 36 A84-38309

KOCH, K. R.

Estimation of variances and covariances in the multivariate and in the incomplete multivariate model
p 20 N84-26073

KODAIRA, N.

A SAR image auto-focusing using linear distortion azimuth matched filter
p 58 A84-38304

KOENIG, G.

RABIVE - A real time program system for radiometric image processing
p 58 A84-37773

KOEPKE, P.

Effective reflectance of oceanic whitecaps
p 35 A84-36119

KOERBER, B. W.

A theoretical study of an airborne laser technique for determining sea water turbidity
p 31 A84-33774

KOLODII, N. V.

The use of remote sensing in the search for hydrocarbons in the Kerch peninsula
p 23 A84-34782

KOLSKY, H. G.

Analysis and processing of Landsat-4 sensor data using advanced image processing techniques and technologies
p 56 A84-33527

KOMBERG, B. V.

Correlations between the nonthermal emission of quasarlike nuclei and their Balmer-line widths
p 58 A84-33629

KOMURA, F.

Performance evaluation and a dedicated system for SAR image data processing
p 58 A84-38300

KONDO, M.

Microwave scatterometer
p 66 A84-38310

KONDRAEV, K. IA.

Satellite climatology
p 13 A84-31024

KOSCO, W. J.

Antarctic mapping and international coordination
p 19 N84-23935

KOSHIISHI, H.

Image analysis researches of remotely sensed data at NAL
p 59 A84-38315

KOSTKOWSKI, H. J.

High-precision atmospheric ozone measurements using wavelengths between 290 and 305 nm
p 67 A84-39447

KOZAK, R. C.

Radar backscatter modelling
p 25 N84-23525

KOZMA, A.

Modeling of SAR signatures of shallow water ocean topography
p 47 N84-27302

KOZODEROV, V. V.

A regression analysis of data from aircraft and ground measurements of a vegetative cover
p 6 A84-34784

KRABILL, W.

Determining forest canopy characteristics using airborne laser data
p 7 A84-37202

KRABILL, W. B.

Airborne laser topographic mapping results
p 8 A84-38998

PERSONAL AUTHOR INDEX

KRAUSS, W. Mean circulation and eddy kinetic energy in the eastern North Atlantic p 32 A84-34501

KRISCHE, E. U. Application of Landsat data in the exploration of 'Calcrete' uranium deposits p 24 A84-37775

KROEN, M. L. A rapid method for obtaining frequency-response functions for multiple input photogrammetric data [AIAA PAPER 84-1060] p 65 A84-31741

KUBO, Y. Performance evaluation and a dedicated system for SAR image data processing p 58 A84-38300

KUBOTA, I. Fast processing of synthetic aperture radar signal without data transposition p 59 A84-38305

KULKARNI, A. V. Bhaskara-II TV data in resource studies - A case study in a part of Andhra Pradesh, southern India p 54 A84-30234

KUMAR, M. Error analysis for marine geodetic control using the global positioning system [AD-A140566] p 21 N84-26687

KUMARAKULASURIYAR, S. Application of multi-concept in remote sensing technique for identification and mapping of soil units of alluvial plain for land use planning in Sri Lanka p 13 A84-30241

KUNZI, K. F. A summary of results from the first Nimbus 7 SMMR observations p 37 A84-39459

KURTZ, D. O. Katabatic wind forcing of the Terra Nova Bay polynya p 33 A84-34509

KUX, H. J. H. Evaluation of SIR-A (Shuttle Imaging Radar) images from the Tres Marias region (Minas Gerais State, Brazil) using derived spatial features and registration with MSS-LANDSAT images [E84-10148] p 62 N84-26096

KUZINA, A. M. Conditions for the illumination of an area in satellite scanner surveys p 65 A84-34787

L

LAHAIE, I. J. Digital processing considerations for extraction of ocean wave image spectra from raw synthetic aperture radar data p 30 A84-30025

LANGEIL, R. A. Reduction of satellite magnetic anomaly data p 19 A84-38812

LANGLEY, R. B. Geometrical aspects of differential GPS positioning p 17 A84-32494

A forecast of the impact of GPS on surveying p 18 A84-33374

LARSSON, L. Correlating aerial photographs to LANDSAT Multispectral Sensor (MSS) data to measure ground control points p 69 N84-25150

LARSSON, R. General triangulation: Incorporating photogrammetric and other observations p 69 N84-25151

GENTRI: A system for simultaneous adjustment of photogrammetric and other observations p 69 N84-25152

LASCANO, R. CONSERVB: A numerical method to compute soil water content and temperature profiles under a bare surface [E84-10113] p 9 N84-23006

LATTY, R. S. A statistical evaluation of the advantages of Landsat Thematic Mapper data in comparison to Multispectral Scanner data p 57 A84-33537

Classifying northern forests using Thematic Mapper Simulator data p 7 A84-34961

LAUER, D. T. LANDSAT 4 investigations of Thematic Mapper and multispectral scanner applications [E84-10100] p 60 N84-23003

LANDSAT 4 investigations of Thematic Mapper and Multispectral Scanner applications [E84-10152] p 63 N84-27247

LAURENT, J. A sample performance of the grille spectrometer aboard Spacelab [AERONOMICA-ACTA-A-281-1984] p 70 N84-26003

LAVOIETTE, P. E. The depiction of Alboran Sea Gyre during Donde Va? using remote sensing and conventional data p 47 N84-27306

LAYALLE, C. SPOT simulations in Bangladesh flight operations and main results p 2 A84-30253

LEBERL, F. Experiments to correct a digital map data base using scene analysis [AD-A139447] p 61 N84-24499

LEBLOND, P. H. Variations in surface current off the coasts of Canada as inferred from infrared satellite imagery p 47 N84-27305

LEE, C.-M. Analysis of land use changes around Salt Lake City using Landsat digital data - A case study of Sandy area p 13 A84-30242

LEE, D. C. L. Forest inventory using multistage sampling with probability proportional to size [E84-10144] p 11 N84-26092

LEES, R. D. Analysis and processing of Landsat-4 sensor data using advanced image processing techniques and technologies p 56 A84-33527

LEGECKIS, R. A model for the analysis of drifter data with an application to a warm core ring in the Gulf of Mexico p 33 A84-34503

LEISE, J. A. The analysis and digital signal processing of NOAA's surface current mapping system p 30 A84-30024

LEMAITRE, M. P. A sample performance of the grille spectrometer aboard Spacelab [AERONOMICA-ACTA-A-281-1984] p 70 N84-26003

LESTER, M. A study of geomagnetic pulsations using the AFGL (Air Force Geophysics Laboratory) magnetometer network [AD-A140507] p 70 N84-26217

LEWIS, J. K. Lagrangian observations of an anticyclonic ring in the western Gulf of Mexico p 33 A84-34502

A model for the analysis of drifter data with an application to a warm core ring in the Gulf of Mexico p 33 A84-34503

LI, L. The use of Hough transformation for detecting lineaments in satellite imagery p 22 A84-30262

LI, X. The application of Landsat image in the surveying of water resources of Dongting Lake p 51 A84-30255

LI, Z.-R. The use of Hough transformation for detecting lineaments in satellite imagery p 22 A84-30262

LIDIAK, E. G. Application of Magsat lithospheric modeling in South America. Part 1: Processing and interpretation of magnetic and gravity anomaly data [E84-10115] p 24 N84-23008

Application of MAGSAT to lithospheric modeling in South America. Part 2: Synthesis of geologic and seismic data for development of integrated crustal models [E84-10126] p 26 N84-25128

Correlation of tectonic provinces of South America and the Caribbean region with MAGSAT anomalies p 27 N84-25130

Satellite elevation magnetic and gravity models of major South American plate tectonic features p 27 N84-25131

Relation of MAGSAT anomalies to the main tectonic provinces of South America p 28 N84-25137

LIN, H. Typical analysis of regional stability and block structures with remote sensing images p 22 A84-30254

LING, C. H. A comparison of numerical results of Arctic Sea ice modeling with satellite images p 39 N84-23969

LINK, L. E. Airborne laser topographic mapping results p 8 A84-38998

LIPES, R. G. Digital SAR processing using a fast polynomial transform p 55 A84-32093

LIPPENS, C. A sample performance of the grille spectrometer aboard Spacelab [AERONOMICA-ACTA-A-281-1984] p 70 N84-26003

LIU, W. T. Observing ocean-atmosphere exchanges with space-borne sensors, appendix C p 50 N84-28298

LIU, X. The application of Landsat image in the surveying of water resources of Dongting Lake p 51 A84-30255

LOGAN, T. L. Spatial inventory integrating raster databases and point sample data p 4 A84-33340

An analysis of Landsat-4 Thematic Mapper geometric properties p 57 A84-33536

LONGACRE, M. B. Correlation of tectonic provinces of South America and the Caribbean region with MAGSAT anomalies p 27 N84-25130

Satellite elevation magnetic and gravity models of major South American plate tectonic features p 27 N84-25131

Relation of MAGSAT anomalies to the main tectonic provinces of South America p 28 N84-25137

LONGDON, N. Earthnet: The story of images [ESA-BR-18] p 62 N84-26102

LOSQUADRO, G. The radar altimeter for ERS-1 Satellite p 64 A84-30516

LOTSPIECH, J. B. Analysis and processing of Landsat-4 sensor data using advanced image processing techniques and technologies p 56 A84-33527

LOWE, D. Landsat planimetric maps p 54 A84-30264

LOZANO, D. F. Landsat-4 MSS and Thematic Mapper data quality and information content analysis p 56 A84-33528

LU, Y. C. Comparative accuracies of AVHRR and MSS data used for Level I land cover classifications p 14 A84-33344

LUCHININ, A. G. Interpreting the spectra of aerial photographs of the sea surface p 30 A84-30443

LUNDQVIST, S. Computer-automated CO₂-laser long-path absorption system for air quality monitoring in the working environment p 13 A84-30307

LUSCH, D. P. Aerial photography for ecological site mapping p 9 N84-23990

LYDEN, J. D. Analysis of SEASAT SAR imagery collected during the JASIN experiment [AD-A140584] p 49 N84-27320

LYZENGA, D. R. Development of Great Lakes algorithms for the Nimbus-G coastal zone color scanner [NASA-CR-173511] p 53 N84-27258

SAR imagery of ocean-wave swell traveling in an arbitrary direction p 44 N84-27278

Modeling of SAR signatures of shallow water ocean topography p 47 N84-27302

M

MACCOLL, D. ESA activities in the use of microwaves for the remote sensing of the Earth p 42 N84-27264

MACFARLANE, N. Atmospheric correction of Landsat MSS data for a multiday suspended sediment algorithm p 59 A84-38942

MACHETEL, P. Present limitations of accurate satellite Doppler positioning for tectonics - An example: Djibouti p 17 A84-32495

MACLEAN, G. Determining forest canopy characteristics using airborne laser data p 7 A84-37202

MAODY, S. L. H. Applications of the Enviro-pod with KA-85A panoramic cameras in south-eastern historic and pre-historic archaeological survey p 23 A84-33327

MAEDA, K. Data compression of remotely sensed data from space p 59 A84-38314

MAINCENT, G. Description of SEP ground station and Vizir image processing VIPS p 54 A84-30268

MALARET, E. Landsat-4 MSS and Thematic Mapper data quality and information content analysis p 56 A84-33528

MALILA, W. A. Characterization of Landsat-4 MSS and TM digital image data p 56 A84-33526

Study on spectral/radiometric characteristics of the Thematic Mapper for land use applications [E84-10130] p 61 N84-25140

MALMSTROEM, H. Correlating aerial photographs to LANDSAT Multispectral Sensor (MSS) data to measure ground control points p 69 N84-25150

MALTSEVA, I. G. Conditions for the illumination of an area in satellite scanner surveys p 65 A84-34787

MANCHANDA, M. L.

MANCHANDA, M. L.

Multispectral and multitemporal Landsat data for soil surveys - A case study of part of north west India
p 1 A84-30228

MANN, W. P.

Cenozoic tectonics of the Caribbean: Structural and stratigraphic studies in Jamaica and Hispaniola
p 25 N84-23062

MARCONNET, B.

Metallogenesis - Use of remote sensing for ore deposit prospecting indicators linked to nonoutcropping leucogranitic apexes
p 23 A84-30878

MARKHAM, B. L.

A statistical evaluation of the advantages of Landsat Thematic Mapper data in comparison to Multispectral Scanner data
p 57 A84-33537

MARKON, C.

Land cover and terrain mapping for the development of digital data bases for wildlife habitat assessment in the Yukon Flats National Wildlife Refuge, Alaska
p 9 N84-23971

MARSH, B. D.

Petrologic and geophysical sources of long-wavelength crustal magnetic anomalies
[NASA-CR-175245] p 29 N84-28276

MARSIGLIA, G.

X to W band radiometric signatures of natural surfaces
p 35 A84-36289

MARTHINSSON, B.

Computer-automated CO₂-laser long-path absorption system for air quality monitoring in the working environment
p 13 A84-30307

MARTIN, C. F.

Seasat observations of lithospheric flexure seaward of trenches
p 32 A84-34339

MARTINI, P. R.

Project SERGE: Brazil referential field data for the SIR-A experiment
[INPE-2973-NTE/210] p 29 N84-27259

MARUOKA, D.

Analysing forest structures by remote sensing
p 1 A84-30236

MASCARENHAS, N. D. A.

Evaluation of entropy and JM-distance criterions as features selection methods using spectral and spatial features derived from LANDSAT images
[E84-10141] p 62 N84-26089

MASUBUCHI, Y.

Fast processing of synthetic aperture radar signal without data transposition
p 59 A84-38305

MASUKO, H.

Remote sensing of the ocean by the airborne microwave scatterometer/radiometer system
p 36 A84-38307

MATSON, M.

Fire detection using the NOAA (National Oceanic and Atmospheric Administration)-series satellites
[PB84-176890] p 13 N84-27324

MATSUMOTO, K.

Two-stage cluster analysis of a Landsat image
p 58 A84-38302

Image analysis researches of remotely sensed data at NAL
p 59 A84-38315

MATTHEWS, E.

Vegetation, land-use and seasonal albedo data sets: Documentation of archived data tape
[E84-10133] p 10 N84-25142

MAXWELL, M. S.

High resolution observations of low contrast phenomena from an Advanced Geosynchronous Platform (AGP)
p 42 N84-27266

MCADOO, D. C.

Seasat observations of lithospheric flexure seaward of trenches
p 32 A84-34339

MCCLAIN, C. R.

Observations of Gulf Stream-induced and wind-driven upwelling in the Georgia Bight using ocean color and infrared imagery
p 34 A84-34517

MCCLAIN, E. P.

Recent advances in multispectral sensing of ocean surface temperature from space
p 46 N84-27297

MCCORMICK, M. P.

SAGE and SAM II measurements of global stratospheric aerosol optical depth and mass loading
p 15 A84-39455

A comparative study of aerosol extinction measurements made by the SAM II and SAGE satellite experiments
p 15 A84-39457

MCFARLAND, M. J.

Crop moisture estimation over the southern Great Plains with dual polarization 1.66 centimeter passive microwave data from Nimbus 7
[E84-10163] p 12 N84-27255

MCGILLEM, C. D.

Landsat-4 MSS and Thematic Mapper data quality and information content analysis
p 56 A84-33528

MCGOLDRICK, L. F.

Remote sensing for oceanography: Past, present, future
p 42 N84-27263

A new parameterization of an empirical model for wind/ocean scatterometry
p 43 N84-27269

MCHONE, J.

Pinacate-Gran Desierto Region, Mexico: SIR-A data analysis
p 25 N84-23526

MCKIM, H. L.

Integration of Landsat data into the Saginaw River Basin geographic information system
p 51 A84-33339

Integration of LANDSAT land cover data into the Saginaw River basin geographic information system for hydrologic modeling
[AD-A140185] p 53 N84-26106

MCCLAUGHLIN, J. D.

A forecast of the impact of GPS on surveying
p 18 A84-33374

MCLEOD, R. G.

The Pennsylvania defoliation application pilot test
[E84-10111] p 8 N84-23004

MCMILLIN, L. M.

Theory and validation of the multiple window sea surface temperature technique
p 33 A84-34513

MCNAMARA, D. P.

Aircraft measurements of convective draft cores in MONEX
p 31 A84-31821

MCPEHRON, R. D.

Global data assimilation experiments with scatterometer winds from SEASAT-A
p 65 A84-32938

MCSEWEENEY, J.

Experiments in lithography from remote sensor imagery
p 55 A84-33362

MEHTA, S.

Microwave measurements using active and passive sensors
p 1 A84-30229

MEHTA, V. M.

Microwave measurements using active and passive sensors
p 1 A84-30229

MENDOZA, A. A. B.

Identification and estimation of the area planted with irrigated rice based on the visual interpretation of LANDSAT MSS data
[E84-10164] p 12 N84-27256

MENDOZA, E. E.

Simple enhancement techniques in digital image processing
p 58 A84-33798

MEROLA, J. A.

Preliminary digital classification of grazing resources in the Southern Chihuahuan Arid Zone of Mexico
p 5 A84-33349

MERRELL, W. J., JR.

Lagrangian observations of an anticyclonic ring in the western Gulf of Mexico
p 33 A84-34502

A model for the analysis of drifter data with an application to a warm core ring in the Gulf of Mexico
p 33 A84-34503

MERRY, C. J.

Integration of Landsat data into the Saginaw River Basin geographic information system
p 51 A84-33339

Integration of LANDSAT land cover data into the Saginaw River basin geographic information system for hydrologic modeling
[AD-A140185] p 53 N84-26106

MERTZ, F. C.

Thematic Mapper image quality - Registration, noise, and resolution
p 57 A84-33533

METZLER, M. D.

Characterization of Landsat-4 MSS and TM digital image data
p 56 A84-33526

Understanding and utilization of Thematic Mapper and other remotely sensed data for vegetation monitoring
[E84-10150] p 11 N84-26098

MEUNIER, T. K.

Glaciological and geological studies of Antarctica with satellite remote sensing technology
p 38 N84-23956

MEYERHOFF, S.

Application of the GPS (Global Positioning System) Geodetic Receiver System
[AD-A140567] p 21 N84-26688

MILAZZO, V. A.

Findings on the use of Landsat-3 return beam vidicon imagery for detecting land use and land cover changes
p 14 A84-33361

MILLER, M. S.

Integration of Landsat data into the Saginaw River Basin geographic information system
p 51 A84-33339

MILLER, W. F.

Application of remote sensing to state and regional problems
[E84-10128] p 68 N84-23986

MINKEL, D. H.

Establishing hydrographic control using Doppler
p 18 A84-33358

MINNIS, P.

Comparison of longwave diurnal models applied to simulations of the Earth Radiation Budget Experiment
p 65 A84-31947

MINSTER, J. F.

Somali current studied from SEASAT altimetry
p 47 N84-27307

MITCHELL, J. L.

The satellite altimeter as a platform for observation of the oceanic mesoscale
p 46 N84-27299

MIYASHITA, K.

A remote sensing data processing system based on a micro-computer
p 64 A84-30265

MO, T.

Calculations of radar backscattering coefficient of vegetation-covered soils
p 2 A84-30671

MOCCIA, A.

A simulation program for the integration of aerospace remote sensing systems with a digital terrain model
p 59 A84-38316

MOGNARD, N. M.

Wind, waves and swell in the Antarctic marginal ice zone by SEASAT radar altimeter
p 38 N84-23941

MOHAN, S.

Microwave measurements using active and passive sensors
p 1 A84-30229

MOHANTY, B. K.

An analysis of tectonics and metallogeny of Orissa state, India with remote sensing technique
p 22 A84-30247

MOHARANA, R. C.

An analysis of tectonics and metallogeny of Orissa state, India with remote sensing technique
p 22 A84-30247

MOLENAAR, M.

Several aspects of the sequential processing of photogrammetric bundle blocks
p 21 N84-26077

MOLLO-CHRISTENSEN, E.

Remote sensing of air-sea interactions
p 42 N84-27267

MONALDO, F. M.

Tracking ocean wave spectrum from SAR images
p 44 N84-27277

ALTIMETER height measurement errors introduced by the presence of variable cloud and rain attenuation
p 45 N84-27289

Improved resolution rain measurements from spaceborne radar altimeters
p 46 N84-27290

MONTGOMERY, D. R.

The use of satellite observations of the ocean surface in commercial fishing operations
[AD-P003120] p 41 N84-26261

MOORE, H. D.

Non-parallactic stereoscopy using shadow-disparity
p 55 A84-33335

MOREIRA, M. A.

Irrigated rice area estimation using remote sensing techniques: Project's proposal and preliminary results
[E84-10131] p 10 N84-26081

Sampling system for wheat (*Triticum aestivum* L) area estimation using digital LANDSAT MSS data and aerial photographs
[E84-10139] p 10 N84-26087

Identification and estimation of the area planted with irrigated rice based on the visual interpretation of LANDSAT MSS data
[E84-10164] p 12 N84-27256

A sampling system for estimating the cultivation of wheat (*Triticum aestivum* L) from LANDSAT data
[E84-10165] p 12 N84-27257

MOREL, P.

The World Climate Research Programme
p 36 A84-38702

MORETON, G. E.

Irrigated crop inventory by classification of satellite image data
p 8 A84-38999

MORIZUMI, S. J.

Performance study of multicolor visual sensor system
p 66 A84-38312

MORRISON, C. E.

Program for mapping Antarctica
p 19 N84-23954

MORRISON, H.

Analysis of airborne electromagnetic systems for mapping thickness of sea ice
[AD-A139766] p 39 N84-25235

MORSE, A.

Benchmark data on the separability between orchards and vineyards in the southern San Joaquin Valley of California
p 5 A84-33348

MOTT, G.

Classifying northern forests using Thematic Mapper Simulator data
p 7 A84-34961

MOUNTAIN, D.

Rapid evolution of a Gulf Stream warm-core ring
p 32 A84-34164

B-8

PERSONAL AUTHOR INDEX

MUELLER, J. L.

Matrix partitioning and EOF/principal component analysis of Antarctic Sea ice brightness temperatures [NASA-TM-83916] p 49 N84-27319

MULLER, C.

A sample performance of the grille spectrometer aboard Spacelab [AERONOMICA-ACTA-A-281-1984] p 70 N84-26003

MURPHY, D. L.

Land cover and terrain mapping for the development of digital data bases for wildlife habitat assessment in the Yukon Flats National Wildlife Refuge, Alaska p 9 N84-23971

MURPHY, J. M.

Revised radiometric calibration technique for Landsat-4 Thematic Mapper data p 56 A84-33530 Evaluating LANDSAT-4 MSS and TM data [E84-10157] p 63 N84-27249

MURRAY, C. W., JR.

Matrix partitioning and EOF/principal component analysis of Antarctic Sea ice brightness temperatures [NASA-TM-83916] p 49 N84-27319

MYERS, H. J.

Analysis and processing of Landsat-4 sensor data using advanced image processing techniques and technologies p 56 A84-33527

MYSAK, L. A.

Seasonal variability in meanders of the California Current System off Vancouver Island p 33 A84-34507 Variations in surface current off the coasts of Canada as inferred from infrared satellite imagery p 47 N84-27305

N

NAGACHENCHIAH, K.

Design and development of CCD pushbroom camera for earth resources survey p 66 A84-38311

NAKA, M.

Two-stage cluster analysis of a Landsat image p 58 A84-38302

Image analysis researches of remotely sensed data at NAL p 59 A84-38315

NAPOLITANO, D. A.

Synthetic aperture radar images of ocean waves, theories of imaging physics and experimental tests p 43 N84-27275

NEDELMAN, K. S.

Automated vegetation classification using Thematic Mapper Simulation data p 5 A84-3347

NELSON, R.

Determining forest canopy characteristics using airborne laser data p 7 A84-37202

NELSON, R. F.

A statistical evaluation of the advantages of Landsat Thematic Mapper data in comparison to Multispectral Scanner data p 57 A84-33537

Classifying northern forests using Thematic Mapper Simulator data p 7 A84-34961

NELSON, R. M.

NASA Oceanic Processes Program, fiscal year 1983 [NASA-TM-86248] p 39 N84-24078

NESSA, M.

Bay monsoon activities in relation to the monsoon in the western Pacific p 30 A84-30232

NEWTON, R. W.

A microwave systems approach to measuring root zone soil moisture [E84-10114] p 9 N84-23007

NIEBAUER, H. J.

Satellite observations of circulation in the eastern Bering Sea p 33 A84-34514

NIERO, M.

Application of LANDSAT data to the study of urban development in Brasilia [E84-10142] p 16 N84-26090

The use of an image registration technique in the urban growth monitoring [E84-10147] p 16 N84-26095

NISHIKAWA, H.

Classification of snow surface conditions by means of Landsat MSS data under compensation of slope effects p 52 A84-38296

NIWA, S.

Remote sensing of the ocean by the airborne microwave scatterometer/radiometer system p 36 A84-38307

NJOKU, E. J.

Satellite-Derived Sea Surface Temperature: Workshop-2 [NASA-CR-173740] p 50 N84-28355

NORWINE, J. R.

Vegetation monitoring and classification using NOAA/AVHRR satellite data p 4 A84-33343

NOVAES, R. A.

Irrigated rice area estimation using remote sensing techniques: Project's proposal and preliminary results [E84-10131] p 10 N84-26081

Identification and estimation of the area planted with irrigated rice based on the visual interpretation of LANDSAT MSS data [E84-10164] p 12 N84-27256

A report of Ceara Project activities [INPE-2988-RPE/452] p 54 N84-27260

NOVO, E. M. L. M.

Evaluation of the effects of the seasonal variation of solar elevation angle and azimuth on the processes of digital filtering and thematic classification of relief units [E84-10121] p 60 N84-23980

Evaluation of solar angle variation over digital processing of LANDSAT imagery [E84-10140] p 61 N84-26088

O

OBRADCHIKOV, O. S.

Topography interpretation possibilities for satellite photos in regions where the platform mantle has a multilayer structure (on the example of the eastern marginal part of the Caspian depression) p 23 A84-34779

OCHIAI, H.

Joint analysis of Landsat-MSS and NOAA-AVHRR data for marine environmental monitoring p 35 A84-38298

ODONOGHUE, W. J.

Integration of Landsat data into the Saginaw River Basin geographic information system p 51 A84-33339

OGAWA, T.

Space disturbance warning system with the aid of satellites p 15 A84-38301

OHARA, T.

Field data observed during the geological excursion in the west-central region of the Sul-RioGrande Shield [E84-10146] p 29 N84-26094

OHNUKI, I.

Two-stage cluster analysis of a Landsat image p 58 A84-38302

OJIMA, T.

Remote sensing of the ocean by the airborne microwave scatterometer/radiometer system p 36 A84-38307

OKAMOTO, K.

Remote sensing of the ocean by the airborne microwave scatterometer/radiometer system p 36 A84-38307

OLIVIER, R.

Euro-African MAGSAT anomaly-tectonic observations p 27 N84-25129

Reduced to pole long-wavelength magnetic anomalies of Africa and Europe p 27 N84-25132

Satellite magnetic anomalies of Africa and Europe p 27 N84-25133

Long-wavelength magnetic and gravity anomaly correlations of Africa and Europe p 28 N84-25135

OLSON, D.

Rapid evolution of a Gulf Stream warm-core ring p 32 A84-34164

ONDOK, T.

Space disturbance warning system with the aid of satellites p 15 A84-38301

ONEILL, P. E.

Aircraft scatterometer observations of soil moisture on rangeland watersheds p 4 A84-33338

ONEO, M.

Fast processing of synthetic aperture radar signal without data transposition p 59 A84-38305

ONSTOTT, R. G.

Marginal ice zone experiment (1983). Part 1: Ice characterization measurements. Part 2. Helicopter-borne and ship-based radar backscatter measurement of sea ice in the marginal ice zone [AD-A139894] p 40 N84-25238

OSHIMA, T.

A remote sensing data processing system based on a micro-computer p 64 A84-30265

OSWALD, J.

Coastal mapping of the Beaufort Sea coast p 31 A84-33360

OTTERMAN, J.

Albedo of a forest modeled as a plane with dense protrusions p 6 A84-34385

P

PALMER, J.

Spectroradiometric calibration of the Thematic Mapper and multispectral scanner system [E84-10098] p 67 N84-23000

In-flight absolute radiometric calibration of the Thematic Mapper p 68 N84-23002

PARREIRA, E. M. D. M. F.

PALMER, J. M.

In-flight absolute radiometric calibration of the Thematic Mapper p 56 A84-33531

Spectroradiometric calibration of the Thematic Mapper and Multispectral Scanner system [E84-10136] p 70 N84-26084

PALUSKA, A.

Discussion of the design of satellite-laser measurement stations in the eastern Mediterranean under the geological aspect. Contribution to the earthquake prediction research by the Wegener Group and to NASA's Crustal Dynamics Project [NASA-TM-77412] p 26 N84-24031

PALUSZKIEWICZ, T.

Satellite observations of circulation in the eastern Bering Sea p 33 A84-34514

PALUZZI, P. R.

Application of computer image processing to underwater surveys [AD-P003122] p 41 N84-26263

PAMPALONI, P.

X to W band radiometric signatures of natural surfaces p 35 A84-36289

PARADA, N. D.

Utilization of digital LANDSAT imagery for the study of granitoid bodies in Rondonia: Case example of the Pedra Branca massif [E84-10120] p 26 N84-23979

Evaluation of the effects of the seasonal variation of solar elevation angle and azimuth on the processes of digital filtering and thematic classification of relief units [E84-10121] p 60 N84-23980

Irrigated rice area estimation using remote sensing techniques: Project's proposal and preliminary results [E84-10131] p 10 N84-26081

Principal components technique analysis for vegetation and land use discrimination [E84-10135] p 10 N84-26083

Sampling system for wheat (*Triticum aestivum* L) area estimation using digital LANDSAT MSS data and aerial photographs [E84-10139] p 10 N84-26087

Evaluation of solar angle variation over digital processing of LANDSAT imagery [E84-10140] p 61 N84-26088

Evaluation of entropy and JM-distance criterions as features selection methods using spectral and spatial features derived from LANDSAT images [E84-10141] p 62 N84-26089

Application of LANDSAT data to the study of urban development in Brasilia [E84-10142] p 16 N84-26090

An integrated software system for geometric correction of LANDSAT MSS imagery [E84-10143] p 62 N84-26091

Forest inventory using multistage sampling with probability proportional to size [E84-10144] p 11 N84-26092

Multiseasonal variables in digital image enhancements for geological applications [E84-10145] p 29 N84-26093

Field data observed during the geological excursion in the west-central region of the Sul-RioGrande Shield [E84-10146] p 29 N84-26094

The use of an image registration technique in the urban growth monitoring [E84-10147] p 16 N84-26095

Evaluation of SIR-A (Shuttle Imaging Radar) images from the Tres Marias region (Minas Gerais State, Brazil) using derived spatial features and registration with MSS-LANDSAT images [E84-10148] p 62 N84-26096

Identification and estimation of the area planted with irrigated rice based on the visual interpretation of LANDSAT MSS data [E84-10164] p 12 N84-27256

A sampling system for estimating the cultivation of wheat (*Triticum aestivum* L) from LANDSAT data [E84-10165] p 12 N84-27257

PARADELLA, W. R.

Methodological approach in lithological discrimination by digital processing: A case study in the Serra do Ramalho, state of Bahia [INPE-3108-PRE/507] p 29 N84-26101

PARIS, J. F.

A microwave systems approach to measuring root zone soil moisture [E84-10114] p 9 N84-23007

PARKINSON, C.

A comparison of numerical results of Arctic Sea ice modeling with satellite images p 39 N84-23969

PARREIRA, E. M. D. M. F.

The use of an image registration technique in the urban growth monitoring [E84-10147] p 16 N84-26095

Q

QI, C. L.

An inquiry into methods of estimating yields of wheat and autumn crops in the plain region with Landsat images visual interpretation p 2 A84-30239

QUADIR, D. A.

Measurement of boro rice acreage in Nabinagar Thana by remote sensing technique p 1 A84-30227

QUIEL, F.

Application of Landsat data in the exploration of 'Calcrete' uranium deposits p 24 A84-3775

R

RADKE, L. F.

Airborne observations of Arctic aerosol. IV - Optical properties of Arctic haze p 32 A84-34287

RAHMAN, M.

Measurement of boro rice acreage in Nabinagar Thana by remote sensing technique p 1 A84-30227
Measurement of boro rice acreage in Srimangal Thana by remote sensing technique p 1 A84-30235

RAITALA, J.

Locating shoreline changes in the Porttipahta (Finland) water reservoir by using multitemporal Landsat data p 52 A84-33987

RAMM, N. S.

Conditions for the illumination of an area in satellite scanner surveys p 65 A84-34787

RAND, R. S.

Cartographic feature extraction on ETL's (Engineer Topographic Laboratories) DIAL (Digital Image Analysis Laboratory) system [AD-A140230] p 63 A84-26112

RANEY, R. K.

Theory and measure of certain image norms in SAR p 43 A84-2724

RAO, P. P. N.

Identification of brown plant hopper and bacterial leaf blight affected rice crop on Landsat false colour composites p 1 A84-30237

RAO, V. R.

Identification of brown plant hopper and bacterial leaf blight affected rice crop on Landsat false colour composites p 1 A84-30237
Remote sensing for bauxite prospecting p 22 A84-30260

RAPLEY, C. G.

First observations of the interaction of ocean swell with sea ice using satellite radar altimeter data p 35 A84-36684
Observations of sea ice and icebergs from satellite radar altimeters p 48 A84-27311

RASHATASUVAN, N.

Remote sensing as a tool for mineral prospecting p 22 A84-30259

RASOOL, S. I.

Surface albedo and the Sahel drought p 7 A84-36710

REED, I. S.

Digital SAR processing using a fast polynomial transform p 55 A84-32093

REEVES, A. B.

The dual-frequency scatterometer reexamined p 44 A84-27280

REILINGER, R.

Coseismic and postseismic vertical movements associated with the 1940 M7.1 Imperial Valley, California, earthquake p 24 A84-36922

REMSBERG, E. E.

The validation of Nimbus 7 LIMS measurements of ozone p 67 A84-39443
Accuracy and precision of the nitric acid concentrations determined by the limb infrared monitor of the stratosphere experiment on NIMBUS 7 p 67 A84-39444

RENBARGER, K. S.

A crustal structure study of South America p 29 A84-25139

RESTI, A.

X to W band radiometric signatures of natural surfaces p 35 A84-36289

RICE, D. P.

Characterization of Landsat-4 MSS and TM digital image data p 56 A84-33526
Understanding and utilization of Thematic Mapper and other remotely sensed data for vegetation monitoring [E84-10150] p 11 A84-26098

RICHARDS, J. A.

Irrigated crop inventory by classification of satellite image data p 8 A84-38999

RIDD, M. K.

Preliminary digital classification of grazing resources in the Southern Chihuahuan Arid Zone of Mexico p 5 A84-33349

PARREIRAS, E. M. D. M. F.

Application of LANDSAT data to the study of urban development in Brasilia p 16 N84-26090

PARRIS, T. M.

Understanding and utilization of Thematic Mapper and other remotely sensed data for vegetation monitoring [E84-10150] p 11 N84-26098

PATHAN, S. K.

Bhaskara-II TV data in resource studies - A case study in a part of Andhra Pradesh, southern India p 54 A84-30234

PATTILLO, C.

Landsat MSS data used for crop identification at the limit of its spatial resolution p 8 A84-38299

PAVONI, N.

Discussion of the design of satellite-laser measurement stations in the eastern Mediterranean under the geological aspect. Contribution to the earthquake prediction research by the Wegener Group and to NASA's Crustal Dynamics Project [NASA-TM-77412] p 26 N84-24031

PAYOLLA, B. L.

Utilization of digital LANDSAT imagery for the study of granitoid bodies in Rondonia: Case example of the Peda Branca massif [E84-10120] p 26 N84-23979

PELZER, H.

Detection of errors in the functional adjustment model p 20 N84-26074

PEREZ, J. E.

Identification and estimation of the area planted with irrigated rice based on the visual interpretation of LANDSAT MSS data [E84-10164] p 12 N84-27256

PERIGAUD, C.

Somali current studied from SEASAT altimetry p 47 N84-27307

PERSSON, U.

Computer-automated CO2-laser long-path absorption system for air quality monitoring in the working environment p 13 A84-30307

PETEHERYCH, S.

A model function for ocean radar cross sections at 14.6 GHz p 34 A84-34516

Large-scale analysis and forecast experiments with wind data from the Seasat A scatterometer p 66 A84-37873

A new parameterization of an empirical model for wind/ocean scatterometry p 43 N84-27269

New algorithms for microwave measurements of ocean winds p 43 N84-27272

The impact of scatterometer wind data on global weather forecasting p 49 N84-27314

PETERSON, U. K.

Classifying the coefficients of spectral brightness of the forest zone in the European part of the Soviet Union p 6 A84-34783

PETROV, S. E.

Topography interpretation possibilities for satellite photos in regions where the platform mantle has a multilayer structure (on the example of the eastern marginal part of the Caspian depression) p 23 A84-34779

PHILIPSON, W. R.

Analysis of Landsat for monitoring vegetables in New York mucklands p 5 A84-33345

PHILLIPS, B. B.

Applications of airborne remote sensing in atmospheric sciences research p 71 N84-27286

PHILLIPS, D. M.

A theoretical study of an airborne laser technique for determining sea water turbidity p 31 A84-33774

PHILLIPS, O. M.

On the response to ocean surface currents in synthetic aperture radar imagery p 47 N84-27304

PHILPOT, W. D.

Analysis of Landsat for monitoring vegetables in New York mucklands p 5 A84-33345

PICARDI, G.

The radar altimeter for ERS-1 Satellite p 64 A84-30516

PIERI, D. C.

NASA Oceanic Processes Program, fiscal year 1983 [NASA-TM-86248] p 39 N84-24078

PIERSON, W. J., JR.

Vector wind, horizontal divergence, wind stress and wind stress curl from SEASAT-SASS at one degree resolution p 48 N84-27313

PIETRAFESA, L. J.

Observations of Gulf Stream-induced and wind-driven upwelling in the Georgia Bight using ocean color and infrared imagery p 34 A84-34517

PERSONAL AUTHOR INDEX

Riparian habitat on the Humboldt River, Death to Elko, Nevada
[E84-10116] p 53 N84-23976

Enviropod handbook: A guide to preparation and use of the Environmental Protection Agency's light-weight aerial camera system
[E84-10123] p 68 N84-23982

EPA Enviropod. A summary of the use of the Enviropod under a Memorandum of Understanding among EPA Region 8, the State of Utah, and the University of Utah Research Institute
[E84-10124] p 15 N84-23983

RINO, C. L.
Propagation effects in satellite-based synthetic aperture radars
[ADA-138681] p 67 N84-22873

RITTER, I. T.
Identification and estimation of the area planted with irrigated rice based on the visual interpretation of LANDSAT MSS data
[E84-10164] p 12 N84-27256

ROBERTSON, J. B.
Effect of space exposure on pyroelectric infrared detectors (A0135) p 68 N84-24679

ROBINSON, A. R.
Simulation and assimilation of satellite altimeter data at the oceanic mesoscale p 48 N84-27312

ROBINSON, I. S.
Atmospheric correction of Landsat MSS data for a multivariate suspended sediment algorithm p 59 A84-38942

ROMEYN, L. J.
Satellite surveying techniques used within geodetic networks p 18 A84-3364

ROSEN, R. D.
Outlook for improved numerical weather prediction using satellite data with a special emphasis on the hydrological variables
[ADA-141233] p 54 N84-28344

ROSENBERG, N.
Coastal bathymetry and currents from LANDSAT data p 47 N84-27303

ROSENKRANZ, P. W.
Monthly distributions of precipitable water from the Nimbus 7 SMMR data p 37 A84-39458

ROSENTHAL, W. D.
Active microwave responses - An aid in improved crop classification p 3 A84-31498

ROSS, D. B.
A summary of results from the first Nimbus 7 SMMR observations p 37 A84-39459

ROSS, IU. K.
Classifying the coefficients of spectral brightness of the forest zone in the European part of the Soviet Union p 6 A84-34783

ROTH, L. E.
Spaceborne radar subsurface imaging in hyperarid regions p 24 A84-39379

ROTHROCK, D. A.
Remote sensing of floe size distribution and surface topography
[E84-10132] p 39 N84-25141

ROUSSEL, J.
SPOT simulations in Bangladesh flight operations and main results p 2 A84-30253

ROZANOV, L. N.
Distinguishing linear contour elements on satellite photos on the basis of a visual perception model p 24 A84-34789

RUBIN, A. L.
Digital SAR processing using a fast polynomial transform p 55 A84-32093

RUFENACH, C. L.
Optimum backscatter cross section of the ocean as measured by synthetic aperture radars p 44 N84-27276

SAR imagery of ocean-wave swell traveling in an arbitrary direction p 44 N84-27278

RUSSELL, J. M., III
Accuracy and precision of the nitric acid concentrations determined by the limb infrared monitor of the stratosphere experiment on NIMBUS 7 p 67 A84-39444

RUSSELL, J. M., III
The Limb Infrared Monitor of the Stratosphere - Experiment description, performance, and results p 66 A84-39440

The validation of Nimbus 7 LIMS measurements of ozone p 67 A84-39443

RUSSO, S. A.
The statewide forest/nonforest classification of Pennsylvania using Landsat MSS data p 3 A84-33329

RYAN, C. J.
A constrained-clustering approach to the analysis of remote sensing data
[ADA-139124] p 10 N84-23993

RZHIGA, O. N.
An airborne radar station for studying the reflection properties of the earth's surface p 64 A84-31072

S

SAHAI, B.
Identification of water-logged and salt-affected soils through remote sensing techniques p 51 A84-30251

SAKAI, T.
Classification of snow surface conditions by means of Landsat MSS data under compensation of slope effects p 52 A84-38296

SALFI, R. E.
Vector wind, horizontal divergence, wind stress and wind stress curl from SEASAT-SASS at one degree resolution p 48 N84-27313

SALSTEIN, D. A.
Outlook for improved numerical weather prediction using satellite data with a special emphasis on the hydrological variables
[ADA-141233] p 54 N84-28344

SALTER, L.
Description of SEP ground station and Vizir image processing VIPS p 54 A84-30268

SAMPSON, R. E.
Understanding and utilization of Thematic Mapper and other remotely sensed data for vegetation monitoring
[E84-10150] p 11 N84-26098

SANDWELL, D. T.
The GRAVSAT signal over tectonic features p 19 A84-36919

SAPPL, E.
The theory of Earth observation using multiple-frequency radar
[ESA-TT-819] p 63 N84-26105

SARRAT, D.
Description of SEP ground station and Vizir image processing VIPS p 54 A84-30268

SASANUMA, M.
Microwave scatterometer p 66 A84-38310

SATCHWELL, B.
Fire detection using the NOAA (National Oceanic and Atmospheric Administration)-series satellites
[PB84-176890] p 13 N84-27324

SATTERWHITE, M. B.
Discriminating vegetation and soils using LANDSAT MSS and Thematic Mapper bands and band ratios
[ADA-140198] p 11 N84-26108

SAUNDERS, R. D.
High-precision atmospheric ozone measurements using wavelengths between 290 and 305 nm p 67 A84-39447

SAVAGE, R. K.
In-flight absolute radiometric calibration of the Thematic Mapper p 56 A84-33531

In-flight absolute radiometric calibration of the Thematic Mapper p 68 N84-23002

SAXENA, N.
Error analysis for marine geodetic control using the global positioning system
[ADA-140566] p 21 N84-26687

SCHABER, G. G.
Spaceborne radar subsurface imaging in hyperarid regions p 24 A84-39379

Radar backscatter modelling p 25 N84-23525

SCHLINGER, C. M.
Petrologic and geophysical sources of long-wavelength crustal magnetic anomalies
[NASA-CR-175245] p 29 N84-28276

SCHMELING, B.
Contour-to-grid transformation: Development of a method for generation of a sparse grid structure out of terrain elevation contours
[FOA-C-30349-E1] p 16 N84-25156

SCHMUGGE, T. J.
Calculations of radar backscattering coefficient of vegetation-covered soils p 2 A84-30671

SCHNEIDER, S. R.
Fire detection using the NOAA (National Oceanic and Atmospheric Administration)-series satellites
[PB84-176890] p 13 N84-27324

SCHNELL, R. C.
Arctic haze and the Arctic gas and aerosol sampling program (AGASP) p 32 A84-34276

SCHOWENGERDT, R. A.
Thematic Mapper image quality - Registration, noise, and resolution p 57 A84-33533

SCHUESSLER, H.
Ocean wind field measurement performance of the ERS-1 scatterometer p 43 N84-27273

SCHULER, D. L.
An improved dual-frequency technique for the remote sensing of ocean currents and wave spectra p 44 N84-27281

SEKHON, R.
Comparative accuracies of AVHRR and MSS data used for Level I land cover classifications p 14 A84-33344

SERAFIN, R. J.
Applications of airborne remote sensing in atmospheric sciences research p 71 N84-27286

SERRA, P. R. M.
An integrated software system for geometric correction of LANDSAT MSS imagery
[E84-10143] p 62 N84-26091

SEXTON, J. L.
US aeromagnetic and satellite magnetic anomaly comparisons p 28 N84-25136

SHAFIU ALAM, A. K. M.
Digital processing of remote sensing data on Hail Haor, Bangladesh for landuse analysis and development potentiality assessment p 13 A84-30240

SHAIN, W. A.
The use of Landsat imagery in analyzing the vegetation and energy resources of Pickens County, South Carolina p 3 A84-33330

SHASBY, M. B.
Land cover and terrain mapping for the development of digital data bases for wildlife habitat assessment in the Yukon Flats National Wildlife Refuge, Alaska p 9 N84-23971

SHEFER, E. I.U.
Correlations between the nonthermal emission of quasarlike nuclei and their Balmer-line widths p 58 A84-33629

SHEN, S. S.
Evaluation of corn/soybeans separability using Thematic Mapper and Thematic Mapper Simulator data p 5 A84-33539

SHEVTSOV, B. M.
Theory of radio wave propagation over the sea surface p 35 A84-37095

SHIMABUKURO, Y. E.
Forest inventory using multistage sampling with probability proportional to size
[E84-10144] p 11 N84-26092

SHIMADA, M.
Remote sensing of the ocean by the airborne microwave scatterometer/radiometer system p 36 A84-38307

Microwave scatterometer p 66 A84-38310

SHORT, D. A.
Nimbus 7 SMMR derived seasonal variations in the water vapor, liquid water and surface winds over the global oceans
[NASA-TM-86080] p 40 N84-26233

SHUCHMAN, R. A.
SAR imagery of ocean-wave swell traveling in an arbitrary direction p 44 N84-27278

Modeling of SAR signatures of shallow water ocean topography p 47 N84-27302

Analysis of SEASAT SAR imagery collected during the JASIN experiment
[ADA-140584] p 49 N84-27320

SHUGAN, I. V.
Speckle statistics in radar images of sea surface obtained with horizontal polarization p 50 N84-27921

SIEGEL, B. Z.
First estimate of annual mercury flux at the Kilauea main vent p 15 A84-34794

SIEGEL, S. M.
First estimate of annual mercury flux at the Kilauea main vent p 15 A84-34794

SIELKEN, R. L., JR.
Area estimation using multiyear designs and partial crop identification
[E84-10151] p 11 N84-26099

SIKDAR, D. N.
Diagnostics of rainfall anomalies in the Nordeste during the global weather experiment
[SAPR-1] p 40 N84-26235

SIMARD, R.
Evaluating LANDSAT-4 MSS and TM data
[E84-10157] p 63 N84-27249

SIMS, M.
Applications of the GPS (Global Positioning System) Geodetic Receiver System
[AD-140567] p 21 N84-26688

SINCLAIR, P. C.
Detection of marine aerosol particles in coastal zones using satellite imagery p 36 A84-38943

SINGER, H. J.
A study of geomagnetic pulsations using the AFGL (Air Force Geophysics Laboratory) magnetometer network
[AD-140507] p 70 N84-26217

SLADKOPEVTSEV, S. A.
Mapping of exogenic terrain dynamics on the basis of space photographs (on the example of the Baikal region) p 18 A84-34491

SLATER, P.

SLATER, P.
Spectroradiometric calibration of the Thematic Mapper and multispectral scanner system
[E84-10098] p 67 N84-23000

SLATER, P. N.
In-flight absolute radiometric calibration of the Thematic Mapper p 56 A84-33531

In-flight absolute radiometric calibration of the Thematic Mapper p 68 N84-23002

Spectroradiometric calibration of the Thematic Mapper and Multispectral Scanner system
[E84-10136] p 70 N84-26084

SLOAN, C. E.
Hydrology of the North Slope, Alaska p 53 N84-23973

SLUD, E. V.
Reduction of satellite magnetic anomaly data p 19 A84-38812

SMIRNOV, M. V.
Distinguishing linear contour elements on satellite photos on the basis of a visual perception model p 24 A84-34789

SMITH, M. P.
Synthetic aperture radar images of ocean waves, theories of imaging physics and experimental tests p 43 N84-27275

SMITH, P. J.
Reduction of satellite magnetic anomaly data p 19 A84-38812

SMITS, K.
Analysis of airborne electromagnetic systems for mapping thickness of sea ice
[AD-A139786] p 39 N84-25235

SOBIESKI, P.
A tentative unified sea model for scattering and emission p 45 N84-27285

SOLEDAD FERNANDEZ, M.
Landsat MSS data used for crop identification at the limit of its spatial resolution p 8 A84-38299

SOMMA, R.
The radar altimeter for ERS-1 Satellite p 64 A84-30516

SORENSEN, C. T.
Evaluation of corn/soybeans separability using Thematic Mapper and Thematic Mapper Simulator data p 5 A84-33539

SOURIAU, A.
Present limitations of accurate satellite Doppler positioning for tectonics - An example: Djibouti p 17 A84-32495

SOUTHARD, R. B.
Antarctic mapping and international coordination p 19 N84-23935

SOUTHWORTH, C. S.
Glaciological and geological studies of Antarctica with satellite remote sensing technology p 38 N84-23956

SPANNER, M. A.
The use of digital elevation model topographic data for soil erosion modeling within a geographic information system p 4 A84-33342

STAELIN, D.
A summary of results from the first Nimbus 7 SMMR observations p 37 A84-39459

STAELIN, D. H.
Monthly distributions of precipitable water from the Nimbus 7 SMMR data p 37 A84-39458

STANFORD, G.
Microwave radiometric measurement of sea surface salinity
[AD-A141302] p 50 N84-28359

STAUFFER, M. L.
The statewide forest/nonforest classification of Pennsylvania using Landsat MSS data p 3 A84-33329

A statistical evaluation of the advantages of Landsat Thematic Mapper data in comparison to Multispectral Scanner data p 57 A84-33537

STEVENSON, M. R.
Seasonal oscillations of the subtropical convergence between the Brazil and Malvinas currents, using oceanographic and SMS-2 satellite data
[INPE-3092-PRE/497] p 40 N84-26255

STRAHLER, A. H.
Spatial inventory integrating raster databases and point sample data p 4 A84-33340

STROME, W. M.
Evaluating LANDSAT-4 MSS and TM data
[E84-10157] p 63 N84-27249

STURM, B.
CZCS data analysis in turbid coastal water p 37 A84-39427

SUGIMORI, Y.
Remote sensing of the oceans p 35 A84-37299

SUZUKI, Y.
Joint analysis of Landsat-MSS and NOAA-AVHRR data for marine environmental monitoring p 35 A84-38298

SWIFT, C. T.

Microwave remote sensing of ocean surface wind speed and rain rates over tropical storms p 45 N84-27288

SWIFT, R. N.

Airborne laser topographic mapping results p 8 A84-38998

SYLVESTER, W. B.

A SEASAT SASS simulation experiment to quantify the errors related to a + or - 3 hour intermittent assimilation technique

[E84-10129] p 68 N84-23987

Vector wind, horizontal divergence, wind stress and wind stress curl from SEASAT-SASS at one degree resolution p 48 N84-27313

SZEJWACH, G.

Applications of airborne remote sensing in atmospheric sciences research p 71 N84-27286

T

TAKEUCHI, S.

Joint analysis of Landsat-MSS and NOAA-AVHRR data for marine environmental monitoring p 35 A84-38298

TANAKA, S.

Classification of snow surface conditions by means of Landsat MSS data under compensation of slope effects p 52 A84-38296

TANIS, F. J.

Development of Great Lakes algorithms for the Nimbus-G coastal zone color scanner
[NASA-CR-173511] p 53 N84-27258

TARDIN, A. T.

Research and applications of data from environmental satellites: Determining parameters and developing interpretation techniques for applications of environmental satellite data

[INPE-3005-NTE/213] p 13 N84-27261

TAYMAN, W. P.

User guide for the USGS aerial camera report of calibration p 65 A84-34958

TEBBS, B.

Application of remote sensing to state and regional problems
[E84-10128] p 68 N84-23986

THEDY, J. L. O.

Identification and estimation of the area planted with irrigated rice based on the visual interpretation of LANDSAT MSS data

[E84-10164] p 12 N84-27256

THOMAS, L. A.

A model function for ocean radar cross sections at 14.6 GHz p 34 A84-34516

THOMAS, R. H.

Satellite remote sensing over ice p 48 N84-27308

THOMPSON, D. R.

Evaluation of corn/soybeans separability using Thematic Mapper and Thematic Mapper Simulator data p 5 A84-33539

Evaluation of Thematic Mapper for detecting soil properties under grassland vegetation p 6 A84-33540

THOMPSON, J. D.

Sampling strategies and four-dimensional assimilation of altimetric data for ocean monitoring and prediction p 49 N84-27317

The influence of actual and apparent geoid error on ocean analysis and prediction p 49 N84-27318

THOMPSON, R. L.

Inversion of vegetation canopy reflectance models for estimating agronomic variables. III - Estimation using only canopy reflectance data as illustrated by the suits model. IV - Total inversion of the SAIL model p 7 A84-37203

THORNDIKE, A. S.

Remote sensing of floe size distribution and surface topography
[E84-10132] p 39 N84-25141

TILLEY, D. G.

Tracking ocean wave spectrum from SAR images p 44 N84-27277

TINGLE, J.

Application of remote sensing to state and regional problems
[E84-10128] p 68 N84-23986

TJERNBERG, J.

A computer program for mapping regions in a geographic data base with raster structure
[FOA-C-20529-D8] p 16 N84-25340

TOFANI, G.

X to W band radiometric signatures of natural surfaces p 35 A84-36289

TOLL, D. L.

A statistical evaluation of the advantages of Landsat Thematic Mapper data in comparison to Multispectral Scanner data p 57 A84-33537

TOMIMURA, S.

Analysing forest structures by remote sensing p 1 A84-30236

TORLEGAARD, K.

Photogrammetric research at the Royal Institute of Technology, Stockholm, Sweden p 69 N84-25147

Mathematical aspects of digital terrain information. A progress report from ISPRS Working Group III:3

p 61 N84-25148

The question of accuracy in the transition from analogue to analytic photogrammetry p 69 N84-25153

Multi-models to increase accuracy p 70 N84-25154

TRIPP, J. S.

A rapid method for obtaining frequency-response functions for multiple input photogrammetric data
[AIAA PAPER 84-1060] p 65 A84-31741

TRUONG, T. K.

Digital SAR processing using a fast polynomial transform p 55 A84-32093

TSENG, Y. C.

Analysis of SEASAT SAR imagery collected during the JASIN experiment
[AD-A140584] p 49 N84-27320

TSUBOI, A.

A SAR image auto-focusing using linear distortion azimuth matched filter p 58 A84-38304

TSUBOMATSU, M.

Classification of snow surface conditions by means of Landsat MSS data under compensation of slope effects p 52 A84-38296

TSUCHIYA, K.

Joint analysis of Landsat-MSS and NOAA-AVHRR data for marine environmental monitoring p 35 A84-38298

Study on temporal geometric-distortion variation of Landsat MSS and RBV imageries and attitude determination program p 59 A84-38313

TUCKER, C. J.

Intensive forest clearing in Rondonia, Brazil, as detected by satellite remote sensing p 8 A84-37204

TULLY, J.

NASA, the first 25 years: 1958 - 1983
[NASA-EP-182] p 72 N84-26563

U

ULABY, F. T.

Improving crop classification through attention to the timing of airborne radar acquisitions p 8 A84-39000

UNGAR, S. G.

Integration of Landsat data into the Saginaw River Basin geographic information system p 51 A84-33339

Integration of LANDSAT land cover data into the Saginaw River basin geographic information system for hydrologic modeling
[AD-A140185] p 53 N84-26106

USERY, E. L.

Cartographic accuracy of Landsat-4 MSS and TM image data p 57 A84-33535

USIKOV, D. A.

The effect of fluctuations in the optical properties of the atmosphere on spectral brightness ratios in the remote sensing of agricultural areas p 6 A84-34777

V

VAFIN, R. F.

The use of satellite photos for analyzing the structural and dynamic conditions surrounding the formation of ancient deposits of phlogopite and apatite p 23 A84-34781

VALDES, J. A.

Landsat-4 MSS and Thematic Mapper data quality and information content analysis p 56 A84-33528

VALENZUELA, C. R.

Landsat-4 MSS and Thematic Mapper data quality and information content analysis p 56 A84-33528

VAN KONIJNENBURG, R.

Status of the TERS project p 71 A84-34575

VANBAVEL, C. H. M.

CONSERVB: A numerical method to compute soil water content and temperature profiles under a bare surface
[E84-10113] p 9 N84-23006

VANICEK, P.

Geometrical aspects of differential GPS positioning p 17 A84-32494

VANMELLE, A.

Error analysis for marine geodetic control using the global positioning system
[AD-A140566] p 21 N84-26687

VENABLE, D. D.

Sensitivity of airborne fluorosensor measurements to linear vertical gradients in chlorophyll concentration p 30 A84-30302

PERSONAL AUTHOR INDEX

ZHANG, S.

VERCHEVAL, J.
A sample performance of the grille spectrometer aboard Spacelab
[AERONOMICA-ACTA-A-281-1984] p 70 N84-26003

VESECKY, J. F.
Synthetic aperture radar images of ocean waves, theories of imaging physics and experimental tests p 43 N84-27275

VETRELLA, S.
A simulation program for the integration of aerospace remote sensing systems with a digital terrain model p 59 A84-38316

VICKERS, E.
Experiments in lithography from remote sensor imagery p 55 A84-33362

VIOLIER, M.
CZCS data analysis in turbid coastal water p 37 A84-39427

VITORELLO, I.
Multiseasonal variables in digital image enhancements for geological applications [E84-10145] p 29 N84-26093

Methodological approach in lithological discrimination by digital processing: A case study in the Serra do Ramalho, state of Bahia [INPE-3108-PRE/507] p 29 N84-26101

VLCEK, J.
Videography - Some remote sensing applications p 3 A84-33331

VOLYAK, K. I.
Speckle statistics in radar images of sea surface obtained with horizontal polarization p 50 N84-27921

VONDER HAAR, T. H.
Detection of marine aerosol particles in coastal zones using satellite imagery p 36 A84-38943

VONFRESE, R. R. B.
Application of Magsat lithospheric modeling in South America. Part 1: Processing and interpretation of magnetic and gravity anomaly data [E84-10115] p 24 N84-23008

Application of Magsat to lithospheric modeling in South America. Part 2: Synthesis of geologic and seismic data for development of integrated crustal models [E84-10126] p 26 N84-25128

Euro-African Magsat anomaly-tectonic observations p 27 N84-25129

Satellite elevation magnetic and gravity models of major South American plate tectonic features p 27 N84-25131

Reduced to pole long-wavelength magnetic anomalies of Africa and Europe p 27 N84-25132

Satellite magnetic anomalies of Africa and Europe p 27 N84-25133

Do satellite magnetic anomaly data accurately portray the crustal component? p 28 N84-25134

Long-wavelength magnetic and gravity anomalies of Africa and Europe p 28 N84-25135

US aeromagnetic and satellite magnetic anomaly comparisons p 28 N84-25136

VUDHICHTIVANICH, S.
Remote sensing as a tool for mineral prospecting p 22 A84-30259

W

WADSWORTH, J. R., JR.
Surface expression of heavily mantled interstratal Karst bordering Okefenokee Swamp, Georgia p 23 A84-33350

WAGNER, C. A.
The GRAVSAT signal over tectonic features p 19 A84-36919

WALKER, R. E.
An analysis of Landsat-4 Thematic Mapper geometric properties p 57 A84-33536

WALSH, E. J.
Altimeter height measurement errors introduced by the presence of variable cloud and rain attenuation p 45 N84-27289

WARD, J. F.
High-precision atmospheric ozone measurements using wavelengths between 290 and 305 nm p 67 A84-39447

WARNER, C.
Aircraft measurements of convective draft cores in MONEX p 31 A84-31821

Satellite observations of a monsoon depression [NASA-CR-173590] p 40 N84-26232

WARREN, A.
Experiments in lithography from remote sensor imagery p 55 A84-33362

WEISSMAN, D. E.
Two-frequency microwave resonance measurements from an aircraft - A quantitative estimate of the directional ocean surface spectrum p 34 A84-34942

Measurements of ocean wave spectra and modulation transfer function with the airborne two frequency scatterometer p 45 N84-27282

WELCH, R.
Cartographic accuracy of Landsat-4 MSS and TM image data p 57 A84-33535

WELLS, D. E.
Geometrical aspects of differential GPS positioning p 17 A84-32494

A forecast of the impact of GPS on surveying p 18 A84-33374

WELLVING, A.
A computer program for mapping regions in a geographic data base with raster structure [FOA-C-20529-D8] p 16 N84-25340

WENDLING, P.
A bispectral method for the height determination of optically thin ice clouds p 60 A84-39044

WENTZ, F. J.
A model function for ocean radar cross sections at 14.6 GHz p 34 A84-34516

New algorithms for microwave measurements of ocean winds p 43 N84-27272

WERNER, C.
Airborne lidar for oceanography and hydrology (FLOH) [ESA-TT-799] p 37 N84-22955

WESCOTT, T.
Interactive digital image processing for terrain data extraction, phase 4 [AD-A140197] p 11 N84-26107

WHITAKER, R. E.
Lagrangian observations of an anticyclonic ring in the western Gulf of Mexico p 33 A84-34502

A model for the analysis of drifter data with an application to a warm core ring in the Gulf of Mexico p 33 A84-34503

WHITING, J. M.
The effect of groundwater inflow on evaporation from a saline lake p 52 A84-34378

WILHEIT, T. T.
Monthly distributions of precipitable water from the Nimbus 7 SMMR data p 37 A84-39458

A summary of results from the first Nimbus 7 SMMR observations p 37 A84-39459

WILKE, G. D.
Crop moisture estimation over the southern Great Plains with dual polarization 1.66 centimeter passive microwave data from Nimbus 7 [E84-10163] p 12 N84-27255

WILLIAMS, D. L.
A statistical evaluation of the advantages of Landsat Thematic Mapper data in comparison to Multispectral Scanner data p 57 A84-33537

WILLIAMS, O. W.
The geodetic activities of the Department of Defense under IGY programs p 17 A84-30727

WILLIAMS, R. S., JR.
Satellite image atlas of glaciers: The Polar regions p 38 N84-23940

Glaciological and geological studies of Antarctica with satellite remote sensing technology p 38 N84-23956

WILSON, C.
Landsat planimetric maps p 54 A84-30264

WITT, R. G.
Comparative accuracies of AVHRR and MSS data used for Level I land cover classifications p 14 A84-33344

WOICESHYN, P. M.
Large-scale analysis and forecast experiments with wind data from the Seasat A scatterometer p 66 A84-37873

A new parameterization of an empirical model for wind/ocean scatterometry p 43 N84-27269

The impact of scatterometer wind data on global weather forecasting p 49 N84-27314

WONG, C. K.
Intercomparison of the Nimbus 7 SBUV/TOMS total ozone data sets with Dobson and MB3 results p 67 A84-39449

WOODCOCK, C. E.
Spatial inventory integrating raster databases and point sample data p 4 A84-33340

WRIGHT, L. H.
Application of remote sensing to state and regional problems [E84-10128] p 68 N84-23986

WRIGLEY, R. C.
Thematic Mapper image quality - Registration, noise, and resolution p 57 A84-33533

Investigation of several aspects of LANDSAT-4 data quality [E84-10122] p 60 N84-23981

WURTELE, M. G.
A new parameterization of an empirical model for wind/ocean scatterometry p 43 N84-27269

WYATT, F.
High precision measurements in crustal dynamic studies [NASA-CR-173680] p 22 N84-28279

X

XU, G.-Q.
Making false color photomap and its application in thematic mapping by using IR photos p 54 A84-30249

Y

YAMADA, H.
Remote sensing of the ocean by the airborne microwave scatterometer/radiometer system p 36 A84-38307

Microwave scatterometer p 66 A84-38310

YAMAGATA, S.
Performance evaluation and a dedicated system for SAR image data processing p 58 A84-38300

YAMAMOTO, H.
Two-stage cluster analysis of a Landsat image p 58 A84-38302

Image analysis researches of remotely sensed data at NAL p 59 A84-38315

YAMAMOTO, S.
Remote sensing of the ocean by the airborne microwave scatterometer/radiometer system p 36 A84-38307

YAMAURA, Y.
Study on temporal geometric-distortion variation of Landsat MSS and RBV imageries and attitude determination program p 59 A84-38313

YAN, S. Y.
Analysis of Landsat for monitoring vegetables in New York mucklands p 5 A84-33345

YAN, T.-S.
Making false color photomap and its application in thematic mapping by using IR photos p 54 A84-30249

YANG, T.-S.
The use of Hough transformation for detecting lineaments in satellite imagery p 22 A84-30262

YANG, W.
The approximation introduced by representing the earth's gravity field with a finite grid of mascons both at the earth's surface and at the bottom of the earth's crust [IAG PAPER 83-394] p 17 A84-30583

YEN, C. C.
Analysis of Landsat for monitoring vegetables in New York mucklands p 5 A84-33345

YODER, J. A.
Observations of Gulf Stream-induced and wind-driven upwelling in the Georgia Bight using ocean color and infrared imagery p 34 A84-34517

YORK, J. E.
Land cover and terrain mapping for the development of digital data bases for wildlife habitat assessment in the Yukon Flats National Wildlife Refuge, Alaska p 9 N84-23971

YOSHIKADO, S.
Remote sensing of the ocean by the airborne microwave scatterometer/radiometer system p 36 A84-38307

YU, T.-W.
Global data assimilation experiments with scatterometer winds from SEASAT-A p 65 A84-32938

YUAN, D. W.
Correlation of tectonic provinces of South America and the Caribbean region with MAGSAT anomalies p 27 N84-25130

Relation of MAGSAT anomalies to the main tectonic provinces of South America p 28 N84-25137

Relation of MAGSAT and gravity anomalies to the main tectonic provinces of South America p 28 N84-25138

YUE, G. K.
A comparative study of aerosol extinction measurements made by the SAM II and SAGE satellite experiments p 15 A84-39457

Z

ZAITSEV, A. L.
An airborne radar station for studying the reflection properties of the earth's surface p 64 A84-31072

ZAKHAROV, A. I.
An airborne radar station for studying the reflection properties of the earth's surface p 64 A84-31072

ZANG, E.
Experiments in lithography from remote sensor imagery p 55 A84-33362

ZHANG, S.
The application of Landsat image in the surveying of water resources of Dongting Lake p 51 A84-30255

ZHENG, Q.

Dynamics of the slope water off New England and its influence on the Gulf Stream as inferred from satellite IR data p 31 A84-30672

ZHU, M. H.

Analysis of Landsat for monitoring vegetables in New York mucklands p 5 A84-33345

ZIMOV, V. E.

An airborne radar station for studying the reflection properties of the earth's surface p 64 A84-31072

ZINATOV, KH. G.

The use of satellite photos for analyzing the structural and dynamic conditions surrounding the formation of ancient deposits of phlogopite and apatite

p 23 A84-34781

ZLOTNICKI, V.

Somali current studied from SEASAT altimetry p 47 N84-27307

ZOBRIST, A. L.

An analysis of Landsat-4 Thematic Mapper geometric properties p 57 A84-33536

The Pennsylvania defoliation application pilot test [E84-10111] p 8 N84-23004

ZWALLY, H. J.

Arctic Sea ice by passive microwave observations from the Nimbus-5 Satellite p 39 N84-23970

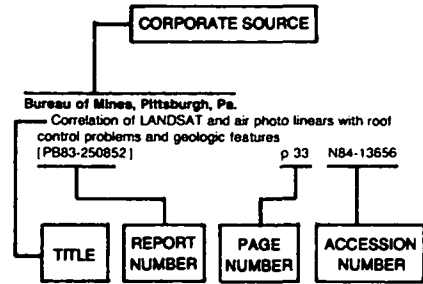
Matrix partitioning and EOF/principal component analysis of Antarctic Sea ice brightness temperatures [NASA-TM-83916] p 49 N84-27319

CORPORATE SOURCE INDEX

EARTH RESOURCES / A Continuing Bibliography (Issue 43)

OCTOBER 1984

Typical Corporate Source Index Listing



The title of the document is used to provide a brief description of the subject matter. The page number and the accession number are included in each entry to assist the user in locating the abstract in the abstract section. If applicable, a report number is also included as an aid in identifying the document.

A

Academy of Sciences (USSR), Moscow.
Scientific activity in oceanography, 1979-1982
p 38 N84-23084

Aerojet ElectroSystems Co., Azusa, Calif.
Digital SAR processing using a fast polynomial transform
p 55 A84-32093

Air Force Inst. of Tech., Wright-Patterson AFB, Ohio.
A constrained-clustering approach to the analysis of remote sensing data
[AD-A139124] p 10 N84-23993

Alaska Pacific Univ.
Vegetation monitoring and classification using NOAA/AVHRR satellite data
p 4 A84-33343

Applied Physics Lab., Johns Hopkins Univ., Laurel, Md.
Remote sensing for oceanography: Past, present, future
p 42 N84-27263

Arizona Univ., Tucson.
In-flight absolute radiometric calibration of the Thematic Mapper
p 56 A84-33531

Thematic Mapper image quality - Registration, noise, and resolution
p 57 A84-33533

Spectroradiometric calibration of the Thematic Mapper and multispectral scanner system
[E84-10098] p 67 N84-23000

Sensor radiance for a midlatitude atmospheric model
p 68 N84-23001

In-flight absolute radiometric calibration of the Thematic Mapper
p 68 N84-23002

Investigation of several aspects of LANDSAT-4 data quality
[E84-10122] p 60 N84-23981

Spectroradiometric calibration of the Thematic Mapper and Multispectral Scanner system
[E84-10136] p 70 N84-26084

Army Cold Regions Research and Engineering Lab., Hanover, N. H.
Integration of Landsat data into the Saginaw River Basin geographic information system
p 51 A84-33339

Integration of LANDSAT land cover data into the Saginaw River basin geographic information system for hydrologic modeling
[AD-A140185] p 53 N84-26106

Army Engineer Topographic Labs., Fort Belvoir, Va.
Discriminating vegetation and soils using LANDSAT MSS and Thematic Mapper bands and band ratios
[AD-A140198] p 11 N84-26108

Cartographic feature extraction on ETL's (Engineer Topographic Laboratories') DIAL (Digital Image Analysis Laboratory) system
[AD-A140230] p 63 N84-26112

Army Engineer Waterways Experiment Station, Vicksburg, Miss.
Airborne laser topographic mapping results
p 8 A84-38998

Survey of automated statewide natural resource information systems
[AD-A139017] p 16 N84-23996

Atmospheric and Environmental Research, Inc., Cambridge, Mass.
Outlook for improved numerical weather prediction using satellite data with a special emphasis on the hydrological variables
[AD-A141233] p 54 N84-28344

Atmospheric Environment Service, Downsview (Ontario).
A model function for ocean radar cross sections at 14.6 GHz
p 34 A84-34516

Large-scale analysis and forecast experiments with wind data from the Seasat A scatterometer
p 66 A84-37873

Accuracy and precision of the nitric acid concentrations determined by the limb infrared monitor of the stratosphere experiment on NIMBUS 7
p 67 A84-39444

Atmospheric Sciences Lab., White Sands Missile Range, N. Mex.
In-flight absolute radiometric calibration of the Thematic Mapper
p 56 A84-33531

Bar-Ilan Univ., Ramat-Gan (Israel).
Method to estimate drag coefficient at the air/ice interface over drifting open pack ice from remotely sensed data
p 48 N84-27310

Battelle Inst., Frankfurt am Main (West Germany).
Applications of laser for climatology and atmospheric research
[BLEV-R-65.169-5] p 70 N84-26237

Fundamentals of spaceborne remote sensing: Applications of lasers, volume 1
p 70 N84-26238

Bayerische Akademie der Wissenschaften, Munich (West Germany).
Seminar on mathematical models of geodetic/photogrammetric point determination with regard to outliers and systematic errors

[SER-A-98] p 20 N84-26069

Correlation calculation in stereoscopic image pairs for the automatic acquisition of digital land models, orthopictures and height line planes
[SER-C-283] p 21 N84-26079

Fisheye objective in the dose range photogrammetry: Theoretical and practical investigations
[SER-C-286] p 21 N84-26080

Bergen Univ. (Norway).

A summary of results from the first Nimbus 7 SMMR observations
p 37 A84-39459

Bern Univ. (Switzerland).

A summary of results from the first Nimbus 7 SMMR observations
p 37 A84-39459

Bonn Univ. (West Germany).

Estimation of variances and covariances in the multivariate and in the incomplete multivariate model
p 20 N84-26073

Boston Univ., Mass.

A study of geomagnetic pulsations using the AFGL (Air Force Geophysics Laboratory) magnetometer network
[AD-A140507] p 70 N84-26217

British Columbia Univ., Vancouver.

Variations in surface current off the coasts of Canada as inferred from infrared satellite imagery
p 47 N84-27305

Business and Technological Systems, Inc., Seabrook, Md.
Potential utility of future satellite magnetic field data
[NASA-CR-175230] p 26 N84-24691

C

California Univ., Berkeley.

Analysis of the quality of image data acquired by the LANDSAT-4 Thematic Mapper and Multispectral Scanners
[E84-10137] p 61 N84-26085

California Univ., Davis.

LANDSAT-D Thematic Mapper image dimensionality reduction and geometric correction accuracy
[E84-10149] p 62 N84-26097

California Univ., La Jolla.

Rapid evolution of a Gulf Stream warm-core ring
p 32 A84-34164

California Univ., San Diego.

High precision measurements in crustal dynamic studies
[NASA-CR-173680] p 22 N84-28279

California Univ., Santa Barbara.

Snow reflectance from Landsat-4 Thematic Mapper
p 52 A84-33541

LANDSAT-D investigations in snow hydrology
[E84-10094] p 53 N84-22997

Atmospheric model development
p 53 N84-22998

Registration of TM data to digital elevation models
p 60 N84-22999

Canada Centre for Remote Sensing, Ottawa (Ontario).
Evaluating LANDSAT-4 MSS and TM data
[E84-10157] p 63 N84-27249

Theory and measure of certain image norms in SAR
p 43 N84-27274

City Coll. of the City Univ. of New York.

Vector wind, horizontal divergence, wind stress and wind stress curl from SEASAT-SASS at one degree resolution
p 48 N84-27313

City Univ. Inst. of Marine and Atmospheric Sciences, New York.

A SEASAT SASS simulation experiment to quantify the errors related to a + or - 3 hour intermittent assimilation technique
[E84-10129] p 68 N84-23987

Clemson Univ., S.C.

Potential benefits of new satellite sensors to wetland mapping
p 7 A84-34960

Computer Sciences Corp., Silver Spring, Md.

Calculations of radar backscattering coefficient of vegetation-covered soils
p 2 A84-30671

The statewide forest/nonforest classification of Pennsylvania using Landsat MSS data
p 3 A84-33329

Comparative accuracies of AVHRR and MSS data used for Level 1 land cover classifications
p 14 A84-33344

A statistical evaluation of the advantages of Landsat Thematic Mapper data in comparison to Multispectral Scanner data
p 57 A84-33537

Cornell Univ., Ithaca, N.Y.

Analysis of Landsat for monitoring vegetables in New York mucklands
p 5 A84-33345

S
O
U
R
C
E

Coseismic and postseismic vertical movements associated with the 1940 M.7.1 Imperial Valley, California, earthquake p 24 N84-36922

Corps of Engineers, Detroit, Mich.

Integration of Landsat data into the Saginaw River Basin geographic information system p 51 N84-33339

Council of State Governments, Washington, D.C.

State remote sensing (LANDSAT) programs catalog [E84-10127] p 71 N84-23985

D

Defense Mapping Agency, Washington, D.C.

Error analysis for marine geodetic control using the global positioning system [AD-A140566] p 21 N84-26687

Applications of the GPS (Global Positioning System) Geodetic Receiver System [AD-A140567] p 21 N84-26688

Delaware Univ., Newark.

Dynamics of the slope water off New England and its influence on the Gulf Stream as inferred from satellite IR data p 31 N84-30672

Evaluation of spatial, radiometric and spectral Thematic Mapper performance for coastal studies [E84-10118] p 9 N84-23978

Evaluation of spatial, radiometric and spectral Thematic Mapper performance for coastal studies [E84-10159] p 12 N84-27251

Department of Agriculture, Beltsville, Md.

Calculations of radar backscattering coefficient of vegetation-covered soils p 2 N84-30671

Aircraft scatterometer observations of soil moisture on rangeland watersheds p 4 N84-33338

Comparison of the information content of data from the Landsat-4 Thematic Mapper and the Multispectral Scanner p 57 N84-33534

Department of Agriculture, Phoenix, Ariz.

In-flight absolute radiometric calibration of the Thematic Mapper p 56 N84-33531

Deutsche Forschungs- und Versuchsanstalt fuer Luft- und Raumfahrt, Oberpfaffenhofen (West Germany).

Preliminary investigations concerning a 90 GHz radiometer satellite experiment [DFVLR-FB-84-02] p 68 N84-24693

Dornier-Werke G.m.b.H., Friedrichshafen (West Germany).

Ocean wind field measurement performance of the ERS-1 scatterometer p 43 N84-27273

E

EG and G Washington Analytical Services Center, Inc., Pocomoke City, Md.

Airborne laser topographic mapping results p 8 N84-38998

EG & G Washington Analytical Services Center, Inc., Riverdale, Md.

Seasat observations of lithospheric flexure seaward of trenches p 32 N84-34339

Environmental Research Inst. of Michigan, Ann Arbor.

Digital processing considerations for extraction of ocean wave image spectra from raw synthetic aperture radar data p 30 N84-30025

Characterization of Landsat-4 MSS and TM digital image data p 56 N84-33526

A physically-based transformation of Thematic Mapper data The TM tasseled cap p 56 N84-33532

Study on spectral/radiometric characteristics of the Thematic Mapper for land use applications [E84-10130] p 61 N84-25140

Understanding and utilization of Thematic Mapper and other remotely sensed data for vegetation monitoring [E84-10150] p 11 N84-26098

Development of Great Lakes algorithms for the Nimbus-G coastal zone color scanner [NASA-CR-173511] p 53 N84-27258

Modeling of SAR signatures of shallow water ocean topography p 47 N84-27302

Analysis of SEASAT SAR imagery collected during the JASIN experiment [AD-A140584] p 49 N84-27320

EROS Data Center, Sioux Falls, S. Dak.

LANDSAT 4 investigations of Thematic Mapper and multispectral scanner applications [E84-10100] p 60 N84-23003

LANDSAT 4 investigations of Thematic Mapper and Multispectral Scanner applications [E84-10152] p 63 N84-27247

European Space Agency, Frascati (Italy).

Proceedings of the Fourth Meeting of the LANDSAT Technical Working Group (LTWG), volume 1 [LIB-PRO-0012-VOL-1] p 69 N84-25144

European Space Agency, Paris (France).

Airborne lidar for oceanography and hydrology (FLOH) [ESA-TT-799] p 37 N84-22955

Earthnet: The story of images [ESA-BR-18] p 62 N84-26102

Digital processing of LANDSAT data for the preparation of a land use map of the rural district surrounding Tuebingen to a scale of 1:50000 [ESA-TT-816] p 16 N84-26104

The theory of Earth observation using multiple-frequency radar [ESA-TT-819] p 63 N84-26105

European Space Technology Center, Noordwijk (Netherlands).

ESA activities in the use of microwaves for the remote sensing of the Earth p 42 N84-27264

G

General Electric Co., Lanham, Md.

Interactive digital image processing for terrain data extraction, phase 4 [AD-A140197] p 11 N84-26107

Geological Survey, Flagstaff, Ariz.

Spaceborne radar subsurface imaging in hyperarid regions Radar backscatter modelling p 24 N84-39379 p 25 N84-23525

Geological Survey, Tacoma, Wash.

A summary of results from the first Nimbus 7 SMMR observations Determination of sea ice parameters with the Nimbus 7 SMMR p 37 N84-39459 p 37 N84-39461

Geological Survey, Washington, D.C.

US Geological Survey Polar Research Symposium. Abstracts with program [USGS-CIRC-911] p 25 N84-23934

Antarctic mapping and international coordination p 19 N84-23935 Satellite image atlas of glaciers: The Polar regions p 38 N84-23940

Wind, waves and swell in the Antarctic marginal ice zone by SEASAT radar altimeter p 38 N84-23941

Surveying in Antarctica during the International Geophysical Year p 25 N84-23942

The Dufek intrusion of Antarctica and a survey of its minor metals related to possible resources p 25 N84-23943

Program for mapping Antarctica p 19 N84-23954

The use of satellite technology in the search for meteorites in Antarctica aut 01Meunier, Tony K. p 26 N84-23955

Glaciological and geological studies of Antarctica with satellite remote sensing technology p 38 N84-23956

Modeling the movement at the polar ice cap at the South Pole p 20 N84-23957

Emerging recognition of the nonfuel mineral resources of Arctic Alaska p 26 N84-23962

Hydrology of the North Slope, Alaska p 53 N84-23973

Georgia Univ., Athens.

Cartographic accuracy of Landsat-4 MSS and TM image data p 57 N84-33535

Comparative assessment of LANDSAT-D MSS and TM data quality for mapping applications in the Southeast [E84-10138] p 61 N84-26086

Guelph Univ. (Ontario).

Improving crop classification through attention to the timing of airborne radar acquisitions p 8 N84-39000

H

Hampton Inst., Va.

Sensitivity of airborne fluorosensor measurements to linear vertical gradients in chlorophyll concentration p 30 N84-30302

Harvard Univ., Cambridge, Mass.

Simulation and assimilation of satellite altimeter data at the oceanic mesoscale p 48 N84-27312

Hawaii Univ., Honolulu.

First estimate of annual mercury flux at the Kilauea main vent p 15 N84-34794

Hofstra Univ., Hempstead, N. Y.

Two-frequency microwave resonance measurements from an aircraft - A quantitative estimate of the directional ocean surface spectrum p 34 N84-34942

Hunter Coll., New York.

Spatial inventory integrating raster databases and point sample data p 4 N84-33340

Institut d'Aeronomie Spatiale de Belgique, Brussels.

A sample performance of the grille spectrometer aboard Spacelab [AERONOMICA-ACTA-A-281-1984] p 70 N84-26003

Institut de Physique du Globe, Paris (France).

Somali current studied from SEASAT altimetry p 47 N84-27307

Institut fuer Angewandte Geodaezie, Frankfurt am Main (West Germany).

Investigation of the combination of geodetic point aggregations [SER-C-285] p 21 N84-28199

Institut Geographique National, Paris (France).

Research on land use cartography by remote sensing p 17 N84-28201

Remote sensing of the Santonge littoral. Processing and interpretation of satellite images [ISBN-2-85929-016-8] p 63 N84-28202

Institute for Atmosphere Optics and Remote Sensing, Hampton, Va.

SAGE and SAM II measurements of global stratospheric aerosol optical depth and mass loading p 15 N84-39455

Institute for Image Processing Computer Mapping, Graz (Austria).

Experiments to correct a digital map data base using scene analysis [AD-A139447] p 61 N84-24499

Institute of Oceanographic Sciences, Birkenhead (England).

Publications and reports of the Institute of Oceanographic Sciences 1979-1982 [IOS-170] p 50 N84-28354

Instituto de Pesquisas Espaciais, Sao Jose dos Campos (Brazil).

Utilization of digital LANDSAT imagery for the study of granitoid bodies in Rondonia: Case example of the Pedra Branca massif [E84-10120] p 26 N84-23979

Evaluation of the effects of the seasonal variation of solar elevation angle and azimuth on the processes of digital filtering and thematic classification of relief units [E84-10121] p 60 N84-23980

Orbital imagery: A cartographic solution [INPE-2820-PRE/374] p 20 N84-25143

Irrigated rice area estimation using remote sensing techniques: Project's proposal and preliminary results [E84-10131] p 10 N84-26061

Principal components technique analysis for vegetation and land use discrimination [E84-10135] p 10 N84-26083

Sampling system for wheat (Triticum aestivum) L area estimation using digital LANDSAT MSS data and aerial photographs [E84-10139] p 10 N84-26087

Evaluation of solar angle variation over digital processing of LANDSAT imagery [E84-10140] p 61 N84-26088

Evaluation of entropy and JM-distance criterions as features selection methods using spectral and spatial features derived from LANDSAT images [E84-10141] p 62 N84-26089

Application of LANDSAT data to the study of urban development in Brasilia p 16 N84-26090

An integrated software system for geometric correction of LANDSAT MSS imagery [E84-10143] p 62 N84-26091

Forest inventory using multistage sampling with probability proportional to size [E84-10144] p 11 N84-26092

Multiseasonal variables in digital image enhancements for geological applications [E84-10145] p 29 N84-26093

Field data observed during the geological excursion in the west-central region of the Sul-Riogrande Shield [E84-10146] p 29 N84-26094

The use of an image registration technique in the urban growth monitoring [E84-10147] p 16 N84-26095

Evaluation of SIR-A (Shuttle Imaging Radar) images from the Tres Marias region (Minas Gerais State, Brazil) using derived spatial features and registration with MSS-LANDSAT images [E84-10148] p 62 N84-26096

Results of field observations of radio waves in alluvial deposits in Cara state from 1:100,000: Fortaleza, Caninde, Taperuaba, Santa Quiteria, Sobral, and Sao Luiz do Curu [INPE-3061-NTE/216] p 53 N84-26100

CORPORATE SOURCE

Methodological approach in lithological discrimination by digital processing: A case study in the Serra do Ramalho, state of Bahia
[INPE-3108-PRE/507] p 29 N84-26101

Seasonal oscillations of the subtropical convergence between the Brazil and Malvinas currents, using oceanographic and SMS-2 satellite data
[INPE-3092-PRE/497] p 40 N84-26255

Maps of favorable areas for tuna fishing to the South and Southeast of Brazil prepared from SMS-2 satellite data
[INPE-3102-PRE/501] p 41 N84-26256

The use of photointerpretation for socio-economic characterization of urban population
[INPE-3067-PRE/484] p 16 N84-26428

Identification and estimation of the area planted with irrigated rice based on the visual interpretation of LANDSAT MSS data
[E84-10164] p 12 N84-27256

A sampling system for estimating the cultivation of wheat (Triticum aestivum L) from LANDSAT data
[E84-10165] p 12 N84-27257

Project SERGE: Brazil referential field data for the SIR-A experiment
[INPE-2973-NTE/210] p 29 N84-27259

A report of Ceara Project activities
[INPE-2988-RPE/452] p 54 N84-27260

Research and applications of data from environmental satellites: Determining parameters and developing interpretation techniques for applications of environmental satellite data
[INPE-3005-NTE/213] p 13 N84-27261

Intergovernmental Oceanographic Commission, Paris (France).

Integrated Global Ocean Services System (IGOSS): Guide to the IGOSS data processing and services system
[WMO-623] p 38 N84-23089

International Inst. for Aerial Survey and Earth Sciences, Enschede (Netherlands).

Several aspects of the sequential processing of photogrammetric bundle blocks
[E84-10112] p 21 N84-26077

Iowa State Univ. of Science and Technology, Ames.

Use of transformed LANDSAT data in regression estimation of crop acreages
[E84-10112] p 11 N84-27246

Iowa Univ., Iowa City.

Use of MAGSAT anomaly data for crustal structure and mineral resources in the US midcontinent
[E84-10112] p 24 N84-23005

J

Jet Propulsion Lab., California Inst. of Tech., Pasadena.

Digital SAR processing using a fast polynomial transform
[AD-A137993] p 55 N84-32093

Spatial inventory integrating raster databases and point sample data
[AD-A137993] p 4 N84-3340

An analysis of Landsat-4 Thematic Mapper geometric properties
[AD-A137993] p 57 N84-33536

Large-scale analysis and forecast experiments with wind data from the Seasat A scatterometer
[AD-A137993] p 66 N84-37873

Spaceborne radar subsurface imaging in hyperarid regions
[AD-A137993] p 24 N84-39379

The Pennsylvania defoliation application pilot test
[E84-10111] p 8 N84-23004

Topex: Observing the oceans from Space
[NASA-CR-173490] p 38 N84-23085

NASA Oceanic Processes Program, fiscal year 1983
[NASA-TM-86248] p 39 N84-24078

Publications of the Jet Propulsion Laboratory 1982
[NASA-CR-173539] p 71 N84-25510

The use of satellite observations of the ocean surface in commercial fishing operations
[AD-P003120] p 41 N84-26261

A new parameterization of an empirical model for wind/ocean scatterometry
[NASA-CR-173490] p 43 N84-27269

Satellite remote sensing over ice
[NASA-CR-173490] p 48 N84-27308

Observing ocean-atmosphere exchanges with space-borne sensors, appendix C
[NASA-CR-173490] p 50 N84-28298

Satellite-Derived Sea Surface Temperature: Workshop-2
[NASA-CR-173740] p 50 N84-28355

Johns Hopkins Univ., Baltimore, Md.

On the response to ocean surface currents in synthetic aperture radar imagery
[NASA-CR-175245] p 47 N84-27304

Petrologic and geophysical sources of long-wavelength crustal magnetic anomalies
[NASA-CR-175245] p 29 N84-28276

Joint Publications Research Service, Arlington, Va.

Speckle statistics in radar images of sea surface obtained with horizontal polarization
[NASA-CR-175245] p 50 N84-27921

NASA. Lyndon B. Johnson Space Center, Houston, Tex.

K

Kansas Univ. Center for Research, Inc., Lawrence.

A scatter model for vegetation up to Ku-band
[NASA-SP-4208] p 7 A84-37201

Improving crop classification through attention to the timing of airborne radar acquisitions
[INPE-3092-PRE/497] p 8 A84-39000

Marginal ice zone experiment (1983), Part 1: Ice characterization measurements. Part 2. Helicopter-borne and ship-based radar backscatter measurement of sea ice in the marginal ice zone
[AD-A139894] p 40 N84-25238

L

Lockheed Engineering and Management Services Co., Inc., Houston, Tex.

Automated vegetation classification using Thematic Mapper Simulation data
[NASA-EP-182] p 5 A84-33347

Evaluation of corn/soybeans separability using Thematic Mapper and Thematic Mapper Simulator data
[E84-10164] p 5 A84-33539

Ludwig-Maximilians-Universitaet, Munich (West Germany).

Accuracy and precision of the nitric acid concentrations determined by the limb infrared monitor of the stratosphere experiment on NIMBUS 7
[NASA-SP-4208] p 67 A84-39444

M

Maine Univ., Orono.

Classifying northern forests using Thematic Mapper Simulator data
[NASA-SP-4208] p 7 A84-34961

Maryland Univ., College Park.

Atmospheric effect on classification of finite fields
[NASA-SP-4208] p 2 A84-30670

A statistical evaluation of the advantages of Landsat Thematic Mapper data in comparison to Multispectral Scanner data
[NASA-SP-4208] p 57 A84-33537

Classifying northern forests using Thematic Mapper Simulator data
[NASA-SP-4208] p 7 A84-34961

Reduction of satellite magnetic anomaly data
[NASA-SP-4208] p 19 A84-38812

Massachusetts Inst. of Tech., Cambridge.

Monthly distributions of precipitable water from the Nimbus 7 SMMR data
[NASA-SP-4208] p 37 A84-39458

A summary of results from the first Nimbus 7 SMMR observations
[NASA-SP-4208] p 37 A84-39459

Massachusetts Univ., Amherst.

Microwave remote sensing of ocean surface wind speed and rain rates over tropical storms
[NASA-SP-4208] p 45 N84-27288

Mathematical Geosciences, Inc., Lexington, Mass.

Geodetic use of GEOSAT-A
[AD-A137993] p 19 N84-23048

Max-Planck-Institut fuer Meteorologie, Hamburg (West Germany).

On the detection of underwater bottom topography by imaging radars
[NASA-SP-4208] p 46 N84-27301

McQuest Marine Research and Development Co. Ltd., Burlington (Ontario).

Application of computer image processing to underwater surveys
[AD-P003122] p 41 N84-26263

Miami Univ., Fla.

Rapid evolution of a Gulf Stream warm-core ring
[NASA-SP-4208] p 32 A84-34164

Michigan State Univ., East Lansing.

Use of remote sensing for land use policy formulation
[E84-10117] p 9 N84-23977

Aerial photography for ecological site mapping
[E84-10117] p 9 N84-23990

Mississippi State Univ., Mississippi State.

Application of remote sensing to state and regional problems
[E84-10128] p 68 N84-23986

Missouri Univ., Columbia.

Contextual classification of remotely sensed data
[NASA-SP-4208] p 63 N84-27245

N

National Academy of Sciences - National Research Council, Washington, D. C.

Proceedings of a workshop: Multidisciplinary Use of the Very Long Baseline Array
[NASA-CR-173541] p 69 N84-25034

National Aeronautics and Space Administration, Washington, D. C.

Discussion of the design of satellite-laser measurement stations in the eastern Mediterranean under the geological aspect. Contribution to the earthquake prediction research by the Wegener Group and to NASA's Crustal Dynamics Project
[NASA-TM-77412] p 26 N84-24031

Living and working in space. A history of Skylab
[NASA-SP-4208] p 72 N84-25737

NASA, the first 25 years: 1958 - 1983
[NASA-EP-182] p 72 N84-26563

National Aeronautics and Space Administration, Ames Research Center, Moffett Field, Calif.

Thematic Mapper image quality - Registration, noise, and resolution
[NASA-SP-4208] p 57 A84-33533

National Aeronautics and Space Administration.

Goddard Inst. for Space Studies, New York.

Integration of Landsat data into the Saginaw River Basin geographic information system
[NASA-SP-4208] p 51 A84-33339

Vegetation, land-use and seasonal albedo data sets: Documentation of archived data tape
[E84-10133] p 10 N84-25142

National Aeronautics and Space Administration.

Goddard Space Flight Center, Greenbelt, Md.

Atmospheric effect on classification of finite fields
[NASA-SP-4208] p 2 A84-30670

Calculations of radar backscattering coefficient of vegetation-covered soils
[NASA-SP-4208] p 2 A84-30671

Active microwave responses - An aid in improved crop classification
[NASA-SP-4208] p 3 A84-31498

Aircraft scatterometer observations of soil moisture on rangeland watersheds
[NASA-SP-4208] p 4 A84-33338

Comparative accuracies of AVHRR and MSS data used for Level I land cover classifications
[NASA-SP-4208] p 14 A84-33344

A statistical evaluation of the advantages of Landsat Thematic Mapper data in comparison to Multispectral Scanner data
[NASA-SP-4208] p 57 A84-33537

Seasat observations of lithospheric flexure seaward of trenches
[NASA-SP-4208] p 32 A84-34339

Albedo of a forest modeled as a plane with dense protrusions
[NASA-SP-4208] p 6 A84-34385

Observations of Gulf Stream-induced and wind-driven upwelling in the Georgia Bight using ocean color and infrared imagery
[NASA-SP-4208] p 34 A84-34517

Potential benefits of new satellite sensors to wetland mapping
[NASA-SP-4208] p 7 A84-34960

Classifying northern forests using Thematic Mapper Simulator data
[NASA-SP-4208] p 7 A84-34961

Determining forest canopy characteristics using airborne laser data
[NASA-SP-4208] p 7 A84-37202

Intensive forest clearing in Rondonia, Brazil, as detected by satellite remote sensing
[NASA-SP-4208] p 8 A84-37204

Large-scale analysis and forecast experiments with wind data from the Seasat A scatterometer
[NASA-SP-4208] p 66 A84-37873

Intercomparison of the Nimbus 7 SBUV/TOMS total ozone data sets with Dobson and M83 results
[NASA-SP-4208] p 67 A84-39449

Monthly distributions of precipitable water from the Nimbus 7 SMMR data
[NASA-SP-4208] p 37 A84-39458

A summary of results from the first Nimbus 7 SMMR observations
[NASA-SP-4208] p 37 A84-39459

Determination of sea ice parameters with the Nimbus 7 SMMR
[NASA-SP-4208] p 37 A84-39461

A comparison of numerical results of Arctic Sea ice modeling with satellite images
[NASA-SP-4208] p 39 N84-23969

Arctic Sea ice by passive microwave observations from the Nimbus-5 Satellite
[NASA-SP-4208] p 39 N84-23970

Nimbus 7 SMMR derived seasonal variations in the water vapor, liquid water and surface winds over the global oceans
[NASA-TM-86080] p 40 N84-26233

Technical publications of the NASA Wallops Flight Facility, 1980 through 1983
[NASA-TM-84421] p 72 N84-26467

Heat Capacity Mapping Radiometer (HCMR) data processing algorithm, calibration, and flight performance evaluation
[E84-10153] p 71 N84-27248

High resolution observations of low contrast phenomena from an Advanced Geosynchronous Platform (AGP)
[NASA-TM-83916] p 42 N84-27266

Remote sensing of air-sea interactions
[NASA-TM-83916] p 42 N84-27267

Some case studies of ocean wave physical processes utilizing the GSFC airborne radar ocean wave spectrometer
[NASA-TM-83916] p 45 N84-27283

Non-Gaussian statistical models of surface wave fields for remote sensing applications
[NASA-TM-83916] p 45 N84-27284

Altimeter height measurement errors introduced by the presence of variable cloud and rain attenuation
[NASA-TM-83916] p 45 N84-27289

The impact of scatterometer wind data on global weather forecasting
[NASA-TM-83916] p 49 N84-27314

Matrix partitioning and EOF/principal component analysis of Antarctic Sea ice brightness temperatures
[NASA-TM-83916] p 49 N84-27319

National Aeronautics and Space Administration.

Lyndon B. Johnson Space Center, Houston, Tex.

Automated vegetation classification using Thematic Mapper Simulation data
[NASA-SP-4208] p 5 A84-33347

Evaluation of corn/soybeans separability using Thematic Mapper and Thematic Mapper Simulator data

p 5 A84-33539

Evaluation of Thematic Mapper for detecting soil properties under grassland vegetation p 6 A84-33540

National Aeronautics and Space Administration.

Langley Research Center, Hampton, Va.

Sensitivity of airborne fluorosensor measurements to linear vertical gradients in chlorophyll concentration

p 30 A84-30302

A rapid method for obtaining frequency-response functions for multiple input photogrammetric data

[AIAA PAPER 84-1060] p 65 A84-31741

Comparison of longwave diurnal models applied to simulations of the Earth Radiation Budget Experiment

p 65 A84-31947

Two-frequency microwave resonance measurements from an aircraft - A quantitative estimate of the directional ocean surface spectrum p 34 A84-34942

The Limb Infrared Monitor of the Stratosphere - Experiment description, performance, and results

p 66 A84-39440

The validation of Nimbus 7 LIMS measurements of ozone

p 67 A84-39443

Accuracy and precision of the nitric acid concentrations determined by the limb infrared monitor of the stratosphere experiment on NIMBUS 7 p 67 A84-39444

SAGE and SAM II measurements of global stratospheric aerosol optical depth and mass loading

p 15 A84-39455

A comparative study of aerosol extinction measurements made by the SAM II and SAGE satellite experiments

p 15 A84-39457

Effect of space exposure on pyroelectric infrared detectors (A0135) p 68 A84-24679

Measurements of ocean wave spectra and modulation transfer function with the airborne two frequency scatterometer p 45 A84-27282

National Aeronautics and Space Administration.

Marshall Space Flight Center, Huntsville, Ala.

Frontiers of Remote Sensing of the Oceans and Troposphere from Air and Space Platforms

[NASA-CP-2303] p 42 A84-27262

National Aeronautics and Space Administration.

Wallop Flight Center, Wallop Island, Va.

Dynamics of the slope water off New England and its influence on the Gulf Stream as inferred from satellite IR data

p 31 A84-30672

Determining forest canopy characteristics using airborne laser data p 7 A84-37202

Airborne laser topographic mapping results

p 8 A84-38998

National Center for Atmospheric Research, Boulder, Colo.

The Limb Infrared Monitor of the Stratosphere - Experiment description, performance, and results

p 66 A84-39440

The validation of Nimbus 7 LIMS measurements of ozone

p 67 A84-39443

Accuracy and precision of the nitric acid concentrations determined by the limb infrared monitor of the stratosphere experiment on NIMBUS 7 p 67 A84-39444

Applications of airborne remote sensing in atmospheric sciences research p 71 A84-27286

National Commission on Libraries and Information

Science, Washington, D. C.

Preserve the sense of Earth from space

[DE84-900854] p 71 A84-25159

National Environmental Satellite Service, Washington, D. C.

Fire detection using the NOAA (National Oceanic and Atmospheric Administration)-series satellites

[PB84-176890] p 13 A84-27324

National Marine Fisheries Service, La Jolla, Calif.

Satellite observations of the 1982-1983 El Nino along the U.S. Pacific coast

p 35 A84-36872

National Marine Fisheries Service, Woods Hole, Mass.

Rapid evolution of a Gulf Stream warm-core ring

p 32 A84-34164

National Oceanic and Atmospheric Administration, Boulder, Colo.

SAR imagery of ocean-wave swell traveling in an arbitrary direction p 44 A84-27278

National Oceanic and Atmospheric Administration,

Miami, Fla.

A summary of results from the first Nimbus 7 SMMR observations p 37 A84-39459

National Oceanic and Atmospheric Administration,

Seattle, Wash.

The variability of the surface wind field in the equatorial Pacific Ocean: Criteria for satellite measurements p 46 A84-27296

National Oceanic and Atmospheric Administration,

Washington, D. C.

The validation of Nimbus 7 LIMS measurements of ozone

p 67 A84-39443

Recent advances in multispectral sensing of ocean surface temperature from space p 46 N84-27297

Naval Ocean Research and Development Activity, Bay St. Louis, Miss.

Analysis of airborne electromagnetic systems for mapping thickness of sea ice

[AD-A139786] p 39 N84-25235

PAME Proceedings, Pattern Analysis in the Marine Environment, An Ocean Science and Technology Workshop

[AD-A140195] p 41 N84-26257

Principal components as a method for atmospherically correcting coastal zone color scanner data

[AD-P003124] p 41 N84-26265

The satellite altimeter as a platform for observation of the oceanic mesoscale p 46 N84-27299

The depiction of Alboran Sea Gyre during Donde Va? using remote sensing and conventional data

p 47 N84-27306

The importance of altimeter and scatterometer data for ocean prediction p 49 N84-27316

Sampling strategies and four-dimensional assimilation of altimetric data for ocean monitoring and prediction

p 49 N84-27317

The influence of actual and apparent geoid error on ocean analysis and prediction p 49 N84-27318

Ocean optical remote sensing capability statement

[AD-A140589] p 49 N84-27321

Microwave radiometric measurement of sea surface salinity

[AD-A141302] p 50 N84-28359

Naval Oceanographic Office, Bay St. Louis, Miss.

Water mass classification in the North Atlantic using IR digital data and Bayesian decision theory

[AD-P003125] p 41 N84-26266

Naval Research Lab., Washington, D. C.

The dual-frequency scatterometer reexamined

p 44 N84-27280

An improved dual-frequency technique for the remote sensing of ocean currents and wave spectra

p 44 N84-27281

Nebraska Univ., Lincoln.

Optimum backscatter cross section of the ocean as measured by synthetic aperture radars

p 44 N84-27276

New York State Univ., Binghamton.

Inversion of vegetation canopy reflectance models for estimating agronomic variables. III - Estimation using only canopy reflectance data as illustrated by the suits model.

IV - Total inversion of the SAIL model p 7 A84-37203

North Carolina State Univ., Raleigh.

Observations of Gulf Stream-induced and wind-driven upwelling in the Georgia Bight using ocean color and infrared imagery p 34 A84-34517

Nova Univ., Dania, Fla.

Rapid evolution of a Gulf Stream warm-core ring

p 32 A84-34164

O

Office National d'Etudes et de Recherches

Aerospatiales, Leclerc (France).

Accuracy and precision of the nitric acid concentrations determined by the limb infrared monitor of the stratosphere experiment on NIMBUS 7 p 67 A84-39444

Office National d'Etudes et de Recherches

Aerospatiales, Toulouse (France).

In-flight absolute radiometric calibration of the Thematic Mapper

p 56 A84-33531

Ohio State Univ., Columbus.

Do satellite magnetic anomaly data accurately portray the crustal component? p 28 N84-25134

Long-wavelength magnetic and gravity anomaly correlations of Africa and Europe p 28 N84-25135

US aeromagnetic and satellite magnetic anomaly comparisons

p 28 N84-25136

P

Pittsburgh Univ., Pa.

Application of Magsat lithospheric modeling in South America. Part 1: Processing and interpretation of magnetic and gravity anomaly data

[E84-10115] p 24 N84-23008

Application of MAGSAT to lithospheric modeling in South America. Part 2: Synthesis of geologic and seismic data for development of integrated crustal models

[E84-10126] p 26 N84-25128

Correlation of tectonic provinces of South America and the Caribbean region with MAGSAT anomalies

p 27 N84-25130

Relation of MAGSAT anomalies to the main tectonic provinces of South America

p 28 N84-25137

Science Applications, Inc., San Diego, Calif.

AVHRR aerosol ground truth experiment

[PB84-157882] p 39 N84-24065

Science Research Council, Chilton (England).

The validation of Nimbus 7 LIMS measurements of ozone

p 67 A84-39443

Accuracy and precision of the nitric acid concentrations determined by the limb infrared monitor of the stratosphere experiment on NIMBUS 7 p 67 A84-39444

Radar altimetry over sea ice p 48 N84-27309

Skidaway Inst. of Oceanography, Savannah, Ga.

Observations of Gulf Stream-induced and wind-driven upwelling in the Georgia Bight using ocean color and infrared imagery

p 34 A84-34517

R

Remote Sensing Systems, Sausalito, Calif.

A model function for ocean radar cross sections at 14.6 GHz

p 34 A84-34516

New algorithms for microwave measurements of ocean winds

p 43 N84-27272

Research Inst. of National Defence, Linkoeping (Sweden).

Contour-to-grid transformation: Development of a method for generation of a sparse grid structure out of terrain elevation contours

[FOA-C-30349-E1] p 16 N84-25156

Research Inst. of National Defence, Stockholm (Sweden).

A computer program for mapping regions in a geographic data base with raster structure

[FOA-C-20529-D8] p 16 N84-25340

Rochester Inst. of Tech., N. Y.

LANDSAT 4 band 6 data evaluation

[E84-10119] p 60 N84-23009

Royal Australian Navy Research Lab., Edgecliff.

Comparisons of sea-surface temperature obtained from ship and satellite data

[AD-A138257] p 38 N84-23087

Royal Inst. of Tech., Stockholm (Sweden).

Photogrammetric research

[TRITA-FMI-47] p 69 N84-25146

Photogrammetric research at the Royal Institute of Technology, Stockholm, Sweden p 69 N84-25147

Mathematical aspects of digital terrain information. A progress report from ISPRS Working Group III:3

p 61 N84-25148

Correlating aerial photographs to LANDSAT Multispectral Sensor (MSS) data to measure ground control points

p 69 N84-25150

General triangulation: Incorporating photogrammetric and other observations

p 69 N84-25151

GENTRI: A system for simultaneous adjustment of photogrammetric and other observations

p 69 N84-25152

The question of accuracy in the transition from analogue to analytic photogrammetry

p 69 N84-25153

Multi-models to increase accuracy

p 70 N84-25154

Royal Norwegian Council for Scientific and Industrial Research, Kjeller.

Ocean waves and turbulence as observed with an adaptive coherent multifrequency radar

p 44 N84-27279

S

Science Applications, Inc., San Diego, Calif.

AVHRR aerosol ground truth experiment

[PB84-157882] p 39 N84-24065

Science Research Council, Chilton (England).

The validation of Nimbus 7 LIMS measurements of ozone

p 67 A84-39443

Accuracy and precision of the nitric acid concentrations determined by the limb infrared monitor of the stratosphere experiment on NIMBUS 7 p 67 A84-39444

Radar altimetry over sea ice p 48 N84-27309

Skidaway Inst. of Oceanography, Savannah, Ga.

Observations of Gulf Stream-induced and wind-driven upwelling in the Georgia Bight using ocean color and infrared imagery

p 34 A84-34517

Societe d'Etudes Techniques et d'Entreprises Generales, Leplessis-Robinson (France).
Comparative study of image data produced by satellites with different characteristics
[ESA-CR(P)-1867] p 62 N84-26103

SOHIO Petroleum Co., Cleveland, Ohio.
Satellite elevation magnetic and gravity models of major South American plate tectonic features
p 27 N84-25131

SRI International Corp., Menlo Park, Calif.
Propagation effects in satellite-based synthetic aperture radars
[AD-A138681] p 67 N84-22873

Stanford Univ., Calif.
Synthetic aperture radar images of ocean waves, theories of imaging physics and experimental tests
p 43 N84-27275

State Univ. of New York, Albany.
Cenozoic tectonics of the Caribbean: Structural and stratigraphic studies in Jamaica and Hispaniola
p 25 N84-23062

Stuttgart Univ. (West Germany).
Mathematical models of photogrammetric point determination
p 20 N84-26070
Stochastic models for point manifolds
p 20 N84-26072

Systems and Applied Sciences Corp., Hampton, Va.
The validation of Nimbus 7 LIMS measurements of ozone
p 67 A84-39443

Accuracy and precision of the nitric acid concentrations determined by the limb infrared monitor of the stratosphere experiment on NIMBUS 7 p 67 A84-39444

Systems and Applied Sciences Corp., Hyattsville, Md.
Intercomparison of the Nimbus 7 SBUV/TOMS total ozone data sets with Dobson and M83 results
p 67 A84-39449

Monthly distributions of precipitable water from the Nimbus 7 SMMR data p 37 A84-39458

T

Technicolor Government Services, Inc., Moffett Field, Calif.
Thematic Mapper image quality - Registration, noise, and resolution p 57 A84-33533

Land cover and terrain mapping for the development of digital data bases for wildlife habitat assessment in the Yukon Flats National Wildlife Refuge, Alaska
p 9 N84-23971

Technische Univ., Hanover (West Germany).
Detection of errors in the functional adjustment model
p 20 N84-26074

Tel-Aviv Univ. (Israel).
Albedo of a forest modeled as a plane with dense protrusions p 6 A84-34385
Coastal bathymetry and currents from LANDSAT data p 47 N84-27303

Texas A&M Univ., Kingsville.
Vegetation monitoring and classification using NOAA/AVHRR satellite data p 4 A84-33343

Texas A&M Univ., College Station.
Active microwave responses - An aid in improved crop classification p 3 A84-31498

Rapid evolution of a Gulf Stream warm-core ring p 32 A84-34164
CONSERVB: A numerical method to compute soil water content and temperature profiles under a bare surface [E84-10113] p 9 N84-23006

A microwave systems approach to measuring root zone soil moisture [E84-10114] p 9 N84-23007
Area estimation using multiyear designs and partial crop identification [E84-10151] p 11 N84-26099

Crop moisture estimation over the southern Great Plains with dual polarization 1.66 centimeter passive microwave data from Nimbus 7 [E84-10163] p 12 N84-27255

Texas Univ., El Paso.
Application of Magsat lithospheric modeling in South America, Part 1: Processing and interpretation of magnetic and gravity anomaly data [E84-10115] p 24 N84-23008

Application of MAGSAT to lithospheric modeling in South America. Part 2: Synthesis of geologic and seismic data for development of integrated crustal models [E84-10126] p 26 N84-25128

A crustal structure study of South America p 29 N84-25139

U

Universite Catholique de Louvain (Belgium).
A tentative unified sea model for scattering and emission p 45 N84-27285

University Coll., Dorking (England).
Observations of sea ice and icebergs from satellite radar altimeters p 48 N84-27311

University of Southern California, Los Angeles.
Digital SAR processing using a fast polynomial transform p 55 A84-32093

Utah Univ., Salt Lake City.
Riparian habitat on the Humboldt River, Deeth to Elko, Nevada [E84-10116] p 53 N84-23976

Enviropod handbook: A guide to preparation and use of the Environmental Protection Agency's light-weight aerial camera system [E84-10123] p 68 N84-23982

EPA Enviropod. A summary of the use of the Enviropod under a Memorandum of Understanding among EPA Region 8, the State of Utah, and the University of Utah Research Institute [E84-10124] p 15 N84-23983

Identifying environmental features for land management decisions [E84-10125] p 15 N84-23984

V

Virginia Univ., Charlottesville.
Satellite observations of a monsoon depression [NASA-CR-173590] p 40 N84-26232

W

Washington Univ., Seattle.
A summary of results from the first Nimbus 7 SMMR observations p 37 A84-39459

Remote sensing of floe size distribution and surface topography [E84-10132] p 39 N84-25141
Scatterometer capabilities in remotely sensing geophysical parameters over the ocean: The status and the possibilities p 42 N84-27268

Wisconsin Univ., Milwaukee.
Diagnostics of rainfall anomalies in the Nordeste during the global weather experiment [SAPR-1] p 40 N84-26235

Woods Hole Oceanographic Institution, Mass.
Rapid evolution of a Gulf Stream warm-core ring p 32 A84-34164

World Meteorological Organization, Geneva (Switzerland).
Integrated Global Ocean Services System (IGOSS): Guide to the IGOSS data processing and services system [WMO-623] p 38 N84-23089

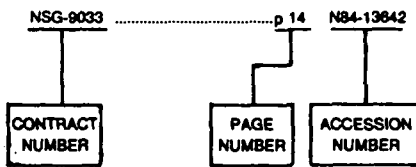
Guide to hydrological practices. Volume 2: Analysis, forecasting and other applications [WMO-168] p 53 N84-25145

CONTRACT NUMBER INDEX

EARTH RESOURCES / A Continuing Bibliography (Issue 43)

OCTOBER 1984

Typical Contract Number Index Listing



Listings in this Index are arranged alphanumerically by contract number. Under each contract number, the accession numbers denoting documents that have been produced as a result of research done under that contract are arranged in ascending order with the AIAA accession numbers appearing first. The accession number denotes the number by which the citation is identified in the abstract section. Preceding the accession number is the page number on which the citation may be found.

| | | | | | | | |
|--------------------------------|------|-----------|-------|-----------|-----------------------------|-------|-----------|
| AF PROJ. 2310 | p 54 | N84-28344 | p 67 | A84-39444 | N00014-83-C-0520 | p 43 | N84-27272 |
| AF PROJ. 3201 | p 19 | N84-23048 | p 44 | N84-27278 | N00014-83-K-0256 | p 33 | A84-34502 |
| AF PROJ. 7601 | p 70 | N84-26217 | p 35 | A84-36872 | | p 33 | A84-34503 |
| AF-AFOSR-80-0151 | p 55 | A84-32093 | p 66 | A84-39440 | N00039-80-C-0641 | p 55 | A84-32093 |
| BMFT-MF-0235 | p 35 | A84-36119 | p 67 | A84-39444 | PROJ. AGRISTARS | p 9 | N84-23006 |
| DA PROJ. IT1-61102-BH-57 | p 61 | N84-24499 | p 34 | A84-34517 | | p 9 | N84-23007 |
| DA PROJ. 4A1-62707-A-855 | p 11 | N84-26107 | p 26 | N84-24031 | STU-83-3307 | p 16 | N84-25156 |
| DAAG29-83-K-0123 | p 44 | N84-27276 | p 34 | A84-34516 | S99-QAXH | p 67 | N84-22873 |
| DAAK70-79-C-0153 | p 11 | N84-26107 | p 43 | N84-27272 | USDA-12-14-5001-38 | p 56 | A84-33531 |
| DAJA45-83-C-0022 | p 61 | N84-24499 | p 15 | A84-39457 | USGS-14-08-0001-20585 | p 24 | A84-36922 |
| DE-AS05-76EV-05163 | p 34 | A84-34517 | p 53 | N84-27258 | 677-00-00-03-89 | p 8 | N84-23004 |
| DE-AS09-76EV-00889 | p 34 | A84-34517 | | | | | |
| DE-AS09-76EV-00901 | p 34 | A84-34517 | | | | | |
| DE-AS09-76EV-00936 | p 34 | A84-34517 | | | | | |
| DE-AS09-76EY-00902 | p 34 | A84-34517 | | | | | |
| DE-OAJ82-00135 | p 34 | A84-34516 | | | | | |
| DEMR-OSQ-80-00169 | p 55 | A84-33335 | | | | | |
| DMA800-78-C-0060 | p 47 | N84-27302 | | | | | |
| DNA001-81-C-0010 | p 67 | N84-22873 | | | | | |
| DSS-08SU-01525-7-0198 | p 8 | A84-39000 | | | | | |
| ESA-4524/81-DJS(SC) | p 62 | N84-26103 | | | | | |
| ESTEC-4868/81/NL-HP(SC) | p 70 | N84-26237 | | | | | |
| ESTEC-4868/81/NL/HP(SC) | p 70 | N84-26238 | | | | | |
| F19628-81-K-0003 | p 70 | N84-26217 | | | | | |
| F19628-82-K-0144 | p 19 | N84-23048 | | | | | |
| F19628-83-C-0027 | p 54 | N84-28344 | | | | | |
| MDA903-83-M-5896 | p 69 | N84-25034 | | | | | |
| NAGW-266 | p 68 | N84-23987 | | | | | |
| NAGW-304 | p 48 | N84-27313 | | | | | |
| NAGW-468 | p 47 | N84-27304 | | | | | |
| NAGW-95 | p 45 | N84-27282 | | | | | |
| NAG05-11 | p 53 | N84-23976 | | | | | |
| NAG5-160 | p 68 | N84-23982 | | | | | |
| NAG5-268 | p 15 | N84-23984 | | | | | |
| NAG5-297 | p 22 | N84-28279 | | | | | |
| NAG5-31 | p 39 | N84-25141 | | | | | |
| NAG5-35 | p 7 | A84-37201 | | | | | |
| NASA ORDER L-36446-A | p 40 | N84-26232 | | | | | |
| NASA ORDER L-86651-A | p 9 | N84-23006 | | | | | |
| NASA ORDER L-9469-B | p 9 | N84-23007 | | | | | |
| NASA ORDER S-10757-C | p 29 | N84-28276 | | | | | |
| NASA ORDER S-10772-C | p 66 | A84-39440 | | | | | |
| NASA ORDER S-70994-A | p 67 | A84-39444 | | | | | |
| NASA ORDER L-86651-A | p 66 | A84-39440 | | | | | |
| NASA ORDER L-9469-B | p 67 | A84-39444 | | | | | |
| NASA ORDER S-10757-C | p 66 | A84-39444 | | | | | |
| NASA ORDER S-10772-C | p 63 | N84-27247 | | | | | |
| NASA ORDER S-70994-A | p 57 | A84-33534 | | | | | |
| NASA ORDER S-70994-A | p 66 | A84-39440 | | | | | |

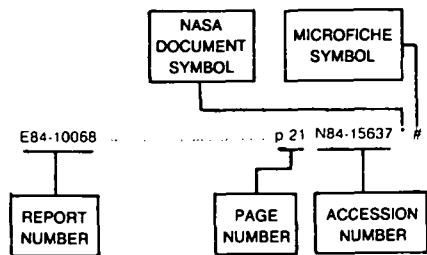
C
O
N
T
R
A
C
T

REPORT/ACCESSION NUMBER INDEX

EARTH RESOURCES / A Continuing Bibliography (Issue 43)

OCTOBER 1984

Typical Report/Accession Number Index Listing



Listings in this index are arranged alphanumerically by report number. The page number indicates the page on which the citation is located. The accession number denotes the number by which the citation is identified. An asterisk (*) indicates that the item is a NASA report. A pound sign (#) indicates that the item is available on microfiche.

| | | | | | | | |
|----------------------------|------|-----------|---|-------------------|------|-----------|---|
| DE84-900854 | p 71 | N84-25159 | # | INPE-2820-PRE/374 | p 20 | N84-25143 | # |
| DFVLR-FB-82-14 | p 37 | N84-22955 | # | INPE-2858-PRE/440 | p 60 | N84-23980 | * |
| DFVLR-FB-82-30 | p 16 | N84-26104 | # | INPE-2941-TDL/150 | p 12 | N84-27257 | # |
| DFVLR-FB-82-31 | p 63 | N84-26105 | # | INPE-2973-NTE/210 | p 29 | N84-27259 | # |
| DFVLR-FB-84-02 | p 68 | N84-24693 | # | INPE-2988-PRE/452 | p 54 | N84-27260 | # |
| DNA-TR-81-253 | p 67 | N84-22873 | # | INPE-2991-NTE/212 | p 12 | N84-27256 | # |
| ERIM-150000-11-F | p 53 | N84-27258 | * | INPE-2995-PRE/447 | p 26 | N84-23979 | * |
| ERIM-155900-16-T | p 49 | N84-27320 | # | INPE-3005-NTE/213 | p 13 | N84-27261 | # |
| ERIM-160300-76-F | p 11 | N84-26098 | # | INPE-3061-NTE/216 | p 53 | N84-26100 | # |
| ERIM-16400-10-P | p 61 | N84-25140 | # | INPE-3063-PRE/480 | p 16 | N84-26090 | # |
| ESA-BR-18 | p 62 | N84-26102 | # | INPE-3067-PRE/484 | p 16 | N84-26428 | # |
| ESA-CR(P)-1867 | p 62 | N84-26103 | # | INPE-3076-PRE/489 | p 10 | N84-26087 | # |
| ESA-CR(P)-1868 | p 70 | N84-26237 | # | INPE-3077-PRE/490 | p 10 | N84-26083 | # |
| ESA-TT-799 | p 37 | N84-22955 | # | INPE-3078-PRE/491 | p 62 | N84-26091 | # |
| ESA-TT-816 | p 16 | N84-26104 | # | INPE-3084-PRE/494 | p 11 | N84-26092 | # |
| ESA-TT-819 | p 63 | N84-26105 | # | INPE-3089-PRE/496 | p 16 | N84-26095 | # |
| ETL-R-060 | p 63 | N84-26112 | # | INPE-3092-PRE/497 | p 40 | N84-26255 | # |
| ETL-R-061 | p 11 | N84-26108 | # | INPE-3098-NTE/218 | p 29 | N84-26094 | # |
| ETL-0348 | p 11 | N84-26107 | # | INPE-3100-PRE/499 | p 29 | N84-26093 | # |
| AAS PAPER 83-394 | p 17 | A84-30583 | # | INPE-3101-PRE/500 | p 61 | N84-26088 | # |
| AD-A137993 | p 19 | N84-23048 | # | INPE-3102-PRE/501 | p 41 | N84-26256 | # |
| AD-A138257 | p 38 | N84-23087 | # | INPE-3105-PRE/504 | p 10 | N84-26081 | * |
| AD-A138681 | p 67 | N84-22873 | # | INPE-3113-PRE/510 | p 62 | N84-26096 | # |
| AD-A139017 | p 16 | N84-23996 | # | INPE-3122-PRE/515 | p 62 | N84-26089 | # |
| AD-A139124 | p 10 | N84-23993 | # | IOS-170 | p 50 | N84-28354 | # |
| AD-A139447 | p 61 | N84-24499 | # | | | | |
| AD-A139786 | p 39 | N84-25235 | # | | | | |
| AD-A139894 | p 40 | N84-25238 | # | | | | |
| AD-A140185 | p 53 | N84-26106 | # | | | | |
| AD-A140195 | p 41 | N84-26257 | # | | | | |
| AD-A140197 | p 11 | N84-26107 | # | | | | |
| AD-A140198 | p 11 | N84-26108 | # | | | | |
| AD-A140230 | p 63 | N84-26112 | # | | | | |
| AD-A140507 | p 70 | N84-26217 | # | | | | |
| AD-A140566 | p 21 | N84-26687 | # | | | | |
| AD-A140567 | p 21 | N84-26688 | # | | | | |
| AD-A140584 | p 49 | N84-27320 | # | | | | |
| AD-A140589 | p 49 | N84-27321 | # | | | | |
| AD-A141233 | p 54 | N84-28344 | # | | | | |
| AD-A141302 | p 50 | N84-28359 | # | | | | |
| AD-E301336 | p 67 | N84-22873 | # | | | | |
| AD-E750826 | p 38 | N84-23087 | # | | | | |
| AD-P003120 | p 41 | N84-26261 | # | | | | |
| AD-P003122 | p 41 | N84-26263 | # | | | | |
| AD-P003124 | p 41 | N84-26265 | # | | | | |
| AD-P003125 | p 41 | N84-26266 | # | | | | |
| AERONOMICA-ACTA-A-281-1984 | p 70 | N84-26003 | # | | | | |
| AFGL-TR-83-0254 | p 19 | N84-23048 | # | | | | |
| AFGL-TR-83-0305 | p 54 | N84-28344 | # | | | | |
| AFGL-TR-84-0027 | p 70 | N84-26217 | # | | | | |
| AFIT/CN/IR-83-80T | p 10 | N84-23993 | # | | | | |
| AIAA PAPER 84-1060 | p 65 | A84-31741 | * | | | | |
| AR-4 | p 39 | N84-24078 | * | | | | |
| BLEV-R-65.169-5 | p 70 | N84-26237 | # | | | | |
| BTS07-84-05/RB | p 26 | N84-24691 | # | | | | |
| CRINC/RSL-TR-331-32 | p 40 | N84-25238 | # | | | | |
| CRREL-SP-84-1 | p 53 | N84-26106 | # | | | | |
| CRSC-83-3 | p 53 | N84-23976 | # | | | | |
| CRSC-84-1 | p 68 | N84-23982 | * | | | | |
| CRSC-84-2 | p 15 | N84-23983 | # | | | | |
| FOA-C-20529-D8 | p 16 | N84-25340 | # | | | | |
| FOA-C-30349-E1 | p 16 | N84-25156 | # | | | | |
| NAS 1.15:77412 | | | | | p 26 | N84-24031 | * |
| NAS 1.15:80258 | | | | | p 71 | N84-27248 | # |
| NAS 1.15:83916 | | | | | p 49 | N84-27319 | # |
| NAS 1.15:84421 | | | | | p 72 | N84-26467 | # |
| NAS 1.15:86080 | | | | | p 40 | N84-26233 | # |
| NAS 1.15:86107 | | | | | p 10 | N84-25142 | # |
| NAS 1.15:86248 | | | | | p 39 | N84-24078 | # |
| NAS 1.19:182 | | | | | p 72 | N84-26563 | # |
| NAS 1.21:4208 | | | | | p 72 | N84-25737 | # |
| NAS 1.26:171781 | | | | | p 11 | N84-26098 | # |
| NAS 1.26:171785 | | | | | p 11 | N84-26099 | # |
| NAS 1.26:171794 | | | | | p 12 | N84-27255 | # |
| NAS 1.26:172507 | | | | | p 10 | N84-26082 | # |
| NAS 1.26:172795 | | | | | p 26 | N84-23979 | # |
| NAS 1.26:172796 | | | | | p 60 | N84-23980 | # |
| NAS 1.26:172797 | | | | | p 60 | N84-23981 | # |
| NAS 1.26:172798 | | | | | p 68 | N84-23982 | # |
| NAS 1.26:172799 | | | | | p 15 | N84-23983 | # |
| NAS 1.26:172800 | | | | | p 15 | N84-23984 | # |
| NAS 1.26:172801 | | | | | p 26 | N84-25128 | # |
| NAS 1.26:172802 | | | | | p 71 | N84-23985 | # |
| NAS 1.26:172803 | | | | | p 68 | N84-23986 | # |
| NAS 1.26:172805 | | | | | p 61 | N84-25140 | # |
| NAS 1.26:172806 | | | | | p 10 | N84-26081 | * |
| NAS 1.26:172808 | | | | | p 10 | N84-26083 | # |

R
E
P
O
R
T

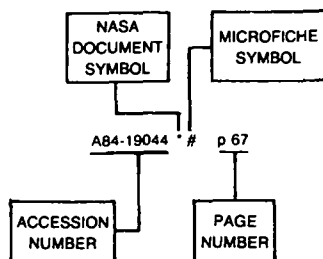
| | | | | | | | |
|-----------------|-------|------|---------------|--------------------|-------|-------|---------------|
| NAS 1.26:172809 | | p 70 | N84-26084 * # | NASA-CR-173640 | | p 12 | N84-27256 * # |
| NAS 1.26:172810 | | p 61 | N84-26085 * # | NASA-CR-173669 | | p 63 | N84-27249 * # |
| NAS 1.26:172811 | | p 61 | N84-26086 * # | NASA-CR-173670 | | p 63 | N84-27250 * # |
| NAS 1.26:172812 | | p 10 | N84-26087 * # | NASA-CR-173671 | | p 12 | N84-27251 * # |
| NAS 1.26:172813 | | p 61 | N84-26088 * # | NASA-CR-173680 | | p 22 | N84-28279 * # |
| NAS 1.26:172814 | | p 62 | N84-26089 * # | NASA-CR-173740 | | p 50 | N84-28355 * # |
| NAS 1.26:172815 | | p 16 | N84-26090 * # | NASA-CR-175155 | | p 39 | N84-25141 * # |
| NAS 1.26:172816 | | p 62 | N84-26091 * # | NASA-CR-175230 | | p 26 | N84-24691 * # |
| NAS 1.26:172817 | | p 11 | N84-26092 * # | NASA-CR-175245 | | p 29 | N84-28276 * # |
| NAS 1.26:172823 | | p 63 | N84-27247 * # | NASA-CR-3799 | | p 68 | N84-23987 * # |
| NAS 1.26:173235 | | p 29 | N84-26093 * # | NASA-EP-182 | | p 72 | N84-26563 * # |
| NAS 1.26:173236 | | p 29 | N84-26094 * # | NASA-SP-4208 | | p 72 | N84-25737 * # |
| NAS 1.26:173237 | | p 16 | N84-26095 * # | NASA-TM-80258 | | p 26 | N84-24031 * # |
| NAS 1.26:173238 | | p 62 | N84-26096 * # | NASA-TM-83916 | | p 71 | N84-27248 * # |
| NAS 1.26:173239 | | p 62 | N84-26097 * # | NASA-TM-84421 | | p 49 | N84-27319 * # |
| NAS 1.26:173367 | | p 67 | N84-23000 * # | NASA-TM-86080 | | p 72 | N84-26467 * # |
| NAS 1.26:173369 | | p 60 | N84-23003 * # | NASA-TM-86107 | | p 40 | N84-26233 * # |
| NAS 1.26:173480 | | p 53 | N84-22997 * # | NASA-TM-86248 | | p 10 | N84-25142 * # |
| NAS 1.26:173481 | | p 8 | N84-23004 * # | NASA-TM-863107 | | p 39 | N84-24078 * # |
| NAS 1.26:173482 | | p 24 | N84-23005 * # | NOAA-84021612 | | p 39 | N84-24065 * # |
| NAS 1.26:173483 | | p 9 | N84-23006 * # | NOAA-84031901 | | p 13 | N84-27324 * # |
| NAS 1.26:173484 | | p 9 | N84-23007 * # | NOAA-TR/NESDIS-7 | | p 13 | N84-27324 * # |
| NAS 1.26:173485 | | p 24 | N84-23008 * # | NORDA-TN-176 | | p 41 | N84-26257 * # |
| NAS 1.26:173486 | | p 53 | N84-23976 * # | NORDA-TN-261 | | p 39 | N84-25235 * # |
| NAS 1.26:173487 | | p 9 | N84-23977 * # | NORDA-TN-264 | | p 49 | N84-27321 * # |
| NAS 1.26:173488 | | p 9 | N84-23978 * # | NORDA-TN-267 | | p 50 | N84-28359 * # |
| NAS 1.26:173489 | | p 60 | N84-23009 * # | NP-4900854 | | p 71 | N84-25159 * # |
| NAS 1.26:173490 | | p 38 | N84-23085 * # | N84-27249 * # | | p 41 | N84-26257 * # |
| NAS 1.26:173511 | | p 53 | N84-27258 * # | N84-27250 * # | | p 39 | N84-24065 * # |
| NAS 1.26:173539 | | p 71 | N84-25510 * # | N84-28279 * # | | p 69 | N84-25034 * # |
| NAS 1.26:173541 | | p 69 | N84-25034 * # | N84-28279 * # | | p 13 | N84-27324 * # |
| NAS 1.26:173590 | | p 40 | N84-26232 * # | N84-28355 * # | | p 50 | N84-28359 * # |
| NAS 1.26:173638 | | p 12 | N84-27257 * # | N84-27256 * # | | p 71 | N84-25159 * # |
| NAS 1.26:173640 | | p 12 | N84-27256 * # | NP-4900854 | | p 71 | N84-25159 * # |
| NAS 1.26:173669 | | p 63 | N84-27249 * # | N84-27249 * # | | p 60 | N84-23009 * # |
| NAS 1.26:173670 | | p 63 | N84-27250 * # | N84-27250 * # | | p 60 | N84-23009 * # |
| NAS 1.26:173671 | | p 12 | N84-27251 * # | N84-28279 * # | | p 61 | N84-24499 * # |
| NAS 1.26:173680 | | p 22 | N84-28279 * # | N84-28279 * # | | p 13 | N84-27324 * # |
| NAS 1.26:173740 | | p 50 | N84-28355 * # | N84-28355 * # | | p 54 | N84-28344 * # |
| NAS 1.26:175155 | | p 39 | N84-25141 * # | PR-3 | | p 63 | N84-27249 * # |
| NAS 1.26:175230 | | p 26 | N84-24691 * # | PR-4 | | p 61 | N84-24499 * # |
| NAS 1.26:175245 | | p 29 | N84-28276 * # | P79-1 | | p 54 | N84-28344 * # |
| NAS 1.26:3799 | | p 68 | N84-23987 * # | QR-5 | | p 67 | N84-23000 * # |
| NAS 1.55:2303 | | p 42 | N84-27262 * # | QR-6 | | p 60 | N84-23009 * # |
| NASA-CP-2303 | | p 42 | N84-27262 * # | QR-6 | | p 70 | N84-26084 * # |
| NASA-CR-171781 | | p 11 | N84-26098 * # | QSTPR-5 | | p 61 | N84-26085 * # |
| NASA-CR-171785 | | p 11 | N84-26099 * # | RANRL-TM(EXT)-8/83 | | p 38 | N84-23087 * # |
| NASA-CR-171794 | | p 12 | N84-27255 * # | RSC-134 | | p 9 | N84-23006 * # |
| NASA-CR-172507 | | p 10 | N84-26082 * # | RSC-138 | | p 9 | N84-23007 * # |
| NASA-CR-172795 | | p 26 | N84-23979 * # | RSC-4854 | | p 12 | N84-27255 * # |
| NASA-CR-172796 | | p 60 | N84-23980 * # | SAI-83/1321 | | p 39 | N84-24065 * # |
| NASA-CR-172797 | | p 60 | N84-23981 * # | SAPR-1 | | p 40 | N84-26235 * # |
| NASA-CR-172798 | | p 68 | N84-23982 * # | SAPR-21 | | p 68 | N84-23986 * # |
| NASA-CR-172799 | | p 15 | N84-23983 * # | SER-A-98 | | p 20 | N84-26069 * # |
| NASA-CR-172800 | | p 15 | N84-23984 * # | SER-C-285 | | p 21 | N84-28199 * # |
| NASA-CR-172801 | | p 26 | N84-25128 * # | SER-C-286 | | p 21 | N84-26080 * # |
| NASA-CR-172802 | | p 71 | N84-23985 * # | SER-C-283 | | p 21 | N84-26079 * # |
| NASA-CR-172803 | | p 68 | N84-23986 * # | SM-3-04447 | | p 9 | N84-23007 * # |
| NASA-CR-172805 | | p 61 | N84-25140 * # | SM-3-04448 | | p 9 | N84-23006 * # |
| NASA-CR-172806 | | p 10 | N84-26081 * # | SR-2 | | p 54 | N84-28344 * # |
| NASA-CR-172808 | | p 10 | N84-26083 * # | TRITA-FMI-47 | | p 69 | N84-25146 * # |
| NASA-CR-172809 | | p 70 | N84-26084 * # | USGS-CIRC-911 | | p 25 | N84-23934 * # |
| NASA-CR-172810 | | p 61 | N84-26085 * # | WES/MP/EL-84-1 | | p 16 | N84-23996 * # |
| NASA-CR-172811 | | p 61 | N84-26086 * # | WMO-168 | | p 53 | N84-25145 |
| NASA-CR-172812 | | p 10 | N84-26087 * # | WMO-623 | | p 38 | N84-23089 |
| NASA-CR-172813 | | p 61 | N84-26088 * # | | | | |
| NASA-CR-172814 | | p 62 | N84-26089 * # | | | | |
| NASA-CR-172815 | | p 16 | N84-26090 * # | | | | |
| NASA-CR-172816 | | p 62 | N84-26091 * # | | | | |
| NASA-CR-172817 | | p 11 | N84-26092 * # | | | | |
| NASA-CR-173223 | | p 63 | N84-27247 * # | | | | |
| NASA-CR-173235 | | p 29 | N84-26093 * # | | | | |
| NASA-CR-173236 | | p 29 | N84-26094 * # | | | | |
| NASA-CR-173237 | | p 16 | N84-26095 * # | | | | |
| NASA-CR-173238 | | p 62 | N84-26096 * # | | | | |
| NASA-CR-173239 | | p 62 | N84-26097 * # | | | | |
| NASA-CR-173367 | | p 67 | N84-23000 * # | | | | |
| NASA-CR-173369 | | p 60 | N84-23003 * # | | | | |
| NASA-CR-173480 | | p 53 | N84-22997 * # | | | | |
| NASA-CR-173481 | | p 8 | N84-23004 * # | | | | |
| NASA-CR-173482 | | p 24 | N84-23005 * # | | | | |
| NASA-CR-173483 | | p 9 | N84-23006 * # | | | | |
| NASA-CR-173484 | | p 9 | N84-23007 * # | | | | |
| NASA-CR-173485 | | p 24 | N84-23008 * # | | | | |
| NASA-CR-173486 | | p 53 | N84-23976 * # | | | | |
| NASA-CR-173487 | | p 9 | N84-23977 * # | | | | |
| NASA-CR-173488 | | p 9 | N84-23978 * # | | | | |
| NASA-CR-173489 | | p 60 | N84-23009 * # | | | | |
| NASA-CR-173490 | | p 38 | N84-23085 * # | | | | |
| NASA-CR-173511 | | p 53 | N84-27258 * # | | | | |
| NASA-CR-173539 | | p 71 | N84-25510 * # | | | | |
| NASA-CR-173541 | | p 69 | N84-25034 * # | | | | |
| NASA-CR-173590 | | p 40 | N84-26232 * # | | | | |
| NASA-CR-173638 | | p 12 | N84-27257 * # | | | | |

ACCESSION NUMBER INDEX

EARTH RESOURCES / A Continuing Bibliography (Issue 43)

OCTOBER 1984

Typical Accession Number Index Listing



Listings in this index are arranged alphanumerically by accession number. The page number listed to the right indicates the page on which the citation is located. An asterisk (*) indicates that the item is a NASA report. A pound sign (#) indicates that the item is available on microfiche.

| | | | |
|------------------|------------------|------------------|------------------|
| A84-30024 # p 30 | A84-31193 # p 31 | A84-38301 # p 15 | N84-23978 # p 9 |
| A84-30025 # p 30 | A84-31431 # p 31 | A84-38302 # p 58 | N84-23979 # p 26 |
| A84-30226 # p 64 | A84-31498 # p 3 | A84-38304 # p 58 | N84-23980 # p 60 |
| A84-30227 # p 1 | A84-31499 # p 3 | A84-38305 # p 59 | N84-23981 # p 60 |
| A84-30228 # p 1 | A84-31741 # p 65 | A84-38307 # p 36 | N84-23982 # p 68 |
| A84-30229 # p 1 | A84-31821 # p 31 | A84-38310 # p 66 | N84-23983 # p 15 |
| A84-30230 # p 30 | A84-31947 # p 65 | A84-38311 # p 66 | N84-23984 # p 15 |
| A84-30232 # p 30 | A84-31948 # p 51 | A84-38312 # p 66 | N84-23985 # p 71 |
| A84-30233 # p 64 | A84-31950 # p 51 | A84-38313 # p 59 | N84-23986 # p 68 |
| A84-30234 # p 54 | A84-32093 # p 55 | A84-38314 # p 59 | N84-23987 # p 68 |
| A84-30235 # p 1 | A84-32266 # p 31 | A84-38315 # p 59 | N84-23990 # p 9 |
| A84-30236 # p 1 | A84-32494 # p 17 | A84-38316 # p 59 | N84-23993 # p 10 |
| A84-30237 # p 1 | A84-32495 # p 17 | A84-38620 # p 36 | N84-23996 # p 16 |
| A84-30238 # p 1 | A84-32590 # p 23 | A84-38702 # p 36 | N84-24031 # p 26 |
| A84-30239 # p 2 | A84-32938 # p 65 | A84-38773 # p 36 | N84-24065 # p 39 |
| A84-30240 # p 13 | A84-33024 # p 17 | A84-38812 # p 19 | N84-24078 # p 39 |
| A84-30241 # p 13 | A84-33226 # p 65 | A84-38922 # p 66 | N84-24499 # p 61 |
| A84-30242 # p 13 | A84-33237 # p 23 | A84-38923 # p 66 | N84-24679 # p 68 |
| A84-30243 # p 13 | A84-3328 # p 3 | A84-38940 # p 24 | N84-24691 # p 26 |
| A84-30246 # p 50 | A84-3329 # p 3 | A84-38941 # p 36 | N84-24693 # p 68 |
| A84-30247 # p 22 | A84-3330 # p 3 | A84-38942 # p 59 | N84-25034 # p 69 |
| A84-30248 # p 54 | A84-33323 # p 4 | A84-38944 # p 36 | N84-25128 # p 26 |
| A84-30249 # p 54 | A84-3333 # p 14 | A84-38945 # p 66 | N84-25129 # p 27 |
| A84-30250 # p 2 | A84-3334 # p 55 | A84-38946 # p 67 | N84-25130 # p 27 |
| A84-30251 # p 51 | A84-3335 # p 55 | A84-3944 # p 67 | N84-25132 # p 27 |
| A84-30252 # p 64 | A84-3337 # p 4 | A84-39447 # p 67 | N84-25133 # p 27 |
| A84-30253 # p 2 | A84-3338 # p 4 | A84-39449 # p 67 | N84-25140 # p 28 |
| A84-30254 # p 22 | A84-3339 # p 51 | A84-3945 # p 67 | N84-25141 # p 39 |
| A84-30255 # p 51 | A84-3340 # p 4 | A84-39450 # p 32 | N84-25142 # p 10 |
| A84-30256 # p 51 | A84-3342 # p 4 | A84-39451 # p 33 | N84-25143 # p 20 |
| A84-30257 # p 51 | A84-3343 # p 4 | A84-39452 # p 34 | N84-25144 # p 69 |
| A84-30258 # p 30 | A84-3344 # p 14 | A84-39453 # p 34 | N84-25145 # p 53 |
| A84-30259 # p 22 | A84-3345 # p 5 | A84-39454 # p 33 | N84-25146 # p 69 |
| A84-30260 # p 22 | A84-3347 # p 5 | A84-39455 # p 15 | N84-25147 # p 69 |
| A84-30261 # p 22 | A84-3348 # p 5 | A84-39456 # p 15 | N84-25148 # p 61 |
| A84-30262 # p 22 | A84-3349 # p 5 | A84-39457 # p 15 | N84-25149 # p 39 |
| A84-30263 # p 22 | A84-3350 # p 23 | A84-22873 # p 67 | N84-25150 # p 69 |
| A84-30264 # p 54 | A84-3352 # p 5 | A84-22995 # p 37 | N84-25151 # p 69 |
| A84-30265 # p 64 | A84-3353 # p 52 | A84-22997 # p 53 | N84-25152 # p 69 |
| A84-30266 # p 64 | A84-3355 # p 52 | A84-34780 # p 6 | N84-22998 # p 60 |
| A84-30268 # p 54 | A84-3356 # p 55 | A84-34781 # p 23 | N84-23000 # p 67 |
| A84-30302 # p 30 | A84-3357 # p 18 | A84-34782 # p 23 | N84-23001 # p 68 |
| A84-30303 # p 22 | A84-3360 # p 31 | A84-34783 # p 6 | N84-23002 # p 68 |
| A84-30304 # p 17 | A84-3361 # p 14 | A84-34784 # p 6 | N84-23003 # p 60 |
| A84-30305 # p 64 | A84-3362 # p 55 | A84-34785 # p 6 | N84-23004 # p 8 |
| A84-30306 # p 22 | A84-3363 # p 55 | A84-34786 # p 58 | N84-23005 # p 24 |
| A84-30307 # p 13 | A84-3364 # p 18 | A84-34787 # p 65 | N84-23006 # p 9 |
| A84-30443 # p 30 | A84-3365 # p 18 | A84-34789 # p 24 | N84-23007 # p 9 |
| A84-30516 # p 64 | A84-3366 # p 55 | A84-34794 # p 15 | N84-23008 # p 24 |
| A84-30583 # p 17 | A84-3367 # p 55 | A84-34942 # p 34 | N84-23009 # p 60 |
| A84-30670 # p 2 | A84-3368 # p 14 | A84-34958 # p 65 | N84-23010 # p 24 |
| A84-30671 # p 2 | A84-3369 # p 18 | A84-34959 # p 58 | N84-23011 # p 9 |
| A84-30672 # p 31 | A84-3370 # p 18 | A84-34960 # p 7 | N84-23012 # p 72 |
| A84-30673 # p 2 | A84-3371 # p 18 | A84-34961 # p 7 | N84-23013 # p 70 |
| A84-30674 # p 3 | A84-3372 # p 5 | A84-35252 # p 34 | N84-23014 # p 20 |
| A84-30727 # p 17 | A84-3373 # p 14 | A84-35542 # p 34 | N84-23015 # p 20 |
| A84-30787 # p 23 | A84-3374 # p 18 | A84-36107 # p 34 | N84-23016 # p 20 |
| A84-31024 # p 13 | A84-3375 # p 56 | A84-36119 # p 35 | N84-23017 # p 20 |
| A84-31072 # p 64 | A84-3376 # p 56 | A84-36289 # p 35 | N84-23018 # p 20 |
| | | A84-36516 # p 7 | N84-23019 # p 21 |
| | | A84-36684 # p 35 | N84-23020 # p 21 |
| | | A84-36686 # p 35 | N84-23021 # p 21 |
| | | A84-36710 # p 7 | N84-23022 # p 21 |
| | | A84-36872 # p 35 | N84-23023 # p 21 |
| | | A84-36919 # p 19 | N84-23024 # p 21 |
| | | A84-36922 # p 24 | N84-23025 # p 39 |
| | | A84-37049 # p 71 | N84-23026 # p 40 |
| | | A84-37069 # p 19 | N84-23027 # p 16 |
| | | A84-37095 # p 35 | N84-23028 # p 71 |
| | | A84-37201 # p 7 | N84-23029 # p 72 |
| | | A84-37202 # p 7 | N84-23030 # p 70 |
| | | A84-37203 # p 7 | N84-23031 # p 70 |
| | | A84-37204 # p 8 | N84-23032 # p 20 |
| | | A84-37299 # p 35 | N84-23033 # p 20 |
| | | A84-37773 # p 58 | N84-23034 # p 61 |
| | | A84-37775 # p 24 | N84-23035 # p 61 |
| | | A84-37873 # p 66 | N84-23036 # p 61 |
| | | A84-38296 # p 52 | N84-23037 # p 61 |
| | | A84-38299 # p 35 | N84-23038 # p 61 |
| | | A84-38300 # p 58 | N84-23039 # p 61 |

A
C
C
E
S
S
I
O
N

N84-26101 # p 29
N84-26102 # p 62
N84-26103 # p 62
N84-26104 # p 16
N84-26105 # p 63
N84-26106 # p 53
N84-26107 # p 11
N84-26108 # p 11
N84-26112 # p 63
N84-26217 # p 70
N84-26232 # p 40
N84-26233 * # p 40
N84-26235 # p 40
N84-26237 # p 70
N84-26238 # p 70
N84-26255 # p 40
N84-26256 # p 41
N84-26257 # p 41
N84-26261 # p 41
N84-26263 # p 41
N84-26265 # p 41
N84-26266 # p 41
N84-26428 # p 16
N84-26467 * # p 72
N84-26563 * # p 72
N84-26687 # p 21
N84-26688 # p 21
N84-27245 # p 63
N84-27246 # p 11
N84-27247 * # p 63
N84-27248 * # p 71
N84-27249 * # p 63
N84-27250 * # p 63
N84-27251 * # p 12
N84-27255 * # p 12
N84-27256 * # p 12
N84-27257 * # p 12
N84-27258 * # p 53
N84-27259 # p 29
N84-27260 # p 54
N84-27261 # p 13
N84-27262 * # p 42
N84-27263 * # p 42
N84-27264 * # p 42
N84-27266 * # p 42
N84-27267 * # p 42
N84-27268 * # p 42
N84-27269 * # p 43
N84-27272 * # p 43
N84-27273 * # p 43
N84-27274 * # p 43
N84-27275 * # p 43
N84-27276 * # p 44
N84-27277 * # p 44
N84-27278 * # p 44
N84-27279 * # p 44
N84-27280 * # p 44
N84-27281 * # p 44
N84-27282 * # p 45
N84-27283 * # p 45
N84-27284 * # p 45
N84-27285 * # p 45
N84-27286 * # p 71
N84-27288 * # p 45
N84-27289 * # p 45
N84-27290 * # p 46
N84-27296 * # p 46
N84-27297 * # p 46
N84-27298 * # p 46
N84-27299 * # p 46
N84-27301 * # p 46
N84-27302 * # p 47
N84-27303 * # p 47
N84-27304 * # p 47
N84-27305 * # p 47
N84-27306 * # p 47
N84-27307 * # p 47
N84-27308 * # p 48
N84-27309 * # p 48
N84-27310 * # p 48
N84-27311 * # p 48
N84-27312 * # p 48
N84-27313 * # p 48
N84-27314 * # p 49
N84-27316 * # p 49
N84-27317 * # p 49
N84-27318 * # p 49
N84-27319 * # p 49
N84-27320 # p 49
N84-27321 # p 49
N84-27324 # p 13
N84-27921 # p 50
N84-28199 # p 21
N84-28201 # p 17
N84-28202 # p 63
N84-28276 * # p 29

| | | | |
|--|--|--|--------------------------|
| 1. Report No. NASA SP-7041 (43) | 2. Government Accession No. | 3. Recipient's Catalog No. | |
| 4. Title and Subtitle EARTH RESOURCES A Continuing Bibliography (Issue 43) | | 5. Report Date October 1984 | |
| 7. Author(s) | | 6. Performing Organization Code | |
| 9. Performing Organization Name and Address National Aeronautics and Space Administration Washington, D.C. 20546 | | 8. Performing Organization Report No. | |
| 12. Sponsoring Agency Name and Address | | 10. Work Unit No. | |
| 15. Supplementary Notes | | 11. Contract or Grant No. | |
| 16. Abstract This bibliography lists 460 reports, articles and other documents introduced into the NASA scientific and technical information system between July 1 and September 30, 1984. Emphasis is placed on the use of remote sensing and geophysical instrumentation in spacecraft and aircraft to survey and inventory natural resources and urban areas. Subject matter is grouped according to agriculture and forestry, environmental changes and cultural resources, geodesy and cartography, geology and mineral resources, hydrology and water management, data processing and distribution systems, instrumentation and sensors, and economical analysis. | | 13. Type of Report and Period Covered | |
| 17. Key Words (Suggested by Author(s)) Bibliographies Earth Resources Remote Sensors | | 18. Distribution Statement Unclassified - Unlimited | |
| 19. Security Classif. (of this report) Unclassified | 20. Security Classif. (of this page) Unclassified | 21. No. of Pages 136 | 22. Price* \$12.00 HC |

* For sale by the National Technical Information Service, Springfield, Virginia 22161

NASA-Langley, 1984

FEDERAL DEPOSITORY LIBRARY PROGRAM

The Federal Depository Library Program provides Government publications to designated libraries throughout the United States. The Regional Depository Libraries listed below receive and retain at least one copy of nearly every Federal Government publication, either in printed or microfilm form, for use by the general public. These libraries provide reference services and inter-library loans; however, they are not sales outlets. You may wish to ask your local library to contact a Regional Depository to help you locate specific publications, or you may contact the Regional Depository yourself.

| | | | |
|---|--|--|--|
| ARKANSAS STATE LIBRARY One Capitol Mall Little Rock, AR 72201 (501) 371-2326 | ILLINOIS STATE LIBRARY Information Services Branch Centennial Building Springfield, IL 62706 (217) 782-5185 | UNIV. OF MISSISSIPPI LIB. Documents Department University, MS 38677 (601) 232-5857 | OKLAHOMA DEPT. OF LIB. Government Documents 200 NE 18th Street Oklahoma City, OK 73105 (405) 521-2502 |
| AUBURN UNIV. AT MONTGOMERY LIBRARY Documents Department Montgomery, AL 36193 (205) 279-9110, ext. 253 | INDIANA STATE LIBRARY Serials Documents Section 140 North Senate Avenue Indianapolis, IN 46204 (317) 232-3686 | UNIV. OF MONTANA Mansfield Library Documents Division Missoula, MT 59812 (406) 243-6700 | OKLAHOMA STATE UNIV. LIB. Documents Department Stillwater, OK 74078 (405) 624-6546 |
| UNIV. OF ALABAMA LIBRARY Documents Dept.—Box S University, AL 35486 (205) 348-7369 | UNIV. OF IOWA LIBRARIES Govt. Documents Department Iowa City, IA 52242 (319) 353-3318 | NEBRAKA LIBRARY COMM. Federal Documents 1420 P Street Lincoln, NE 68508 (402) 471-2045 In cooperation with University of Nebraska-Lincoln | PORLAND STATE UNIV. LIB. Documents Department P.O. Box 1151 Portland, OR 97207 (503) 229-3673 |
| DEPT. OF LIBRARY, ARCHIVES AND PUBLIC RECORDS Third Floor—State Cap. 1700 West Washington Phoenix, AZ 85007 (602) 255-4121 | UNIVERSITY OF KANSAS Doc. Collect—Spencer Lib. Lawrence, KS 66045 (913) 864-4662 | UNIVERSITY OF NEVADA LIB. Govt. Pub. Department Reno, NV 89557 (702) 784-6579 | STATE LIBRARY OF PENN. Government Pub. Section P.O. Box 1601 Harrisburg, PA 17105 (717) 787-3752 |
| UNIVERSITY OF ARIZONA LIB. Government Documents Dept. Tucson, AZ 85721 (602) 626-5233 | UNIV. OF KENTUCKY LIBRARIES Govt. Pub. Department Lexington, KY 40506 (606) 257-3139 | NEWARK PUBLIC LIBRARY 5 Washington Street Newark, NJ 07101 (201) 733-7812 | TEXAS STATE LIBRARY Public Services Department P.O. Box 12927—Cap. Sta. Austin, TX 78753 (512) 471-2996 |
| CALIFORNIA STATE LIBRARY Govt. Publications Section P.O. Box 2037 Sacramento, CA 95809 (916) 322-4572 | LOUISIANA STATE UNIVERSITY Middleton Library Govt. Docs. Dept. Baton Rouge, LA 70803 (504) 388-2570 | UNIVERSITY OF NEW MEXICO Zimmerman Library Government Pub. Dept. Albuquerque, NM 87131 (505) 277-5441 | TEXAS TECH UNIV. LIBRARY Govt. Documents Department Lubbock, TX 79409 (806) 742-2268 |
| UNIV. OF COLORADO LIB. Government Pub. Division Campus Box 184 Boulder, CO 80309 (303) 492-8834 | LOUISIANA TECHNICAL UNIV. LIBRARY Documents Department Ruston, LA 71272 (318) 257-4962 | NEW MEXICO STATE LIBRARY Reference Department 325 Don Gaspar Avenue Santa Fe, NM 87501 (505) 827-2033, ext. 22 | UTAH STATE UNIVERSITY Merrill Library, U.M.C. 30 Logan, UT 84322 (801) 750-2682 |
| DENVER PUBLIC LIBRARY Govt. Pub. Department 1357 Broadway Denver, CO 80203 (303) 571-2131 | UNIVERSITY OF MAINE Raymond H. Fogler Library Tri-State Regional Documents Depository Orono, ME 04469 (207) 581-1680 | NEW YORK STATE LIBRARY Empire State Plaza Albany, NY 12230 (518) 474-5563 | UNIVERSITY OF VIRGINIA Alderman Lib.—Public Doc. Charlottesville, VA 22901 (804) 924-3133 |
| CONNECTICUT STATE LIBRARY Government Documents Unit 231 Capitol Avenue Hartford, CT 06106 (203) 566-4971 | UNIVERSITY OF MARYLAND McKeldin Lib.—Doc. Div. College Park, MD 20742 (301) 454-3034 | UNIVERSITY OF NORTH CAROLINA AT CHAPEL HILL Wilson Library BA/SS Documents Division Chapel Hill, NC 27515 (919) 962-1321 | WASHINGTON STATE LIBRARY Documents Section Olympia, WA 98504 (206) 753-4027 |
| UNIV. OF FLORIDA LIBRARIES Library West Documents Department Gainesville, FL 32611 (904) 392-0367 | BOSTON PUBLIC LIBRARY Government Docs. Dept. Boston, MA 02117 (617) 536-5400 ext. 226 | UNIVERSITY OF NORTH DAKOTA Chester Fritz Library Documents Department Grand Forks, ND 58202 (701) 777-2617, ext. 27 (In cooperation with North Dakota State Univ. Library) | WEST VIRGINIA UNIV. LIB. Documents Department Morgantown, WV 26506 (304) 293-3640 |
| UNIV. OF GEORGIA LIBRARIES Government Reference Dept. Athens, Ga 30602 (404) 542-8951 | DETROIT PUBLIC LIBRARY Sociology Department 5201 Woodward Avenue Detroit, MI 48202 (313) 833-1409 | STATE LIBRARY OF OHIO Documents Department 65 South Front Street Columbus, OH 43215 (614) 462-7051 | MILWAUKEE PUBLIC LIBRARY 814 West Wisconsin Avenue Milwaukee, WI 53233 (414) 278-3000 |
| UNIV. OF HAWAII LIBRARY Govt. Documents Collection 2550 The Mall Honolulu, HI 96822 (808) 948-8230 | MICHIGAN STATE LIBRARY P.O. Box 30007 Lansing, MI 48909 (517) 373-0640 | UNIVERSITY OF MINNESOTA Government Pubs. Division 408 Wilson Library 309 19th Avenue South Minneapolis, MN 55455 (612) 373-7813 | ST. HIST LIB. OF WISCONSIN Government Pub. Section 816 State Street Madison, WI 53706 (608) 262-4347 |
| UNIV. OF IDAHO LIBRARY Documents Section Moscow, ID 83843 (208) 885-6344 | | | WYOMING STATE LIBRARY Supreme Ct. & Library Bld. Cheyenne, WY 82002 (307) 777-6344 |

National Aeronautics and
Space Administration

Washington, D.C.
20546

Official Business

Penalty for Private Use, \$300

THIRD-CLASS BULK RATE

Postage and Fees Paid
National Aeronautics and
Space Administration
NASA-451



10 I SP-7041, 841106 S90569ASR850630
NASA

SCIEN & TECH INFO FACILITY
ATTN: ACCESSIONING DEPT
P O BOX 8757 BWI ARPRT
BALTIMORE MD 21240

NASA

POSTMASTER: If Undeliverable (Section 158
Postal Manual) Do Not Return
